



저작자표시-비영리-변경금지 2.0 대한민국

이용자는 아래의 조건을 따르는 경우에 한하여 자유롭게

- 이 저작물을 복제, 배포, 전송, 전시, 공연 및 방송할 수 있습니다.

다음과 같은 조건을 따라야 합니다:



저작자표시. 귀하는 원저작자를 표시하여야 합니다.



비영리. 귀하는 이 저작물을 영리 목적으로 이용할 수 없습니다.



변경금지. 귀하는 이 저작물을 개작, 변형 또는 가공할 수 없습니다.

- 귀하는, 이 저작물의 재이용이나 배포의 경우, 이 저작물에 적용된 이용허락조건을 명확하게 나타내어야 합니다.
- 저작권자로부터 별도의 허가를 받으면 이러한 조건들은 적용되지 않습니다.

저작권법에 따른 이용자의 권리는 위의 내용에 의하여 영향을 받지 않습니다.

이것은 [이용허락규약\(Legal Code\)](#)을 이해하기 쉽게 요약한 것입니다.

[Disclaimer](#)

이학박사학위논문

**[3,3]-Sigmatropic Rearrangement of N-Hydroxyindole: Synthetic Study towards Rhazimal and Method Development**

N-하이드록시인돌의 [3,3] 시그마 결합 자리  
옮김 반응: 라지말의 합성 연구 및 관련 방법론  
개발

2023년 8월

서울대학교 대학원

화학부 유기화학 전공

이 유 진

**[3,3]-Sigmatropic Rearrangement of N-  
Hydroxyindole: Synthetic Study towards  
Rhazimal and Method Development**

Yujin Lee

A DISSERTATION  
IN CANDIDACY FOR THE DEGREE  
OF DOCTOR OF PHILOSOPHY

Supervisor: Prof. Hong Geun Lee

August 2023

**Department of Chemistry**  
**Graduate School**  
**Seoul National University**

**[3,3]-Sigmatropic Rearrangement of N-  
Hydroxyindole: Synthetic Study towards Rhazimal  
and Method Development**

지도교수 이 홍 근

이 논문을 이학박사학위논문으로 제출함

2023년 8월

서울대학교 대학원

화학부 유기화학 전공

이유진

이유진의 박사학위논문을 인준함

2023년 8월

위 원 장	_____	(인)
부 위 원 장	_____	(인)
위 원	_____	(인)
위 원	_____	(인)
위 원	_____	(인)

# ABSTRACT

Indole, whose importance will never fade among myriad types of small molecules and heterocycles, is a “privileged” scaffold that has been of interest to laboratories and related industries from the dawn of organic chemistry.

Aside from the biological and pharmacological values of indole itself, numerous noble molecular architectures that can be accessed by dearomatization of indole further enhance the value of research on indole. Remarkable advances in chemistry over decades has enabled the application of various converging technologies and innovative tools in the field of organic chemistry, and as a result it has become possible to materialize various ideas that have not been realized before, and different approaches have been able to be developed at an increasing pace on indole functionalization.

Amid the tide of these various strategies available, the use of *N*-hydroxyindole for the dearomatization of indole is still in the minority. Only recently has the inherent reactivity of *N*-hydroxyindole been re-examined and inspired the related studies to be actively published. However, it is undeniable that the potential of *N*-hydroxyindole has not yet been fully explored. This thesis describes efforts and attempts to extend the [3,3]-sigmatropic rearrangement of *N*-hydroxyindole from a total synthetic and methodological viewpoint.

In Chapter 1, the synthetic contribution towards total synthesis of rhazimal is presented. A new biosynthetic hypothesis that *N*-hydroxyl geissoschizine is generated as a result of oxidation of geissoschizine and promotes selective C7–C16 bond formation via intramolecular [3,3]-sigmatropic rearrangement, was proposed. To prove this hypothesis, a three-step synthetic plan with stepwise increase in molecular complexity was devised, ultimately aiming at the biomimetic synthesis of rhazimal.

In Chapter 2, C3-hetero-functionalization of indole derivatives via [3,3]-sigmatropic rearrangement of *N*-hydroxyindole is discussed. [3,3]-Sigmatropic rearrangement of *N*-hydroxyindole was extended as an integrated means of conjugating various heteroatoms to the C3-position of indole scaffold by exploiting the reactivity discovered during the investigations of the total synthesis of rhazimal. It was experimentally observed that two distinct mechanisms operate simultaneously, and the electronic properties of the substrate determine the relative contributions and energy barrier of these mechanistic pathways.

**Keyword** : Dearomatization • *N*-Hydroxyindole • Nitrogen heterocycles • Substituent effect • Sigmatropic rearrangement

**Student Number** : 2018-39895

## PREFACE

Certain section of this thesis has been adapted from the published articles co-authored by the author and other researchers, which are the outcome of substantial collaborations between the author and other researchers. The author's individual contributions are delineated below.

**Chapter 2:** Yujin Lee, Yun Seung Nam, Soo Young Kim, Jeong Eun Ki, and Hong Geun Lee, “Mechanistic Duality of Indolyl 1,3-Heteroatom Transposition”, *Chem. Sci.*, **2023**, accepted article. DOI: 10.1039/D3SC00716B

### *Respective contributions*

H.G.L. initiated and supervised the project. Y.L. designed the experiments and performed the reaction optimization for the preliminary results. Y.S.N. performed optimization of the reaction utilizing imidoyl chloride. Y.L., Y.S.N., S.Y.K., and J.E.K. carried out the synthetic experiments and Y.L. conducted the mechanistic investigations ( $^{18}\text{O}$  isotope labelling and related calculations, crossover experiment, radical trap experiment and reaction with indolyl *N*-carbamate). All the authors analyzed and discussed the experimental data. H.G.L. and Y.L. wrote the manuscript, and Y.L. and Y.S.N. wrote the supplementary information.

# CONTENTS

**Abstract**

**Preface**

**Table of Contents**

**List of Abbreviations**

<b>Chapter 1. Synthetic Studies towards Rhazimal</b> .....	1
<b>1.1. Introduction</b> .....	2
<b>1.1.1 Background and Biosynthesis</b> .....	2
<b>1.1.2. Past Synthetic Works towards C7–C16 Bond Connection from Geissoschizine via Biomimetic Approaches</b> .....	5
<b>1.1.3. [3,3]-Sigmatropic Rearrangement of <i>N</i>-Hydroxyindole</b> .....	12
1.1.3.1. C–O bond formation.....	14
1.1.3.2. C–C bond formation.....	17
1.1.3.3. Similar Applications in Different Framework.....	21
<b>1.2. A Controlled C7–C16 Bond Formation via [3,3]-Sigmatropic Rearrangement Strategy</b> .....	24
<b>1.2.1. Model Study Development for [3,3]-Sigmatropic Rearrangement</b> .....	25
<b>1.2.2. Implementation of the Key Strategy in the Intramolecular System and Synthetic Attempt for Rhazimal</b> .....	32
<b>1.3. Conclusions</b> .....	45
<b>1.4. References</b> .....	46
<b>1.5. Experimental Section</b> .....	50
<b>Chapter 2. C3-Hetero-functionalization of Indole Scaffolds via Facilitated Indolyl 1,3-Heteroatom Transposition Reaction</b> .....	80
<b>2.1. C3-Hetero-functionalization of Indole Scaffolds</b> .....	81



<b>2.1.1. Electrophilic Substitution of Indole Derivatives</b> .....	86
2.1.1.1. C3-Oxygenation of Indole derivatives .....	86
2.1.1.2. C3-Amination of Indole derivatives .....	91
<b>2.1.2. C3-Functionalization of Indole via Umpolung Strategy</b> .....	107
<b>2.1.3 Radical Addition to 3-Position of Indole</b> .....	124
<b>2.2. Development of C3-Hetero-Functionalization of Indole via [3,3]-Sigmatropic Rearrangement of <i>N</i>-Hydroxyindole</b> .....	134
<b>2.2.1. Initial Findings and C3-Acyloxylation of Indole Scaffolds</b> .....	136
<b>2.2.2. C3-Amidation of Indole Scaffolds</b> .....	139
<b>2.3. Mechanistic Considerations</b> .....	144
<b>2.3.1. Mechanistic Insights I: <sup>18</sup>O-Labeling Studies</b> .....	145
<b>2.3.2. Mechanistic Insights II: Additional Mechanistic Studies</b> .....	152
<b>2.4. Conclusions</b> .....	159
<b>2.5. References</b> .....	160
<b>2.6. Experimental Section</b> .....	171

## List of Abbreviations

AcOH	acetic acid
AQN	anthraquinone
BHT	2,6-di-tert-butyl-4-methylphenol
brsm	based on recovered starting material
CAN	ceric ammonium nitrate
Cbz	benzyloxycarbonyl
CPA	chiral phosphoric acid
DABCO	1,4-diazabicyclo[2.2.2]octane
DBU	1,8-diazabicyclo(5.4.0)undec-7-ene
DCC	<i>N,N'</i> -dicyclohexylcarbodiimide
DCE	1,2-dichloroethane
DEAD	diethyl azodicarboxylate
DIPEA	<i>N,N</i> -diisopropylethylamine
DMAP	4-(dimethylamino)pyridine
DMDO	dimethyldioxirane
DME	1,2-dimethoxyethane
DMF	<i>N,N</i> -dimethylformamide
DMP	Dess–Martin periodinane

DMSO	dimethyl sulfoxide
DPH	2,4-dinitrophenylhydrazine
dr	diastereomeric ratio
DtBPF	1,1'-bis(di-tert-butylphosphino)ferrocene
EA	ethyl acetate
EDC·HCl	1-ethyl-3-(3-dimethylaminopropyl)-carbodiimide hydro-chloride
ee	enantiomeric excess
er	enantiomeric ratio
HOBt	hydroxybenzotriazole
HPLC	high-performance liquid chromatography
HRMS	high-resolution mass spectrometry
IHT	indolyl 1,3-heteroatom transposition
LAH	lithium aluminium hydride
LC-MS	liquid chromatography–mass spectrometry
LDA	lithium diisopropylamide
LiHMDS	lithium bis(trimethylsilyl)amide
Me	methyl
MeCN	acetonitrile
MTAD	4-methyl-1,2,4-triazoline-3,5-dione

NADP	nicotinamide adenine dinucleotide phosphate
NIS	<i>N</i> -iodosuccinimide
NMO	4-methylmorpholine <i>N</i> -oxide
PCET	proton-coupled electron transfer
PMB	<i>p</i> -methoxybenzyl
ppm	parts per million
PPTS	pyridinium <i>p</i> -toluenesulfonate
SEM	2-(trimethylsilyl)ethoxymethyl
SEMCI	2-(trimethylsilyl)ethoxymethyl chloride
SET	single-electron transfer
<i>S</i> -TCPTTL	<i>N</i> -tetrachlorophthaloyl-( <i>S</i> )- <i>tert</i> -leucinate
	tris(dimethylamino)sulfonium
TASF	difluorotrimethylsilicate
TBAF	tetrabutylammonium fluoride
TBSCl	<i>tert</i> -butyldimethylsilyl chloride
TCE	1,1,2,2-tetrachloroethane
TEA	triethylamine
TEMPO	(2,2,6,6-tetramethylpiperidin-1-yl)oxyl
TFA	trifluoroacetic acid
TFAA	trifluoroacetic anhydride

TMG	1,1,3,3-tetramethylguanidine
Tr	trityl, triphenylmethyl
THF	tetrahydrofuran
TLC	thin-layers chromatography
<i>p</i> -TsOH	<i>para</i> -toluenesulfonic acid

**Chapter 1.**  
**Synthetic Studies towards Rhazimal**

## 1.1. Introduction

### 1.1.1 Background and Biosynthesis

*Rhazya stricta*, the a small evergreen shrub which is widespread in Western and South Asia, has been used as a traditional medication method since ancient times and exhibits various bioactivities including antioxidant and anticarcinogenic activities. This garnered the interest of numerous research groups in the source of its medicinal effects, leading to active research on the subject. As part of ongoing effort to identify various metabolites in *R. stricta*, an unique indole alkaloid named rhazimal was first isolated from the leaves of *R. stricta* in 1979 and its structural elucidation was confirmed in 1985.<sup>1</sup>

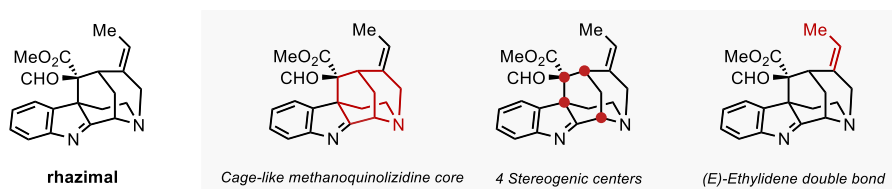


**Figure 1.1.** Rhazimal and its structural features.

The intricate molecular architecture of rhazimal features pentacyclic framework which includes a characteristic cage-like methanoquinolizidine core with an (*E*)-ethylidene moiety (Figure 1.1). In addition, four stereocenters with two contiguous quaternary stereocenters highlights the complexity of the molecule. This structural complexity has made rhazimal a molecule of interest for many synthetic laboratories.

Aside from the synthetically challenging nature of rhazimal's complex structure, the structural importance of rhazimal from a metabolic perspective has intrigued researchers in related fields of study. This importance can be more easily understood by considering the biosynthetic pathways to rhazimal and second metabolites accessible from rhazimal, as shown in Figure 1.2.<sup>2</sup> Tryptamine and secologanine undergo Pictet-Spengler-type cyclization mediated by strictosidine synthase to provide strictosidine. After deglycosylation of the secologanine-derived moiety in strictosidine, the corresponding 3,4-dihydropyranol ring is converted to a chain-tethered aldehyde by spontaneous ring opening. The aldehyde forms a

tetracyclic skeleton through a rapid condensation with a secondary amine and completes most of the structural features of geissoschizine. Geissoschizine, obtained by reduction from 4,21-dehydro-geissoschizine, immediately acquires a high level of structural complexity via single-step bond formation, thereby providing access to rhazimal. Rhazimal is a first natural product that is encountered when geissoschizine undergoes structural complexation via C7–C16 bond formation. Thus, rhazimal serves as the central hub of a metabolic pathway that leads not only to alkaloids that share a similar methanoquinolizidine core such as akuammiline, echitamine, and picraline, but also to indole alkaloids with more complex molecular architectures such as strychnan and secocuran alkaloids.

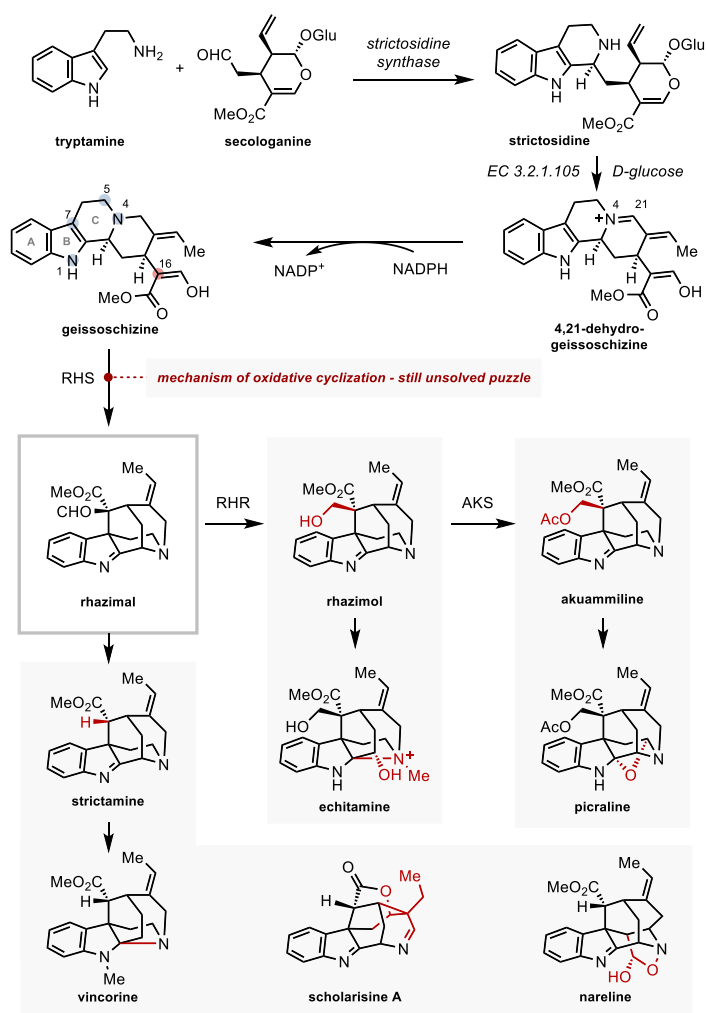


**Figure 1.2.** The importance of rhazimal as a branching point to several families of indole alkaloids.



The direct connection between C7 and C16 of geissoschizine mentioned above enables the facile synthesis of the unique methanoquinolizidine core of the akuammiline family via single step of oxidative cyclization. However, the detailed mechanism for this oxidative coupling is yet to be known.

### 1.1.2. Past Synthetic Works towards C7–C16 Bond Connection from Geissoschizine via Biomimetic Approaches

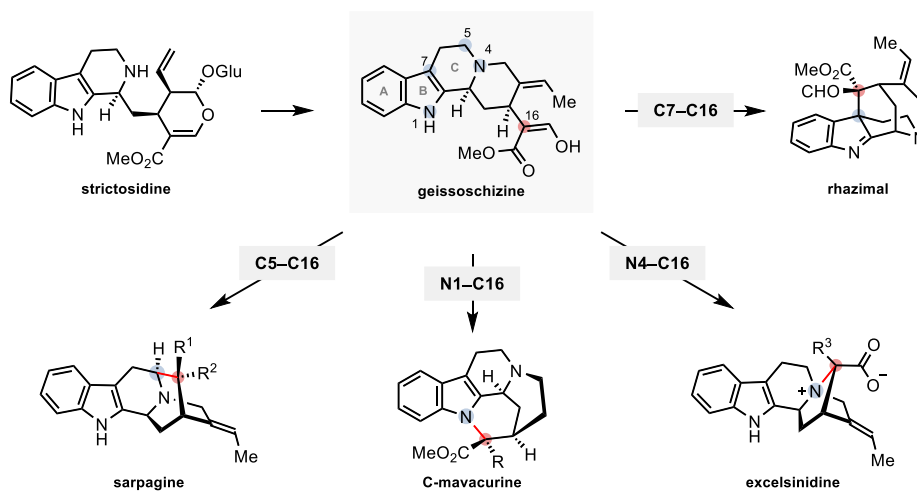


**Figure 1.3.** Indole alkaloids accessible from geissoschizine via oxidative cyclization.

Geissoschizine is a very powerful intermediate that can visit diverse core structures of a wide range of related indole alkaloids, as evidenced by the long history of indole alkaloids. The oxidation in highly regioselective and/or chemoselective manner, which is delicately controlled by enzymes, can differentiate the oxidation site of the ABC tricyclic structure and eventually achieve the desired complexity by trapping of oxidized position with nucleophilic C16, such as N1–C16 bond for mavacurine, C5–C16 bond for sarpagine, N4–C16 bond for excelsinidine, and C7–C16 bond for akuammiline.<sup>2h</sup>

The potential of geissoschizine as a versatile intermediate for the synthesis of various natural products has led to intensive efforts towards a biomimetic synthesis via geissoschizine in the last few decades. As part of this continuing effort, the a successful application of bio-inspired strategy towards total syntheses of alkaloids such as mavacuran, sarpagine, and excelsinidine through intramolecular coupling of geissoschizine under oxidative conditions were reported.<sup>3</sup> However, to the best of our knowledge, the biomimetic synthesis of rhazimal via oxidative formation of C7–C16 bond has not reported up to date.

In this section, noteworthy attempts at C7–C16 bond formation using geissoschizine and

various total syntheses of related natural products achieved during this journey are presented. In addition, the importance of problem-solving process on the basis of systematic approach with design-thinking processes to pursue high selectivity with the target C7-position is introduced. Other biomimetic syntheses via geissoschizine outside of attempts at C7–C16 bond formation are not discussed in this thesis.

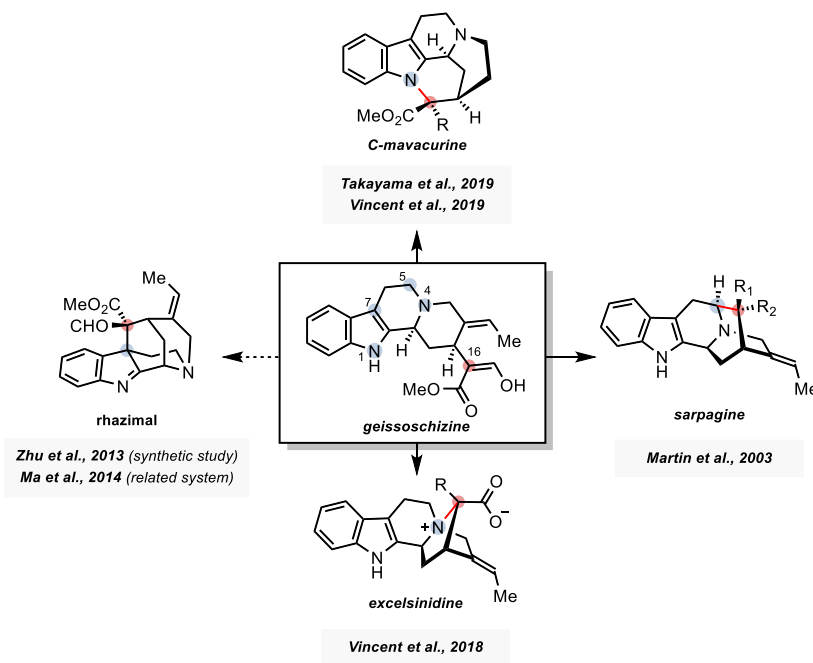


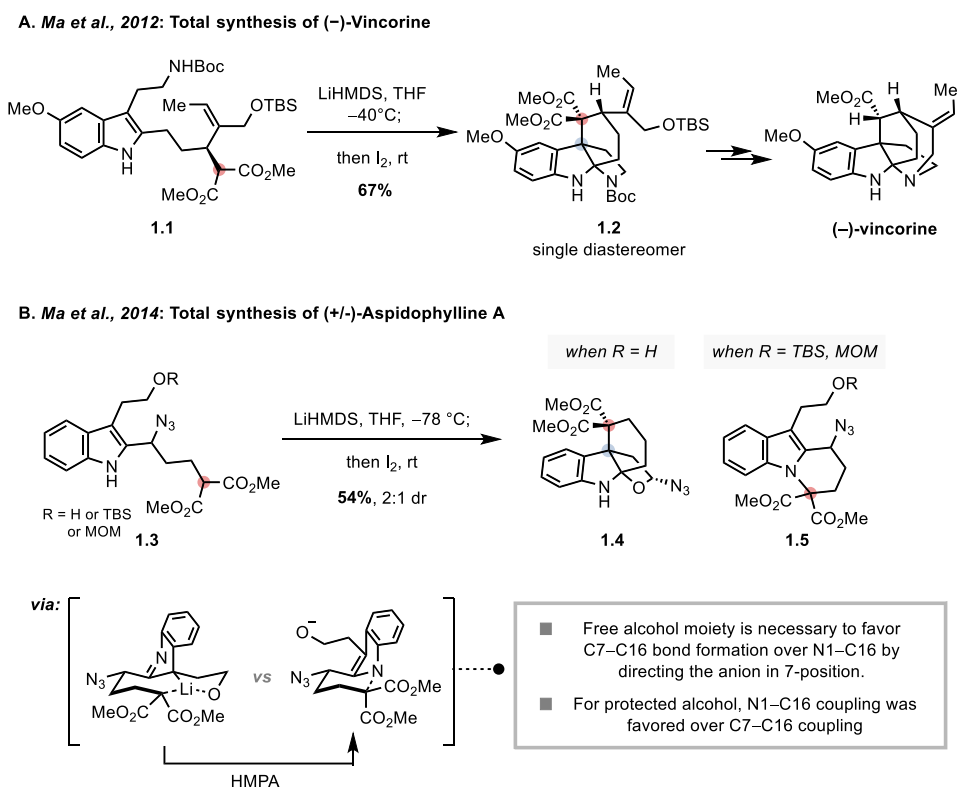
**Figure 1.4.** Biomimetic syntheses towards the mavacurines, akuammilines, and excelsinidines via single-step functionalization of geissoschizine.

An oxidative coupling between the indole and dicarbonyl moieties was chosen as the key strategy in various total syntheses those indole-framed secondary metabolites derived from geissoschizine. The nucleophilicity of the 7-position of the molecule, which corresponds to the C3 position of the indole, raised logical decision to use the nucleophilic substitution approach for the desired transformation. Based on this logic, Ma and co-workers established C7–C16 bond in well-designed indole substrate **1.1** and **1.3** by adopting iodination conditions as the oxidative method to complete the total synthesis of two renowned indole alkaloids, vincorine and aspidophylline A (Scheme 1.1).<sup>3a,3f</sup>

Unlike the case of vincorine which showed high site-selectivity at the 7-position in the key

step (**1.1** to **1.2**, Scheme 1.1A), two structural isomers **1.4** and **1.5** were formed when the same oxidative conditions was applied to the precursor **1.3** during the synthesis of aspidophylline A (Scheme 1.1B). The authors explained the special role of the free alcohol moiety in exclusively C7-selective bond formation when the free alcohol is linked to the substrate. The hydroxyl group along with the lithium ion chelates with the enolate after deprotonation by LiHMDS, allowing it to be placed closer to the 7-position. This pre-arrangement allows selective bond formation as desired. This cooperative structural arrangement enabled by the hydroxyl group and the lithium ion was further proven by demonstrating selective N1–C16 bond formation from an alcohol-protected substrate or the use of HMPA.

**Scheme 1.1.** Synthetic approach towards bioinspired C7–C16 oxidative coupling and application in total synthesis of aspidophylline A.

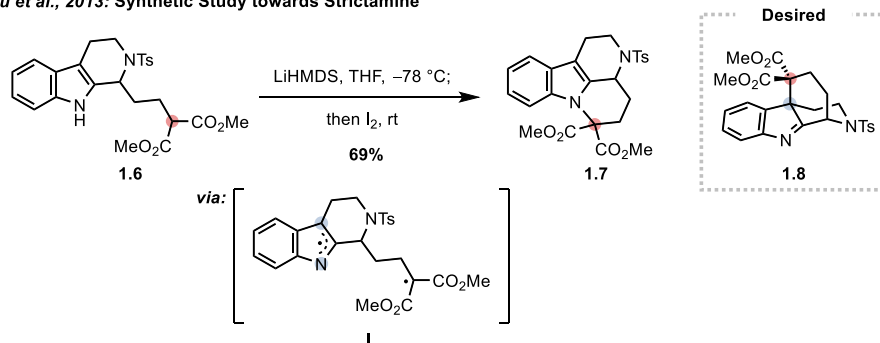


Early work on exploiting biomimetic oxidative coupling in a substrate modeled after geissoschizine was performed by Zhu and co-workers (Scheme 1.2).<sup>4</sup> The  $\alpha$ -carbon of the

pendant dicarbonyl in **1.6**, which is corresponding to the 16-position of geissoschizine, was converted into an electrophile under the same iodination conditions utilized in Ma's synthetic works. Interestingly, the formation of **1.7** with N1–C16 bonds instead of **1.8** with intended C7–C16 bonds suggests that a different approach is required to achieve high site-selectivity in systems with multiple potential reaction sites.

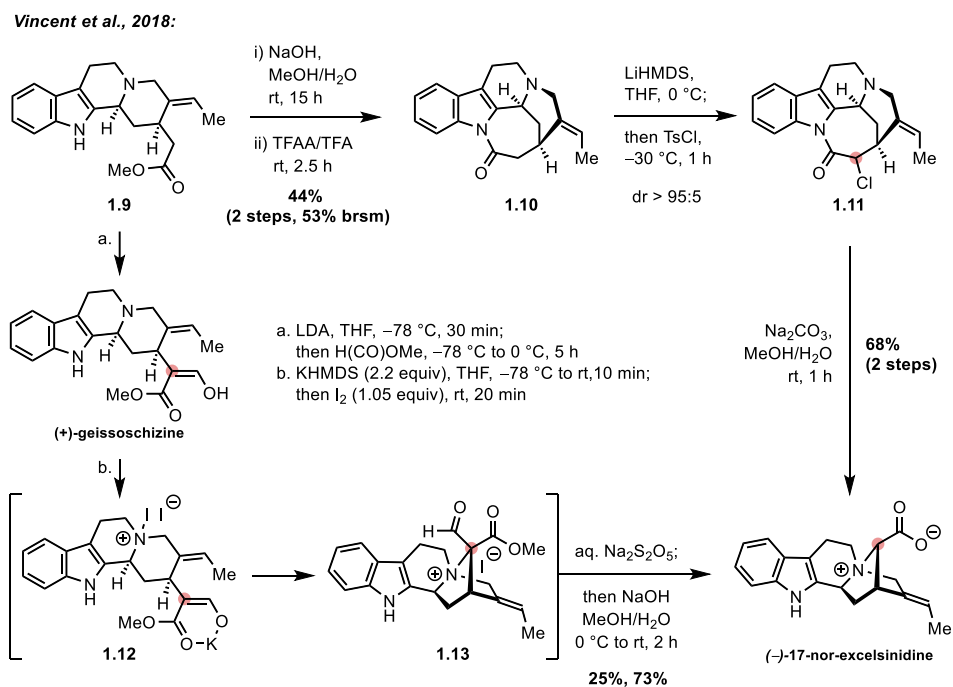
**Scheme 1.2.** The work done by Zhu and coworkers, 2013.

Zhu et al., 2013: Synthetic Study towards Strictamine



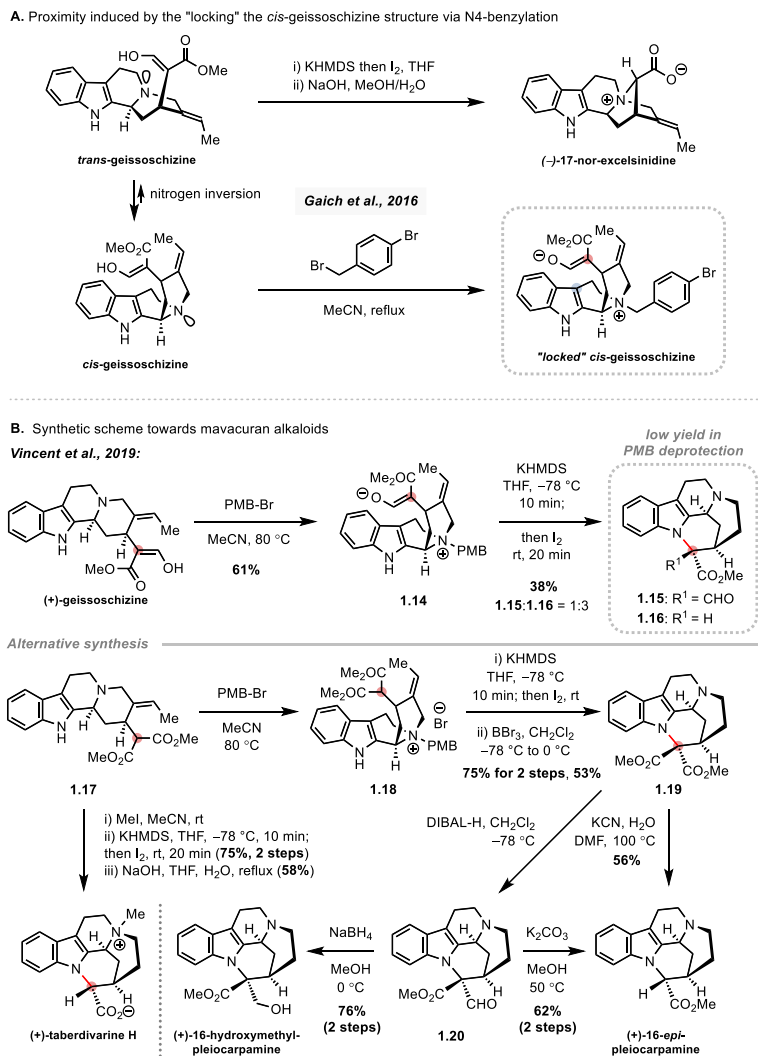
In 2018, Vincent group secured two new synthetic schemes towards 17-nor-excelsinidine, including a biomimetic synthetic route from geissoschizine (Scheme 1.3).<sup>3c</sup> In the initial route, **1.10**, obtained from intramolecular amidation of 16-deformyl-geissoschizine **1.9**, undergoes chlorination to give an umpolung reactivity to the C16 of **1.11**. Under the conditions of sodium carbonate in wet methanol, the corresponding  $\alpha$ -chlorolactam **1.11** then undergoes nucleophilic substitution of C16 by N4 followed by simultaneous lactam cleavage, delivering enantiopure (-)-17-nor-excelsinidine. Harnessing the similar strategy, umpolung approach to change the electronics of C16 was applied to geissoschizine. The iodination conditions by Zhu and Ma was employed to effectively achieve the N4–C16 bond formation. The authors hypothesized that instead of desired iodination at the  $\alpha$ -carbon position of the dicarbonyl, oxidation occurred selectively at the tertiary amine moiety, triggering rapid bond formation by the C16 enolate.

**Scheme 1.3.** The work done by Vincent and coworkers, 2018.



In 2016, Gaich disclosed the rationale behind the configuration of geissoschizine and the configuration-biased cyclization of geissoschizine (Scheme 1.4A).<sup>5</sup> The group focused on the fact that intramolecular cyclization only occurs to geissoschizine with (*E*)-ethylidene, and elucidated that the ethylidene with (*E*)-configuration favors the formation of *cis*-geissoschizine to avoid additional *gauche* interactions. The curved structure of *cis*-geissoschizine allows close alignment of the C16 enolate and indole rings, providing insight into how bond formation occurs between C16 and indole, which appear relatively far apart in the planar depiction. At the same time, *cis*-geissoschizine was able to be isolated as “locked” form aided by the increased nucleophilicity of N4 by its rigid cage-like structure.

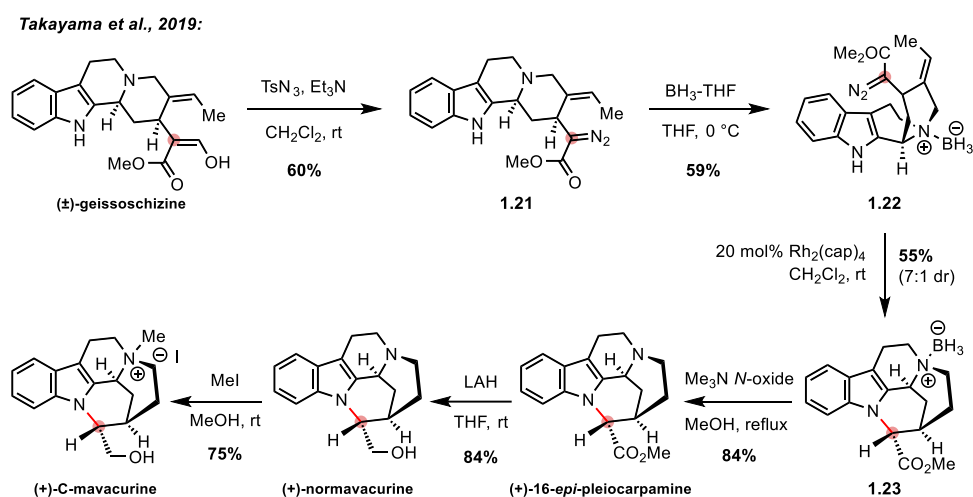
**Scheme 1.4.** Selective acquisition of *cis*-geissoschizine by structure fixation (Gaich and Eckermann, 2016) and total synthesis of the mavacuran family of indole alkaloids (Vincent and coworkers, 2019).



Inspired by the work of Gaich, Vincent and coworkers further extended the research towards the biomimetic synthesis from geissoschizine, in which “locked” strategy was applied to extend the reach of the C16 enolate to the indole motif (Scheme 1.4B).<sup>3d</sup> After obtaining the bent structure of *cis*-geissoschizine, the same oxidative conditions used in the synthesis of excelsinidine by the authors (*vide supra*, Scheme 1.3) was applied to the *cis*-geissoschizine-like structure. Aided by this rigid system, successful N1–C16 coupling was

achieved to provide **1.15** and **1.16** with the core structure of the mavacuran alkaloids. (+)-16-*epi*-Pleiocarpamine was able to be synthesized by PMB deprotection of **1.16**, however, low yielding prevented the reaction from being feasible. Therefore, an alternative scheme using **1.17**, a modified geissoschizine with dimethyl malonate tail, was proposed. Starting from **1.17**, N4-benylation afforded **1.18** and **1.19** was obtained by key cyclization and PMB deprotection of **1.18**. From **1.19**, various mavacuran alkaloids were synthesized by placing reduction, oxidation, and deformylation steps in the right place.

**Scheme 1.5.** The work done by Takayama and co-workers, 2019.



A similar approach utilizing the structural fixation of geissoschizine was undertaken by Kabat and co-workers in 2019 to complete a total synthesis of (±)-pleiocarpamine, (±)-normavacurine, and (±)-C-mavacurine (Scheme 1.5). Instead of iodide species, the authors utilized a carbene species **1.21** for the desired carbene insertion reaction. After providing the sufficient proximity between indole nucleus and C16 by treating BH<sub>3</sub>-THF complex, resulting cyclization precursor **1.22** was successfully undergoes ring closure to generate **1.23** by Rh<sub>2</sub>(cap)<sub>4</sub>-catalyzed carbene N-H insertion. Cleavage of N-B bond under thermal conditions in the presence of trimethylamine oxide and subsequent reduction, N-methylation provided (±)-pleiocarpamine, (±)-normavacurine, and (±)-C-mavacurine, respectively.



### 1.1.3. [3,3]-Sigmatropic Rearrangement of *N*-Hydroxyindole

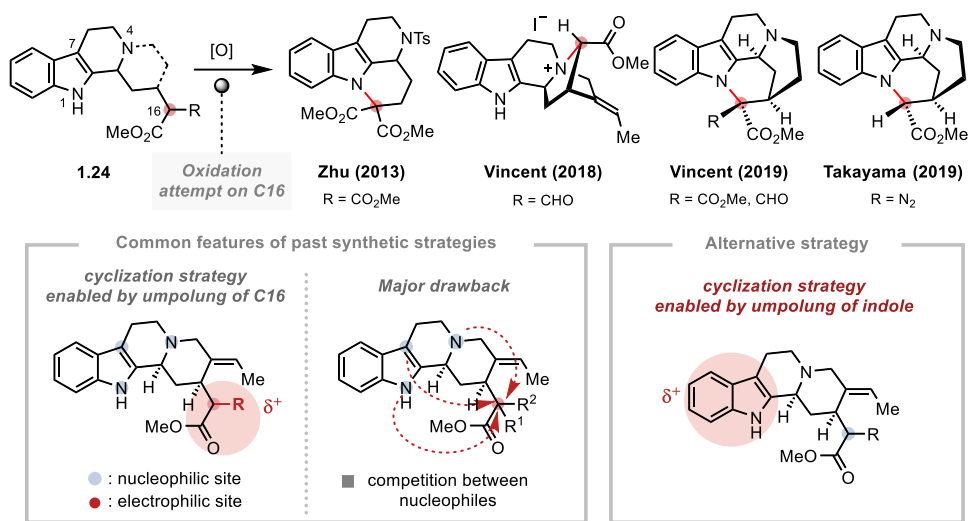


**Figure 1.5.** Major drawbacks of previous strategies and an alternative strategy to address previous limitations.

Based on the past pioneering work described in the previous section, the utilized strategies and chemical intuitions for bond formation between C16 and other atoms in geissoschizine and/or other variants of geissoschizine under oxidative conditions are fundamentally identical in terms of the inducing interaction between nucleophilic species and electrophilic C16 carbon (Figure 1.5).<sup>6</sup> One noticeable drawback of these rather classic approaches is in its site-selectivity. When C16 acts as an electrophile, all nucleophilic sites inherently embedded in the ABC tricycle backbone have the potential to undergo nucleophilic substitution with C16, which could compromise the high regioselectivity of the reaction.

The [3,3] sigmatropic rearrangement is a class of pericyclic reactions in which a  $\sigma$ -bond breaks and results in the formation of a new  $\sigma$ -bond. The reaction is typically thermally driven, while various catalysts such as transition metal species or Lewis acids, are able to drive the reaction in the enantioselective and effective manner, thus making it an attractive and efficient transformation in organic synthesis.<sup>7</sup>

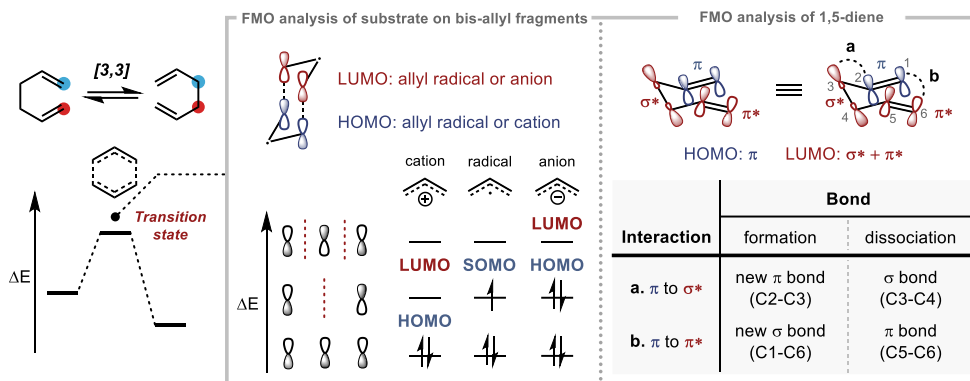


**Figure 1.6.** [3,3] sigmatropic rearrangement and its FMO analysis.

Several mechanisms can explain the nature of the rearrangement, while the most well-known mechanistic explanation is characterized by a concerted mechanism where all the electrons involved move simultaneously without the formation of any intermediate species (Figure 1.6). In terms of molecular orbital interaction, the transition state of the [3,3] sigmatropic rearrangement can be interpreted as the interaction of two separated species, allyl radical-allyl radical or allyl anion-allyl cation. The SOMO orbital of the allyl radical, the LUMO of the allyl cation, and the HOMO of the allyl anion share the same  $\pi_2$  molecular orbital configuration. Different phases of the orbital lobes at each end enables the interactions between allyl radicals or between allyl cation-anion pairs, rendering the reaction as symmetry-allowed. Even without specifically dividing the substrate into bis-allyl fragments, performing a Frontier Molecular Orbital (FMO) analysis on a 1,5-diene allows for an explanation of bond formation and cleavage during the reaction process, by considering one of the  $\pi$  orbitals as the HOMO and the  $\sigma^*$  orbital and  $\pi^*$  orbital of the remaining part as the LUMO. This unique pericyclic mechanism accounts for the high stereoselectivity and regioselectivity observed in [3,3] sigmatropic rearrangements.

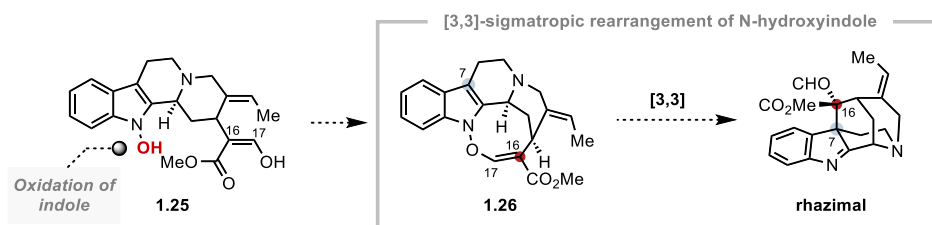


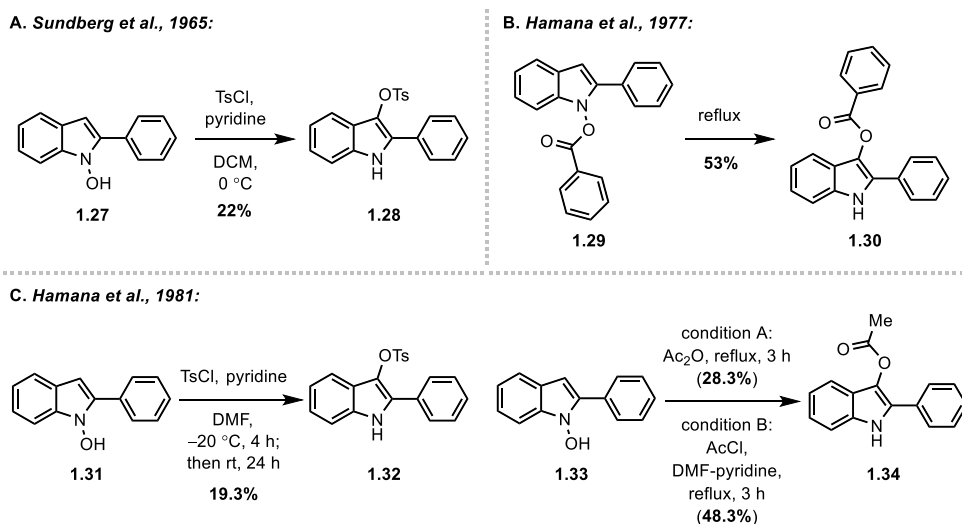
**Figure 1.7.** Alternative strategy towards rhazimal and revisiting biosynthetic hypothesis.

Our synthetic plan began with the contemplation of solving the enigma of nature's high site-selectivity for its oxidative cyclization. In our effort to combine the oxidative process and exclusive site-selectivity into a single protocol, our attention turned to a rare, but not uncommon, cases of indole alkaloids with an *N*-hydroxyindole core, *e.g.*, stephacidin B. From this, it was envisioned that [3,3]-sigmatropic rearrangement of *N*-hydroxyindole can be the resolution which fits these critical requirements. The delineation of this strategy in geissoschizine system is in Figure 1.7. Installation of the  $\pi$ -bonded system containing C16 on 1-hydroxyl-geissoschizine **1.25** could enable access to precursor **1.26** required for [3,3]-sigmatropic rearrangement.

This naturally gave rise of the fundamental question of whether (perhaps rather unfamiliar) *N*-hydroxyindole can undergo such transformation. In fact, the field of *N*-hydroxyindole has its rich history, which includes sporadic works on the [3,3]-sigmatropic rearrangement of *N*-hydroxyindole system. In order to realize the downstream applications of this chemistry, the understanding the reactivity pattern from the state-of-the-art examples should be a priority.

### 1.1.3.1. C–O bond formation

**Scheme 1.6.** Early examples of [3,3]-sigmatropic rearrangement of *N*-hydroxyindole (Sundberg and co-workers, 1965 / Hamana and co-workers, 1977 / Hamana and co-workers, 1981).



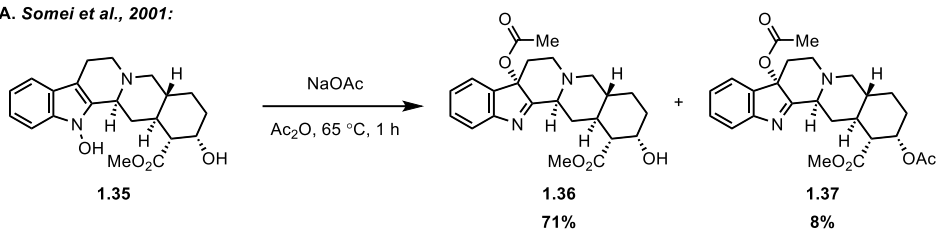
The first discovery of this unique reactivity was made by Sundberg and co-workers in 1965

(Scheme 1.6A).<sup>8</sup> Upon examining the chemistry of *N*-hydroxyindole, tosyl protection on the hydroxyl group of *N*-hydroxy-2-phenylindole **1.27** led the rapid migration of the tosyl group to the 3-position of indole. Hamana and co-workers later extended the work to benzoate by demonstrating the conversion of indolyl benzoate **1.29** to 3-benzyloxyated indole **1.30** (Scheme 1.6B).<sup>9</sup>

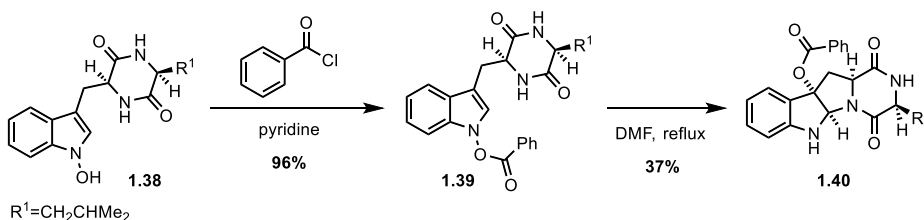
In 1981, Hamana and co-workers reenacted Sundberg's discovery and confirmed that an identical rearrangement could occur even with the acetyl group (**1.34**) instead of the tosyl or benzoyl group (Scheme 1.6C).<sup>10</sup> These seminal works are the first moment of recognition of the [3,3] rearrangement of *N*-hydroxyindole and demonstrates the possibility of the reaction as the pivotal starting point that can undergo the C3-oxygenation reaction with the intermediacy of the corresponding ester, phosphonate, or sulfonate.

**Scheme 1.7.** The works done by Somei and co-workers, 2001.

**A. Somei et al., 2001:**



**B. Somei et al., 2001:**



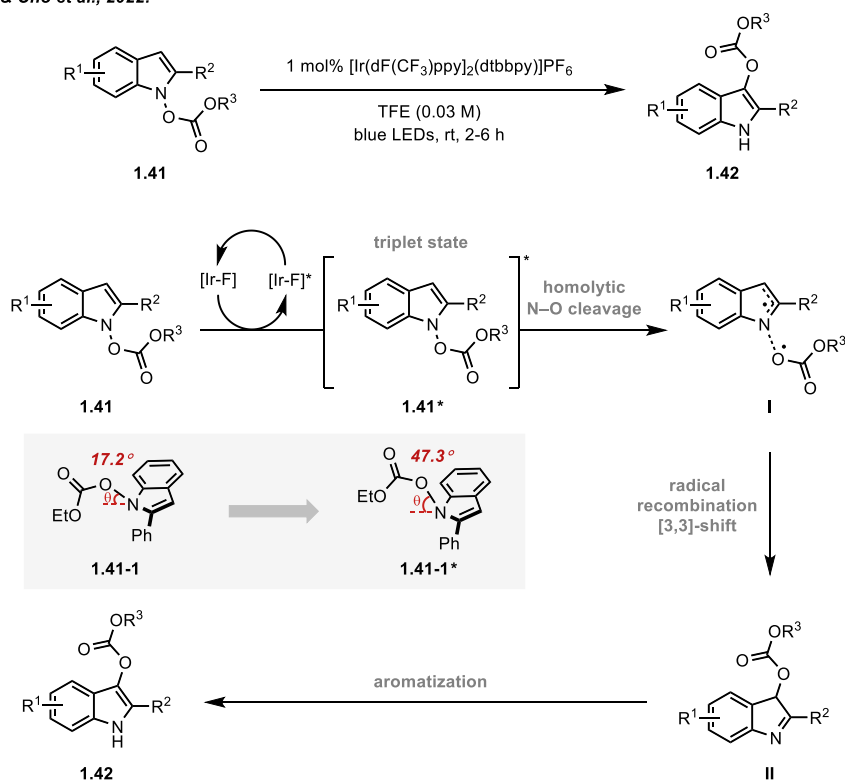
Since then, much effort has been devoted to exploit the field of *N*-hydroxyindole by the Somei group in the late 20th century. Among numerous studies on *N*-hydroxyindole, the group has detailed several report on observing the [3,3]-sigmatropic rearrangement of *N*-hydroxyindole. In 2001, Somei and co-workers reported the C3-oxygenation of yohimbine, representative indole alkaloid possessing a pentacyclic indole skeleton (Scheme 1.7A).<sup>11</sup> Treatment of NaOAc with acetic anhydride successfully converted the *N*-hydroxyl derivative of yohimbine **1.35** to C3-acetyloxyated yohimbine **1.36** and **1.37**, presumably via *N*-acetoxy

yohimbine as a reactive intermediate.

In the same year, a similar reaction was performed by the Somei group in the *N*-hydroxyindole derivative with 2,5-piperazinedione moiety to form a pyrroloindoline structure via [3,3]-sigmatropic rearrangement (Scheme 1.7B).<sup>12</sup> Benzoylation to the hydroxyl moiety of *N*-hydroxyindole **1.38** yielded indolyl benzoate **1.39**, and the application of thermal conditions completed the construction of pyrroloindoline along with the simultaneous C3-benzyloxylation to provide pyrroloindoline **1.40**. 2,5-Piperazinedione can be frequently seen in natural product families such as okaramine, sporidesmin, and breviramide family and many of the aforementioned natural product families share the pyrroloindoline structure as main architecture. Demonstration of such chemistry on this intricate natural product-related structure proved the compatibility of the reaction.

**Scheme 1.8.** The work done by Shin, Cho and co-workers, 2022.

*Shin & Cho et al., 2022:*



Shin and Cho reinterpreted the [3,3]-sigmatropic rearrangement of *N*-hydroxyindole from a photochemical viewpoint (Scheme 1.8).<sup>13</sup> Based on their continued interest and expertise in energy-transfer catalysis, the group performed effective N–O bond homolysis by excitation of indolyl *N*-carbonate **1.41** into a high triplet state.

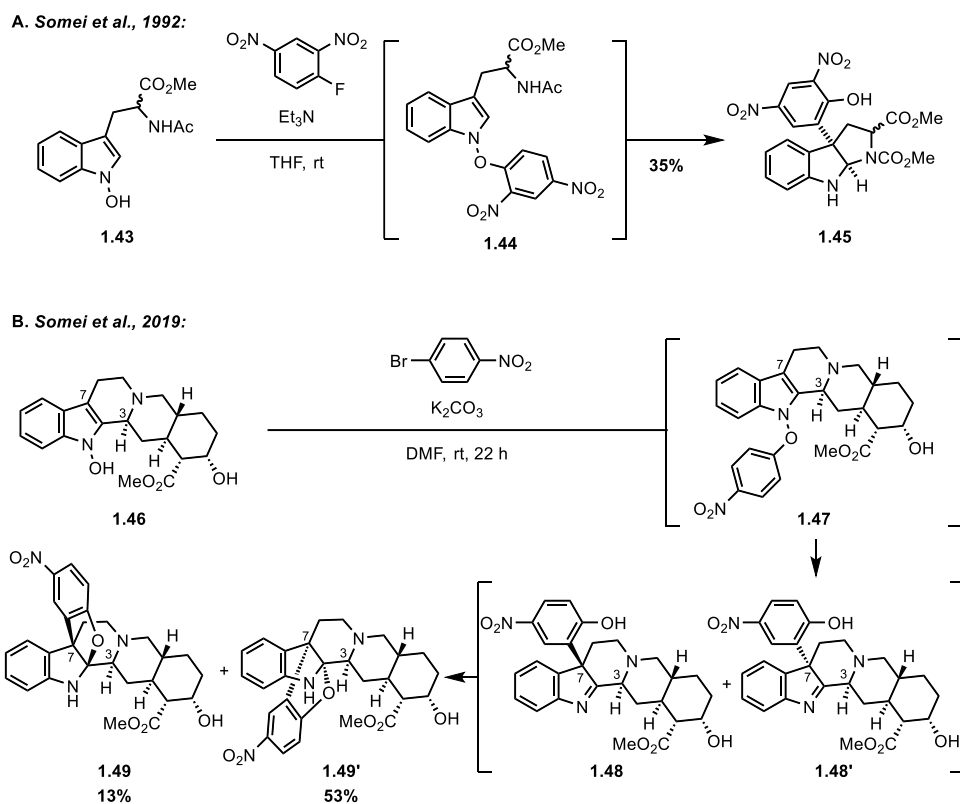
The DFT calculation was performed using **1.41-1** as a model structure and showed that photoexcitation induced a structural modification where the angle between the indole plane and the N–O bond increased from around 17° to 47°. The expansion of this angle allows the nitrogen atom of the indole core to exhibit *sp*<sup>3</sup> hybridization character, allowing for more favorable dissociation of the N–O bond. The resulted N-centered, and O-centered radicals were ultimately able to undergo rapid radical recombination to provide C3-acyloxyindole **1.42**.

#### 1.1.3.2. C–C bond formation

One of the practical attractiveness of the functional group-transposition in *N*-hydroxyindole system is that the strategy can provide an unified platform for the synthesis of C3-functionalized indole derivatives by simply changing the coupling partner. Over time, this transposition strategy and its variants in *N*-hydroxyindole system have proven their competence as effective toolkits for the functionalization of the 3-position of indole derivatives by expanding the reaction to C–C bond formation.

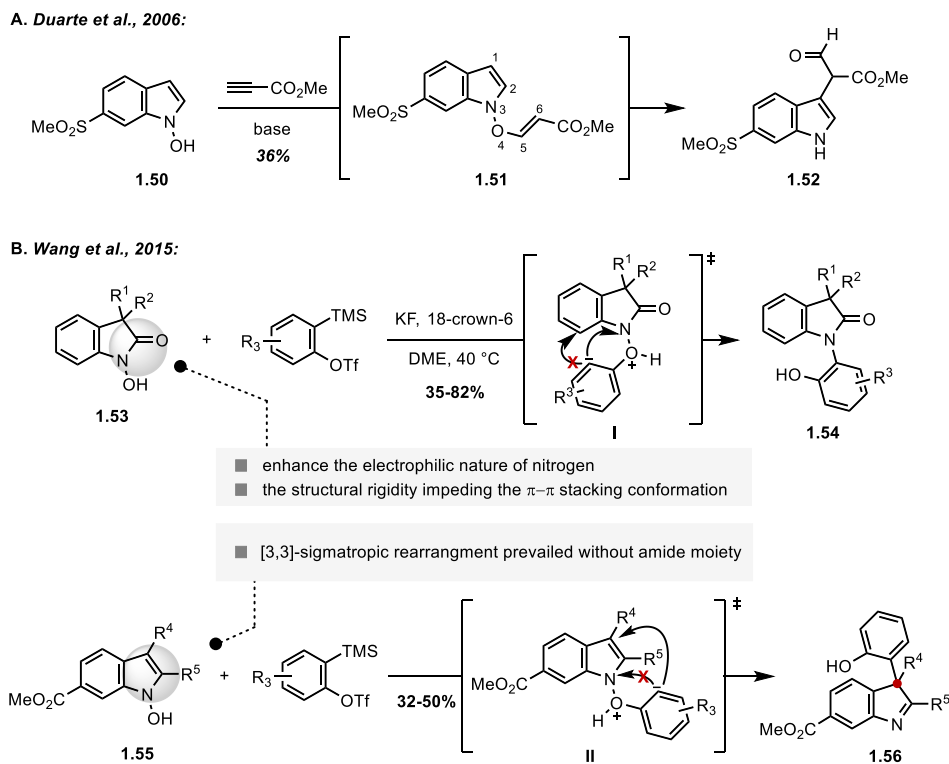
In 1992, the Somei group observed the formation of C3-arylated pyrroloindoline **1.45** via the coupling of *N*-hydroxyindole **1.43** and 1-fluoro-2,4-dinitrobenzene (Scheme 1.9A).<sup>14</sup> When 1-fluoro-2,4-dinitrobenzene, an electron-deficient arene motif, was treated with *N*-hydroxyindole **1.43**, C3-arylated pyrroloindoline **1.45** was obtained as sole product, presumably via the formation of transient intermediate, 1-phenoxy-1H-indole **1.44** by the S<sub>N</sub>Ar reaction and spontaneous [3,3]-sigmatropic rearrangement.

**Scheme 1.9.** The works done by Somei and co-workers, 1992 and 2019.



Having recognized the possibility as a new C–C bond formation strategy, the base-promoted  $S_NAr$  reaction was demonstrated in the yohimbine **1.46** and 1-bromo-4-nitrobenzene to promote the formation of a new C–C bond between yohimbine and the aryl moiety (Scheme 1.9B).<sup>15</sup> [3,3]-Sigmatropic rearrangement of intermediate **1.47** led to C7-arylation of yohimbine and the resulting indolenines **1.48** and **1.48'** underwent intramolecular cyclization with newly formed phenol motif to construct the bridged benzofuro[2,3-b]indoline **1.49** and **1.49'**, which shares the same bridged skeleton found in various indole alkaloids such as diazonamide and pleiocraline. Regarding the stark yield difference between **1.49** and **1.49'**, it is inferred that the stereochemical orientation of the [3,3]-sigmatropic rearrangement is determined by the stereogenic 3-position closest to the N–O bond.

**Scheme 1.10.** The works done by Duarte and co-workers, 2006 and Wang and co-workers, 2015.

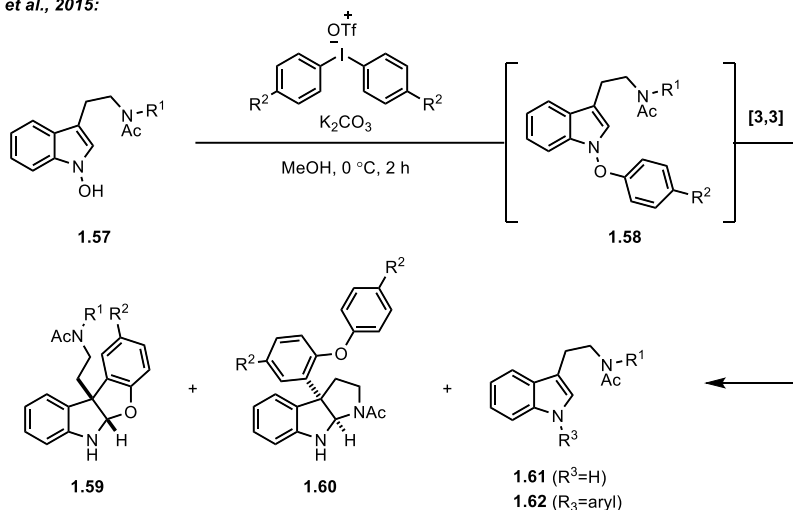


In 2006, Duarte and co-workers reported an extension of the [3,3]-sigmatropic rearrangement of *N*-hydroxyindole from traditional C3-aryl coupling to C3-alkyl coupling, by using methyl propiolate as a coupling partner albeit in a very limited scope (Scheme 1.10A).<sup>16</sup> Wang group developed the development of a metal-free aryne insertion approach to access *o*-aminophenols from hydroxyindolinones (Scheme 1.10B).<sup>17</sup> The original gist of this paper was that a unique regioselective [1,3]-rearrangement occurs when benzyne generated *in situ* from 2-(trimethylsilyl)phenyl trifluoromethanesulfonate was applied to *N*-hydroxyindolinone **1.53**. However, a few examples of *N*-hydroxyindole applied to the newly developed strategy were also enlisted: An interesting shift from [1,3]-rearrangement to [3,3]-sigmatropic rearrangement occurred in case of *N*-hydroxyindole **1.55**, providing C3-arylated product **1.56**.



**Scheme 1.11.** The work done by Vincent and co-workers, 2015.

Vincent *et al.*, 2015:



R <sup>1</sup>	R <sup>2</sup>	1.59	1.60	1.61+1.62
H	H	44%	20%	36%
H	Cl	22%	trace	40%
Bn	H	17%	-	41%
Bn	Cl	18%	-	30%
Bn	OMe	15%	-	27%

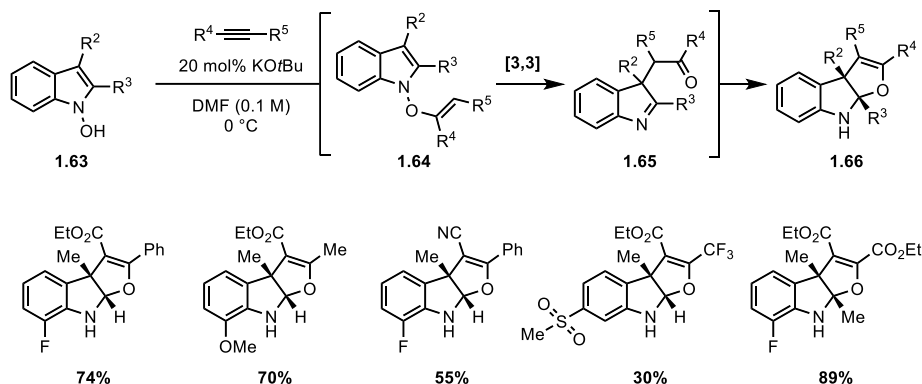
By employing a similar rearrangement strategy, the Vincent group developed a new protocol for O-arylation/[3,3]-sigmatropic rearrangement sequence of *N*-hydroxyindole for the construction of benzofuroindoline (Scheme 1.11).<sup>18</sup> 1-Phenoxy tryptamine **1.58** could be generated *in situ* by using biaryliodonium salt to *N*-hydroxytryptamine **1.57** and spontaneous [3,3]-sigmatropic rearrangement of **1.58** delivered the benzofuroindoline **1.59**. However, it was unable to increase the ratio of benzofuroindoline **1.59** over pyrroloindoline **1.60** when mono-substituted amide was tethered, due to the competition between two potential nucleophiles, *i.e.*, tethered amide and phenol. In order to avoid the formation of unwanted pyrroloindolines **1.60**, the use of *N*-hydroxyindole with fully substituted tethered amide chain was required.

In 2021, the Anderson group reported the [3,3]-sigmatropic rearrangement of *N*-hydroxyindole using an alkyne as a coupling partner instead of an aryl counterpart (Scheme

1.12).<sup>19</sup> Conjugate addition of *N*-hydroxyindole **1.63** to the activated alkyne provided facile access to the transient indolyl enol ether **1.64**, which underwent rapid [3,3]-sigmatropic rearrangement followed by tautomerization and intramolecular imine trapping of **1.65** to provide a variety of furo[2,3-*b*]indolines **1.66**.

**Scheme 1.12.** The work done by Anderson and co-workers, 2021.

Anderson et al., 2021:

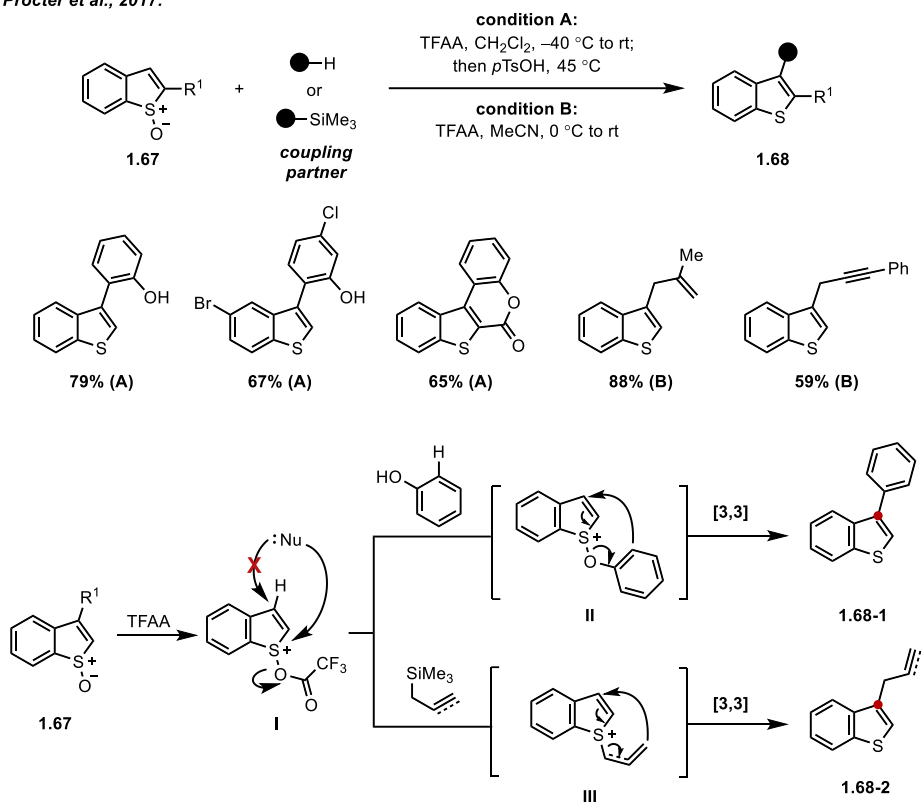


### 1.1.3.3. Similar Applications in Different Framework

Similar intrinsic reactivity was observed for benzothiophene S-oxide, a structural analogue of *N*-hydroxyindole. In 2017, Procter and co-workers detailed an interrupted Pummerer/charged-accelerated [3,3]-sigmatropic rearrangement protocol to synthesize C3-functionalized benzothiophenes (Scheme 1.13).<sup>20</sup> Activation of S–O bonds embedded in benzothiophene S-oxide **1.67** via an interrupted Pummerer reaction enabled direct intermolecular  $C(sp^2)-C(sp^2)$  or  $C(sp^2)-C(sp^3)$  coupling in high regioselective fashion. The acyl group attached to the O-acylated sulfoxide **I** was utilized as a handle for instant polarity reversal of benzothiophene core, thereby facilitating the charged-accelerated [3,3]-sigmatropic rearrangement to successfully provide C3-functionalized benzothiophene **1.68**.

**Scheme 1.13.** The work done by Procter and co-workers, 2017.

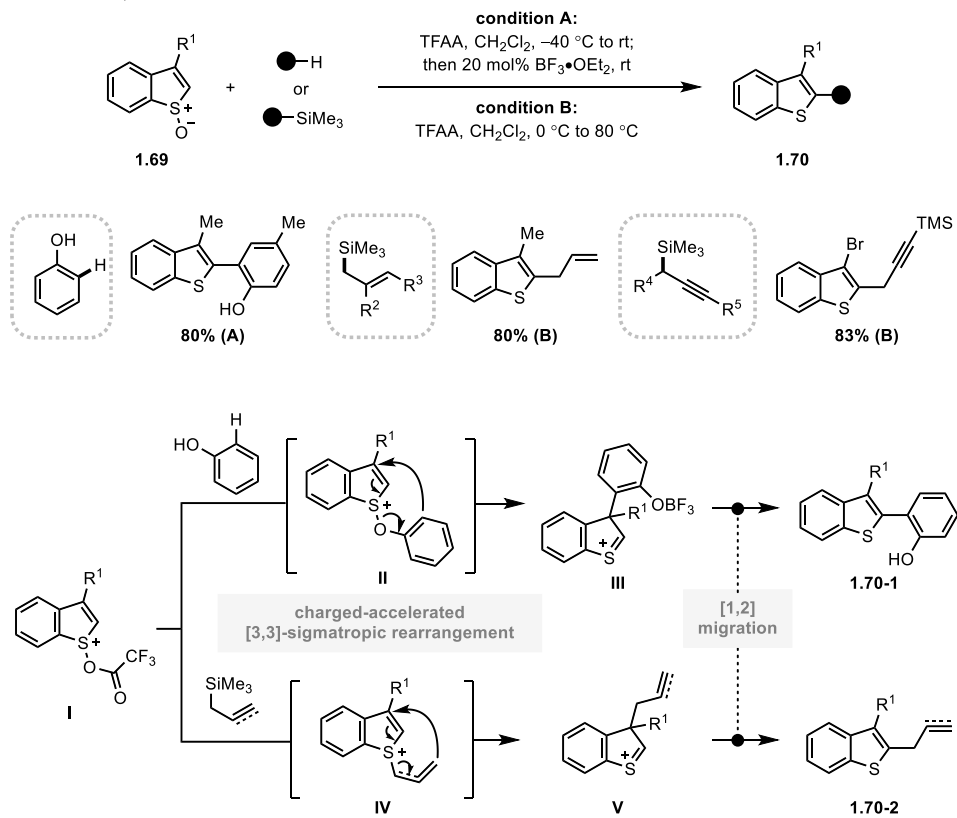
*Procter et al., 2017:*



The potential of benzothiophene S-oxide was once again exploited by Procter and co-workers to achieve C2-aryl/alkylation of benzothiophene (Scheme 1.14).<sup>21</sup> When the trademark protocol, interrupted Pummerer reaction/[3,3]-sigmatropic rearrangement sequence, is performed on C3-substituted benzothiophene S-oxide **1.69**, a transient benzothiophenium species **III** or **V** with C2-quaternary center can be formed via O-aryl sulfoxide **II** or O-alkyl sulfoxide **IV**, respectively. This benzothiophenium **III** or **V** undergoes a spontaneous 1,2-migration to access the C2-functionalized benzothiophene **1.70**, presumably facilitated by a positive charge on the sulfur atom.

**Scheme 1.14.** The work done by Procter and co-workers, 2018.

*Procter et al., 2018:*



## 1.2. A Controlled C7–C16 Bond Formation via [3,3]-Sigmatropic Rearrangement Strategy

As briefly mentioned in Section 1.1.3, a bio-inspired strategy towards accessing rhazimal was envisioned through the [3,3]-sigmatropic rearrangement of *N*-hydroxyindole (Figure 1.8). We hypothesized that, under the carefully-designed conditions, a variant of 1-hydroxygeissoschizine **1.71** derived from chemoselective oxidation of indole nucleus would be able to undergo [3,3]-sigmatropic rearrangement through intermediacy of **1.72** with a labile N-O group as a driving force. Implementation of this bio-inspired strategy can not only address the issue of intervention of other potential reacting sites in a site-selective manner, but also can contribute to the alternative mechanistic hypothesis for the details of this biosynthetic cyclization.

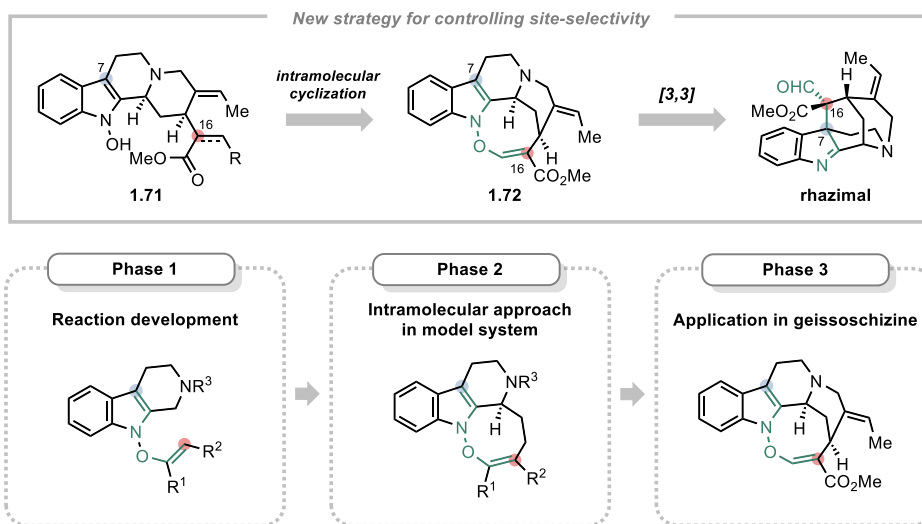


**Figure 1.8.** Biomimetic C7–C16 coupling as key reaction of the total synthesis and implementation of the idea via 3-phased synthetic plan.

We subdivided this synthetic project towards rhazimal into three phases. The first phase is the reaction development for the C–C bond formation via [3,3]-sigmatropic rearrangement of *N*-hydroxyindole (Figure 1.7, Phase 1). In the second phase, the developed reaction will

be carried out in the intramolecular manner using geissoschizine-like model substrate, but in a more simplified structure (Figure 1.7, Phase 2). In the third phase, biomimetic synthesis will be commenced by the direct implementation of the corresponding strategy in geissoschizine (Figure 1.7, Phase 3).

The following section will highlight the efforts to expand the [3,3]-sigmatropic rearrangement of *N*-hydroxyindole to build C(*sp*<sup>3</sup>)-C(*sp*<sup>3</sup>) bond,<sup>22</sup> and establishing a viable, high-yielding synthetic sequence of precursor for [3,3]-sigmatropic rearrangement so as to expedite the realization of the desired rearrangement of *N*-hydroxyindole, and to further exploit this newly observed reactivity in the biomimetic C7-C16 bond formation in more complex system, geissoschizine.

### 1.2.1. Model Study Development for [3,3]-Sigmatropic Rearrangement

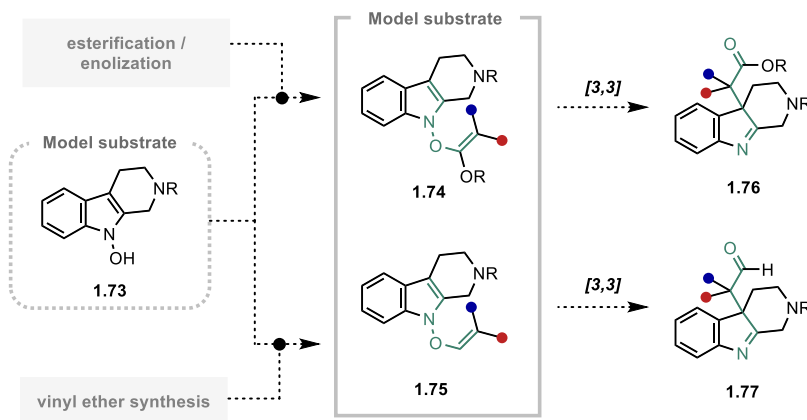
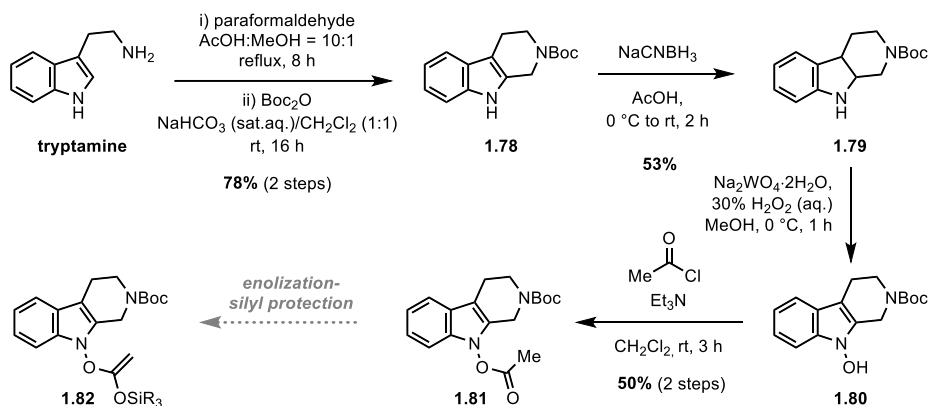


**Figure 1.9.** Structural design of the precursor to form the desired C7(*sp*<sup>3</sup>)-C16(*sp*<sup>3</sup>) bond.

Since there was no general methods reported that could achieve C-C bond formation with  $\pi$  system other than aryl ring, a new breakthrough to install the olefin moiety in *N*-hydroxyindole to enable the stable supply of indolyl enol ether should be preceded.<sup>22</sup> Before embarking on the exploration, **1.73** was chosen as the model substrate and two candidates were the targeted as a potential candidates for the ideal precursor (Figure 1.9). Since both ester and aldehyde groups are placed at the 16-position of rhazimal, precursors in any

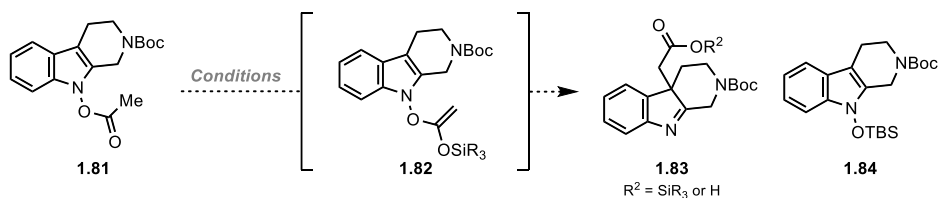
oxidation state, *i.e.*, indolyl *N*-carboxylate **1.74** and indolyl enol ether **1.75**, can smoothly provide the desired core structure with necessary functional groups placing in the desired position. Considering the compatibility of resulting functional groups with further chemistry, we targeted **1.74** as a feasible intermediate for [3,3]-sigmatropic rearrangement and a synthetic route to **1.74** is depicted in Scheme 1.15.

**Scheme 1.15.** A short synthesis of indolyl *N*-carboxylate **1.81**.



The synthetic route started from commercially available tryptamine, which was treated with formaldehyde under acidic conditions followed by Boc protection to give ABC tricyclic compound **1.78**. Indoline **1.79** could be prepared by reduction of **1.78** with NaCNBH<sub>4</sub>. The resulting indoline **1.79** then underwent a Somei oxidation upon treatment with H<sub>2</sub>O<sub>2</sub> in the presence of catalytic amount of Na<sub>2</sub>WO<sub>4</sub>·2H<sub>2</sub>O to yield *N*-hydroxyindole **1.80**, and subsequent esterification afforded indolyl acetate **1.81**. Silyl ketene acetal, a traditional substrate used in the [3,3]-sigmatropic rearrangement - Ireland-Claisen rearrangement to be more precise, is one of the easiest subclasses of enol ethers to synthesize. Simple enolization and silyl protection can provide the facile access to the precursor, which makes indolyl *N*-carboxylate substrate more attractive.

**Table 1.1.** Screening for the enolization of indolyl acetate **1.81**.



entry	conditions	result
1	LiHMDS, THF, $-78\text{ }^{\circ}\text{C}$ ; then TBSCl, THF, $-78\text{ }^{\circ}\text{C}$ to rt	<b>1.84</b> (33%)
2	LiHMDS, THF, $-78\text{ }^{\circ}\text{C}$ ; then TBSOTf, $-78\text{ }^{\circ}\text{C}$ to rt	<b>1.84</b> (28%)
3	NaH, TBSOTf, $\text{CH}_2\text{Cl}_2$ , $0\text{ }^{\circ}\text{C}$	decomposition
4	$\text{Et}_3\text{N}$ , TBSOTf, THF, $0\text{ }^{\circ}\text{C}$ to rt	side reaction
5	pyridine, TBSOTf, $\text{CH}_2\text{Cl}_2$ , $0\text{ }^{\circ}\text{C}$ to rt	side reaction
6	$\text{K}_2\text{CO}_3$ , TBSOTf, MeOH (2 drops), $\text{CH}_2\text{Cl}_2$ , $0\text{ }^{\circ}\text{C}$ to rt	s.m. recovered

With **1.81** in hand, enolization conditions to achieve the silyl ketene acetal **1.82** or, if possible, the *in situ* rearranged product **1.83** were screened using indolyl acetate **1.81** as a model substrate (Table 1.1). The initial effort was devoted to observing the silyl enol ether via hard enolization. However, silyl protected *N*-hydroxyindole **1.84** was obtained instead of the desired silyl enol ether **1.82** or **1.83** (entries 1 and 2). The plausible mechanism for the formation of **1.84** is described in Figure 1.10.

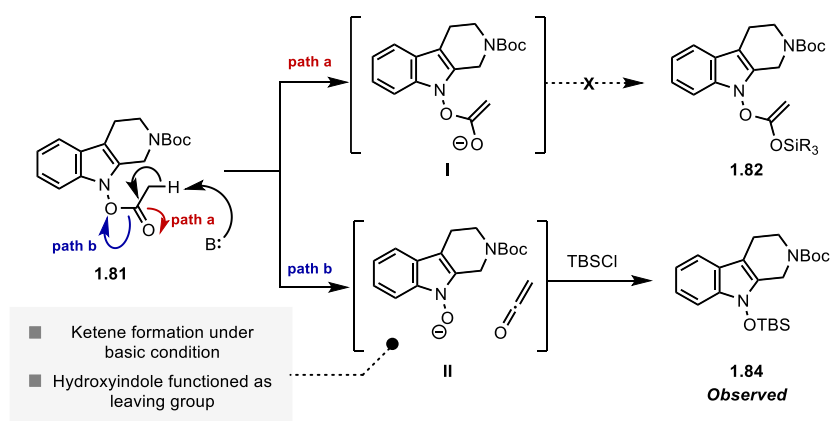


**Figure 1.10.** Rationale for the formation of **1.84**.



In most cases, the lone pair of electrons formed by  $\alpha$ -deprotonation go to the carbonyl side to form enolate (**path a, I**), but for certain substrates with good leaving groups attached adjacent to carbonyl, *i.e.*, acyl chloride, it is well-known that such substrates can form ketene upon subsequent detachment of leaving groups after  $\alpha$ -deprotonation (**path b, II**). In the case of indolyl acetate system, it is speculated that ketene formation prevailed over the desired enolate formation presumably due to the *N*-hydroxyindole unit acting as a good leaving group, as the anionic character formed in the oxygen atom could be delocalized over indole  $\pi$  system by inductive effect. An extensive survey of various soft enolization methods was also performed, but neither the desired silyl ketene acetal **1.82** nor the rearranged product **1.83** could be observed (entries 3, 4, 5 and 6).

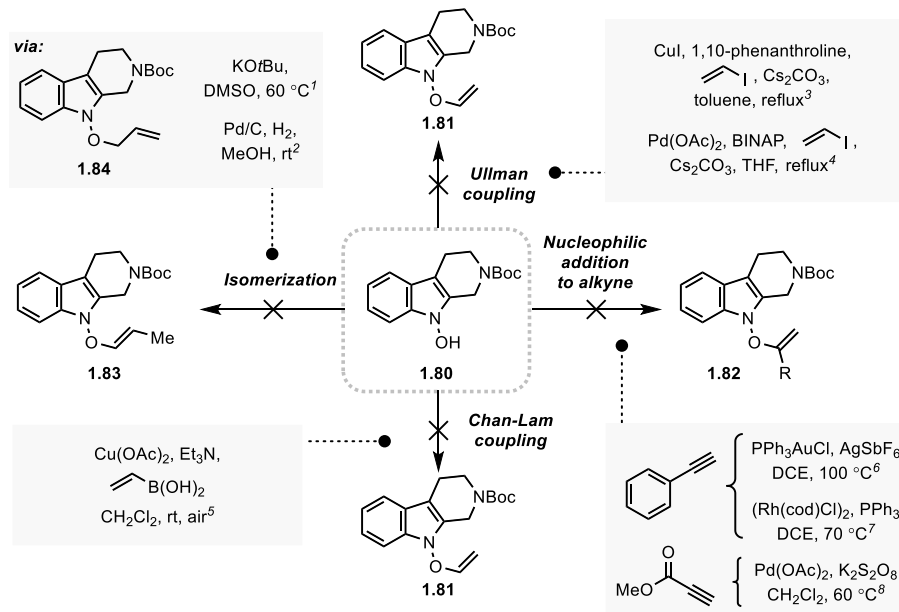


**Figure 1.11.** Failed attempts towards the synthesis of indolyl enol ether.

Moving on from the Ireland-Claisen rearrangement approach, we decided to lower the oxidation state of substrate and focused on the next challenge: indolyl enol ether approach (Figure 1.11). Extensive efforts have been dedicated to finding a generic method to synthesize indolyl enol ether, whose general structure is depicted as **1.75** (*vide supra*, Figure 1.8).

Various approaches including Chan-Lam coupling, Ullman-type coupling, alkene isomerization and nucleophilic addition of *N*-hydroxyindole to alkyne in the presence of  $\pi$  bond-activating catalysts were examined, but turned out to be fruitless. These results were not entirely surprising given the fragile nature of the *N*-hydroxyindole *i.e.*, complete decomposition of *N*-hydroxyindole when interacting with transition-metal catalyst.

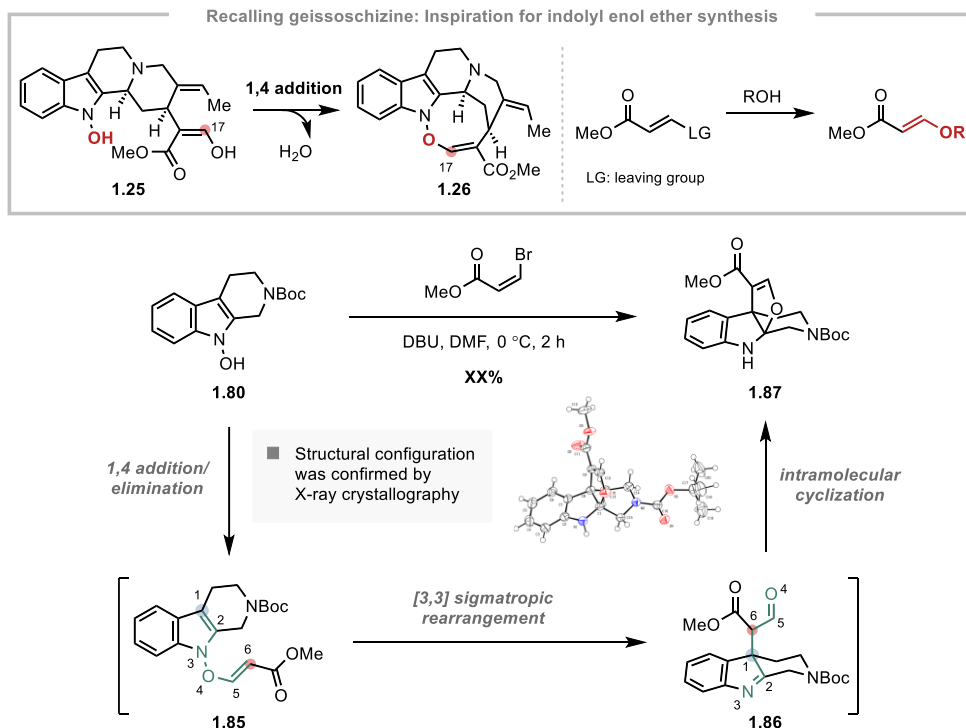
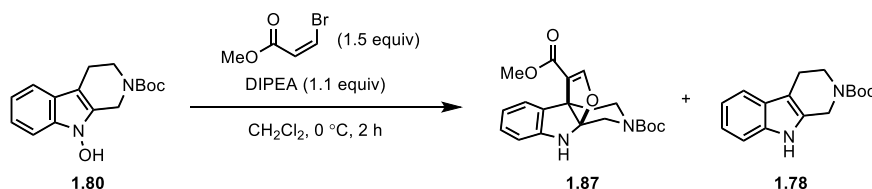


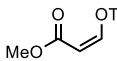
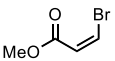
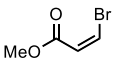
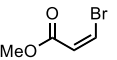
**Figure 1.12.** Successful installation of C=C bond and simultaneous [3,3]-sigmatropic rearrangement.

We eventually decided to introduce the desired alkene in the form of the highest structural relevance to the targeted system, *i.e.*, geissoschizine (Figure 1.12). When a precursor for the [3,3]-sigmatropic rearrangement **1.26** is constructed from *N*-hydroxyl geissoschizine **1.25**, vestiges of a unique dicarbonyl moiety derived from geissoschizine could be remained in the newly formed octagonal framework, which is structurally reminiscent of 3-oxo-enolate resulting from a nucleophilic conjugate addition–elimination process. Inspired by this structural feature in **1.26**, we suspected that employment of an  $\alpha,\beta$ -unsaturated ester

containing an appropriate leaving group as a coupling partner would arise an feasible 1,4-addition and subsequent removal of the leaving group, which can establish the desired alkene as a similar form to that of **1.26**. Using methyl (*Z*)-3-bromoacrylate as coupling partner, a 1,4-addition/elimination sequence was implemented on *N*-hydroxyindole **1.80**. When *N*-hydroxyindole **1.80** and methyl (*Z*)-3-bromoacrylate were combined under basic conditions, surprisingly, immediate [3,3]-sigmatropic rearrangement (**1.85**) and subsequent 1,2-addition to imine (**1.86**) occurred to yield bridged indoline **1.87** instead of the expected indolyl enol ether **1.85**. The structural configuration of **1.87** was confirmed by X-ray crystallographic analysis.

**Table 1.2.** Optimization of [3,3]-sigmatropic rearrangement in *N*-hydroxyindole **1.80**.<sup>a</sup>



entry	variation from optimized conditions	yield of <b>1.87</b> <sup>b</sup>	yield of <b>1.78</b> <sup>b</sup>
1	none	58% (55%)	6%
2	 instead of 	0%	71%
3	Cs <sub>2</sub> CO <sub>3</sub> instead of DIPEA	27%	18%
4	Et <sub>3</sub> N instead of DIPEA	43%	12%
5	rt instead of 0 °C	52%	9%
6	DBU, DMF, 0 °C	45%	18%
7	THF instead of CH <sub>2</sub> Cl <sub>2</sub>	12%	58%
8	1.0 equiv 	39%	10%
9	2.0 equiv 	53%	8%

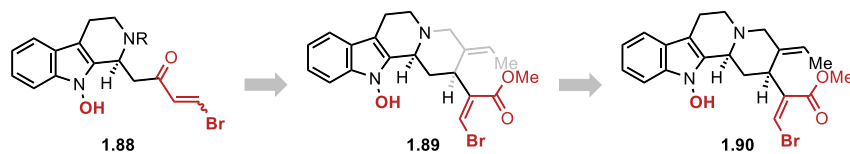
<sup>a</sup>Reactions performed with methyl (*Z*)-3-bromoacrylate (1.5 equiv.), DIPEA (0.1 equiv.) in solvent (0.05 M) at indicated temperature on 0.2 mmol scale. <sup>b</sup>Determined by <sup>1</sup>H NMR analysis of the crude mixture using TCE as an internal standard and the isolated yield was included in the parentheses.

Using these findings as milestones, an examination of various conditions was commenced and details of the optimization for 1,4-addition/elimination/[3,3]-sigmatropic rearrangement

protocol are summarized in Table 1.2. Screening of reaction conditions revealed that DIPEA in CH<sub>2</sub>Cl<sub>2</sub> conditions can provide the bridged indoline **1.87** with yield up to 55% (entry 1). When methyl (*Z*)-3-bromoacrylate was replaced with methyl (*Z*)-3-(tosyloxy)acrylate, the desired reaction did not occur (entry 2). The reaction sequence was highly compatible across different types of bases, solvents, and temperatures (entries 3-5). Entry 6 is a case in point showing that the desired reaction can proceed in various combinations of bases and solvents. Even in the completely different combination of base and solvent compared with the optimized condition, a rearranged product **1.87** was obtained with 50% yield. One of the few exceptions of this compatibility is the use of THF: diminished yield was observed when THF was used as solvent (entry 7). Increasing the equivalent of coupling partner did not significantly affect the yield, whereas reducing the amount to 1.0 equivalent was deleterious to the reaction (entries 8, and 9). By virtue of these early investigations, prototype of the pivotal bio-inspired C6–C17 bond formation could be established.

## 1.2.2. Implementation of the Key Strategy in the Intramolecular System and Synthetic Attempt for Rhazimal

### A. Possible candidates listed by complexity



### B. Retrosynthetic analysis

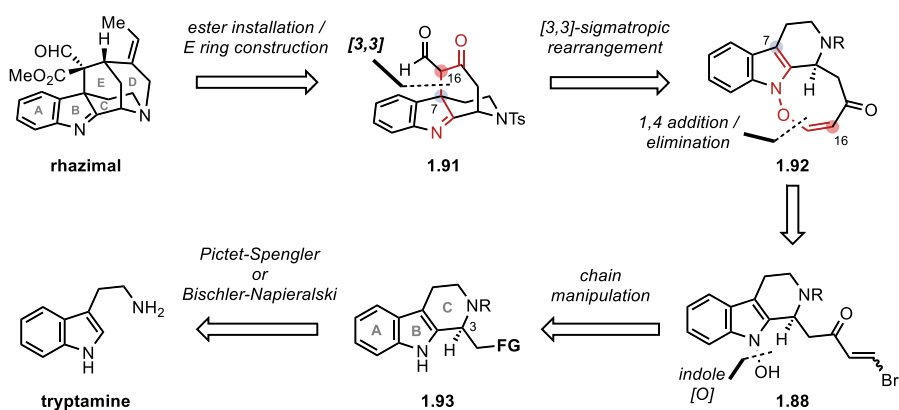


**Figure 1.13.** Phase 2: retrosynthetic analysis.

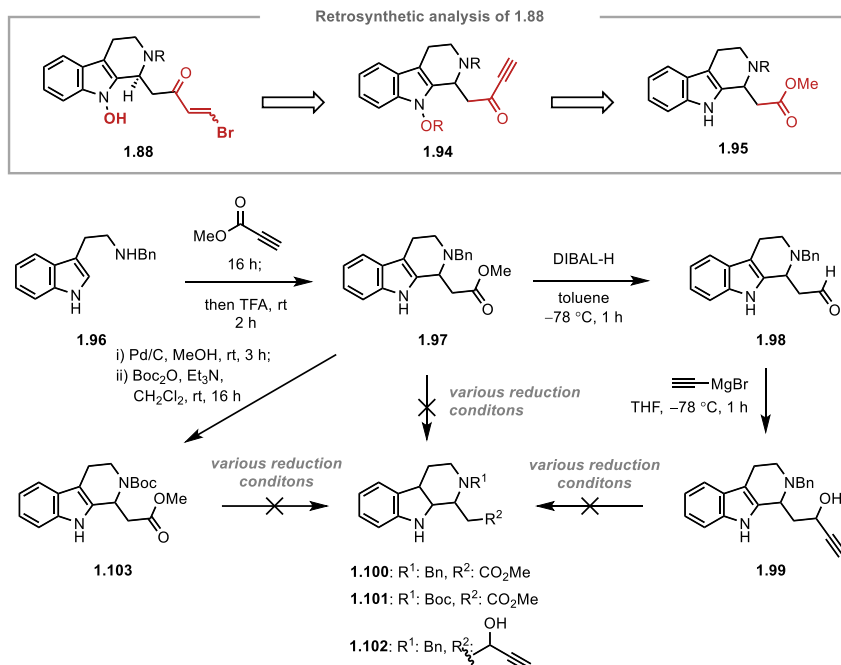
After completing the reaction optimization, we first enumerated the possible candidates for the intramolecular cyclization which could lead to the C7–C16 bond formation after the vital rearrangement step (Figure 1.13A). We envisioned that 1.88 is the most suitable precursor for this purpose for several reasons: two quaternary centers will be directly connected if [3,3]-sigmatropic rearrangement takes place in 1.89 or 1.90, and the formation of such vicinal quaternary-quaternary carbon centers is scarcely preceded, due to the presence of two bulky groups in close proximity.<sup>23</sup> Taking the steric aspect into account, it was expected that 1.88, in which the reaction position is less substituted, would be more advantageous than 1.89 or 1.90 in implementing the key reaction. In addition, the tethered chain of 1.88 was expected to add flexibility to the structure, which would allow for a more

viable approach between C7 and C16. Accordingly, **1.88** was chosen as an intermediate for the total synthesis of rhazimal. However, the possibility of replacing the targeted intermediate to **1.89** or **1.90**, depending on synthetic progress, should not be neglected.

Our retrosynthetic plan was initiated with removal of D ring motif of geissoschizine to increase the structural flexibility for the better access to [3,3]-sigmatropic rearrangement (Figure 1.13B). This led us to arrive at compound **1.91**, an analogue of geissoschizine but with more simplified architecture. Completing the central ABC tricyclic framework could be accomplished by well-known Pictet-Spengler reaction or Bischler-Napieralski reaction while successfully installing tethered chain to the C3 position. Compound **1.93** was then retrosynthetically dissected as a chain moiety and an indole moiety, and orthogonal functionalization in the indole and tethered chain was envisioned to furnish **1.88**. While this seems very logical from the viewpoint of strategy, not much has been known about the compatibility of *N*-hydroxyindole to the various synthetic conditions and the observed susceptibility of the related molecule, *i.e.*, **1.80**, made us doubt about the viability of compound **1.88**, thus careful synthetic design is needed. After successful oxidation of the indole and installation of  $\alpha,\beta$ -unsaturated carbonyl moiety (**1.88**), the 1,4-addition/elimination sequence could be proceeded in an intramolecular manner (**1.90**). Implementation of the developed protocol would allow the successful formation of C7–C16 bonds by spontaneous [3,3]-sigmatropic rearrangement. The resulting **1.91** could be subjected to a series of functionalization for late-stage E ring construction to complete rhazimal.

For the synthesis of **1.88**, a key precursor for [3,3]-sigmatropic rearrangement, we envisioned that  $\alpha,\beta$ -unsaturated bromoketone tethered in C ring would be easily synthesized through ynone **1.94** (Scheme 1.16). Accordingly, ester **1.95** was determined to be the flexible precursor for the synthesis of ynone **1.94**, and in the worst case, would provide stable mid-point for the detour.

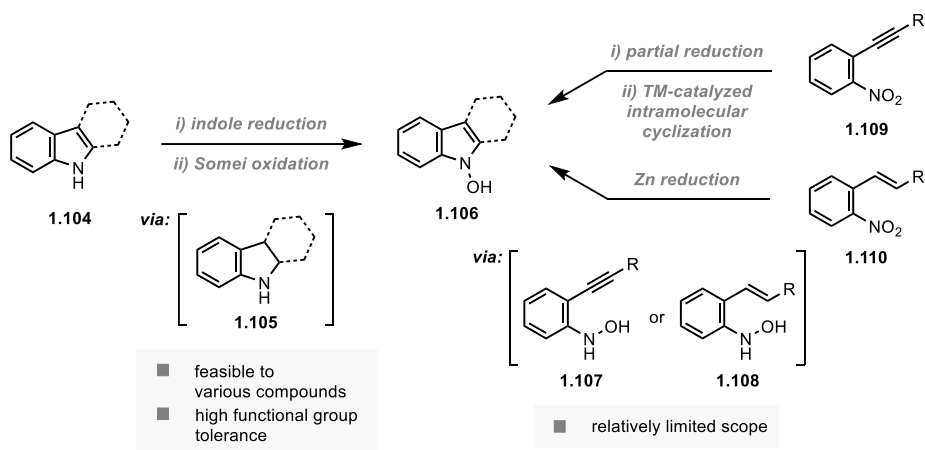
**Scheme 1.16.** General strategies for construction of the key intermediate **1.88** and failed routes to access to indoline.



Synthesis of ynone **1.94** began with the condensation of benzyl-protected tryptamine **1.96** with methyl propiolate. After treating with TFA, tricyclic compound **1.97** was successfully synthesized within 2 steps. The initial plan was to access to indoline **1.100** which is the prerequisite for the synthesis of *N*-hydroxyindole. Even after the extensive screening for the suitable reduction conditions, it was impossible to obtain the desired indoline **1.100** with affordable yield, only observing the mixture of multiple compounds. We reasoned that the functional groups in C ring motif, either N4-protecting group or functional groups in chain moiety, is important for the compatibility of the reduction to the corresponding system. Thus, we decided to transform the tethered ester before conducting the indole reduction-oxidation sequence. From **1.97**, propargyl alcohol **1.99** was successfully prepared by treatment of DIBAL-H to furnish aldehyde **1.98**, followed by alkyne addition to the corresponding aldehyde. The resulted alcohol **1.99** was then subjected to a number of reducing conditions, expecting for indoline **1.102**. However, to our disappointment, only the mixture of unidentified compounds were obtained. Putative reason for this incompatibility might stem from the electronics of the C ring motif. Thus, different amine protection group with electron-

withdrawing nature was assessed (**1.103**), but also failed to provide the desired indoline **1.102**.

**Scheme 1.17.** Two general methods to access *N*-hydroxyindole.



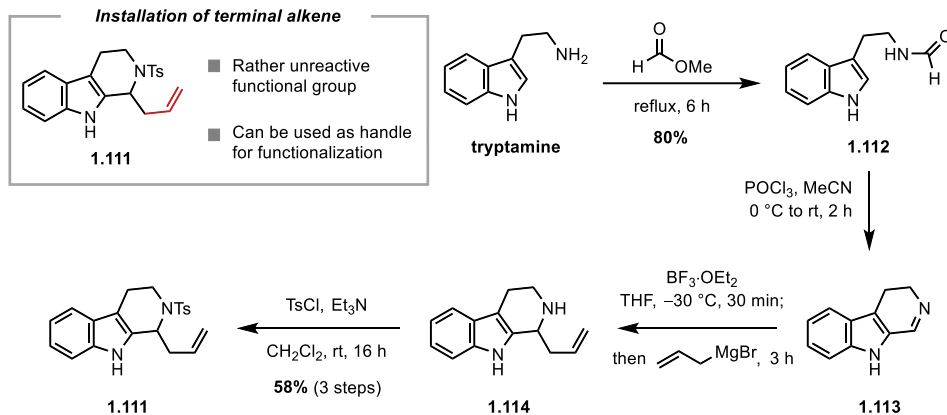
The obvious difficulty surrounding the competent synthesis of *N*-hydroxyindole **1.106** lies in the limited synthetic methods available (Scheme 1.17). Only two general strategies are utilized to access *N*-hydroxyindole, and could be even more narrowed when starting from indole framework. The approach starting from nitrobenzene **1.109** or **1.110** to reach phenylhydroxylamine **1.107** or **1.108**, respectively, by partial reduction of the nitro group followed by intramolecular cyclization is a widely used method for *N*-hydroxyindole synthesis. However, there are several difficulties in that only the limited scope is available and more importantly, functionalization of the C-ring motif has to go through much more tedious synthetic steps than when synthesizing from tryptamine. On the other hand, the reduction/oxidation sequence starting from indole **1.104** has the advantage of utilizing indole framework as a starting point and its attendant effortlessness of C-ring functionalization. Thus, reduction/oxidation sequence was considered more appropriate for our synthetic endeavors which in other words, access to indoline was inevitable to our synthetic plan.

We recognized that reduction of indole to indoline is an essential component in achieving access to *N*-hydroxyindole, thus sought a solution for a reliable supply of indoline. To achieve this goal, it was unavoidable to scrutinize the manipulation of the functional groups of the C ring, *i.e.*, the amine-protecting group and tethered chain, and the compatibility of each



combination in the reducing conditions.

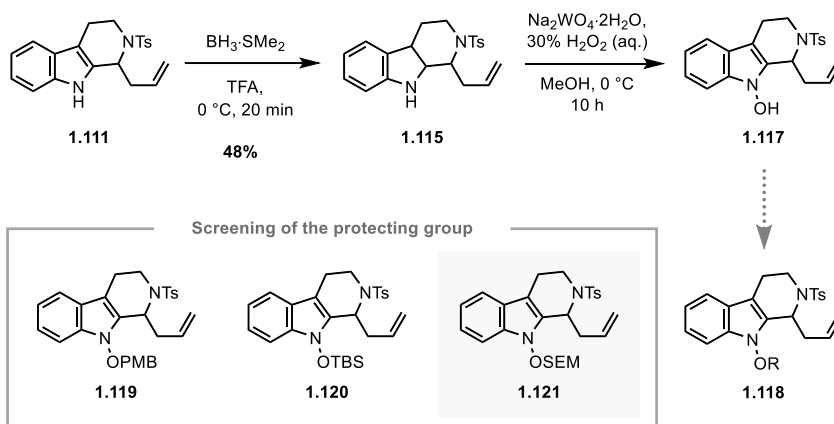
**Scheme 1.18.** Constructing the tricyclic framework with homoallylic chain for further functionalization.



Consequently, tosyl group and homoallylic chain were installed as a functional group that could be a stepping stone to advance to various functional groups while being less affected by external conditions (Scheme 1.18). To generate compound **1.111**, we imagined that simple Grignard addition to an imine group in tricyclic **1.113** would yield the desired overall structure. Starting from tryptamine, treatment of methyl formate would result in a formylation of the primary amine chain. The resulted formamide **1.112** was transformed into an imine **1.113** via Bischler-Napieralski reaction, which was then undergone subsequent Grignard addition and protection of secondary amine (**1.114**) to furnish indole **1.111**.



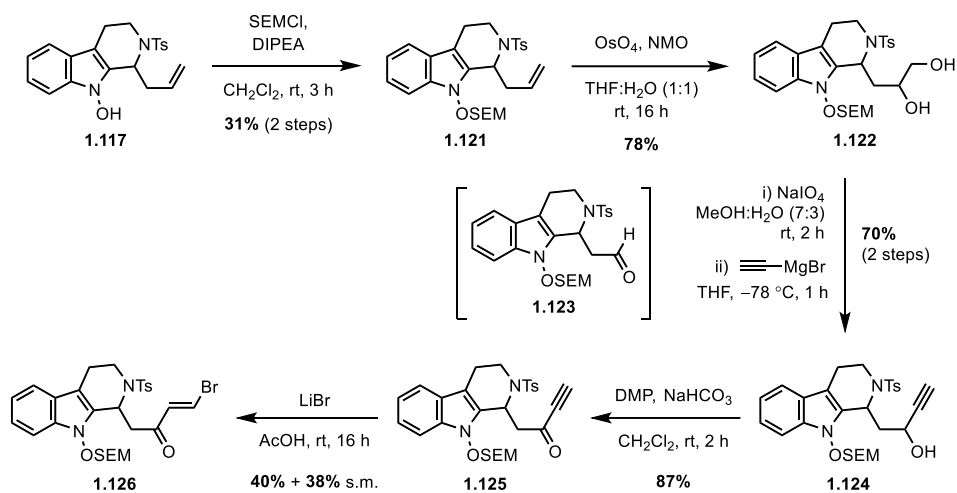
**Scheme 1.19.** Access to *N*-hydroxyindole **1.117** and evaluation of suitable hydroxyl-protecting group.



After successfully reducing the indole **1.111** to indoline **1.115**, indoline **1.115** was treated with Somei oxidation conditions to yield *N*-hydroxyindole **1.117** (Scheme 1.19). *N*-hydroxyindoles are in most cases sufficiently pure to be used as crude for further reaction. At the same time, most of them are unstable, supported by the previous report<sup>24</sup> and empirical evidence. Due to this critical issue, *N*-hydroxyindole **1.117** needed protection for safely bringing to the late-stage functionalization. Thus, the assessment of adequate protection groups for *N*-hydroxyindole **1.117** was commenced. The first and foremost aspect to consider is the reliable deprotection of the protecting group, which should not be detrimental to the resulting *N*-hydroxyindole and should be able to be conducted in the presence of several delicate functionalities, including a rather vulnerable  $\alpha,\beta$ -unsaturated bromoketone.

Following the examination of various protecting groups including PMB group, TBS group as the representative of silicon-based protection, and lastly SEM group among the acetal-based protection groups, it was revealed that the use of SEM protecting group safely provided the naked *N*-hydroxyindole after deprotection and SEM protected tricycle **1.121** was chosen for further synthetic journey.

**Scheme 1.20.** Synthetic route to an intermediate **1.126**.



The synthesis moving forward from *N*-hydroxyindole **1.117** was thus started from the SEM protection of corresponding *N*-hydroxyl group (Scheme 1.20). By stirring with SEMCl and DIPEA in  $\text{CH}_2\text{Cl}_2$ , desired SEM-protected *N*-hydroxyindole **1.121** was obtained with 58% yield from indoline **1.115**. Dihydroxylation with  $\text{OsO}_4$  led to diol **1.122**, which was then cleaved by  $\text{NaIO}_4$  to furnish aldehyde **1.123**. Aldehyde **1.123** was then used directly for the subsequent Grignard addition to provide propargyl alcohol **1.124**. Oxidation of propargyl alcohol formed **1.125**, generating the requisite ynone for the synthesis of  $\alpha,\beta$ -unsaturated bromoketone moiety. To our delight, combination of LiBr and acetic acid furnished the desired intermediate **1.126** with an  $\alpha,\beta$ -unsaturated bromoketone moiety in affordable yield.

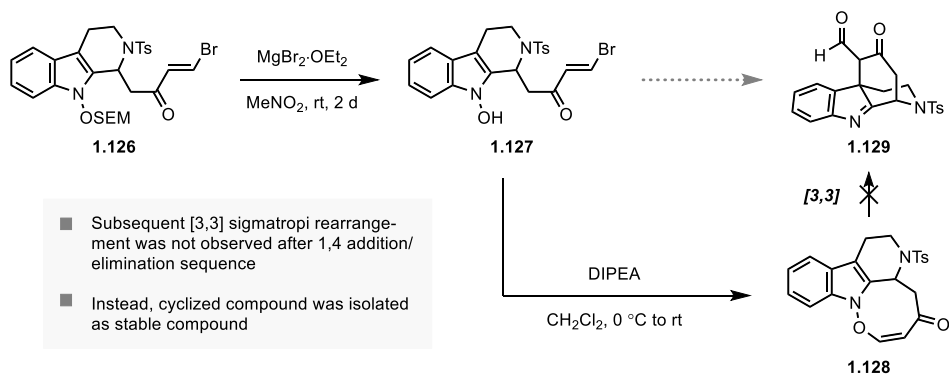
**Table 1.4.** Screening for the SEM deprotection of **1.126**.

entry	conditions	result
1	CsF, DMF, 60°C, 1 h	< 5%
2	TBAF, THF, 0°C to rt, 1 h	< 5%
3	TASF, CH <sub>2</sub> Cl <sub>2</sub> , rt, 1 h	< 5%
4	PPTS, <i>t</i> BuOH, reflux, 1 h	< 5%
5	<i>p</i> -TsOH, <i>t</i> BuOH, reflux, 1 h	< 5%
6	TfOH, CH <sub>2</sub> Cl <sub>2</sub> , rt, 1 h	35%
7	TMSOTf, 2,2'-bipyridyl, CH <sub>2</sub> Cl <sub>2</sub> , 0°C, 2 h	< 5%
<b>8</b>	<b>MgBr<sub>2</sub>·Et<sub>2</sub>O, MeNO<sub>2</sub>, Et<sub>2</sub>O, rt, 1 d</b>	<b>55%</b>

A thorough screening of additives and solvents to achieve SEM deprotection was performed (Table 1.4). Aided by the silyl group attached to the end of the protecting group, two general conditions could be applied to the detachment of the SEM group: the acidic conditions commonly employed for acetal deprotection, and the use of a fluoride source which is widely used in the removal of silyl group. However, as already observed in the previous attempt to deprotect the TBS group in TBS-protected *N*-hydroxyindole **1.120** under various sources of nucleophilic fluoride including TBAF, KF, CsF and DAST (*vide supra*, Scheme 1.19), we suspected that nucleophilic fluoride appears to be a major culprit for the destruction of the *N*-hydroxyindole moiety. As expected, rapid decomposition was observed in the presence of nucleophilic fluoride reagent (entries 1-3). Accordingly, the switch of the deprotection method to the acidic conditions was done and various acidic conditions were screened regardless of the degree of acidity (entries 4-6). Access to *N*-hydroxyindole **1.127** was finally realized by treatment of TfOH. However, the practicality of the reaction conditions became problematic since a sharp decrease in yield occurred when the reaction scale became larger (< 0.1 mmol). The diminishing yield of deprotection with increasing scale made it difficult to access **1.127** efficiently, and thus was not suited for our synthetic dedication. Thus, our attention shifted towards utilizing the mild Lewis acidic reagents as a

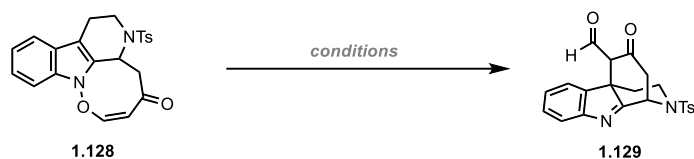
potential alternative method to access **1.27** (entries 7, and 8) and the desired *N*-hydroxyindole **1.27** could be safely obtained by using  $\text{MgBr}_2 \cdot \text{Et}_2\text{O}$ .<sup>25</sup>

**Scheme 1.21.** Initial attempt for 1,4-addition/elimination/[3,3]-sigmatropic rearrangement sequence.



The stimulating outcome of deprotection prompted us to proceed with the key transformation, which is the 1,4-addition/elimination/[3,3]-sigmatropic rearrangement protocol (Scheme 1.21). Having naked *N*-hydroxyindole **1.127** in hand, 1,4-addition/elimination sequence was commenced via treatment of DIPEA in  $\text{CH}_2\text{Cl}_2$  (Scheme 1.21). Preliminary trials of 1,4-addition/elimination sequence in intermolecular system (*vide supra*, Figure 1.11 and Table 1.2) were always accompanied with [3,3]-sigmatropic rearrangement. However, the expected [3,3]-sigmatropic rearrangement was not initiated in this intramolecular system: Instead, 1,4-addition/elimination sequence yielded **1.128** which could be isolated as a stable intermediate, while [3,3]-sigmatropic rearrangement to reach the desired **1.129** was put on hold.

**Table 1.5.** Screening thermal conditions for [3,3]-sigmatropic rearrangement.

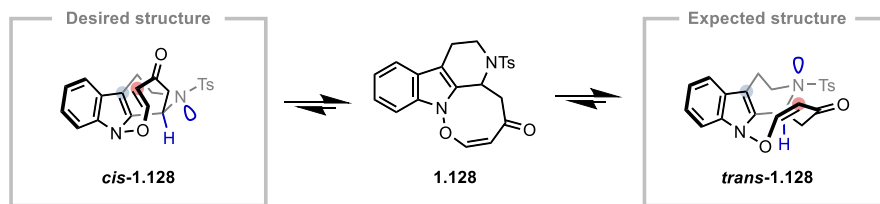


entry	conditions	result
1	benzene, 120 °C	no reaction
2	BF <sub>3</sub> -OEt <sub>2</sub> , benzene, 120 °C	no reaction
3	quinoline, 200 °C	decomposed
4	nitrobenzene, 200 °C	decomposed
5	cumene, 150 °C	decomposed

Given that the substrate **1.128** does not possess the envisioned flexibility necessary for facile approach of each reacting sites, we expected that more forcing conditions might be required for the desired transformation to overcome the rigidity of the system (Table 1.5). Exhaustive screening of different solvents and additives, however, ended with unsuccessful results. Cyclized enone **1.128** turned out to be inert towards desired [3,3]-sigmatropic rearrangement, presumably because significant ring strain must be overcome to bring the two reacting sites within the effective reaction distance.

The detailed mechanistic rationale for the failure of the [3,3]-sigmatropic rearrangement step is as follows (Figure 1.14). Depending on inversion of nitrogen lone pair, *cis*-**1.128** and *trans*-**1.128** can coexist in an equilibrium state as shown below (Figure 1.14A). In this case, *trans*-**1.128** is expected to be the dominant one, which can avoid steric congestion between the octagonal skeleton and indole moiety. Such avoidance eventually led C7 and C16 sites unable to be placed within an effective reaction distance, thus obviating the possibility for the desired reaction to occur.

A. Conformational isomers of **1.128** by nitrogen inversion



B. Conformational isomers of (*E*)- and (*Z*)-geissoschizine and different preferences arose from 1,3-allylic strain.

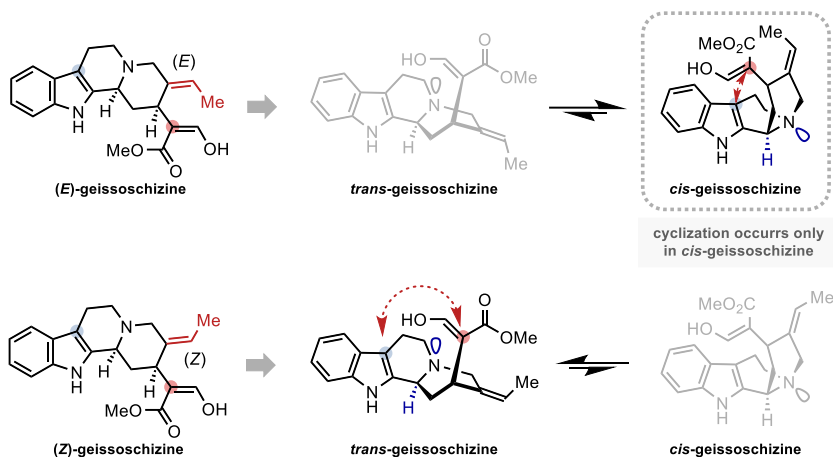


**Figure 1.14.** Proposed mechanistic rationale for failed [3,3]-sigmatropic rearrangement step.

We envisaged that a solution to these structural defects could be found in targeted natural product, rhazimal and its precursor, geissoschizine. Fascinating work done by Gaich, which was briefly presented earlier (*vide supra*, Scheme 1.4A and discussion thereof), disclosed the impact of the ethylidene moiety in the structural determination of geissoschizine (Figure 1.14B). Basically, geissoschizine exists in two forms, *cis*-geissoschizine and *trans*-geissoschizine, depending on the inversion of the lone pair of nitrogen. The *E/Z* configuration of ethylidene is the key to control such *cis* and *trans* conformation of quinolizidine system of the geissoschizine: *cis*-geissoschizine predominates when ethylidene has *E* conformation, and *trans*-geissoschizine predominates when ethylidene has *Z* conformation. By being in *cis*-form, C16 site in geissoschizine can be located closer to potential reaction sites, which becomes the driving force of intramolecular cyclization.

The same logic could be key to a successful synthetic design of rhazimal. We did not prioritize using geissoschizine as a starting material as it was viewed as "high risk, high



return" strategy. However, it appears that the nature-arranged flexural structure of geissoschizine can be used as an accelerator to evoke a crucial C7–C16 bond formation. A new synthetic approach that reflects these observations will be revisited in the future.

### 1.3. Conclusions

The extensive studies towards total synthesis of rhazimal was presented. The synthetic program was divided into three phases: the reaction development (Phase 1), the application of developed reaction in simple model system in intramolecular manner (Phase 2), and the biomimetic synthesis via direct C7–C16 bond formation in geissoschizine (Phase 3).

In Phase 1, [3,3]-Sigmatropic rearrangement of *N*-hydroxyindole to build C(*sp*<sup>3</sup>)–C(*sp*<sup>3</sup>) bond was newly materialized. Inspired by the structure of geissoschizine, 1,4-addition/elimination/[3,3]-sigmatropic rearrangement sequence could deliberately achieve the desired transformation in model system.

To successfully complete Phase 2, we established a concise synthesis of appropriate precursors to intramolecularly implement the initially discovered [3,3]-sigmatropic rearrangement of *N*-hydroxyindole. This synthetic route, alongside with the numerous optimizations of protecting group chemistry and functional group manipulations, led us to acquire **1.127** as a key precursor for the developed protocol. Application of the developed sequence, however, could not deliver the rearranged product and instead the octacyclic system was isolated as stable compound.

Take-home messages to ruminate for successful future total synthesis of rhazimal include:

1. The experimental evidences ascertained that the synthetic attempt towards rhazimal from a geissoschizine-mimicked simple model system is inherently flawed, regardless of retaining the current key strategy.
2. Internal and external measures are required to position C7 and C16, which occupy the opposite ends of the targeted C–C bond, close to each other.
3. Despite above difficulties, it is believed that the aforementioned problem can be solved by biomimetic logic if the inherent propensity for *cis*-decalin structure of geissoschizine is exploited.

## 1.4. References

- (1) (a) Ahmad, Y.; Fatima, K.; Le Quesne, P., Atta-ur-Rahman.: The isolation and structure of rhazimal, rhazimol and rhazinol from the leaves of *Rhazya stricta*. *J. Chem. Soc. Pak* **1979**, *1*, 69. (b) Ahmad, Y.; Fatima, K.; Le Quesne, P. W.; Atta ur, R., Further alkaloidal constituents of the leaves of *Rhazya stricta*. *Phytochemistry* **1983**, *22*, 1017.
- (2) (a) Wang, Z.; Xiao, Y.; Wu, S.; Chen, J.; Li, A.; Tatsis, E. C., Deciphering and reprogramming the cyclization regioselectivity in bifurcation of indole alkaloid biosynthesis. *Chem. Sci.* **2022**, *13*, 12389. (b) Zhao, S.; Sirasani, G.; Andrade, R. B. In *The Alkaloids: Chemistry and Biology*; Knölker, H.-J., Ed.; Academic Press: 2021; Vol. 86, p 1. (c) Pandey, K.; Shevkar, C.; Bairwa, K.; Kate, A. S., Pharmaceutical perspective on bioactives from *Alstonia scholaris*: ethnomedicinal knowledge, phytochemistry, clinical status, patent space, and future directions. *Phytochemistry Reviews* **2020**, *19*, 191. (d) Basha, A. *Biosynthesis of indole alkaloids*; Oxford University Press, USA, 1983; Vol. 7. (e) Scott, A. I., Biosynthesis of the indole alkaloids. *Acc. Chem. Res.* **1970**, *3*, 151. (f) Wenkert, E.; Wickberg, B., General Methods of Synthesis of Indole Alkaloids. IV. A Synthesis of DI-Eburnamonine1, 2. *J. Am. Chem. Soc.* **1965**, *87*, 1580. (g) Benayad, S.; Ahamada, K.; Lewin, G.; Evanno, L.; Poupon, E., Preakuammicine: A Long-Awaited Missing Link in the Biosynthesis of Monoterpene Indole Alkaloids. *Eur. J. Org. Chem.* **2016**, *2016*, 1494. (h) Eckermann, R.; Gaich, T., The Akuammiline Alkaloids; Origin and Synthesis. *Synthesis* **2013**, *45*, 2813.
- (3) (a) Zi, W.; Xie, W.; Ma, D., Total Synthesis of Akuammiline Alkaloid (–)-Vincorine via Intramolecular Oxidative Coupling. *J. Am. Chem. Soc.* **2012**, *134*, 9126. (b) Deiters, A.; Chen, K.; Eary, C. T.; Martin, S. F., Biomimetic Entry to the Sarpagan Family of Indole Alkaloids: Total Synthesis of (+)-Geissoschizine and (+)-N-Methylvellosimine. *J. Am. Chem. Soc.* **2003**, *125*, 4541. (c) Jarret, M.; Tap, A.; Kouklovsky, C.; Poupon, E.; Evanno, L.; Vincent, G., Bioinspired Oxidative Cyclization of the Geissoschizine Skeleton for the Total Synthesis of (–)-17-nor-Excelsinidine. *Angew. Chem. Int. Ed.* **2018**, *57*, 12294. (d) Jarret, M.; Turpin, V.; Tap, A.; Gallard, J.-F.; Kouklovsky, C.; Poupon, E.; Vincent, G.; Evanno, L., Bioinspired Oxidative Cyclization of the Geissoschizine Skeleton for Enantioselective Total Synthesis of Mavacuran Alkaloids. *Angew. Chem. Int. Ed.* **2019**, *58*, 9861. (e) Sato, K.; Kogure, N.; Kitajima, M.; Takayama, H., Total Syntheses of Pleiocarpamine, Normavacurine, and C-Mavacurine. *Org. Lett.* **2019**, *21*, 3342. (f) Teng, M.; Zi, W.; Ma, D., Total Synthesis of the

- Monoterpenoid Indole Alkaloid ( $\pm$ )-Aspidophylline A. *Angew. Chem. Int. Ed.* **2014**, *53*, 1814.
- (4) Ren, W.; Tappin, N.; Wang, Q.; Zhu, J., Synthetic Study towards Strictamine: The Oxidative Coupling Approach. *Synlett* **2013**, *24*, 1941.
- (5) Eckermann, R.; Gaich, T., The Double-Bond Configuration of Corynanthean Alkaloids and Its Impact on Monoterpenoid Indole Alkaloid Biosynthesis. *Chem. Eur. J.* **2016**, *22*, 5749.
- (6) In the case of Vincent's work in 2018, the mechanism for direct N4-C16 bond formation by iodination is explained as oxidation of N4, not C16. However, considering the discussion of C16 umpolung permeating the entire work and the fact that the adopted oxidative conditions is the conditions used by Ma and Zhu to iodinate the  $\alpha$ -carbon of carbonyl, it can be assertable that the original intention of the step was polarity-reversal of C16 position.
- (7) For selected reviews, see: (a) Nubbemeyer, U., Recent Advances in Asymmetric [3,3]-Sigmatropic Rearrangements. *Synthesis* **2003**, *2003*, 0961. (b) Nubbemeyer, U., Recent advances in charge-accelerated Aza-Claisen rearrangements. *Natural products synthesis II* **2005**, 149. (c) Hiersemann, M.; Nubbemeyer, U. *The Claisen rearrangement: methods and applications*; John Wiley & Sons, 2007. (d) Ilardi, E. A.; Stivala, C. E.; Zakarian, A., [3,3]-Sigmatropic rearrangements: recent applications in the total synthesis of natural products. *Chem. Soc. Rev.* **2009**, *38*, 3133. (e) Lee, H.; Kim, K. T.; Kim, M.; Kim, C. In *Catalysts* 2022; Vol. 12. (f) Liu, Y.; Liu, X.; Feng, X., Recent advances in metal-catalysed asymmetric sigmatropic rearrangements. *Chem. Sci.* **2022**, *13*, 12290.
- (8) Sundberg, R., Deoxygenation of nitro groups by trivalent phosphorus. Indoles from o-nitrostyrenes. *J. Org. Chem.* **1965**, *30*, 3604.
- (9) Nagayoshi, T.; Saeki, S.; Hamana, M., Some Reactions of 1-Hydroxy-2-phenylindole. *Heterocycles* **1977**, *6*, 1666.
- (10) Nagayoshi, T.; Saeki, S.; Hamana, M., Some Reactions of 1-Hydroxy-2-phenylindole. *Heterocycles* **1977**, *6*, 1666.
- (11) Somei, M.; Noguchi, K.; Yamada, F., Synthesis of 1-Hydroxy-yohimbine and Its Novel Skeletal Rearrangement Reaction into Oxindole Derivatives. *Heterocycles* **2001**, *55*, 1237.
- (12) Fukui, Y.; Somei, M., Simple Synthesis of 1, 3, 4, 5a, 6, 10b, 11, 11a-Octahydro-2H-pyrazino[1', 2':1, 5]pyrrolo[2, 3-b]indole Derivatives Based on 1-Hydroxyindole Chemistry. *Heterocycles* **2001**, *55*, 2055.
- (13) Bera, M.; Hwang, H. S.; Um, T.-W.; Oh, S. M.; Shin, S.; Cho, E. J., Energy Transfer

- Photocatalytic Radical Rearrangement in N-Indolyl Carbonates. *Org. Lett.* **2022**, *24*, 1774.
- (14) Somei, M.; Kawasaki, T.; Fukui, Y.; Yamada, F.; Kobayashi, T.; Aoyama, H., The Chemistry of 1-Hydroxyindole Derivatives: Nucleophilic Substitution Reactions on Indole Nucleus. *Heterocycles* **1992**, *34*, 1877.
- (15) Fukui, Y.; Kobayashi, T.; Kawasaki, T.; Yamada, F.; Somei, M., A [3, 3] Sigmatropic and Novel Ipso [3,3] Sigmatropic Rearrangement of 1-Hydroxyindole Chemistry, *Heterocycles* **2019**, *99*, 465.
- (16) Duarte, M. P.; Mendonça, R. F.; Prabhakar, S.; Lobo, A. M., N-Hydroxy Indoles as Flexible Substrates in Rearrangements—a Novel Reaction with Activated Triple Bonds. *Tetrahedron Lett.* **2006**, *47*, 1173.
- (17) Chen, Z.; Wang, Q., Synthesis of o-Aminophenols via a Formal Insertion Reaction of Arynes into Hydroxyindolinones. *Org. Lett.* **2015**, *17*, 6130.
- (18) Tomakinian, T.; Kouklovsky, C.; Vincent, G., Investigation of the Synthesis of Benzofuroindolines from N-Hydroxyindoles: An O-Arylation/[3,3]-Sigmatropic Rearrangement Sequence. *Synlett* **2015**, *26*, 1269.
- (19) Shevlin, M.; Strotman, N. A.; Anderson, L. L., Concise Synthesis of Furo[2,3-b]indolines via [3,3]-Sigmatropic Rearrangement of N-Alkenyloxyindoles. *Synlett* **2021**, *32*, 197.
- (20) Shrivs, H. J.; Fernández-Salas, J. A.; Hedtke, C.; Pulis, A. P.; Procter, D. J., Regioselective Synthesis of C3 Alkylated and Arylated Benzothiophenes. *Nat. Commun.* **2017**, *8*, 14801.
- (21) He, Z.; Shrivs, H. J.; Fernández-Salas, J. A.; Abengózar, A.; Neufeld, J.; Yang, K.; Pulis, A. P.; Procter, D. J., Synthesis of C2 Substituted Benzothiophenes via an Interrupted Pummerer/[3,3]-Sigmatropic/1,2-Migration Cascade of Benzothiophene S-Oxides. *Angew. Chem. Int. Ed.* **2018**, *57*, 5759.
- (22) The work done by Anderson (see ref 18) was published after the investigation of the key step was finished.
- (23) Pierrot, D.; Marek, I., Synthesis of Enantioenriched Vicinal Tertiary and Quaternary Carbon Stereogenic Centers within an Acyclic Chain. *Angew. Chem. Int. Ed.* **2020**, *59*, 36.
- (24) Somei, M. In *Bioactive Heterocycles I*; Eguchi, S., Ed.; Springer Berlin Heidelberg: Berlin, Heidelberg, 2006, p 77.
- (25) (a) Fujioka, H.; Minamitsuji, Y.; Kubo, O.; Senami, K.; Maegawa, T., The reaction of

acetal-type protective groups in combination with TMSOTf and 2,2'-bipyridyl; mild and chemoselective deprotection and direct conversion to other protective groups. *Tetrahedron* **2011**, *67*, 2949. (b) Vakalopoulos, A.; Hoffmann, H. M. R., Novel Deprotection of SEM Ethers: A Very Mild and Selective Method Using Magnesium Bromide. *Org. Lett.* **2000**, *2*, 1447.

## 1.5. Experimental Section

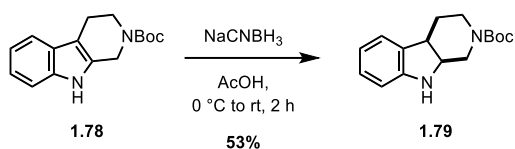
### General Information

Reactions were performed in oven-dried or flame-dried glassware under N<sub>2</sub> atmosphere with dry solvents under anhydrous conditions, unless otherwise stated. Tetrahydrofuran (THF) and dichloromethane (CH<sub>2</sub>Cl<sub>2</sub>) were initially degassed by sonication, and subsequently dried by passing them through a PureSolv solvent purification system and toluene was dried over CaH<sub>2</sub> and distilled under N<sub>2</sub> atmosphere. *N,N*-Dimethylformamide (DMF), dimethyl sulfoxide (DMSO), 1,2-dichloroethane (DCE), acetonitrile (MeCN), and 1,4-dioxane were purchased in anhydrous form from a commercial source (Sigma-Aldrich). Nitromethane was dried over molecular sieves (4Å) and degassed prior to use. Acetone, ethyl acetate (EtOAc), diethyl ether (Et<sub>2</sub>O), CH<sub>2</sub>Cl<sub>2</sub>, hexanes, and water (H<sub>2</sub>O) were purchased from a commercial source (Samchun Chemical) and used without further purification. H<sub>2</sub><sup>18</sup>O (97 atom% <sup>18</sup>O) was purchased from Sigma-Aldrich and used as received. Other reagents were purchased from commercial sources (Sigma-Aldrich, Alfa Aesar, Acros Organics, and TCI) and used as received. Yields refer to chromatographically and spectroscopically (<sup>1</sup>H NMR) homogeneous materials, unless otherwise stated. Reactions were monitored by thin-layers chromatography (TLC) using 0.25 mm E. Merck silica gel plates (60 F<sub>254</sub>) and the developed chromatogram was visualized by using UV light or an acidic ethanolic anisaldehyde or potassium permanganate (KMnO<sub>4</sub>) stain with heating. Intertec Silica gel (60, particle size 60–200 μm) was used for flash column chromatography. <sup>1</sup>H, <sup>13</sup>C and <sup>19</sup>F NMR spectra were recorded on an Agilent 400-MR DD2 Magnetic Resonance System, Varian/Oxford As-500 instrument, or Bruker 500 MHz instrument and calibrated using residual un-deuterated solvent signal (CHCl<sub>3</sub> in CDCl<sub>3</sub>: δ 7.26 ppm for <sup>1</sup>H, δ 77.16 ppm for <sup>13</sup>C; CH<sub>3</sub>OH in MeOD: δ 3.31 ppm for <sup>1</sup>H, δ 49.00 ppm for <sup>13</sup>C) as the internal reference. <sup>19</sup>F NMR spectra were calibrated to an external standard of neat PhCF<sub>3</sub> (δ –63.72 ppm). Data for NMR spectra were reported as follows: chemical shift (multiplicities, coupling constant (Hz), and integration) and chemical shifts are reported in ppm. The following abbreviations were used to explain the multiplicities: s = singlet, d = doublet, t = triplet, q = quartet, p = pentet, dd = doublet of doublets, td = triplet of doublets, tt = triplet of triplets, dq = doublet of quartets, ddd = doublet of doublet of doublets, ddt = doublet of doublet of triplets, dtd = doublet of triplet of doublets, dtt = doublet of triplet of triplets, tdd = triplet of doublet of doublets, m = multiplet, br = broad. High-

resolution mass spectrometry (HRMS) was performed using a HRMS-ESI Q-TOF 5600 spectrometer at National Instrumentation Center for Environmental Management (NICEM) in Seoul National University, Ultra High Resolution ESI Q-TOF mass spectrometer (Bruker compact) at the Organic Chemistry Research Center in Sogang University, or ThermoFisher Scientific mass spectrometer (Orbitrap Exploris 120) at Department of Chemistry at Seoul National University. The crystal structure was determined by single-crystal X-ray diffractometer at the Instrumental Analysis Center of Gyeongsang National University.



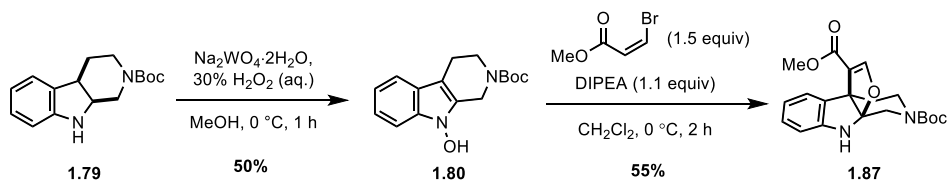
## Indoline 1.79



To an oven-dried round-bottom flask equipped with a stir bar and septum were added indole **1.78** (1.00 g, 3.67 mmol) and AcOH (40 mL) at 23 °C. The resulting solution was cooled to 0 °C, and NaBH<sub>3</sub>CN (461 mg, 7.34 mmol) was added to the solution. The reaction mixture was warmed up to rt and stirred while the reaction was monitored by TLC. After completion of reaction (1–2 h), the reaction mixture was directly concentrated under reduced pressure. The crude product was re-dissolved in CH<sub>2</sub>Cl<sub>2</sub> and basified to pH 9–10 using NH<sub>3</sub>·H<sub>2</sub>O (25.0–30.0 wt% in H<sub>2</sub>O). The layers were separated and the aqueous layer was extracted with CH<sub>2</sub>Cl<sub>2</sub> (3 × 30 mL). The combined organic layer was washed with brine (1 × 20 mL), dried over anhydrous MgSO<sub>4</sub>, filtered, and concentrated under reduced pressure. The resulting residue was purified by flash column chromatography (silica gel, hexanes:EtOAc = 1:0 → 7:3) to afford indoline **1.79** (534 mg, 53%) as a pale yellow oil. Analytic data is in agreement with the reported literature values.<sup>1</sup>

<sup>1</sup>H NMR (500 MHz, CDCl<sub>3</sub>): δ 7.07 – 7.01 (m, 2H), 6.73 (t, *J* = 7.2 Hz, 1H), 6.62 (d, *J* = 7.7 Hz, 1H), 3.97 – 3.86 (m, 2H), 3.58 – 3.53 (m, 1H), 3.39 – 3.34 (m, 3H), 2.06 – 1.95 (m, 1H), 1.88 – 1.81 (m, 1H), 1.44 (s, 9H); <sup>13</sup>C NMR (126 MHz, CDCl<sub>3</sub>): δ 155.8, 150.6, 131.2, 127.9, 123.8, 119.0, 109.8, 79.6, 57.5, 43.7, 41.3, 39.4, 28.6, 26.4.

## Bridged indoline 1.87



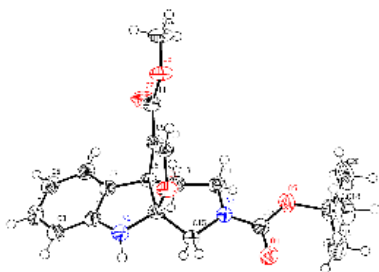
*N*-Hydroxyindole **1.80** was synthesized according to a known literature procedure.<sup>2</sup> To an oven-dried round-bottom flask equipped with a stir bar and septum were added indoline **1.79** (0.100 g, 0.364 mmol) and MeOH (10 mL) at 23 °C. The resulting solution was cooled to

0 °C, and sodium tungstate dihydrate (6.0 mg, 18.2  $\mu\text{mol}$ ) and  $\text{H}_2\text{O}_2$  (30 wt% in  $\text{H}_2\text{O}$ , 1.0 mL) were added to the solution. The resulting mixture was stirred for 2 h before it was quenched with  $\text{H}_2\text{O}$  (10 mL). The layers were separated and the aqueous layer was extracted with  $\text{CH}_2\text{Cl}_2$  ( $3 \times 10$  mL). The combined organic layer was washed with  $\text{H}_2\text{O}$  ( $3 \times 10$  mL), dried over anhydrous  $\text{MgSO}_4$ , filtered, and concentrated under reduced pressure to afford *N*-hydroxyindole **1.80** (52.5 mg, 0.182 mmol) as a colorless oil. The resulting crude was pure enough to be used directly in the subsequent reaction without further purification.

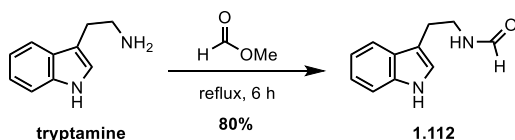
To an oven-dried round-bottom flask equipped with a stir bar and septum were added crude *N*-hydroxyindole **1.80** obtained above and  $\text{CH}_2\text{Cl}_2$  (4 mL) at 23 °C. The resulting solution was cooled to 0 °C, and methyl (*Z*)-3-bromoacrylate (45.0 mg, 0.273 mmol) and DIPEA (34.9  $\mu\text{L}$ , 0.200 mmol) were added to the solution. The resulting mixture was stirred for 2 h at 0 °C before it was quenched with  $\text{H}_2\text{O}$  (5 mL). The layers were separated and the aqueous layer was extracted with  $\text{CH}_2\text{Cl}_2$  ( $3 \times 5$  mL). The combined organic layer was washed with  $\text{H}_2\text{O}$  ( $1 \times 20$  mL), dried over anhydrous  $\text{MgSO}_4$ , filtered, and concentrated under reduced pressure. The resulting residue was purified by flash column chromatography (silica gel, hexanes:EtOAc = 1:0  $\rightarrow$  7:3) to afford indoline **1.87** (37.3 mg, 55%) as a pale yellow oil.

$^1\text{H NMR}$  (400 MHz, MeOD, ca. 55:45 mixture of rotamers):  $\delta$  7.52 (s, 1H), 7.39 (d,  $J = 7.3$  Hz, 1H), 7.01 (t,  $J = 7.7$  Hz, 1H), 6.66 (t,  $J = 7.5$  Hz, 1H), 6.58 (d,  $J = 7.8$  Hz, 1H), 4.01 – 3.82 (m, 1H), 3.78 – 3.63 (m, 1H), 3.72 (s, 3H), 3.36 – 3.26 (m, 1H), 3.20 – 3.09 (m, 1H), 2.64 and 2.55 (dt,  $J = 14.1, 5.3$  Hz, 1H), 2.33 – 2.13 (m, 1H), 1.47 and 1.42 (s, 9H);  $^{13}\text{C NMR}$  (101 MHz, MeOD):  $\delta$  166.6, 159.8, 149.4, 132.4, 132.1, 129.5, 125.5, 119.9, 111.4, 111.3, 109.5, 81.5, 81.4, 57.2, 51.5, 45.7, 44.4, 41.4, 40.7, 28.7.

**X-ray crystal structure of bridged indoline 1.87.** For more information, see page 56.



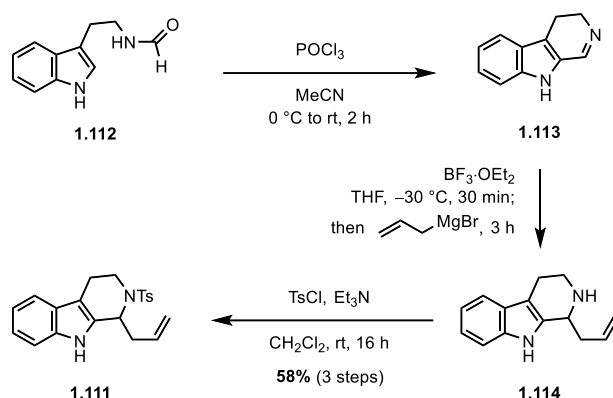
### N-Formyl tryptamine 1.112



To an oven-dried round-bottom flask equipped with a stir bar and septum were added tryptamine (5.00g, 31.2 mmol) and methyl formate (50 mL) at 23 °C. The reaction solution was heated to reflux and stirred for 6 h, before it was cooled to rt and directly concentrated under reduced pressure. The resulting residue was purified by flash column chromatography (silica gel, hexanes:EtOAc = 1:0  $\rightarrow$  3:7) to afford product **1.112** (4.70 g, 80%) as a pale yellow oil.

**<sup>1</sup>H NMR** (500 MHz, CDCl<sub>3</sub>, ca. 80:20 mixture of rotamers):  $\delta$  8.35 (br s, 1H), 8.06 (br s, 0.8H), 7.81 (d,  $J$  = 12.0 Hz, 0.2H), 7.59 and 7.56 (d,  $J$  = 7.9 Hz, 1H), 7.36 (d,  $J$  = 8.2 Hz, 1H), 7.21 (t,  $J$  = 8.0 Hz, 1H), 7.14–7.11 (m, 1H), 7.01 and 6.97 (s, 1H) 5.95 and 5.75 (br s, 1H), 3.63 and 3.48 (q,  $J$  = 6.5 Hz, 2H), 2.98 and 2.96 (t,  $J$  = 6.8 Hz, 2H); **<sup>13</sup>C NMR** (101 MHz, CDCl<sub>3</sub>):  $\delta$  164.9, 161.5, 136.7, 136.5, 127.3, 126.9, 122.9, 122.4, 122.3, 122.2, 119.7, 119.6, 118.6, 118.4, 112.4, 111.6, 111.6, 111.5, 42.1, 38.4, 27.4, 25.2.

## N-Tosyl tricycle **1.111**



To an oven-dried round-bottom flask equipped with a stir bar and septum were added **1.112** (2.00 g, 12.3 mmol, 1.0 equiv) at  $23\text{ }^\circ\text{C}$ , cooled to  $0\text{ }^\circ\text{C}$ , and  $\text{POCl}_3$  (40 mL) was added. The reaction solution warmed up to  $23\text{ }^\circ\text{C}$  and stirred for 2 h, before it was directly concentrated under reduced pressure to afford crude **1.113**, which was used directly in the subsequent reaction without further purification.

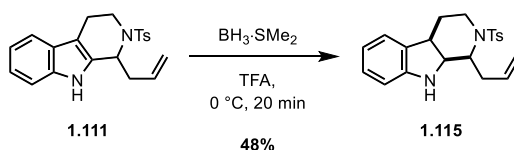
To an oven-dried round-bottom flask equipped with a stir bar and septum were added crude **1.113** and  $\text{THF}$  (40 mL) at  $23\text{ }^\circ\text{C}$ . The resulting solution was cooled to  $-30\text{ }^\circ\text{C}$ , and  $\text{BF}_3 \cdot \text{OEt}_2$  (3.08 mL, 25.0 mmol) was added dropwise to the solution. After the reaction mixture was stirred for 30 min, allylmagnesium bromide solution (1.0 M in diethyl ether, 50.0 mL) was added dropwise over 30 min. The resulting mixture was stirred for additional 3 h before it was quenched with brine (20 mL). The layers were separated and the aqueous layer was extracted with  $\text{EtOAc}$  ( $3 \times 50\text{ mL}$ ). The combined organic layer was washed with brine ( $3 \times 30\text{ mL}$ ), dried over anhydrous  $\text{MgSO}_4$ , filtered, and concentrated under reduced pressure to afford crude **1.114**, which was used directly in the subsequent reaction without further purification.

To an oven-dried round-bottom flask equipped with a stir bar and septum were added crude **1.114** and  $\text{CH}_2\text{Cl}_2$  (40 mL) at  $23\text{ }^\circ\text{C}$ , followed by  $\text{TsCl}$  (4.77 g, 25.0 mmol) and  $\text{Et}_3\text{N}$  (3.5 mL, 25.0 mmol). The resulting mixture was stirred for 16 h before it was quenched with brine (20 mL). The layers were separated and the aqueous layer was extracted with  $\text{CH}_2\text{Cl}_2$  ( $3 \times 50\text{ mL}$ ). The combined organic layer was washed with brine ( $1 \times 30\text{ mL}$ ), dried over anhydrous  $\text{MgSO}_4$ , filtered, and concentrated under reduced pressure. The resulting residue was purified by flash column chromatography (silica gel, hexanes: $\text{EtOAc}$  = 1:0  $\rightarrow$  7:3) to afford product

**1.111** (5.31 g, 58% for 3 steps) as a red-brown oil.

<sup>1</sup>H NMR (500 MHz, CDCl<sub>3</sub>): δ 8.14 (br s, 1H), 7.68 (d, *J* = 7.9 Hz, 2H), 7.35 (d, *J* = 7.9 Hz, 1H), 7.30 (d, *J* = 8.0 Hz, 1H), 7.17 – 7.12 (m, 3H), 7.07 (t, *J* = 7.4 Hz, 1H), 6.01 – 5.90 (m, 2H), 5.23 (br d, *J* = 6.3 Hz, 1H), 5.16 (br d, *J* = 16.3 Hz, 1H), 5.22 – 5.16 (m, 1H), 4.15 (dd, *J* = 14.5, 5.6 Hz, 1H), 3.43 (t, *J* = 13.1 Hz, 1H), 2.69 (t, *J* = 6.9 Hz, 2H), 2.56 (dd, *J* = 15.5, 4.4 Hz, 1H), 2.50 – 2.36 (m, 1H), 2.31 (s, 3H); <sup>13</sup>C NMR (126 MHz, CDCl<sub>3</sub>): δ 143.4, 138.2, 136.0, 134.1, 132.6, 129.7, 126.8, 126.6, 122.1, 119.5, 119.0, 118.2, 111.1, 108.1, 52.8, 40.5, 40.1, 21.5, 20.2.

### N-Tosyl indoline **1.115**

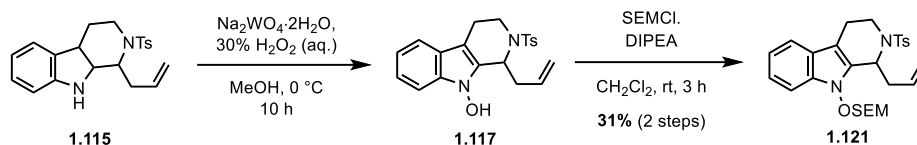


To an oven-dried round-bottom flask equipped with a stir bar and septum were added **1.111** (830 mg, 2.26 mmol) and TFA (10 mL) at 23 °C. The resulting solution was cooled to 0 °C, and BH<sub>3</sub>·SMe<sub>2</sub> (0.43 mL, 4.53 mmol) was added to the solution. The reaction mixture was stirred for 1 h before it was directly concentrated under reduced pressure. The crude product was re-dissolved in CH<sub>2</sub>Cl<sub>2</sub> (20 mL) and basified to pH 9–10 using NH<sub>3</sub>·H<sub>2</sub>O (25.0–30.0 wt% in H<sub>2</sub>O). The layers were separated and the aqueous layer was extracted with CH<sub>2</sub>Cl<sub>2</sub> (3 × 20 mL). The combined organic layer was washed with brine (1 × 20 mL), dried over anhydrous MgSO<sub>4</sub>, filtered, and concentrated under reduced pressure. The resulting residue was purified by flash column chromatography (silica gel, hexanes:EtOAc = 1:0 → 7:3) to afford product **1.115** (400 mg, 48%) as a reddish oil.

<sup>1</sup>H NMR (500 MHz, CDCl<sub>3</sub>): δ 7.76 (d, *J* = 8.3 Hz, 2H), 7.23 (d, *J* = 8.1 Hz, 2H), 7.02 (d, *J* = 7.3 Hz, 1H), 6.99 (td, *J* = 7.7, 1.1 Hz, 1H), 6.67 (td, *J* = 7.4, 1.0 Hz, 1H), 6.43 (d, *J* = 7.7 Hz, 1H), 5.84 (dddd, *J* = 16.8, 10.2, 7.9, 6.3 Hz, 1H), 5.10 (br dd, *J* = 15.5, 1.3 Hz, 1H), 5.08 (br d, *J* = 7.2 Hz, 1H), 4.13 (ddd, *J* = 8.1, 6.0, 1.7 Hz, 1H), 3.80 (dd, *J* = 7.5, 1.7 Hz, 1H), 3.44 (br s, 1H), 3.30 (ddd, *J* = 12.9, 6.3, 4.1 Hz, 1H), 3.22 – 3.13 (m, 2H), 2.54 – 2.48 (m, 1H), 2.40 (s, 3H), 2.38 – 2.34 (m, 1H), 1.83 (dtd, *J* = 14.0, 6.3, 3.0 Hz, 1H), 1.46 – 1.36 (m, 1H); <sup>13</sup>C NMR (126 MHz, CDCl<sub>3</sub>): δ 149.9, 143.0, 137.4, 134.8, 133.1, 129.4, 127.9, 127.7,

123.8, 119.1, 118.0, 109.7, 60.0, 54.7, 38.8, 38.5, 36.1, 28.2, 21.6

### SEM-Protected tricycle **1.121**



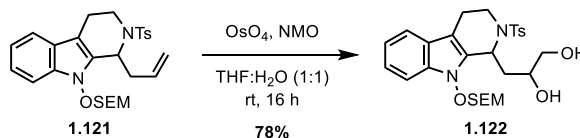
**1.117** was synthesized according to a known literature procedure.<sup>2</sup> To an oven-dried round-bottom flask equipped with a stir bar and septum were added indoline **1.115** (400 mg, 1.09 mmol) and MeOH (20 mL) at 23 °C. The resulting solution was cooled to 0 °C, and sodium tungstate dihydrate (17.9 mg, 0.054 mmol) and  $\text{H}_2\text{O}_2$  (30 wt% in  $\text{H}_2\text{O}$ , 2.5 mL) were added to the solution. The resulting mixture was stirred for 2 h before it was quenched with  $\text{H}_2\text{O}$  (20 mL). The layers were separated and the aqueous layer was extracted with  $\text{CH}_2\text{Cl}_2$  (3 × 20 mL). The combined organic layer was washed with  $\text{H}_2\text{O}$  (3 × 20 mL), dried over anhydrous  $\text{MgSO}_4$ , filtered, and concentrated under reduced pressure to afford crude *N*-hydroxyindole **1.117** which was used directly in the subsequent reaction without further purification.

To an oven-dried round-bottom flask equipped with a stir bar and septum were added crude **1.117** and  $\text{CH}_2\text{Cl}_2$  (20 mL) at 23 °C, followed by SEMCl (0.21 mL, 1.20 mmol) and DIPEA (0.17 mL, 1.30 mmol). The resulting mixture was stirred for 3 h before it was quenched with  $\text{H}_2\text{O}$  (10 mL). The layers were separated and the aqueous layer was extracted with  $\text{CH}_2\text{Cl}_2$  (3 × 10 mL). The combined organic layer was washed with  $\text{H}_2\text{O}$  (1 × 10 mL), dried over anhydrous  $\text{MgSO}_4$ , filtered, and concentrated under reduced pressure. The resulting residue was purified by flash column chromatography (silica gel, hexanes:EtOAc = 1:0 → 8:2) to afford product **1.121** (173 mg, 31% for 2 steps) as an orange oil.

<sup>1</sup>H NMR (500 MHz,  $\text{CDCl}_3$ ):  $\delta$  7.70 (d,  $J$  = 8.3 Hz, 2H), 7.33 (d,  $J$  = 8.1 Hz, 1H), 7.25 (d,  $J$  = 8.2 Hz, 1H), 7.06 – 7.02 (m, 1H), 7.04 (d,  $J$  = 8.0 Hz, 2H), 5.97 (ddt,  $J$  = 17.1, 10.2, 7.0 Hz, 1H), 5.47 (dd,  $J$  = 9.8, 3.6 Hz, 1H), 5.25 (d,  $J$  = 7.6 Hz, 1H), 5.22 (d,  $J$  = 7.5 Hz, 1H), 5.14 (br dd,  $J$  = 15.3, 1.6 Hz, 1H), 5.12 (br d,  $J$  = 6.8 Hz, 1H), 4.18 – 4.08 (m, 2H), 3.83 (ddd,  $J$  = 11.6, 9.7, 5.7 Hz, 1H), 3.41 (ddd,  $J$  = 14.8, 12.1, 4.8 Hz, 1H), 2.79 (dddd,  $J$  = 14.9, 7.1, 3.6, 1.2 Hz, 1H), 2.58 (dddd,  $J$  = 14.9, 9.7, 6.7, 1.4 Hz, 1H), 2.43 (dd,  $J$  = 15.7, 4.4 Hz, 1H), 2.29 – 2.21 (m, 1H), 2.24 (s, 3H), 1.29 – 1.21 (m, 1H), 1.14 (ddd,  $J$  = 13.8, 11.6, 5.7 Hz, 1H),

0.07 (s, 9H);  $^{13}\text{C}$  NMR (126 MHz,  $\text{CDCl}_3$ ):  $\delta$  143.2, 138.4, 134.5, 133.7, 132.6, 129.5, 127.1, 123.1, 122.5, 120.1, 118.5, 117.7, 108.6, 104.5, 101.3, 69.0, 52.0, 39.3, 38.8, 21.5, 19.3, 18.0, -1.2.

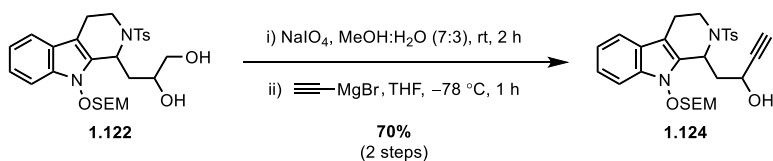
### Diol **1.122**



To an oven-dried round-bottom flask equipped with a stir bar and septum were added **1.121** (110 mg, 0.215 mmol) and THF:H<sub>2</sub>O (1:1, 10 mL) at 23 °C, followed by OsO<sub>4</sub> (4% in H<sub>2</sub>O, 68  $\mu\text{L}$ , 0.0107 mmol) and NMO (37.7 mg, 0.322 mmol). The reaction mixture was stirred for 16 h before it was quenched with H<sub>2</sub>O (5 mL). The layers were separated and the aqueous layer was extracted with EtOAc (3  $\times$  5 mL). The combined organic layer was washed with H<sub>2</sub>O (1  $\times$  5 mL), dried over anhydrous MgSO<sub>4</sub>, filtered, and concentrated under reduced pressure. The resulting residue was purified by flash column chromatography (silica gel, hexanes:EtOAc = 1:0  $\rightarrow$  6:4) to afford product **1.122** (91.5 mg, 78%) as a yellow oil.

$^1\text{H}$  NMR (500 MHz, MeOD, 60:40 mixture of diastereomers):  $\delta$  7.71 (d,  $J$  = 8.2 Hz, 2H), 7.35 (d,  $J$  = 8.2 Hz, 1H), 7.21 (d,  $J$  = 7.8 Hz, 1H), 7.14 (t,  $J$  = 7.5 Hz, 1H), 7.10 (d,  $J$  = 8.3 Hz, 2H), 6.98 (t,  $J$  = 7.4 Hz, 1H), 5.77 (dd,  $J$  = 9.9, 3.8 Hz, 0.6H), 5.54 (dd,  $J$  = 10.2, 4.3 Hz, 0.4H), 5.38 (d,  $J$  = 7.8 Hz, 1H), 5.33 (d,  $J$  = 7.5 Hz, 1H), 4.28 – 4.18 (m, 2H), 4.03 – 3.87 (m, 2H), 3.81 – 3.44 (m, 3H), 2.59 – 2.38 (m, 2H), 2.36 – 2.19 (m, 1H), 2.21 (s, 3H), 2.05 – 1.93 (m, 1H), 1.18 – 1.06 (m, 2H), 0.04 (s, 9H);  $^{13}\text{C}$  NMR (126 MHz,  $\text{CDCl}_3$ ):  $\delta$  143.7, 137.6, 137.3, 133.9, 133.3, 132.6, 132.2, 129.7, 129.6, 127.1, 126.9, 123.1, 123.0, 122.7, 122.5, 120.3, 120.1, 118.5, 118.4, 108.8, 108.6, 104.5, 103.9, 101.4, 70.9, 69.3, 69.1, 67.9, 66.5, 66.2, 51.2, 49.6, 39.3, 39.2, 37.4, 37.1, 29.8, 21.5, 19.1, 18.1, 18.0, -1.2.

### Propargyl alcohol **1.124**

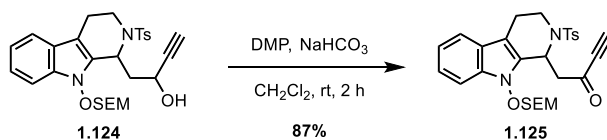


To an oven-dried round-bottom flask equipped with a stir bar and septum were added **1.122** (91.5 mg, 0.167 mmol) and MeOH:H<sub>2</sub>O (7:3, 10 mL) at 23 °C, followed by NaIO<sub>4</sub> (53.7 mg, 0.251 mmol). The reaction mixture was stirred for 2 h before it was quenched with H<sub>2</sub>O (5 mL). The layers were separated and the aqueous layer was extracted with CH<sub>2</sub>Cl<sub>2</sub> (3 × 5 mL). The combined organic layer was washed with H<sub>2</sub>O (1 × 5 mL), dried over anhydrous MgSO<sub>4</sub>, filtered, and concentrated under reduced pressure to afford crude aldehyde, which was used directly in the subsequent reaction without further purification.

To an oven-dried round-bottom flask equipped with a stir bar and septum were added crude aldehyde and THF (6 mL) at 23 °C. The resulting solution was cooled to -78 °C, and ethynylmagnesium bromide (0.5 M in THF, 0.34 mL, 0.167 mmol) was added dropwise to the solution. The resulting mixture was stirred for 1 h before it was quenched with brine (5 mL). The layers were separated and the aqueous layer was extracted with EtOAc (3 × 5 mL). The combined organic layer was washed with brine (1 × 3 mL), dried over anhydrous MgSO<sub>4</sub>, filtered, and concentrated under reduced pressure. The resulting residue was purified by flash column chromatography (silica gel, hexanes:EtOAc = 1:0 → 7:3) to afford product **1.124** (63.3 mg, 70% for 2 steps) as a pale yellow oil.

<sup>1</sup>H NMR (500 MHz, MeOD): δ 7.70 (d, *J* = 8.2 Hz, 2H), 7.37 (d, *J* = 8.2 Hz, 1H), 7.19 (d, *J* = 8.0 Hz, 1H), 7.14 (t, *J* = 7.3 Hz, 1H), 7.09 (d, *J* = 8.5 Hz, 2H), 6.99 (t, *J* = 7.8 Hz, 1H), 5.47 (dd, *J* = 10.7, 2.8 Hz, 1H), 5.31 (d, *J* = 7.7 Hz, 1H), 5.27 (d, *J* = 7.4 Hz, 1H), 4.60 – 4.56 (m, 1H), 4.16 (dd, *J* = 15.1, 6.2 Hz, 1H), 4.12 – 4.05 (m, 2H), 3.98 – 3.91 (m, 1H), 3.53 (ddd, *J* = 15.0, 11.9, 5.2 Hz, 1H), 2.97 (d, *J* = 2.0 Hz, 1H), 2.44 (dd, *J* = 15.9, 5.1 Hz, 1H), 2.38 – 2.25 (m, 2H), 2.23 – 2.14 (m, 1H), 2.20 (s, 3H), 1.10 (t, *J* = 8.0 Hz, 2H), 0.05 (s, 9H); <sup>13</sup>C NMR (126 MHz, CDCl<sub>3</sub>): δ 143.7, 137.5, 133.6, 131.1, 129.7, 126.9, 122.9, 122.6, 120.0, 118.6, 108.8, 104.7, 101.4, 84.4, 76.1, 73.5, 60.2, 49.4, 41.6, 39.5, 21.6, 19.6, 17.5, -1.2.

### Ynone 1.125



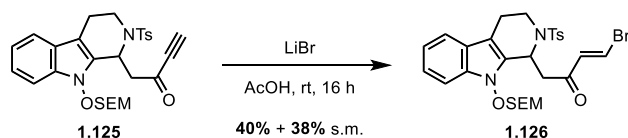
To an oven-dried round-bottom flask equipped with a stir bar and septum were added **1.124**



(63.3 mg, 0.117 mmol) and CH<sub>2</sub>Cl<sub>2</sub> (8 mL) at 23 °C, followed by DMP (64.6 mg, 0.152 mmol) and NaHCO<sub>3</sub> (29.5 mg, 0.351 mmol). The reaction mixture was stirred for 2 h before it was quenched with NaHCO<sub>3</sub> (5 mL, sat. aq.). The layers were separated and the aqueous layer was extracted with CH<sub>2</sub>Cl<sub>2</sub> (3 × 5 mL). The combined organic layer was washed with H<sub>2</sub>O (1 × 5 mL), dried over anhydrous MgSO<sub>4</sub>, filtered, and concentrated under reduced pressure. The resulting residue was purified by flash column chromatography (silica gel, hexanes:EtOAc = 1:0 → 7:3) to afford product **1.125** (54.9 mg, 87%) as a pale yellow oil.

<sup>1</sup>H NMR (500 MHz, CDCl<sub>3</sub>): δ 7.71 (d, *J* = 8.3 Hz, 1H), 7.38 (d, *J* = 7.9 Hz, 1H), 7.34 (d, *J* = 8.1 Hz, 1H), 7.22 (t, *J* = 7.8 Hz, 1H), 7.19 (d, *J* = 8.2 Hz, 2H), 7.08 (t, *J* = 7.5 Hz, 1H), 5.79 (dd, *J* = 8.3, 3.9 Hz, 1H), 5.23 (d, *J* = 7.6 Hz, 1H), 5.19 (d, *J* = 7.7 Hz, 1H), 4.29 – 4.22 (m, 1H), 4.21 – 4.14 (m, 1H), 3.33 (ddd, *J* = 14.6, 11.7, 4.6 Hz, 1H), 3.28 (s, 1H), 3.20 (dd, *J* = 15.7, 3.9 Hz, 1H), 3.10 (dd, *J* = 15.7, 8.1 Hz, 1H), 2.74 (ddd, *J* = 16.4, 12.3, 5.8 Hz, 1H), 2.62 (ddd, *J* = 15.8, 4.7, 1.2 Hz, 1H), 2.34 (s, 3H), 1.24 – 1.20 (m, 2H), 0.09 (s, 9H); <sup>13</sup>C NMR (126 MHz, CDCl<sub>3</sub>): δ 182.9, 143.8, 137.4, 133.6, 130.3, 129.7, 127.4, 122.8, 120.2, 118.7, 108.9, 105.3, 81.4, 79.8, 76.3, 50.5, 47.6, 40.0, 29.8, 21.6, 20.3, 17.5, –1.3.

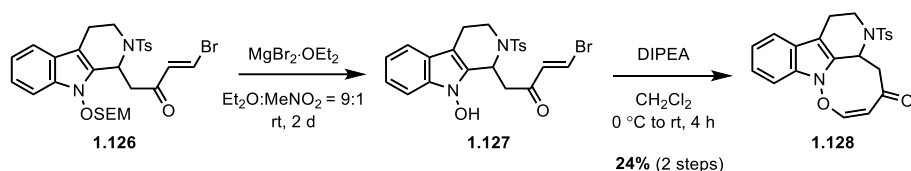
#### α,β-Unsaturated bromoketone **1.126**



To an oven-dried round-bottom flask equipped with a stir bar and septum were added **1.125** (35.0 mg, 0.065 mmol) and AcOH (3 mL) at 23 °C, followed by LiBr (8.5 mg, 0.097 mmol). The reaction mixture was stirred for 16 h before it was directly concentrated under reduced pressure to remove most of AcOH. The crude product was re-dissolved in CH<sub>2</sub>Cl<sub>2</sub> (5 mL) and diluted with H<sub>2</sub>O (5 mL). The layers were separated and the aqueous layer was extracted with CH<sub>2</sub>Cl<sub>2</sub> (3 × 5 mL). The combined organic layer was washed with H<sub>2</sub>O (1 × 5 mL), dried over anhydrous MgSO<sub>4</sub>, filtered, and concentrated under reduced pressure. The resulting residue was purified by flash column chromatography (silica gel, hexanes:EtOAc = 1:0 → 8:2) to afford α,β-unsaturated bromoketone **1.126** (16.1 mg, 40%, 78% brsm) as a colorless oil.

**<sup>1</sup>H NMR** (500 MHz, MeOD):  $\delta$  7.79 (d,  $J$  = 14.1 Hz, 1H), 7.70 (d,  $J$  = 8.3 Hz, 2H), 7.34 (d,  $J$  = 8.2 Hz, 1H), 7.23 (d,  $J$  = 7.9 Hz, 1H), 7.21 (t,  $J$  = 7.5 Hz, 1H), 7.16 (t,  $J$  = 7.7 Hz, 1H), 7.11 (d,  $J$  = 8.5 Hz, 2H), 7.01 (t,  $J$  = 7.5 Hz, 1H), 6.88 (d,  $J$  = 14.1 Hz, 1H), 5.93 (dd,  $J$  = 9.8, 3.5 Hz, 1H), 5.33 (d,  $J$  = 7.7 Hz, 1H), 5.28 (d,  $J$  = 7.7 Hz, 1H), 4.20 – 4.07 (m, 2H), 3.88 (ddd,  $J$  = 11.4, 9.8, 5.7 Hz, 1H), 3.55 (ddd,  $J$  = 14.8, 12.0, 5.0 Hz, 1H), 3.27 (dd,  $J$  = 15.0, 9.9 Hz, 1H), 3.04 (dd,  $J$  = 15.1, 3.4 Hz, 1H), 2.49 (dd,  $J$  = 16.1, 4.7 Hz, 1H), 2.39 – 2.29 (m, 1H), 2.23 (s, 3H), 1.27 – 1.20 (m, 1H), 1.18 – 1.08 (m, 1H), 0.07 (s, 9H); **<sup>13</sup>C NMR** (126 MHz, CDCl<sub>3</sub>):  $\delta$  197.4, 143.8, 137.4, 136.2, 133.6, 130.3, 129.7, 127.4, 125.5, 122.8, 120.2, 118.7, 108.9, 105.3, 76.3, 50.5, 47.6, 40.0, 29.8, 21.6, 20.3, 17.5, –1.3.

### Octacycle **1.128**

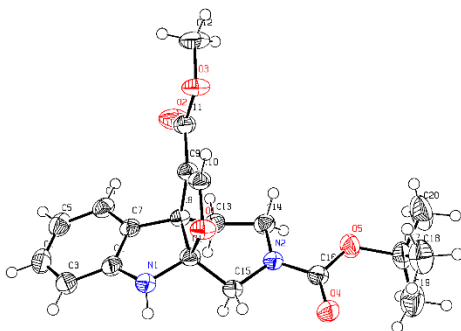


To an oven-dried round-bottom flask equipped with a stir bar and septum were added **1.126** (16.1 mg, 0.026 mmol) and Et<sub>2</sub>O:MeNO<sub>2</sub> (9:1, 1 mL) at 23 °C, followed by MgBr<sub>2</sub>·OEt<sub>2</sub> (134 mg, 0.520 mmol). The reaction mixture was stirred for 2 d before it was quenched with H<sub>2</sub>O (3 mL). The layers were separated and the aqueous layer was extracted with CH<sub>2</sub>Cl<sub>2</sub> (3 × 3 mL). The combined organic layer was washed with H<sub>2</sub>O (2 × 2 mL), dried over anhydrous MgSO<sub>4</sub>, filtered, and concentrated under reduced pressure to afford crude *N*-hydroxyindole **1.127** which was used directly in the subsequent reaction without further purification.

To an oven-dried round-bottom flask equipped with a stir bar and septum were added crude **1.127** and CH<sub>2</sub>Cl<sub>2</sub> (1 mL) at 23 °C. The resulting solution was cooled to 0 °C, and DIPEA (4.5 μL, 0.026 mmol) was added to the solution. The resulting mixture was warmed up to 23 °C and stirred for 4 h before it was quenched with H<sub>2</sub>O (1 mL). The layers were separated and the aqueous layer was extracted with CH<sub>2</sub>Cl<sub>2</sub> (3 × 1 mL). The combined organic layer was washed with H<sub>2</sub>O (1 × 1 mL), dried over anhydrous MgSO<sub>4</sub>, filtered, and concentrated under reduced pressure. The resulting residue was purified by preparative thin layer chromatography (hexanes:EtOAc = 1:0 → 6:4) to afford product **1.128** (2.5 mg, 24% for 2 steps) as an orange oil.

**<sup>1</sup>H NMR** (500 MHz, CDCl<sub>3</sub>): δ 7.81 (t, *J* = 7.7 Hz, 1H), 7.75 (dd, *J* = 7.7, 1.5 Hz, 1H), 7.71 (d, *J* = 8.2 Hz, 2H), 7.64 (d, *J* = 11.5 Hz, 1H), 7.48 (t, *J* = 7.6 Hz, 1H), 7.35 (d, *J* = 8.1 Hz, 1H), 7.19 (d, *J* = 8.0 Hz, 2H), 6.44 (d, *J* = 11.6 Hz, 1H), 4.81 (dd, *J* = 4.7, 3.3 Hz, 1H), 3.95 (ddd, *J* = 11.3, 10.1, 7.0 Hz, 1H), 3.73 (ddd, *J* = 10.1, 8.5, 1.8 Hz, 2H), 3.69 – 3.60 (m, 1H), 3.05 (ddd, *J* = 13.1, 3.3, 1.9 Hz, 1H), 2.98 (dd, *J* = 13.1, 4.8 Hz, 1H), 2.50 (ddd, *J* = 13.4, 11.4, 8.6 Hz, 1H), 2.22 (s, 3H), 2.07 – 2.01 (m, 1H).

### X-ray crystallographic data of bridged indoline 1.87:



Identification code	YJL-Interm-I	
Empirical formula	C <sub>20</sub> H <sub>24</sub> N <sub>2</sub> O <sub>5</sub>	
Formula weight	372.41	
Temperature	223(2) K	
Wavelength	0.71073 Å	
Crystal system	Triclinic	
Space group	P-1	
Unit cell dimensions	a = 8.0642(7) Å	α = 71.872(2)°.
	b = 10.8485(9) Å	β = 89.750(3)°.
	c = 12.1132(11) Å	γ = 71.677(3)°.
Volume	950.91(14) Å <sup>3</sup>	
Z	2	
Density (calculated)	1.301 Mg/m <sup>3</sup>	
Absorption coefficient	0.094 mm <sup>-1</sup>	
F(000)	396	
Crystal size	0.191 x 0.179 x 0.157 mm <sup>3</sup>	
Theta range for data collection	2.675 to 28.507°.	
Index ranges	-10 ≤ h ≤ 10, -14 ≤ k ≤ 14, -16 ≤ l ≤ 16	
Reflections collected	26827	
Independent reflections	4785 [R(int) = 0.0542]	
Completeness to theta = 25.242°	99.7 %	

Absorption correction	Semi-empirical from equivalents
Max. and min. transmission	0.7457 and 0.7131
Refinement method	Full-matrix least-squares on F <sup>2</sup>
Data / restraints / parameters	4785 / 0 / 252
Goodness-of-fit on F <sup>2</sup>	1.023
Final R indices [I > 2σ(I)]	R1 = 0.0455, wR2 = 0.0995
R indices (all data)	R1 = 0.0877, wR2 = 0.1213
Extinction coefficient	n/a
Largest diff. peak and hole	0.214 and -0.209 e.Å <sup>-3</sup>

Table 2. Atomic coordinates ( $\times 10^4$ ) and equivalent isotropic displacement parameters ( $\text{\AA}^2 \times 10^3$ ) for YJL-Interm-I.  $U(\text{eq})$  is defined as one third of the trace of the orthogonalized  $U^{ij}$  tensor.

	x	y	z	$U(\text{eq})$
C(1)	3263(2)	3107(2)	1513(1)	31(1)
N(1)	3195(2)	2560(2)	592(1)	36(1)
C(2)	1607(2)	2310(2)	524(1)	35(1)
C(3)	1003(3)	1847(2)	-288(2)	43(1)
C(4)	-635(3)	1677(2)	-194(2)	47(1)
C(5)	-1636(3)	1939(2)	684(2)	45(1)
C(6)	-1024(2)	2399(2)	1500(2)	39(1)
C(7)	600(2)	2584(2)	1414(1)	32(1)
C(8)	1564(2)	3104(2)	2139(1)	30(1)
C(9)	2333(2)	2101(2)	3348(1)	31(1)
C(10)	4076(2)	1644(2)	3385(1)	33(1)
O(1)	4756(1)	2155(1)	2400(1)	37(1)
C(11)	1294(2)	1764(2)	4313(1)	36(1)
O(2)	-282(2)	2202(2)	4250(1)	56(1)
O(3)	2304(2)	914(1)	5312(1)	44(1)
C(12)	1363(3)	555(2)	6316(2)	56(1)
C(13)	545(2)	4551(2)	2150(2)	36(1)
C(14)	1699(2)	5156(2)	2649(2)	36(1)
N(2)	3276(2)	5114(1)	2025(1)	34(1)
C(15)	3546(2)	4483(2)	1111(1)	34(1)
C(16)	4333(2)	5826(2)	2140(1)	36(1)
O(4)	5526(2)	5957(1)	1540(1)	46(1)
O(5)	3894(2)	6355(1)	3007(1)	45(1)
C(17)	4803(3)	7234(2)	3273(2)	47(1)
C(18)	6748(3)	6478(2)	3568(2)	63(1)
C(19)	4388(3)	8560(2)	2267(2)	72(1)

C(20)

3987(3)

7474(3)

4351(2)

82(1)

---

Table 3. Bond lengths [ $\text{\AA}$ ] and angles [ $^\circ$ ] for YJL-Interm-I.

---

C(1)-N(1)	1.425(2)
C(1)-O(1)	1.4863(19)
C(1)-C(15)	1.510(2)
C(1)-C(8)	1.564(2)
N(1)-C(2)	1.398(2)
N(1)-H(1)	0.85(2)
C(2)-C(3)	1.386(2)
C(2)-C(7)	1.396(2)
C(3)-C(4)	1.389(3)
C(3)-H(3)	0.9400
C(4)-C(5)	1.378(3)
C(4)-H(4)	0.9400
C(5)-C(6)	1.391(3)
C(5)-H(5)	0.9400
C(6)-C(7)	1.385(2)
C(6)-H(6)	0.9400
C(7)-C(8)	1.511(2)
C(8)-C(9)	1.517(2)
C(8)-C(13)	1.530(2)
C(9)-C(10)	1.331(2)
C(9)-C(11)	1.456(2)
C(10)-O(1)	1.3440(18)
C(10)-H(10)	0.9400
C(11)-O(2)	1.202(2)
C(11)-O(3)	1.349(2)
O(3)-C(12)	1.446(2)
C(12)-H(12A)	0.9700
C(12)-H(12B)	0.9700
C(12)-H(12C)	0.9700
C(13)-C(14)	1.516(2)
C(13)-H(13A)	0.9800



C(13)-H(13B)	0.9800
C(14)-N(2)	1.472(2)
C(14)-H(14A)	0.9800
C(14)-H(14B)	0.9800
N(2)-C(16)	1.351(2)
N(2)-C(15)	1.455(2)
C(15)-H(15A)	0.9800
C(15)-H(15B)	0.9800
C(16)-O(4)	1.2212(19)
C(16)-O(5)	1.342(2)
O(5)-C(17)	1.478(2)
C(17)-C(18)	1.508(3)
C(17)-C(19)	1.509(3)
C(17)-C(20)	1.517(3)
C(18)-H(18A)	0.9700
C(18)-H(18B)	0.9700
C(18)-H(18C)	0.9700
C(19)-H(19A)	0.9700
C(19)-H(19B)	0.9700
C(19)-H(19C)	0.9700
C(20)-H(20A)	0.9700
C(20)-H(20B)	0.9700
C(20)-H(20C)	0.9700
N(1)-C(1)-O(1)	109.44(13)
N(1)-C(1)-C(15)	113.35(13)
O(1)-C(1)-C(15)	106.70(13)
N(1)-C(1)-C(8)	106.86(13)
O(1)-C(1)-C(8)	105.83(11)
C(15)-C(1)-C(8)	114.35(13)
C(2)-N(1)-C(1)	110.00(14)
C(2)-N(1)-H(1)	118.8(14)
C(1)-N(1)-H(1)	116.4(14)

C(3)-C(2)-C(7)	120.74(16)
C(3)-C(2)-N(1)	127.74(17)
C(7)-C(2)-N(1)	111.52(15)
C(2)-C(3)-C(4)	118.03(18)
C(2)-C(3)-H(3)	121.0
C(4)-C(3)-H(3)	121.0
C(5)-C(4)-C(3)	121.70(18)
C(5)-C(4)-H(4)	119.1
C(3)-C(4)-H(4)	119.1
C(4)-C(5)-C(6)	120.16(18)
C(4)-C(5)-H(5)	119.9
C(6)-C(5)-H(5)	119.9
C(7)-C(6)-C(5)	118.88(18)
C(7)-C(6)-H(6)	120.6
C(5)-C(6)-H(6)	120.6
C(6)-C(7)-C(2)	120.49(16)
C(6)-C(7)-C(8)	130.58(16)
C(2)-C(7)-C(8)	108.91(14)
C(7)-C(8)-C(9)	114.93(13)
C(7)-C(8)-C(13)	113.55(13)
C(9)-C(8)-C(13)	112.98(13)
C(7)-C(8)-C(1)	102.55(13)
C(9)-C(8)-C(1)	101.36(12)
C(13)-C(8)-C(1)	110.10(12)
C(10)-C(9)-C(11)	126.48(15)
C(10)-C(9)-C(8)	109.33(14)
C(11)-C(9)-C(8)	124.12(14)
C(9)-C(10)-O(1)	116.04(14)
C(9)-C(10)-H(10)	122.0
O(1)-C(10)-H(10)	122.0
C(10)-O(1)-C(1)	107.43(12)
O(2)-C(11)-O(3)	122.90(15)
O(2)-C(11)-C(9)	124.78(16)

O(3)-C(11)-C(9)	112.31(15)
C(11)-O(3)-C(12)	115.46(14)
O(3)-C(12)-H(12A)	109.5
O(3)-C(12)-H(12B)	109.5
H(12A)-C(12)-H(12B)	109.5
O(3)-C(12)-H(12C)	109.5
H(12A)-C(12)-H(12C)	109.5
H(12B)-C(12)-H(12C)	109.5
C(14)-C(13)-C(8)	111.74(14)
C(14)-C(13)-H(13A)	109.3
C(8)-C(13)-H(13A)	109.3
C(14)-C(13)-H(13B)	109.3
C(8)-C(13)-H(13B)	109.3
H(13A)-C(13)-H(13B)	107.9
N(2)-C(14)-C(13)	110.55(14)
N(2)-C(14)-H(14A)	109.5
C(13)-C(14)-H(14A)	109.5
N(2)-C(14)-H(14B)	109.5
C(13)-C(14)-H(14B)	109.5
H(14A)-C(14)-H(14B)	108.1
C(16)-N(2)-C(15)	118.19(13)
C(16)-N(2)-C(14)	122.00(14)
C(15)-N(2)-C(14)	118.99(13)
N(2)-C(15)-C(1)	111.15(12)
N(2)-C(15)-H(15A)	109.4
C(1)-C(15)-H(15A)	109.4
N(2)-C(15)-H(15B)	109.4
C(1)-C(15)-H(15B)	109.4
H(15A)-C(15)-H(15B)	108.0
O(4)-C(16)-O(5)	125.11(16)
O(4)-C(16)-N(2)	124.30(15)
O(5)-C(16)-N(2)	110.59(14)
C(16)-O(5)-C(17)	121.12(13)

O(5)-C(17)-C(18)	110.80(16)
O(5)-C(17)-C(19)	109.47(16)
C(18)-C(17)-C(19)	112.78(19)
O(5)-C(17)-C(20)	102.05(15)
C(18)-C(17)-C(20)	109.87(19)
C(19)-C(17)-C(20)	111.4(2)
C(17)-C(18)-H(18A)	109.5
C(17)-C(18)-H(18B)	109.5
H(18A)-C(18)-H(18B)	109.5
C(17)-C(18)-H(18C)	109.5
H(18A)-C(18)-H(18C)	109.5
H(18B)-C(18)-H(18C)	109.5
C(17)-C(19)-H(19A)	109.5
C(17)-C(19)-H(19B)	109.5
H(19A)-C(19)-H(19B)	109.5
C(17)-C(19)-H(19C)	109.5
H(19A)-C(19)-H(19C)	109.5
H(19B)-C(19)-H(19C)	109.5
C(17)-C(20)-H(20A)	109.5
C(17)-C(20)-H(20B)	109.5
H(20A)-C(20)-H(20B)	109.5
C(17)-C(20)-H(20C)	109.5
H(20A)-C(20)-H(20C)	109.5
H(20B)-C(20)-H(20C)	109.5

---

Symmetry transformations used to generate equivalent atoms:

Table 4. Anisotropic displacement parameters ( $\text{\AA}^2 \times 10^3$ ) for YJL-Interm-I. The anisotropic displacement factor exponent takes the form:  $-2\pi^2 [ h^2 a^{*2} U^{11} + \dots + 2 h k a^* b^* U^{12} ]$

	U <sup>11</sup>	U <sup>22</sup>	U <sup>33</sup>	U <sup>23</sup>	U <sup>13</sup>	U <sup>12</sup>
C(1)	36(1)	28(1)	26(1)	-5(1)	3(1)	-9(1)
N(1)	47(1)	36(1)	32(1)	-12(1)	10(1)	-18(1)
C(2)	43(1)	25(1)	31(1)	-3(1)	-2(1)	-10(1)
C(3)	60(1)	33(1)	34(1)	-7(1)	-1(1)	-16(1)
C(4)	60(1)	34(1)	45(1)	-7(1)	-14(1)	-18(1)
C(5)	46(1)	37(1)	49(1)	-3(1)	-10(1)	-16(1)
C(6)	40(1)	32(1)	38(1)	-2(1)	-2(1)	-13(1)
C(7)	37(1)	24(1)	29(1)	-1(1)	-2(1)	-8(1)
C(8)	32(1)	28(1)	27(1)	-5(1)	3(1)	-10(1)
C(9)	36(1)	27(1)	27(1)	-5(1)	3(1)	-10(1)
C(10)	38(1)	29(1)	26(1)	-3(1)	1(1)	-9(1)
O(1)	33(1)	39(1)	31(1)	-4(1)	4(1)	-8(1)
C(11)	40(1)	37(1)	31(1)	-6(1)	4(1)	-15(1)
O(2)	38(1)	77(1)	40(1)	-3(1)	8(1)	-16(1)
O(3)	44(1)	46(1)	29(1)	4(1)	4(1)	-13(1)
C(12)	59(1)	66(1)	33(1)	4(1)	11(1)	-27(1)
C(13)	36(1)	28(1)	37(1)	-6(1)	3(1)	-7(1)
C(14)	39(1)	32(1)	36(1)	-11(1)	9(1)	-11(1)
N(2)	42(1)	35(1)	30(1)	-13(1)	10(1)	-18(1)
C(15)	46(1)	33(1)	26(1)	-9(1)	8(1)	-18(1)
C(16)	44(1)	34(1)	31(1)	-12(1)	8(1)	-15(1)
O(4)	56(1)	53(1)	44(1)	-22(1)	21(1)	-32(1)
O(5)	50(1)	57(1)	47(1)	-32(1)	16(1)	-28(1)
C(17)	46(1)	56(1)	56(1)	-34(1)	10(1)	-24(1)
C(18)	51(1)	70(2)	78(2)	-38(1)	-2(1)	-18(1)
C(19)	84(2)	49(1)	89(2)	-29(1)	-4(1)	-24(1)
C(20)	78(2)	128(2)	92(2)	-86(2)	34(2)	-53(2)

---

Table 5. Hydrogen coordinates ( $\times 10^4$ ) and isotropic displacement parameters ( $\text{\AA}^2 \times 10^3$ ) for YJL-Interm-I.

	x	y	z	U(eq)
H(1)	3580(30)	2920(20)	-34(18)	49(6)
H(3)	1682	1654	-884	52
H(4)	-1071	1376	-743	56
H(5)	-2735	1807	731	55
H(6)	-1702	2581	2100	47
H(10)	4789	1002	4061	40
H(12A)	638	1386	6452	84
H(12B)	2196	-17	6997	84
H(12C)	624	56	6173	84
H(13A)	68	5147	1351	43
H(13B)	-444	4517	2618	43
H(14A)	1036	6109	2578	43
H(14B)	2050	4635	3479	43
H(15A)	4743	4362	892	41
H(15B)	2727	5092	419	41
H(18A)	6939	5555	4095	95
H(18B)	7269	6961	3940	95
H(18C)	7287	6433	2858	95
H(19A)	4842	8365	1575	107
H(19B)	4930	9158	2461	107
H(19C)	3126	9008	2120	107
H(20A)	2723	7888	4174	123
H(20B)	4455	8084	4590	123
H(20C)	4262	6604	4978	123

Table 6. Torsion angles [°] for YJL-Interm-I.

---

O(1)-C(1)-N(1)-C(2)	118.25(14)
C(15)-C(1)-N(1)-C(2)	-122.78(15)
C(8)-C(1)-N(1)-C(2)	4.10(17)
C(1)-N(1)-C(2)-C(3)	176.47(16)
C(1)-N(1)-C(2)-C(7)	-3.66(19)
C(7)-C(2)-C(3)-C(4)	0.5(2)
N(1)-C(2)-C(3)-C(4)	-179.60(16)
C(2)-C(3)-C(4)-C(5)	-0.8(3)
C(3)-C(4)-C(5)-C(6)	0.6(3)
C(4)-C(5)-C(6)-C(7)	-0.1(3)
C(5)-C(6)-C(7)-C(2)	-0.2(2)
C(5)-C(6)-C(7)-C(8)	177.97(16)
C(3)-C(2)-C(7)-C(6)	0.0(2)
N(1)-C(2)-C(7)-C(6)	-179.93(14)
C(3)-C(2)-C(7)-C(8)	-178.57(14)
N(1)-C(2)-C(7)-C(8)	1.55(18)
C(6)-C(7)-C(8)-C(9)	73.6(2)
C(2)-C(7)-C(8)-C(9)	-108.09(15)
C(6)-C(7)-C(8)-C(13)	-58.6(2)
C(2)-C(7)-C(8)-C(13)	119.68(15)
C(6)-C(7)-C(8)-C(1)	-177.39(16)
C(2)-C(7)-C(8)-C(1)	0.93(16)
N(1)-C(1)-C(8)-C(7)	-3.00(15)
O(1)-C(1)-C(8)-C(7)	-119.58(13)
C(15)-C(1)-C(8)-C(7)	123.28(14)
N(1)-C(1)-C(8)-C(9)	116.02(14)
O(1)-C(1)-C(8)-C(9)	-0.56(15)
C(15)-C(1)-C(8)-C(9)	-117.70(14)
N(1)-C(1)-C(8)-C(13)	-124.15(14)
O(1)-C(1)-C(8)-C(13)	119.27(14)
C(15)-C(1)-C(8)-C(13)	2.13(19)



C(7)-C(8)-C(9)-C(10)	109.64(16)
C(13)-C(8)-C(9)-C(10)	-117.86(16)
C(1)-C(8)-C(9)-C(10)	-0.10(17)
C(7)-C(8)-C(9)-C(11)	-73.1(2)
C(13)-C(8)-C(9)-C(11)	59.4(2)
C(1)-C(8)-C(9)-C(11)	177.19(15)
C(11)-C(9)-C(10)-O(1)	-176.37(15)
C(8)-C(9)-C(10)-O(1)	0.8(2)
C(9)-C(10)-O(1)-C(1)	-1.21(19)
N(1)-C(1)-O(1)-C(10)	-113.79(14)
C(15)-C(1)-O(1)-C(10)	123.21(14)
C(8)-C(1)-O(1)-C(10)	1.04(16)
C(10)-C(9)-C(11)-O(2)	179.56(19)
C(8)-C(9)-C(11)-O(2)	2.7(3)
C(10)-C(9)-C(11)-O(3)	0.8(2)
C(8)-C(9)-C(11)-O(3)	-176.01(14)
O(2)-C(11)-O(3)-C(12)	0.0(3)
C(9)-C(11)-O(3)-C(12)	178.83(16)
C(7)-C(8)-C(13)-C(14)	-167.11(13)
C(9)-C(8)-C(13)-C(14)	59.72(18)
C(1)-C(8)-C(13)-C(14)	-52.79(17)
C(8)-C(13)-C(14)-N(2)	54.21(18)
C(13)-C(14)-N(2)-C(16)	166.70(15)
C(13)-C(14)-N(2)-C(15)	-2.7(2)
C(16)-N(2)-C(15)-C(1)	142.69(15)
C(14)-N(2)-C(15)-C(1)	-47.5(2)
N(1)-C(1)-C(15)-N(2)	169.24(14)
O(1)-C(1)-C(15)-N(2)	-70.23(16)
C(8)-C(1)-C(15)-N(2)	46.40(19)
C(15)-N(2)-C(16)-O(4)	-1.3(3)
C(14)-N(2)-C(16)-O(4)	-170.79(16)
C(15)-N(2)-C(16)-O(5)	179.08(14)
C(14)-N(2)-C(16)-O(5)	9.6(2)

O(4)-C(16)-O(5)-C(17)	3.3(3)
N(2)-C(16)-O(5)-C(17)	-177.13(15)
C(16)-O(5)-C(17)-C(18)	-58.5(2)
C(16)-O(5)-C(17)-C(19)	66.5(2)
C(16)-O(5)-C(17)-C(20)	-175.44(18)

---

Symmetry transformations used to generate equivalent atoms:

Table 7. Hydrogen bonds for YJL-Interm-I [ $\text{\AA}$  and  $^\circ$ ].

D-H...A	d(D-H)	d(H...A)	d(D...A)	$\angle(\text{DHA})$
N(1)-H(1)...O(4)#1	0.85(2)	2.12(2)	2.9590(19)	172.7(19)

Symmetry transformations used to generate equivalent atoms:

#1  $-x+1, -y+1, -z$

## Reference

- (1) Guan, H.; Tung, C.-H.; Liu, L., Methane Monooxygenase Mimic Asymmetric Oxidation: Self-Assembling  $\mu$ -Hydroxo, Carboxylate-Bridged Diiron(III)-Catalyzed Enantioselective Dehydrogenation. *J. Am. Chem. Soc.* **2022**, *144*, 5976.
- (2). Yamada, F.; Kawanishi, A.; Tomita, A.; Somei, M., The First Preparation of the Unstable 1-Hydroxy-2, 3-dimethylindole. *Arkivoc* **2003**, *8*, 102.

## **Chapter 2.**

### **C3-Hetero-functionalization of Indole Scaffolds via Facilitated Indolyl 1,3-Heteroatom Transposition Reaction**

## 2.1. C3-Hetero-functionalization of Indole Scaffolds

Among many other pharmaceutically interesting molecules, indole can be described as one of the most fascinating scaffolds which are closely related to various medicinal properties.<sup>1</sup> Embedded in numerous natural products, the ubiquity of the indole motif ranges from headache pills to anti-cancer reagents, such as vinca alkaloids.

The importance of indole scaffold is not limited to the structure of indole itself. Indolenine and indoline, the representative examples of the indole dearomatization, can provide the direct access to essential framework of various natural alkaloids. Amid a myriad of indole-derived compounds, C3-hetero-functionalized indole derivatives, regardless of their form of indole (**A**), indolenine (**B**), or indoline (**C**) are the privileged structures constituting the basic frameworks many medicines and natural products (Figure 2.1).<sup>2</sup>

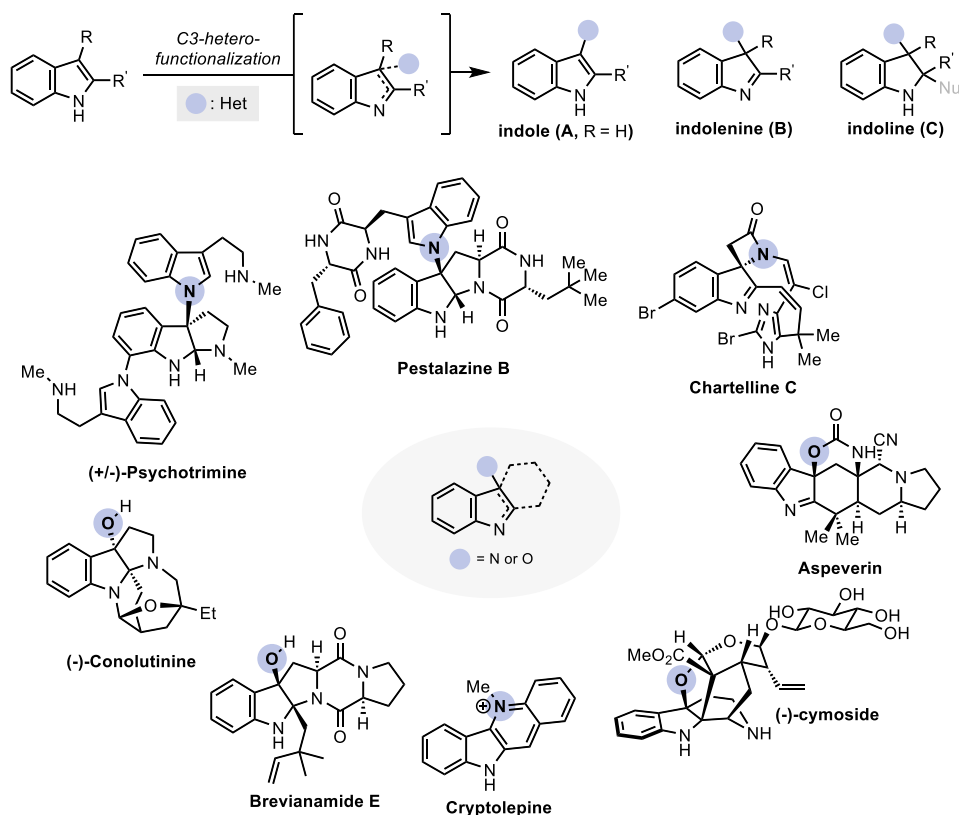


**Figure 2.1.** C3-Hetero-functionalization of indole: structural diversity and representative examples of C3-hetero-functionalized indole derivatives.

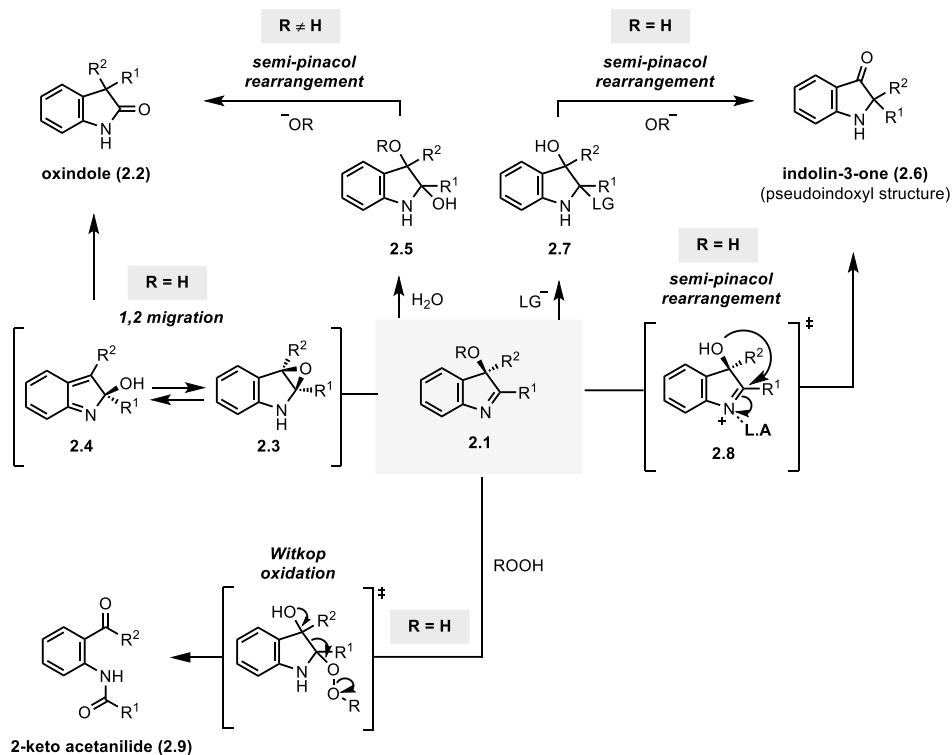


**Figure 2.2.** C3-hydroxylation of indole

A classic example of the exquisite flexibility of C3-hetero-functionalized indole derivatives towards other important backbone structures is the C3-hydroxylated indole (Figure 2.2). The C3-hydroxylation of indole has attracted considerable attention of researchers because the C3-hydroxylation of indole is closely related to the biosynthetic pathway of a few classes of indole-derived natural products. C3-hydroxyindolenine **2.1**, the primary structure derived from C3-hydroxylation, can access to a oxindole **2.2** directly via two very similar yet distinctive pathways: 1) 1,2 Migration of hydroxyl group to 2-position to access intermediate **2.3** or **2.4** and subsequent isomerization or 2) semi-pinacol rearrangement of 2,3-dialkoxyindoline **2.5** after the addition of H<sub>2</sub>O in imine group. A pseudoindoxyl **2.6** is another structure that can be approached from indolenine **2.1**, via semi-pinacol rearrangement of either indoline **2.7** or Lewis acid-activated indolenine **2.8**. Witkop–Winterfeldt-type oxidation of C3-hydroxyindolenine **2.1** provides 2-keto acetanilide **2.9**, which is well-known structure to access other valuable backbone structure such as pyrroloquinolones.

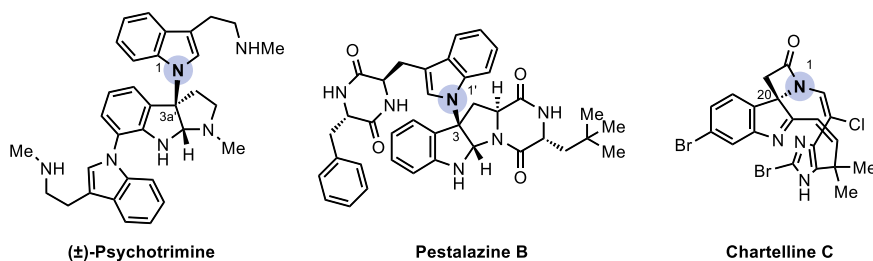


**Figure 2.3.** Representative examples of indole alkaloids with C–N bond positioned in C3.

C3-aminated indole also accounts for a substantial proportion of the field of indole functionalization. Although not as versatile as C3-hydroxylated indole derivatives, C3-aminated indole derivatives are also very closely related to certain classes of natural products (Figure 2.3). For instance, psychotrimine, one of the polypyrroloindoline natural products which comprises 3 repeated sequences of pyrroloindoline units, contains a very characteristic N1-C3a' bond connection. Same N1'–C3 linkage appears in pestalazine B, representative example of dimeric diketopiperazine alkaloids, wherein two tryptamine-derived subunits are adjoining by this N1'–C3 bridge. Chartelline C which is the first example of natural products containing the hallmark indolenine- $\beta$ -lactam structure, also possess distinctive C–N bond in 3-position. Given these numerous examples, the preparation of the C3-hetero-functionalized indole derivatives via dearomatization strategies have been an important subject of investigation.



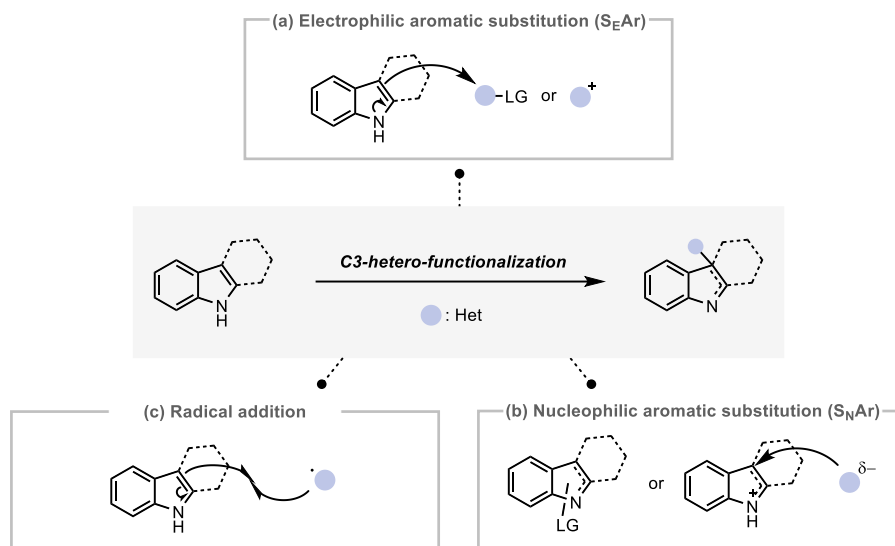


**Figure 2.4.** Previous synthetic approaches.

As summarized in Figure 2.4, C3-functionalization of indole can be classified into three general approaches: (1) electrophilic substitution of indole derivatives, which utilizes the intrinsic nucleophilicity of indole with the electrophilic source of heteroatom (Figure 2.4, Approach (a)), (2) nucleophilic substitution of indole derivatives via the umpolung reactivity of indole under oxidative conditions so as to employ the nucleophilic reagents as a source of heteroatoms (Figure 2.4, Approach (b)) and (3) regioselective radical addition to indole 2,3  $\pi$  bond (Figure 2.4, Approach (c)).

All of these approaches have been studied extensively and each has been greatly devoted to the fundamental understanding of the nature of indole scaffolds. The electrophilic substitution approach permits direct access to C3-functionalized indole derivatives without the need of modification of indole substrates. The umpolung strategy, on the other hand, can provide the unified protocol of C3-functionalization of indole which various nucleophiles can be applied in a single method. The radical-based approach can not only aim for high regioselectivity, but also induce complete conversion of site-selectivity by delicately adjusting the properties of indole and radical coupling partners. In addition, an indole-radical intermediate obtained by radical addition can be used as an intermediate for further di-functionalization.

In this dissertation, historical findings, representative examples and recently developed methodologies for the C3-functionalization of indoles were enlisted to introduce the various tools used in this field, *i.e.*, stoichiometric reagents and photochemical, electrochemical instruments, and to emphasize the importance of reaction design and mechanistic insights. Many remarkable achievements have been made in this field related to the introduction of heteroatoms at the 3-position of indole. However, particular emphasis will be on the C–O bond and C–N bond formation and other variants of C3-hetero-functionalization of indole were not covered in this thesis.

### 2.1.1. Electrophilic Substitution of Indole Derivatives

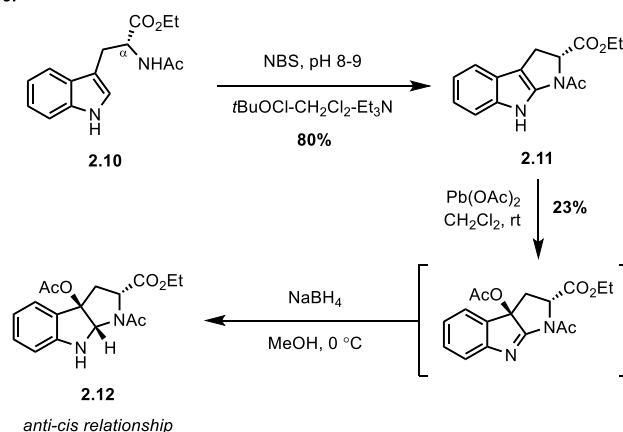
Without doubt, electrophilic substitution of indole is one of the most exemplified reactions in the field of indole functionalization. The use of electrophilic heteroatom sources for indole C3-functionalization has a long history in the field of indole chemistry, and still remains as one of the most widely used approaches to synthesize C3-hetero-functionalized indole derivatives.

#### 2.1.1.1. C3-Oxygenation of Indole derivatives

Considering the large section of natural products bearing an oxygen atom at the 3-position of indole-derived substructures, C3-hydroxylation of indole is closely related to the total syntheses and pharmaceutical/material examination with natural product-related architecture. Electrophilic approaches have been widely used especially for such syntheses in that no prior modification of indole scaffold is required for the desired transformation. As evidence of the above assertion, there are many cases in which electrophilic oxidation has been attempted to achieve C3-oxidation on complex natural products from past to present. By providing the relatively recent examples of such application in natural product syntheses, the versatility and practicality of the dearomatization strategy promoted by electrophilic oxygen atom can be verified.

**Scheme 2.1.** Synthesis of 3a-acyloxy-pyrroloindoline via lead acetate oxidation. (Witkop and co-workers, 1968)

*Witkop et al., 1968:*

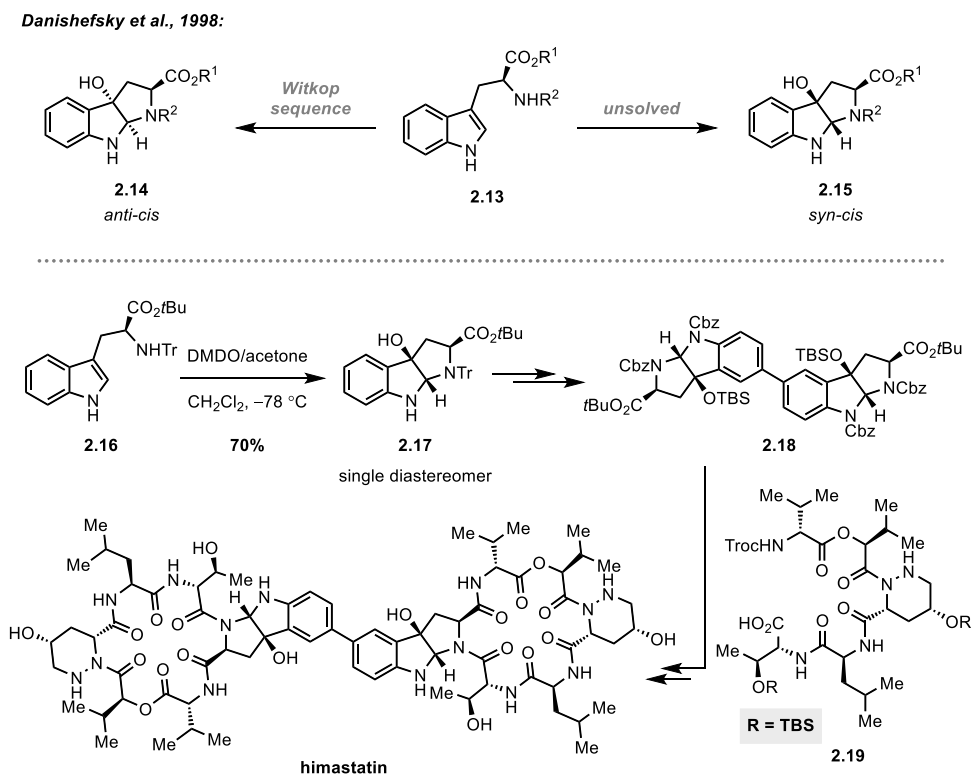


In the early report of introducing oxygen atom to the 3-position of indole via electrophilic

substitution, Witkop and co-workers accomplished the synthesis of 3a-acyloxy-pyrroloindoline structure from protected tryptophan **2.10** (Scheme 2.1).<sup>3</sup> Oxidative cyclization via *in situ* generation of bromonium species followed by elimination afforded cyclized tryptophan **2.11**. Treatment of  $\text{Pb}(\text{OAc})_2$  successfully introduces the acetyl group at the 3-position and subsequent reduction of imine yielded pyrroloindoline **2.12** with an *anti-cis* relationship. This stepwise elimination-addition sequence led to high stereo-selectivity in an *anti-cis* manner.

The pioneering discovery made by Witkop showed the possibility of diastereoselective cyclization induced by the embedded stereocenter in tryptophan. Inspired by the work of Witkop, Danishefsky and co-workers achieved the stereoselective access to pyrrolo[2,3-b]indolines in both the *anti-cis* (**2.14**) and *syn-cis* (**2.15**) manner en route to the total synthesis of himastatin (Scheme 2.2).<sup>4</sup>

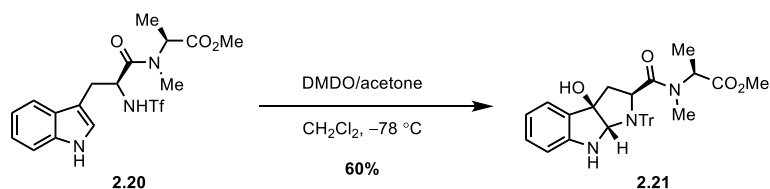
**Scheme 2.2.** C3-hydroxylation of tryptophan derivatives using DMDO as an electrophilic oxygen source (Danishefsky and co-workers, 1998)



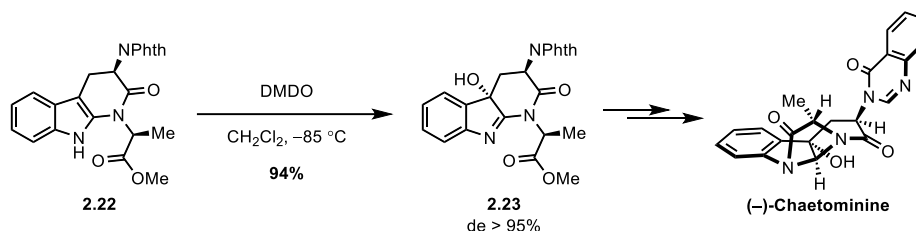
The key to solving a synthetic problem with himastatin lied in the achievement of stereospecific access to *syn-cis*-pyrrolo[2,3-*b*]indoline framework. Tryptophan **2.16** with appropriate setting of protecting group was found to be essential for the desired transformation to be happened in the high yield. After extensive screening, the tryptophan congener with *tert*-butyl ester and trityl protection at the aliphatic amine, was able to undergo oxidative cyclization in a highly diastereoselective manner. Pyrroloindoline **2.17** was then dimerized to give **2.18**, and coupling of **2.18** with two units of **2.19** under carefully controlled conditions eventually gave rise to himastatin.

**Scheme 2.3.** Diastereoselective C3-hydroxylation using DMDO as electrophilic oxygen source (Patrick, Perrin and co-workers, 2005 / Evano and co-workers, 2008)

Patrick and Perrin et al., 2005:



Evano et al., 2008:

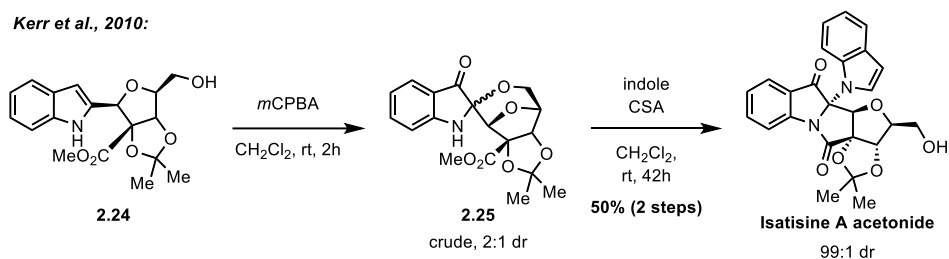


The valuable work of Danishefsky and Witkop demonstrated that the chiral information of  $\text{C}_\alpha$  position of tryptophan can be transferred and involved in determining the chirality of other adjacent parts. Various examples of related diastereoselective C3-hydroxylation have been actively used in the similar system. In 2005, Perrin and co-workers also followed the precedent of Danishefsky for the synthesis of 3a-hydroxypyrrolo[2,3-*b*]indoline dipeptide methyl esters **2.21** (Scheme 2.3).<sup>5</sup> Similar C3-hydroxylation strategy was harnessed using DMDO and demonstrated efficient elaboration to the corresponding pyrroloindolines. Another representative example is the synthesis of **(-)-chaetominin** reported in 2005 by the Evano group.<sup>6</sup> The main features of the synthesis include the diastereoselective C3-hydroxylation of indole **2.22** to furnish indolenine **2.23** whose high level of

diastereoselectivity was most likely induced by steric interactions between phthalimide moiety in **2.22** and DMDO.

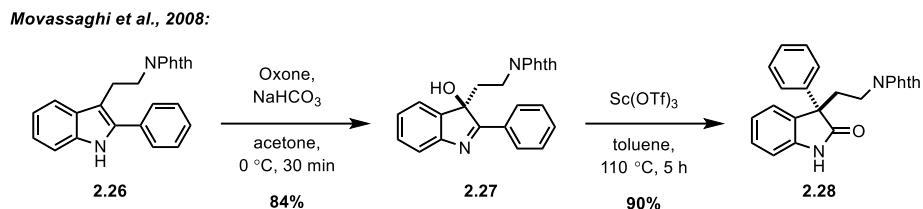
The Kerr group reported the enantiospecific total synthesis of (+)-Isatisine A in 2010 utilizing the intrinsic nucleophilicity of the indole motif (Scheme 2.4).<sup>7</sup> The unique indolin-3-one structure was constructed by double oxidation of the **2.24** using *m*CPBA as the electrophilic oxygen reagent, followed by the nucleophilic addition of the internal hydroxyl group to 2-position.<sup>8</sup> A 2:1 diastereomeric mixture of the aminal **2.25** was used directly for the next step and indole could be successfully installed in 2-position under the proton-mediated equilibrium of aminal and *N*-acyliminium ion. The high diastereoselectivity of obtained Isatisine A acetone results from the chiral resolution occurred during the process of the reversible indole addition.

**Scheme 2.4.** Total synthesis of (+)-Isatisine A and indole oxidation utilizing *m*CPBA as an electrophilic oxygen source (Kerr and co-workers, 2010)

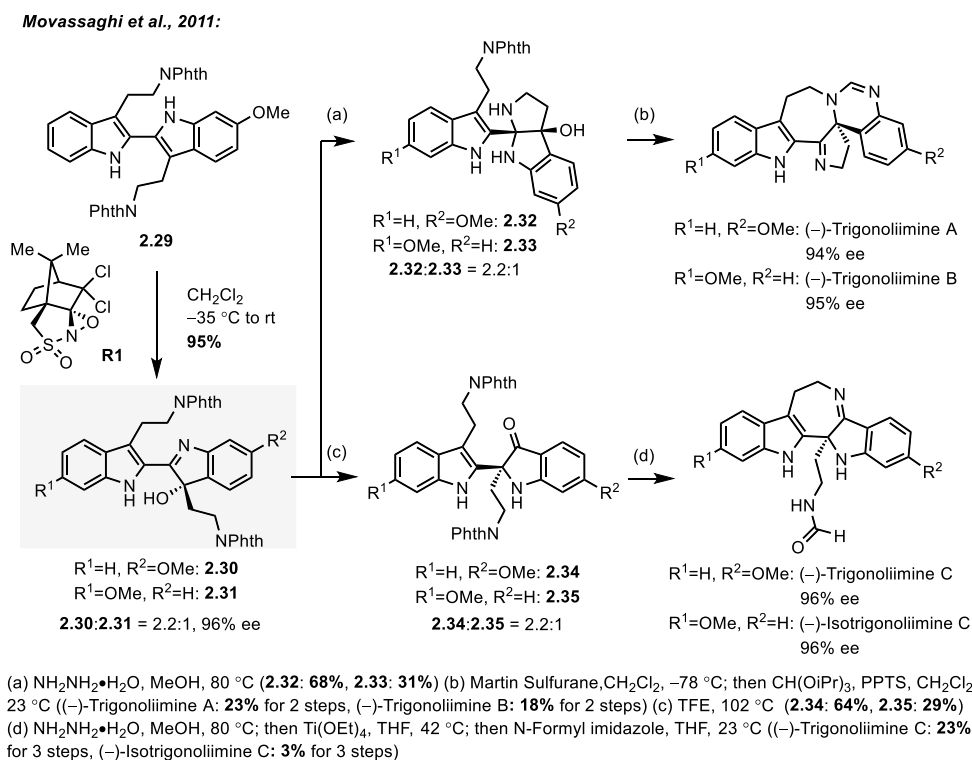


The Movassaghi group has been dedicated to the development of elegant indole dearomatization reactions assisted by various electrophilic oxygen sources for total syntheses of related natural products. In 2008, Movassaghi and co-workers investigated the efficient formation of oxindole with a quaternary center via stereoselective 1,2 migration with the aim of the stereoselective synthesis of hexahydropyrroloindole alkaloids (Scheme 2.5).<sup>9</sup> 2-Phenyl-3-hydroxyindolenine **2.27** was chosen as a substrate, which is accessible from tryptamine **2.26**. The essence of this method lies in the discovery of the optimal Lewis acid catalyst which selectively converts **2.27** to oxindole **2.28** while avoiding the semi-pinacol rearrangement leading to a pseudoindoxyl structure. After extensive screening of acids, scandium trifluoromethanesulfonate proved most favorable, leading to the exclusive formation of **2.28**.

**Scheme 2.5.** C3-Hydroxylation and stereoselective oxidative rearrangement of 2-aryl tryptamine derivatives (Movassaghi and co-workers, 2008)



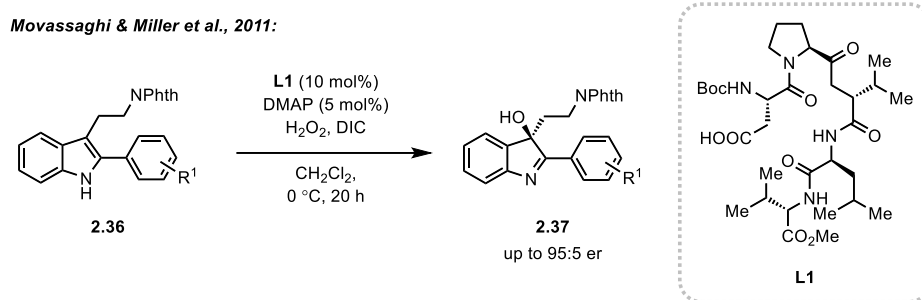
**Scheme 2.6.** Total syntheses of trigonoliimine A, B and C (Movassaghi and co-workers, 2011)



In 2011, a streamlined syntheses of trigonoliimine A, B and C were reported by Movassaghi and co-workers (Scheme 2.6).<sup>10</sup> The bis-tryptamine heterodimer **2.29** was selected as an starting point for the synthesis of these unique dimeric natural products, and hydroxyindolenine **2.30** and **2.31** was obtained through desymmetrization via chemoselective oxidation of bis-tryptamine **2.29**. An exception level of enantioselectivity for both isomers was achieved using (+)-((8,8-dichlorocamphoryl)sulfonyl)oxaziridine (Davis' oxaziridine, **R1**) for chemoselective C3-hydroxylation. Given the characteristics of hydroxyindolenine

capable of transforming into various structures, hydroxyindolenine **2.30** and **2.31** were contributed as a branching point, completing two distinct core structures that goes to different natural products, *i.e.*, (–)-Trigonoliimine A, B and (–)-Trigonoliimine C, (–)-Isotrigonoliimine C, respectively. Advancement of hydroxyindolenine **2.30** and **2.31** via intramolecular imine cyclization provided pyrroloindoline **2.32** and **2.33**, which went to (–)-Trigonoliimine A and B whereas 1,2-migration of **2.30** and **2.31** constructed pseudoindoxyl core in **2.34** and **2.35** for (–)-Trigonoliimine C and (–)-Isotrigonoliimine C.

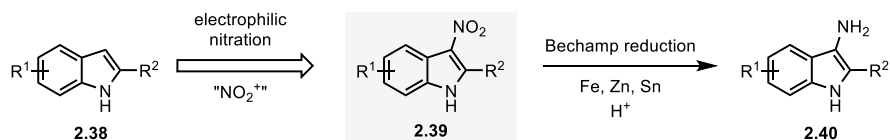
**Scheme 2.7.** Enantioselective C3-hydroxylation of tryptamine with peptide-based catalysis (Movassaghi, Miller and co-workers, 2011)



In the same year, an elegant organocatalytic asymmetric C3-hydroxylation of tryptamine congeners was introduced by Movassaghi and Miller, utilizing the novel aspartyl peptide-based catalyst (Scheme 2.7).<sup>11</sup> The transient generation of chiral peracids in a peptide-based catalytic system **L1** enables asymmetric epoxidation of tryptamine derivative **2.36** to indolenine **2.37** with a rare level of efficiency.

### 2.1.1.2. C3-Amination of Indole derivatives

**Scheme 2.8.** 3-nitroindole as a handle for the 3-aminoindole.

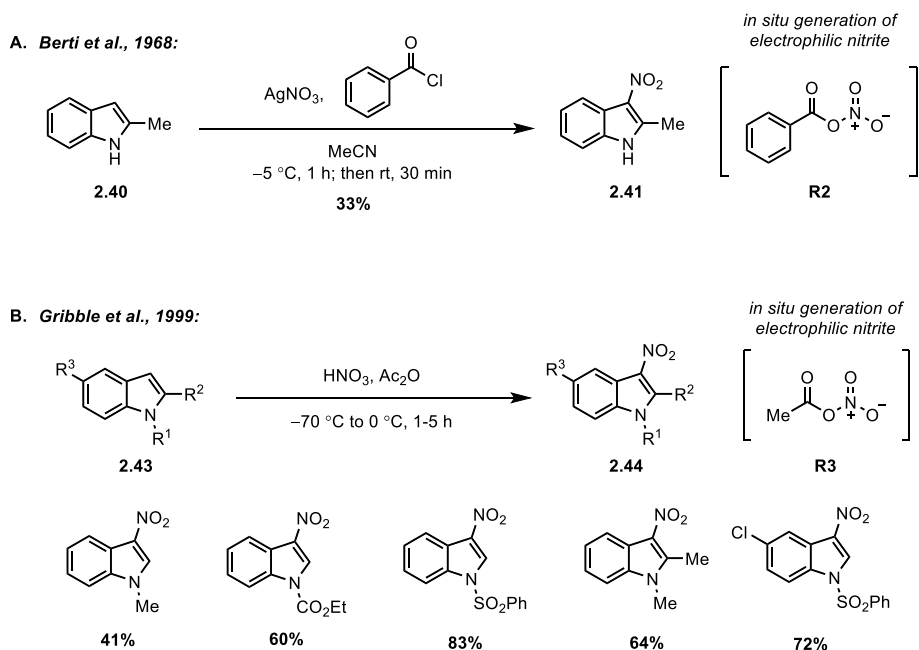


The electrophilic C3-amination of indole has mainly been achieved using two general approaches: (1) Utilizing an electrophilic amine reagent and (2) Formation of electrophilic



nitrene under a transition metal catalyst. The primary aim of the research in the former approach has been to develop a source of electrophilic amines that can be used with ease and efficiency. The early example of electrophilic amine source used for C–N bond formation in 3-position of indole was nitrate (Scheme 2.8). One of the negatively charged oxygens in the nitrate can be functionalized to become a labile leaving group, so that the nitrate can act as an electrophile to which the indole **2.38** initiates a nucleophilic attack and successfully garners the nitrite at the 3-position. Since 3-nitroindole **2.39** can be easily transformed into the corresponding 3-aminoindole **2.40** under acidic conditions with a reducing metal such as Fe or Zn, it can serve as a handle that connects to C3-functionalized indole with various nitrogen-related functional groups.

**Scheme 2.9.** Pioneering examples using electrophilic nitrogen oxide as amine source in indole C3-functionalization (Berti and co-workers, 1968) and application of nitrite activation mode (Gribble and co-workers, 1999)



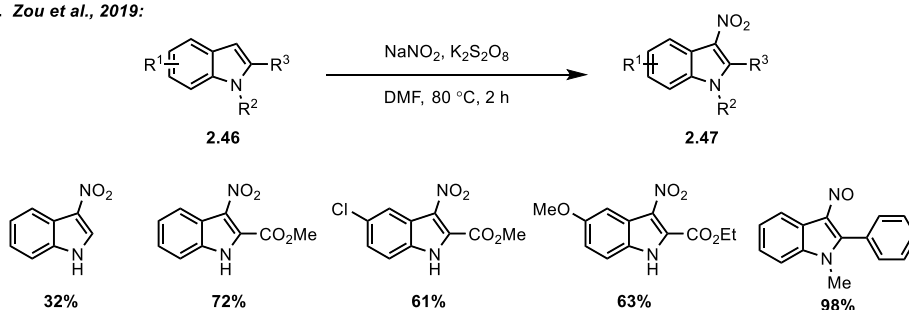
The synthetic utility of electrophilic nitrite for the C3-functionalization of the indole is first validated by Berti in 1968 (Scheme 2.9A).<sup>12</sup> In the reaction system, the transiently formed electrophilic nitrite **R2** with the benzoyl group as a leaving group participated to transform 2-methylindole **2.40** to 3-nitroindole **2.41**. Since then, plentiful follow-on studies have

utilized aforementioned activation mode with the *in situ* generation of reactive nitrite electrophile. One of the representative examples is the C3-nitration of indole reported by Gribble in 1999 (Scheme 2.9B).<sup>13</sup>

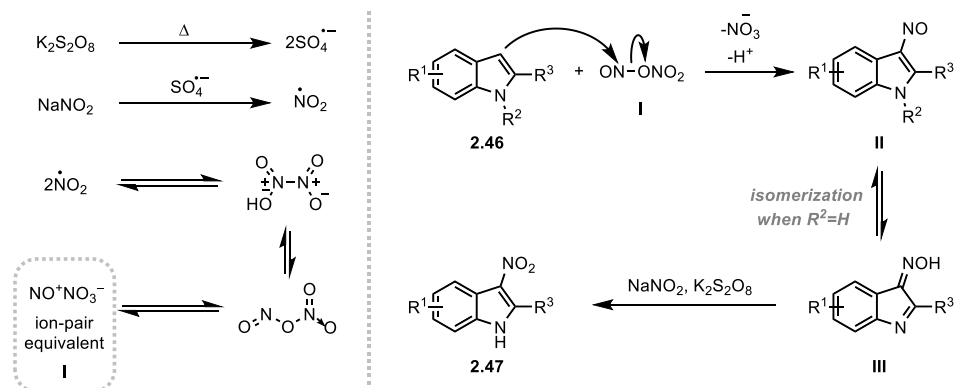
In addition to the method of using nitrate as a tool to access towards activated nitrite by combination between nitrate and potential leaving group, the other method of using nitrate as an electrophilic amine source has been addressed.

**Scheme 2.10.** Alternative approach to utilize the nitrate as potential electrophilic amine source (Zou and co-workers, 2019).

**A. Zou et al., 2019:**



**B.**

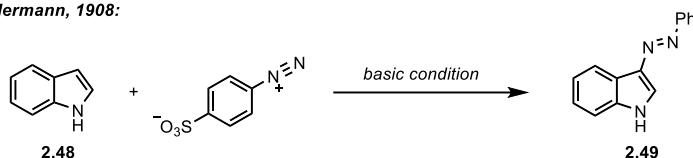


In 2019, Zou and co-workers reported C3-nitration of indole under the conditions of using  $\text{NaNO}_2$  and  $\text{K}_2\text{S}_2\text{O}_8$  (Scheme 2.10A).<sup>14</sup> Despite the involvement of the  $\text{NO}_2$  radical during the reaction, the possibility of radical addition to indole 2,3- $\pi$  bond was ruled out due to the fact that 1) the initial formation of oxime intermediates in the reactions was observed, and 2) the generation of 3-nitrosoindole instead of 3-nitroindole was observed in a few indole substrates with appropriate setting. The proposed mechanism suggested that the electrophilic

NO ion pair **I**, dimeric form of the NO<sub>2</sub> radical, undergoes electrophilic addition to the indole **2.46** (Scheme 2.10B). It can be interpreted that nitroso compound **II** is obtained by the nucleophilic attack of the indole (at the electron-rich 3-position) to NO ion pair, while 3-nitroindole **2.47** is obtained by isomerization of **II** to oxime **III** and further oxidation of oxime **III** when the indole is unprotected.

**Scheme 2.11.** The early example of C3-diazenylation of indole (Pauly and Gundermann, 1908)

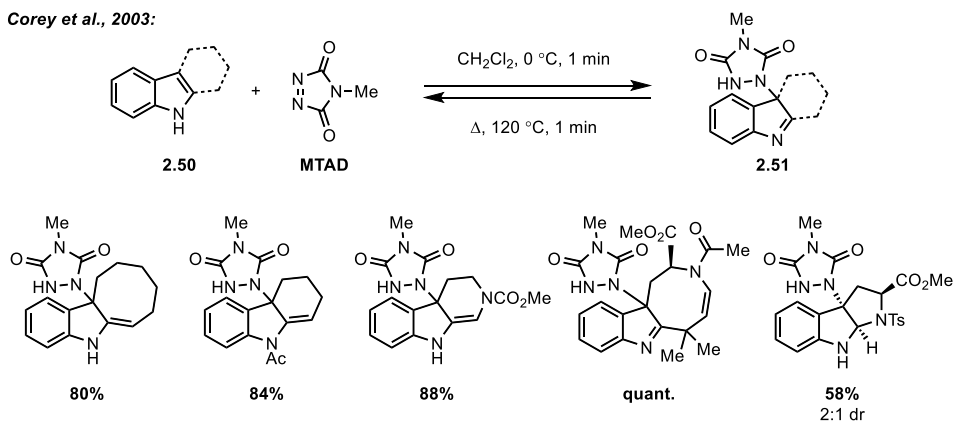
*Pauly & Gundermann, 1908:*



Successful employment of reagents containing nitrogen-nitrogen multiple bonds, such as diazene (R–N=N–R) or azide (N=N=N), has expanded the region of C3-amination of indole derivatives (Scheme 2.11). The first report of a reaction between a diazonium salt and indole should be dated back to 1886.<sup>15</sup> The solid verification of Fischer's observation that reaction occurs preferentially at the indole 3-position was later confirmed by Pauly and Gundermann after an array of experiments with various indole substrates **2.48** and diazobenzenesulfonic acid (Scheme 2.11).<sup>16</sup>

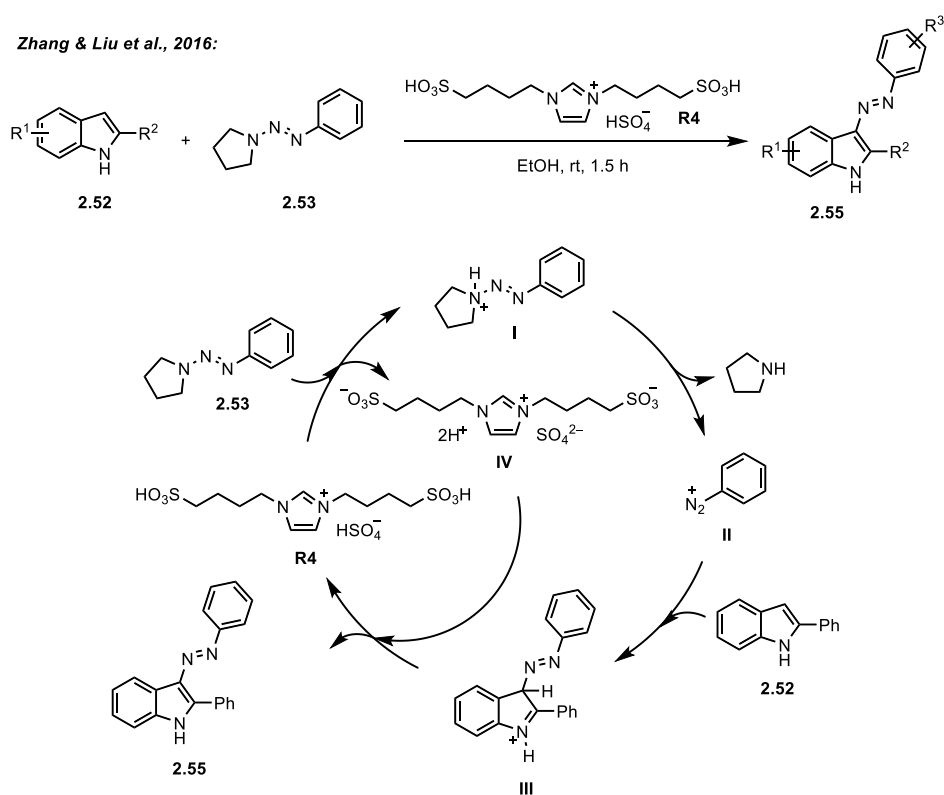
**Scheme 2.12.** Protection–Deprotection method of the Indole 2,3- $\pi$  Bond via ene reaction (Corey and co-workers, 2003)

*Corey et al., 2003:*



The exploitation of the diazonium salt in the functionalization of the indole scaffold has continued up to date. In 2003, Corey reports an effective method to mask the indole 2,3- $\pi$  bond with triazoline by selectively introducing C–N bond in 3-position of indole (Scheme 2.12).<sup>17</sup> By utilizing 4-methyl-1,2,4-triazoline-3,5-dione (MTAD) as an electrophile, MTAD was effectively attached to the 3-position of indole **2.50** by regioselective ene reaction, delivering the protected indolenine **2.51** with ease. The attached MTAD can be removed under thermal conditions and the corresponding double bond can be regenerated.

**Scheme 2.13.** Ionic liquid-promoted C3-diazenylation of 2-substituted indole (Zhang, Liu and co-workers, 2016)



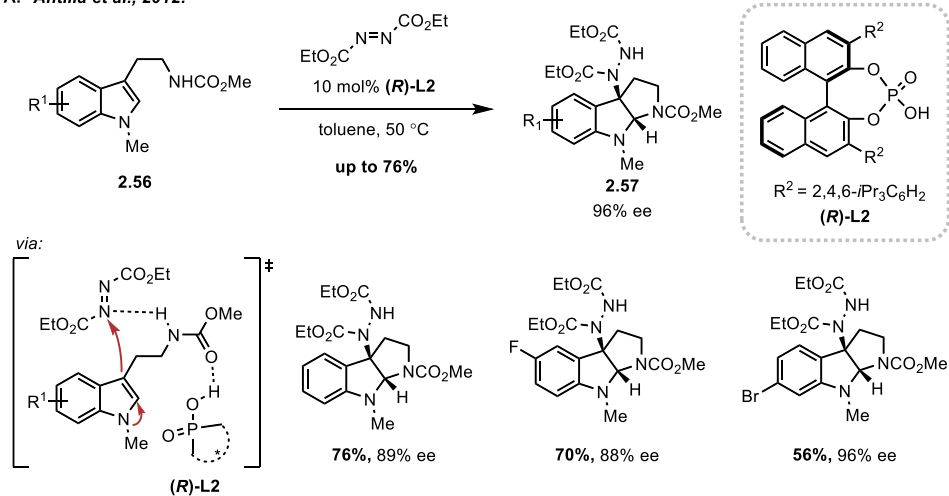
Zhang and Liu described a Brønsted acidic ionic liquid-promoted diazenylation of indole derivatives with triazene (Scheme 2.13).<sup>18</sup> In this reaction, aryltriazenes **2.53** was used as a precursor to form transient diazonium species **II**, by effective releasing of pyrrolidine under the aid of ionic liquid **R4**. The electrophilic addition of indole **2.52** to the diazonium species **II** would result the formation of intermediate **III**, which simultaneously aromatized to

product **2.55**. The ionic liquid **R4** served as a shuttle for the effective circulation of protons, and contributed to deprotonation and aromatization of intermediate **III** as a deprotonated form, **IV**.

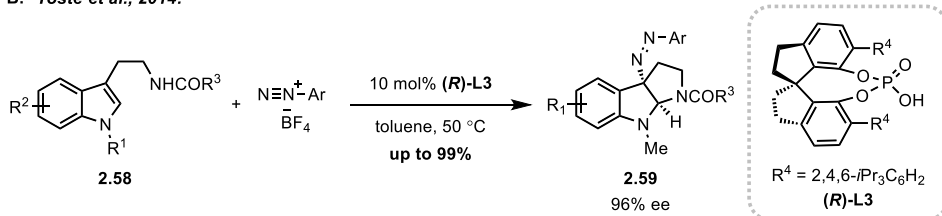
Since it was revealed that chiral phosphoric acid can deliver an outstanding level of enantioselectivity in asymmetric reaction of indole derivatives<sup>19</sup>, numerous asymmetric dearomatization strategies of indole derivatives began to utilize chiral phosphoric acid catalysis.

**Scheme 2.14.** Enantioselective construction of pyrroloindolines catalyzed by chiral phosphoric acids (Antilla and co-workers, 2012 / Toste and coworker, 2014)

**A. Antilla et al., 2012:**



**B. Toste et al., 2014:**

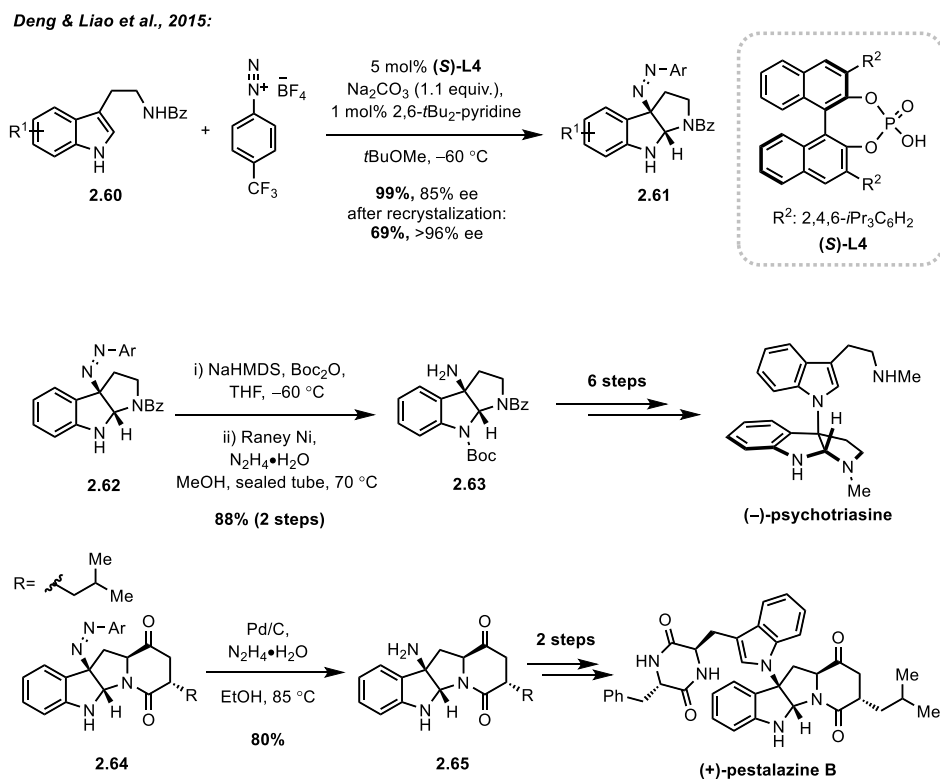


The first successful example of application of such catalysis in the C3-hetero-functionalization of indole is the chiral phosphoric acid-catalyzed enantioselective construction of pyrroloindolines via C3-amination of tryptamine reported by Antilla in 2012 (Scheme 2.14A).<sup>20</sup> Diethyl azodicarboxylate (DEAD) was selected as a suitable electrophile and various functionalized C3-hydrazinated pyrroloindolines were obtained with high

enantioselectivity by aid of BINOL-derived chiral phosphoric acid. Extensive NMR experiments clarified that the hydrogen bonding between tryptamine and chiral phosphoric acid and between the coupling partner and tryptamine is the key for the exclusive chirality transfer.

Similar organocatalytic strategy was undertaken by the Toste group as a part of their longstanding interest in phase transfer catalysis, to construct C3-diazenated pyrroloindolines in the presence of chiral phosphoric acid (Scheme 2.14B).<sup>21</sup> Instead of azodicarboxylate used in Antilla's work, diazonium salt was used as the electrophilic nitrogen source.

**Scheme 2.15.** Chiral phosphoric acid-catalyzed diazenylation (Deng, Liao and co-workers, 2015).



The activation mode utilized by Deng and Liao in 2015 is also similar to the previously introduced chiral acid-catalyzed C–N bond formation (Scheme 2.15).<sup>22</sup> This newly reported method has fundamental similarity with Toste's work in terms of the activation method, the substrate used (**2.60**), diazonium species, catalyst (**L4**), and resulted product (**2.61**). The particular specialty of this work is that the present work demonstrated the versatility and

practicality of organo-catalyzed dearomatization by disclosing the total synthesis of psychotriasine and (+)-pestalazine B with this protocol. The group envisioned that the stereoselective diazenylation-cyclization cascade reactions could be employed a unified strategy for the total synthesis of indole alkaloids with the novel C3–N1 linkage, and presented the efficient construction of the core structures by ion-pairing induction or via diastereoselective diazenylation of tryptophan derivatives. The resulted diazanyl groups in **2.62** and **2.64** were successfully reduced to naked primary amines in **2.63** and **2.65**, respectively, which permitted the facile connection with other subunit to complete the total syntheses of (-)-psychotriasine and (+)-pestalazine B.

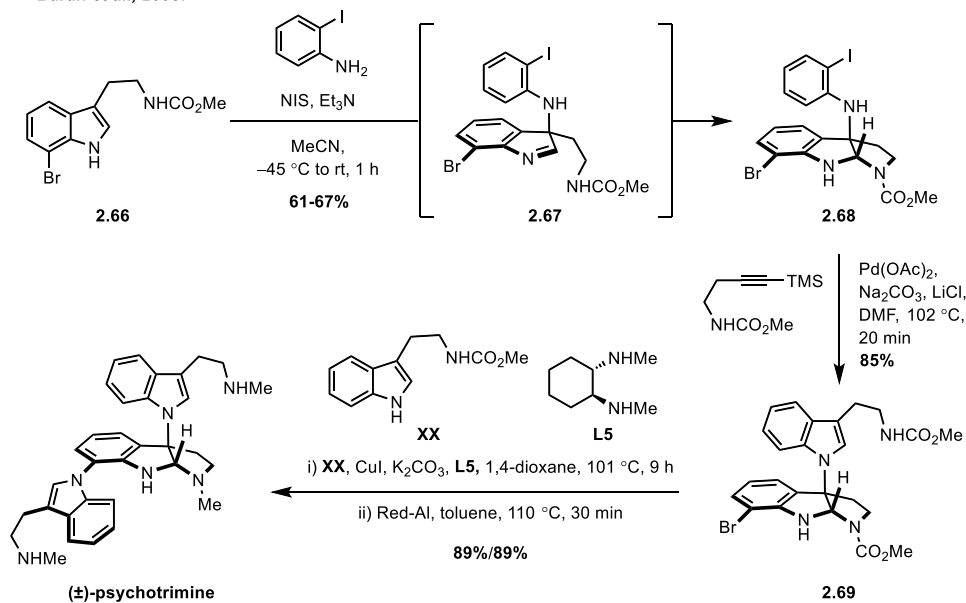
The method of taking advantage of the intrinsic electrophilicity inherent in the diazonium salt or triazoline is an inventive method of delivering nitrogen atom to the indole. However, additional synthetic steps must be followed in order to transform the attached diazanyl or hydrazide group to amine. On the other hand, the umpolung strategy of inverting the electronics of amines made the direct amination of indole derivatives possible. One of the commonly used reagents is *N*-hydroxylamine, in which a hydroxyl group can be modified to the suitable leaving group. In addition, an approach to render unstable *N*-haloamine *in situ* has also been explored.

In 2008, the Baran group utilized the novel electrophilic amination strategy for the total synthesis of psychotrimine (Scheme 2.16A).<sup>23</sup> While investigating a method to achieve a direct connection of N1 and C3 of two independent indole subunits in psychotrimine, it was found that 2-iodoaniline and tryptamine derivatives **2.66** can exhibit highly chemoselective coupling in the presence of stoichiometric amounts of NIS, furnishing C3-N-functionalized pyrroloindoline **2.68**. Using this reaction as a key transformation, total synthesis of psychotrimine with an overall yield of over 40% was achieved in 4 steps from readily available **2.66**. Later in 2010, an additional article elucidating the mechanism of NIS-mediated indole-aniline coupling through an in-depth mechanistic investigation was published (Scheme 2.16B).<sup>24</sup> As a result of comparing the aspect of the reaction with various *N*-halosuccinimides, it is suggested that the oxidation of aniline occurs instead of halogenation of indole, and the desired pyrroloindoline is formed by the electrophilic addition of a transient *N*-haloaniline species to the indole via reversible formation of intermediate **2.71**

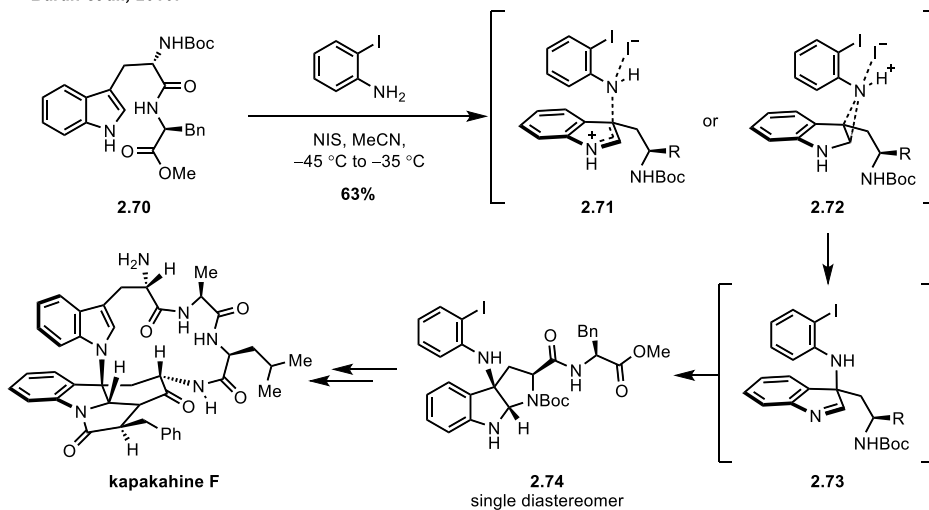
or **2.72**. Further synthetic utility of the NIS-mediated oxidative coupling has been showcased by the multi-gram scale synthesis of three different indole alkaloids: psychotrimine, kapakahines F and B.

**Scheme 2.16.** Total synthesis of psychotrimine (Baran and co-workers, 2008 and 2010).

**A. Baran et al., 2008:**



**B. Baran et al., 2010:**



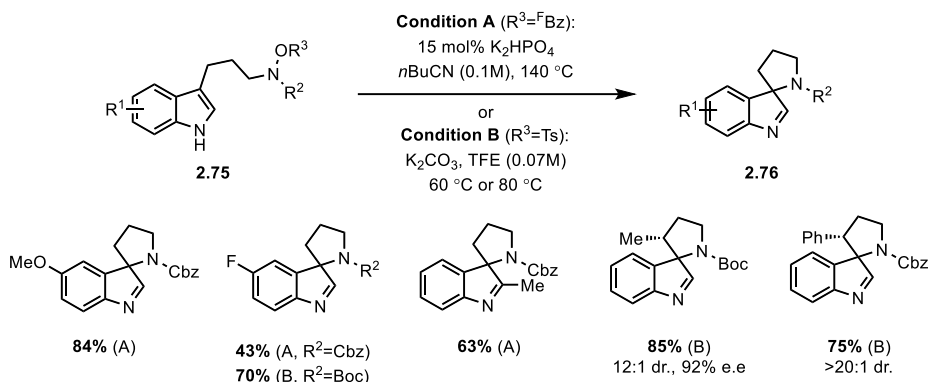
In 2017, the Bower group developed an intramolecular cyclization of elongated tryptamine



derivatives **2.75** to access spiro-indolenines **2.76** by the modification of the tethered *N*-hydroxylamine (Scheme 2.17).<sup>25</sup> This dearomatization protocol activates the weak N–O bond of *N*-hydroxylamine through the electronic manipulation, thereby utilizing protected *N*-hydroxyamine as a useful nitrenium equivalent while blocking the possibility of competing oxidation in the electron-rich indole moiety.

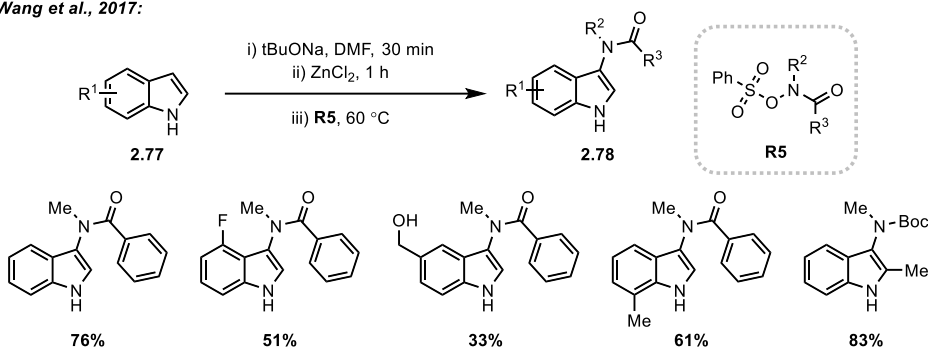
**Scheme 2.17.** Spiroindolenine synthesis via nucleophilic substitution of indole (Bower and co-workers, 2017).

*Bower et al., 2017:*



**Scheme 2.18.** Electrophilic C3-amination enabled by electrophilic nitrogen reagent (Wang and co-workers, 2017)

*Wang et al., 2017:*



In the same year, a stable electrophilic nitrogen reagent for intermolecular C3-amidation of indole was introduced by the Wang group (Scheme 2.18).<sup>26</sup> The conversion of *N*-hydroxyamide into an effective electrophilic nitrogen reagent, *i.e.*, *N*-[(arylsulfonyl)oxy]-substituted amides **R5**, was made possible by attaching a benzenesulfonyl group to the

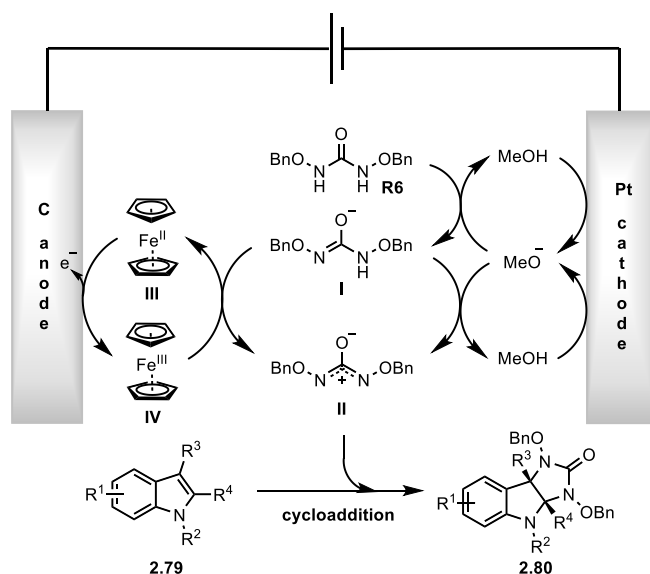
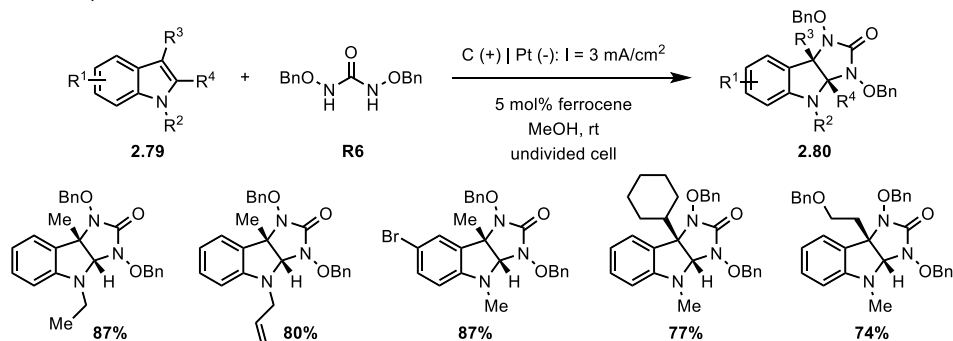
hydroxyl group. Through this reaction, the amide group could be successfully installed at the 3-position of the indole **2.77** to furnish 3-amidated indole **2.78**. The use of ZnCl<sub>2</sub> as an activating agent was found to be crucial in preventing undesired side reactions, enabling the high yielding of corresponding 3-amidated indole derivatives.

The predominant methods of electrophilic C3-amination rely on the pre-installation of the leaving group on the nitrogen atom with use of the stoichiometric amount of reagents. Within this context, the formation of nitrenium ions *in situ* by direct loss of electrons should be the powerful tool in terms of atom-economy, while underlining the new direction not only to the related field but also to the field of synthetic chemistry in general. One of the important methods to realize the aforementioned strategy is electrochemistry.

In 2018, Luo and co-workers disclosed the electrochemical method to generate the diaza-oxyallylic cation from N,N'-dibenzoyloxyurea **R6** under electrochemical conditions and its application to the [3+2] cycloaddition of indole derivatives (Scheme 2.19).<sup>27</sup> The plausible mechanism suggested that the reaction was initialized by simultaneous anodic oxidation of Cp<sub>2</sub>Fe **III** to [Cp<sub>2</sub>Fe]<sup>+</sup> **IV** and cathodic reduction of methanol to methoxide and H<sub>2</sub>. The catalytic amount of methoxide formed in the reaction system not only played an important role in facilitating ferrocene-catalyzed oxidation by deprotonating N,N'-dibenzoyloxyurea **R6**, but also directly participated in the oxidation of anion **I** to zwitterion **II**. The corresponding zwitterion **II** then underwent [3+2] cycloaddition with indole **2.79** to form product **2.80**.

**Scheme 2.19.** Electrochemical [3+2] cycloaddition of indole derivatives (Luo and co-workers, 2018)

Luo et al., 2018:

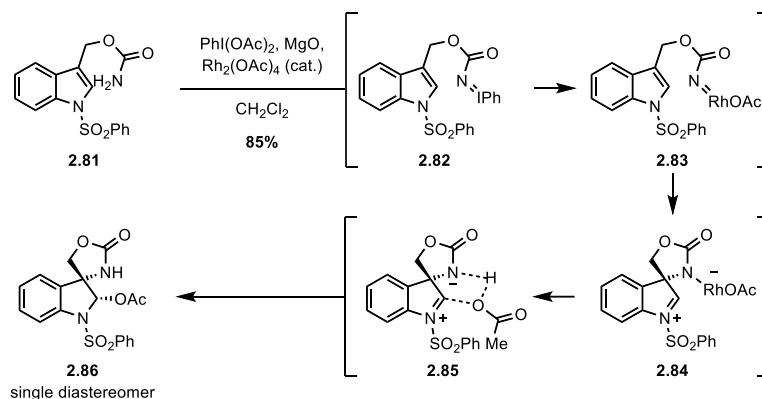


Another foundational method of exploiting the intrinsic nucleophilicity of indole was the Rh-catalyzed aza-spiro-cyclization of indole carbamate using electrophilic nitrenoid species reported by Padwa and co-workers in 2002 (Scheme 2.20).<sup>28</sup> During the exploration of rhodium(II)-catalyzed aziridination of various allyl-substituted sulfonamides and carbamates, the group observed distinct reactivity when it comes to indole 2,3- $\pi$  bond. When the reaction was conducted with protected 3-indolyl carbamate **2.81**, spiro-cyclization at 3-position and stereoselective acetylation at 2-position were observed instead of expected aziridination. Given the *syn*-configuration of the newly generated substituents of the resulting product, the

possibility of aziridine formation and consecutive  $S_N2$  opening of aziridine was excluded. The newly proposed mechanism is as follows: The reaction initiated with the formation of an iminoiodinane intermediate **2.82**, followed by loss of iodobenzene to furnish nitrenoid **2.83**. Addition of tethered nitrenoid to the indole  $\pi$ -bond generated a zwitterion **2.84** and concurrent deprotonation of acetic acid and nucleophilic attack of corresponding acetate anion on the *N*-sulfonyliminium ion **2.85** ultimately led to the spiro-indoline **2.86**.

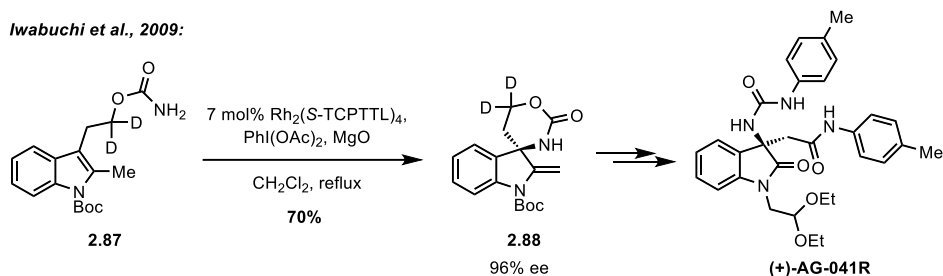
**Scheme 2.20.** Rh-catalyzed aza-spiro-cyclization of indole carbamates (Padwa and co-workers, 2002).

*Padwa et al., 2002:*

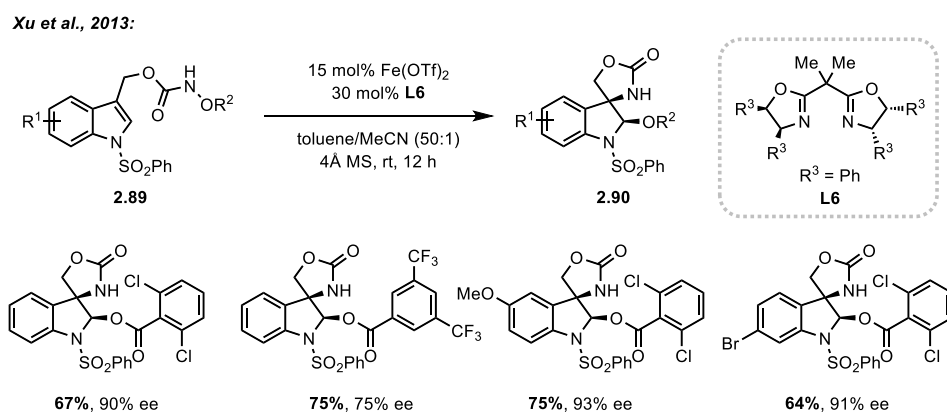


In 2009, An asymmetric synthesis of (+)-AG-041R, a potent gastrin/CCK-B receptor antagonist, was achieved by Iwabuchi and co-workers via chiral rhodium(II)-catalyzed intramolecular aza-spiro-cyclization (Scheme 2.21).<sup>29</sup> As a result of extending various rhodium-catalyzed enantioselective approaches to the work of Padwa mentioned above, the highly enantioselective cyclization of indolyl carbamate **2.87** was enabled by employing  $\text{Rh}_2(\text{S-TCPTTL})_4$ , one of the well-known chiral dirhodium(II) catalyst, was achieved to furnish indoline **2.88** with aza-quaternary center in a highly enantioselective manner. Meanwhile, the introduction of deuterium in the tethered chain was found to be an essential component for the efficient promotion of the spiro-cyclization.<sup>30</sup>

**Scheme 2.21.** Rh-catalyzed aza-spiro-cyclization utilized in the synthesis of (+)-AG-041R (Iwabuchi and co-workers, 2009).



**Scheme 2.22.** Spirocyclized indoline synthesis via Fe catalysis (Xu and co-workers, 2013).



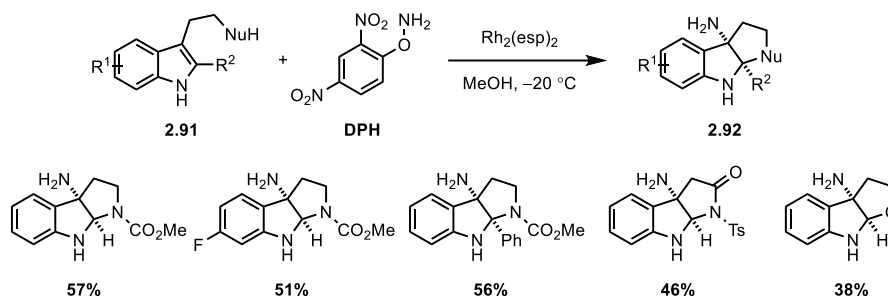
In 2013, the Xu group developed the Fe-catalyzed asymmetric intramolecular aminohydroxylation of indoles (Scheme 2.22).<sup>31</sup> By using *N*-hydroxycarbamate **2.89**, similar yet distinct from the substrate used in Padwa's work, an additional hydroxyl group attached to the carbamate nitrogen could be tuned for the efficient generation of nitrenoid. The additional advantages from the employment of *N*-hydroxycarbamate are that 1) the use of an external oxidant *i.e.*, hypervalent iodine, was avoided and 2) the unavoidable addition of acetate in the previous literature precedent, a byproduct of the hypervalent iodine reagent, could be prevented and at the same time, such reactivity *i.e.*, nucleophilic addition to indolenine, was further extended to C2-functionalization with various benzoate resulting from cleavage of protected *N*-hydroxycarbamate to yield indoline **2.90**.

In 2015, Lai, Zhu and Xie described the first direct synthesis of unprotected 3a-amino-pyrroloindoline via aminocyclization of tryptamine derivatives (Scheme 2.23).<sup>32</sup> The reaction

is presumably proceeds via the interaction of O-(2,4-dinitrophenyl)hydroxylamine (DPH) with the Rh catalyst to generate a metallonitrene species which is responsible for the facilitation of intramolecular cyclization.

**Scheme 2.23.** Direct synthesis of unprotected 3a-amino-pyrroloindolines enabled by intervention of nitrenoid (Lai, Zhu, Xie and co-workers, 2015).

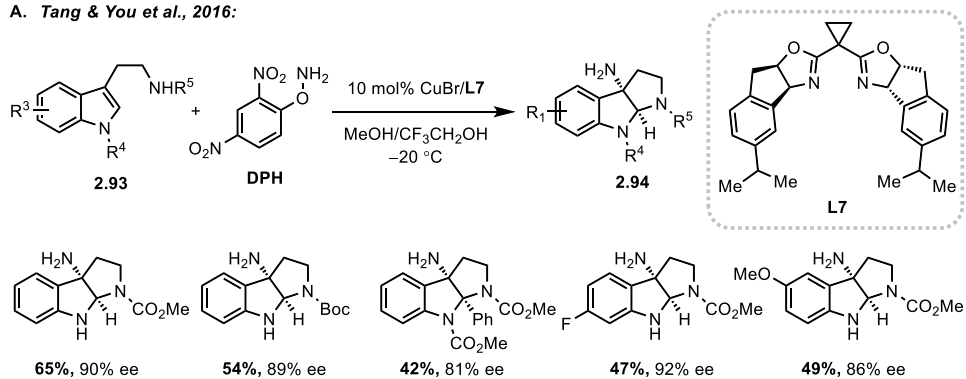
*Lai, Zhu & Xie et al., 2015:*



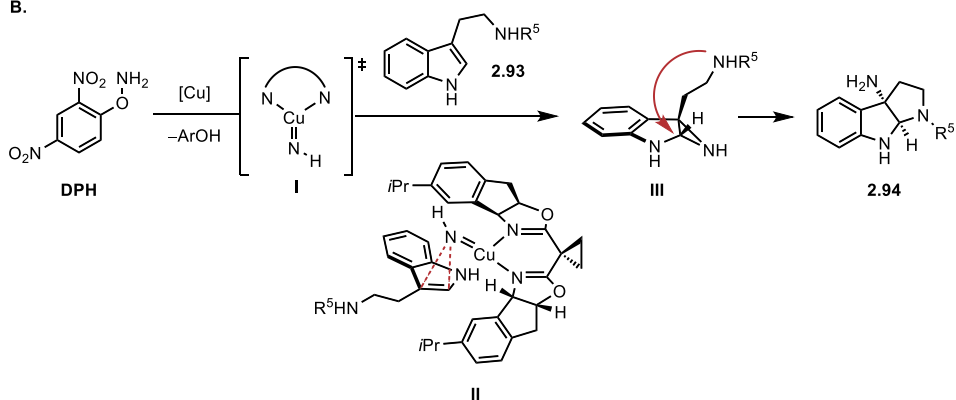
Shortly after this racemic synthesis, an enantioselective version of the identical reaction was reported by Tang, You and co-workers (Scheme 2.24A).<sup>33</sup> The key to disclosing an asymmetric construction of naked amino-pyrroloindoline was the employment of CuBr with bisoxazoline **L7** as a catalyst. A plausible reaction mechanism and the transition state for the asymmetric aziridination step is as follows (Scheme 2.24B). Initially, Cu-nitrene intermediate **I** was generated from the DPH and the Cu(I)-catalyst, and the generated chiral Cu-nitrene species was inserted to the 2,3  $\pi$  bond of the tryptamine **2.93**. The resulted aziridine intermediate **III** facilitated prompt intramolecular cyclization and aziridine ring opening process, affording the product **2.94**. The facial selectivity is presumably derived from the steric hindrance between the tryptamine and the chiral BOX ligand.

**Scheme 2.24.** Enantioselective synthesis of unprotected 3a-amino-pyrroloindolines enabled by Cu catalysis (Tang, You and co-workers, 2016).

**A. Tang & You et al., 2016:**



**B.**



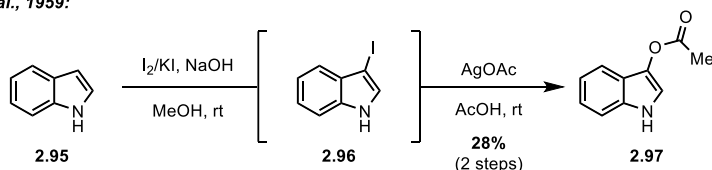
### 2.1.2. C3-Functionalization of Indole via Umpolung Strategy

Majority of the effort for indole C3-hetero-functionalization has been focused on utilizing the innate nucleophilic character of the indole. However, the recent interest on the umpolung reactivity of the indole, *i.e.*, electrophilic indole, has grown with time, and contributed to expanding the current portfolio of indole C3-hetero-functionalization. This approach was made possible by fine-tuning the electronics of indole via chemical conversion or catalytic direct one-electron oxidation.

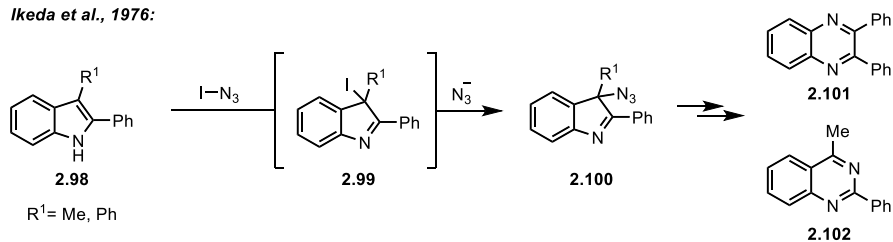
The first example of using an electrophilic indole for C3-hetero-functionalization of indole dates back to 1951 (Scheme 2.25A).<sup>34</sup> Stepp and co-workers were able to increase the oxidation state of indole **2.95** by iodination of electron-rich indole motif. This rather unstable 3-iodoindole **2.96** could react as an electrophile and generate indolyl 3-acetate **2.97** in the presence of silver acetate with acetic acid. Another example employing a similar approach was the C3-azidation of indole reported by Ikeda and co-workers in 1976 (Scheme 2.25B).<sup>35</sup> The iodination of 2-substituted indole **2.98** was performed using iodine azide to form iodoindolenine **2.99**, which immediately substituted with azide anion to generate 3-azidoindolenine **2.100**. The resulted 3-azido-2,3-substituted indolenine **2.100** could be transformed into diphenylquinoxaline **2.101** or 4-methyl-2-phenylquinoxaline **2.102** by Curtius-type rearrangement under refluxing conditions.

**Scheme 2.25.** C3-hetero-functionalization via indolyl iodide (Stepp and co-workers, 1959 / Ikeda and co-workers, 1976).

A. *Stepp et al., 1959:*



B. *Ikeda et al., 1976:*

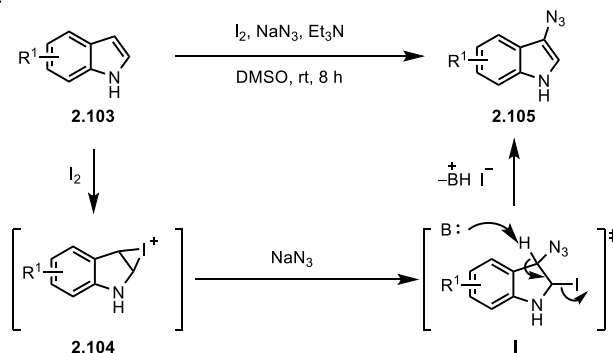




In 2016, the Sudalai group described the C3-azidation of indole by taking advantage of the combination of iodine and NaN<sub>3</sub> (Scheme 2.26).<sup>36</sup> Similar with the Ikeda's strategy, azide anion was used to act as the nucleophilic nitrogen source, while the iodine reversed the polarity of the indole nucleus to generate electrophilic **2.104**.

**Scheme 2.26.** C3-azidation via electrophilic indole species (Sudalai and co-workers, 2016).

Sudalai et al., 2016:

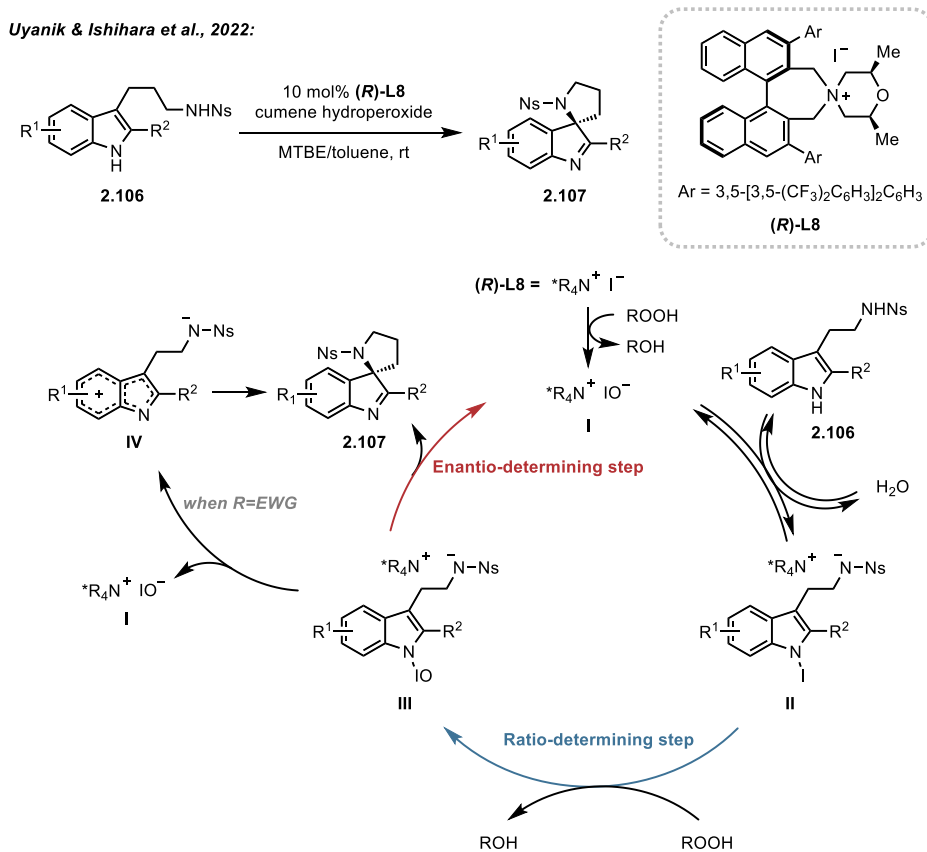


Mechanistically, it is generally explained that the direct activation of indole is involved in the reaction pathway for the hetero-functionalization of indole by iodine. However, the precise mechanism remains controversial and other mechanistic explanations have been proposed. For instance, the indole-aniline coupling, a key reaction for the elegant synthesis of psychotrimine and kapakahines by the Baran group as illustrated in Scheme 2.16, was initiated with NIS-mediated activation in aniline rather than in indole. Given this precedent, a cascade of oxidation of the nucleophile and electrophilic substitution/addition cannot be excluded as a potential mechanistic hypothesis.

In 2022, Uyanik and Ishihara were able to extend the conventional iodination of indoles with stoichiometric usage of iodine source to a catalytic process (Scheme 2.27).<sup>37</sup> This elegantly designed strategy allowed the catalytic iodination of homo-tryptamine derivatives **2.106** at N1 aided by ammonium hypoiodite catalyst, providing the corresponding spiro-indolenine **2.107** in high enantioselectivity. Detailed mechanistic studies revealed that ammonium hypoiodite **I**, an active species generated *in situ* from the oxidation of ammonium iodide **L8** with cumene hydroperoxide, reacted with indole to generate *N*-iodoindole **II** via a reversible iodination of indole N–H position or iodination of the sulfonamide N–H followed

by intramolecular iodo-transfer. Electrophilic *N*-iodoso intermediate **III** generated by rate-determining oxidation of **II** could initiate the intramolecular cyclization under chiral environment to furnish the desired **2.107**. The dissociation of ammonium hypoiodite which generated the zwitterion **IV** to participate in the identical reaction in racemic fashion was hypothesized as a background reaction mechanism.

**Scheme 2.27.** Hypoiodite-catalyzed oxidative cyclization of indoles (Uyanik and Ishihara, 2022).



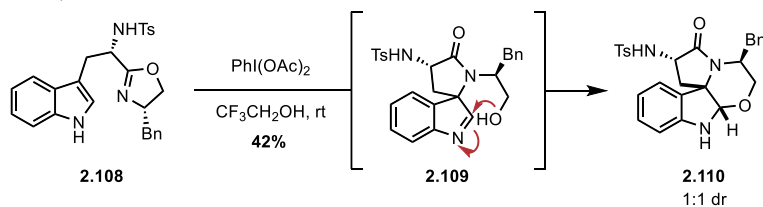
As a complementary approach to activate the indole motif, hypervalent iodine has been actively involved in C3-hetero-functionalization as an alternative method to iodine. In 1999, Ciufolini performed an intramolecular cyclization of indole derivative **2.108** using  $\text{PhI}(\text{OAc})_2$ , one of the most well-known hypervalent iodine reagent (Scheme 2.28A).<sup>38</sup> Oxazoline moiety in the substrate served as a masked form of the nucleophile that provides the two different nucleophiles sequentially. The nitrogen atom of oxazoline first attacked the 3-position, and

the alcohol moiety which is newly released from oxazoline by ring opening of oxazoline was added to the C=N bond of indolenine **2.109** to furnish **2.110**.

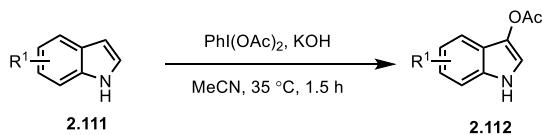
The Huang group reported C3-acetoxylation of indole in 2010, in which an additional acetate group produced after the reaction between  $\text{PhI}(\text{OAc})_2$  and indole acts as a nucleophile (Scheme 2.28B).<sup>39</sup> Later in 2018, the same strategy was applied to achieve the intramolecular spiro-cyclization of indole derivatives **2.113** to access the corresponding spiro-indolenines **2.114** using hypervalent iodine (Scheme 2.28C).<sup>40</sup>

**Scheme 2.28.**  $\text{PhI}(\text{OAc})_2$ -mediated dearomative C3-hetero-functionalization of indole in various systems (Ciufolini and co-workers, 1999 / Huang and co-workers, 2010 / Huang and co-workers, 2018).

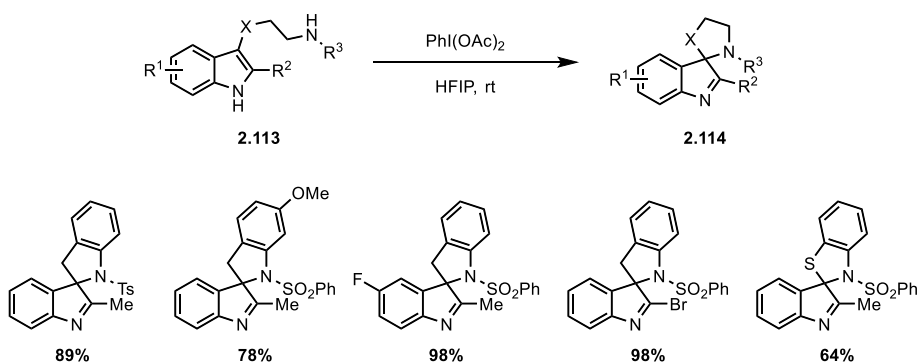
**A. Ciufolini et al., 1999:**



**B. Huang et al., 2010:**



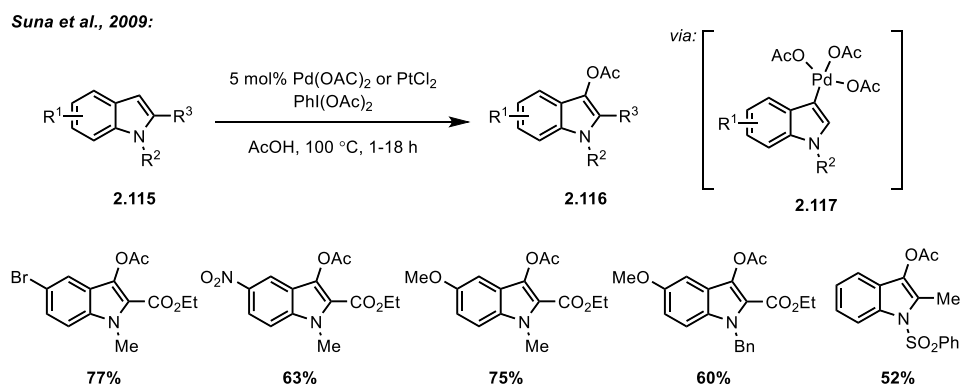
**C. Huang & Zhu et al., 2018:**



The ability of hypervalent iodine, especially with two carbon-based substituents such as the diaryliodonium salt, to function in place of organohalides has sparked the interest of

application in transition-metal catalyzed reactions. Following the unique reactivity of diaryliodonium salts, indolyl  $\lambda$ 3-iodane, in which the hypervalent iodine is substituted at 3-position of indole, was adopted for the new strategy of introducing various functional groups in designated position via transition-metal catalysis. Oxidative addition could lead to an intermediate with a metal coordinated at the 3-position, and subsequent reductive elimination could install a hetero-functional group to furnish the functionalized indole derivatives. The newly introduced hetero-functional groups can be varied depending on the nucleophile used during the reaction.

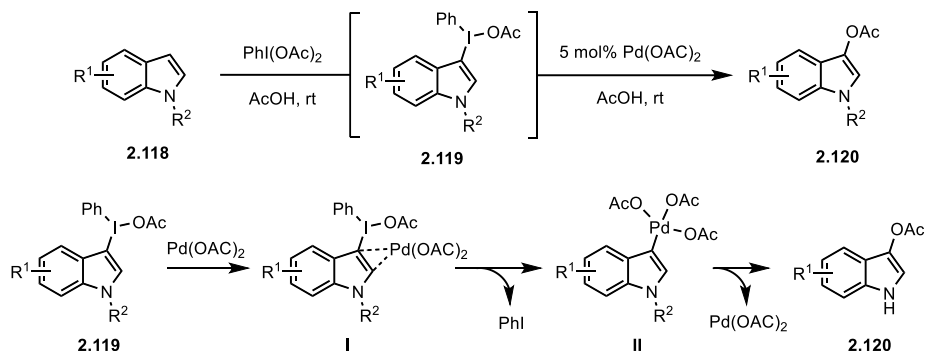
**Scheme 2.29.** C3-Acetoxylation of Indoles via Pd catalyzed coupling (Suna and co-workers, 2009).



The Suna group has been one of the leading pioneers in the hypervalent iodine-mediated C3-hetero-functionalization of indole (Scheme 2.29).<sup>41</sup> Using Pd(OAc)<sub>2</sub> and PhI(OAc)<sub>2</sub>, Suna and co-workers developed C3-acetoxylation of indole wherein the cooperative utilization of a hypervalent iodine reagent and a transition metal catalyst in indole-based system gave rise to intermediate **2.117** as a result of electrophilic C3-palladation of indole. Subsequent reductive elimination of corresponding intermediate led to C3-acyloxyated **2.116**. The group has shown that the presence of Pd(OAc)<sub>2</sub> was critical for the product formation, which was in the sharp contrast with the previous works using PhI(OAc)<sub>2</sub> (*vide supra*). Although it has been established that hypervalent iodine-activated indole is not a key electrophile which reacts directly with the nucleophile in the reaction, the possibility of such an intermediate being involved in the reaction pathway cannot be ruled out.

**Scheme 2.30.** C3-Acetoxylation of Indoles via umpolung indole iodanes (Suna and co-workers, 2011).

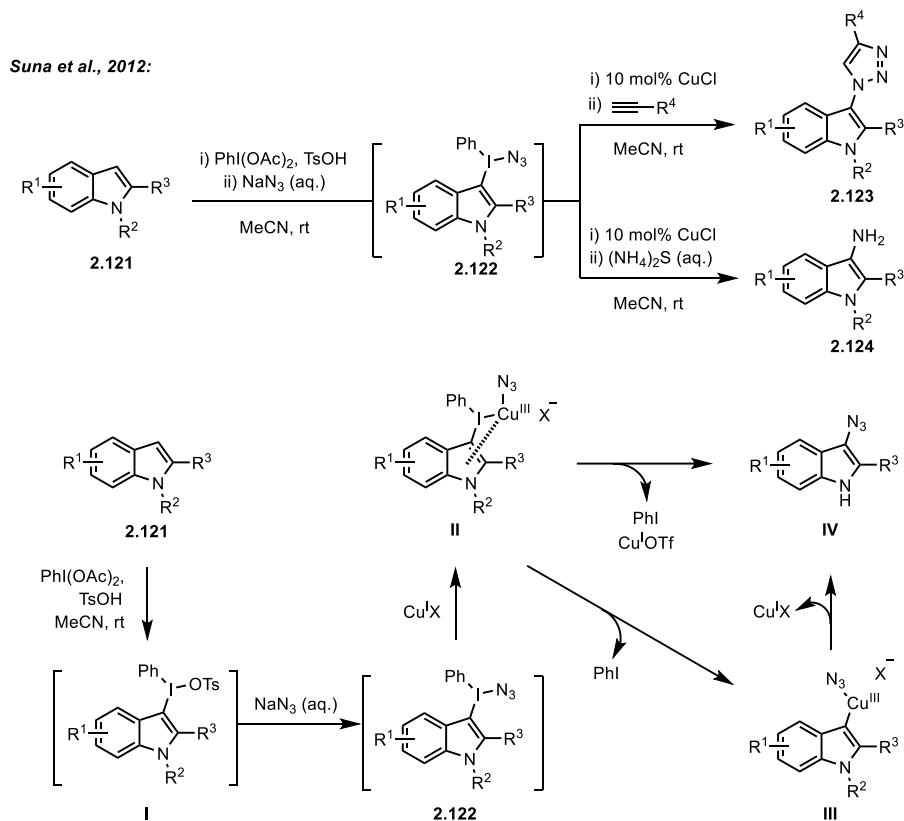
*Suna et al., 2011:*



In the course of their in-depth studies on indole functionalization by hypervalent iodine, Suna and coworker presented the mechanistic basis for the above-mentioned C3-acetoxylation developed by the same group (Scheme 2.30).<sup>42</sup> Initially it was believed that Pd(IV)-indole species could be formed by direct C–H activation or a sequence of palladation of an aryl C–H bond with Pd(II) species followed by oxidation to dinuclear Pd(III) complexes. However, by expanding the substrate scope of the reaction to pyrrole and successfully isolating pyrrolyliodonium acetate in the process, the group demonstrated that the Pd(IV)-indole species **II** responsible for the desired transformation originated in the formation of heteroaryliodonium acetates **I**, providing evidence that a different mechanism is operating from previous examples of C–H activation.

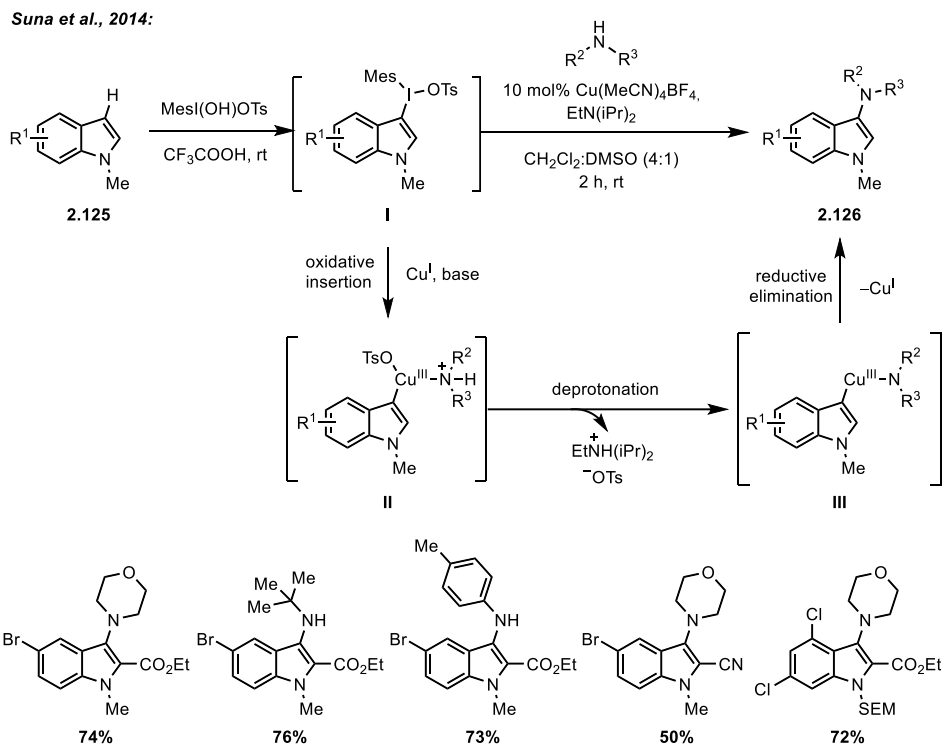
In a further demonstration of the utility of hypervalent iodine-assisted activation strategy, Suna and co-workers successfully extended the reaction to hetero-functionalization other than acetate by exploiting the properties of newly discovered heteroaryliodonium acetates (Scheme 2.31).<sup>43</sup> Under the assumption that using other counterions instead of acetate would be able to provide the differently substituted indole, C3-azidation of indole derivatives **2.121** was accomplished via access to iodonium azide **2.122** by exchanging acetate for azide. The practicality of the reaction was demonstrated by application of Cu-catalyzed click chemistry to furnish 1,2,3-triazoles **2.123** and *in situ* reduction to provide C3-aminoindole **2.124**.

**Scheme 2.31.** C3-Azidation of indole derivatives via copper-catalyzed regioselective fragmentation of Unsymmetrical  $\lambda^3$ -iodanes (Suna and co-workers, 2012).



The underlying mechanism for the C3-azidation of indole is outlined as follows: Indole **2.121** reacting with PhI(OAc)<sub>2</sub> and TsOH provided heteroaryliodonium salt **I**, and subsequent anion exchange would result in iodonium azide **2.122**. Oxidative addition of iodonium azide **2.122** to Cu(I) generated Cu(III) species **II**. Complex **II** could provide azide **IV** directly via regioselective coupling of the heterocycle with the azide. The heteroaryl copper(III) species **III** could also intervene in the reaction pathway as another potential intermediate responsible for the desired transformation. Reductive elimination of **III** would result in azide **IV** while regenerating Cu(I) species.

**Scheme 2.32.** C3-Amination of indole derivatives via copper-catalyzed fragmentation (Suna and co-workers, 2014).

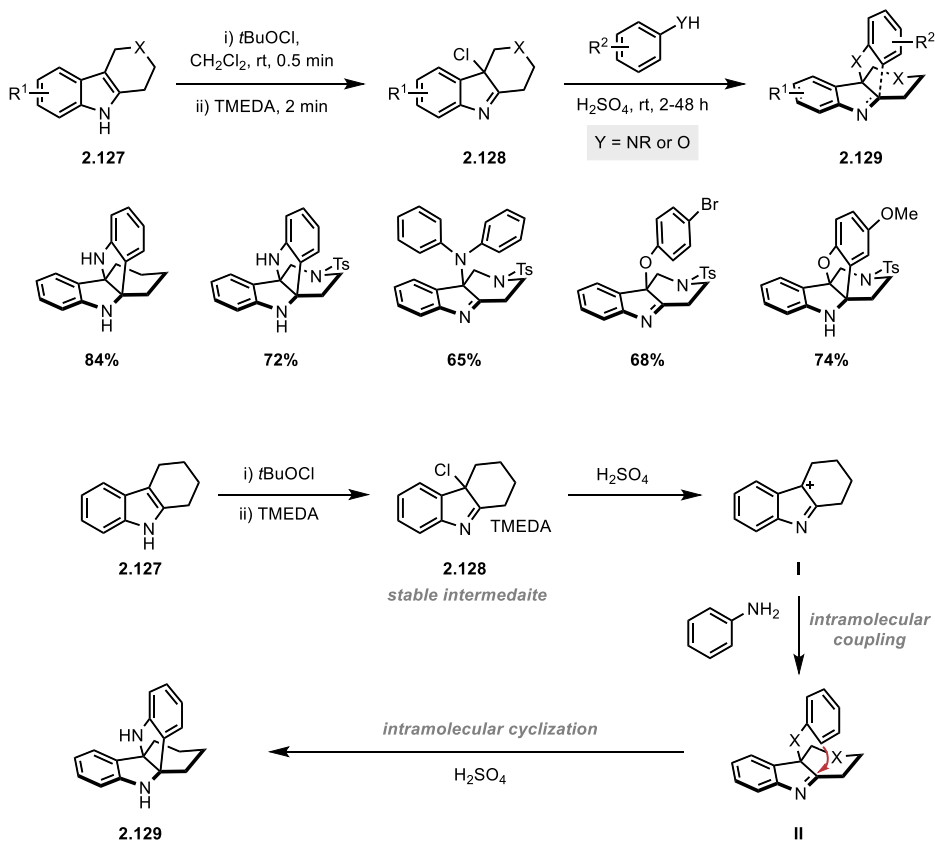


In 2014, Suna and co-workers developed a new protocol for C3-amination between the indolyl- $\lambda$ 3-iodanes formed *in situ* and a wide range of unprotected amines as a nucleophilic nitrogen source (Scheme 2.32).<sup>44</sup> The mechanism of the developed C3-amination was consistent with previously reported methods from the same group, but distinctive features lay within the reaction. Instead of substitution of tosylate in iodonium I to amine and sequential coordination of Cu(I) species to indole moiety, which are the early steps of the previously proposed mechanism, the reaction involves direct oxidative addition of the  $\lambda$ 3-iodane I to Cu(I)-amine complex to form the Cu(III) intermediate II. For this unsymmetrical diaryl- $\lambda$ 3-iodanes, regioselectivity of the oxidative addition to Cu(I) species can be controlled by the use of a mesityl group as a nontransferable aryl ligand. Deprotonation of the Cu(III)-coordinated amine followed by reductive elimination from the resulting Cu(III)-amide complex III would afford aminoindole 2.126 and regenerate a Cu(I) species to complete the catalytic cycle.

One of the unique advantages of the oxidative umpolung strategy is that the reaction can proceed with different nucleophiles as long as it is ensured that the nucleophiles do not interfere with the oxidation process. This is quite distinct from methods using the inherent nucleophilicity of indole in that the syntheses of each different electrophilic heteroatom reagents must be prioritized in order to allow various heteroatoms to participate in C3-substitution of indole.

**Scheme 2.33.** Construction of various bisindoline via 3-chloroindolenine as versatile intermediate (Chen and co-workers, 2020).

Chen et al., 2020:

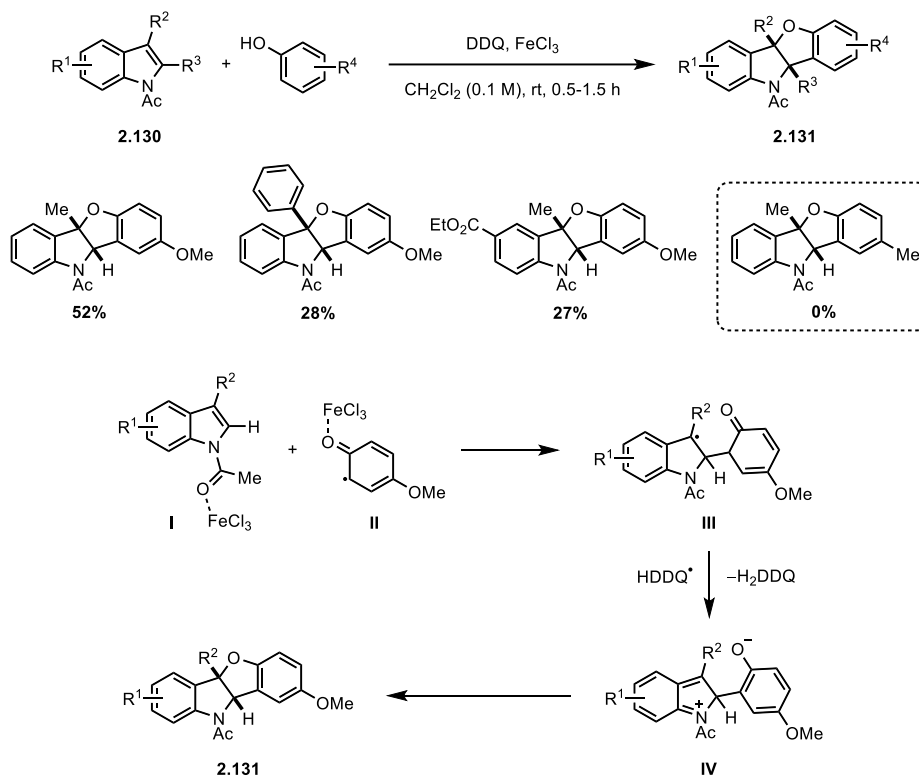


Chen's work in 2020 highlighted this specificity (Scheme 2.33).<sup>45</sup> The group validated the synthetic versatility of electrophilic indole derivatives by constructing various C3-hetero-functionalized indolenines and indolines via oxidative coupling. 3-Chloroindolenine **2.128** obtained by halogenation of indole derivative **2.127** was used as a precursor for the diverse hetero-C3-functionalization.



**Scheme 2.34.** Generation of C3-electrophilic Indoles via FeCl<sub>3</sub>-mediated activation and regioselective synthesis of benzofuroindoline (Vincent and co-workers, 2014).

Vincent et al., 2014:



A more sophisticated activation strategy to reverse the electronics of the indole was developed by Vincent and co-workers, wherein the elegant approach for the regioselective synthesis of benzofuro[3,2-*b*]indolines was realized (Scheme 2.34).<sup>46</sup> The catalytic generation of the active indole substrate was embodied via noncovalent interaction between *N*-acetyl indole **2.130** and FeCl<sub>3</sub>, which facilitated the regioselective radical addition to furnish the benzofuroindoline **2.131**. The dual activation of the *N*-acetyl indole and phenol radical by FeCl<sub>3</sub> favors the coupling between the two species (**I** and **II**, respectively) in 2-position, delivering adduct **III**. This radical adduct **III** could be oxidized by HDDQ which results from the oxidation of phenol with DDQ, and subsequent cyclization of intermediate **IV** would lead to benzofuroindolines **2.131**.

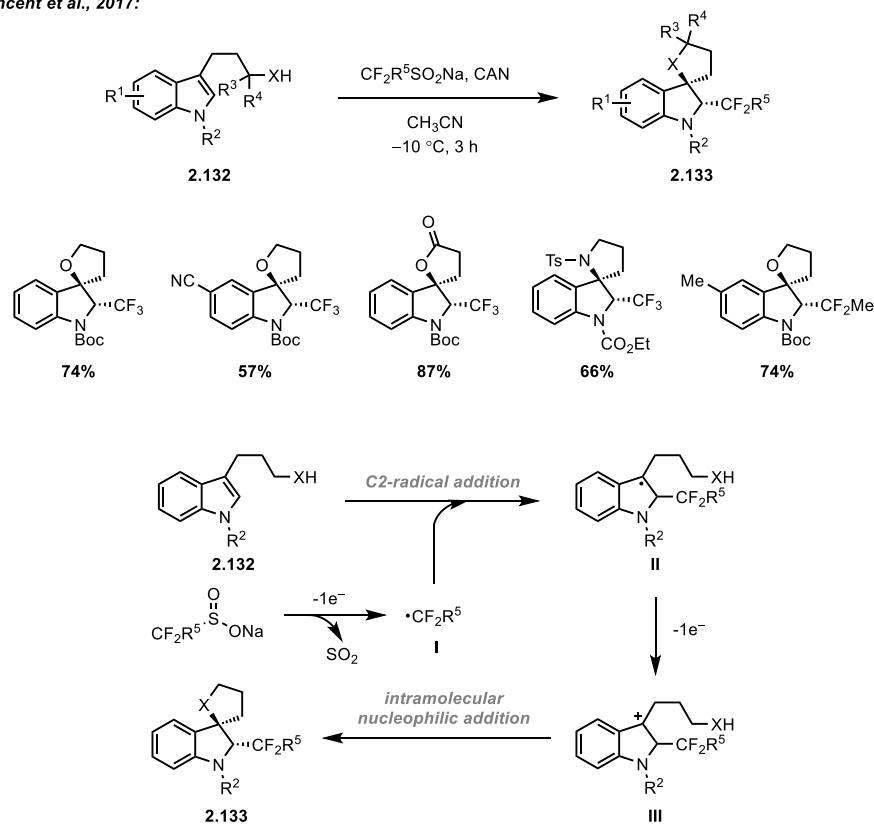
What should be noted here is that unlike most of the previous examples, the oxidation itself took place in the phenol moiety rather than the indole moiety, and FeCl<sub>3</sub>-activation

significantly altered the properties of indole even without the aid of oxidation. The high regioselectivity derived from the well-documented reactivity of the radical with indole, that radicals displays a penchant for attaching to the 2-position of the indole ring. However, a few combinations of indole and phenol showed reversed reactivity, presumably due to steric hindrance or the different stability of the resulting radical intermediates.

In 2017, the Vincent group achieved intramolecular cyclization of indole derivatives with tethered nucleophile wherein ceric ammonium nitrate (CAN)-mediated generation of tri- or difluoromethyl radical **I** enabled the regioselective radical addition to 2-position of indole derivative **2.132** (Scheme 2.35).<sup>47</sup> This justified the localization of the newly formed radical at C3 as a form of **II**, which was oxidized to the corresponding cation **III** and ultimately allowed the regioselective addition of the tethered nucleophile to the 3-position after one-electron oxidation, to generate the spiro-indoline **2.133**.

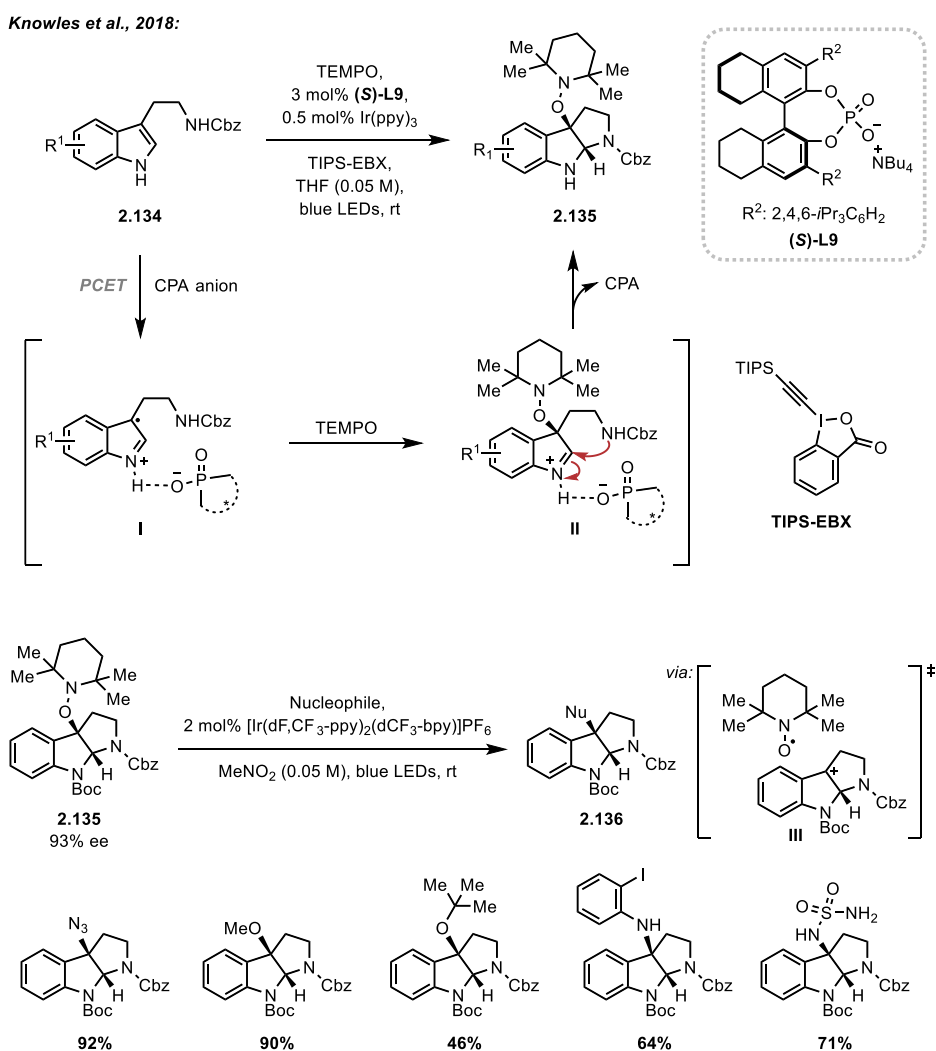
**Scheme 2.35.** Spirocyclization of indole enabled by fluoromethyl radical (Vincent and co-workers, 2017).

Vincent et al., 2017:



If direct electron loss in the indole moiety could be realized without undergoing additional chemical oxidation to change the oxidation state of the indole, the use of excess reagent can be minimized and a more environmentally benign synthetic design can be pursued. Photochemical and electrochemical techniques as a new activation tool have become the answer for this longstanding question. The introduction of photochemistry and electrochemistry presented an opportunity to discover a new reactivity of indole motif which was difficult to access in conventional organic chemistry.

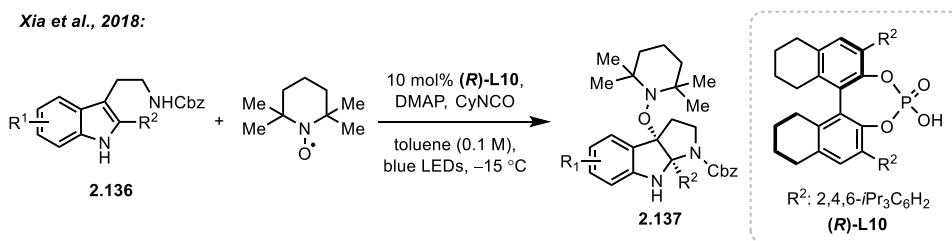
**Scheme 2.36.** Enantioselective synthesis of pyrroloindolines enabled by chiral phosphoric acid-assisted PCET (Knowles and co-workers, 2018).



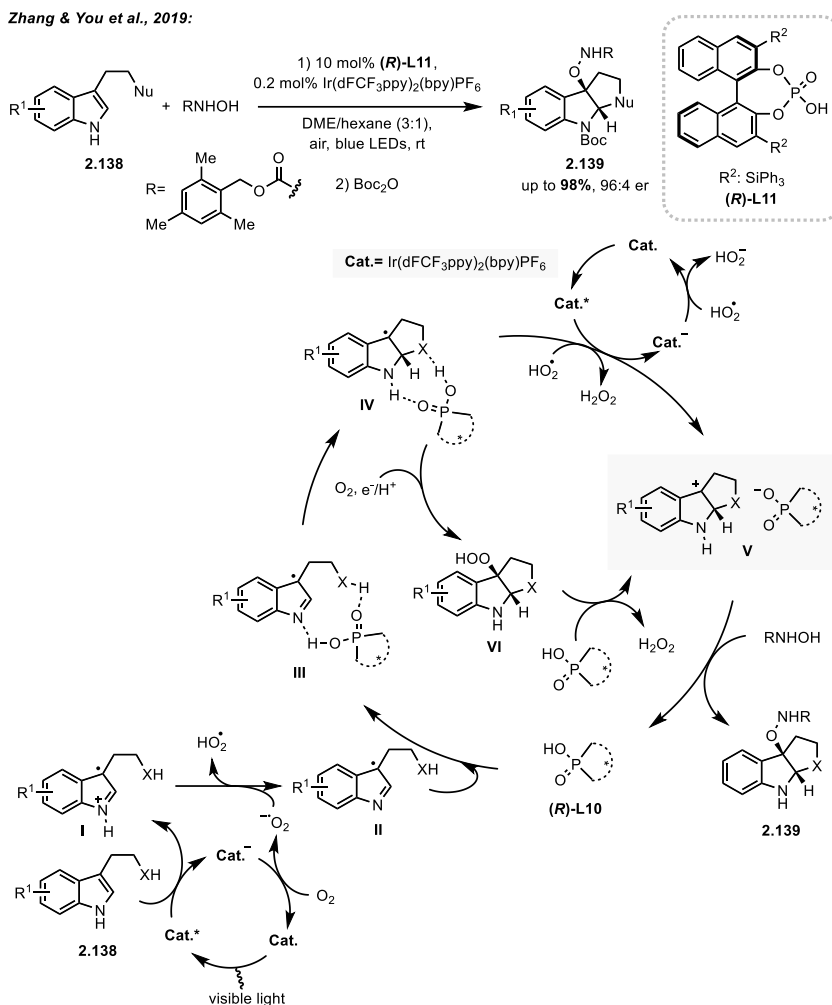
In 2018, the Knowles group presented the enantioselective synthesis of pyrroloindolines via the catalytic oxidation of the indole motif, wherein the hydrogen bonding between chiral phosphate and tryptamine variant facilitates proton-coupled electron transfer (PCET) (Scheme 2.36).<sup>48</sup> This weakly coordinated complex of tryptamine derivative **2.134** and chiral phosphate **L9** could engage in a one-electron oxidation under photochemical conditions to yield an indole radical cation **I**. The indole radical cation **I**, stabilized by chiral phosphate, effectively bounded to TEMPO to yield **II** and subsequently cyclized to form a stable TEMPO-substituted pyrroloindoline **2.135** with high enantioselectivity. Further elaboration of the TEMPO-substituted pyrroloindoline **2.135** was demonstrated via one-electron oxidation/mesolytic cleavage cascade reaction, to furnish transient carbocation intermediates **III** that could be trapped by a wide range of nucleophiles.

In same year, Xia group reported the identical synthetic protocol to that of the Knowles group (Scheme 2.37).<sup>49</sup> In the presence of chiral phosphoric acid **L10**, intercepting the indole radical cation by TEMPO to obtain TEMPO-trapped pyrroloindoline **2.137** was demonstrated. However, the paper did not discuss further application of TEMPO-adduct **2.137**, *i.e.*, oxidation and subsequent nucleophilic addition at the 3-position of pyrroloindoline.

**Scheme 2.37.** Enantioselective synthesis of C3-TEMPO pyrroloindoline (Xia and co-workers, 2018).



**Scheme 2.38.** Asymmetric dearomatization of indoles via photoredox catalysis (Zhang, You and co-workers, 2019).



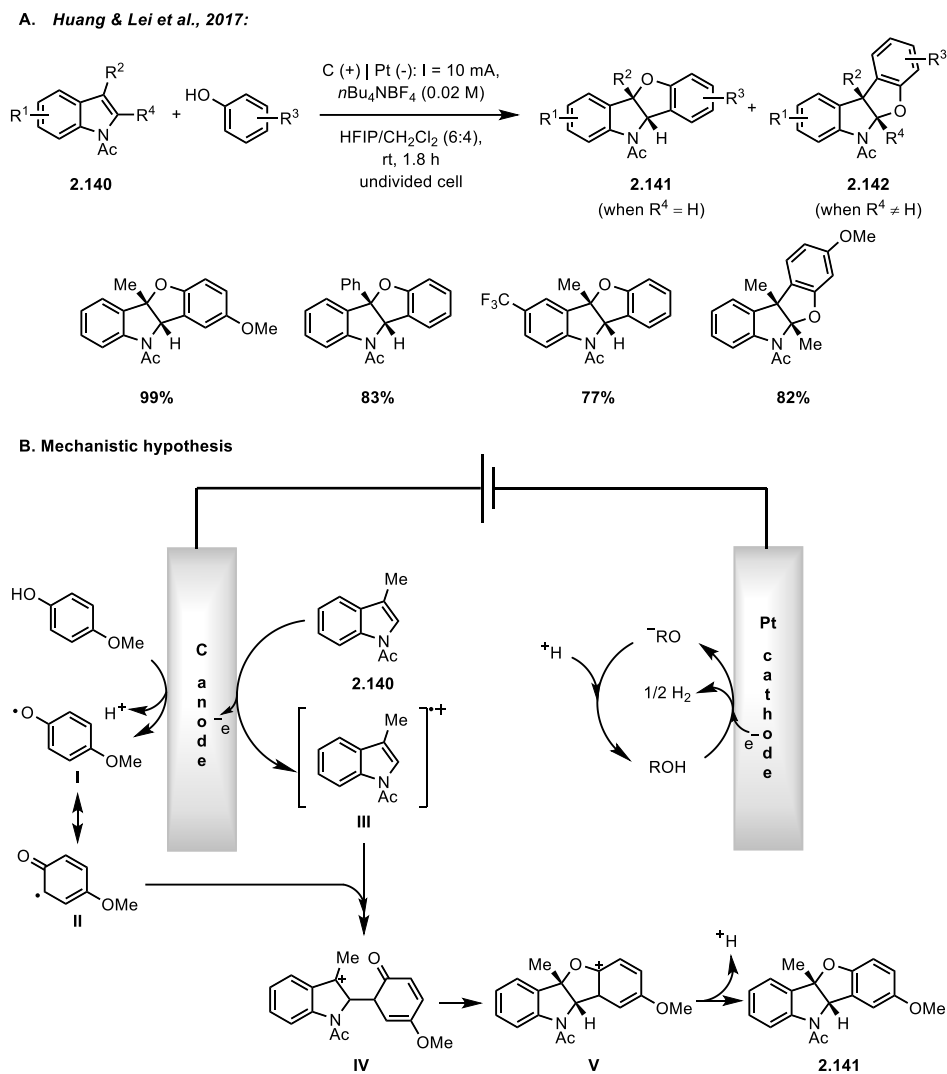
Asymmetric dearomatization of indole derivatives reported by Zhang and You used an approach analogous to the work of Knowles and Xia in combining a photocatalytic system and organocatalyst to elicit the umpolung reactivity of indole, but has unique strengths that set it apart from the rest (Scheme 2.38).<sup>50</sup> First, indole oxidation was proposed to occur without the aid of a chiral phosphoric acid. Previous observations suggested that activation of indole by chiral phosphoric acid is an essential factor for direct loss of electrons in the indole ring. In this case, direct oxidation occurred under the photochemical conditions to form radical cation **I** and superoxide provoked from the photocatalysis acted as a base to deprotonate radical cation **I** to generate radical **II**. Second, molecular oxygen—whether in

the form of activated superoxide or hydroperoxyl radical—is involved not only in the oxidation of indole but also in the regeneration of the catalyst, thereby completing the overall reaction cycle. Finally, two consecutive oxidations allow the tryptamine variants to easily reach the C3-cationic pyrroloindolines without additional trapping and isolation of intermediate. In previous methods, the isolation of the TEMPO-adduct should be prior in order to commence the further C3-hetero-functionalization of pyrroloindolines. In this new protocol, however, the generated indole radical cation **IV** could undergo additional one-electron oxidation *in situ* to become a cationic pyrroloindoline **V**. This sequential dual-oxidation to cationic pyrroloindoline **V** made it possible to circumvent inconvenience of obtaining an intermediate separately, and rapid construction of enantio-enriched C3-substituted pyrroloindoline **2.139** directly from prochiral tryptamine derivative **2.138**.

Introduction of electrochemical tools for oxidation of indole was exploited by Huang and Lei for the synthesis of benzofuroindoline reported in 2017 (Scheme 2.39A)<sup>51</sup> Distinguishing the two regioisomers that can be generated from the electrooxidative [3 + 2] annulation of indole and phenol, *i.e.*, benzofuro[3,2-b]indoline **2.141** and benzofuro[2,3-b]indoline **2.142**, was determined based on the C2 and C3-substitution of the indole. When there is no substituent bulkier than hydrogen at 2-position, benzofuro[3,2-b]indoline **2.141** was obtained with an oxygen atom positioned at C3, whereas an alkyl or aryl substituent positioned at C3 led to benzofuro[2,3-b]indoline **2.142** which is consistent with the observed results from the Vincent's report (*vide supra*).

The basic mechanism underlying the reaction is the two orthogonal electro-oxidation of indole and phenol (Scheme 2.39B). The resultant indole radical cation **III** and the phenol C-radical **II** generated by radical relocation in the phenoxy radical **I** formed the cationic intermediate **IV** via indole-phenol radical cross-coupling. The intermediate **IV** then underwent an intramolecular cyclization by trapping the cation located at the C3-position of the indole with a nearby oxygen atom, thereby completing the structure of benzofuroindoline.

**Scheme 2.39.** Electrochemical [3 + 2] annulation between phenol and indole to access benzofuroindolines (Huang, Lei and co-workers, 2017).

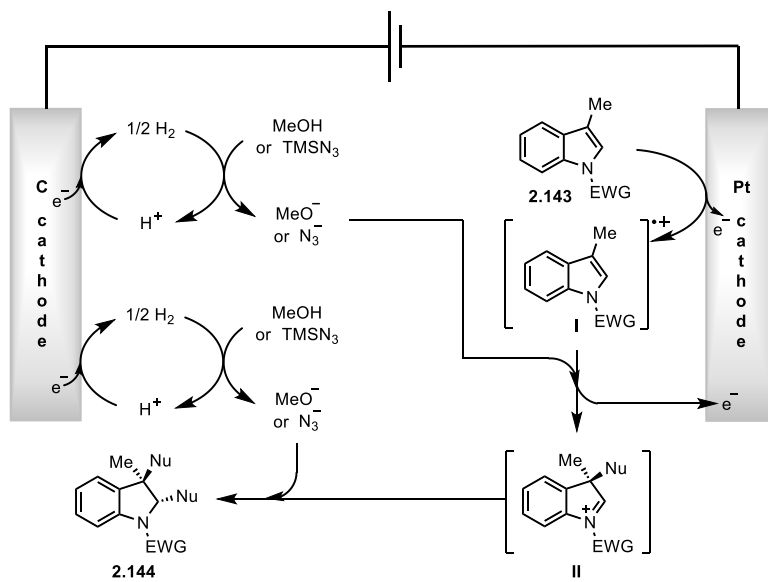
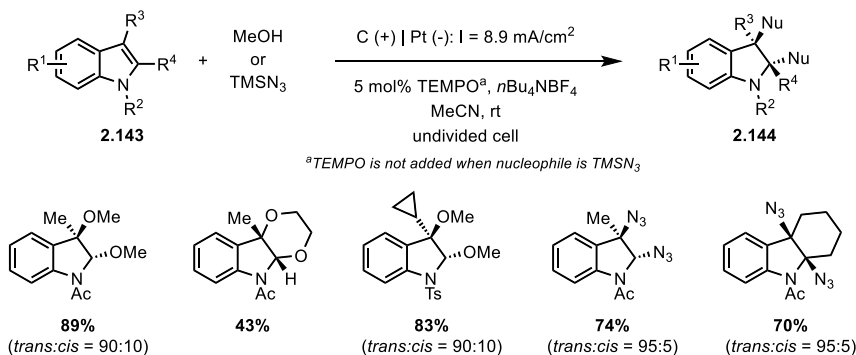


The Vincent group has an outstanding insight for unlocking the potential of indole by making the most of the tools available to the field of organic chemistry, and contributed to the formation of complex indole-embedded architecture. As an extension of their interest in the dearomatization of indole, Vincent and co-workers developed an electrochemical method for the indole dearomatization, thereby making indole an electrophilic platform capable of reacting with various nucleophiles (Scheme 2.40).<sup>52</sup> The formation of the 2,3-disubstituted indoline **2.144** with two C–O or C–N bonds is believed to arise from the anodic oxidation of the *N*-substituted indole **2.143** to give a radical cation **I**. Methoxide or azide anion generated

by cathodic reduction reacts with intermediate **I**, accompanied by an additional oxidation process at the anode either in simultaneous or stepwise process, generating iminium ion **II**. Intercepting the resulting iminium ion **II** by the methoxide or azide anion eventually delivers the product **2.143**.

**Scheme 2.40.** Electrochemical 2,3-difunctionalization of indoles (Vincent and co-workers, 2019).

Vincent et al., 2019:





### 2.1.3 Radical Addition to 3-Position of Indole

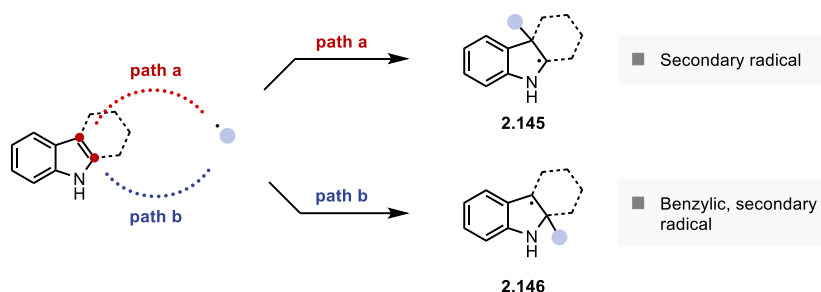


**Figure 2.5.** Reactivity of radicals biased by C2-addition.

The involvement of radical species in the functionalization of indole also has a long history, comparable to the previous two approaches in Section 1.1.1 and 1.1.2. However, one of the most prominent problems of the reaction to be actively used for the C3-heterofunctionalization is the regioselectivity issue (Figure 2.5). When a radical species approaches an indole and radical-engaged dearomatization occurs, the resulting radical within the indole motif is formed at C2 or C3 depending on the position of addition. Radical addition at the 2-position would lead to an intermediate **2.146** with a benzylic secondary radical which gains considerable stabilization from the aryl group. In the case of a radical bound to the 3-position, such a stabilizing effect is missed in an intermediate **2.145**. Considering the difference in the relative energies of the two radical intermediates, it is unobjectionable that the radical tends to be added at the C2-position of the indole ring, which has been empirically proven throughout the history of radical-involved functionalization of indole. For these reasons, the regioselective engagement of radicals at the 3-position has encountered several obstacles. However, methods that overcome this intrinsic reactivity and demonstrate regioselective C3-heterofunctionalization of indole have been reported.

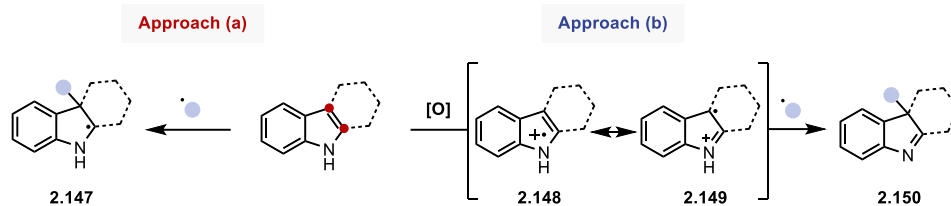


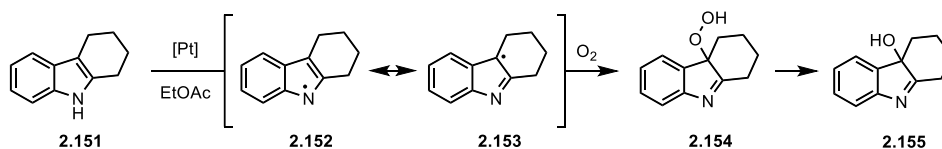
**Figure 2.6.** Two approaches in radical addition strategy.

C3-hetero-functionalization of indole via radical addition to the indole 2,3  $\pi$  bond can be classified into two types of approaches (Figure 2.6). First approach is the radical addition to the 2,3  $\pi$  bond of neutral indole core (Approach (a), Figure 2.6). Since there is no mechanistic factors which could override thermodynamic driving force to reverse the native preference of radical bound to 2-position, substrates with a specific substituents, or systems deliberately designed to place the nucleophile close to the 3-position, have been utilized. The other is the preceding conversion of indole nucleus into the corresponding radical or radical cation prior to the radical addition (Approach (b), Figure 2.6). This “pre-treatment” process intentionally generates C3-benzylic radical owing to the above-mentioned reasons, thereby allowing the participation of the external radical to 3-position in a highly regioselective manner.<sup>53</sup>

The most well-documented example of radical addition of indole 2,3  $\pi$  bond would be the reaction with triplet oxygen. The first observation of this reactivity was reported by Beer over 70 years ago, from which the precise chemical structure was confirmed in 1950 and later re-explored by Witkop and co-workers in 1951 (Scheme 2.41).<sup>54</sup> A Pt-catalyzed oxidation of tetrahydrocarbazole in the presence of molecular oxygen led to the construction of 3-hydroxyindolenine **2.155**, the product of an instantaneous reduction of 3-hydroperoxyindolenine **2.154**.

**Scheme 2.41.** Early literature precedents of C3-hetero-functionalization via radical addition (Beer and co-workers, 1949, 1950 / Witkop and co-workers, 1951).

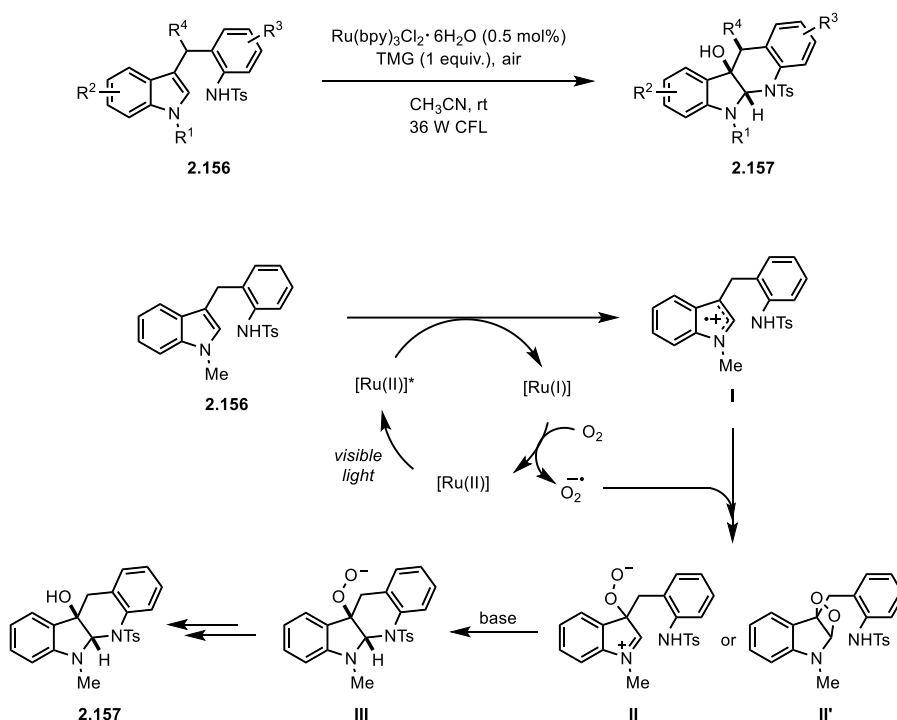
*Beer et al., 1949 / Beer et al., 1950 / Witkop et al., 1951:*



In 2013, the Xiao group reported a new method to form tetrahydro-5H-indolo[2,3-b]quinolinols using molecular oxygen as a source for oxygenation at 3-position by expanding the indole reactivity shown in the previous literature precedents (Scheme 2.42).<sup>55</sup> The photocatalytic protocol proceeds with oxidation of indole **2.156** and activation of molecular oxygen in the presence of a  $\text{Ru}^*(\text{bpy})_3\text{Cl}_2 \cdot 6\text{H}_2\text{O}$  catalyst. Subsequently, the radical cross-coupling of the resulting indole radical cation **I** and superoxide anion could be induced to deliver intermediate **II** or **II'**. The obtained intermediate, either in the form of **II** or **II'**, undergoes an intramolecular cyclization to yield intermediate **III**. Reductive cleavage of the O–O bond of intermediate **III** led to the formation of tetracycle **2.157**.

**Scheme 2.42.** Synthesis of tetrahydro-5H-indolo[2,3-b]quinolinols via C3-oxygenation (Xiao and co-workers, 2013).

*Xiao et al., 2013:*

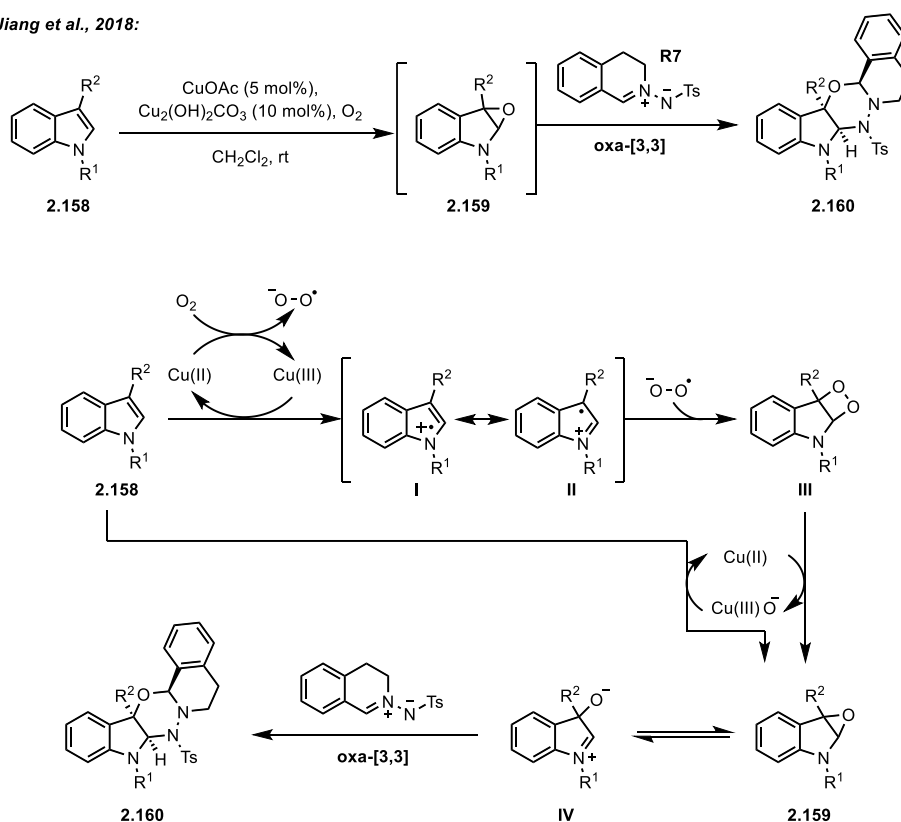


In 2018, the Jiang group reports the aerobic [3+3] cycloaddition of 3-substituted indoles and C,N-cyclic azomethine imines (Scheme 2.43).<sup>56</sup> What should be emphasized most is the synchronized action of the copper catalyst and molecular oxygen to oxidize indole to generate

**2.159** as a counterpart for [3+3] cycloaddition. First, copper(II) catalyst is oxidized by molecular oxygen to afford a copper(III) species with the generation of a superoxide anion. The copper(III) species generates indole radical cation **I**, which is immediately trapped by superoxide, leading to oxacycle **III**. Upon copper(II)-catalyzed reduction, **III** converts to the intermediate **2.159**, and the resulting copper(III)–oxygen complex participates in the alternative pathway to form **2.159** and regenerates copper(II) by reacting with indole **2.158**. Reversible opening/closing of epoxide allows **2.159** to equilibrate with zwitterion **IV**, which combines C,N-cyclic azomethine imine **R7** to construct [2,3]-fused indoline O-heterocycle **2.160**.

**Scheme 2.43.** Aerobic [3+3] cycloaddition of 3-substituted indoles (Jiang and co-workers, 2018).

Jiang *et al.*, 2018:



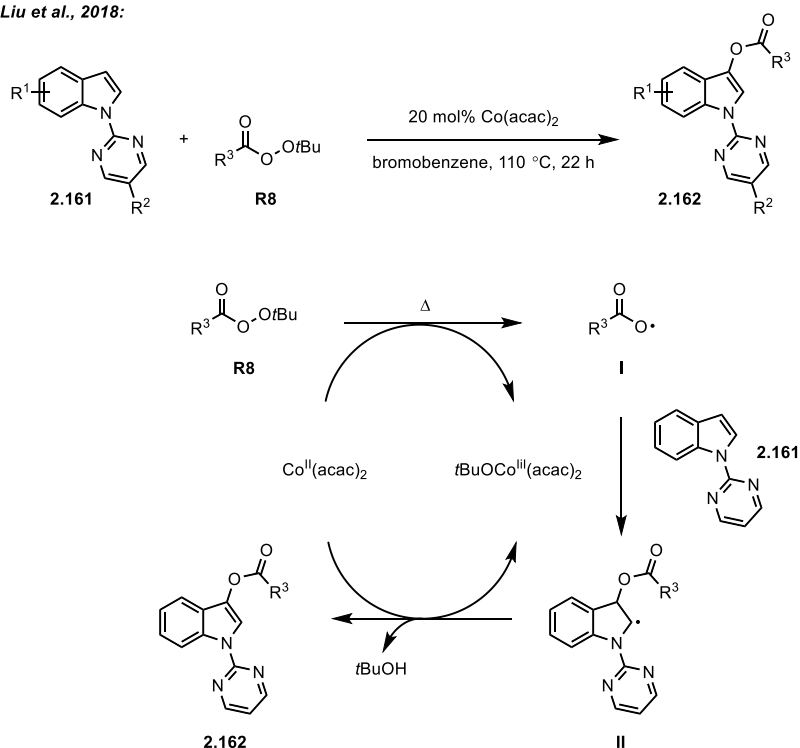
In 2018, Liu and Liu described a Co(II)-catalyzed C3-acyloxylation of indoles (Scheme 2.44).<sup>57</sup> The reaction is initiated by the Co(acac)<sub>2</sub>-facilitated homolytic cleavage of *tert*-butyl peroxybenzoate **R8**, generating a carboxylic radical **I**. Trapping of the carboxylic radical **I**

with 1-pyrimidinylindole **2.161** specifically creates a new bond positioned at C3, leading to the radical intermediate **II**. Intermediate **II** is then oxidized to the corresponding cation via SET while Co(II) species are regenerated through this process. Finally, a C3-deprotonation takes place to reincorporate the double bond, providing the C3-acyloxyated product **2.162**.

Of particular interest is that the highly regioselective C3-transformation was made possible, surmounting the innate C2-preference of radical species. Although the detailed elucidation of this observation was not described in detail, the existence of the pyrimidine ring attached to indole N1 is considered to be the dominating factor. The pyrimidine moiety might provide additional steric hindrance at the 2-position, while making the 3-position a kinetically more favored reaction site, and at the same time electronic modification derived from the attached pyrimidine motif might also be involved.

**Scheme 2.44.** Co(II)-catalyzed C3-acyloxylation of indoles (Liu, Liu and co-workers, 2018).

*Liu & Liu et al., 2018:*

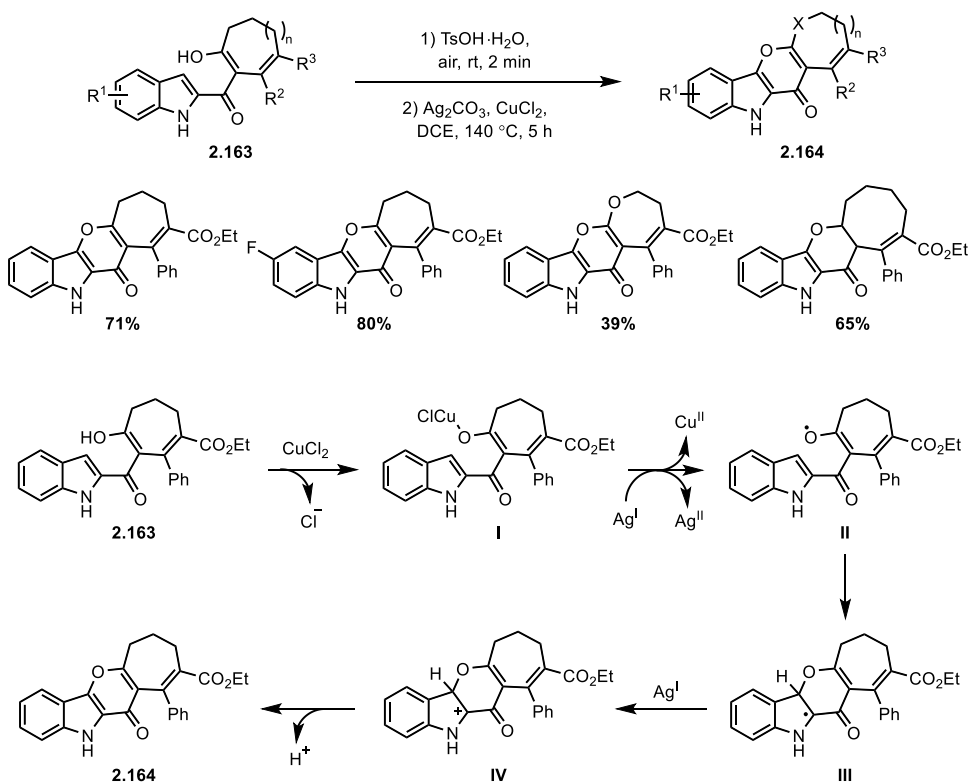


The new protocol to access pyrano[3,2-b]indoles reported by the Li group was also mechanistically explained as radical addition to 2,3  $\pi$  bond of neutral indole moiety (Scheme

2.45).<sup>58</sup> The reaction is initiated from the enol tautomer of the 1,3-dicarbonyl **2.163** reacting with the  $\text{CuCl}_2$ . O-radical **II** is then generated from the *in situ* generated complex **I** by aid of copper catalyst and silver oxidant. The molecular structure of the substrate **2.163** is designed in such a way that the generated O radical is accessible exclusively at the 3-position, while undesired C2-addition is prevented in advance. Thus, the O-radical is intramolecularly added at the 3-position of **II** and the yielded radical intermediate **III** undergoes additional oxidation followed by deprotonation to provide desired product **2.164**.

**Scheme 2.45.** Synthesis of pyrano[3,2-b]indoles via selective C3-radical addition (Li and co-workers, 2021).

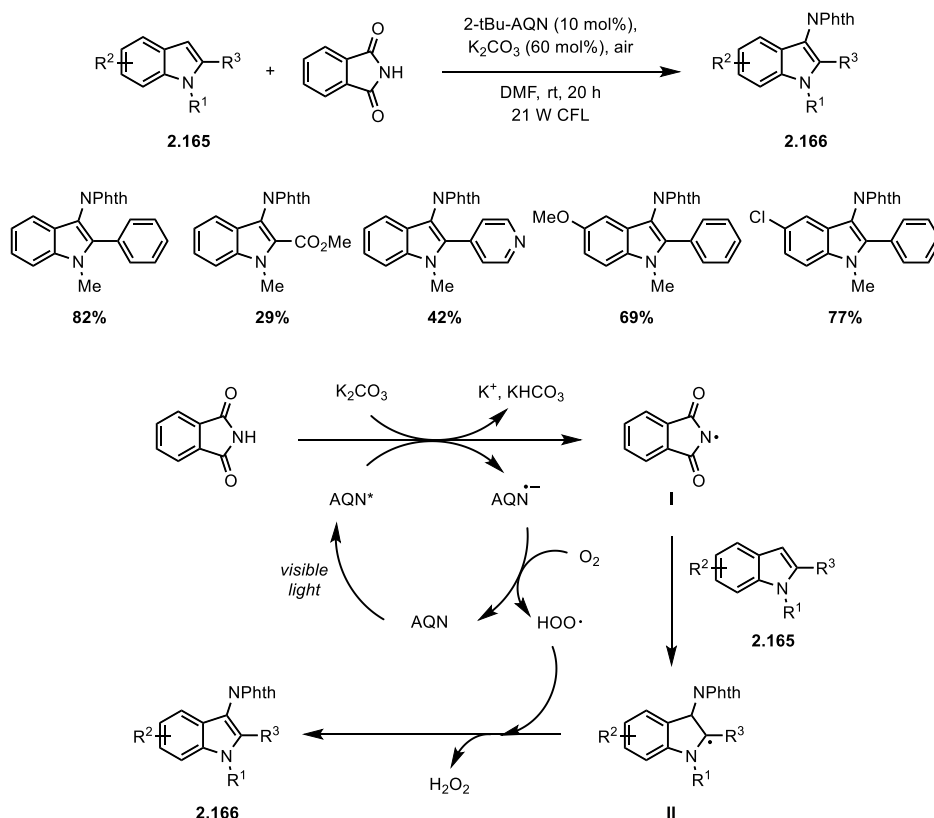
*Li et al., 2021:*



In 2017, the Itoh group achieved C3-amidation of indoles via catalytic formation of N-centered radical under organo-photocatalytic conditions (Scheme 2.46).<sup>59</sup> Initially, the N-centered radical **I** is formed from phthalimide via SET to AQN\*. The resulted radical species **II** adds to indole derivative **2.165** to generate intermediate **II**, which would undergo one-electron oxidation and aromatization to furnish **2.166**. On the other hand, AQN•- resulted from SET is oxidized to AQN by molecular oxygen, which is then converted by visible light to AQN\* to complete the catalytic system. The C3-regioselectivity is presumably due to the steric effect induced by the substituent at the 2-position, and addition to the kinetically favored 3-position appears to occur rapidly.

**Scheme 2.46.** Aerobic C3-amidation of indoles via *in situ* formation of N-centered radical (Itoh and co-workers, 2017).

*Itoh et al., 2017:*



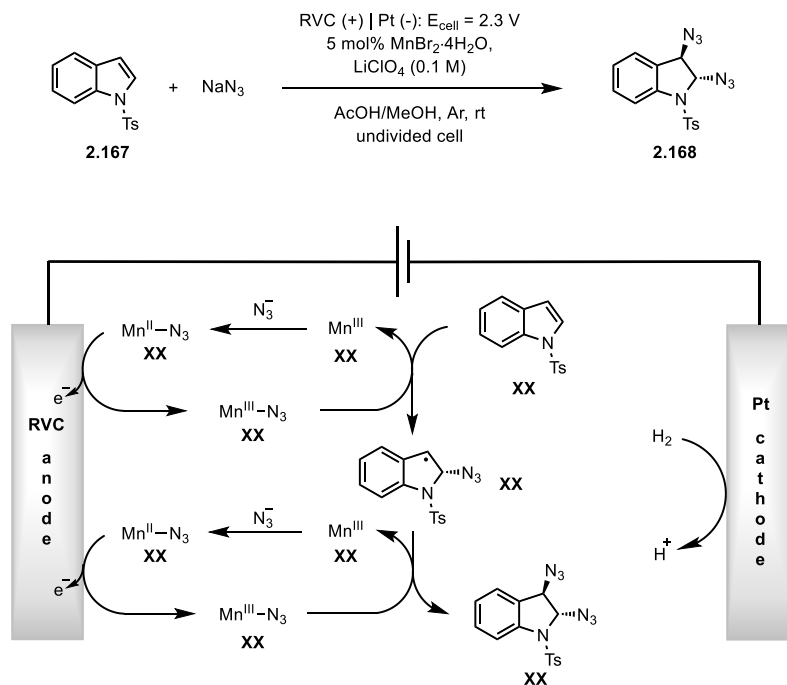
A method to realize the electrochemical 2,3-difunctionalization of indole by addition of an electrochemically generated radical species to indole was first observed by the Lin group in

2017 (Scheme 2.47).<sup>60</sup> Although the reaction is not designed to selectively induce regioselectivity, the thermodynamic approach unravels the reaction mechanism leading to the formation of a C3-benzylic radical, which is worth discussing in the dedicated section.

The main essence of the mechanism is the double addition of the azidyl radical to the indole via Mn-catalyzed radical transport. Great emphasis was placed on the role of the Mn catalyst, which has been instrumental in the production of azidyl equivalents in the form of Mn(III)-N<sub>3</sub> to preserve the radical properties required to induce desired addition while reducing other side reactions such as dimerization.

**Scheme 2.47.** Electrochemical 2,3-diazidation of indole via Mn catalysis (Lin and co-workers, 2017)

*Lin et al., 2017:*

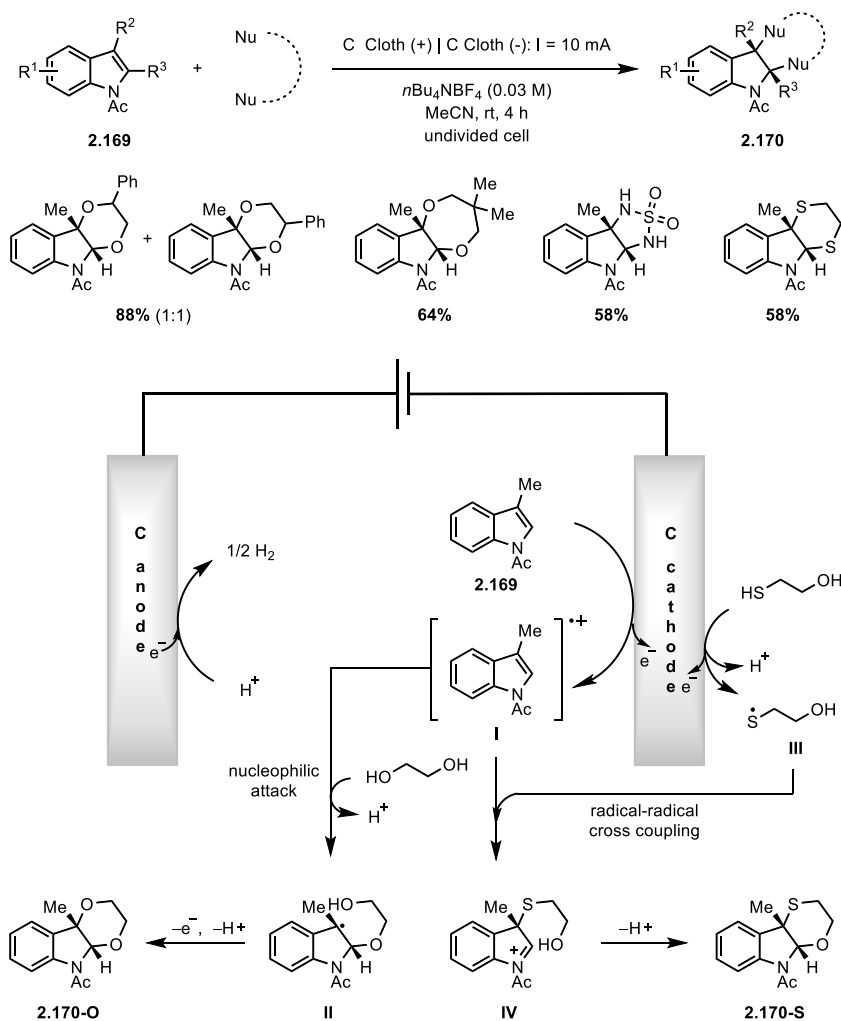




In 2020, another 2,3-difunctionalization method of indole under electrochemical conditions was discovered by the Lei group. The corresponding work by the Lei group is synthetically comparable to earlier work by Lin in terms of the product, but the reaction is elucidated from slightly different mechanistic aspects (Scheme 2.48).<sup>61</sup> Indole, previously reported in Lin's work to be inert to both anodic oxidation and cathodic reduction, is oxidized to the indole radical cation **I** under the newly modified electrochemical conditions. The coupling of the resulting radical cation **I** with the nucleophile occurs in two possible ways, depending on which dinucleophile is introduced in the reaction.

**Scheme 2.48.** Electrochemical 2,3-difunctionalization of indole with bis-nucleophile (Lei and co-workers, 2020)

Lei et al., 2020:



If both nucleophilic sites are derived from oxygen atoms, *i.e.*, ethane-1,2-diol, the indole radical cation **I** preferentially undergoes nucleophilic addition with the coupling partner to form a new bond at the C2-position to yield radical intermediate **II**. The site selectivity is thought to arise from the preference of the indole radical cation **I** as a C3-benzyl radical bearing an iminium ion rather than as an N-centered radical cation. Thereafter, additional oxidation is applied to the C3-benzyl radical to generate a cation, completing the product **2.170-O** by intramolecular cyclization.

When a mercaptan-containing nucleophile is adopted, *i.e.*, mercaptoethanol or dithiol, the indolyl radical cation **I** is converted to the iminium ion **III** via radical cross-coupling at the 3-position followed by iminium capture with the internal nucleophile to furnish indoline **2.170**. In contrast to the previous example in which the C-radical of the phenol is selectively added to the 2-position of indole radical cation (*vide supra*, Scheme 2.39), the selective radical addition occurs to the 3-position if the coupling partner contains a mercapto group. This is the unique regioselectivity observed also in the previous radical addition cases that the hetero-radical and the C-centered radical prefer different addition sites in indole.

## 2.2. Development of C3-Hetero-Functionalization of Indole via [3,3]-Sigmatropic Rearrangement of *N*-Hydroxyindole

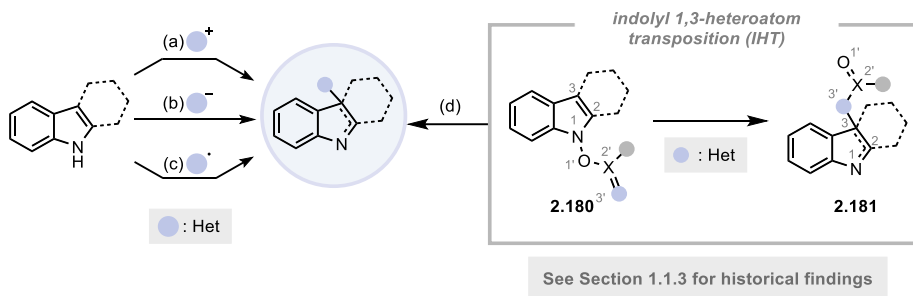


**Figure 2.7.** Synthetic strategies for the C3-hetero-functionalization.

In the previous section (*vide supra*, Section 2.1), we discussed the importance of the C3-heterofunctionalized indole derivatives and the synthetic methods to access such compounds. In the rich history of their synthetic development, the vast majority of approaches have relied on the intrinsic nucleophilicity of indole at the 3-position to react with an electrophilic source of heteroatoms (Figure 2.7, (a)). More recently, alternative strategies that exploit the nucleophilic sources of heteroatoms under oxidative conditions (Figure 2.7, (b)) or radical precursors (Figure 2.7, (c)) have emerged as useful toolkits to embellish the indolyl framework. Despite these remarkable advances, however, general access to all three types of products, *i.e.*, A-C, has yet to be established, primarily because of the highly reactive nature of the products and the chemical compatibility of the reagents used for the preparation of each type of product.

An entirely orthogonal approach that can address these synthetic challenges is the indolyl 1,3-heteroatom transposition (**IHT**, Figure 2.7, (d), See Section 1.1.3 for historical findings). This method can be termed as a [3,3]-sigmatropic rearrangement type reaction, in which the labile N–O bond provides a significant driving force for the desired transformation.<sup>62</sup> The methodological importance of this reaction lies in the ability for highly regioselective bond formation in the 3-position and potential as a unified platform for the introduction of different heteroatoms in the 3-position, since the indolyl precursors **2.180** with different heteroatomic

components in the 2'-position are readily accessible from *N*-hydroxyindole. These significant advantages have demonstrated that the field of **IHT** can be a valuable synthetic tools. The accompanying disruption of aromaticity, however, sometimes requires harsh reaction conditions. Considering this deficit, The advancement of **IHT** chemistry with a new activation mode is crucial to the pursuit of a practical protocol of C3-hetero-functionalization. Given our goal of developing an unified strategy that would allow the synthesis of various C3-hetero-functionalized indole derivatives, we focused on developing an activation strategy to lower the overall activation energy of the reaction, so as to overcome the major limitation *i.e.*, harsh reaction condition, which impede the further application.

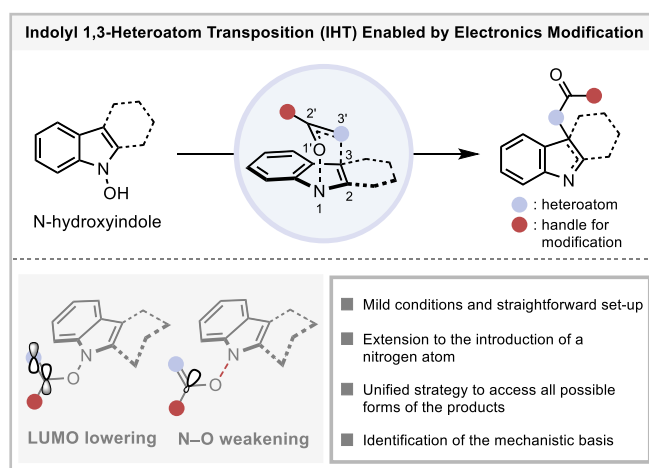


**Figure 2.8.** Design principle for the facilitated indolyl 1,3-heteroatom transposition (**IHT**).

Although the mechanism of the **IHT** reaction has not been systematically surveyed, analogous rearrangements of *N*-oxyenamines have historically been viewed as symmetry-allowed [3,3]-sigmatropic rearrangement.<sup>62</sup> The Bartoli indole synthesis, one of the most famous examples of this rearrangement, clearly demonstrates such mechanism. Therefore, it was envisioned that the general rate-enhancing elements of the concerted pericyclic process should improve the synthetic efficiency of the targeted rearrangement process (Figure 2.8). Specifically, the established substituent effect at the 2- or 2'-position of the system, either through radical stabilization or electronic induction, was recognized as an attractive means of promoting the bond reorganization from the *N*-hydroxyindole derivatives.<sup>63</sup> Furthermore, the proposed weakening of the N–O bond by a neighboring functional group should help

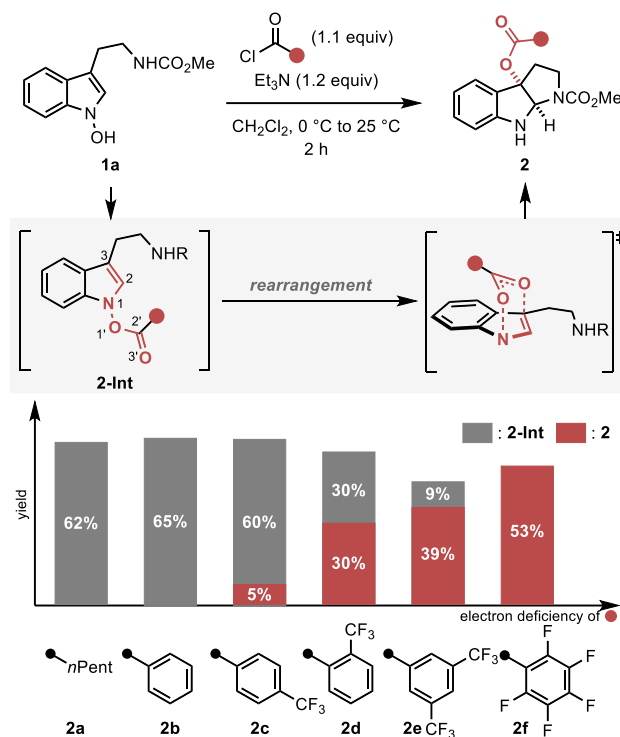
lower the activation barrier of the rearrangement reaction.<sup>64</sup> Overall, it was envisaged that the functional modification of the 2'-position of the *N*-hydroxyindole system should be the key to solving the synthetic problems by accelerating the desired rearrangement.

Herein, we report a general dearomative strategy for the introduction of a heteroatom at the 3-position of an indole via the **IHT** process, which is enabled by the facilitated rearrangement of *N*-hydroxyindole derivatives. By applying the substituent-based rate-enhancement protocol, all possible forms of the oxygenated products can be conveniently accessed via *in situ* generated indolyl ester intermediates. Moreover, an extension of the strategy allowed the introduction of a nitrogen atom to produce classes of products that could not be accessed using the classical reactivity. In contrast to conventional approaches, the method obviates the use of synthetically nonideal reaction conditions, such as extreme reaction temperature and/or the use of a large excess of reagents, thereby greatly expanding the applicability of the strategy. Finally, in-depth studies were carried out to identify the unique mechanistic basis of the facilitated **IHT** reaction.

### 2.2.1. Initial Findings and C3-Acyloxylation of Indole Scaffolds

To evaluate our hypothesis of reaction facilitation via substituent modification at 2'-position, the *N*-hydroxytryptamine derivative (**1a**) was subjected to the room temperature rearrangement reaction via acylation with carboxylic acids possessing different electronic properties (Scheme 2.49). When the *n*-hexanoic acid (**2a**) or unsubstituted benzoic acid (**2b**) was used as the coupling partner, only the direct O-acylation products were obtained as the product. The products could be isolated and purified by silica gel column chromatography, and independent thermal activation of the acylation intermediates revealed that extensive heating was required to initiate the rearrangement process. However, as the arene portion of the acyl donor becomes more electron-deficient, the rearrangement products begin to form as a mixture with the acylation intermediate (**2c-2e**). Ultimately, the use of pentafluorobenzoic acid furnished the rearrangement product as an exclusive product of the reaction in 53% yield (**2f**).<sup>65</sup> The result clearly demonstrates the strong correlation of the reaction efficiency with the electron deficiency of the substituent at the 2'-position.

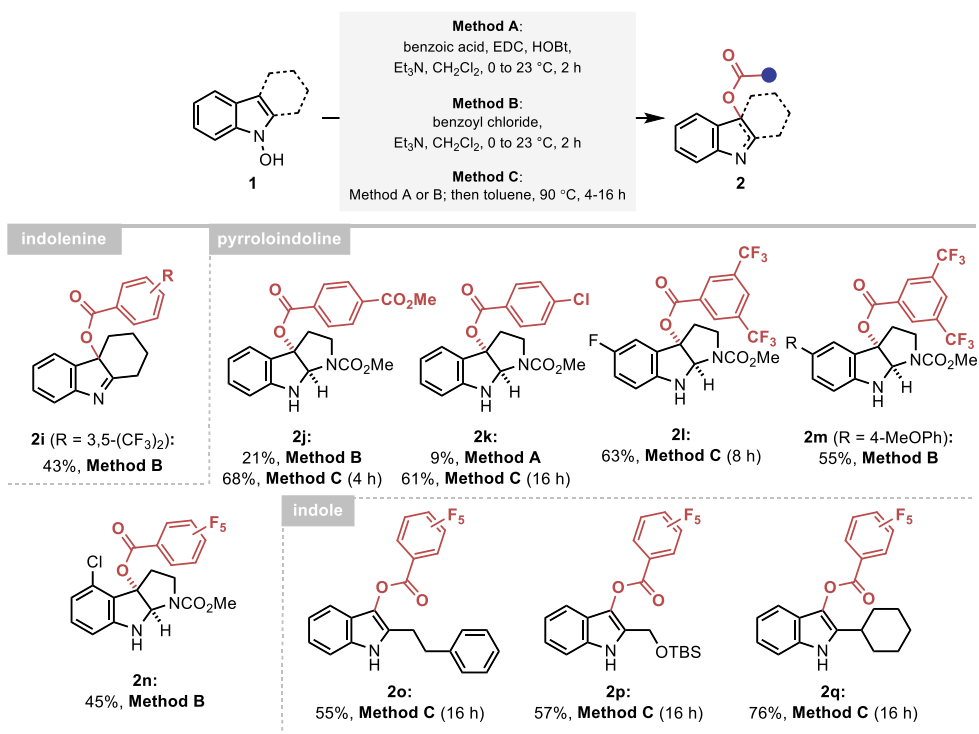
**Scheme 2.49.** Initial finding of electronic effect in facilitating the [3,3]-sigmatropic rearrangement in indolyl ester system.



<sup>a</sup>Reactions performed with benzoyl chloride (1.1 equiv) and Et<sub>3</sub>N (1.2 equiv) in CH<sub>2</sub>Cl<sub>2</sub> (0.05 M) at 0 °C to rt for 2 h on 0.1–0.3 mmol scale. Yields of the isolated product are reported and the ratio of **2-Int** and **2** was determined by <sup>1</sup>H NMR.

The optimized reactivity could be utilized as an efficient synthetic platform to provide the functionalized products in all possible forms, *i.e.*, indole, indolenine, and indoline (Scheme 2.50). In contrast to conventional approaches, the use of a large excess of the acylating reagent and/or harsh thermal activation was not required. A delicate indolenine product could be smoothly formed at ambient temperature (**2i**). Also, various pyrroloindolines could be obtained using the developed method (**2j-2n**). In agreement with our mechanistic proposal, however, higher reaction temperature was required for electronically under-activated cases (**2j-2l**). In addition, the formation of 3-acyl indole products containing a range of C2 substituents, including primary and secondary alkyl groups, could be realized in a highly straightforward manner (**2o-2q**). It should be noted that an identical reaction with an acetyl or benzoyl group failed to yield the 3-acyl indole products, indicating the importance of electronic activation at the 2'-position (See SI for details).

**Scheme 2.50.** Substrate Scope of C3-acyloxylation.<sup>a</sup>

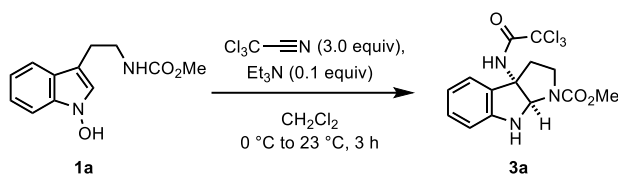


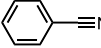
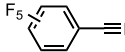
<sup>a</sup>**Method A:** Reactions performed with benzoyl chloride (1.1 equiv) and Et<sub>3</sub>N (1.2 equiv) in CH<sub>2</sub>Cl<sub>2</sub> (0.05 M) at 0 °C to rt for 2 h on 0.1–0.3 mmol scale. **Method B:** Reactions performed with benzoic acid (1.0 equiv), EDC·HCl (1.1 equiv), HOBT (1.1 equiv) and Et<sub>3</sub>N (2.2 equiv) in CH<sub>2</sub>Cl<sub>2</sub> (0.05 M) at 0 °C to rt for 2 h on 0.2–0.6 mmol scale. **Method C:** Reactions performed via **Method A** or **B** at rt for 16 h on 0.1–0.7 mmol scale. After filtration through silica gel, the solvent was exchanged to toluene (0.05 M) and the system was heated to 90 °C. Yields of the isolated product are reported. EDC·HCl= 1-ethyl-3-(3-dimethylaminopropyl)-carbodiimide hydrochloride, HOBT= 1-hydroxybenzotriazole.

## 2.2.2. C3-Amidation of Indole Scaffolds

The results obtained from the accelerated oxygenation reaction led us to the new hypothesis that an identical inductive rate enhancement strategy can facilitate other types of rearrangements in the indolyl frameworks. Thus, we next tried to extend the developed strategy to the introduction of a nitrogen atom at the 3-position of indole via **IHT** process. A summarized outline of the optimization for C3-amidation is depicted in Table 2.1.

**Table 2.1.** Optimization of C3-amidation.<sup>a</sup>



entry	variation from optimized condition	yield of <b>3a</b> <sup>b</sup>
1	none	78%
2	 instead of $\text{Cl}_3\text{C}-\text{C}\equiv\text{N}$	0%
3	 instead of $\text{Cl}_3\text{C}-\text{C}\equiv\text{N}$	0%
4	DBU instead of $\text{Et}_3\text{N}$	70%
5	pyridine instead of $\text{Et}_3\text{N}$	<5%
6	1.0 equiv $\text{Et}_3\text{N}$	37%
7	1.0 equiv $\text{Cl}_3\text{C}-\text{C}\equiv\text{N}$	36%
8	2.0 equiv $\text{Cl}_3\text{C}-\text{C}\equiv\text{N}$	55%
9	4.0 equiv $\text{Cl}_3\text{C}-\text{C}\equiv\text{N}$	48%
10	THF instead of $\text{CH}_2\text{Cl}_2$	4%
11	$23\text{ }^\circ\text{C}$ instead of $0\text{ }^\circ\text{C}$ to $23\text{ }^\circ\text{C}$	67%

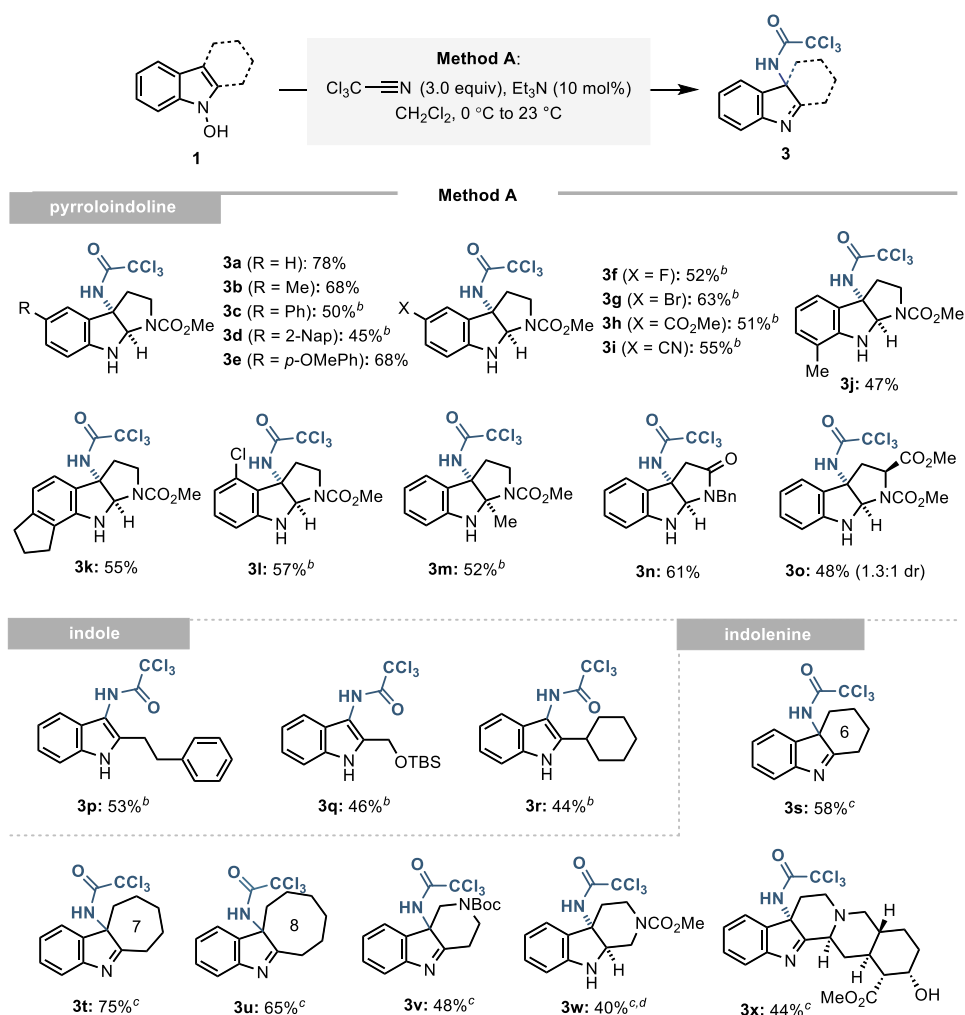
<sup>a</sup>Reactions performed with nitrile reagent (3.0 equiv) and base (0.1 equiv) in solvent (0.05 M) at indicated temperature on 0.5 mmol scale. <sup>b</sup>Yields of the isolated product are reported. DBU= 1,8-diazabicyclo(5.4.0)undec-7-ene, THF= tetrahydrofuran.

Direct extension with unsubstituted benzonitrile or electron deficient benzonitrile derivatives, such as pentafluorobenzonitrile, failed to provide the desired product, presumably due to insufficient nucleophilicity of the *N*-hydroxyindole to initiate the formation of the imidate intermediate (entries 2 and 3). After extensive investigations, it was identified that the trichloroacetimidate system, which can be readily accessed by reaction of the *N*-hydroxyindole precursor with trichloroacetonitrile, is an excellent embodiment of the



envisioned strategy. In addition to the choice of trichloroacetonitrile as a suitable nitrogen source, other reaction parameters were further optimized. Using a catalytic amount of triethylamine as the base was critical to achieve the best performance in the overall reaction (entries 4-6). Also, the use of three equivalents of the trichloroacetonitrile was the most desirable (entries 7-9). Lastly, the identification of a suitable solvent system and reaction temperature completed the optimal reaction conditions (entries 10-11).

**Scheme 2.51.** Substrate scope of C3-amidation of indole derivatives.<sup>a</sup>



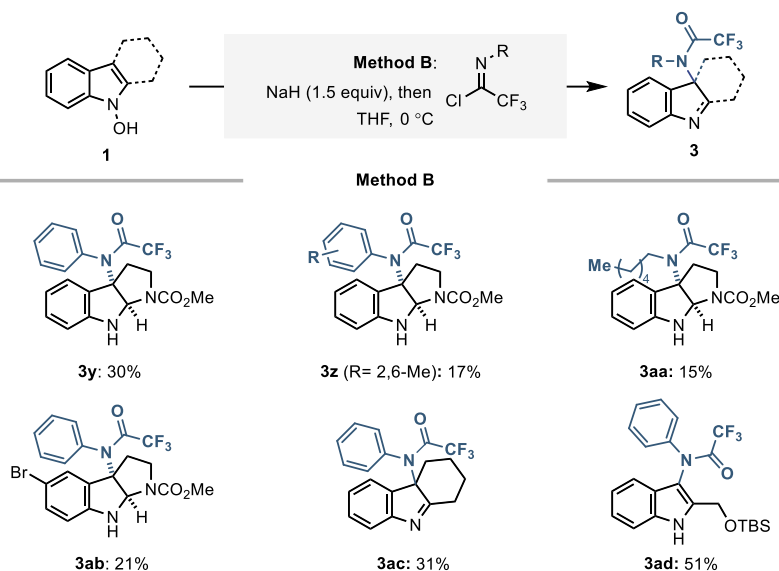
<sup>a</sup>**Method A:** Reactions performed with trichloroacetonitrile (3.0 equiv) and  $\text{Et}_3\text{N}$  (0.1 equiv) in  $\text{CH}_2\text{Cl}_2$  (0.05 M) at 0 °C to 23 °C for 3 h on 0.1–0.7 mmol scale. <sup>b</sup>The reaction performed with trichloroacetonitrile (3.0 equiv) and  $\text{Et}_3\text{N}$  (0.1 equiv) in DCE (0.05 M) at 23 °C to 90 °C for 2 h on 0.1–0.3 mmol scale. <sup>c</sup>Reactions performed at 0 °C instead of 0 °C to 23 °C. <sup>d</sup>Yield of the isolated product after reduction with  $\text{NaBH}_4$  in MeOH. Yields of the isolated product are reported.

The related 1,3-allylic O/N transposition reaction using the trichloroacetimidate intermediate, originally reported by Overman, has been utilized as a preferred method for preparing allylamines and their derivatives.<sup>66</sup> The reaction has been classically identified as a [3,3]-sigmatropic rearrangement and usually requires extensive heating or transition-metal catalysis to accomplish a reasonable level of synthetic efficiency. In our aza-allylic O/N transposition in the indolyl framework, however, the rearrangement process could be mediated in an extremely efficient fashion without any external assistance at ambient temperature.

With the optimized conditions in hand, the applicability of the reaction was assessed (Scheme 2.51). First, starting from *N*-hydroxytryptamines, preparation of a diverse array of functionalized pyrroloindolines with a nitrogen substituent at the 3-position was demonstrated (**3a-3m**). Functional groups with varying electronic properties could be installed at 5-position of the indole framework without diminishing the synthetic efficiency (**3a-3i**). Also, various substituents at 4-, 6-, or 7-position were also tolerated (**3j-3l**). Of note, synthetically convertible functional handles, such as halogen atoms, could be installed to allow future diversifications (**3g, 3l**). Interestingly, when the indole skeleton contains a substituent with an electron-withdrawing nature (**3f-3i**) or a steric congestion near the reaction center (**3m**), mild thermal activation was required to achieve full conversion of the starting material. Finally, the interception of the initially formed imine intermediate could be realized by a pendant amide (**3n**) or a substituted carbamate (**3o**).

Expanding the scope of the developed reaction to indole scaffolds without an internal nucleophile provided a new opportunity to access the unexplored structural diversity. 3-Amidated indoles could be conveniently synthesized by aid of the developed strategy (**3p-3r**). Of particular interest is that the developed method could be utilized to furnish indolenine products containing a sensitive C=N bond. Tricyclic indolenines with various carbocycles or with a piperidine ring were also formed in a highly straightforward manner (**3s-3v**). The *in situ* addition of a hydride nucleophile was also achieved to provide a hexahydropyridoindole structure (**3w**). Finally, the method was applied to the diversification of a complex natural product, *i.e.*, yohimbine, without the use of protecting groups, demonstrating the synthetic robustness of the strategy (**3x**).<sup>67</sup>

**Scheme 2.52.** Substrate scope of C3-amidation of indole derivatives.<sup>a</sup>



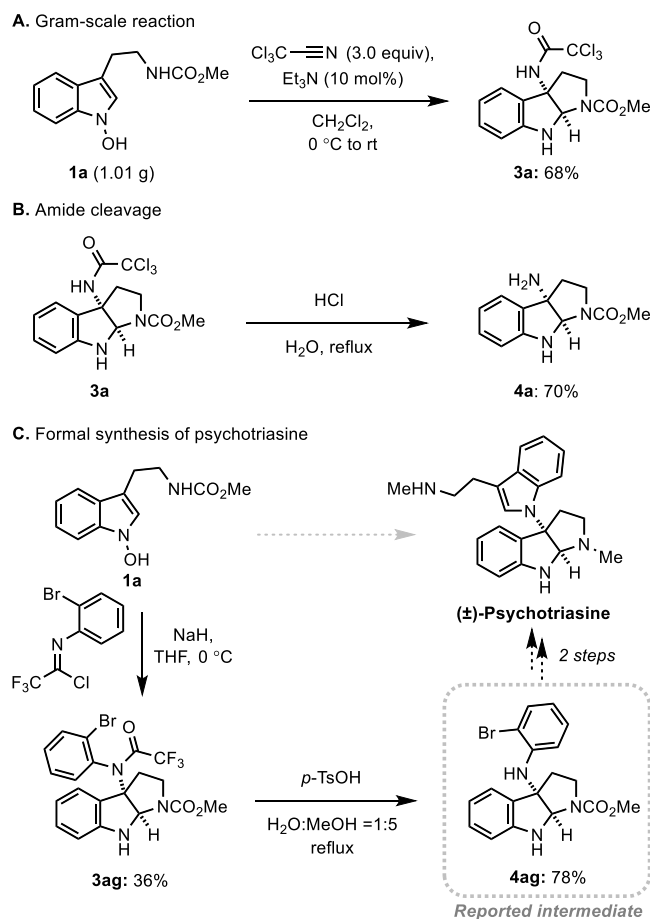
<sup>a</sup>**Method B**: Reactions performed with imidoyl chloride (1.5 equiv), NaH (1.5 equiv) in THF (0.05 M) at 0 °C on 0.3~1.2 mmol scale. Yields of the isolated product are reported.

An even higher level of structural diversity could be attained using trifluoroimidoyl chloride as a coupling partner (Scheme 2.52). The presence of an even more electron-withdrawing trifluoromethyl group enabled the installation of an additional carbon-based substituent at the C3-nitrogen atom. The phenyl group and the sterically demanding 2,6-dimethyl phenyl group could be appended to the nitrogen substituent of the pyrroloindoline products (**3y**, **3z**). Also, an aliphatic alkyl chain, such as a *n*-hexyl group, was able to be attached to the product (**3aa**). The reaction could also be accomplished in the presence of the electron-withdrawing substituent on the 5-position of indole (**3ab**). Finally, an identical diversity amplification strategy was applied to the preparation of indolenine (**3ac**) and indole structures (**3ad**).

Next, we assessed the practicality of the developed method (Scheme 2.53). First, the reaction scale was conveniently increased to the gram-scale without a significant loss of efficiency, demonstrating the robustness of the system (Scheme 2.53A). Also, the conversion of the trichloromethyl acetamide to the corresponding amine was realized in a single step via simple acidic hydrolysis, allowing for future conversion to a variety of amine derivatives (Scheme 2.53B). Finally, the preparation of a key intermediate for the alkaloid natural

product psychotriazine was achieved in a highly convergent way (Scheme 2.53C). Starting from the *N*-hydroxyindole **1a**, the introduction of nitrogen atom at 3-position, the pyrroloindoline formation, and the installation of *ortho*-bromo phenyl group was achieved in a single step. After straightforward removal of the trifluoroacetamide group, the key intermediate for psychotriazine could be accessed.<sup>22,33,48,68</sup>

**Scheme 2.53.** Practicality and versatility of the amidative IHT reaction.



### 2.3. Mechanistic Considerations

Over the last decades, the mechanism of the [3,3]-sigmatropic rearrangement has been extensively investigated using various experimental and computational methods.<sup>69</sup> Consequently, the mechanism of the related 1-aza-1'-oxa Cope rearrangement has been revealed in a number of systems by virtue of several pioneering studies.<sup>62,70</sup> However, no comprehensive studies on the rearrangement of the *N*-hydroxyindole skeleton have been performed to date. Due to the unique electronic nature of the *N*-hydroxyindolyl framework as well as the involvement of a dearomatization process during the reaction, we speculated that a special feature might be in action during the rearrangement reaction. Therefore, we systematically analyzed the mechanism for the **IHT** reaction.

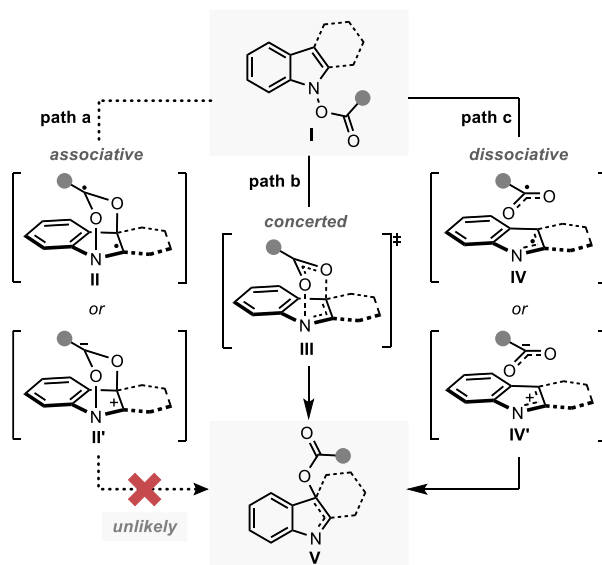


**Figure 2.9.** Mechanistic possibilities for indolyl 1,3-heteroatom transposition reaction.

The plausible mechanism of the transformation from the acyl or imidoyl *N*-hydroxyindole starting material (**I**) to the rearrangement product (**V**) can be divided into three different pathways (Figure 2.9).<sup>71</sup> First, a mechanism involving the early formation of the C–X bond to afford either a diradical (**II**) or a zwitterionic (**II'**) intermediate could be conceived (path **a**, associative mechanism). Alternatively, a classical pathway was postulated in which C–X bond formation and N–O bond cleavage occur in a concerted manner without forming any

intermediates (path **b**, concerted mechanism). The last possibility proceeds through the initial cleavage of the N–O bond of the starting material (**I**), and the subsequent formation of intermediates in the form of either a radical pair (**IV**) or an ion pair (**IV'**) (path **c**, dissociative mechanism). Of the three major candidates, the associative pathway (path **a**) is highly unlikely, considering the lability of the N–O bond (~57 kcal/mol) compared to that of the newly formed C–X bond (X=O, N; 69-91 kcal/mol).<sup>72</sup> In fact, the cleavage of the weak N–O bond is one of the major driving forces of the overall transformation in related systems, supported by computational analysis.<sup>73</sup> Accordingly, we assessed the mechanism with special emphasis on the concerted (path **b**) and the dissociative (path **c**) mechanism.

### 2.3.1. Mechanistic Insights I: <sup>18</sup>O-Labeling Studies

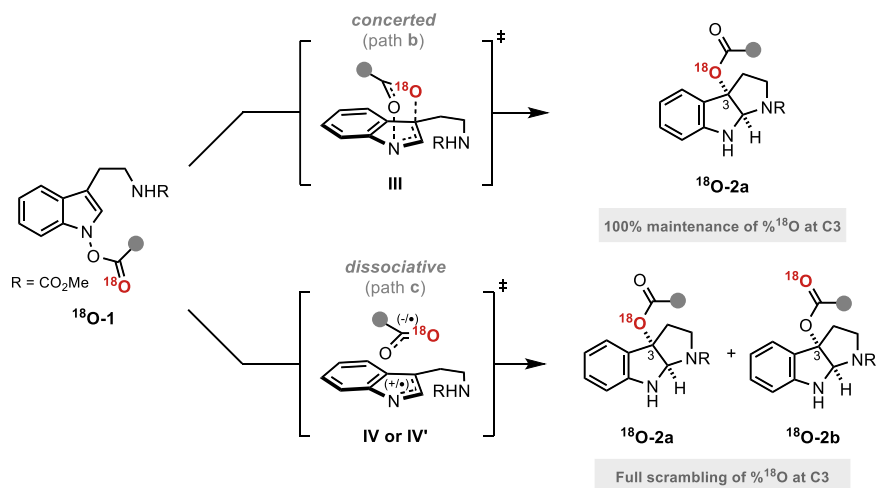


**Figure 2.10.** Projected migration of <sup>18</sup>O isotope during the IHT.

Our mechanistic investigation was initiated with the isotope labeling studies of the carbonyl oxygen on the acyl *N*-hydroxyindoles with the <sup>18</sup>O atom (Figure 2.10). With the position-specific placement of the <sup>18</sup>O atom through acylation with the isotopically enriched acyl donor, the intervention of a specific pathway can be traced (Figure 4, A).<sup>74</sup> While the involvement of the concerted pathway should result in exclusive <sup>18</sup>O migration to the 3-position of pyrroloindoline (**18O-2a**), the involvement of the dissociative pathway should produce a mixture of products **18O-2a** and **18O-2b** in which the <sup>18</sup>O labeling is evenly distributed between the C3-oxygen and the carbonyl oxygen.

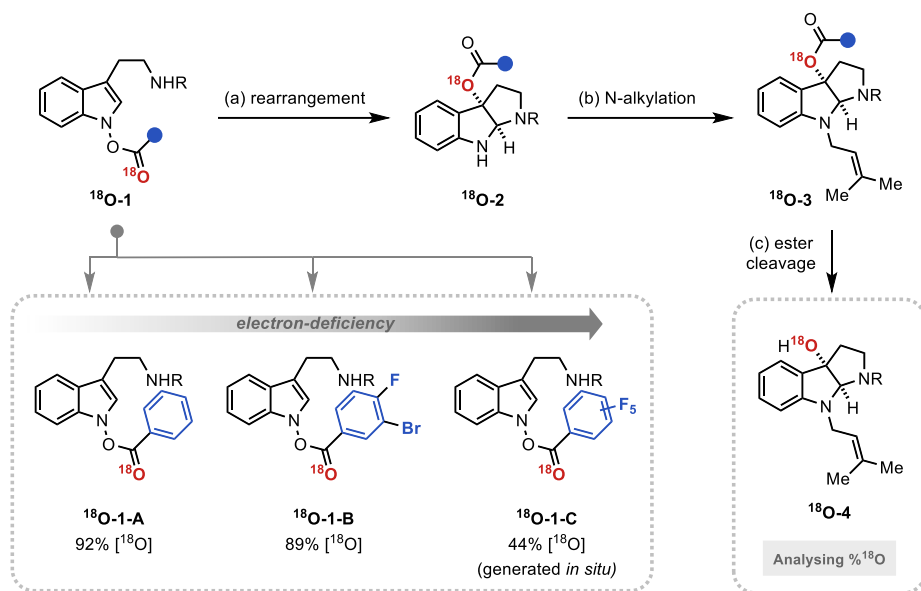


**Figure 2.11.** Experimental design for  $^{18}\text{O}$  labeling experiment.

Based on these assumptions, a series of  $^{18}\text{O}$ -enriched indolyl benzoates with different electron-withdrawing capacities were prepared (Figure 2.11). Benzoates with a phenyl group ( $^{18}\text{O-1-A}$ ), a 3-bromo-4-fluorophenyl group ( $^{18}\text{O-1-B}$ ), and a pentafluorophenyl group ( $^{18}\text{O-1-C}$ ) were independently exposed to the synthetically relevant rearrangement reaction conditions for each precursor. The products subsequently underwent *N*-alkylation and ester cleavage to furnish 3-hydroxypyrroloindoline products  $^{18}\text{O-4}$ , which were subjected to HRMS analysis to determine the degree of  $^{18}\text{O}$  enrichment.

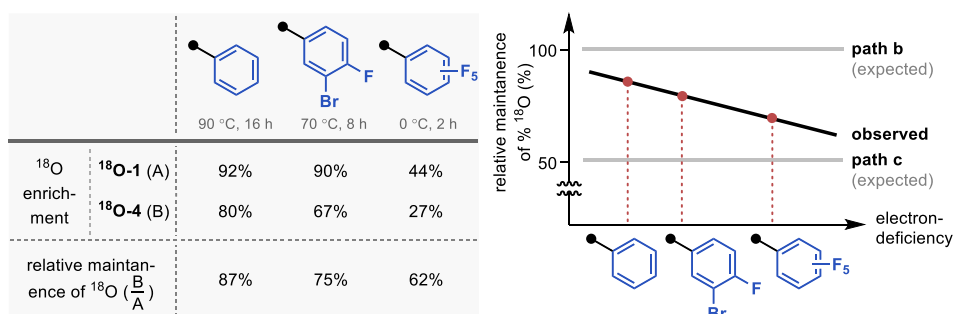


**Figure 2.12.** Result of the  $^{18}\text{O}$  labeling experiment and the influence of electronic property.

The experimental results revealed a number of unique features of the rearrangement process (Figure 2.12). Most importantly, the rearrangement reactions featured a non-zero, but

at the same time only partial conservation with respect to the position of the  $^{18}\text{O}$  labeling. The expected complete maintenance (**path b**) or full scrambling (**path c**) of  $^{18}\text{O}$  was not observed in any tested cases. Based on the report that even the most asynchronous concerted pathway exhibits complete preservation of the isotopically labeled atom during the analogous rearrangement process, the contribution of a single border-line mechanism cannot explain the observed experimental outcome.<sup>75</sup> Thus, the isotope labeling experiment indicates the involvement of at least two independent reaction mechanisms, one of which induces a position-specific delivery of the oxygen atom (**path b**) and another which leads to complete scrambling of the position (**path c**).

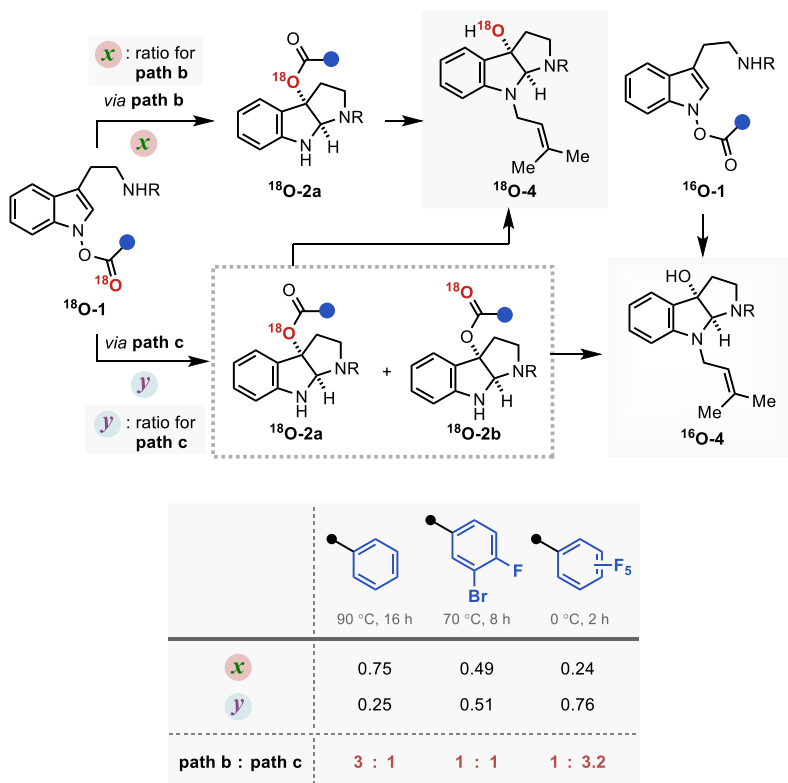


**Figure 2.13.** Definition of  $x$ ,  $y$  and schematic explanation for the calculation of the mechanistic ratio.

The second and even more remarkable characteristics of the rearrangement process were identified on the basis of a quantitative analysis of the degree of  $^{18}\text{O}$  labeling. Assuming **path b** and **path c** are primarily operating for the **IHT** process, the relative contribution of each



pathway was determined (Figure 2.13). The formation of  $^{18}\text{O-4}$  is attributed to the action of **path b** from  $^{18}\text{O-1}$  in total, and half the participation of **path c** from the identical starting material. The other half of the involvement of **path c** from  $^{18}\text{O-1}$ , along with the rearrangement from  $^{18}\text{O}$ -free starting material,  $^{16}\text{O-1}$ , generates the unlabeled oxygenation product  $^{16}\text{O-4}$ . With the relative degrees of participation for **path b** and **path c** denoted as  $x$  and  $y$ , respectively, the ratio of  $x:y$  could be derived from the ratio of  $^{18}\text{O-4}$  and  $^{16}\text{O-4}$  in the final product (See the SI for details). As a result, the contribution of each pathway to the overall reaction could be expressed as a numerical term. The calculated values revealed that the contribution of each pathway was directly affected by the electronic nature of the substituent at the 2'-position. As benzoate became more electron deficient, a greater level of isotope mixing was observed, indicating that the dissociative pathway (**path c**) predominates. More importantly, the major pathway that dominantly contributed to product formation changed from the pericyclic pathway (**path b**) to the stepwise pathway (**path c**). It is believed that the inductive stabilization of the fragment pair is responsible for the observed preference, although the exact structural identity of the pair is unclear at this point. Also, kinetic facilitation through the weakening of the N–O bond during the formation of the fragment pair (**path c**) could be particularly more effective than that in the pericyclic process.

The observed mechanistic duality in our **IHT** is particularly notable in several aspects. The idea of the participation of multiple types of mechanisms in a [3,3]-sigmatropic rearrangement has been introduced since the pioneering contributions of Houk, Doering, and Gajewski.<sup>76</sup> The chameleonic character of the mechanism is expressed as a nature in which the single operating mechanism shifts from one type to another by the electronic perturbation of the system when the electronics of the substituents change. In our **IHT**, however, the overall transformation is supported by the coexistence of two independent mechanisms simultaneously, in which their weighted average can be shifted based on the effect of the electronics. Such a unique mechanistic duality of [3,3]-sigmatropic rearrangement has been reported only in a specially substituted O-benzoyl aniline *N*-oxides system, wherein the isotope scrambling pathway was detected as an insignificant side pathway that contributes minimally to product formation.<sup>70a-e</sup> In the current system, the special mechanistic duality is inherently present in general. Furthermore, either of the mechanistic pathways can be the

dominant pathway for product formation depending on the electronics of the substrate, suggesting that special engineering of the system could be possible.

The third and the final note regarding the observed characteristics is the overall rate enhancement. The change in the electronics at the 2'-position not only altered the composition of the contributing mechanism but also lowered the activation energy required for both pathways. While  $^{18}\text{O-1-A}$  is incapable of generating the rearrangement product at room temperature, the pentafluorophenyl variant  $^{18}\text{O-1-C}$  smoothly furnished the product with a 1:3 ratio of the concerted and stepwise mechanisms. Both processes could be operated at room temperature, indicating a significant reduction in the required activation energies. Therefore, facilitated product formation could be rationalized in both mechanistic pathways in action.

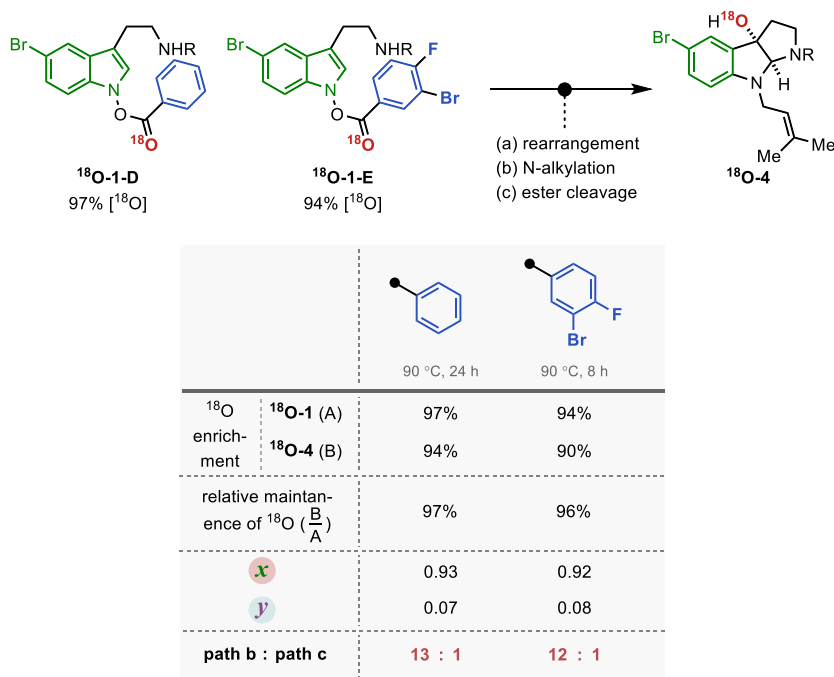


**Figure 2.14.** The influence of electronic distribution in indole scaffold.

Having the results of the electronic effect of the benzoyl group in hand, an electronic effect of the indole scaffold, the remaining reacting site other than benzoyl group in the substrate, was evaluated after replacement of *N*-hydroxytryptamine to the more electron-deficient 5-bromo-*N*-hydroxytryptamine (Figure 2.14).  $^{18}\text{O}$ -enriched benzoic acid and 3-bromo-4-fluorobenzoic acid were reacted with 5-bromo-*N*-hydroxytryptamine, respectively, and 3-

hydroxypyrrroloindoline products **<sup>18</sup>O-4-D** and **<sup>18</sup>O-4-E** were synthesized following the established procedures.

The change in <sup>18</sup>O enrichment level was clearly distinctive with that of the unsubstituted *N*-hydroxytryptamine variant. Comparing with the partial conservation of <sup>18</sup>O enrichment from 92% to 80% in case of unsubstituted indolyl benzoate (*vide supra*, Figure 2.12), 5-bromo-indolyl benzoate variant showed almost no loss of <sup>18</sup>O enrichment, maintaining 97% of its <sup>18</sup>O enrichment level to 94% after ester cleavage. This increased incorporation of <sup>18</sup>O isotope in 3-position clearly shows the significant suppression of the dissociative pathway (path **c**) and full involvement of concerted pathway (path **b**) in electron-deficient indole system.

Changing the benzoyl group to the more electron-deficient 3-bromo-4-fluorobenzoyl group couldn't affect the maintenance level of <sup>18</sup>O isotope during the **IHT** reaction when indole scaffold remains electron-deficient. 5-bromo-indolyl benzoate with 3-bromo-4-fluorophenyl group (**<sup>18</sup>O-1-E**) with 94% <sup>18</sup>O enrichment provided **<sup>18</sup>O-4-E** with 90% <sup>18</sup>O enrichment level. This result indicates that electronics of indole scaffold is undoubtedly important for the dissociative mechanism to occur. The rationale for the observed trend is consistent with the afore-established hypothesis from the shifting contribution of pathways affected by the electronics of the benzoyl group (*vide supra*, Figure 2.12, Figure 2.13 and the discussion thereof). The presence of the electron-withdrawing group in indole ring resulted in the lack of stabilization of indolyl fragment, thus presumably inhibited the formation of either a radical pair (**IV**) or an ion pair (**IV'**) intermediate.

The high energy barrier for the titled reaction in electron-deficient indole system is another example showing the importance of electronics of the substrate. Under the same reaction condition, 5-bromo indolyl benzoate **<sup>18</sup>O-1-D** needs much longer reaction time than unsubstituted indolyl benzoate **<sup>18</sup>O-1-A** to reach its full conversion, indicating the higher activation energy is involved. The electron-deficiency of the indole system increases the TS energy of the reaction in general, which is completely opposing effect with the effect of electron-deficiency in benzoyl group. In particular, the decreased ratio of the dissociative pathway (path **c**) implies that the increase in TS energy of the dissociative mechanism (path **c**) is significantly larger than that in TS energy of the concerted pathway (path **b**).

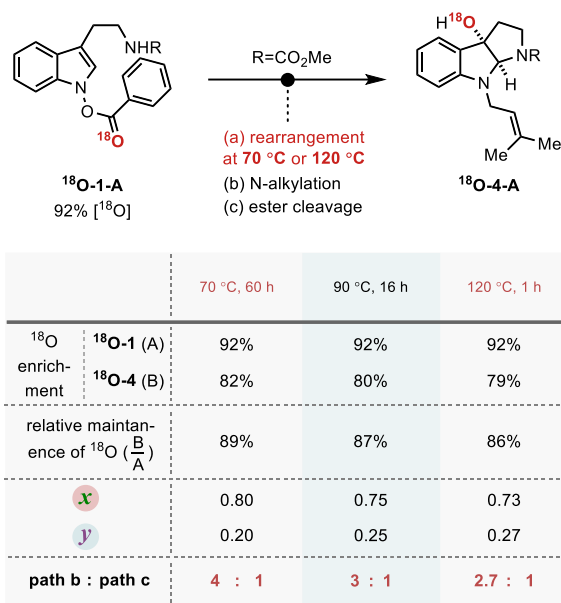


**Figure 2.15.** The influence of reaction temperature.

Additionally, the effect of reaction temperature on the mechanistic duality of the **IHT** reaction was examined (Figure 2.15). When precursor **<sup>18</sup>O-1-A** with 92% <sup>18</sup>O enrichment underwent the **IHT** reaction at 70, 90, or 120 °C, no significant change in the degree of <sup>18</sup>O scrambling was recorded. Only up to 3% difference in isotope enrichment, which translates to a change from 4:1 to 2.7:1 ratio between concerted and dissociative mechanism, was observed. These results indicate that the activation barriers for both mechanistic pathways undergo a similar level of modification as the reaction temperature changes within a given range. Of note, the slight increase in the degree of participation in the dissociative mechanism (**path c**) can be attributed to the greater entropic contribution at an increased reaction temperature.

### 2.3.2. Mechanistic Insights II: Additional Mechanistic Studies

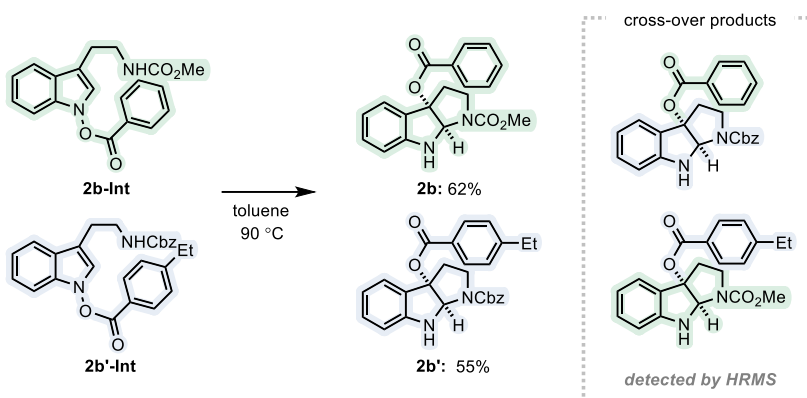


**Figure 2.16.** Crossover experiment.

Additional experiments were performed to further delineate the mechanistic details of the **IHT** reaction. First, a crossover experiment was conducted using **2b-Int** and **2b'-Int** (Figure 2.16). Under standard conditions, no appreciable amount of the crossover product was observed, as confirmed by the thin-layer chromatography (TLC) or  $^1\text{H}$  nuclear magnetic resonance (NMR) analysis using all four possible products, which were prepared independently. Only the rearrangement products **2b** and **2b'** were formed as major products, indicating that no significant crossover of fragments was accompanied during the reaction. However, thorough analysis of the reaction mixture using HRMS showed traces of both crossover products. The low abundance of the crossover product demonstrates the rapid recombination of dissociated fragments, either in the form of an ion pair or a radical pair, formed after N–O bond cleavage (**path c**).

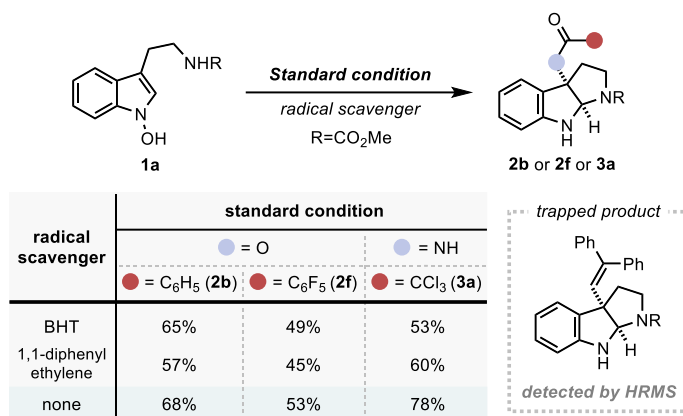


**Figure 2.17.** Radical-trapping experiment.

Subsequently, a series of trapping experiments were carried out in the presence of various radical scavengers to identify the nature of the fragments involved (Figure 2.17).<sup>77</sup> When *N*-hydroxytryptamine **1a** was subjected to the standard C–O or C–N bond-forming conditions, no significant decrease in the reaction yield was observed in the presence of a radical scavenger. Notwithstanding the sustained yield of the product, the presence of a radical intermediate was suggested by HRMS. When the C–O bond formation reaction of the benzoate precursor BHT was conducted together with 1,1-diphenylethylene, a small amount of the trapping product was detected based on HRMS analysis. Taken together, the formation of the radical pair that undergoes rapid recombination over diffusion is considered as a non-significant but existing contributing factor for the dissociative mechanism (**path c**).<sup>78</sup>

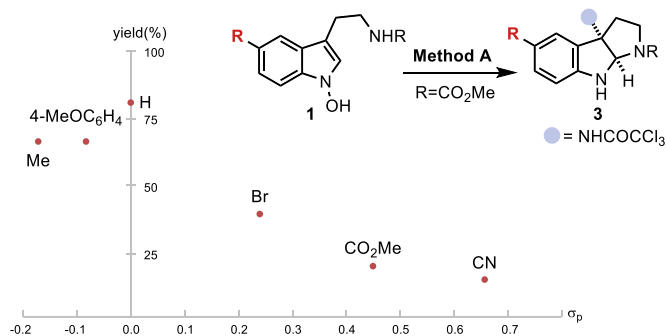


**Figure 2.18.** The substituent effect at 5-position.

Finally, the dependence of the activation energy on the electronics of the substrate was reaffirmed by examining the substituent effect of the indole framework based on the electronic variations at the 5-position (Figure 2.18). *N*-hydroxytryptamines with C5-substituents with varying electronic properties was subjected to the C3-amidation, and the resulted yields were enumerated by the Hammett constant of the corresponding indole substituent. A generally unfavorable reactivity was noted as the C5-substituent becomes more electron withdrawing. The observation is consistent with the participation of an intermediate with positive charge partitioned in the indolyl part such as intermediate **IV'** in Figure 2.9. Therefore, the identity of the of the “intermediate pair” can be two-fold, although the composition of each pair is unclear at this point.

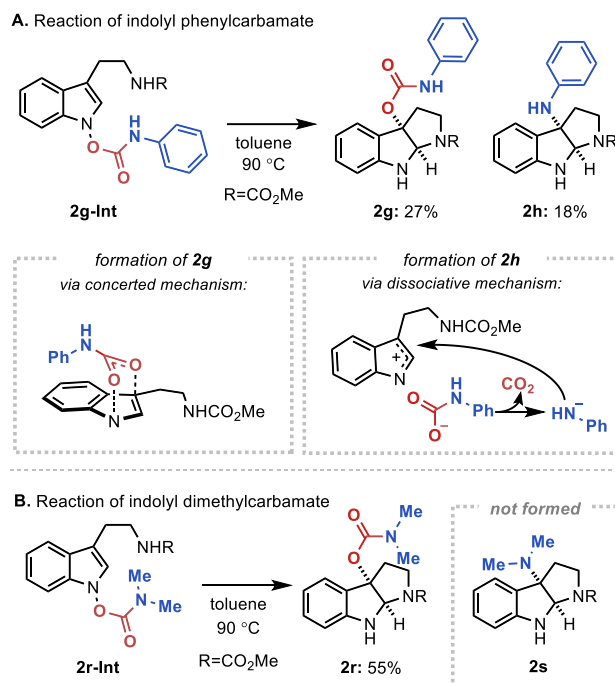


**Figure 2.19.** Reaction of indolyl carbamate.

Finally, the mechanistic duality of the **IHT** reaction was examined in the context of the rearrangement of the indolyl carbamates (Figure 2.19). While the direct operation of the concerted pathway should generate a C3-oxygenation product, the engagement of a dissociative mechanism should result in the C3-amination via a rapid decarboxylation of the initially formed carbamate anion.<sup>79</sup> Indeed, indolyl *N*-phenyl carbamate **2g-Int** successfully furnished a 2:1 mixture of the C3-oxygenation (**2g**) and C3-amination (**2h**) products, indicating the presence of two independently operating mechanisms (Figure 2.19A).<sup>80</sup>

Interestingly, the submission of the identical transformation with an indolyl *N,N*-dimethyl carbamate (**2r-Int**) afforded the oxygenation product (**2r**) as an exclusive product (Figure 2.19B). The contrasting result is attributed to the modified electronics of the system originating from the highly electron-rich dimethylamino group at the 2'-position, which induces the participation of the concerted pathway. However, an alternative explanation can arise on the basis of the stability of the dissociated carbamate anion: The stability of the carbamate is exceedingly increased as the basicity of the parent amine increases.<sup>79</sup> Since the basicity of dimethylamine ( $\text{p}K_a$  of conjugate acid = 10.7)<sup>81</sup> is considerably greater than that



of aniline ( $pK_a$  of conjugate acid = 4.6)<sup>82</sup>, the carbamate anion could be maintained in its native form and thus could provide carbamate **2r** exclusively.

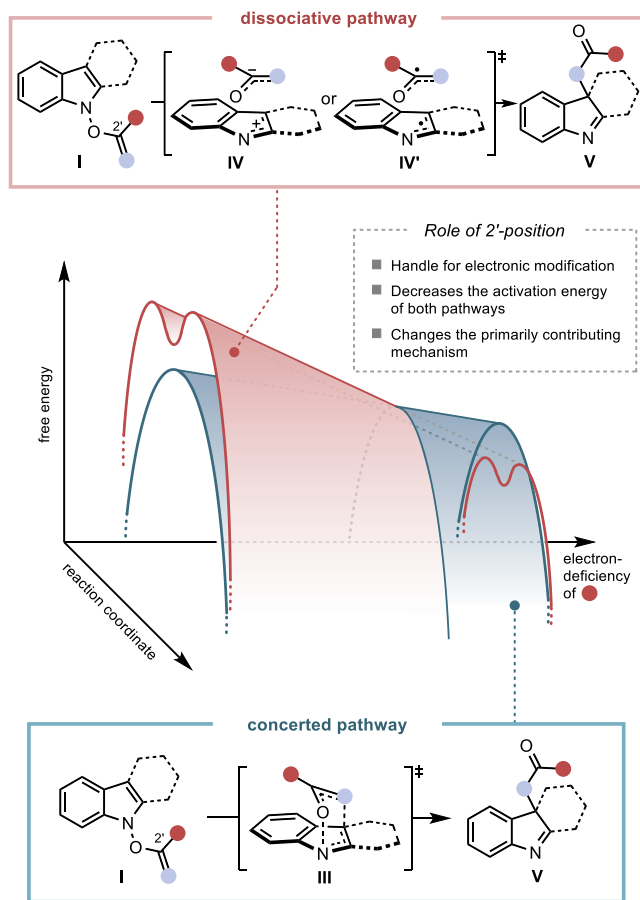


**Figure 2.20.** Plausible mechanistic scenario of **IHT** reaction.

The conclusions drawn from the above experimental investigations are as follows (Figure 2.20). (A) Two separate mechanisms, concerted and dissociative mechanism, operate simultaneously in the **IHT** reaction system. (B) The degree of mechanistic contribution of each pathway can be shifted by modifying the electronic properties of the substituents at the 2' substituent and indole backbone. Either mechanistic pathway can be the dominant pathway for the product formation. (C) During the course of electronic modification, the level of the activation energy for both pathways of **IHT** reaction can be adjusted. (D) The identity of the fragment pair in the dissociative pathway is unclear; both evidence supporting the

involvement of a radical pair and evidence supporting the participation of an ion pair were identified.

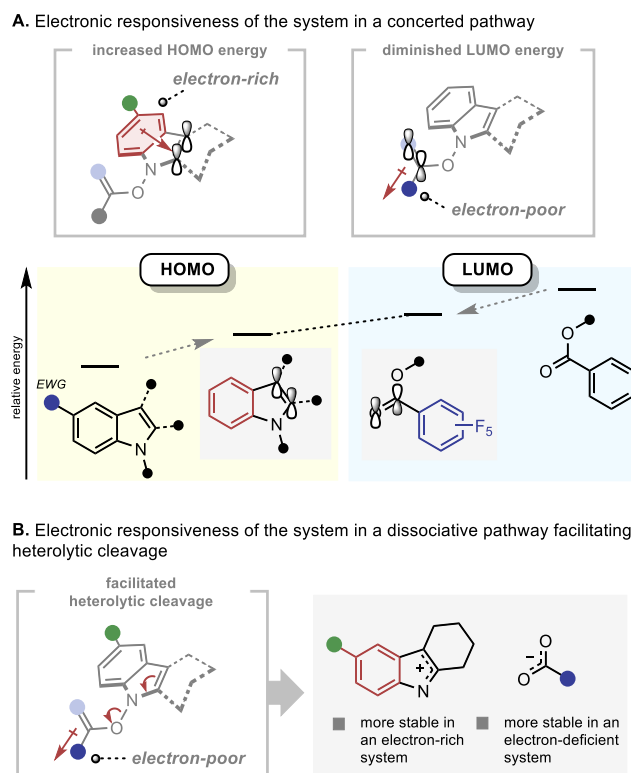


**Figure 2.21.** Mechanistic rationale of **IHT** reaction.

The electronic responsiveness consistently observed in the **IHT** reaction can be rationalized from both concerted and dissociative mechanistic point of view (Figure 2.21). In the case of the concerted mechanism, the observed trend can be explained from the perspective of frontier molecular orbital theory (Figure 2.21A). The energy level of the highest occupied molecular orbital (HOMO), which is located mainly in the indole framework, can be increased by the incorporation of electron-donating groups in indole nucleus. On the other hand, the energy level of the lowest unoccupied molecular orbital (LUMO), which lies primarily in the C=O bond of the benzoate can be lowered by installing electron-withdrawing groups next to the C=O bond. Thus, electronic polarization within the substrate should reduce the HOMO-LUMO gap. In the dissociation mechanism, the increased electron density on the indolyl backbone and the electron-withdrawing nature of the benzoate should facilitate formation of the indolyl cation and benzoate anion through heterolytic cleavage of the N–O bond (Figure 2.21B). The electronic responsiveness of the **IHT** reaction

could also provide an acceptable rationale for homolysis-induced dissociation pathways. On the other hand, the basis for the influence of the electronic polarization in favor of radical pair formation through N–O homolysis is unclear.

## 2.4. Conclusions

In summary, an efficient method of C3-hetero-functionalization for indoles via [3,3]-sigmatropic rearrangement of *N*-hydroxyindole has been developed. The discovery of a significant electron-withdrawing effect at the 2'-position was crucial for the development of a mild reaction condition, allowing access to a wide range of indole derivatives. Specifically, an effortless approach towards rather vulnerable indolenine derivatives emphasizes a distinctive advantage of our protocol. A detailed investigation of the mechanistic aspects revealed that the reaction proceeds via two concurrent reaction pathways, concerted and dissociative mechanism, whose weighted average can be shifted depending on the electronic nature of the substituents. Throughout the reaction, electron-deficiency in either benzo-ate or imidate group plays an important role in both reducing the activation energy and changing major mechanistic pathway from concerted mechanism to dissociative mechanism. From a synthetic perspective, this new method would ensure reliable access towards diversified structures derived from indole scaffolds. Based on the mechanistic understanding, future engineering for catalysis should be made possible.

## 2.5. References

- (1) (a) Ban, Y.; Murakami, Y.; Iwasawa, Y.; Tsuchiya, M.; Takano, N., Indole alkaloids in medicine. *Med. Res. Rev.* **1988**, *8*, 231. (b) Taylor, R. D.; MacCoss, M.; Lawson, A. D. G., Rings in Drugs. *J. Med. Chem.* **2014**, *57*, 5845. (c) Vitaku, E.; Smith, D. T.; Njardarson, J. T., Analysis of the Structural Diversity, Substitution Patterns, and Frequency of Nitrogen Heterocycles among U.S. FDA Approved Pharmaceuticals. *J. Med. Chem.* **2014**, *57*, 10257. (d) Wan, Y.; Li, Y.; Yan, C.; Yan, M.; Tang, Z., Indole: A privileged scaffold for the design of anti-cancer agents. *Eur. J. Med. Chem.* **2019**, *183*, 111691. (e) Seigler, D. S. In *Plant Secondary Metabolism*; Springer: 1998, p 628.
- (2) (a) Sandtorv, A. H., Transition Metal-Catalyzed C–H Activation of Indoles. *Adv. Synth. Catal.* **2015**, *357*, 2403. (b) Liu, S.; Zhao, F.; Chen, X.; Deng, G.-J.; Huang, H., Aerobic Oxidative Functionalization of Indoles. *Adv. Synth. Catal.* **2020**, *362*, 3795. (c) Sheng, F.-T.; Wang, J.-Y.; Tan, W.; Zhang, Y.-C.; Shi, F., Progresses in organocatalytic asymmetric dearomatization reactions of indole derivatives. *Org. Chem. Front.* **2020**, *7*, 3967. (d) Urbina, K.; Tresp, D.; Sipps, K.; Szostak, M., Recent Advances in Metal-Catalyzed Functionalization of Indoles. *Adv. Synth. Catal.* **2021**, *363*, 2723. (e) Abou-Hamdan, H.; Kouklovsky, C.; Vincent, G., Dearomatization Reactions of Indoles to Access 3D Indoline Structures. *Synlett* **2020**, *31*, 1775.
- (3) Ohno, M.; Spande, T. F.; Witkop, B., Cyclization of tryptophan and tryptamine derivatives to pyrrolo[2,3-b]indoles. *J. Am. Chem. Soc.* **1968**, *90*, 6521.
- (4) (a) Kamenecka, T. M.; Danishefsky, S. J., Total Synthesis of Himastatin: Confirmation of the Revised Stereostructure. *Angew. Chem. Int. Ed.* **1998**, *37*, 2995. (b) Kamenecka, T. M.; Danishefsky, S. J., Discovery through Total Synthesis: A Retrospective on the Himastatin Problem. *Chem. Eur. J.* **2001**, *7*, 41.
- (5) May, J. P.; Fournier, P.; Pellicelli, J.; Patrick, B. O.; Perrin, D. M., High Yielding Synthesis of 3a-Hydroxypyrrolo[2,3-b]indoline Dipeptide Methyl Esters: Synthons for Expedient Introduction of the Hydroxypyrroloindoline Moiety into Larger Peptide-Based Natural Products and for the Creation of Tryptathionine Bridges. *J. Org. Chem.* **2005**, *70*, 8424.
- (6) Toumi, M.; Couty, F.; Marrot, J.; Evano, G., Total Synthesis of Chaetominine. *Org. Lett.* **2008**, *10*, 5027.
- (7) Karadeolian, A.; Kerr, M. A., Total Synthesis of (+)-Isatisine A. *J. Org. Chem.* **2010**, *75*,

6830.

- (8) Buller, M. J.; Cook, T. G.; Kobayashi, Y., Versatile synthesis of 2, 2-disubstituted indolinones via protected indolones generated by one-pot multi-oxidation of 2-substituted indoles. *Heterocycles* **2007**, *72*, 163.
- (9) Movassaghi, M.; Schmidt, M. A.; Ashenurst, J. A., Stereoselective Oxidative Rearrangement of 2-Aryl Tryptamine Derivatives. *Org. Lett.* **2008**, *10*, 4009.
- (10) Han, S.; Movassaghi, M., Concise Total Synthesis and Stereochemical Revision of all (–)-Trigonoliimines. *J. Am. Chem. Soc.* **2011**, *133*, 10768.
- (11) Kolundzic, F.; Noshi, M. N.; Tjandra, M.; Movassaghi, M.; Miller, S. J., Chemoselective and Enantioselective Oxidation of Indoles Employing Aspartyl Peptide Catalysts. *J. Am. Chem. Soc.* **2011**, *133*, 9104.
- (12) Berti, G.; Settimo, A. D.; Nannipieri, E., The reactions of some indole derivatives with benzoyl nitrate. Novel oxidative coupling reactions of 2-methylindoles. *J. Chem. Soc. (C)* **1968**, 2145.
- (13) Pelkey, E. T.; Gribble, G. W., Synthesis and reactions of N-protected 3-nitroindoles. *Synthesis* **1999**, *1999*, 1117.
- (14) Shoberu, A.; Li, C.-K.; Tao, Z.-K.; Zhang, G.-Y.; Zou, J.-P., NaNO<sub>2</sub>/K<sub>2</sub>S<sub>2</sub>O<sub>8</sub>-mediated Selective Radical Nitration/Nitrosation of Indoles: Efficient Approach to 3-Nitro- and 3-Nitrosoindoles. *Adv. Synth. Catal.* **2019**, *361*, 2255.
- (15) Fischer, O.; Hepp, E., Zur Kenntniss der Nitrosamine. *Ber. Deutsch. Chem. Ges.* **1886**, *19*, 2991.
- (16) Pauly, H.; Gundermann, K., Über jodbindende Systeme in den Eiweiß-Spaltkörpern. *Ber. Deutsch. Chem. Ges.* **1908**, *41*, 3999.
- (17) Baran, P. S.; Guerrero, C. A.; Corey, E. J., The First Method for Protection–Deprotection of the Indole 2,3- $\pi$  Bond. *Org. Lett.* **2003**, *5*, 1999.
- (18) Cao, D.; Zhang, Y.; Liu, C.; Wang, B.; Sun, Y.; Abdukadera, A.; Hu, H.; Liu, Q., Ionic Liquid Promoted Diazenylation of N-Heterocyclic Compounds with Aryltriazenes under Mild Conditions. *Org. Lett.* **2016**, *18*, 2000.
- (19) Terada, M.; Sorimachi, K., Enantioselective Friedel–Crafts Reaction of Electron-Rich Alkenes Catalyzed by Chiral Brønsted Acid. *J. Am. Chem. Soc.* **2007**, *129*, 292.
- (20) Zhang, Z.; Antilla, J. C., Enantioselective Construction of Pyrroloindolines Catalyzed

by Chiral Phosphoric Acids: Total Synthesis of (–)-Debromoflustramine B. *Angew. Chem. Int. Ed.* **2012**, *51*, 11778.

(21) Nelson, H. M.; Reisberg, S. H.; Shunatona, H. P.; Patel, J. S.; Toste, F. D., Chiral Anion Phase Transfer of Aryldiazonium Cations: An Enantioselective Synthesis of C3-Diazenated Pyrroloindolines. *Angew. Chem. Int. Ed.* **2014**, *53*, 5600.

(22) Li, Q.; Xia, T.; Yao, L.; Deng, H.; Liao, X., Enantioselective and diastereoselective azo-coupling/iminium-cyclizations: a unified strategy for the total syntheses of (–)-psychotriasine and (+)-pestalazine B. *Chem. Sci.* **2015**, *6*, 3599.

(23) Newhouse, T.; Baran, P. S., Total Synthesis of (±)-Psychotrimine. *J. Am. Chem. Soc.* **2008**, *130*, 10886.

(24) Newhouse, T.; Lewis, C. A.; Eastman, K. J.; Baran, P. S., Scalable Total Syntheses of N-Linked Tryptamine Dimers by Direct Indole–Aniline Coupling: Psychotrimine and Kapakahines B and F. *J. Am. Chem. Soc.* **2010**, *132*, 7119.

(25) Ma, X.; Farndon, J. J.; Young, T. A.; Fey, N.; Bower, J. F., A Simple and Broadly Applicable C–N Bond Forming Dearomatization Protocol Enabled by Bifunctional Amino Reagents. *Angew. Chem. Int. Ed.* **2017**, *56*, 14531.

(26) Ortiz, G. X.; Hemric, B. N.; Wang, Q., Direct and Selective 3-Amidation of Indoles Using Electrophilic N-[(Benzenesulfonyl)oxy]amides. *Org. Lett.* **2017**, *19*, 1314.

(27) Li, L.; Luo, S., Electrochemical Generation of Diaza-oxyallyl Cation for Cycloaddition in an All-Green Electrolytic System. *Org. Lett.* **2018**, *20*, 1324.

(28) (a) Padwa, A.; Stengel, T., Stereochemical Aspects of the Iodine(III)-Mediated Aziridination Reaction of Some Cyclic Allylic Carbamates. *Org. Lett.* **2002**, *4*, 2137. (b) Padwa, A.; Flick, A. C.; Leverett, C. A.; Stengel, T., Rhodium(II)-Catalyzed Aziridination of Allyl-Substituted Sulfonamides and Carbamates. *J. Org. Chem.* **2004**, *69*, 6377.

(29) Sato, S.; Shibuya, M.; Kanoh, N.; Iwabuchi, Y., An Expedient Route to a Potent Gastrin/CCK-B Receptor Antagonist (+)-AG-041R. *J. Org. Chem.* **2009**, *74*, 7522.

(30) (a) Kim, M.; Mulcahy, J. V.; Espino, C. G.; Du Bois, J., Expanding the Substrate Scope for C–H Amination Reactions: Oxidative Cyclization of Urea and Guanidine Derivatives. *Org. Lett.* **2006**, *8*, 1073. (b) Gupta, R.; Sogi, K. M.; Bernard, S. E.; Decatur, J. D.; Rojas, C. M., Protecting Group and Solvent Control of Stereo- and Chemoselectivity in Glucal 3-Carbamate Amidoglycosylation. *Org. Lett.* **2009**, *11*, 1527.

- (31) Liu, G.-S.; Zhang, Y.-Q.; Yuan, Y.-A.; Xu, H., Iron(II)-Catalyzed Intramolecular Aminohydroxylation of Olefins with Functionalized Hydroxylamines. *J. Am. Chem. Soc.* **2013**, *135*, 3343.
- (32) Shen, Z.; Xia, Z.; Zhao, H.; Hu, J.; Wan, X.; Lai, Y.; Zhu, C.; Xie, W., Synthesis of naked amino-pyrroloindoline via direct aminocyclization of tryptamine. *Org. Biomol. Chem.* **2015**, *13*, 5381.
- (33) Liu, C.; Yi, J.-C.; Zheng, Z.-B.; Tang, Y.; Dai, L.-X.; You, S.-L., Enantioselective Synthesis of 3a-Amino-Pyrroloindolines by Copper-Catalyzed Direct Asymmetric Dearomative Amination of Tryptamines. *Angew. Chem. Int. Ed.* **2016**, *55*, 751.
- (34) Arnold, R.; Nutter, W.; Stepp, W., Indoxyl acetate from indole. *J. Org. Chem.* **1959**, *24*, 117.
- (35) Ikeda, M.; Tabusa, F.; Nishimura, Y.; Kwon, S.; Tamura, Y., The reactions of some indoles with iodine azide: syntheses of 3-azidoindolenines, 2-azidomethylindoles, and 3a-azido-furo- and pyrrolo-[2,3-b]indoles. *Tetrahedron Lett.* **1976**, *17*, 2347.
- (36) Prasad, P. K.; Kalshetti, R. G.; Reddi, R. N.; Kamble, S. P.; Sudalai, A., I<sub>2</sub>-mediated regioselective C–3 azidation of indoles. *Org. Biomol. Chem.* **2016**, *14*, 3027.
- (37) Tanaka, H.; Ukegawa, N.; Uyanik, M.; Ishihara, K., Hypoiodite-Catalyzed Oxidative Umpolung of Indoles for Enantioselective Dearomatization. *J. Am. Chem. Soc.* **2022**, *144*, 5756.
- (38) Braun, N. A.; Bray, J. D.; Ciufolini, M. A., Hypervalent iodine oxidation of indolic 2-oxazolines. *Tetrahedron Lett.* **1999**, *40*, 4985.
- (39) Liu, K.; Wen, P.; Liu, J.; Huang, G., A Novel and Efficient Method for the Synthesis of 1H-Indol-3-yl Acetates. *Synthesis* **2010**, *2010*, 3623.
- (40) Zhou, Y.; Li, D.; Tang, S.; Sun, H.; Huang, J.; Zhu, Q., PhI(OAc)<sub>2</sub>-mediated dearomative C–N coupling: facile construction of the spiro[indoline-3,2'-pyrrolidine] skeleton. *Org. Biomol. Chem.* **2018**, *16*, 2039.
- (41) Mutule, I.; Suna, E.; Olofsson, K.; Pelcman, B., Catalytic Direct Acetoxylation of Indoles. *J. Org. Chem.* **2009**, *74*, 7195.
- (42) Lubriks, D.; Sokolovs, I.; Suna, E., Iodonium Salts Are Key Intermediates in Pd-Catalyzed Acetoxylation of Pyrroles. *Org. Lett.* **2011**, *13*, 4324.
- (43) Lubriks, D.; Sokolovs, I.; Suna, E., Indirect C–H Azidation of Heterocycles via Copper-



Catalyzed Regioselective Fragmentation of Unsymmetrical  $\lambda^3$ -Iodanes. *J. Am. Chem. Soc.* **2012**, *134*, 15436.

(44) Sokolovs, I.; Lubriks, D.; Suna, E., Copper-Catalyzed Intermolecular C–H Amination of (Hetero)arenes via Transient Unsymmetrical  $\lambda^3$ -Iodanes. *J. Am. Chem. Soc.* **2014**, *136*, 6920.

(45) Cui, R.; Ye, J.; Li, J.; Mo, W.; Gao, Y.; Chen, H., Construction of Bisindolines via Oxidative Coupling Cyclization. *Org. Lett.* **2020**, *22*, 116.

(46) Tomakinian, T.; Guillot, R.; Kouklovsky, C.; Vincent, G., Direct Oxidative Coupling of N-Acetyl Indoles and Phenols for the Synthesis of Benzofuroindolines Related to Phalarine. *Angew. Chem. Int. Ed.* **2014**, *53*, 11881.

(47) Ryzhakov, D.; Jarret, M.; Guillot, R.; Kouklovsky, C.; Vincent, G., Radical-Mediated Dearomatization of Indoles with Sulfinates Reagents for the Synthesis of Fluorinated Spirocyclic Indolines. *Org. Lett.* **2017**, *19*, 6336.

(48) Gentry, E. C.; Rono, L. J.; Hale, M. E.; Matsuura, R.; Knowles, R. R., Enantioselective synthesis of pyrroloindolines via noncovalent stabilization of indole radical cations and applications to the synthesis of alkaloid natural products. *J. Am. Chem. Soc.* **2018**, *140*, 3394.

(49) Liang, K.; Tong, X.; Li, T.; Shi, B.; Wang, H.; Yan, P.; Xia, C., Enantioselective Radical Cyclization of Tryptamines by Visible Light-Excited Nitroxides. *J. Org. Chem.* **2018**, *83*, 10948.

(50) Cheng, Y.-Z.; Zhao, Q.-R.; Zhang, X.; You, S.-L., Asymmetric Dearomatization of Indole Derivatives with N-Hydroxycarbamates Enabled by Photoredox Catalysis. *Angew. Chem. Int. Ed.* **2019**, *58*, 18069.

(51) Liu, K.; Tang, S.; Huang, P.; Lei, A., External oxidant-free electrooxidative [3 + 2] annulation between phenol and indole derivatives. *Nat. Commun.* **2017**, *8*, 775.

(52) Wu, J.; Dou, Y.; Guillot, R.; Kouklovsky, C.; Vincent, G., Electrochemical Dearomative 2,3-Difunctionalization of Indoles. *J. Am. Chem. Soc.* **2019**, *141*, 2832.

(53) In the case of Knowles and Xia's works (vide supra), in which the photochemically generated indole radical cation combines with TEMPO, it would be correct to consider it as a radical addition to one electron-oxidized indole motif. However, one of the greatest advantages in Knowles' work is the additional oxidation of TEMPO-trapped pyrroloindoline to obtain C3-carbocation to derive the coupling with various nucleophiles, thus it was

introduced in Section 1.1.2. Xia's work was introduced following Knowles' work to emphasize the similarity with Knowles' work.

(54) (a) Beer, R. J. S.; McGrath, L.; Robertson, A.; Woodier, A. B., Tetrahydrocarbazole Peroxides. *Nature* **1949**, *164*, 362. (b) Beer, R.; McGrath, L.; Robertson, A., 638. Peroxides of tetrahydrocarbazole and related compounds. Part II. *J. Chem. Soc.* **1950**, 3283. (c) Witkop, B.; Patrick, J., The Course and Kinetics of the Acid-Base-Catalyzed Rearrangements of 11-Hydroxytetrahydrocarbazolenine1. *J. Am. Chem. Soc.* **1951**, *73*, 2188.

(55) An, J.; Zou, Y.-Q.; Yang, Q.-Q.; Wang, Q.; Xiao, W.-J., Visible Light-Induced Aerobic Oxyamidation of Indoles: A Photocatalytic Strategy for the Preparation of Tetrahydro-5H-indolo[2,3-b]quinolinols. *Adv. Synth. Catal.* **2013**, *355*, 1483.

(56) Yu, L.; Zhong, Y.; Yu, J.; Gan, L.; Cai, Z.; Wang, R.; Jiang, X., Highly diastereoselective oxa-[3+3] cyclization with C,N-cyclic azomethine imines via the copper-catalyzed aerobic oxygenated C–C bond of indoles. *Chem. Commun.* **2018**, *54*, 2353.

(57) Zhou, Y.; Chen, G.; Li, C.; Liu, X.; Liu, P., Cobalt (II)-catalyzed direct C3-selective C–H acyloxylation of indoles with tert-butyl peresters. *Synth. Commun.* **2018**, *48*, 2912.

(58) Wang, M.; Yang, Y.; Yin, L.; Feng, Y.; Li, Y., Selective Synthesis of Pyrano[3,2-b]indoles or Cyclopenta[b]indoles Tethered with Medium-Sized Rings via Cascade C–C  $\sigma$ -Bond Cleavage and C–H Functionalization. *J. Org. Chem.* **2021**, *86*, 683.

(59) Yamaguchi, T.; Yamaguchi, E.; Itoh, A., Cross-Dehydrogenative C–H Amination of Indoles under Aerobic Photo-oxidative Conditions. *Org. Lett.* **2017**, *19*, 1282.

(60) Fu, N.; Sauer, G. S.; Saha, A.; Loo, A.; Lin, S., Metal-catalyzed electrochemical diazidation of alkenes. *Science* **2017**, *357*, 575.

(61) Liu, K.; Song, W.; Deng, Y.; Yang, H.; Song, C.; Abdelilah, T.; Wang, S.; Cong, H.; Tang, S.; Lei, A., Electrooxidation enables highly regioselective dearomative annulation of indole and benzofuran derivatives. *Nat. Commun.* **2020**, *11*, 3.

(62) Tabolin, A. A.; Ioffe, S. L., Rearrangement of N-Oxyenamines and Related Reactions. *Chem. Rev.* **2014**, *114*, 5426.

(63) (a) Burrows, C. J.; Carpenter, B. K., Substituent effects on the aliphatic Claisen rearrangement. 1. Synthesis and rearrangement of cyano-substituted allyl vinyl ethers. *J. Am. Chem. Soc.* **1981**, *103*, 6983. (b) Gajewski, J. J.; Gee, K. R.; Jurayj, J., Energetic and rate effects of the trifluoromethyl group at C–2 and C–4 on the aliphatic Claisen rearrangement.

*J. Org. Chem.* **1990**, *55*, 1813. (c) Aviyente, V.; Houk, K. N., Cyano, Amino, and Trifluoromethyl Substituent Effects on the Claisen Rearrangement. *J. Phys. Chem. A* **2001**, *105*, 383. (d) Aviyente, V.; Yoo, H. Y.; Houk, K. N., Analysis of Substituent Effects on the Claisen Rearrangement with Ab Initio and Density Functional Theory. *J. Org. Chem.* **1997**, *62*, 6121. (e) Gajewski, J. J., The Claisen Rearrangement. Response to Solvents and Substituents: The Case for Both Hydrophobic and Hydrogen Bond Acceleration in Water and for a Variable Transition State. *Acc. Chem. Res.* **1997**, *30*, 219.

(64) Davies, J.; Booth, S. G.; Essafi, S.; Dryfe, R. A. W.; Leonori, D., Visible-Light-Mediated Generation of Nitrogen-Centered Radicals: Metal-Free Hydroimination and Iminohydroxylation Cyclization Reactions. *Angew. Chem. Int. Ed.* **2015**, *54*, 14017.

(65) Reactions with extremely electron deficient acyl donors, such as trifluoroacetic anhydride, resulted in extensive decomposition to produce a mixture of untractable products.

(66) (a) Overman, L. E.; Carpenter, N. E., The Allylic Trihaloacetimidate Rearrangement. *Org. React.* **2005**, *1*. (b) Nomura, H.; Richards, C. J., Allylic Imidate Rearrangements Catalyzed by Planar Chiral Palladacycles. *Chem. Asian. J.* **2010**, *5*, 1726. (c) Fernandes, R. A.; Kattanguru, P.; Gholap, S. P.; Chaudhari, D. A., Recent advances in the Overman rearrangement: synthesis of natural products and valuable compounds. *Org. Biomol. Chem.* **2017**, *15*, 2672.

(67) The stereochemical outcome at the C3 position was tentatively assigned on the basis of the analogous rearrangement in the yohimbine system. see: Somei, M.; Noguchi, K.; Yamada, F., Synthesis of 1-Hydroxyyohimbine and Its Novel Skeletal Rearrangement Reaction into Oxindole Derivatives. *Heterocycles* **2001**, *55*, 1237.

(68) (a) Adhikari, A. A.; Chisholm, J. D., Lewis Acid Catalyzed Displacement of Trichloroacetimidates in the Synthesis of Functionalized Pyrroloindolines. *Org. Lett.* **2016**, *18*, 4100. (b) Gallego, S.; Lorenzo, P.; Alvarez, R.; de Lera, A. R., Total synthesis of naturally occurring (+)-psychotriazine and the related tetrahydro- $\beta$ -carboline, dimeric tryptamines with NC connectivities. *Tetrahedron Lett.* **2017**, *58*, 210.

(69) (a) Ganem, B., The Mechanism of the Claisen Rearrangement: Déjà Vu All Over Again. *Angew. Chem. Int. Ed.* **1996**, *35*, 936. (b) Martín Castro, A. M., Claisen Rearrangement over the Past Nine Decades. *Chem. Rev.* **2004**, *104*, 2939. (c) Graulich, N., The Cope rearrangement—the first born of a great family. *Wiley Interdiscip. Rev. Comput. Mol. Sci.*

**2011**, *1*, 172. (d) Hiersemann, M.; Nubbemeyer, U. *The Claisen rearrangement: methods and applications*; John Wiley & Sons, 2007. (e) Nubbemeyer, U., Recent Advances in Asymmetric [3,3]-Sigmatropic Rearrangements. *Synthesis* **2003**, *2003*, 0961. (f) Majumdar, K. C.; Bhattacharyya, T.; Chattopadhyay, B.; Sinha, B., Recent Advances in the Aza-Claisen Rearrangement. *Synthesis* **2009**, *2009*, 2117. (g) Houk, K. N.; Gonzalez, J.; Li, Y., Pericyclic reaction transition states: passions and punctilios, 1935-1995. *Acc. Chem. Res.* **1995**, *28*, 81.

(70) (a) Tissue, G.; Grassmann, M.; Lwowski, W., Rearrangement of O-arenesulfonyl phenylhydroxylamines. *Tetrahedron* **1968**, *24*, 999. (b) Gutschke, D.; Heesing, A., Arylnitrenium-Ionen bei der Umlagerung von O-(Arylsulfonyl) phenylhydroxylaminen. *Chem. Ber.* **1973**, *106*, 2379. (c) Binding, N.; Heesing, A., Memory-Effekt und 1, 3-Diazepin-Ringschluß bei Arylnitrenium-Ionen. *Chem. Ber.* **1983**, *116*, 1822. (d) Oae, S.; Sakurai, T.; Kimura, H.; Kozuka, S., OXYGEN-18 TRACER STUDY OF THE REARRANGEMENT OF O-BENZOYL-N-(p-TOLUENESULFONYL) ARYLHYDROXYLAMINES. *Chem. Lett.* **1974**, *3*, 671. (e) Oae, S.; Sakurai, T., Mechanism of the exclusive cyclic 1, 3-rearrangement of O-benzoyl-N-(p-toluenesulfonyl)-n-arylhydroxylamines. *Tetrahedron* **1976**, *32*, 2289. (f) Koenig, T., The Reaction of 2-Picoline N-Oxide with Substituted Acetic Anhydrides. *J. Am. Chem. Soc.* **1966**, *88*, 4045. (g) Bodalski, R.; Katritzky, A. R., N-oxides and related compounds. Part XXXIII. The mechanism of the acetic anhydride rearrangement of 2-alkylpyridine 1-oxides. *J. Chem. Soc. B* **1968**, 831. (h) Oae, S.; Kitao, T.; Kitaoka, Y., The Mechanism of the Reaction of 2-Picoline N-Oxide with Acetic Anhydride. *J. Am. Chem. Soc.* **1962**, *84*, 3359.

(71) The [1,3]-sigmatropic shift has been ruled out due to the high activation energy involved due to structural rigidity constraining orbital alignment.

(72) Luo, Y.-R. *Comprehensive handbook of chemical bond energies*; CRC press, 2007.

(73) (a) Çelebi-Ölçüm, N.; Lam, Y.-h.; Richmond, E.; Ling, K. B.; Smith, A. D.; Houk, K. N., Pericyclic Cascade with Chirality Transfer: Reaction Pathway and Origin of Enantioselectivity of the Hetero-Claisen Approach to Oxindoles. *Angew. Chem. Int. Ed.* **2011**, *50*, 11478. (b) Sączewski, J.; Fedorowicz, J.; Gdaniec, M.; Wiśniewska, P.; Sieniawska, E.; Drażba, Z.; Rzewnicka, J.; Balewski, Ł., The Elusive Paal-Knorr Intermediates in the Trofimov Synthesis of Pyrroles: Experimental and Theoretical Studies. *J. Org. Chem.* **2017**, *82*, 9737.

(74) (a) Mauleón, P.; Krinsky, J. L.; Toste, F. D., Mechanistic Studies on Au(I)-Catalyzed [3,3]-Sigmatropic Rearrangements using Cyclopropane Probes. *J. Am. Chem. Soc.* **2009**, *131*, 4513. (b) Lu, B.-L.; Wei, Y.; Shi, M., Gold(I) and Brønsted Acid Catalyzed Intramolecular Rearrangements of Vinylidene-cyclopropanes. *Chem. Eur. J.* **2010**, *16*, 10975. (c) Nakamura, I.; Owada, M.; Jo, T.; Terada, M., Concerted [1,3]-Rearrangement in Cationic Cobalt-Catalyzed Reaction of O-(Alkoxy-carbonyl)-N-arylhydroxylamines. *Org. Lett.* **2017**, *19*, 2194. (d) Sekar Kulandai Raj, A.; Liu, R.-S., Gold-catalyzed [4+3]-Annulations of Benzopyriliums with Vinylidazo Carbonyls to Form Bicyclic Heptatriene Rings with Skeletal Rearrangement. *Adv. Synth. Catal.* **2020**, *362*, 2517.

(75) Agirre, M.; Henrion, S.; Rivilla, I.; Miranda, J. I.; Cossío, F. P.; Carboni, B.; Villalgorido, J. M.; Carreaux, F., 1,3-Dioxa-[3,3]-sigmatropic Oxo-Rearrangement of Substituted Allylic Carbamates: Scope and Mechanistic Studies. *J. Org. Chem.* **2018**, *83*, 14861.

(76) (a) Doering, W. v. E.; Wang, Y., Perturbation of Cope's Rearrangement: 1,3,5-Triphenylhexa-1,5-diene. Chameleonic or Centauric Transition Region? *J. Am. Chem. Soc.* **1999**, *121*, 10112. (b) Borden, W. T. In *Theory and Applications of Computational Chemistry*; Dykstra, C. E., Frenking, G., Kim, K. S., Scuseria, G. E., Eds.; Elsevier: Amsterdam, 2005, p 859. (c) Doering, W. v. E.; Wang, Y., CryptoCope Rearrangement of 1,3-Dicyano-5-phenyl-4,4-d<sub>2</sub>-hexa-2,5-diene. Chameleonic or Centauric? *J. Am. Chem. Soc.* **1999**, *121*, 10967. (d) Hrovat, D. A.; Beno, B. R.; Lange, H.; Yoo, H.-Y.; Houk, K. N.; Borden, W. T., A Becke3LYP/6-31G\* Study of the Cope Rearrangements of Substituted 1,5-Hexadienes Provides Computational Evidence for a Chameleonic Transition State. *J. Am. Chem. Soc.* **1999**, *121*, 10529. (e) Black, K. A.; Wilsey, S.; Houk, K. N., Dissociative and Associative Mechanisms of Cope Rearrangements of Fluorinated 1,5-Hexadienes and 2,2'-Bis-methylenecyclopentanes. *J. Am. Chem. Soc.* **2003**, *125*, 6715. (f) Gajewski, J. J.; Conrad, N. D., Variable transition state structure in 3,3-sigmatropic shifts from .alpha.-secondary deuterium isotope effects. *J. Am. Chem. Soc.* **1979**, *101*, 6693. (g) Vidhani, D. V.; Krafft, M. E.; Alabugin, I. V., Gold(I)-Catalyzed Allenyl Cope Rearrangement: Evolution from Asynchronicity to Trappable Intermediates Assisted by Stereoelectronic Switching. *J. Am. Chem. Soc.* **2016**, *138*, 2769. (h) Vidhani, D. V.; Alabugin, I. V., Controlled Evolution of the Cope Rearrangement: Transition from Concerted to Interrupted and Aborted Pericyclic Reactions Regulated by a Switch Built from an Intramolecular Frustrated Lewis Pair. *J. Org.*

*Chem.* **2019**, *84*, 14844. (i) Gajewski, J. J.; Gilbert, K. E., Empirical approach to substituent effects in [3, 3]-sigmatropic shifts utilizing the thermochemistry of coupled nonconcerted alternative paths. *J. Org. Chem.* **1984**, *49*, 11. (j) Gajewski, J. J., Substituent effects in concerted reactions. A nonlinear free-energy relationship for the 3, 3-shift and the Diels-Alder reaction. *J. Am. Chem. Soc.* **1979**, *101*, 4393.

(77) TEMPO could not be used due to vigorous decomposition of N-hydroxyindole (1a) when TEMPO was added to 1a. However, in the case of indolyl benzoate (2a), which is stable at room temperature, could be isolated and subjected to a rearrangement conditions with TEMPO. The result was almost identical to the result using 1,1-diphenylethylene. No noticeable yield loss was observed and a trace of product trapped by TEMPO was detected by HRMS.

(78) (a) Braden, D. A.; Parrack, E. E.; Tyler, D. R., Solvent cage effects. I. Effect of radical mass and size on radical cage pair recombination efficiency. II. Is geminate recombination of polar radicals sensitive to solvent polarity? *Coord. Chem. Rev.* **2001**, *211*, 279. (b) Barry, J. T.; Berg, D. J.; Tyler, D. R., Radical Cage Effects: Comparison of Solvent Bulk Viscosity and Microviscosity in Predicting the Recombination Efficiencies of Radical Cage Pairs. *J. Am. Chem. Soc.* **2016**, *138*, 9389. (c) Barry, J. T.; Berg, D. J.; Tyler, D. R., Radical Cage Effects: The Prediction of Radical Cage Pair Recombination Efficiencies Using Microviscosity Across a Range of Solvent Types. *J. Am. Chem. Soc.* **2017**, *139*, 14399.

(79) (a) da Silva, E. F.; Svendsen, H. F., Study of the Carbamate Stability of Amines Using ab Initio Methods and Free-Energy Perturbations. *Ind. Eng. Chem. Res.* **2006**, *45*, 2497. (b) McCann, N.; Phan, D.; Fernandes, D.; Maeder, M., A systematic investigation of carbamate stability constants by <sup>1</sup>H NMR. *Int. J. Greenh. Gas Control.* **2011**, *5*, 396. (c) Gupta, M.; Svendsen, H. F., Modeling temperature dependent and absolute carbamate stability constants of amines for CO<sub>2</sub> capture. *Int. J. Greenh. Gas Control.* **2020**, *98*, 103061.

(80) The possibility of an involvement of the C=N tautomer of the carbamate for the generation of compound 2p was excluded, since the C=N tautomer is highly unstable compared to the corresponding carbamate.

(81) (a) Bergström, S.; Olofsson, G., Thermodynamic quantities for the dissociation of the methylammonium ions between 273 and 398 K. *J. Chem. Thermodyn.* **1977**, *9*, 143. (b) Casado, J.; Castro, A.; Lorenzo, F. M.; Meijide, F., Kinetic studies on the formation of N-

nitroso compounds XI. Nitrosation of dimethylamine by nitrite esters in aqueous basic media. *Monatsh. Chem.* **1986**, *117*, 335.

(82) (a) Gross, K. C.; Seybold, P. G., Substituent effects on the physical properties and pKa of aniline. *Int. J. Quantum Chem* **2000**, *80*, 1107. (b) Albert, A.; Serjeant, E. P. *Ionization constants of acids and bases: a laboratory manual*; Methuen, 1962.

## 2.6. Experimental Section

### Table of Contents

<b>1. General Information</b> .....	174
<b>2. Preparation of Starting Materials</b> .....	176
<b>2.1. Preparation of Indole Derivatives</b> .....	177
<b>2.2. Preparation of Indoline Derivatives</b> .....	182
<b>2.3. Preparation of N-Hydroxyindole Derivatives</b> .....	197
<b>3. C–O Bond Formation via Indolyl 1,3-Heteroatom Transposition (IHT)</b> .....	211
<b>3.1. Identification of 2'-Substituent Effect in the Facilitated IHT Reaction (Scheme 2.49)</b> .....	211
<b>3.2. Optimization of the C3-Acyloxylation Conditions</b> .....	216
<b>3.3. General Procedures for C3-Acyloxylation of Indole Derivatives (Scheme 2.50)</b> .....	217
<b>4. C–N Bond Formation via Indolyl 1,3-Heteroatom Transposition (IHT)</b> .....	226
<b>4.1. Optimization of the C3-Amidation Reaction Conditions (Table 2.1)</b> .....	226
<b>4.2. Preparation of Trifluoroacetimidoyl Chloride</b> .....	230
<b>4.3. General Procedure for C3-Amidation of Indole Derivatives (Scheme 2.51 and scheme 2.52)</b> .....	231
<b>4.4. Evaluation of Practicality and Versatility of the C3-Amidation (Scheme 2.53)</b> .....	251
<b>4.4.1. Gram-scale Reaction</b> .....	251
<b>4.4.2. Conversion to the 3-Aminopyrroloindoline</b> .....	251
<b>4.4.3. Formal Synthesis of Psychotriasine</b> .....	252
<b>5. Mechanistic Investigations</b> .....	255



<b>5.1. <sup>18</sup>O Isotope Experiment (Figure 2.10 and 2.11)</b> .....	255
<b>5.1.1. Preparation of <sup>18</sup>O Labeled Compounds</b> .....	256
5.1.1.1 Benzoyl substituent.....	256
5.1.1.2 3-Bromo-4-fluorobenzoyl substituent .....	261
5.1.1.3 Pentafluorobenzoyl substituent .....	268
5.1.1.4 Bromotryptamine with benzoyl substituent .....	273
5.1.1.5 Bromotryptamine with 3-bromo-4-fluorobenzoyl substituent .....	277
<b>5.1.2. Determination of <sup>18</sup>O Saturation</b> .....	282
<b>5.1.3. Quantitative Analysis of <sup>18</sup>O-Labeling Experiment Results (Figures 2.12 and 2.13)</b> .....	306
5.1.3.1. Dependence of the electronic properties.....	306
5.1.3.2. The influence of electronic properties of the indole backbone (Figure 2.14).....	314
5.1.3.3. The influence of reaction temperature (Figure 2.15).....	319
<b>5.2. Crossover Experiment (Figure 2.16)</b> .....	324
<b>5.2.1 Preparation of Compound 2b-Int and 2b'-Int</b> .....	324
<b>5.2.2. Preparation of Crossover Products</b> .....	326
<b>5.2.2 Crossover Experiment</b> .....	328
<b>5.2.3. Analysis of Crossover Experiment Results</b> .....	330
5.2.3.1. TLC analysis of the crossover experiment.....	330
5.2.3.2. HRMS/HPLC analysis of the crossover experiment .....	331
<b>5.3. Radical-trapping Experiment (Figure 2.17)</b> .....	333
<b>5.3.1. Radical-trapping Experiment with Indolyl <i>N</i>-Carboxylate 2b-Int</b> ....	333
5.3.1.1. HRMS results using TEMPO as a radical scavenger .....	334

5.3.1.2. HRMS results using 1,1-diphenylethylene as a radical scavenger	335
<b>5.3.2. Radical-trapping Experiment with Electron-deficient Indolyl <i>N</i>-carboxylate</b>	<b>336</b>
5.3.2.1. Control experiment using TEMPO as a radical scavenger	337
5.3.2.2. HRMS results using 1,1-diphenylethylene as a radical scavenger	338
<b>5.3.3. Radical-trapping Experiment with Indolyl Acetimidate</b>	<b>339</b>
5.3.3.1. HRMS results using 1,1-diphenylethylene as a radical scavenger	340
<b>5.4. [3,3]-Sigmatropic Rearrangement of Indolyl Carbamate (Figure 2.19A)</b>	<b>341</b>
5.4.1. Preparation of Indolyl Carbamate	341
5.4.2. [3,3]-Sigmatropic Rearrangement of indolyl <i>N</i> -carboxylate <b>2g-Int (Figure 8A)</b>	<b>343</b>
5.4.3. [3,3]-Sigmatropic Rearrangement of indolyl <i>N</i> -carboxylate <b>2r-Int (Figure 2.19B)</b>	<b>345</b>
<b>6. References</b>	<b>346</b>

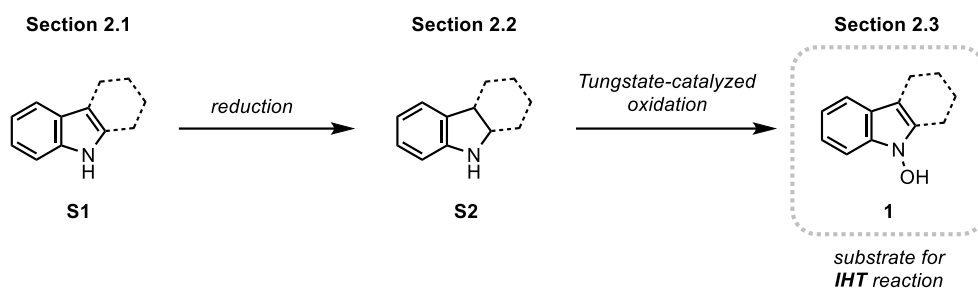
## 1. General Information

Reactions were performed in oven-dried or flame-dried glassware under N<sub>2</sub> atmosphere with dry solvents under anhydrous conditions, unless otherwise stated. Tetrahydrofuran (THF) and dichloromethane (CH<sub>2</sub>Cl<sub>2</sub>) were initially degassed by sonication, and subsequently dried by passing them through a PureSolv solvent purification system and toluene was dried over CaH<sub>2</sub> and distilled under N<sub>2</sub> atmosphere. *N,N*-Dimethylformamide (DMF), dimethyl sulfoxide (DMSO), 1,2-dichloroethane (DCE), acetonitrile (MeCN), and 1,4-dioxane were purchased in anhydrous form from a commercial source (Sigma-Aldrich). Nitromethane was dried over molecular sieves (4Å) and degassed prior to use. Acetone, ethyl acetate (EtOAc), diethyl ether (Et<sub>2</sub>O), CH<sub>2</sub>Cl<sub>2</sub>, hexanes, and water (H<sub>2</sub>O) were purchased from a commercial source (Samchun Chemical) and used without further purification. H<sub>2</sub><sup>18</sup>O (97 atom% <sup>18</sup>O) was purchased from Sigma-Aldrich and used as received. Other reagents were purchased from commercial sources (Sigma-Aldrich, Alfa Aesar, Acros Organics, and TCI) and used as received. Yields refer to chromatographically and spectroscopically (<sup>1</sup>H NMR) homogeneous materials, unless otherwise stated. Reactions were monitored by thin-layers chromatography (TLC) using 0.25 mm E. Merck silica gel plates (60 F<sub>254</sub>) and the developed chromatogram was visualized by using UV light or an acidic ethanolic anisaldehyde or potassium permanganate (KMnO<sub>4</sub>) stain with heating. Intertec Silica gel (60, particle size 60–200 μm) was used for flash column chromatography. <sup>1</sup>H, <sup>13</sup>C and <sup>19</sup>F NMR spectra were recorded on an Agilent 400-MR DD2 Magnetic Resonance System, Varian/Oxford As-500 instrument, or Bruker 500 MHz instrument and calibrated using residual un-deuterated solvent signal (CHCl<sub>3</sub> in CDCl<sub>3</sub>: δ 7.26 ppm for <sup>1</sup>H, δ 77.16 ppm for <sup>13</sup>C; CH<sub>3</sub>OH in MeOD: δ 3.31 ppm for <sup>1</sup>H, δ 49.00 ppm for <sup>13</sup>C) as the internal reference. <sup>19</sup>F NMR spectra were calibrated to an external standard of neat PhCF<sub>3</sub> (δ –63.72 ppm). Data for NMR spectra were reported as follows: chemical shift (multiplicities, coupling constant (Hz), and integration) and chemical shifts are reported in ppm. The following abbreviations were used to explain the multiplicities: s = singlet, d = doublet, t = triplet, q = quartet, p = pentet, dd = doublet of doublets, td = triplet of doublets, tt = triplet of triplets, dq = doublet of quartets, ddd = doublet of doublet of doublets, ddt = doublet of doublet of triplets, dtd = doublet of triplet of doublets, dtt = doublet of triplet of triplets, tdd = triplet of doublet of doublets, m = multiplet, br = broad. High-resolution mass spectrometry (HRMS) was performed using a HRMS-ESI Q-TOF 5600

spectrometer at National Instrumentation Center for Environmental Management (NICEM) in Seoul National University, Ultra High Resolution ESI Q-TOF mass spectrometer (Bruker compact) at the Organic Chemistry Research Center in Sogang University, or ThermoFisher Scientific mass spectrometer (Orbitrap Exploris 120) at Department of Chemistry at Seoul National University.

## 2. Preparation of Starting Materials

**Scheme S1.** Synthetic scheme for N-hydroxyindole **1**.



The synthetic scheme of the preparation of N-hydroxyindole **1**, the substrate of indolyl 1,3-heteroatom transposition (**IHT**) reaction, is depicted in Scheme 1. The two-step sequence, reduction of indole **S1** followed by tungstate-catalyzed oxidation, was utilized to provide a series of N-hydroxyindole **1**.<sup>13</sup> Detailed information on the preparation and characterization of **S1**, **S2** and **1** is described in Section 2.1, 2.2 and 2.3, respectively.

## 2.1. Preparation of Indole Derivatives

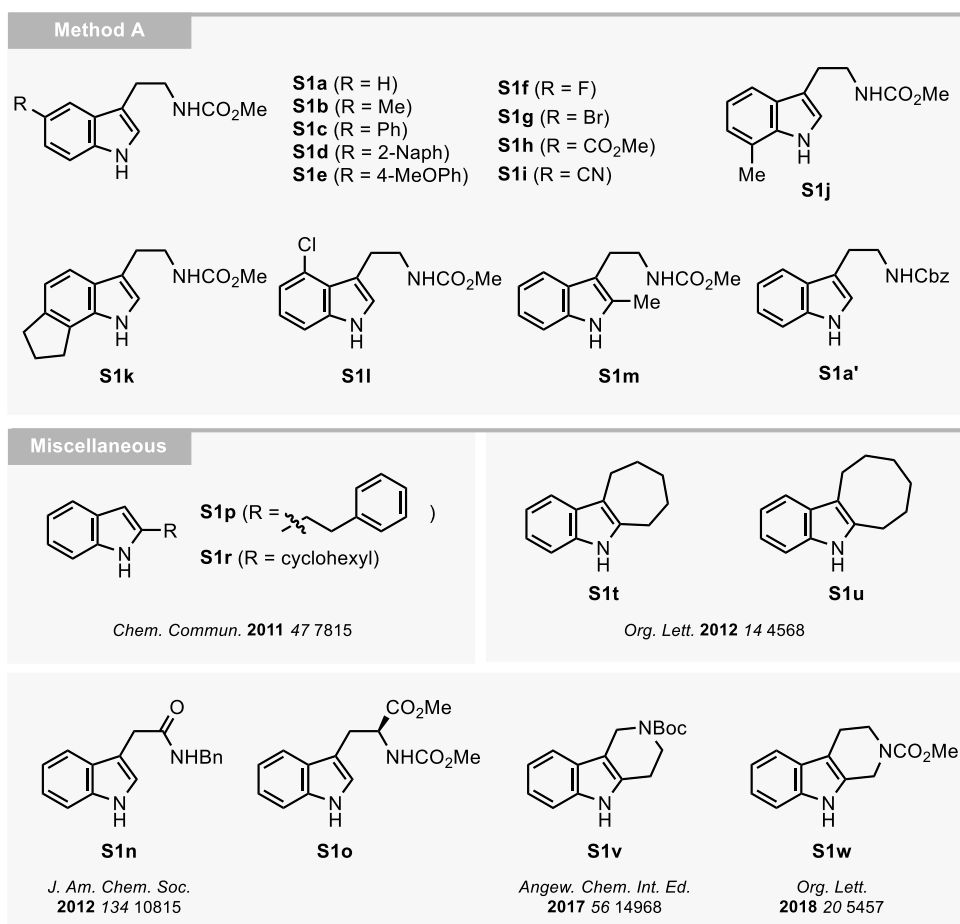
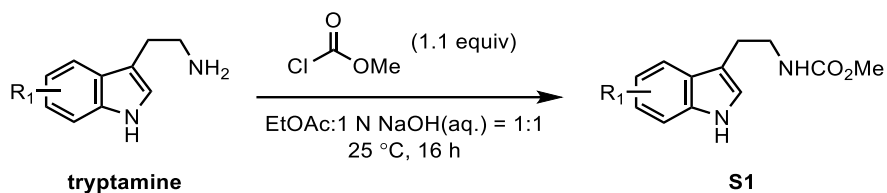


**Figure S1.** List of indole derivatives categorized by methods of preparation.

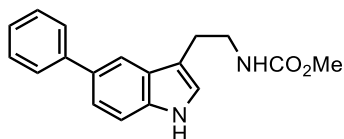
**The spectral data matched to those reported in the literature:** S1a<sup>1</sup>, S1b<sup>1</sup>, S1f<sup>1</sup>, S1g<sup>2</sup>, S1j<sup>2</sup>, S1l<sup>1</sup>, S1m<sup>3</sup>, S1n<sup>4</sup>, S1o, S1p<sup>5</sup>, S1r<sup>5</sup>, S1t<sup>6</sup>, S1u<sup>6</sup>, S1v<sup>7</sup>, S1w<sup>8</sup>, S1a<sup>9</sup>.

## General procedure A



To an oven-dried round-bottom flask equipped with a stir bar and septum were added tryptamine (1.0 equiv) and EtOAc:1 N NaOH (1:1, 0.2 M in tryptamine) at 23 °C, followed by methyl chloroformate (1.1 equiv). The resulting mixture was stirred for 16 h, before it was diluted with H<sub>2</sub>O. The layers were separated and the aqueous layer was extracted with CH<sub>2</sub>Cl<sub>2</sub> three times. The combined organic layer was washed with brine, dried over anhydrous MgSO<sub>4</sub>, filtered, and concentrated under reduced pressure. The resulting residue was purified by flash column chromatography to afford the desired product.

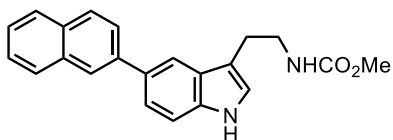
### Methyl (2-(5-phenyl-1H-indol-3-yl)ethyl)carbamate (S1c)



Following the **general procedure A**, 5-phenyl tryptamine (0.580 g, 1.97 mmol) afforded tryptamine **S1c** (465 mg, 80%) as a pale yellow oil after purification by flash column chromatography (silica gel, hexanes:EtOAc = 1:0 → 7:3).

$R_f$ =0.40 (silica gel, hexanes:EtOAc = 1:1); **<sup>1</sup>H NMR** (400 MHz, CDCl<sub>3</sub>): δ 8.42 (br s, 1H), 7.84 (s, 1H), 7.71 (d,  $J$  = 7.6 Hz, 2H), 7.51 – 7.47 (m, 3H), 7.42 (d,  $J$  = 8.4 Hz, 1H), 7.37 (t,  $J$  = 7.4 Hz, 1H), 7.06 – 6.96 (m, 1H), 4.94 (br s, 1H), 3.70 (s, 3H), 3.60 – 3.55 (m, 2H), 3.03 (t,  $J$  = 6.8 Hz, 2H); **<sup>13</sup>C NMR** (101 MHz, CDCl<sub>3</sub>): δ 157.3, 142.5, 135.9, 132.8, 128.7, 127.8, 127.3, 126.3, 123.0, 121.7, 117.0, 112.9, 111.6, 52.0, 41.5, 25.6; **HRMS** calcd. for C<sub>18</sub>H<sub>19</sub>N<sub>2</sub>O<sub>2</sub><sup>+</sup> [M + H]<sup>+</sup> 295.1441, found 295.1438.

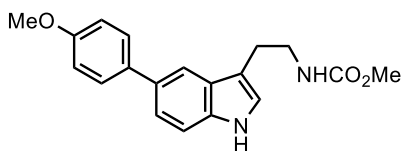
### Methyl (2-(5-(naphthalen-2-yl)-1H-indol-3-yl)ethyl)carbamate (S1d)



Following the **general procedure A**, 5-(naphthalen-2-yl)-tryptamine (0.490 g, 1.71 mmol) afforded tryptamine **S1d** (0.340 g, 58%) as a pale yellow amorphous solid after purification by flash column chromatography (silica gel, hexanes:EtOAc = 1:0 → 7:3).

$R_f=0.4$  (silica gel, hexanes:EtOAc = 7:3);  $^1\text{H NMR}$  (400 MHz,  $\text{CDCl}_3$ ):  $\delta$  8.11 (br s, 1H), 8.09 (s, 1H), 7.94 – 7.90 (m, 3H), 7.88 – 7.83 (m, 2H), 7.60 (d,  $J = 8.3$  Hz, 1H), 7.53 – 7.45 (m, 3H), 7.09 (s, 1H), 4.80 (s, 1H), 3.67 (s, 3H), 3.61 – 3.58 (br q,  $J = 6.5$  Hz, 2H), 3.05 (t,  $J = 6.8$  Hz, 2H);  $^{13}\text{C NMR}$  (101 MHz,  $\text{CDCl}_3$ ):  $\delta$  157.2, 139.9, 136.1, 134.0, 133.1, 132.3, 128.4, 128.2, 128.1, 127.8, 126.4, 126.3, 125.7, 125.6, 123.0, 122.4, 117.7, 113.5, 111.7, 52.2, 41.5, 25.9; **HRMS** calcd. for  $\text{C}_{22}\text{H}_{21}\text{N}_2\text{O}_2^+$   $[\text{M} + \text{H}]^+$  345.1598, found 345.1591.

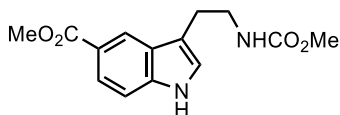
#### Methyl (2-(5-(4-methoxyphenyl)-1H-indol-3-yl)ethyl)carbamate (**S1e**)



Following the **general procedure A**, 5-(4-methoxyphenyl)-tryptamine (0.750 g, 2.82 mmol) afforded tryptamine **S1e** (0.630 g, 69%) as a pale yellow oil after purification by flash column chromatography (silica gel, hexanes:EtOAc = 1:0 → 7:3).

$R_f=0.27$  (silica gel, hexanes:EtOAc = 1:1);  $^1\text{H NMR}$  (500 MHz,  $\text{CDCl}_3$ ):  $\delta$  8.15 (br s, 1H), 7.74 (s, 1H), 7.58 (d,  $J = 8.6$  Hz, 1H), 7.44 – 7.38 (m, 2H), 7.04 (s, 1H), 7.00 (d,  $J = 8.6$  Hz, 2H), 4.81 (br s, 1H), 3.87 (s, 3H), 3.67 (s, 3H), 3.57 – 3.53 (m, 2H), 3.01 (t,  $J = 6.8$  Hz, 2H);  $^{13}\text{C NMR}$  (126 MHz,  $\text{CDCl}_3$ ):  $\delta$  158.65, 157.21, 135.73, 135.26, 132.96, 128.47, 127.95, 122.87, 121.99, 116.87, 114.25, 113.35, 111.54, 55.50, 52.15, 41.48, 25.88; **HRMS** calcd. for  $\text{C}_{19}\text{H}_{21}\text{N}_2\text{O}_3^+$   $[\text{M} + \text{H}]^+$  325.1547, found 325.1556.

#### Methyl 3-(2-((methoxycarbonyl)amino)ethyl)-1H-indole-5-carboxylate (**S1h**)

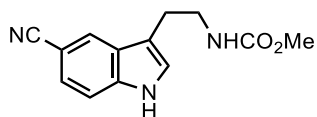




Following the **general procedure A**, Methyl tryptamine-5-carboxylate (0.300 g, 1.36 mmol) afforded tryptamine **S1h** (0.210 g, 56%) as a pale yellow amorphous solid after purification by flash column chromatography (silica gel, hexanes:EtOAc = 1:0 → 6:4).

$R_f=0.4$  (silica gel, hexanes:EtOAc = 4:6);  $^1\text{H NMR}$  (400 MHz,  $\text{CDCl}_3$ ):  $\delta$  8.78 (br s, 1H), 8.35 (s, 1H), 7.89 (d,  $J = 8.6$  Hz, 1H), 7.35 (d,  $J = 8.5$  Hz, 1H), 7.06 (s, 1H), 4.88 (br s, 1H), 3.93 (s, 3H), 3.65 (s, 3H), 3.53 – 3.48 (m, 2H), 2.97 (t,  $J = 6.5$  Hz, 2H);  $^{13}\text{C NMR}$  (101 MHz,  $\text{CDCl}_3$ ):  $\delta$  168.4, 157.3, 139.1, 127.0, 123.6, 123.5, 121.7, 121.4, 114.3, 111.1, 52.2, 52.0, 41.4, 25.7; **HRMS** calcd. for  $\text{C}_{14}\text{H}_{17}\text{N}_2\text{O}_4^+$   $[\text{M} + \text{H}]^+$  277.1187, found 277.1182.

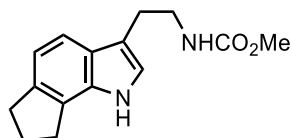
### Methyl (2-(5-cyano-1H-indol-3-yl)ethyl)carbamate (**S1i**)



Following the **general procedure A**, 5-cyanotryptamine (352 mg, 1.88 mmol) afforded tryptamine **S1i** (0.250 g, 55%) as a pale yellow oil after purification by flash column chromatography (silica gel, hexanes:EtOAc = 1:0 → 6:4).

$R_f=0.2$  (silica gel, hexanes:EtOAc = 4:6);  $^1\text{H NMR}$  (400 MHz,  $\text{CDCl}_3$ ):  $\delta$  8.58 (br s, 1H), 7.94 (s, 1H), 7.42 (s, 2H), 7.16 (s, 1H), 4.81 (br s, 1H), 3.67 (s, 3H), 3.53 – 3.48 (m, 2H), 2.97 (t,  $J = 6.5$  Hz, 2H);  $^{13}\text{C NMR}$  (101 MHz,  $\text{CDCl}_3$ ):  $\delta$  157.2, 138.1, 127.4, 125.2, 124.6, 124.3, 120.9, 114.2, 112.3, 102.7, 52.3, 41.4, 25.7; **HRMS** calcd. for  $\text{C}_{13}\text{H}_{14}\text{N}_3\text{O}_2^+$   $[\text{M} + \text{H}]^+$  244.1076, found 244.1081.

### Methyl (2-(1,6,7,8-tetrahydrocyclopenta[g]indol-3-yl)ethyl)carbamate (**S1k**)



Following the **general procedure A**, 2-(1,6,7,8-tetrahydrocyclopenta[g]indol-3-yl)ethan-1-amine (0.230 g, 1.14 mmol) afforded tryptamine **S1k** (191 mg, 65%) as a pale yellow oil after purification by flash column chromatography (silica gel, hexanes:EtOAc = 1:0 → 7:3).

$R_f=0.6$  (silica gel, hexanes:EtOAc = 6:4);  $^1\text{H NMR}$  (400 MHz,  $\text{CDCl}_3$ ):  $\delta$  7.93 (br s, 1H), 7.42 (d,  $J = 8.1$  Hz, 1H), 7.07 (d,  $J = 8.0$  Hz, 1H), 6.97 (s, 1H), 4.77 (br s, 1H), 3.66 (s, 3H),

3.52 (d,  $J = 6.6$  Hz, 2H), 3.05 (q,  $J = 8.0$  Hz, 4H), 2.97 (t,  $J = 6.9$  Hz, 2H), 2.22 (p,  $J = 7.3$  Hz, 2H);  $^{13}\text{C}$  NMR (101 MHz,  $\text{CDCl}_3$ ):  $\delta$  157.2, 138.9, 133.7, 126.0, 125.7, 121.4, 116.9, 116.6, 113.6, 52.1, 41.4, 33.2, 29.9, 26.1, 25.5; **HRMS** calcd. for  $\text{C}_{15}\text{H}_{20}\text{N}_2\text{O}_2^+$   $[\text{M} + \text{H}]^+$  259.1441, found 259.1439.

## 2.2. Preparation of Indoline Derivatives

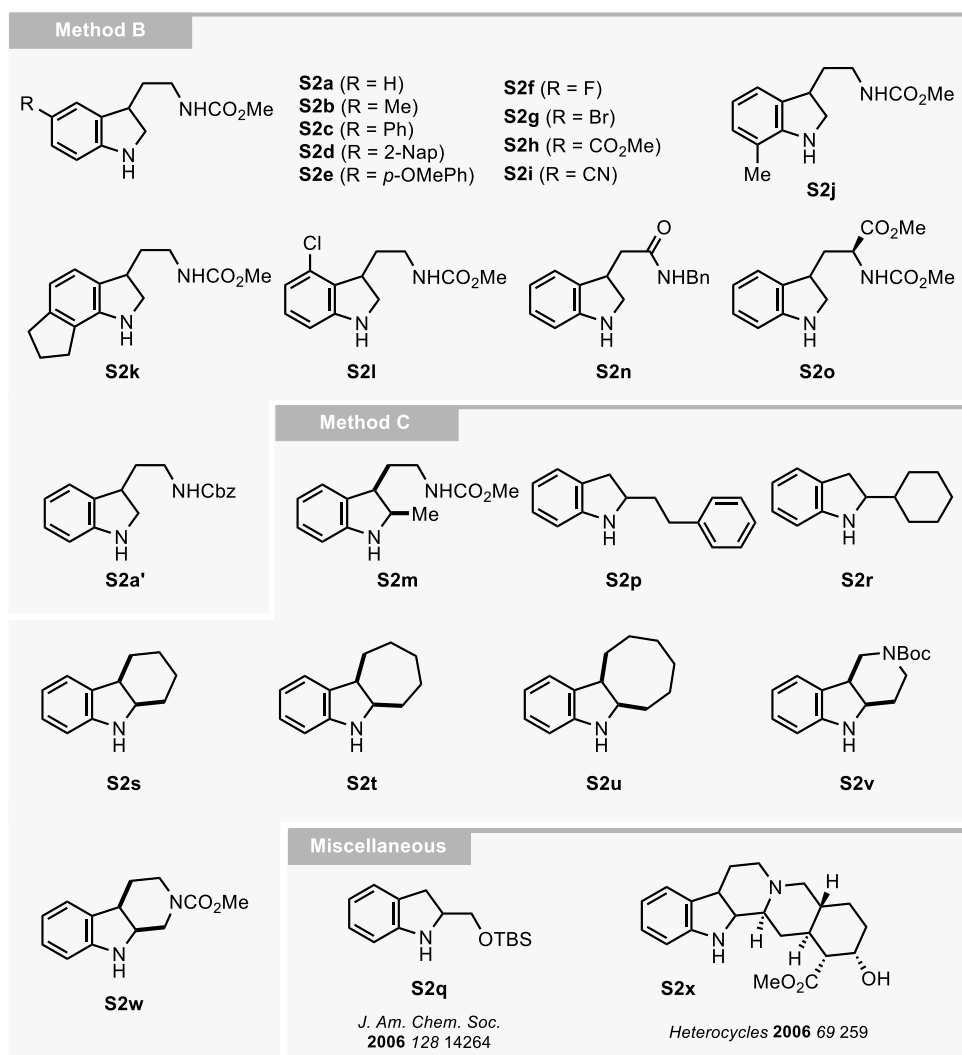
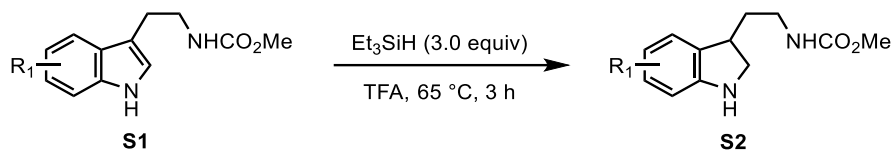


**Figure S2.** List of indoline derivatives categorized by methods of preparation.

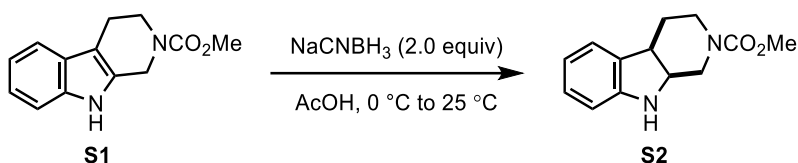
The spectral data matched to those reported in the literature: S2p<sup>10</sup>, S2q<sup>10</sup>, S2r<sup>11</sup>, S2s<sup>10</sup>, S2t<sup>10</sup>, S2u<sup>12</sup>, S2x<sup>13</sup>

### General procedure B



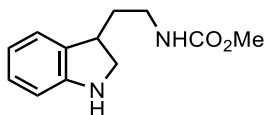
To an oven-dried round-bottom flask equipped with a stir bar and septum were added indole **S1** (1.0 equiv) and TFA (0.3 M in **S1**) at  $23\text{ }^\circ\text{C}$ , followed by  $Et_3SiH$  (3.0 equiv). The resulting mixture was heated to  $65\text{ }^\circ\text{C}$  in a pre-heated oil bath and stirred for 3 h, before it was cooled to rt and directly concentrated under reduced pressure to remove most of TFA. The crude product was re-dissolved in  $CH_2Cl_2$  and basified to pH 9–10 using  $NH_3 \cdot H_2O$  (25.0–30.0 wt% in  $H_2O$ ). The layers were separated and the aqueous layer was extracted with  $CH_2Cl_2$  three times. The combined organic layer was washed with brine, dried over anhydrous  $MgSO_4$ , filtered, and concentrated under reduced pressure. The resulting residue was purified by flash column chromatography to afford indoline **S2**.

### General procedure C



To an oven-dried round-bottom flask equipped with a stir bar and septum were added indole **S1** (1.0 equiv) and AcOH (0.1 M in **S1**) at  $23\text{ }^\circ\text{C}$ . The resulting solution was cooled to  $0\text{ }^\circ\text{C}$ , and  $NaBH_3CN$  (2.0 equiv) was added to the solution. The reaction mixture was warmed up to rt and stirred while the reaction was monitored by TLC. After completion of reaction (1–2 h), the reaction mixture was directly concentrated under reduced pressure. The crude product was re-dissolved in  $CH_2Cl_2$  and basified to pH 9–10 using  $NH_3 \cdot H_2O$  (25.0–30.0 wt% in  $H_2O$ ). The layers were separated and the aqueous layer was extracted with  $CH_2Cl_2$  three times. The combined organic layer was washed with brine, dried over anhydrous  $MgSO_4$ , filtered, and concentrated under reduced pressure. The resulting residue was purified by flash column chromatography to afford indoline **S2**.

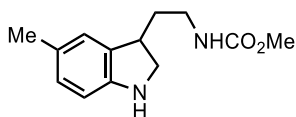
### Methyl (2-(indolin-3-yl)ethyl)carbamate (S2a)



Following the **general procedure B**, tryptamine **S1a** (3.50 g, 16.0 mmol) afforded indoline **S2a** (3.30 g, 94%) as a pale yellow amorphous amorphous solid after purification by flash column chromatography (silica gel, hexanes:EtOAc = 8:2 → 6:4).

$R_f=0.2$  (silica gel, hexanes:EtOAc = 1:1);  $^1\text{H NMR}$  (500 MHz,  $\text{CDCl}_3$ ):  $\delta$  7.08 (d,  $J = 7.3$  Hz, 1H), 7.03 (t,  $J = 7.6$  Hz, 1H), 6.72 (t,  $J = 7.4$  Hz, 1H), 6.64 (d,  $J = 7.7$  Hz, 1H), 5.03 (s, 1H), 3.78 – 3.62 (m, 5H), 3.35 – 3.26 (m, 2H), 3.22 (m, 2H), 2.04 – 1.93 (m, 1H), 1.73 (m, 1H);  $^{13}\text{C NMR}$  (126 MHz,  $\text{CDCl}_3$ ):  $\delta$  157.2, 151.3, 132.1, 127.7, 123.9, 118.8, 109.7, 53.3, 52.1, 39.6, 39.1, 34.5; **HRMS** calcd. for  $\text{C}_{12}\text{H}_{17}\text{N}_2\text{O}_2^+$   $[\text{M} + \text{H}]^+$  221.1285, found 221.1278.

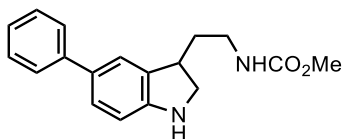
### Methyl (2-(5-methylindolin-3-yl)ethyl)carbamate (S2b)



Following the **general procedure B**, tryptamine **S1b** (0.100 g, 0.431 mmol) afforded indoline **S2b** (75.0 mg, 74%) as a pale yellow oil after purification by flash column chromatography (silica gel, hexanes:EtOAc = 8:2 → 6:4).

$R_f=0.34$  (silica gel, hexanes:EtOAc = 2:8);  $^1\text{H NMR}$  (400 MHz,  $\text{CDCl}_3$ ):  $\delta$  6.91 (s, 1H), 6.85 (d,  $J = 7.9$  Hz, 1H), 6.57 (d,  $J = 7.8$  Hz, 1H), 4.86 (br s, 1H), 3.68 (t,  $J = 7.3$  Hz, 2H), 3.66 (s, 3H), 3.35 – 3.18 (m, 4H), 2.26 (s, 3H), 2.04 – 1.95 (m, 1H), 1.78 – 1.69 (m, 1H);  $^{13}\text{C NMR}$  (101 MHz,  $\text{CDCl}_3$ ):  $\delta$  157.2, 148.8, 132.5, 128.1, 127.9, 124.5, 109.7, 53.4, 51.9, 39.5, 39.0, 34.3, 20.8; **HRMS** calcd. for  $\text{C}_{13}\text{H}_{19}\text{N}_2\text{O}_2^+$   $[\text{M} + \text{H}]^+$  235.1442, found 235.1441.

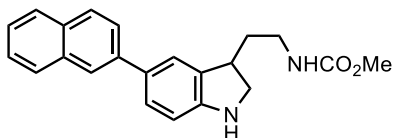
### Methyl (2-(5-phenylindolin-3-yl)ethyl)carbamate (S2c)



Following the **general procedure B**, tryptamine **S1c** (0.300 g, 1.02 mmol) afforded indoline **S2c** (0.265 g, 88%) as a pale yellow amorphous solid after purification by flash column chromatography (silica gel, hexanes:EtOAc = 8:2 → 6:4).

$R_f$ =0.38 (silica gel, hexanes:EtOAc = 2:8);  $^1\text{H NMR}$  (500 MHz,  $\text{CDCl}_3$ ):  $\delta$  7.54 (d,  $J$  = 7.7 Hz, 2H), 7.41 (t,  $J$  = 7.6 Hz, 2H), 7.34 (s, 1H), 7.33 – 7.27 (m, 2H), 6.71 (d,  $J$  = 8.0 Hz, 1H), 5.01 (br s, 1H), 3.75 (t,  $J$  = 8.7 Hz, 1H), 3.68 (s, 3H), 3.41 – 3.35 (m, 1H), 3.33 – 3.24 (m, 3H), 2.09 – 2.03 (m, 1H), 1.79 (dt,  $J$  = 14.2, 7.1 Hz, 1H);  $^{13}\text{C NMR}$  (126 MHz,  $\text{CDCl}_3$ ):  $\delta$  157.2, 150.7, 141.6, 132.9, 132.2, 128.7, 126.8, 126.6, 126.2, 122.8, 109.8, 53.5, 52.1, 39.5, 39.1, 34.6; **HRMS** calcd. for  $\text{C}_{18}\text{H}_{21}\text{N}_2\text{O}_2^+$   $[\text{M} + \text{H}]^+$  297.1592, found 297.1598.

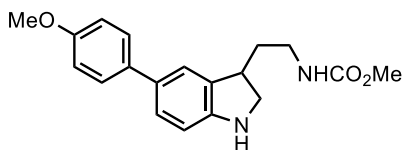
#### Methyl (2-(5-(naphthalen-2-yl)indolin-3-yl)ethyl)carbamate (**S2d**)



Following the **general procedure B**, tryptamine **S1d** (0.450 g, 1.31 mmol) afforded indoline **S2d** (0.330 g, 73%) as a pale yellow amorphous solid after purification by flash column chromatography (silica gel, hexanes:EtOAc = 8:2 → 6:4).

$R_f$ =0.38 (silica gel, hexanes:EtOAc = 2:8);  $^1\text{H NMR}$  (500 MHz,  $\text{CDCl}_3$ ):  $\delta$  7.97 (s, 1H), 7.87 (d,  $J$  = 8.2 Hz, 2H), 7.84 (d,  $J$  = 8.0 Hz, 1H), 7.71 (dd,  $J$  = 8.5, 1.8 Hz, 1H), 7.52 – 7.40 (m, 4H), 6.74 (d,  $J$  = 8.0 Hz, 1H), 4.92 (s, 1H), 3.77 (t,  $J$  = 8.7 Hz, 1H), 3.68 (s, 3H), 3.45 – 3.37 (m, 1H), 3.37 – 3.24 (m, 3H), 2.15 – 2.03 (m, 1H), 1.88 – 1.76 (m, 1H);  $^{13}\text{C NMR}$  (126 MHz,  $\text{CDCl}_3$ ):  $\delta$  157.3, 150.9, 139.1, 134.0, 133.0, 132.2, 132.0, 128.3, 128.0, 127.7, 127.2, 126.2, 125.6, 125.5, 124.6, 123.1, 109.9, 53.5, 52.2, 39.7, 39.2, 34.7; **HRMS** calcd. for  $\text{C}_{22}\text{H}_{23}\text{N}_2\text{O}_2^+$   $[\text{M} + \text{H}]^+$  347.1754, found 347.1748.

#### Methyl (2-(5-(4-methoxyphenyl)indolin-3-yl)ethyl)carbamate (**S2e**)

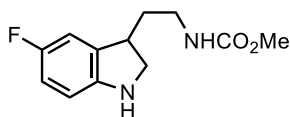


Following the **general procedure B**, tryptamine **S1e** (0.370 g, 1.14 mmol) afforded indoline

**S2e** (0.280 g, 75%) as a pale yellow oil after purification by flash column chromatography (silica gel, hexanes:EtOAc = 8:2 → 6:4).

$R_f=0.1$  (silica gel, hexanes:EtOAc = 1:1);  $^1\text{H NMR}$  (500 MHz,  $\text{CDCl}_3$ ):  $\delta$  7.44 (d,  $J = 8.3$  Hz, 2H), 7.21 (d,  $J = 6.5$  Hz, 1H), 6.92 (d,  $J = 8.2$  Hz, 2H), 6.61 (d,  $J = 8.0$  Hz, 1H), 5.33 (br s, 1H), 3.85 (s, 1H), 3.77 (s, 3H), 3.64 (s, 3H), 3.32 – 3.12 (m, 4H), 2.02 – 1.96 (m, 1H), 1.73 – 1.66 (m, 1H);  $^{13}\text{C NMR}$  (126 MHz,  $\text{CDCl}_3$ ):  $\delta$  158.1, 157.1, 150.2, 134.1, 132.7, 131.3, 127.2, 126.0, 122.1, 113.9, 109.5, 55.1, 53.2, 51.8, 39.3, 38.9, 34.2; **HRMS** calcd. for  $\text{C}_{19}\text{H}_{23}\text{N}_2\text{O}_3^+$   $[\text{M} + \text{H}]^+$  327.1701, found 327.1703.

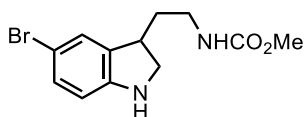
#### Methyl (2-(5-fluoroindolin-3-yl)ethyl)carbamate (**S2f**)



Following the **general procedure B**, tryptamine **S1f** (1.80 g, 7.62 mmol) afforded indoline **S2f** (1.30 g, 72%) as a brown oil after purification by flash column chromatography (silica gel, hexanes:EtOAc = 8:2 → 1:1).

$R_f=0.28$  (silica gel, hexanes:EtOAc = 2:8);  $^1\text{H NMR}$  (400 MHz,  $\text{CDCl}_3$ ):  $\delta$  6.81 (d,  $J = 8.3$  Hz, 1H), 6.73 (t,  $J = 8.8$  Hz, 1H), 6.54 (dd,  $J = 8.5, 4.3$  Hz, 1H), 4.88 (br s, 1H), 3.71 (t,  $J = 8.0$  Hz, 2H), 3.66 (s, 3H), 3.35 – 3.17 (m, 4H), 2.03 – 1.90 (m, 1H), 1.79 – 1.68 (m, 1H);  $^{13}\text{C NMR}$  (101 MHz,  $\text{CDCl}_3$ ):  $\delta$  157.2 (d,  $J = 235.6$  Hz), 157.2, 147.3 (d,  $J = 1.4$  Hz), 134.0 (d,  $J = 6.1$  Hz), 113.8 (d,  $J = 23.4$  Hz), 111.4 (d,  $J = 23.9$  Hz), 110.0 (d,  $J = 8.2$  Hz), 53.9, 52.2, 40.0, 39.0, 34.4;  $^{19}\text{F NMR}$  (376 MHz,  $\text{CDCl}_3$ ):  $\delta$  -126.1; **HRMS** calcd. for  $\text{C}_{12}\text{H}_{16}\text{FN}_2\text{O}_2^+$   $[\text{M} + \text{H}]^+$  239.1188, found 239.1190.

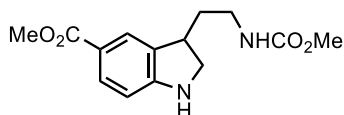
#### Methyl (2-(5-bromoindolin-3-yl)ethyl)carbamate (**S2g**)



Following the **general procedure B**, tryptamine **S1g** (0.500 g, 1.68 mmol) afforded indoline **S2g** (0.400 g, 80%) as a yellow oil after purification by flash column chromatography (silica gel, hexanes:EtOAc = 8:2 → 1:1).

$R_f=0.23$  (silica gel, hexanes:EtOAc = 1:1);  $^1\text{H NMR}$  (400 MHz,  $\text{CDCl}_3$ ):  $\delta$  7.16 (s, 1H), 7.12 (d,  $J = 7.9$  Hz, 1H), 6.50 (d,  $J = 8.2$  Hz, 1H), 4.80 (br s, 1H), 3.75 – 3.65 (m, 4H), 3.36 – 3.20 (m, 4H), 2.01 – 1.93 (s, 1H), 1.80 – 1.69 (m, 1H);  $^{13}\text{C NMR}$  (101 MHz,  $\text{CDCl}_3$ )  $\delta$  157.2, 150.4, 134.6, 130.4, 127.0, 110.9, 110.3, 53.5, 52.2, 39.6, 39.0, 34.5; **HRMS** calcd. for  $\text{C}_{12}\text{H}_{16}\text{BrN}_2\text{O}_2^+ [\text{M} + \text{H}]^+$  299.0390, found 299.0390.

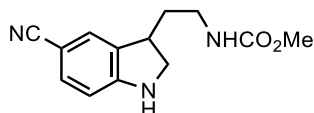
### Methyl 3-(2-((methoxycarbonyl)amino)ethyl)indoline-5-carboxylate (**S2h**)



Following the **general procedure B**, tryptamine **S1h** (0.340 g, 1.23 mmol) afforded indoline **S2h** (0.212 g, 76%) as a colorless oil after purification by flash column chromatography (silica gel, hexanes:EtOAc = 8:2  $\rightarrow$  1:1).

$R_f=0.45$  (silica gel, hexanes:EtOAc = 2:8);  $^1\text{H NMR}$  (400 MHz,  $\text{CDCl}_3$ ):  $\delta$  8.78 (s, 1H), 8.35 (s, 1H), 7.89 (d,  $J = 8.6$  Hz, 1H), 7.35 (d,  $J = 8.5$  Hz, 1H), 7.06 (s, 1H), 4.88 (s, 1H), 3.93 (s, 3H), 3.65 (s, 3H), 3.57 – 3.42 (m, 2H), 2.97 (t,  $J = 6.5$  Hz, 2H);  $^{13}\text{C NMR}$  (101 MHz,  $\text{CDCl}_3$ ):  $\delta$  168.4, 157.3, 139.1, 127.0, 123.6, 123.5, 121.8, 121.4, 114.3, 111.1, 52.2, 52.0, 41.4, 25.7; **HRMS** calcd. for  $\text{C}_{14}\text{H}_{19}\text{N}_2\text{O}_4^+ [\text{M} + \text{H}]^+$  279.1341, found 279.1339.

### Methyl (2-(5-cyanoindolin-3-yl)ethyl)carbamate (**S2i**)

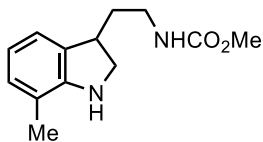


Following the **general procedure B**, tryptamine **S1i** (0.900 g, 3.70 mmol) afforded indoline **S2i** (0.700 g, 77%) as a pale yellow amorphous solid after purification by flash column chromatography (silica gel, hexanes:EtOAc = 8:2  $\rightarrow$  1:1).

$R_f=0.34$  (silica gel, hexanes:EtOAc = 2:8);  $^1\text{H NMR}$  (400 MHz, MeOD):  $\delta$  7.33 – 7.26 (m, 2H), 6.54 (d,  $J = 8.2$  Hz, 1H), 3.79 – 3.72 (m, 1H), 3.63 (s, 3H), 3.35 – 3.27 (m, 2H), 3.19 (t,  $J = 7.6$  Hz, 2H), 1.97 – 1.90 (m, 1H), 1.75 – 1.65 (m, 1H);  $^{13}\text{C NMR}$  (101 MHz,  $\text{CDCl}_3$ ):  $\delta$  157.3, 155.1, 133.5, 132.6, 127.6, 120.8, 108.4, 99.7, 53.0, 52.3, 38.8, 38.7, 34.8; **HRMS** calcd. for  $\text{C}_{13}\text{H}_{16}\text{N}_3\text{O}_2^+ [\text{M} + \text{H}]^+$  246.1234, found 246.1237.



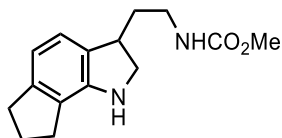
### Methyl (2-(7-methylindolin-3-yl)ethyl)carbamate (S2j)



Following the **general procedure B**, tryptamine **S1j** (0.450 g, 1.94 mmol) afforded indoline **S2j** (0.345 g, 76%) as a pale yellow amorphous solid after purification by flash column chromatography (silica gel, hexanes:EtOAc = 8:2 → 6:4).

$R_f$ =0.34 (silica gel, hexanes:EtOAc = 2:8);  $^1\text{H NMR}$  (400 MHz,  $\text{CDCl}_3$ ):  $\delta$  6.96 (d,  $J = 7.4$  Hz, 1H), 6.89 (d,  $J = 7.5$  Hz, 1H), 6.69 (t,  $J = 7.4$  Hz, 1H), 4.91 (br s, 1H), 3.76 – 3.69 (m, 2H), 3.67 (s, 2H), 3.39 – 3.30 (m, 1H), 3.30 – 3.17 (m, 3H), 2.13 (s, 3H), 2.06 – 1.93 (m, 1H), 1.81 – 1.68 (m, 1H);  $^{13}\text{C NMR}$  (101 MHz,  $\text{CDCl}_3$ ):  $\delta$  157.2, 149.8, 131.5, 128.7, 121.5, 119.3, 119.1, 53.2, 52.2, 40.0, 39.2, 34.7, 16.9; **HRMS** calcd. for  $\text{C}_{13}\text{H}_{19}\text{N}_2\text{O}_2^+$   $[\text{M} + \text{H}]^+$  235.1441, found 235.1441.

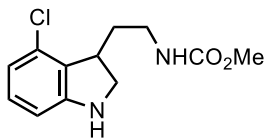
### Methyl (2-(1,2,3,6,7,8-hexahydrocyclopenta[g]indol-3-yl)ethyl)carbamate (S2k)



Following the **general procedure B**, tryptamine **S1k** (0.230 g, 0.891 mmol) afforded indoline **S2k** (0.210 g, 91%) as a pale yellow oil after purification by flash column chromatography (silica gel, hexanes:EtOAc = 8:2 → 6:4).

$R_f$ =0.24 (silica gel, hexanes:EtOAc = 7:3);  $^1\text{H NMR}$  (500 MHz,  $\text{CDCl}_3$ ):  $\delta$  6.91 (d,  $J = 7.4$  Hz, 1H), 6.66 (d,  $J = 7.4$  Hz, 1H), 4.83 (br s, 1H), 3.73 (t,  $J = 8.2$  Hz, 1H), 3.67 (s, 3H), 3.57 (s, 1H), 3.37 – 3.15 (m, 4H), 2.86 (t,  $J = 7.5$  Hz, 2H), 2.70 (t,  $J = 7.3$  Hz, 2H), 2.17 (s, 1H), 2.08 (p,  $J = 7.5$  Hz, 2H), 1.99 (dq,  $J = 13.9, 7.0$  Hz, 1H), 1.74 (dq,  $J = 14.4, 7.6$  Hz, 1H);  $^{13}\text{C NMR}$  (126 MHz,  $\text{CDCl}_3$ ):  $\delta$  157.2, 147.3, 144.8, 129.7, 125.2, 121.9, 114.8, 77.4, 77.2, 76.9, 53.9, 52.2, 39.7, 39.3, 34.9, 32.9, 31.1, 29.5, 25.6; **HRMS** calcd. for  $\text{C}_{15}\text{H}_{21}\text{N}_2\text{O}_2^+$   $[\text{M} + \text{H}]^+$  261.1598, found 261.1590.

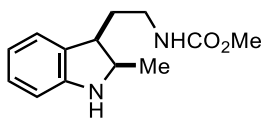
### Methyl (2-(4-chloroindolin-3-yl)ethyl)carbamate (S2l)



Following the **general procedure B**, tryptamine **S1l** (0.100 g, 0.396 mmol) afforded indoline **S2l** (80.0 mg, 89%) as a pale yellow oil after purification by flash column chromatography (silica gel, hexanes:EtOAc = 8:2 → 1:1).

$R_f$ =0.34 (silica gel, hexanes:EtOAc = 2:8);  $^1\text{H NMR}$  (400 MHz,  $\text{CDCl}_3$ ):  $\delta$  6.95 (t,  $J = 7.9$  Hz, 1H), 6.65 (d,  $J = 8.0$  Hz, 1H), 6.50 (d,  $J = 7.8$  Hz, 1H), 4.97 (s, 1H), 3.87 (s, 1H), 3.68 (d,  $J = 8.8$  Hz, 1H), 3.65 (s, 3H), 3.51 – 3.34 (m, 2H), 3.31 – 3.07 (m, 2H), 2.00 – 1.81 (m, 2H);  $^{13}\text{C NMR}$  (101 MHz,  $\text{CDCl}_3$ )  $\delta$  157.2, 152.8, 130.8, 129.6, 129.4, 119.1, 107.9, 77.5, 77.2, 76.8, 52.2, 52.1, 39.3, 38.7, 32.6; **HRMS** calcd. for  $\text{C}_{12}\text{H}_{16}\text{ClN}_2\text{O}_2^+$   $[\text{M} + \text{H}]^+$  255.0895, found 255.0892.

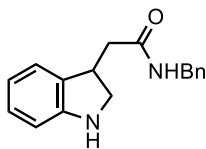
### Methyl (2-(2-methylindolin-3-yl)ethyl)carbamate (S2m)



Following the **general procedure C**, tryptamine **S1m** (0.500 g, 2.15 mmol) afforded indoline **S2m** (0.430 g, 85%) as a pale yellow oil after purification by flash column chromatography (silica gel, hexanes:EtOAc = 8:2 → 1:1).

$R_f$ =0.48 (silica gel, hexanes:EtOAc = 2:8);  $^1\text{H NMR}$  (400 MHz,  $\text{CDCl}_3$ ):  $\delta$  7.09 – 7.04 (m, 1H), 7.02 (t,  $J = 7.6$  Hz, 1H), 6.70 (q,  $J = 6.9$  Hz, 1H), 6.59 (t,  $J = 8.7$  Hz, 1H), 5.09 (br s, 1H), 3.95 and 3.59 (t,  $J = 6.1$  Hz, 1H), 3.80 – 3.70 (m, 1H), 3.65 (s, 3H), 3.23 – 3.18 (m, 2H), 3.10 and 2.84 (q,  $J = 6.2$  Hz, 1H), 1.91 – 1.73 (m, 2H), 1.22 and 1.16 (d,  $J = 6.4$  Hz, 3H);  $^{13}\text{C NMR}$  (101 MHz,  $\text{CDCl}_3$ ):  $\delta$  157.2, 150.4, 150.0, 131.8, 131.3, 127.7, 127.5, 124.3, 124.3, 118.6, 118.5, 109.6, 109.4, 60.4, 58.3, 52.0, 47.1, 42.2, 39.3, 38.7, 34.3, 28.4, 22.2, 16.0; **HRMS** calcd. for  $\text{C}_{13}\text{H}_{19}\text{N}_2\text{O}_2^+$   $[\text{M} + \text{H}]^+$  235.1442, found 235.1441.

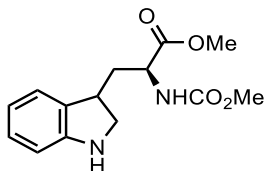
### N-benzyl-2-(indolin-3-yl)acetamide (S2n)



Following the **general procedure B**, indole **S1n** (2.30 g, 8.70 mmol) afforded indoline **S2n** (1.37 g, 59%) as a pale yellow oil after purification by flash column chromatography (silica gel, hexanes:EtOAc = 1:0 → 1:1).

$R_f$ =0.26 (silica gel, hexanes:EtOAc = 6:4);  $^1\text{H NMR}$  (500 MHz,  $\text{CDCl}_3$ ):  $\delta$  7.36 – 7.27 (m, 3H), 7.26 – 7.21 (m, 2H), 7.07 (d,  $J$  = 7.6 Hz, 2H), 6.75 (t,  $J$  = 7.3 Hz, 1H), 6.67 (d,  $J$  = 7.5 Hz, 1H), 6.34 (s, 1H), 5.12 (s, 1H), 4.40 (d,  $J$  = 5.8 Hz, 2H), 3.80 – 3.74 (m, 1H), 3.70 (t,  $J$  = 9.0 Hz, 1H), 3.30 – 3.22 (m, 1H), 2.50 (ddd,  $J$  = 61.3, 14.5, 7.3 Hz, 2H);  $^{13}\text{C NMR}$  (126 MHz,  $\text{CDCl}_3$ )  $\delta$  171.4, 150.0, 138.2, 138.2, 132.1, 132.1, 128.7, 128.1, 127.8, 127.5, 124.3, 119.7, 110.6, 110.6, 52.8, 43.6, 41.2, 38.9; **HRMS** calcd. for  $\text{C}_{17}\text{H}_{19}\text{N}_2\text{O}^+$   $[\text{M} + \text{H}]^+$  267.1492, found 267.1491.

### Methyl (2S)-3-(indolin-3-yl)-2-((methoxycarbonyl)amino)propanoate (S2o)

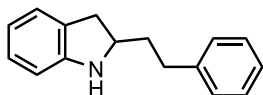


Following the **general procedure B**, tryptophan **S1o** (1.50 g, 5.43 mmol) afforded indoline **S2o** (1.07 g, 71%) as an inconsequential 1:1 mixture of diastereomers in the form of a pale yellow oil after purification by flash column chromatography (silica gel, hexanes:EtOAc = 1:0 → 1:1). The resulting diastereomeric mixture were used directly in the subsequent reaction without separation. The diastereomeric ratio was determined by  $^1\text{H NMR}$  analysis of the crude reaction mixture.

$R_f$ =0.25 (silica gel, hexanes:EtOAc = 1:1);  $^1\text{H NMR}$  (500 MHz,  $\text{CDCl}_3$ ):  $\delta$  7.15 (d,  $J$  = 7.3 Hz, 0.5H), 7.05 (d,  $J$  = 7.3 Hz, 0.5H), 7.03 (t,  $J$  = 7.6 Hz, 1H), 6.74 – 6.69 (m, 1H), 6.63 (t,  $J$  = 7.2 Hz, 1H), 5.61 (br s, 1H), 4.52 – 4.43 (m, 1H), 3.80-3.70 (m, 1H), 3.72 and 3.69 (s, 6H), 3.39 – 3.33 (m, 1H), 3.28 (t,  $J$  = 7.4 Hz, 0.5H), 3.21 (t,  $J$  = 7.4 Hz, 0.5H), 2.29 (dt,  $J$  = 13.3, 6.1 Hz, H), 2.10 – 2.01 (m, 1H), 1.87 (dt,  $J$  = 15.6, 8.2 Hz, 0.5H);  $^{13}\text{C NMR}$  (126

MHz, CDCl<sub>3</sub>):  $\delta$  173.2, 156.9, 156.7, 151.2, 151.1, 131.7, 131.4, 127.9, 127.8, 124.3, 123.6, 118.9, 118.7, 109.8, 109.7, 53.7, 52.9, 52.6, 52.5, 52.4, 38.8, 38.6, 37.2; **HRMS** calcd. for C<sub>14</sub>H<sub>19</sub>N<sub>2</sub>O<sub>4</sub><sup>+</sup> [M + H]<sup>+</sup> 279.1339, found 279.11340.

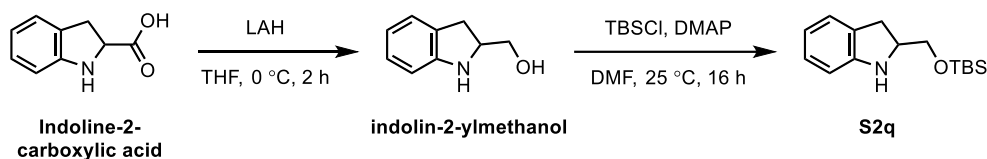
### 2-Phenethylindoline (S2p)



Following the **general procedure C**, indole **S1p** (0.280 g, 1.27 mmol) afforded indoline **S2p** (0.230 g, 81%) as a pale yellow oil after purification by flash column chromatography (silica gel, hexanes:EtOAc = 1:0  $\rightarrow$  95:5). Analytic data is in agreement with the reported literature values.<sup>10</sup>

$R_f$ =0.24 (silica gel, hexanes:EtOAc = 7:3); **<sup>1</sup>H NMR** (400 MHz, CDCl<sub>3</sub>):  $\delta$  7.39 – 7.32 (m, 2H), 7.28 – 7.24 (m, 3H), 7.05 (d,  $J$  = 7.4 Hz, 1H), 6.99 (t,  $J$  = 7.6 Hz, 1H), 6.67 (t,  $J$  = 7.4 Hz, 1H), 6.61 (d,  $J$  = 7.7 Hz, 1H), 3.96 – 3.87 (m, 1H), 3.20 (dd,  $J$  = 15.4, 8.7 Hz, 1H), 2.80 – 2.73 (m, 3H), 2.03 – 1.97 (m, 2H); **<sup>13</sup>C NMR** (101 MHz, CDCl<sub>3</sub>):  $\delta$  151.0, 141.9, 128.8, 128.6, 128.4, 127.4, 126.1, 124.8, 118.7, 109.3, 59.6, 38.6, 36.2, 33.0.

### 2-(((tert-Butyldimethylsilyl)oxy)methyl)indoline (S2q)

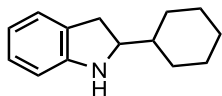


To an oven-dried round-bottom flask equipped with a stir bar and septum were added indoline-2-carboxylic acid (2.00 g, 12.3 mmol, 1.0 equiv) and THF (30 mL) at 23 °C. The resulting solution was cooled to 0 °C, and LAH (0.412 g, 13.7 mmol, 1.11 equiv) was added to the solution. The reaction mixture was stirred for 2 h before it was quenched with brine (20 mL). The layers were separated and the aqueous layer was extracted with EtOAc (3  $\times$  30 mL). The combined organic layer was washed with brine (3  $\times$  20 mL), dried over anhydrous MgSO<sub>4</sub>, filtered, and concentrated under reduced pressure to afford crude indolin-2-ylmethanol, which was used directly in the subsequent reaction without further purification. To an oven-dried round-bottom flask equipped with a stir bar and septum were added crude

indolin-2-ylmethanol and DMF (20 mL) at 23 °C, followed by TBSCl (1.88 g, 12.5 mmol, 1.01 equiv) and DMAP (1.50 g, 12.3 mmol, 1.0 equiv). The resulting mixture was stirred for 16 h before it was quenched with brine (20 mL). The layers were separated and the aqueous layer was extracted with CH<sub>2</sub>Cl<sub>2</sub> (3 × 20 mL). The combined organic layer was washed with brine (3 × 20 mL), dried over anhydrous MgSO<sub>4</sub>, filtered, and concentrated under reduced pressure. The resulting residue was purified by flash column chromatography (silica gel, hexanes:EtOAc = 1:0 → 95:5) to afford product **S2q** (2.09 g, 73%) as a pale yellow oil. Analytic data is in agreement with the reported literature values.<sup>10</sup>

*R<sub>f</sub>*=0.24 (silica gel, hexanes:EtOAc = 95:5); <sup>1</sup>H NMR (400 MHz, CDCl<sub>3</sub>): δ 7.10 (d, *J* = 7.3 Hz, 1H), 7.05 (t, *J* = 7.6 Hz, 1H), 6.72 (t, *J* = 7.4 Hz, 1H), 6.65 (d, *J* = 7.7 Hz, 1H), 4.01 – 3.93 (m, 1H), 3.67 – 3.54 (m, 2H), 3.14 (dd, *J* = 15.8, 9.1 Hz, 1H), 2.68 (dd, *J* = 15.8, 5.8 Hz, 1H), 0.96 (s, 9H), 0.11 (s, 6H); <sup>13</sup>C NMR (101 MHz, CDCl<sub>3</sub>): δ 150.6, 128.2, 127.5, 124.9, 118.5, 109.4, 66.7, 60.5, 32.2, 26.0, 18.4, –5.2.

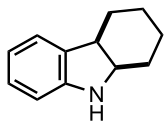
### 2-Cyclohexylindoline (**S2r**)



Following the **general procedure C**, indole **S1r** (0.100 g, 0.502 mmol) afforded indoline **S2r** (82.0 mg, 81%) as a pale yellow oil after purification by flash column chromatography (silica gel, hexanes:EtOAc = 1:0 → 95:5). Analytic data is in agreement with the reported literature values.<sup>11</sup>

*R<sub>f</sub>*=0.24 (silica gel, hexanes:EtOAc = 7:3); <sup>1</sup>H NMR (400 MHz, CDCl<sub>3</sub>): δ 7.08 (d, *J* = 7.3 Hz, 1H), 7.01 (t, *J* = 7.6 Hz, 1H), 6.68 (t, *J* = 7.4 Hz, 1H), 6.61 (d, *J* = 7.7 Hz, 1H), 3.94 (br s, 1H), 3.56 (q, *J* = 8.8 Hz, 1H), 3.07 (dd, *J* = 15.5, 8.7 Hz, 1H), 2.75 (dd, *J* = 15.5, 9.8 Hz, 1H), 1.89 (d, *J* = 12.3 Hz, 1H), 1.51 – 1.41 (m, 1H), 1.34 – 1.13 (m, 3H), 1.06 – 0.94 (m, 2H); <sup>13</sup>C NMR (101 MHz, CDCl<sub>3</sub>): δ 151.3, 129.2, 127.3, 124.6, 118.5, 109.0, 65.7, 44.0, 34.3, 30.3, 29.7, 26.6, 26.2, 26.1.

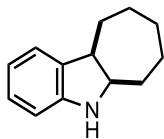
### 2,3,4,4a,9,9a-Hexahydro-1H-carbazole (S2s)



Following the **general procedure C**, 1,2,3,4-tetrahydrocarbazole (3.00 g, 17.5 mmol) afforded indoline **S2s** (2.37 g, 78%) as a white amorphous solid after purification by flash column chromatography (silica gel, hexanes:EtOAc = 1:0 → 95:5). Analytic data is in agreement with the reported literature values.<sup>10</sup>

$R_f=0.68$  (silica gel, hexanes:EtOAc = 9:1);  $^1\text{H NMR}$  (300 MHz,  $\text{CDCl}_3$ ):  $\delta$  7.10 (d,  $J = 7.3$  Hz, 1H), 7.04 (t,  $J = 7.6$  Hz, 1H), 6.76 (t,  $J = 7.4$  Hz, 1H), 6.69 (d,  $J = 7.7$  Hz, 1H), 3.74 (q,  $J = 6.1$  Hz, 1H), 3.11 (q,  $J = 6.7$  Hz, 1H), 1.72 – 1.65 (m, 1H), 1.62 – 1.53 (m, 2H), 1.58 (dq,  $J = 12.5, 7.0, 5.5$  Hz, 2H), 1.48 – 1.32 (m, 3H);  $^{13}\text{C NMR}$  (75 MHz,  $\text{CDCl}_3$ ):  $\delta$  150.9, 133.9, 127.1, 123.3, 118.9, 110.3, 59.8, 41.1, 29.3, 27.1, 22.7, 21.8.

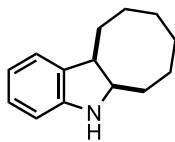
### 5,5a,6,7,8,9,10,10a-Octahydrocyclohepta[b]indole (S2t)



Following the **general procedure C**, indole **S1t** (0.300 g, 1.62 mmol) afforded indoline **S2t** (0.280 g, 92%) as a white amorphous solid after purification by flash column chromatography (silica gel, hexanes:EtOAc = 1:0 → 95:5). Analytic data is in agreement with the reported literature values.<sup>10</sup>

$R_f=0.68$  (silica gel, hexanes:EtOAc = 9:1);  $^1\text{H NMR}$  (400 MHz,  $\text{CDCl}_3$ ):  $\delta$  7.01 – 6.93 (m, 2H), 6.68 (t,  $J = 7.3$  Hz, 1H), 6.55 (d,  $J = 7.6$  Hz, 1H), 4.07 – 4.01 (m, 1H), 3.47 (td,  $J = 10.4, 3.9$  Hz, 1H), 2.00 – 1.93 (m, 1H), 1.89 – 1.69 (m, 6H), 1.44 – 1.32 (m, 3H);  $^{13}\text{C NMR}$  (101 MHz,  $\text{CDCl}_3$ ):  $\delta$  150.3, 133.7, 127.5, 124.3, 118.3, 108.6, 63.6, 47.5, 33.7, 31.5, 30.0, 26.2.

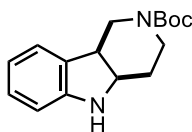
### 5a,6,7,8,9,10,11,11a-Octahydro-5H-cycloocta[b]indole (S2u)



Following the **general procedure C**, indole **S1u** (0.250 g, 1.25 mmol) afforded indoline **S2u** (0.221 g, 88%) as a pale yellow oil after purification by flash column chromatography (silica gel, hexanes:EtOAc = 1:0 → 95:5). Analytic data is in agreement with the reported literature values.<sup>12</sup>

$R_f$ =0.68 (silica gel, hexanes:EtOAc = 9:1); **<sup>1</sup>H NMR** (500 MHz, CDCl<sub>3</sub>): δ 7.07 (d,  $J$  = 7.4 Hz, 1H), 7.01 (t,  $J$  = 7.6 Hz, 1H), 6.71 (t,  $J$  = 7.4 Hz, 1H), 6.57 (d,  $J$  = 7.7 Hz, 1H), 3.88 (t,  $J$  = 9.9 Hz, 1H), 3.21 (t,  $J$  = 9.7 Hz, 1H), 2.01 (dq,  $J$  = 45.0, 12.4, 11.5 Hz, 2H), 1.78 – 1.50 (m, 10H); **<sup>13</sup>C NMR** (126 MHz, CDCl<sub>3</sub>): δ 149.5, 135.4, 127.3, 124.3, 118.6, 108.6, 63.9, 46.2, 30.3, 30.1, 28.8, 27.7, 25.9, 25.5.

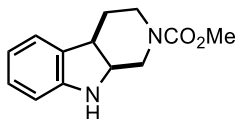
### tert-Butyl 1,3,4,4a,5,9b-hexahydro-2H-pyrido[4,3-b]indole-2-carboxylate (S2v)



Following the **general procedure C**, indole **S1v** (0.200 g, 0.734 mmol) afforded indoline **S2v** (0.127 g, 63%) as a pale yellow oil after purification by flash column chromatography (silica gel, hexanes:EtOAc = 1:0 → 7:3).

$R_f$ =0.24 (silica gel, hexanes:EtOAc = 7:3); **<sup>1</sup>H NMR** (400 MHz, CDCl<sub>3</sub>): δ 7.12 (d,  $J$  = 7.1 Hz, 1H), 7.05 (td,  $J$  = 7.7, 1.3 Hz, 1H), 6.73 (td,  $J$  = 7.4, 1.0 Hz, 1H), 6.66 (d,  $J$  = 7.8 Hz, 1H), 3.99 – 3.95 (dd,  $J$  = 8.7, 3.7 Hz, 1H), 3.45 – 3.27 (m, 5H), 1.93 – 1.84 (m, 1H), 1.77 – 1.71 (m, 1H), 1.45 (s, 9H); **<sup>13</sup>C NMR** (101 MHz, CDCl<sub>3</sub>): δ 155.1, 151.0, 128.1, 124.4, 119.1, 110.1, 79.6, 57.6, 43.9, 41.2, 40.1, 39.5, 28.6, 28.2; **HRMS** calcd. for C<sub>16</sub>H<sub>23</sub>N<sub>2</sub>O<sub>2</sub><sup>+</sup> [M + H]<sup>+</sup> 275.1754, found 275.1759.

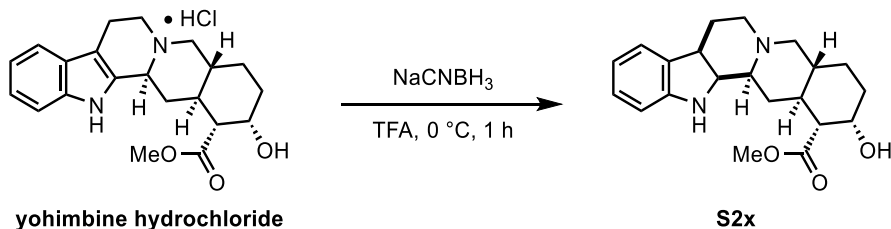
### Methyl 1,3,4,4a,9,9a-hexahydro-2H-pyrido[3,4-b]indole-2-carboxylate (**S2w**)



Following the **general procedure C**, indole **S1w** (0.500 g, 1.84 mmol) afforded indoline **S2w** (0.262 g, 52%) as a white amorphous solid after purification by flash column chromatography (silica gel, hexanes:EtOAc = 1:0 → 7:3).

$R_f$ =0.24 (silica gel, hexanes:EtOAc = 7:3);  $^1\text{H NMR}$  (400 MHz,  $\text{CDCl}_3$ ):  $\delta$  7.07 – 7.01 (m, 2H), 6.73 (t,  $J$  = 7.4 Hz, 1H), 6.62 (d,  $J$  = 7.7 Hz, 1H), 3.97 – 3.86 (m, 2H), 3.68 (s, 3H), 3.58 – 3.53 (m, 1H), 3.39 – 3.34 (m, 3H), 2.04 – 1.96 (m, 1H), 1.87 – 1.79 (m, 1H);  $^{13}\text{C NMR}$  (101 MHz,  $\text{CDCl}_3$ ):  $\delta$  150.6, 131.2, 127.9, 123.7, 119.0, 109.8, 57.4, 52.6, 44.4, 41.1, 39.3, 26.4; **HRMS** calcd. for  $\text{C}_{13}\text{H}_{17}\text{N}_2\text{O}_2^+$  [ $\text{M} + \text{H}$ ] $^+$  233.1285, found 233.1288.

### Methyl (1R,2S,4aR,13bS,14aS)-2-hydroxy-1,2,3,4,4a,5,7,8,8a,13,13a,13b,14,14a-tetradecahydroindolo[2',3':3,4]pyrido [1,2-b]isoquinoline-1-carboxylate (**S2x**)



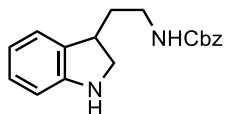
To an oven-dried round-bottom flask equipped with a stir bar and septum were added yohimbine hydrochloride (0.100 g, 0.256 mmol, 1.0 equiv) and TFA (5 mL) at 23 °C. The resulting solution was cooled to 0 °C, and  $\text{NaBH}_3\text{CN}$  (48.2 mg, 0.767 mmol, 3.0 equiv) was added to the solution. The reaction mixture was stirred for 1 h before it was directly concentrated under reduced pressure. The crude product was re-dissolved in  $\text{CH}_2\text{Cl}_2$  (20 mL) and basified to pH 9–10 using  $\text{NH}_3 \cdot \text{H}_2\text{O}$  (25.0–30.0 wt% in  $\text{H}_2\text{O}$ ). The layers were separated and the aqueous layer was extracted with  $\text{CH}_2\text{Cl}_2$  (3 × 30 mL). The combined organic layer was washed with brine (1 × 20 mL), dried over anhydrous  $\text{MgSO}_4$ , filtered, and concentrated under reduced pressure. The resulting residue was purified by flash column chromatography (silica gel,  $\text{CH}_2\text{Cl}_2$ :MeOH = 1:0 → 9:1) to afford indoline **S2x** (83.0 mg, 91%) as a pale yellow viscous oil as a single diastereomer, which is consistent with the literature



observations.<sup>13</sup>

$R_f=0.31$  (silica gel,  $\text{CH}_2\text{Cl}_2:\text{MeOH} = 9:1$ );  $^1\text{H NMR}$  (500 MHz, MeOD):  $\delta$  7.05 (d,  $J = 7.2$  Hz, 1H), 6.97 (t,  $J = 7.7$  Hz, 1H), 6.67 – 6.64 (m, 2H), 4.25 (s, 1H), 3.69 (s, 3H), 3.55 (d,  $J = 4.8$  Hz, 1H), 2.99 (dt,  $J = 12.5, 6.6$  Hz, 1H), 2.88 (d,  $J = 11.4$  Hz, 1H), 2.83 (d,  $J = 11.8$  Hz, 1H), 2.51 (d,  $J = 11.6$  Hz, 1H), 2.35 – 2.27 (m, 2H), 2.13 (t,  $J = 10.3$  Hz, 1H), 1.91 – 1.89 (m, 3H), 1.79 (dd,  $J = 14.1, 6.3$  Hz, 1H), 1.65 (t,  $J = 12.6$  Hz, 1H), 1.55 – 1.43 (m, 3H), 1.38 – 1.28 (m, 2H);  $^{13}\text{C NMR}$  (126 MHz, MeOD):  $\delta$  175.0, 151.5, 135.6, 128.5, 124.1, 119.8, 111.5, 68.4, 64.2, 64.0, 62.4, 54.7, 53.7, 52.0, 49.8, 41.0, 40.6, 37.1, 35.0, 33.3, 30.1, 24.0; **HRMS** calcd. for  $\text{C}_{21}\text{H}_{29}\text{N}_2\text{O}_3^+$   $[\text{M} + \text{H}]^+$  357.2173, found 357.2180.

### Benzyl (2-(indolin-3-yl)ethyl)carbamate (**S2a'**)

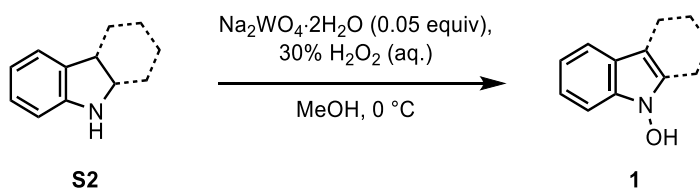


Following the **general procedure B**, tryptamine **S1a'** (3.50 g, 16.0 mmol) afforded indoline **S2a'** (3.30 g, 94%) as a pale yellow oil after purification by flash column chromatography (silica gel, hexanes:EtOAc = 1:0 → 6:4).

$R_f=0.18$  (silica gel, hexanes:EtOAc = 6:4);  $^1\text{H NMR}$  (500 MHz,  $\text{CDCl}_3$ ): 7.36 (d,  $J = 4.3$  Hz, 4H), 7.34 – 7.28 (m, 1H), 7.10 (d,  $J = 7.3$  Hz, 1H), 7.05 (t,  $J = 7.6$  Hz, 1H), 6.74 (t,  $J = 7.5$  Hz, 1H), 6.68 (d,  $J = 7.8$  Hz, 1H), 5.10 (s, 2H), 4.89 (s, 1H), 3.71 (t,  $J = 8.7$  Hz, 1H), 3.33 (q,  $J = 7.2$  Hz, 1H), 3.27 (t,  $J = 7.4$  Hz, 1H), 2.01 (dq,  $J = 13.2, 6.3$  Hz, 1H), 1.77 (dt,  $J = 13.8, 7.0$  Hz, 1H);  $^{13}\text{C NMR}$  (126 MHz,  $\text{CDCl}_3$ ):  $\delta$  156.5, 151.2, 136.6, 132.0, 128.4, 128.0, 127.6, 123.8, 118.6, 109.6, 66.5, 53.1, 39.4, 39.0, 34.3; **HRMS** calcd. for  $\text{C}_{12}\text{H}_{17}\text{N}_2\text{O}_2^+$   $[\text{M} + \text{H}]^+$  221.1285, found 221.1278.

## 2.3. Preparation of N-Hydroxyindole Derivatives

### General procedure D



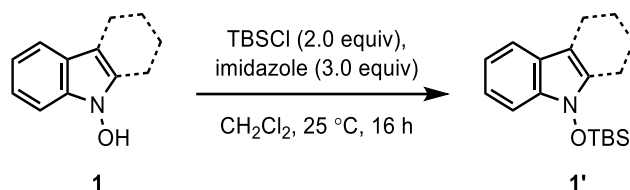
The compounds were synthesized according to a known literature procedure.<sup>14</sup> To an oven-dried round-bottom flask equipped with a stir bar and septum were added indoline **S2** (1.0 equiv) and MeOH (0.1 M in **S2**) at 23 °C. The resulting solution was cooled to 0 °C, and sodium tungstate dihydrate (0.05 equiv) and H<sub>2</sub>O<sub>2</sub> (30 wt% in H<sub>2</sub>O, 10.0 equiv) were added to the solution. The reaction mixture was stirred while the reaction was monitored by TLC. After completion of reaction, the reaction mixture was quenched with H<sub>2</sub>O. The layers were separated and the aqueous layer was extracted with CH<sub>2</sub>Cl<sub>2</sub> three times. The combined organic layer was washed with H<sub>2</sub>O three times, dried over anhydrous MgSO<sub>4</sub>, filtered, and concentrated under reduced pressure to afford N-hydroxyindole **1**. The resulting crude was used directly in the subsequent reaction without further purification.

**note:** In most cases, *N*-hydroxyindoles are unstable and slowly undergo decomposition, thus was unable to be stored for an extended period of time. However, most of *N*-hydroxyindoles could be obtained in excellent state which are clean enough to be characterized without purification. *N*-hydroxyindoles enlisted in this section were characterized without further purification (**1a–1o**, **1s**, **1x**) or otherwise protected with TBS group (**1p'**, **1q'**, **1r'**, **1v'**, **1w'**, **1a''**) for characterization. In case of the *N*-hydroxyindoles **1t** and **1u**, the products could be obtained in affordable quality. However, they could not be fully characterized due to their fast decomposition.

**Determination of the reaction yield for the preparation of *N*-hydroxyindoles:** The crude product was dissolved in CH<sub>2</sub>Cl<sub>2</sub> to provide a solution with a total volume of 10.0 mL. 1.0 mL of the resulting solution was syringed out and dried separately in a 4 mL vial. To the 4 mL vial containing the separated sample was added 10.0 μL of 1,1,2,2-tetrachloroethane (TCE) as an internal standard and the resulting mixture was dissolved entirely in d<sub>4</sub>-methanol.

The yield of product was determined by the integration of peaks from the  $^1\text{H}$  NMR spectra relative to the internal standard, TCE. The calculated amount of the product in the sample (A) was then multiplied by 10 to provide the total mass of the *N*-hydroxyindole product. The remaining 9.0 mL of the stock solution was dried under reduced pressure and used directly for the next step. The calculated amount of the product in the sample (A) was multiplied by 9 to provide the quantity of the starting material for the next reaction.

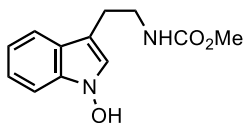
### General Procedure E



For compounds **1p'**, **1q'**, **1r'**, **1v'**, **1w'**, **1a''**:

To an oven-dried round-bottom flask equipped with a stir bar and septum were added crude *N*-hydroxyindole **1** (1.0 equiv) and  $\text{CH}_2\text{Cl}_2$  (0.2 M in **1**) at 23 °C, followed by TBSCl (2.0 equiv) and imidazole (3.0 equiv). The resulting mixture was stirred for 16 h before it was quenched with  $\text{H}_2\text{O}$ . The layers were separated and the aqueous layer was extracted with  $\text{CH}_2\text{Cl}_2$  three times. The combined organic layer was dried over anhydrous  $\text{MgSO}_4$ , filtered, and concentrated under reduced pressure. The resulting residue was purified by flash column chromatography to afford TBS protected *N*-hydroxyindole.

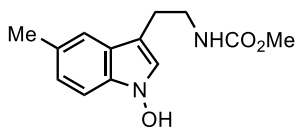
### Methyl (2-(1-hydroxy-1H-indol-3-yl)ethyl)carbamate (**1a**)



Following the **general procedure D** for 2 h, indoline **S2a** (0.120 g, 0.545 mmol) afforded N-hydroxyindole **1a** (93.0 mg, 73%) as a yellow oil and was used directly in the subsequent reaction without further purification.

$R_f$ =0.45 (silica gel, hexanes:EtOAc = 1:1);  $^1\text{H NMR}$  (500 MHz, MeOD):  $\delta$  7.53 (d,  $J$  = 8.1 Hz, 1H), 7.34 (d,  $J$  = 8.2 Hz, 1H), 7.13 (t,  $J$  = 7.7 Hz, 1H), 7.10 (s, 1H), 6.99 (t,  $J$  = 7.5 Hz, 1H), 3.62 (s, 3H), 3.36 (t,  $J$  = 7.5 Hz, 2H), 2.89 (t,  $J$  = 7.7 Hz, 2H);  $^{13}\text{C NMR}$  (126 MHz, MeOD):  $\delta$  159.6, 135.7, 125.0, 124.4, 122.7, 119.7, 119.5, 109.2, 108.8, 75.8, 52.4, 42.8, 26.6; **HRMS** calcd. for  $\text{C}_{12}\text{H}_{15}\text{N}_2\text{O}_3^+$  [ $\text{M} + \text{H}$ ] $^+$  235.1077, found 235.1077.

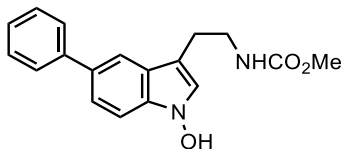
### Methyl (2-(1-hydroxy-5-methyl-1H-indol-3-yl)ethyl)carbamate (**1b**)



Following the **general procedure D** for 2 h, indoline **S2b** (75.0 mg, 0.320 mmol) afforded N-hydroxyindole **1b** (48.0 mg, 60%) as a pale yellow oil and was used directly in the subsequent reaction without further purification.

$R_f$ =0.24 (silica gel, hexanes:EtOAc = 7:3);  $^1\text{H NMR}$  (500 MHz, MeOD):  $\delta$  7.32 (s, 1H), 7.23 (d,  $J$  = 8.3 Hz, 1H), 7.04 (s, 1H), 6.97 (dd,  $J$  = 8.4, 1.6 Hz, 1H), 3.62 (s, 3H), 3.34 (t,  $J$  = 7.4 Hz, 2H), 2.85 (t,  $J$  = 7.4 Hz, 2H), 2.41 (s, 3H);  $^{13}\text{C NMR}$  (126 MHz, MeOD):  $\delta$  159.6, 134.3, 128.8, 125.3, 124.5, 124.3, 119.1, 109.0, 108.2, 52.4, 42.8, 26.6, 21.6; **HRMS** calcd. for  $\text{C}_{13}\text{H}_{17}\text{N}_2\text{O}_3^+$  [ $\text{M} + \text{H}$ ] $^+$  249.1234, found 249.1233.

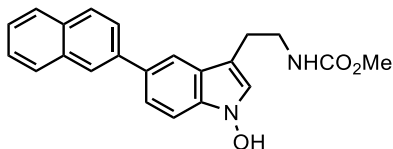
**Methyl (2-(1-hydroxy-5-phenyl-1H-indol-3-yl)ethyl)carbamate (1c)**



Following the **general procedure D** for 2 h, indoline **S2c** (60.0 mg, 0.202 mmol) afforded N-hydroxyindole **1c** (29.0 mg, 47%) as a pale yellow oil and was used directly in the subsequent reaction without further purification.

$R_f=0.40$  (silica gel, hexanes:EtOAc = 1:1);  $^1\text{H NMR}$  (500 MHz, MeOD):  $\delta$  7.76 (s, 1H), 7.64 (d,  $J = 7.7$  Hz, 2H), 7.44 – 7.37 (m, 4H), 7.26 (t,  $J = 7.4$  Hz, 1H), 7.14 (s, 1H), 3.60 (s, 3H), 3.39 (t,  $J = 7.3$  Hz, 2H), 2.94 (t,  $J = 7.4$  Hz, 2H);  $^{13}\text{C NMR}$  (126 MHz, MeOD):  $\delta$  159.6, 144.0, 135.1, 133.6, 129.6, 128.1, 127.2, 125.6, 125.1, 122.4, 118.0, 109.6, 109.4, 52.4, 43.0, 26.6; **HRMS** calcd. for  $\text{C}_{18}\text{H}_{17}\text{N}_2\text{O}_3^-$   $[\text{M} - \text{H}]^-$  309.1245, found 309.1241.

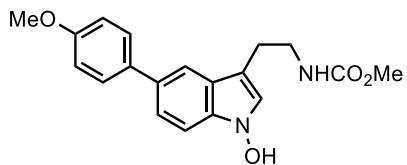
**Methyl (2-(1-hydroxy-5-(naphthalen-2-yl)-1H-indol-3-yl)ethyl)carbamate (1d)**



Following the **general procedure D** for 4 h, indoline **S2d** (75.0 mg, 0.216 mmol) afforded N-hydroxyindole **1d** (56.0 mg, 72%) as a brown oil and was used directly in the subsequent reaction without further purification.

$R_f=0.24$  (silica gel, hexanes:EtOAc = 7:3);  $^1\text{H NMR}$  (400 MHz, MeOD):  $\delta$  8.10 (s, 1H), 7.91 (d,  $J = 7.8$  Hz, 3H), 7.87 – 7.83 (m, 2H), 7.59 (dd,  $J = 8.5, 1.7$  Hz, 1H), 7.50 – 7.42 (m, 3H), 7.17 (s, 1H), 3.61 (s, 3H), 3.42 (t,  $J = 7.3$  Hz, 2H), 2.97 (t,  $J = 7.3$  Hz, 2H);  $^{13}\text{C NMR}$  (126 MHz, MeOD):  $\delta$  159.7, 141.4, 135.4, 135.2, 133.7, 133.3, 129.2, 129.0, 128.6, 127.1, 127.1, 126.4, 126.1, 125.7, 125.2, 122.6, 118.4, 109.7, 109.5, 52.4, 43.1, 26.6; **HRMS** calcd. for  $\text{C}_{22}\text{H}_{21}\text{N}_2\text{O}_3^+$   $[\text{M} + \text{H}]^+$  361.1547, found 361.1545.

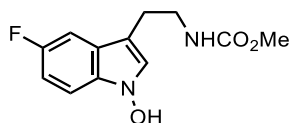
### Methyl (2-(1-hydroxy-5-(4-methoxyphenyl)-1H-indol-3-yl)ethyl)carbamate (**1e**)



Following the **general procedure D** for 2 h, indoline **S2e** (75.0 mg, 0.230 mmol) afforded N-hydroxyindole **1e** (44.6 mg, 57%) as a pale yellow oil and was used directly in the subsequent reaction without further purification.

$R_f=0.27$  (silica gel, hexanes:EtOAc = 1:1);  $^1\text{H NMR}$  (500 MHz, MeOD):  $\delta$  7.70 (s, 1H), 7.55 (d,  $J = 8.7$  Hz, 2H), 7.38 (s, 2H), 7.12 (s, 1H), 6.97 (d,  $J = 8.7$  Hz, 2H), 3.81 (s, 3H), 3.60 (s, 3H), 3.38 (t,  $J = 7.3$  Hz, 2H), 2.92 (t,  $J = 7.4$  Hz, 2H);  $^{13}\text{C NMR}$  (126 MHz, MeOD):  $\delta$  159.9, 159.6, 136.6, 134.9, 133.3, 129.1, 125.6, 125.0, 122.2, 117.4, 115.1, 109.5, 109.3, 55.7, 52.4, 43.0, 26.6; **HRMS** calcd. for  $\text{C}_{19}\text{H}_{21}\text{N}_2\text{O}_4^+$   $[\text{M} + \text{H}]^+$  341.1496, found 341.1504.

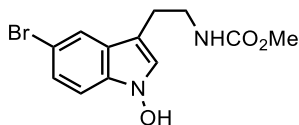
### Methyl (2-(5-fluoro-1-hydroxy-1H-indol-3-yl)ethyl)carbamate (**1f**)



Following the **general procedure D** for 4 h, indoline **S2f** (50.0 mg, 0.210 mmol) afforded N-hydroxyindole **1f** (34.0 mg, 64%) as a pale yellow oil and was used directly in the subsequent reaction without further purification.

$R_f=0.27$  (silica gel, hexanes:EtOAc = 1:1);  $^1\text{H NMR}$  (500 MHz, MeOD):  $\delta$  7.31 (dd,  $J = 8.9$ , 4.5 Hz, 1H), 7.22 (dd,  $J = 9.9$ , 2.4 Hz, 1H), 7.17 (s, 1H), 6.91 (td,  $J = 9.1$ , 2.4 Hz, 1H), 3.62 (s, 3H), 3.35 (t,  $J = 8.0$  Hz, 2H), 2.85 (t,  $J = 7.4$  Hz, 2H);  $^{13}\text{C NMR}$  (126 MHz, MeOD):  $\delta$  159.6, 158.9 (d,  $J = 232.4$  Hz), 132.4, 126.1, 125.2 (d,  $J = 9.7$  Hz), 110.9 (d,  $J = 26.7$  Hz), 110.2 (d,  $J = 9.7$  Hz), 108.7, 104.2 (d,  $J = 23.8$  Hz), 52.4, 42.7, 26.5;  $^{19}\text{F NMR}$  (376 MHz, MeOD):  $\delta$  -128.0 (td,  $J = 9.3$ , 4.2 Hz); **HRMS** calcd. for  $\text{C}_{12}\text{H}_{12}\text{FN}_2\text{O}_3^-$   $[\text{M} - \text{H}]^-$  251.0837, found 251.0832.

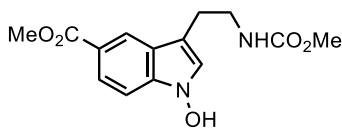
### Methyl (2-(5-bromo-1-hydroxy-1H-indol-3-yl)ethyl)carbamate (**1g**)



Following the **general procedure D** for 2.5 h, indoline **S2g** (0.100 g, 0.334 mmol) afforded N-hydroxyindole **1g** (57.0 mg, 54%) as a pale yellow oil and was used directly in the subsequent reaction without further purification.

$R_f=0.41$  (silica gel, hexanes:EtOAc = 1:1);  $^1\text{H NMR}$  (500 MHz, MeOD):  $\delta$  7.68 (s, 1H), 7.26 (d,  $J = 8.7$  Hz, 1H), 7.21 (dd,  $J = 8.7, 1.8$  Hz, 1H), 7.14 (s, 1H), 3.61 (s, 3H), 3.33 (t,  $J = 7.3$  Hz, 2H), 2.84 (t,  $J = 7.3$  Hz, 2H);  $^{13}\text{C NMR}$  (126 MHz, MeOD):  $\delta$  159.6, 134.1, 126.7, 125.7, 125.4, 122.1, 112.8, 110.9, 108.6, 52.4, 42.8, 26.3; **HRMS** calcd. for  $\text{C}_{12}\text{H}_{12}\text{BrN}_2\text{O}_3^- [\text{M} - \text{H}]^-$  311.0037, found 311.0033.

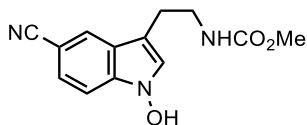
### Methyl 1-hydroxy-3-(2-((methoxycarbonyl)amino)ethyl)-1H-indole-5-carboxylate (**1h**)



Following the **general procedure D** for 6 h, indoline **S2h** (70.0 mg, 0.252 mmol) afforded N-hydroxyindole **1h** (45.0 mg, 61%) as a pale yellow oil and was used directly in the subsequent reaction without further purification.

$R_f=0.24$  (silica gel, hexanes:EtOAc = 7:3);  $^1\text{H NMR}$  (500 MHz, MeOD):  $\delta$  8.32 (s, 1H), 7.83 (dd,  $J = 8.7, 1.4$  Hz, 1H), 7.39 (d,  $J = 8.7$  Hz, 1H), 7.23 (s, 1H), 3.90 (s, 3H), 3.62 (s, 3H), 3.37 (t,  $J = 7.2$  Hz, 2H), 2.94 (t,  $J = 7.2$  Hz, 2H);  $^{13}\text{C NMR}$  (126 MHz, MeOD):  $\delta$  170.0, 159.6, 137.4, 126.1, 124.5, 123.9, 122.9, 121.6, 110.9, 109.0, 52.4, 52.3, 42.8, 26.3; **HRMS** calcd. for  $\text{C}_{14}\text{H}_{15}\text{N}_2\text{O}_5^- [\text{M} - \text{H}]^-$  291.0987, found 291.0985.

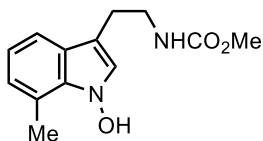
### Methyl (2-(5-cyano-1-hydroxy-1H-indol-3-yl)ethyl)carbamate (**1i**)



Following the **general procedure D** for 6 h, indoline **S2i** (25.3 mg, 0.103 mmol) afforded N-hydroxyindole **1i** (17.1 mg, 64%) as a pale yellow oil and was used directly in the subsequent reaction without further purification.

$R_f=0.24$  (silica gel, hexanes:EtOAc = 7:3);  $^1\text{H NMR}$  (500 MHz, MeOD):  $\delta$  8.02 (s, 1H), 7.49 (d,  $J = 8.5$  Hz, 1H), 7.41 (dd,  $J = 8.4, 1.5$  Hz, 1H), 7.31 (s, 1H), 3.61 (s, 3H), 3.36 (t,  $J = 7.2$  Hz, 3H), 2.92 (t,  $J = 7.2$  Hz, 3H);  $^{13}\text{C NMR}$  (126 MHz, MeOD):  $\delta$  159.6, 136.4, 126.9, 125.8, 125.3, 124.8, 121.8, 110.5, 110.3, 102.2, 52.4, 42.7, 26.2 ; **HRMS** calcd. for  $\text{C}_{13}\text{H}_{14}\text{N}_3\text{O}_3^+$   $[\text{M} + \text{H}]^+$  260.1030, found 260.1024.

### Methyl (2-(1-hydroxy-7-methyl-1H-indol-3-yl)ethyl)carbamate (**1j**)

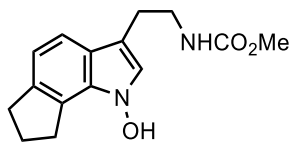


Following the **general procedure D** for 2 h, indoline **S2j** (80.0 mg, 0.341 mmol) afforded N-hydroxyindole **1j** (39.6 mg, 47%) as a pale yellow oil and was used directly in the subsequent reaction without further purification.

$R_f=0.24$  (silica gel, hexanes:EtOAc = 7:3);  $^1\text{H NMR}$  (400 MHz, MeOD):  $\delta$  7.33 (d,  $J = 7.6$  Hz, 1H), 7.03 (s, 1H), 6.90 – 6.80 (m, 2H), 3.62 (s, 3H), 3.35 (t,  $J = 7.5$  Hz, 2H), 2.85 (t,  $J = 7.4$  Hz, 2H), 2.67 (s, 3H);  $^{13}\text{C NMR}$  (101 MHz, MeOD):  $\delta$  159.6, 134.3, 125.7, 125.3, 124.7, 121.7, 120.0, 117.2, 108.8, 52.4, 42.7, 26.6, 18.3; **HRMS** calcd. for  $\text{C}_{13}\text{H}_{17}\text{N}_2\text{O}_3^+$   $[\text{M} + \text{H}]^+$  249.1234, found 249.1234.



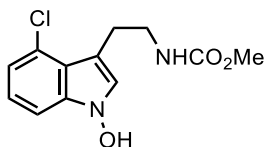
**Methyl (2-(1-hydroxy-1,6,7,8-tetrahydrocyclopenta[g]indol-3-yl)ethyl)carbamate (1k)**



Following the **general procedure D** for 2 h, indoline **S2k** (50.0 mg, 0.192 mmol) afforded N-hydroxyindole **1k** (40.5 mg, 77%) as a pale yellow oil and was used directly in the subsequent reaction without further purification.

$R_f=0.24$  (silica gel, hexanes:EtOAc = 7:3);  $^1\text{H NMR}$  (500 MHz, MeOD):  $\delta$  7.29 (d,  $J = 8.1$  Hz, 1H), 6.97 (s, 1H), 6.88 (d,  $J = 8.1$  Hz, 1H), 3.61 (s, 3H), 3.35 – 3.27 (m, 4H), 2.94 (t,  $J = 7.4$  Hz, 2H), 2.84 (t,  $J = 7.5$  Hz, 2H), 2.14 (qui,  $J = 7.4$  Hz, 2H);  $^{13}\text{C NMR}$  (126 MHz, MeOD):  $\delta$  159.6, 139.6, 132.9, 125.4, 124.1, 123.9, 117.6, 116.7, 109.2, 52.4, 42.7, 33.6, 31.4, 26.8, 26.5; **HRMS** calcd. for  $\text{C}_{15}\text{H}_{19}\text{N}_2\text{O}_3^+$   $[\text{M} + \text{H}]^+$  275.1390, found 275.1389.

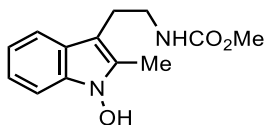
**Methyl (2-(4-chloro-1-hydroxy-1H-indol-3-yl)ethyl)carbamate (1l)**



Following the **general procedure D** for 5 h, indoline **S2l** (50.0 mg, 0.196 mmol) afforded N-hydroxyindole **1l** (37.1 mg, 70%) as a pale yellow oil and was used directly in the subsequent reaction without further purification.

$R_f=0.24$  (silica gel, hexanes:EtOAc = 7:3);  $^1\text{H NMR}$  (500 MHz, MeOD):  $\delta$  7.30 (dd,  $J = 8.2$ , 0.7 Hz, 1H), 7.17 (s, 1H), 7.05 (t,  $J = 7.9$  Hz, 1H), 6.96 (d,  $J = 7.5$  Hz, 1H), 3.61 (s, 3H), 3.40 (t,  $J = 7.3$  Hz, 2H), 3.12 (t,  $J = 7.3$  Hz, 2H);  $^{13}\text{C NMR}$  (126 MHz, MeOD):  $\delta$  159.6, 137.0, 127.1, 126.1, 123.1, 121.3, 120.6, 108.8, 108.3, 52.4, 43.8, 27.5; **HRMS** calcd. for  $\text{C}_{12}\text{H}_{14}\text{ClN}_2\text{O}_3^+$   $[\text{M} + \text{H}]^+$  269.0688, found 269.0685.

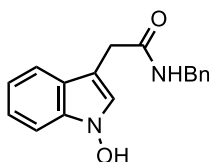
### Methyl (2-(1-hydroxy-2-methyl-1H-indol-3-yl)ethyl)carbamate (**1m**)



Following the **general procedure D** for 2 h, indoline **S2m** (33.6 mg, 0.143 mmol) afforded N-hydroxyindole **1m** (23.7 mg, 67%) as a pale yellow oil and was used directly in the subsequent reaction without further purification.

$R_f=0.60$  (silica gel, hexanes:EtOAc = 1:1);  $^1\text{H NMR}$  (500 MHz, MeOD):  $\delta$  7.46 (d,  $J = 7.4$  Hz, 1H), 7.30 (d,  $J = 8.1$  Hz, 1H), 7.06 (t,  $J = 7.6$  Hz, 1H), 6.96 (t,  $J = 7.4$  Hz, 1H), 3.62 (s, 1H), 3.27 (t,  $J = 7.3$  Hz, 2H), 2.87 (t,  $J = 7.2$  Hz, 2H), 2.36 (s, 3H);  $^{13}\text{C NMR}$  (126 MHz, MeOD):  $\delta$  159.6, 135.3, 133.1, 124.9, 121.6, 119.7, 118.4, 108.6, 104.6, 52.3, 42.8, 25.8, 8.9; **HRMS** calcd. for  $\text{C}_{13}\text{H}_{17}\text{N}_2\text{O}_3^+$   $[\text{M} + \text{H}]^+$  249.1234, found 249.1233.

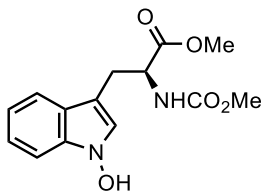
### N-Benzyl-2-(1-hydroxy-1H-indol-3-yl)acetamide (**1n**)



Following the **general procedure D** for 1.5 h, indoline **S2n** (40.8 mg, 0.153 mmol) afforded N-hydroxyindole **1n** (23.2 mg, 54%) as a pale yellow oil and was used directly in the subsequent reaction without further purification.

$R_f=0.58$  (silica gel, hexanes:EtOAc = 1:1);  $^1\text{H NMR}$  (500 MHz, MeOD):  $\delta$  7.52 (dt,  $J = 8.0$ , 1.0 Hz, 1H), 7.37 (dt,  $J = 8.2$ , 1.0 Hz, 1H), 7.26 – 7.18 (m, 6H), 7.16 (ddd,  $J = 8.2$ , 7.0, 1.1 Hz, 1H), 7.00 (ddd,  $J = 8.0$ , 6.9, 1.0 Hz, 1H), 4.35 (s, 2H), 3.66 (s, 2H);  $^{13}\text{C NMR}$  (126 MHz, MeOD):  $\delta$  174.6, 139.9, 135.6, 129.4, 128.5, 128.1, 125.6, 124.8, 122.9, 120.0, 119.7, 109.3, 104.8, 44.2, 33.7; **HRMS** calcd. for  $\text{C}_{17}\text{H}_{17}\text{N}_2\text{O}_2^+$   $[\text{M} + \text{H}]^+$  281.1285, found 281.1282.

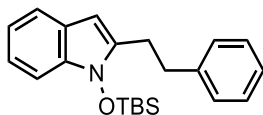
**Methyl (S)-3-(1-hydroxy-1H-indol-3-yl)-2-((methoxycarbonyl)amino)propanoate (1o)**



Following the **general procedure D** for 2 h, indoline **S2o** (70.0 mg, 0.252 mmol) afforded N-hydroxyindole **1o** (48.5 mg, 66%) as a pale yellow oil and was used directly in the subsequent reaction without further purification.

$R_f$ =0.44 (silica gel, hexanes:EtOAc = 1:1);  $^1\text{H NMR}$  (400 MHz, MeOD):  $\delta$  7.50 (d,  $J$  = 7.9 Hz, 1H), 7.36 (d,  $J$  = 8.1 Hz, 1H), 7.17 – 7.12 (m, 2H), 7.01 (t,  $J$  = 7.5 Hz, 1H), 4.47 (t,  $J$  = 6.7 Hz, 1H) 3.64 (s, 3H), 3.59 (s, 3H), 3.25 (dd,  $J$  = 14.6, 5.7 Hz, 1H), 3.10 (dd,  $J$  = 14.6, 7.9 Hz, 1H);  $^{13}\text{C NMR}$  (101 MHz, MeOD):  $\delta$  174.3, 159.0, 135.4, 125.2, 124.9, 122.8, 119.9, 119.3, 109.3, 106.1, 56.5, 52.7, 28.4; **HRMS** calcd. for  $\text{C}_{14}\text{H}_{17}\text{N}_2\text{O}_5^+$  [ $\text{M} + \text{H}$ ] $^+$  293.1132, found 293.1138.

**1-((tert-Butyldimethylsilyloxy)-2-phenethyl-1H-indole (1p')**

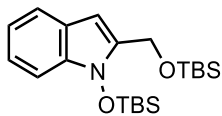


Following the **general procedure D** for 1.5 h, indoline **S2p** (30.0 mg, 0.134 mmol) afforded N-hydroxyindole **1p** as a pale yellow oil and was used directly in the subsequent reaction without further purification. For characterization, crude N-hydroxyindole **1p** underwent TBS protection following the **general procedure E** to afford TBS-protected N-hydroxyindole **1p'** (27.4 mg, 0.0781 mmol, 58% for 2 steps) as a colorless oil after purification by flash column chromatography (silica gel, hexanes:EtOAc = 1:0  $\rightarrow$  1:1).

$R_f$ =0.24 (silica gel, hexanes:EtOAc = 7:3);  $^1\text{H NMR}$  (400 MHz,  $\text{CDCl}_3$ ):  $\delta$  7.49 (d,  $J$  = 7.8 Hz, 1H), 7.34 – 7.30 (m, 3H), 7.26 – 7.21 (m, 3H), 7.14 (t,  $J$  = 7.5 Hz, 1H), 7.05 (t,  $J$  = 7.4 Hz, 1H), 6.16 (s, 1H), 3.06 (s, 4H), 1.14 (s, 9H), 0.27 (s, 6H);  $^{13}\text{C NMR}$  (126 MHz,  $\text{CDCl}_3$ ):  $\delta$  141.5, 139.2, 134.8, 128.6, 128.5, 126.2, 124.1, 121.0, 120.0, 119.6, 109.0, 95.5, 34.6, 27.9, 26.1, 18.4, -3.7; **HRMS** calcd. for  $\text{C}_{22}\text{H}_{30}\text{NOSi}^+$  [ $\text{M} + \text{H}$ ] $^+$  352.2091, found 352.2091.

### 1-((tert-Butyldimethylsilyl)oxy)-2-(((tert-butyldimethylsilyl)oxy)methyl)-1H-indole

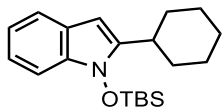
(1q')



Following the **general procedure D** for 1.5 h, indoline **S2q** (70.0 mg, 0.266 mmol) afforded N-hydroxyindole **1q** as a pale yellow oil and was used directly in the subsequent reaction without further purification. For characterization, crude N-hydroxyindole **1q** underwent TBS protection following the **general procedure E** to afford TBS-protected N-hydroxyindole **1q'** (71.9 mg, 0.190mmol, 72% for 2 steps) as a colorless oil after purification by flash column chromatography (silica gel, hexanes:EtOAc = 1:0 → 1:1).

$R_f$ =0.24 (silica gel, hexanes:EtOAc = 7:3);  $^1\text{H NMR}$  (400 MHz,  $\text{CDCl}_3$ ):  $\delta$  7.53 (d,  $J$  = 7.8 Hz, 1H), 7.32 (d,  $J$  = 8.2 Hz, 1H), 7.16 (t,  $J$  = 7.6 Hz, 1H), 7.06 (t,  $J$  = 7.4 Hz, 1H), 6.33 (s, 1H), 4.84 (s, 2H), 1.14 (s, 9H), 0.95 (s, 9H), 0.29 (s, 6H), 0.11 (s, 6H);  $^{13}\text{C NMR}$  (126 MHz,  $\text{CDCl}_3$ ):  $\delta$  138.9, 135.3, 124.1, 121.5, 120.6, 119.8, 109.2, 96.9, 57.3, 26.1, 18.5, 18.5, -4.0, -5.1; **HRMS** calcd. for  $\text{C}_{21}\text{H}_{38}\text{NO}_2\text{Si}_2^+$   $[\text{M} + \text{H}]^+$  392.2436, found 392.2435.

### 1-((tert-Butyldimethylsilyl)oxy)-2-cyclohexyl-1H-indole (1r')

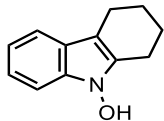


Following the **general procedure D** for 1.5 h, indoline **S2r** (20.0 mg, 0.0993 mmol) afforded N-hydroxyindole **1r** as a pale yellow oil and was used directly in the subsequent reaction without further purification. For characterization, crude N-hydroxyindole **1r** underwent TBS protection following the **general procedure E** to afford TBS-protected N-hydroxyindole **1r'** (18.4 g, 0.0558 mmol, 56% for 2 steps) as a colorless oil after purification by flash column chromatography (silica gel, hexanes:EtOAc = 1:0 → 1:1).

$R_f$ =0.24 (silica gel, hexanes:EtOAc = 7:3);  $^1\text{H NMR}$  (500 MHz,  $\text{CDCl}_3$ ):  $\delta$  7.48 (d,  $J$  = 7.8 Hz, 1H), 7.28 (d,  $J$  = 8.2 Hz, 1H), 7.10 (td,  $J$  = 7.1, 0.9 Hz, 1H), 7.02 (td,  $J$  = 7.5, 0.8 Hz, 1H), 6.08 (s, 1H), 2.81 – 2.75 (m, 1H), 2.08 (d,  $J$  = 8.4 Hz, 2H), 1.86 – 1.84 (m, 2H), 1.76 (d,  $J$  = 11.7 Hz, 1H), 1.42 – 1.24 (m, 6H), 1.14 (s, 9H), 0.24 (s, 6H);  $^{13}\text{C NMR}$  (126 MHz,

CDCl<sub>3</sub>):  $\delta$  145.0, 134.1, 124.0, 120.6, 120.0, 119.3, 108.9, 92.8, 35.1, 32.8, 26.7, 26.3, 26.1, 18.4, -3.8; **HRMS** calcd. for C<sub>20</sub>H<sub>32</sub>NOSi<sup>+</sup> [M + H]<sup>+</sup> 330.2248, found 330.2246.

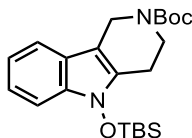
### 1,2,3,4-Tetrahydro-9H-carbazol-9-ol (**1s**)



Following the **general procedure D** for 1.5 h, indoline **S2s** (30.0 mg, 0.173 mmol) afforded N-hydroxyindole **1s** (25.0 mg, 77%) as a pale yellow oil and was used directly in the subsequent reaction without further purification.

**R<sub>f</sub>**=0.65 (silica gel, hexanes:EtOAc = 9:1); **<sup>1</sup>H NMR** (400 MHz, MeOD):  $\delta$  7.30 (dd, *J* = 14.5, 7.9 Hz, 2H), 7.04 (t, *J* = 7.6 Hz, 1H), 6.92 (t, *J* = 7.4 Hz, 1H), 2.69 (dt, *J* = 36.8, 4.8 Hz, 4H), 1.91 – 1.82 (m, 4H); **<sup>13</sup>C NMR** (101MHz, MeOD):  $\delta$  135.9, 135.15 124.6, 121.5, 119.4, 118.3, 108.6, 105.9, 24.5, 24.0, 21.9, 21.8; **HRMS** calcd. for C<sub>12</sub>H<sub>14</sub>NO<sup>+</sup> [M + H]<sup>+</sup> 188.1070, found 188.1067.

### tert-Butyl 5-((tert-butyldimethylsilyloxy)-1,3,4,5-tetrahydro-2H-pyrido[4,3-b]indole-2-carboxylate (**1v'**)

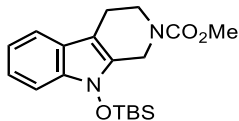


Following the **general procedure D** for 2 h, indoline **S2v** (50.0 mg, 0.182 mmol) afforded N-hydroxyindole **1v** as a pale yellow oil and was used directly in the subsequent reaction without further purification. For characterization, N-hydroxyindole **1v** underwent TBS protection following the **general procedure E** to afford TBS-protected N-hydroxyindole **1v'** (55.6 mg, 0.138 mmol, 76% for 2 steps) as a colorless oil after purification by flash column chromatography (silica gel, hexanes:EtOAc = 1:0 → 7:3).

**R<sub>f</sub>**=0.24 (silica gel, hexanes:EtOAc = 7:3); **<sup>1</sup>H NMR** (400 MHz, CDCl<sub>3</sub>):  $\delta$  7.40 (d, *J* = 7.8 Hz, 1H), 7.29 (d, *J* = 8.2 Hz, 1H), 7.17 (t, *J* = 7.6 Hz, 1H), 7.09 (d, *J* = 7.5 Hz, 1H), 4.61 (br s, 2H), 3.78 (br s, 2H), 2.79 (br s, 2H), 1.51 (s, 9H), 1.11 (s, 9H), 0.29 (s, 6H); **<sup>13</sup>C NMR** (126 MHz, CDCl<sub>3</sub>):  $\delta$  136.6, 121.7, 119.9, 117.7, 109.5, 80.1, 41.4, 40.6, 28.7, 26.0, 22.7, 18.3, –

4.0; **HRMS** calcd. for  $C_{22}H_{35}N_2O_3Si^+$   $[M + H]^+$  403.24115, found 403.2412.

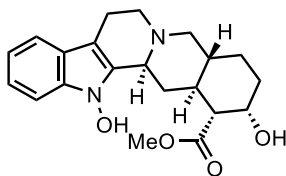
**Methyl 9-((tert-butyldimethylsilyloxy)-1,3,4,9-tetrahydro-2H-pyrido[3,4-b]indole-2-carboxylate (1w')**



Following the **general procedure D** for 2 h, indoline **S2w** (50.0 mg, 0.215 mmol) afforded N-hydroxyindole **1w** as a pale yellow oil and was used directly in the subsequent reaction without further purification. For characterization, N-hydroxyindole **1w** underwent TBS protection following the **general procedure E** to afford TBS-protected N-hydroxyindole **1w'** (55.8 mg, 0.155 mmol, 72% for 2 steps) as a colorless oil after purification by flash column chromatography (silica gel, hexanes:EtOAc = 1:0 → 1:1).

$R_f$ =0.24 (silica gel, hexanes:EtOAc = 7:3); **<sup>1</sup>H NMR** (400 MHz, CDCl<sub>3</sub>): δ 7.43 (d,  $J$  = 7.8 Hz, 1H), 7.30 (d,  $J$  = 8.1 Hz, 1H), 7.18 (t,  $J$  = 7.6 Hz, 1H), 7.09 (t,  $J$  = 7.4 Hz, 1H), 4.64 (d,  $J$  = 19.6 Hz, 2H), 3.83 – 3.76 (m, 2H), 3.77 (s, 3H), 2.79 (t,  $J$  = 5.8 Hz, 2H), 1.12 (s, 9H), 0.32 (s, 6H); **<sup>13</sup>C NMR** (126 MHz, CDCl<sub>3</sub>): δ 156.5, 136.9, 132.3, 123.8, 122.0, 120.0, 118.2, 109.6, 106.3, 105.7, 53.0, 42.2, 41.4, 26.0, 21.5, 21.0, 18.3, -3.9; **HRMS** calcd. for  $C_{19}H_{29}N_2O_3Si^+$   $[M + H]^+$  361.1942, found 361.1941.

**Methyl (1R,2S,4aR,13bS,14aS)-2,13-dihydroxy-1,2,3,4,4a,5,7,8,13,13b,14,14a-dodecahydroindolo[2',3':3,4]pyrido[1,2-b]isoquinoline-1-carboxylate (1x)**

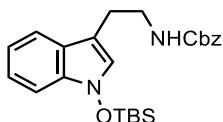


Following the **general procedure D** for 30 min, indoline **S2x** (40.0 mg, 0.112 mmol) afforded N-hydroxyindole **1x** (29.9 mg, 72%) as a pale yellow oil and was used directly in the subsequent reaction without further purification. Analytic data is in agreement with the reported literature values.<sup>13</sup>

$R_f$ =0.39 (silica gel, CH<sub>2</sub>Cl<sub>2</sub>:MeOH = 9:1); **<sup>1</sup>H NMR** (500 MHz, MeOD): δ 7.37 (d,  $J$  = 7.8

Hz, 1H), 7.30 (d,  $J = 8.1$  Hz, 1H), 7.10 (t,  $J = 7.5$  Hz, 1H), 6.98 (t,  $J = 7.4$  Hz, 1H), 4.23 (q,  $J = 2.9$  Hz, 1H), 3.74 (s, 3H), 3.64 (d,  $J = 11.7$  Hz, 1H), 3.17 – 3.10 (m, 1H), 2.98 – 2.91 (m, 3H), 2.76 – 2.65 (m, 2H), 2.41 (t,  $J = 11.2$  Hz, 1H), 2.33 (dd,  $J = 11.7, 2.6$  Hz, 1H), 2.00 (qd,  $J = 11.5, 3.1$  Hz, 1H), 1.92 (dq,  $J = 14.3, 3.3$  Hz, 1H), 1.71 – 1.63 (m, 1H), 1.60 – 1.44 (m, 2H), 1.41 – 1.34 (m, 1H), 1.21 (q,  $J = 11.8$  Hz, 1H);  $^{13}\text{C}$  NMR (126 MHz, MeOD):  $\delta$  175.4, 137.3, 134.8, 123.8, 122.4, 120.2, 118.7, 109.3, 105.1, 68.6, 62.3, 60.9, 54.0, 52.7, 52.0, 40.3, 37.6, 33.6, 33.5, 24.4, 22.5; HRMS calcd. for  $\text{C}_{19}\text{H}_{29}\text{N}_2\text{O}_3\text{Si}^+$   $[\text{M} + \text{H}]^+$  361.1942, found 361.1941.

### Benzyl (2-(1-((tert-butyldimethylsilyloxy)-1H-indol-3-yl)ethyl)carbamate (1a'')



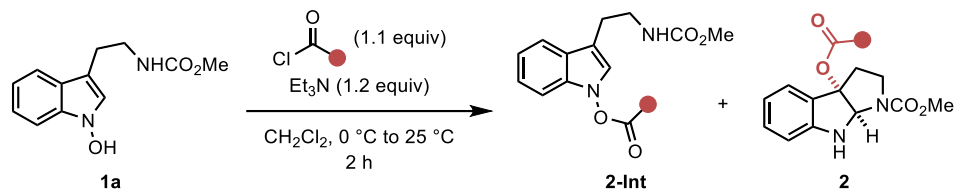
Following the **general procedure D** for 2 h, indoline **S2a'** (70.0 mg, 0.236 mmol) afforded N-hydroxyindole **1a'** as a pale yellow oil and was used directly in the subsequent reaction without further purification. For characterization, N-hydroxyindole **1a'** underwent TBS protection following the **general procedure E** to afford TBS-protected N-hydroxyindole **1a''** (66.2 mg, 0.156 mmol, 66% for 2 steps) as a colorless oil after purification by flash column chromatography (silica gel, hexanes:EtOAc = 1:0  $\rightarrow$  7:3).

$R_f$ =0.63 (silica gel, hexanes:EtOAc = 7:3);  $^1\text{H}$  NMR (500 MHz, MeOD):  $\delta$  7.56 (d,  $J = 8.0$  Hz, 1H), 7.35 – 7.26 (m, 5H), 7.26 (d,  $J = 8.2$  Hz, 1H), 7.15 (t,  $J = 7.5$  Hz, 1H), 7.07 (s, 1H), 7.01 (t,  $J = 7.5$  Hz, 1H), 5.06 (s, 2H), 3.39 (t,  $J = 7.1$  Hz, 2H), 2.91 (t,  $J = 7.1$  Hz, 2H), 1.10 (s, 9H), 0.22 (s, 6H);  $^{13}\text{C}$  NMR (126 MHz, MeOD):  $\delta$  158.9, 138.5, 136.0, 129.5, 128.9, 128.7, 125.1, 124.9, 123.1, 122.6, 120.2, 119.8, 110.0, 109.8, 67.3, 42.7, 26.4, 26.2, 18.8, –4.7; HRMS calcd. for  $\text{C}_{24}\text{H}_{33}\text{N}_2\text{O}_3\text{Si}^+$   $[\text{M} + \text{H}]^+$  425.2255, found 425.2269.

### 3. C–O Bond Formation via Indolyl 1,3-Heteroatom Transposition (IHT)

#### 3.1. Identification of 2'-Substituent Effect in the Facilitated IHT Reaction (Scheme 2.49)

**Table S1.** Evaluation of 2'-substituents.<sup>a</sup>



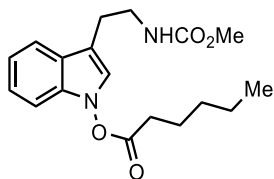
entry	2'-substituent (●)	yield of <b>2-Int</b> (%) <sup>b</sup>	yield of <b>2</b> (%) <sup>b</sup>
1		62	0
2		65	0
3		60	5
4		30	30
5		9	39
6 <sup>c</sup>		0	53

<sup>a</sup>Reactions performed with benzoyl chloride (1.1 equiv) and Et<sub>3</sub>N (1.2 equiv) in CH<sub>2</sub>Cl<sub>2</sub> (0.05 M) at 0 °C to 23 °C for 2 h on 0.201 mmol scale. <sup>b</sup>Yields of the isolated product are reported and the ratio of **2-Int** and **2** was determined by <sup>1</sup>H NMR.

For characterization, the mixture obtained in entries 3, 4 and 5 was converted to pyrroloindoline **2** under separately performed thermal conditions since indolyl *N*-benzoate **2-Int** and pyrroloindoline **2** co-eluted under the various solvent systems.



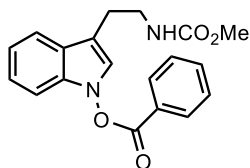
**Methyl 3a-(hexanoyloxy)-3,3a,8,8a-tetrahydropyrrolo[2,3-b]indole-1(2H)-carboxylate (2a-Int)**



Purified by silica gel column chromatography (silica gel, hexanes:EtOAc = 1:0 → 7:3) to indolyl *N*-carboxylate **2a-Int** (41.1 mg, 62%) as a pale yellow oil.

$R_f=0.60$  (silica gel, hexanes:EtOAc = 6:4);  $^1\text{H NMR}$  (400 MHz,  $\text{CDCl}_3$ ):  $\delta$  7.58 (d,  $J = 7.9$  Hz, 1H), 7.28 – 7.22 (m, 1H), 7.19 – 7.13 (m, 2H), 6.98 (br s, 1H), 4.83 (s, 1H), 3.66 (s, 3H), 3.51 (q,  $J = 6.7$  Hz, 2H), 2.94 (t,  $J = 6.8$  Hz, 2H), 2.63 (t,  $J = 7.5$  Hz, 2H), 1.82 (p,  $J = 7.4$  Hz, 2H), 1.50 – 1.35 (m, 4H), 0.95 (t,  $J = 6.9$  Hz, 3H);  $^{13}\text{C NMR}$  (101 MHz,  $\text{CDCl}_3$ ):  $\delta$  171.8, 157.2, 135.4, 124.7, 123.9, 123.5, 120.8, 119.3, 111.5, 108.9, 52.2, 41.1, 31.7, 31.3, 25.8, 24.7, 22.4; **HRMS** calcd. for  $\text{C}_{18}\text{H}_{25}\text{N}_2\text{O}_4^+$   $[\text{M} + \text{H}]^+$  333.1809, found 333.1810.

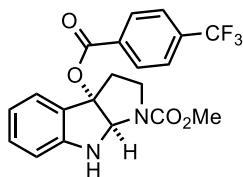
**3-(2-((Methoxycarbonyl)amino)ethyl)-1H-indol-1-yl benzoate (2b-Int)**



Purified by silica gel column chromatography (silica gel, hexanes:EtOAc = 1:0 → 7:3) to indolyl *N*-carboxylate **2b-Int** (44.2 mg, 65%) as a pale yellow oil.

$R_f=0.31$  (silica gel, hexanes:EtOAc = 7:3);  $^1\text{H NMR}$  (500 MHz,  $\text{CDCl}_3$ ):  $\delta$  8.22 (d,  $J = 7.2$  Hz, 2H), 7.72 (t,  $J = 7.5$  Hz, 1H), 7.62 (d,  $J = 7.8$  Hz, 1H), 7.57 (t,  $J = 7.8$  Hz, 2H), 7.26 (d,  $J = 3.5$  Hz, 2H), 7.18 (ddd,  $J = 8.1, 4.6, 3.5$  Hz, 1H), 7.10 (s, 1H), 4.83 (s, 1H), 3.67 (s, 3H), 3.55 (q,  $J = 6.6$  Hz, 2H), 2.98 (t,  $J = 6.8$  Hz, 2H);  $^{13}\text{C NMR}$  (126 MHz,  $\text{CDCl}_3$ ):  $\delta$  164.9, 157.2, 135.9, 134.7, 130.4, 129.1, 126.6, 125.0, 124.2, 123.7, 121.1, 119.4, 112.0, 109.2, 52.2, 41.1, 25.9; **HRMS** calcd. for  $\text{C}_{19}\text{H}_{19}\text{N}_2\text{O}_4^+$   $[\text{M} + \text{H}]^+$  339.1339, found 339.1338.

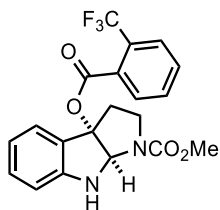
**Methyl 3a-((4-(trifluoromethyl)benzoyl)oxy)-3,3a,8,8a-tetrahydropyrrolo[2,3-b]indole-1(2H)-carboxylate (2c)**



Purified by silica gel column chromatography (silica gel, hexanes:EtOAc = 1:0 → 7:3) to an inseparable mixture of indolyl *N*-carboxylate **2c-Int** and pyrroloindoline **2c** (53.1 mg, 12:1, overall 65%) as a pale yellow oil. For characterization, the pure sample of **2c** was obtained as a sole product by the reaction of **1a** at 90 °C (**general procedure H**, Section 3.3).

$R_f$ =0.63 (silica gel, hexanes:EtOAc = 1:1);  $^1\text{H NMR}$  (500 MHz,  $\text{CDCl}_3$ , 60:40 mixture of rotamers):  $\delta$  8.10 (d,  $J$  = 8.1 Hz, 2H), 7.67 (d,  $J$  = 8.1 Hz, 2H), 7.61 and 7.55 (d,  $J$  = 7.6 Hz, 1H), 7.21 (t,  $J$  = 7.7 Hz, 1H), 6.81 (q,  $J$  = 6.9 Hz, 1H), 6.69 (d,  $J$  = 7.9 Hz, 1H), 5.77 (s, 1H), 3.94 and 3.82 (t,  $J$  = 9.6 Hz, 1H), 3.80 and 3.73 (s, 3H), 3.26 – 3.20 (m, 1H), 3.09 and 2.99 (dd,  $J$  = 12.6, 5.9 Hz, 1H), 2.71 (q,  $J$  = 11.2 Hz, 1H);  $^{13}\text{C NMR}$  (126 MHz,  $\text{CDCl}_3$ ):  $\delta$  164.3, 155.7, 154.9, 151.1, 150.9, 134.8 (q,  $J$  = 32.5 Hz), 133.5, 131.4, 130.3, 126.7, 126.2, 125.5 (q,  $J$  = 4.2 Hz), 123.5 (q,  $J$  = 272.7 Hz), 119.8, 119.6, 110.6, 110.4, 95.1, 93.8, 80.4, 79.6, 53.0, 52.7, 45.6, 35.8, 35.7;  $^{19}\text{F NMR}$  (471 MHz,  $\text{CDCl}_3$ ):  $\delta$  -63.2; **HRMS** calcd. for  $\text{C}_{20}\text{H}_{18}\text{F}_3\text{N}_2\text{O}_4^+$  [ $\text{M} + \text{H}$ ] $^+$  407.1213, found 407.1206.

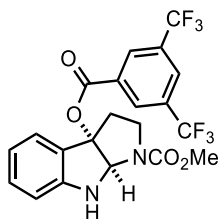
**Methyl 3a-((2-(trifluoromethyl)benzoyl)oxy)-3,3a,8,8a-tetrahydropyrrolo[2,3-b]indole-1(2H)-carboxylate (2d)**



Purified by silica gel column chromatography (silica gel, hexanes:EtOAc = 1:0 → 7:3) to an inseparable mixture of indolyl *N*-carboxylate **2d-Int** and pyrroloindoline **2d** (49.0 mg, 1:1, overall 60%) as a pale yellow oil. For characterization, the pure sample of **2d** was obtained as a sole product by the reaction of **1a** at 90 °C (**general procedure H**, Section 3.3).

$R_f=0.50$  (silica gel, hexanes:EtOAc = 1:1);  $^1\text{H NMR}$  (500 MHz,  $\text{CDCl}_3$ , 60:40 mixture of rotamers):  $\delta$  7.74 – 7.68 (m, 2H), 7.62 and 7.58 (d,  $J=7.5$  Hz, 1H), 7.60 – 7.54 (m, 2H), 7.21 (t,  $J=7.8$  Hz, 1H), 6.82 (q,  $J=7.2$  Hz, 1H), 6.68 (d,  $J=7.9$  Hz, 1H), 5.71 and 5.70 (s, 1H), 3.92 and 3.81 (t,  $J=9.8$  Hz, 1H), 3.80 and 3.73 (s, 3H), 3.25 – 3.19 (m, 1H), 3.05 and 2.96 (dd,  $J=12.9, 6.3$  Hz, 1H), 2.78 – 2.69 (m, 1H);  $^{13}\text{C NMR}$  (126 MHz,  $\text{CDCl}_3$ ):  $\delta$  165.6, 155.7, 154.9, 151.1, 150.8, 131.9, 131.5, 131.3, 131.2, 130.7, 128.7 (q,  $J=32.6$  Hz), 126.8 (q,  $J=5.6$  Hz), 126.6, 126.2, 125.5, 125.4, 123.5 (q,  $J=272.7$  Hz), 119.8, 119.5, 110.5, 110.4, 95.5, 94.3, 80.0, 79.3, 53.0, 52.7, 45.6, 35.2, 35.1;  $^{19}\text{F NMR}$  (471 MHz,  $\text{CDCl}_3$ ):  $\delta$  –58.9; **HRMS** calcd. for  $\text{C}_{20}\text{H}_{18}\text{F}_3\text{N}_2\text{O}_4^+$   $[\text{M} + \text{H}]^+$  407.1213, found 407.1204.

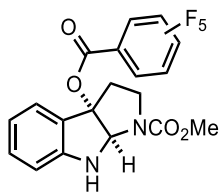
**Methyl 3a-((3,5-bis(trifluoromethyl)benzoyl)oxy)-3,3a,8,8a-tetrahydropyrrolo[2,3-b]indole-1(2H)-carboxylate (2e)**



Purified by silica gel column chromatography (silica gel, hexanes:EtOAc = 1:0 → 7:3) to an inseparable mixture of indolyl *N*-carboxylate **2e-Int** and pyrroloindoline **2e** (45.8 mg, 1:4, overall 48%) as a pale yellow oil. For characterization, the pure sample of **2e** was obtained as a sole product by the reaction of **1a** at 90 °C (**general procedure H**, Section 3.3).

$R_f=0.70$  (silica gel, hexanes:EtOAc = 1:1);  $^1\text{H NMR}$  (500 MHz,  $\text{CDCl}_3$ , 60:40 mixture of rotamers):  $\delta$  8.54 and 8.42 (s, 2H), 8.11 and 8.05 (s, 1H), 7.60 (dd,  $J=20.2, 7.6$  Hz, 1H), 7.22 (t,  $J=7.7$  Hz, 1H), 6.82 (q,  $J=7.0$  Hz, 1H), 6.71 (d,  $J=7.9$  Hz, 1H), 5.80 and 5.77 (s, 1H), 5.78 (d,  $J=13.8$  Hz, 1H), 3.96 and 3.86 (t,  $J=9.5$  Hz, 1H), 3.82 and 3.74 (s, 3H), 3.24 (tt,  $J=11.5, 6.0$  Hz, 1H), 3.13 and 3.07 (dd,  $J=12.7, 6.2$  Hz, 1H), 2.77 – 2.65 (m, 1H);  $^{13}\text{C NMR}$  (126 MHz,  $\text{CDCl}_3$ ):  $\delta$  162.8, 155.7, 154.8, 151.2, 151.0, 132.7, 132.4, 132.35 (q,  $J=26.0$  Hz), 131.7, 130.4, 130.0, 127.0, 126.8, 126.7, 126.4, 125.0, 125.0, 122.93 (q,  $J=272.9$  Hz), 120.0, 119.7, 110.6, 110.5, 95.8, 94.6, 80.4, 79.7, 53.1, 52.8, 45.7, 35.7;  $^{19}\text{F NMR}$  (471 MHz,  $\text{CDCl}_3$ ):  $\delta$  –63.0, –63.0; **HRMS** calcd. for  $\text{C}_{21}\text{H}_{17}\text{F}_6\text{N}_2\text{O}_4^+$   $[\text{M} + \text{H}]^+$  475.1087, found 475.1077.

**Methyl 3a-((perfluorobenzoyl)oxy)-3,3a,8,8a-tetrahydropyrrolo[2,3-b]indole-1(2H)-carboxylate (2f)**

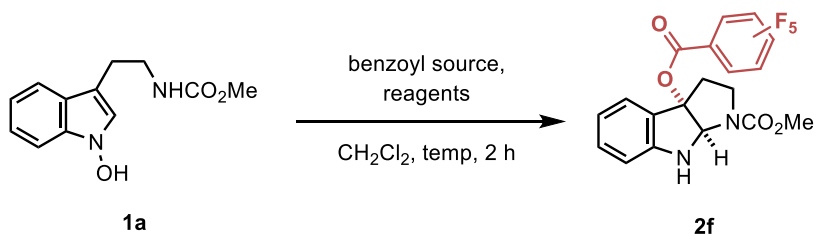


Purified by silica gel column chromatography (silica gel, hexanes:EtOAc = 1:0 → 7:3) to pyrroloindoline **2f** (45.6 mg, 53%) as a pale yellow oil.

$R_f$ =0.56 (silica gel, hexanes:EtOAc = 1:1);  $^1\text{H NMR}$  (400 MHz,  $\text{CDCl}_3$ , 60:40 mixture of rotamers):  $\delta$  7.56 and 7.53 (d,  $J$  = 8.7 Hz, 1H), 7.22 (t,  $J$  = 7.7 Hz, 1H), 6.83 (q,  $J$  = 7.2, 6.7 Hz, 1H), 6.69 (d,  $J$  = 8.0 Hz, 1H), 5.71 (d,  $J$  = 3.3 Hz, 1H), 3.92 and 3.82 (t,  $J$  = 9.7 Hz, 1H), 3.80 and 3.73 (s, 3H), 3.25 – 3.16 (m, 1H), 3.03 and 2.96 (dd,  $J$  = 12.6, 6.2 Hz, 1H), 2.70 (q,  $J$  = 10.7 Hz, 1H);  $^{13}\text{C NMR}$  (101 MHz,  $\text{CDCl}_3$ ):  $\delta$  157.8, 155.6, 154.8, 151.2, 151.0, 147.2 – 144.0 (dm,  $J$  = 262.7 Hz), 145.1 – 141.9 (dm,  $J$  = 260.2 Hz), 139.5 – 136.1 (dm,  $J$  = 257.6 Hz), 131.7, 126.4, 126.1, 124.8, 124.7, 122.6, 120.5, 120.0, 119.7, 110.7, 110.5, 108.2 (t,  $J$  = 15.7 Hz), 96.6, 95.4, 80.1, 79.4, 53.0, 52.8, 45.5, 35.7, 35.6;  $^{19}\text{F NMR}$  (376 MHz,  $\text{CDCl}_3$ ):  $\delta$  –139.6 (dp,  $J$  = 17.0, 5.8 Hz), –149.6 (dtt,  $J$  = 57.4, 20.7, 4.8 Hz), –161.8 – –162.0 (m); **HRMS** calcd. for  $\text{C}_{19}\text{H}_{14}\text{F}_5\text{N}_2\text{O}_4^+$   $[\text{M} + \text{H}]^+$  429.0868, found 429.0873.

### 3.2. Optimization of the C3-Acyloxylation Conditions

**Table S2.** Evaluation of esterification conditions for pentafluorobenzoyl sources.<sup>a</sup>



entry	benzoyl source	conditions	temperature	yield of <b>2f</b> (%) <sup>b</sup>
1	C <sub>6</sub> F <sub>5</sub> COOH	EDC·HCl (1.1 equiv), HOBt (1.1 equiv), Et <sub>3</sub> N (2.2 equiv)	23 °C	31%
2	C <sub>6</sub> F <sub>5</sub> COOH	DCC (1.1 equiv), DMAP (1.1 equiv)	23 °C	27%
3	C <sub>6</sub> F <sub>5</sub> COCl	Et <sub>3</sub> N (1.2 equiv)	23 °C	38%
<b>4</b>	<b>C<sub>6</sub>F<sub>5</sub>COCl</b>	<b>Et<sub>3</sub>N (1.2 equiv)</b>	<b>0 °C to 23 °C</b>	<b>55%</b>

<sup>a</sup>Reactions performed with N-hydroxyindole **1a** (1.0 equiv), benzoyl source (1.1 equiv) in CH<sub>2</sub>Cl<sub>2</sub> (0.05 M) at indicated temperature on 0.5–1.0 mmol scale. <sup>b</sup>Yields were determined by <sup>1</sup>H NMR using TCE as an internal standard.

### 3.3. General Procedures for C3-Acyloxylation of Indole Derivatives (Scheme 2.50)

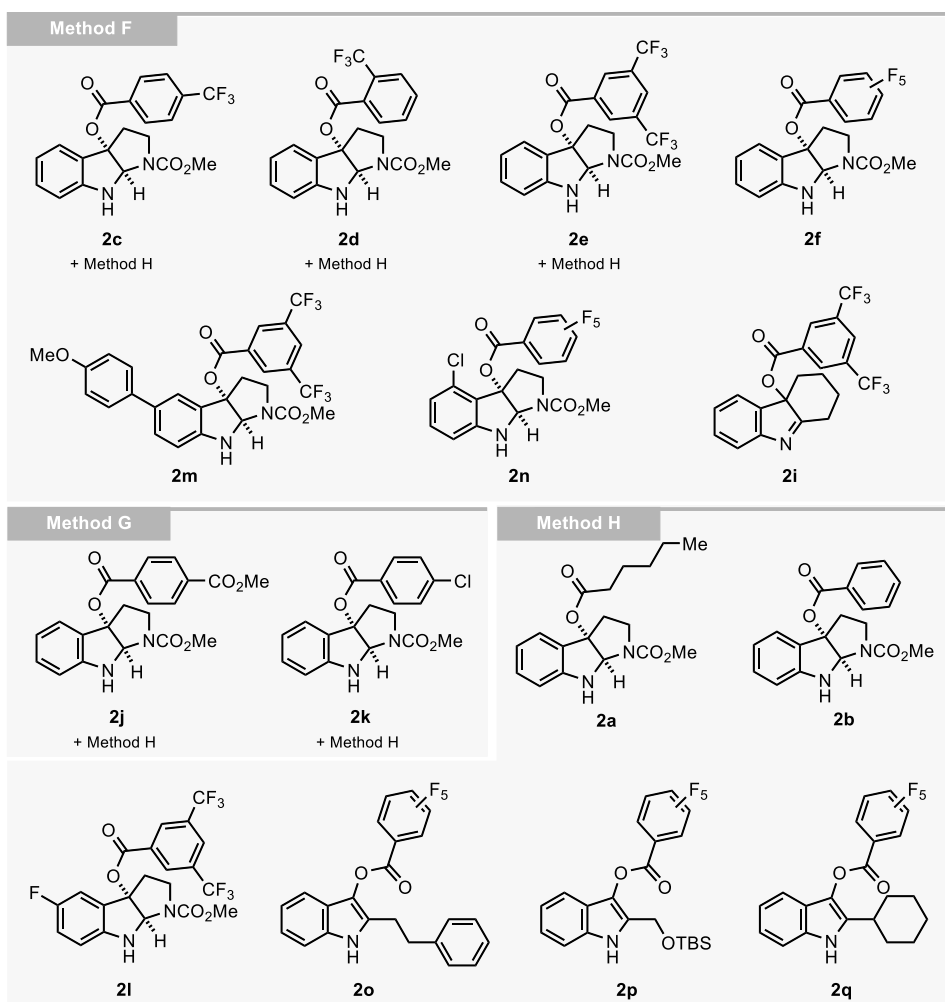
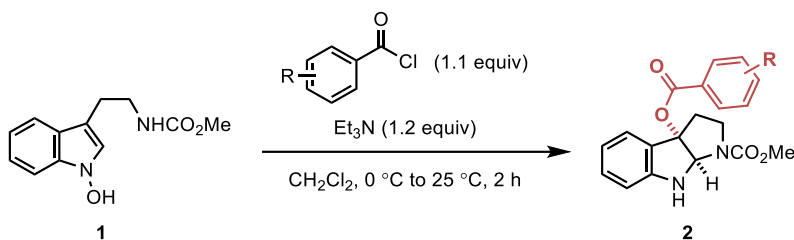


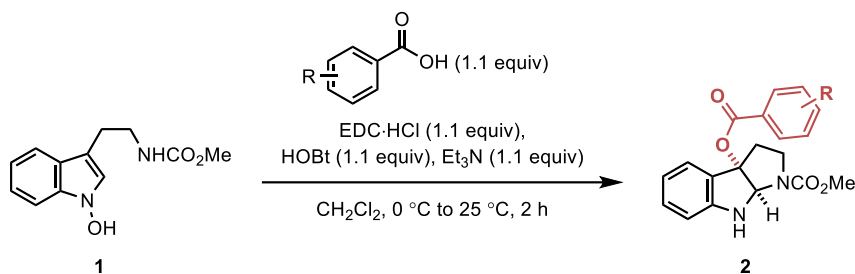
**Figure S3.** List of C3-acyloxyated products categorized by methods of C3-acyloxylation.

### General procedure F



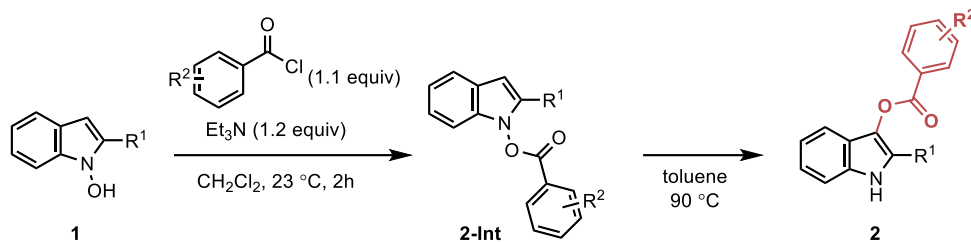
To an oven-dried round-bottom flask equipped with a stir bar and septum were added N-hydroxyindole **1** (1.0 equiv) and CH<sub>2</sub>Cl<sub>2</sub> (0.05 M in **1**) at 23 °C. The resulting solution was cooled to 0 °C, and benzoyl chloride (1.1 equiv) and Et<sub>3</sub>N (1.2 equiv) were added to the solution. The reaction mixture was warmed up to rt and stirred for 2 h, before it was diluted with H<sub>2</sub>O. The layers were separated, and the aqueous layer was extracted with CH<sub>2</sub>Cl<sub>2</sub> three times. The combined organic layer was washed with brine, dried over anhydrous MgSO<sub>4</sub>, filtered, and concentrated under reduced pressure. The resulting residue was purified by flash column chromatography to afford the product **2**.

### General procedure G



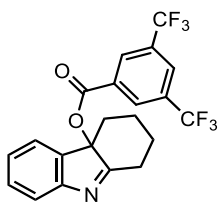
To an oven-dried round-bottom flask equipped with a stir bar and septum were added N-hydroxyindole **1** (1.0 equiv) and CH<sub>2</sub>Cl<sub>2</sub> (0.05 M in **1**) at The resulting solution was cooled to 0 °C, and benzoic acid (1.1 equiv), EDC·HCl (1.1 equiv), HOBT (1.1 equiv) and Et<sub>3</sub>N (2.2 equiv) were added to the solution. The reaction mixture was warmed up to rt and stirred for 2 h, before it was diluted with H<sub>2</sub>O. The layers were separated and the aqueous layer was extracted with CH<sub>2</sub>Cl<sub>2</sub> three times. The combined organic layer was washed with brine, dried over anhydrous MgSO<sub>4</sub>, filtered, and concentrated under reduced pressure. The resulting residue was purified by flash column chromatography to afford the product **2**.

## General procedure H



To an oven-dried round-bottom flask equipped with a stir bar and septum were added *N*-hydroxyindole **1** (1.0 equiv) and  $\text{CH}_2\text{Cl}_2$  (0.05 M in **1**) at 23 °C, followed by benzoyl chloride (1.1 equiv) and  $\text{Et}_3\text{N}$  (1.2 equiv). The resulting mixture was stirred for 2 h, before it was quenched with  $\text{NaHCO}_3$  (20 mL, sat. aq.). The layers were separated and the aqueous layer was extracted with  $\text{CH}_2\text{Cl}_2$  three times. The combined organic layer was washed with  $\text{NaHCO}_3$  (sat. aq.), dried over anhydrous  $\text{MgSO}_4$ , filtered, and concentrated under reduced pressure. The resulting crude was filtered through a short pad of silica gel using  $\text{CH}_2\text{Cl}_2$  as eluent, concentrated under reduced pressure and re-dissolved in toluene (0.05 M in **1**). The resulting solution was then heated to 90 °C in a pre-heated oil bath and stirred while the reaction was monitored by TLC. After completion of reaction (2–16 h), the reaction mixture was cooled to 23 °C, the crude mixture was concentrated under reduced pressure and directly purified by column chromatography to afford the product **2**.

### 1,2,3,4-Tetrahydro-4aH-carbazol-4a-yl 3,5-bis(trifluoromethyl)benzoate (**2i**)



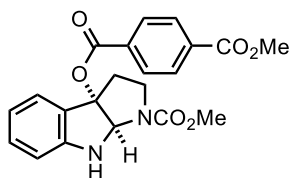
Following the **general procedure G**, *N*-hydroxyindole **1s** (86.6mg, 0.463 mmol) afforded indolenine **2i** (85.0 mg, 43%) as a pale yellow oil after purification by flash column chromatography (silica gel, hexanes:EtOAc = 1:0 → 9:1).

$R_f$ =0.27 (silica gel, hexanes:EtOAc = 9:1);  $^1\text{H NMR}$  (500 MHz,  $\text{CDCl}_3$ ):  $\delta$  8.45 (s, 2H), 8.08 (s, 1H), 7.62 (d,  $J$  = 7.7 Hz, 1H), 7.43 – 7.40 (m, 2H), 7.20 (t,  $J$  = 7.5 Hz, 1H), 3.00 (d,  $J$  = 15.0 Hz, 2H), 2.51 (td,  $J$  = 13.2, 5.9 Hz, 1H), 2.22 (br d,  $J$  = 10.9 Hz, 1H), 1.90 (tt,  $J$  = 13.3,



3.5 Hz, 1H), 1.85 – 1.81 (m, 1H), 1.62 – 1.49 (m, 1H), 1.36 (td,  $J = 14.1, 4.1$  Hz, 1H);  $^{13}\text{C}$  NMR (126 MHz,  $\text{CDCl}_3$ ):  $\delta$  182.3, 161.7, 154.3, 137.2, 132.6 (q,  $J = 34.2$  Hz), 131.7, 130.3, 130.0, 129.9, 126.9 (p,  $J = 3.8$  Hz), 126.0, 122.9 (d,  $J = 273.0$  Hz), 122.0, 121.2, 87.7, 38.4, 30.0, 28.6, 21.0;  $^{19}\text{F}$  NMR (471 MHz,  $\text{CDCl}_3$ ):  $\delta$  -63.0; HRMS calcd. for  $\text{C}_{12}\text{H}_{16}\text{N}^+ [\text{M} + \text{H}]^+$  174.1279, found 174.1277.

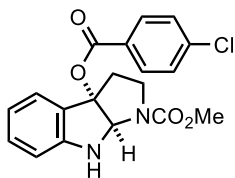
**1-(Methoxycarbonyl)-2,3,8,8a-tetrahydropyrrolo[2,3-b]indol-3a(1H)-yl methyl terephthalate (2j)**



Following the **general procedure G**, *N*-hydroxyindole **1a** (91.2 mg, 0.389 mmol) afforded an inseparable mixture of pyrroloindoline **2j-Int** and indolyl *N*-carboxylate **2j** (122 mg, 2.7:1, overall 79%) as a pale yellow oil after purification by flash column chromatography (silica gel, hexanes:EtOAc = 1:0 → 7:3). When following the **general procedure H** for 4 h, *N*-hydroxyindole **1a** (71.0 mg, 0.303 mmol) afforded pyrroloindoline **2j** (81.7 mg, 68%) as a sole product.

$R_f$ =0.27 (silica gel, hexanes:EtOAc = 1:1);  $^1\text{H}$  NMR (400 MHz,  $\text{CDCl}_3$ , 60:40 mixture of rotamers):  $\delta$  8.06 (m, 1H), 7.62 and 7.56 (d,  $J = 7.5$  Hz, 1H), 7.21 (t,  $J = 7.6$  Hz, 1H), 6.84 – 6.76 (m, 1H), 6.70 (d,  $J = 8.0$  Hz, 1H), 5.78 (s, 1H), 3.96 – 3.91 and 3.85 – 3.80 (m, 1H), 3.94 (s, 3H), 3.80 and 3.73 (s, 3H), 3.27 – 3.20 (m, 1H), 3.08 and 2.99 (dd,  $J = 12.8, 6.2$  Hz, 1H), 2.72 (q,  $J = 10.7$  Hz, 1H);  $^{13}\text{C}$  NMR (101 MHz,  $\text{CDCl}_3$ ):  $\delta$  166.3, 164.7, 155.7, 154.9, 151.0, 150.7, 134.3, 134.0, 131.4, 129.9, 129.7, 126.7, 126.2, 125.8, 125.7, 122.4, 119.9, 119.7, 111.3, 110.6, 110.5, 94.9, 93.7, 80.4, 79.6, 53.0, 52.7, 52.6, 45.6, 35.8, 35.7; HRMS calcd. for  $\text{C}_{21}\text{H}_{21}\text{N}_2\text{O}_6^+ [\text{M} + \text{H}]^+$  397.1394, found 397.1383.

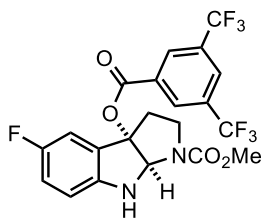
**Methyl 3a-((4-chlorobenzoyl)oxy)-3,3a,8,8a-tetrahydropyrrolo[2,3-b]indole-1(2H)-carboxylate (2k)**



Following the **general procedure G**, *N*-hydroxyindole **1a** (88.0 mg, 0.376 mmol) afforded an inseparable mixture of pyrroloindoline **2k-Int** and indolyl *N*-carboxylate **2k** (109 mg, 7.7:1, overall 78%) as a pale yellow oil after purification by flash column chromatography (silica gel, hexanes:EtOAc = 1:0 → 7:3). When following the **general procedure H** for 16 h, *N*-hydroxyindole **1a** (70.9 mg, 0.303 mmol) afforded pyrroloindoline **2k** (68.8 mg, 61%) as a sole product.

$R_f$ =0.53 (silica gel, hexanes:EtOAc = 1:1);  $^1\text{H NMR}$  (500 MHz,  $\text{CDCl}_3$ , 60:40 mixture of rotamers):  $\delta$  7.91 (d,  $J$  = 8.4 Hz, 2H), 7.61 and 7.54 (d,  $J$  = 7.6 Hz, 1H), 7.38 (d,  $J$  = 8.2 Hz, 2H), 7.20 (t,  $J$  = 7.8 Hz, 1H), 6.80 (q,  $J$  = 6.9 Hz, 1H), 6.68 (d,  $J$  = 7.9 Hz, 1H), 5.75 (s, 1H), 3.93 and 3.81 (t,  $J$  = 9.8 Hz, 1H), 3.79 and 3.72 (s, 3H), 3.25 – 3.19 (m, 1H), 3.06 and 2.96 (dd,  $J$  = 13.0, 6.3 Hz, 0H), 2.73 – 2.65 (m, 1H);  $^{13}\text{C NMR}$  (126 MHz,  $\text{CDCl}_3$ ):  $\delta$  164.6, 155.7, 154.9, 151.0, 150.8, 139.8, 139.8, 131.3, 128.8, 128.7, 128.0, 128.0, 126.7, 126.1, 125.9, 125.7, 119.8, 119.5, 110.5, 110.3, 94.7, 93.5, 80.4, 79.6, 52.9, 52.7, 45.6, 45.6, 35.8, 35.7; **HRMS** calcd. for  $\text{C}_{19}\text{H}_{18}\text{ClN}_2\text{O}_4^+$  [ $\text{M} + \text{H}$ ] $^+$  373.0950, found 373.0947.

**Methyl 3a-((3,5-bis(trifluoromethyl)benzoyl)oxy)-5-fluoro-3,3a,8,8a-tetrahydropyrrolo[2,3-b]indole-1(2H)-carboxylate (2l)**

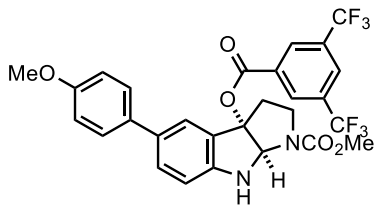


Following the **general procedure H** for 8 h, *N*-hydroxyindole **1f** (43.0 mg, 0.170 mmol) afforded pyrroloindoline **2l** (52.8 mg, 63%) as a pale yellow oil after purification by flash column chromatography (silica gel, hexanes:EtOAc = 1:0 → 7:3).

$R_f$ =0.57 (silica gel, hexanes:EtOAc = 1:1);  $^1\text{H NMR}$  (400 MHz,  $\text{CDCl}_3$ , 55:45 mixture of rotamers):  $\delta$  8.42 (s, 2H), 8.06 (s, 1H), 7.35 and 7.31 (d,  $J$  = 8.2 Hz, 1H), 6.94 (t,  $J$  = 8.8 Hz,

1H), 6.64 and 6.62 (d,  $J = 4.2$  Hz, 1H), 5.80 and 5.78 (s, 1H), 5.19 and 4.83 (s, 1H), 3.97 and 3.85 (t,  $J = 9.9$  Hz, 1H), 3.81 and 3.74 (s, 3H), 3.29 – 3.21 (m, 1H), 3.11 – 3.01 (m, 1H), 2.73 – 2.65 (m, 1H);  $^{13}\text{C NMR}$  (101 MHz,  $\text{CDCl}_3$ ):  $\delta$  162.8, 157.2 (d,  $J = 237.3$  Hz), 157.1 (d,  $J = 237.0$  Hz), 155.6, 154.7, 147.3, 147.1, 132.4 (q,  $J = 34.1$  Hz), 132.2, 130.0 (d,  $J = 3.9$  Hz), 126.8, 126.1 (br t,  $J = 9.4$  Hz), 122.9 (q,  $J = 273.1$  Hz), 118.4 (d,  $J = 24.0$  Hz), 113.8 (d,  $J = 24.9$  Hz), 113.5 (d,  $J = 24.6$  Hz), 111.3 (d,  $J = 8.1$  Hz), 111.2 (d,  $J = 7.8$  Hz), 113.3, 111.4, 111.3, 111.2, 95.5, 94.3, 81.1, 80.4, 53.1, 52.8, 45.6, 45.6, 35.7, 31.0;  $^{19}\text{F NMR}$  (376 MHz,  $\text{CDCl}_3$ ):  $\delta$  -63.0, -124.1 (q,  $J = 4.5$  Hz), -124.5 (q,  $J = 4.5$  Hz); **HRMS** calcd. for  $\text{C}_{21}\text{H}_{16}\text{F}_7\text{N}_2\text{O}_4^+$   $[\text{M} + \text{H}]^+$  493.0993, found 493.0990.

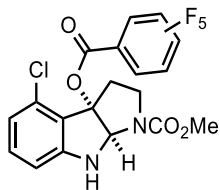
**Methyl 3a-((3,5-bis(trifluoromethyl)benzoyl)oxy)-5-(4-methoxyphenyl)-3,3a,8,8a-tetrahydropyrrolo[2,3-b]indole-1(2H)-carboxylate (2m)**



Following the **general procedure F**, *N*-hydroxyindole **1e** (51.0 mg, 0.150 mmol) afforded pyrroloindoline **2m** (47.8 mg, 55%) as a pale yellow oil after purification by flash column chromatography (silica gel, hexanes:EtOAc = 1:0 → 8:2).

$R_f$ =0.43 (silica gel, hexanes:EtOAc = 1:1);  $^1\text{H NMR}$  (400 MHz,  $\text{CDCl}_3$ , 60:40 mixture of rotamers):  $\delta$  8.56 and 8.44 (s, 2H), 8.11 and 8.05 (s, 1H), 7.83 and 7.78 (s, 1H), 7.47 – 7.43 (m, 2H), 6.95 (d,  $J = 8.4$  Hz, 2H), 6.78 (d,  $J = 8.3$  Hz, 1H), 5.86 and 5.83 (s, 1H), 4.00 and 3.88 (t,  $J = 8.2$  Hz, 1H), 3.84 and 3.77 (s, 3H), 3.34 – 3.26 (m, 1H), 3.20 and 3.14 (dd,  $J = 12.7, 6.0$  Hz, 1H), 2.79 – 2.70 (m, 1H);  $^{13}\text{C NMR}$  (101 MHz,  $\text{CDCl}_3$ ):  $\delta$  166.9, 162.9, 158.8, 158.8, 155.8, 154.9, 150.2, 149.9, 133.7, 133.6, 133.2, 132.9, 132.8, 132.4, 132.4 (q,  $J = 34.0$  Hz), 132.3 (q,  $J = 34.0$  Hz), 130.4, 130.3, 130.2, 130.1, 130.0, 127.7, 126.7, 126.7, 127.1 – 126.8 (m), 126.3, 125.7, 125.6, 125.0, 124.6, 123.0 (q,  $J = 273.1$  Hz), 122.91 (q,  $J = 273.1$  Hz), 115.1, 114.3, 110.9, 110.7, 95.8, 94.6, 80.7, 80.0, 55.5, 53.2, 52.9, 45.7, 35.8, 35.8;  $^{19}\text{F NMR}$  (376 MHz,  $\text{CDCl}_3$ ):  $\delta$  -62.9, -63.0; **HRMS** calcd. for  $\text{C}_{28}\text{H}_{23}\text{F}_6\text{N}_2\text{O}_5^+$   $[\text{M} + \text{H}]^+$  581.1506, found 581.1499.

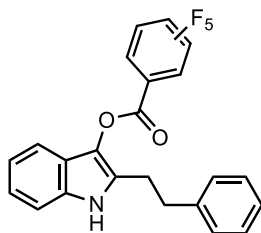
**Methyl 4-chloro-3a-((perfluorobenzoyl)oxy)-3,3a,8,8a-tetrahydropyrrolo[2,3-b]indole-1(2H)-carboxylate (2n)**



Following the **general procedure F**, *N*-hydroxyindole **11** (75.0 mg, 0.279 mmol) afforded pyrroloindoline **2n** (58.1 mg, 45%) as a pale yellow oil after purification by flash column chromatography (silica gel, hexanes:EtOAc = 1:0 → 8:2).

$R_f$ =0.57 (silica gel, hexanes:EtOAc = 1:1);  $^1\text{H NMR}$  (400 MHz,  $\text{CDCl}_3$ , 60:40 mixture of rotamers):  $\delta$  7.13 (t,  $J$  = 7.9 Hz, 1H), 6.73 (d,  $J$  = 7.8 Hz, 1H), 6.57 (d,  $J$  = 8.0 Hz, 1H), 5.97 and 5.91 (s, 1H), 5.30 (s, 1H), 3.92 – 3.87 and 3.83 – 3.79 (m, 1H), 3.79 and 3.75 (s, 3H), 3.32 (q,  $J$  = 9.7 Hz, 1H), 2.88 – 2.72 (m, 2H);  $^{13}\text{C NMR}$  (101 MHz,  $\text{CDCl}_3$ ):  $\delta$  157.7, 157.6, 155.8, 154.9, 152.2, 152.1, 145.9 (dm,  $J$  = 257.6 Hz), 143.6 (dm,  $J$  = 259.0 Hz), 137.8 (ddd,  $J$  = 256.1, 18.2, 12.4, 5.3 Hz), 132.5, 130.4, 121.9, 120.3, 120.0, 108.7, 108.6, 107.7 (t,  $J$  = 14.2 Hz), 96.7, 95.6, 79.8, 79.2, 53.0, 52.9, 44.3, 44.2, 35.8, 35.4;  $^{19}\text{F NMR}$  (376 MHz,  $\text{CDCl}_3$ ):  $\delta$  -137.1 (tt,  $J$  = 20.3, 6.0 Hz), -147.5 (t,  $J$  = 20.7 Hz), -147.8 (t,  $J$  = 20.7 Hz), -160.2 (dtd,  $J$  = 32.6, 20.2, 6.2 Hz); **HRMS** calcd. for  $\text{C}_{19}\text{H}_{13}\text{ClF}_5\text{N}_2\text{O}_4^+$  [ $\text{M} + \text{H}$ ] $^+$  463.0479, found 463.0475.

**2-Phenethyl-1H-indol-3-yl 2,3,4,5,6-pentafluorobenzoate (2o)**

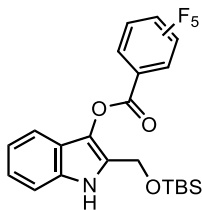


Following the **general procedure H** for 16 h, *N*-hydroxyindole **1p** (30.0 mg, 0.126 mmol) afforded indole **2o** (32.1 mg, 59%) as a pale yellow oil after purification by flash column chromatography (silica gel, hexanes:EtOAc = 1:0 → 95:5).

$R_f$ =0.24 (silica gel, hexanes:EtOAc = 7:3);  $^1\text{H NMR}$  (500 MHz,  $\text{CDCl}_3$ ):  $\delta$  7.59 (br s, 1H), 7.45 (d,  $J$  = 7.6 Hz, 1H), 7.36 – 7.31 (m, 2H), 7.29 – 7.15 (m, 6H), 3.11 – 2.98 (m, 4H);  $^{13}\text{C}$

**NMR** (126 MHz, CDCl<sub>3</sub>):  $\delta$  157.6, 145.7 (dm,  $J = 258.2$  Hz), 143.6 (dm,  $J = 255.2$  Hz), 140.8, 138.0 (dm,  $J = 255.8$  Hz), 132.8, 128.8, 128.5, 127.9, 126.6, 126.1, 122.4, 120.8, 120.5, 117.0, 111.2, 107.9 (td,  $J = 16.2, 4.1$  Hz), 35.1, 27.1; **<sup>19</sup>F NMR** (471 MHz, CDCl<sub>3</sub>):  $\delta$  -137.3 (dp,  $J = 16.9, 5.8$  Hz), -147.6 (tt,  $J = 20.9, 4.8$  Hz), -159.7 – -159.8 (m); **HRMS** calcd. for C<sub>23</sub>H<sub>15</sub>F<sub>5</sub>NO<sub>2</sub><sup>+</sup> [M + H]<sup>+</sup> 432.1018, found 432.1021.

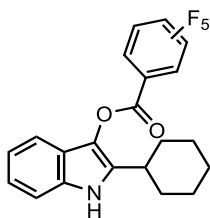
**2-(((*tert*-Butyldimethylsilyl)oxy)methyl)-1H-indol-3-yl 2,3,4,5,6-pentafluorobenzoate (2p)**



Following the **general procedure H** for 16 h, *N*-hydroxyindole **1q** (51.1 mg, 0.184 mmol) afforded indole **2p** (52.9 mg, 61%) as a pale yellow oil after purification by flash column chromatography (silica gel, hexanes:EtOAc = 1:0 → 95:5).

**R<sub>f</sub>**=0.45 (silica gel, hexanes:EtOAc = 8:2); **<sup>1</sup>H NMR** (500 MHz, CDCl<sub>3</sub>):  $\delta$  8.20 (br s, 1H), 7.45 (d,  $J = 7.9$  Hz, 1H), 7.38 (d,  $J = 8.2$  Hz, 1H), 7.22 (t,  $J = 7.6$  Hz, 1H), 7.16 (t,  $J = 7.5$  Hz, 1H), 4.87 (s, 2H), 0.94 (s, 9H), 0.12 (s, 6H); **<sup>13</sup>C NMR** (126 MHz, CDCl<sub>3</sub>):  $\delta$  157.2, 145.8 (dm,  $J = 244.4$  Hz), 143.8 (dm,  $J = 261.0$  Hz), 138.0 (dm,  $J = 256.0$  Hz), 132.9, 127.0, 124.5, 122.8, 120.8, 120.6, 117.5, 111.6, 56.5, 26.0, -5.3; **<sup>19</sup>F NMR** (471 MHz, CDCl<sub>3</sub>):  $\delta$  -137.2 (dp,  $J = 17.2, 6.0$  Hz), -147.4 (tt,  $J = 20.9, 4.6$  Hz), -159.6 – -159.8 (m); **HRMS** calcd. for C<sub>22</sub>H<sub>23</sub>F<sub>5</sub>NO<sub>3</sub>Si<sup>+</sup> [M + H]<sup>+</sup> 472.1362, found 472.1365.

**2-Cyclohexyl-1H-indol-3-yl 2,3,4,5,6-pentafluorobenzoate (2q)**



Following the **general procedure H** for 16 h, *N*-hydroxyindole **1r** (28.8 mg, 0.134 mmol) afforded indole **2q** (43.3 mg, 76%) as a pale yellow oil after purification by flash column

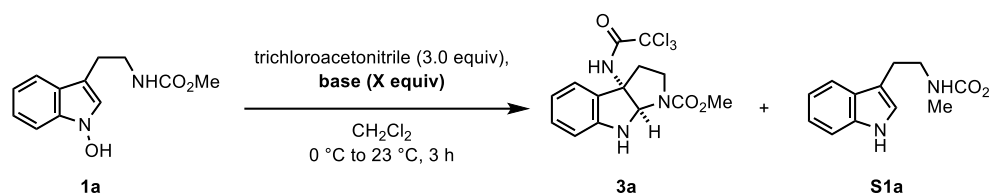
chromatography (silica gel, hexanes:EtOAc = 1:0 → 95:5).

$R_f=0.45$  (silica gel, hexanes:EtOAc = 8:2);  $^1\text{H NMR}$  (400 MHz,  $\text{CDCl}_3$ ):  $\delta$  7.83 (s, 1H), 7.40 (d,  $J=7.7$  Hz, 1H), 7.29 (d,  $J=7.9$  Hz, 1H), 7.18 (t,  $J=7.5$  Hz, 1H), 7.14 (t,  $J=7.2$  Hz, 1H), 2.85 (tt,  $J=12.0, 3.5$  Hz, 1H), 2.02 (dd,  $J=12.5, 3.4$  Hz, 2H), 1.88 (dt,  $J=13.1, 3.3$  Hz, 2H), 1.79 (dt,  $J=13.1, 3.4$  Hz, 1H), 1.54 – 1.37 (m, 4H), 1.29 (ddt,  $J=12.3, 8.0, 3.6$  Hz, 1H);  $^{13}\text{C NMR}$  (126 MHz,  $\text{CDCl}_3$ ):  $\delta$  157.8, 145.6 (dm,  $J=257.0$  Hz), 143.6 (d,  $J=252.5$  Hz), 138.0 (dddd,  $J=250.9, 15.8, 12.6, 4.8$  Hz), 133.1, 132.6, 124.8, 122.2, 121.0, 120.4, 116.9, 111.3, 108.2 (t,  $J=16.7$  Hz), 35.3, 32.2, 26.5, 26.0;  $^{19}\text{F NMR}$  (376 MHz,  $\text{CDCl}_3$ ):  $\delta$  -137.5 (dp,  $J=16.9, 5.5, 5.1$  Hz), -148.0 (tt,  $J=21.1, 4.8$  Hz), -159.7 – -159.9 (m); **HRMS** calcd. for  $\text{C}_{21}\text{H}_{17}\text{F}_5\text{NO}_2^+$   $[\text{M} + \text{H}]^+$  410.1174, found 410.1176.

## 4. C–N Bond Formation via Indolyl 1,3-Heteroatom Transposition (IHT)

### 4.1. Optimization of the C3-Amidation Reaction Conditions (Table 2.1)

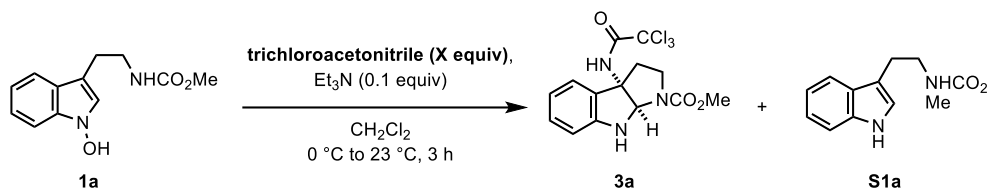
**Table S3.** Evaluation of bases.<sup>a</sup>



entry	base	equiv	yield of 3a <sup>b</sup>	yield of S1a <sup>b</sup>
1	DIPEA	0.1	51%	7%
2	DBU	0.1	70%	5%
3	DABCO	0.1	59%	6%
4	pyridine	0.1	<5%	54%
5	NaH	1.1	68%	5%
<b>6</b>	<b>Et<sub>3</sub>N</b>	<b>0.1</b>	<b>75% (71%)</b>	<b>&lt;1%</b>
7	Et <sub>3</sub> N	1.0	37%	21%

<sup>a</sup>Reactions were performed with trichloroacetonitrile (3.0 equiv) and base in CH<sub>2</sub>Cl<sub>2</sub> (0.05 M) at 0 °C to 23 °C on 0.3–1.2 mmol scale. <sup>b</sup>Determined by <sup>1</sup>H NMR analysis of the crude mixture using TCE as an internal standard and the isolated yield was included in the parentheses.

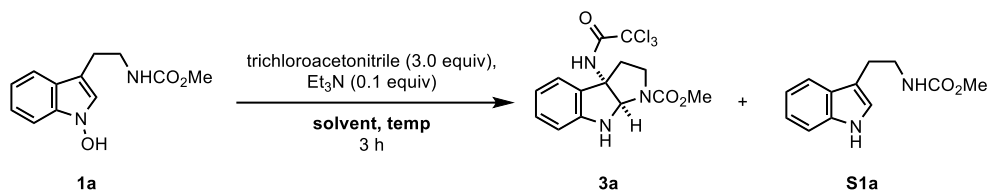
**Table S4.** Evaluation of equivalent of trichloroacetonitrile.<sup>a</sup>



entry	equiv	yield of <b>3a</b> (%) <sup>b</sup>	yield of <b>S1a</b> (%) <sup>b</sup>
1	1.0	36%	22%
2	2.0	55%	9%
<b>3</b>	<b>3.0</b>	<b>79% (78%)</b>	<b>&lt;1%</b>
4	4.0	48%	11%

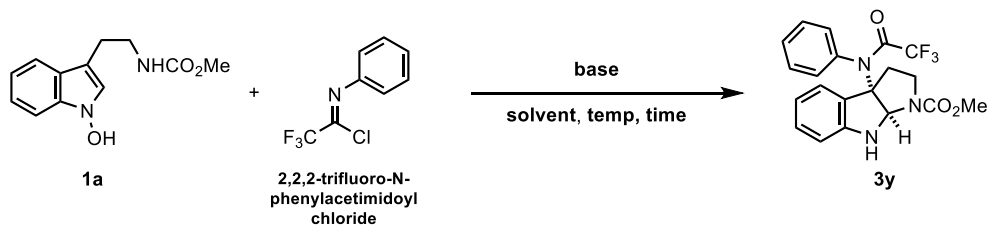
<sup>a</sup>Reactions performed with trichloroacetonitrile and  $\text{Et}_3\text{N}$  (0.1 equiv) in  $\text{CH}_2\text{Cl}_2$  (0.05 M) at 0 to  $23\text{ }^\circ\text{C}$  on 0.3–1.2 mmol scale. <sup>b</sup>Determined by  $^1\text{H}$  NMR analysis of the crude mixture using TCE as an internal standard and the yield of the isolated product was given in the parentheses.



**Table S5.** Evaluation of solvents and temperatures.<sup>a</sup>

entry	solvent	temperature	time	yield of <b>3a</b> (%) <sup>b</sup>	yield of <b>S1a</b> (%) <sup>b</sup>
1	THF	0 to 23 °C	3 h	4%	48%
2	toluene	0 to 23 °C	3 h	11%	63%
3	MeCN	0 to 23 °C	3 h	16%	72%
4	DMF	0 to 23 °C	3 h	<5%	56%
<b>5</b>	<b>CH<sub>2</sub>Cl<sub>2</sub></b>	<b>0 to 23 °C</b>	<b>3 h</b>	<b>75% (73%)</b>	<b>&lt;1%</b>
6	CH <sub>2</sub> Cl <sub>2</sub>	23 °C	3 h	67%	<1%
7	CH <sub>2</sub> Cl <sub>2</sub>	0 °C	24 h	38%	33%

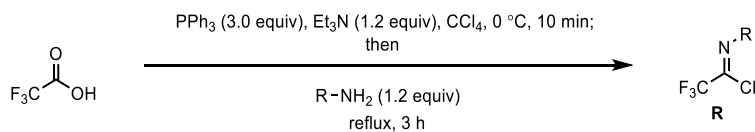
<sup>a</sup>Reactions performed with trichloroacetonitrile (3.0 equiv) and Et<sub>3</sub>N (0.1 equiv) in solvent (0.05 M) at indicated temperature on 0.3–1.2 mmol scale. <sup>b</sup>Determined by <sup>1</sup>H NMR analysis of the crude mixture using TCE as an internal standard and the yield of the isolated product was given in the parentheses.

**Table S6.** Evaluation of reaction conditions using trifluoroacetimidoyl chloride.<sup>a</sup>

entry	base (equiv)	equiv of imidoyl chloride	solvent	temperature	time	yield of <b>3y</b> <sup>b</sup>
1	Et <sub>3</sub> N (1.1 equiv)	1.5	THF	0 °C	1 h	8%
2	LDA (1.1 equiv)	1.5	THF	0 °C	1 h	13%
3	LiHMDS (1.1 equiv)	1.5	THF	0 °C	1 h	17%
4	NaHMDS (1.1 equiv)	1.5	THF	0 °C	1 h	16%
<b>5</b>	<b>NaH (1.1 equiv)</b>	<b>1.5</b>	<b>THF</b>	<b>0 °C</b>	<b>1 h</b>	<b>34% (28%)</b>
6	NaH (1.1 equiv)	1.5	CH <sub>2</sub> Cl <sub>2</sub>	0 °C	1 h	26% (20%)
7	NaH (2.0 equiv)	1.5	THF	0 °C	1 h	24%
8	NaH (1.1 equiv)	3.0	THF	0 °C	1 h	21%
9	NaH (1.1 equiv)	1.5	THF	-20 °C	12 h	11%
10	NaH (1.1 equiv)	1.5	THF	-78 °C	24 h	19%

<sup>a</sup>Reactions performed with imidoyl chloride and base in solvent (0.05 M) at indicated temperature on 0.3–1.2 mmol scale. <sup>b</sup>Determined by <sup>1</sup>H NMR analysis of the crude mixture using TCE as an internal standard and the isolated yield was included in the parentheses.

## 4.2. Preparation of Trifluoroacetimidoyl Chloride



Trifluoroacetimidoyl chlorides were prepared according to the literature procedure.<sup>15</sup> To an oven-dried round-bottom flask equipped with a stir bar, septum, and condenser were added TFA (1.0 equiv),  $\text{PPh}_3$  (3.0 equiv),  $\text{Et}_3\text{N}$  (1.2 equiv), and  $\text{CCl}_4$  (5.0 equiv) at  $23\text{ }^\circ\text{C}$ . The resulting solution was cooled to  $0\text{ }^\circ\text{C}$  and stirred for 10 min before the solution of amine (1.2 equiv) in  $\text{CCl}_4$  (5.0 equiv) was added. The reaction mixture was heated to reflux in a pre-heated oil bath and stirred for 2 h, before it was cooled to  $23\text{ }^\circ\text{C}$  and directly concentrated under reduced pressure. The crude product was re-dissolved in hexanes and filtered, and the filter cake was washed with hexanes three times. The resulting filtrate was concentrated under reduced pressure, and the crude product was distilled to afford the imidoyl chloride **R**.

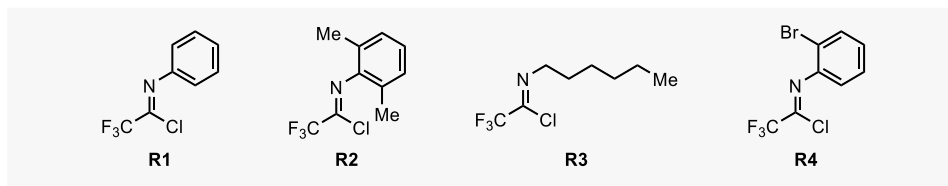


**Figure S4.** List of trifluoroacetimidoyl chlorides.

**The spectral data matched to those reported in the literature:** 2,2,2-trifluoro-*N*-phenylacetimidoyl chloride (**R1**)<sup>15</sup>, *N*-(2,6-dimethylphenyl)-2,2,2-trifluoroacetimidoyl chloride (**R2**)<sup>15</sup>, 2,2,2-trifluoro-*N*-hexylacetimidoyl chloride (**R3**)<sup>15</sup>, *N*-(2-bromophenyl)-2,2,2-trifluoroacetimidoyl chloride (**R4**)<sup>16</sup>

### 4.3. General Procedure for C3-Amidation of Indole Derivatives (Scheme 2.51 and scheme 2.52)

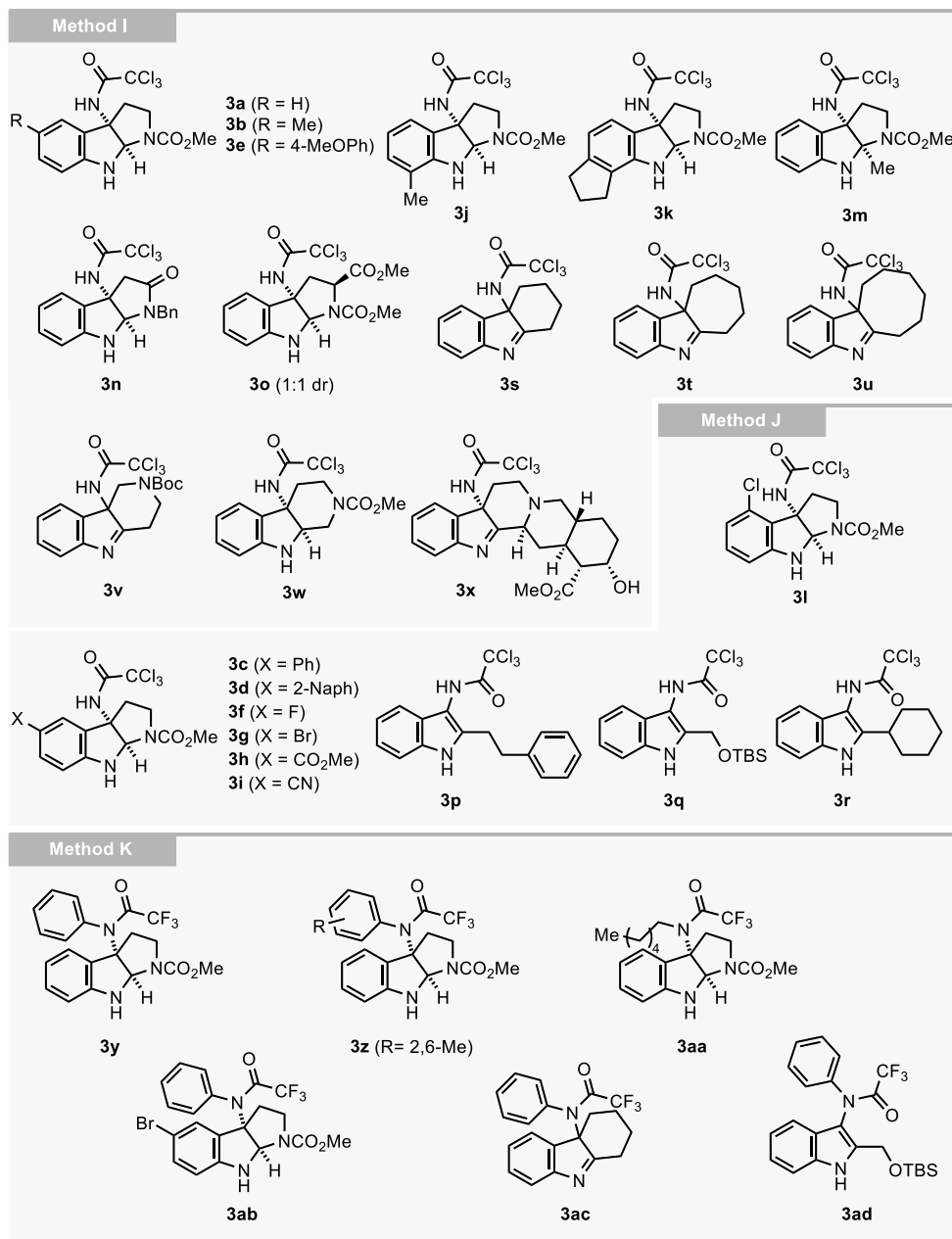
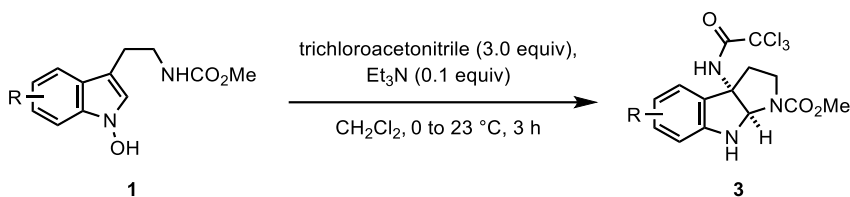


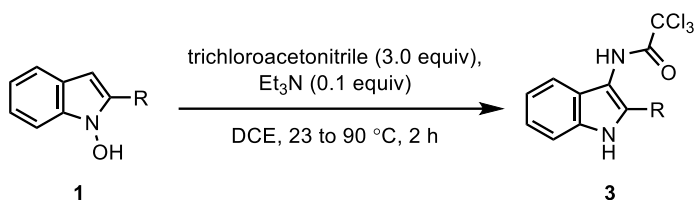
**Figure S5.** List of C3-amidated products categorized by methods of C3-amidation.

### General procedure I



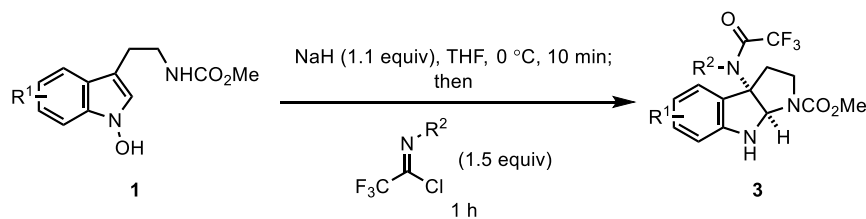
To an oven-dried round-bottom flask equipped with a stir bar and septum were added *N*-hydroxyindole **1** (1.0 equiv) and CH<sub>2</sub>Cl<sub>2</sub> (0.05 M in **1**) at 23 °C. The resulting solution was cooled to 0 °C, and trichloroacetonitrile (3.0 equiv) and Et<sub>3</sub>N (0.1 equiv) were successively added to the solution. The reaction mixture was warmed up to 23 °C and stirred for 3 h before it was quenched with H<sub>2</sub>O. The layers were separated and the aqueous layer was extracted with CH<sub>2</sub>Cl<sub>2</sub> three times. The combined organic layer was dried over anhydrous MgSO<sub>4</sub>, filtered, and concentrated under reduced pressure. The resulting residue was purified by flash column chromatography to afford the desired product **3**.

### General procedure J



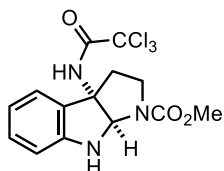
To an oven-dried heavy-wall pressure tube equipped with a stir bar and septum were successively added *N*-hydroxyindole **1** (1.0 equiv) and DCE (0.05 M in **1**) at 23 °C, followed by trichloroacetonitrile (3.0 equiv) and Et<sub>3</sub>N (0.1 equiv). The resulting mixture was heated to 90 °C in a pre-heated oil bath and stirred for 2 h, before it was cooled to 23 °C and quenched with H<sub>2</sub>O. The layers were separated and the aqueous layer was extracted with CH<sub>2</sub>Cl<sub>2</sub> three times. The combined organic layer was dried over anhydrous MgSO<sub>4</sub>, filtered, and concentrated under reduced pressure. The resulting residue was purified by flash column chromatography to afford the desired product **3**.

### General procedure K



To an oven-dried round-bottom flask equipped with a stir bar and septum were successively added *N*-hydroxyindole **1** (1.0 equiv) and THF (0.05 M in **1**) at 23 °C. The resulting solution was cooled to 0 °C, and NaH (60% in mineral oil, 1.1 equiv) was added to the solution. The reaction mixture was stirred for 10 min, then imidoyl chloride (1.5 equiv) was added. The resulting mixture was stirred for additional 1 h at 0 °C before it was quenched with brine. The layers were separated and the aqueous layer was extracted with EtOAc three times. The combined organic layer was washed with brine, dried over anhydrous MgSO<sub>4</sub>, filtered, and concentrated under reduced pressure. The resulting residue was purified by flash column chromatography to afford the desired product **3**.

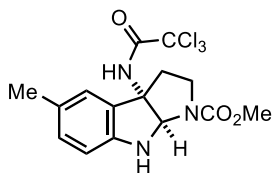
**Methyl 3a-(2,2,2-trichloroacetamido)-3,3a,8,8a-tetrahydropyrrolo[2,3-*b*]indole-1(2H)-carboxylate (3a)**



Following the **general procedure I**, *N*-hydroxyindole **1a** (133 mg, 0.568 mmol) afforded pyrroloindoline **3a** (168 mg, 78%) as a pale yellow oil after purification by flash column chromatography (silica gel, hexanes:EtOAc = 1:0 → 7:3).

*R<sub>f</sub>*=0.51 (silica gel, hexanes:EtOAc = 1:1); <sup>1</sup>H NMR (500 MHz, CDCl<sub>3</sub>): δ 7.34 and 7.30 (d, *J* = 7.5 Hz, 1H), 7.23 – 7.19 (m, 1H), 6.88 – 6.80 (m, 2H), 6.68 (d, *J* = 7.3 Hz, 1H), 5.70 and 5.68 (s, 1H), 3.88 and 3.78 (t, *J* = 9.9 Hz, 1H), 3.77 and 3.70 (s, 3H), 3.16 – 3.08 (m, 1H), 3.01 – 2.91 (m, 1H), 2.50 and 2.41 (dd, *J* = 12.5, 6.5 Hz, 1H); <sup>13</sup>C NMR (101 MHz, CDCl<sub>3</sub>): δ 161.0, 155.5, 154.6, 149.9, 149.7, 131.1, 131.1, 127.0, 126.8, 123.8, 123.5, 120.0, 119.8, 110.5, 110.4, 92.3, 78.3, 78.2, 72.0, 70.9, 52.9, 52.6, 45.4, 45.3, 33.0; **HRMS** calcd. for **HRMS** calcd. for C<sub>14</sub>H<sub>15</sub>Cl<sub>3</sub>N<sub>3</sub>O<sub>3</sub><sup>+</sup> [M + H]<sup>+</sup> 378.0174, found 378.0173.

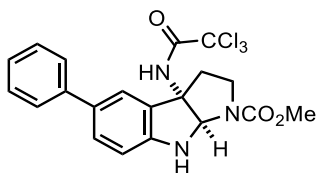
**Methyl 5-methyl-3a-(2,2,2-trichloroacetamido)-3,3a,8,8a-tetrahydropyrrolo[2,3-b]indole-1(2H)-carboxylate (3b)**



Following the **general procedure I**, N-hydroxyindole **1b** (72.0 mg, 0.290 mmol) afforded pyrroloindoline **3b** (77.2 mg, 68%) as a pale yellow oil after purification by flash column chromatography (silica gel, hexanes:EtOAc = 1:0 → 7:3).

$R_f$ =0.56 (silica gel, hexanes:EtOAc = 1:1);  $^1\text{H NMR}$  (500 MHz,  $\text{CDCl}_3$ ):  $\delta$  7.14 and 7.10 (s, 1H), 7.03 (d,  $J$  = 8.0 Hz, 1H), 6.80 and 6.76 (s, 1H), 6.60 (d,  $J$  = 8.0 Hz, 1H), 5.69 and 5.67 (s, 1H), 3.89 and 3.77 (t,  $J$  = 9.7 Hz, 1H), 3.77 and 3.70 (s, 3H), 3.12 (tt,  $J$  = 10.9, 6.8 Hz, 1H), 3.01 – 2.91 (m, 1H), 2.47 and 2.39 (dd,  $J$  = 12.4, 6.1 Hz, 1H), 2.30 (s, 3H);  $^{13}\text{C NMR}$  (101 MHz,  $\text{CDCl}_3$ ):  $\delta$  161.0, 155.6, 154.7, 147.7, 147.5, 131.8, 131.7, 129.7, 129.5, 127.2, 127.0, 124.2, 123.9, 110.7, 110.5, 92.3, 78.5, 72.1, 71.0, 52.9, 52.6, 45.5, 45.3, 32.7, 32.6, 21.0; **HRMS** calcd. for  $\text{C}_{15}\text{H}_{17}\text{Cl}_3\text{N}_3\text{O}_3^+$   $[\text{M} + \text{H}]^+$  392.0330, found 392.0330.

**Methyl 5-phenyl-3a-(2,2,2-trichloroacetamido)-3,3a,8,8a-tetrahydropyrrolo[2,3-b]indole-1(2H)-carboxylate (3c)**

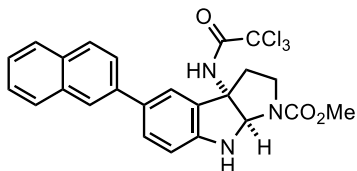


Following the **general procedure J**, N-hydroxyindole **1c** (35.6 mg, 0.115 mmol) afforded pyrroloindoline **3c** (26.1 mg, 50%) as a pale yellow oil after purification by flash column chromatography (silica gel, hexanes:EtOAc = 1:0 → 7:3).

$R_f$ =0.44 (silica gel, hexanes:EtOAc = 1:1);  $^1\text{H NMR}$  (500 MHz,  $\text{CDCl}_3$ ):  $\delta$  7.57 and 7.52 (s, 1H), 7.53 (d,  $J$  = 7.5 Hz, 2H), 7.48 (d,  $J$  = 7.5 Hz, 1H), 7.42 (t,  $J$  = 7.5 Hz, 2H), 7.31 (t,  $J$  = 7.4 Hz, 1H), 6.87 and 6.84 (s, 1H), 6.76 (d,  $J$  = 8.1 Hz, 1H), 5.76 and 5.74 (s, 1H), 3.94 and 3.83 (t,  $J$  = 9.6 Hz, 1H), 3.80 and 3.72 (s, 3H), 3.20 (tt,  $J$  = 11.0, 5.6 Hz, 1H), 3.00 (dq,  $J$  =

21.9, 10.9 Hz, 1H), 2.57 and 2.49 (dd,  $J = 12.5, 6.5$  Hz, 1H);  $^{13}\text{C NMR}$  (126 MHz,  $\text{CDCl}_3$ ):  $\delta$  161.2, 155.6, 154.7, 149.3, 149.2, 140.9, 140.8, 133.7, 133.5, 130.3, 130.2, 129.0, 127.9, 127.7, 126.9, 126.7, 122.5, 122.2, 110.9, 110.7, 92.3, 78.7, 72.1, 71.0, 53.0, 52.7, 45.5, 45.4, 33.0; **HRMS** calcd. for  $\text{C}_{20}\text{H}_{19}\text{Cl}_3\text{N}_3\text{O}_3^+$   $[\text{M} + \text{H}]^+$  454.0487, found 454.0487.

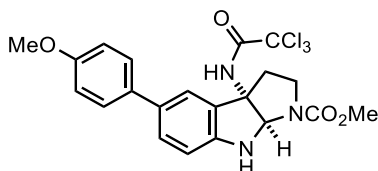
**Methyl 5-(naphthalen-2-yl)-3a-(2,2,2-trichloroacetamido)-3,3a,8,8a-tetrahydropyrrolo[2,3-b]indole-1(2H)-carboxylate (3d)**



Following the **general procedure J**, N-hydroxyindole **1d** (47.2 mg, 0.131 mmol) afforded pyrroloindoline **3d** (29.7 mg, 45%) as a pale yellow oil after purification by flash column chromatography (silica gel, hexanes:EtOAc = 1:0  $\rightarrow$  7:3).

$R_f$ =0.41 (silica gel, hexanes:EtOAc = 1:1);  $^1\text{H NMR}$  (500 MHz, MeOD):  $\delta$  7.98 (s, 1H), 7.87 (d,  $J = 8.2$  Hz, 2H), 7.82 (d,  $J = 8.0$  Hz, 1H), 7.76 – 7.70 (m, 2H), 7.58 (d,  $J = 8.3$  Hz, 1H), 7.44 (dt,  $J = 19.7, 7.1$  Hz, 2H), 6.78 (d,  $J = 8.2$  Hz, 1H), 5.84 and 5.83 (s, 1H), 3.83 (t,  $J = 10.3$  Hz, 1H), 3.80 and 3.74 (s, 3H), 3.22 (td,  $J = 10.9, 10.4, 6.9$  Hz, 1H), 2.80 – 2.60 (m, 2H);  $^{13}\text{C NMR}$  (126 MHz, MeOD):  $\delta$  163.5, 157.2, 156.9, 151.4, 140.0, 135.4, 133.7, 133.5, 133.4, 130.4, 130.0, 129.9, 129.3, 129.0, 128.6, 127.2, 126.5, 126.2, 125.3, 123.7, 123.6, 111.3, 111.1, 93.9, 81.2, 80.7, 73.8, 72.8, 53.4, 53.2, 46.1, 46.0, 37.0, 36.6; **HRMS** calcd. for  $\text{C}_{24}\text{H}_{21}\text{Cl}_3\text{N}_3\text{O}_3^+$   $[\text{M} + \text{H}]^+$  504.0643, found 504.0648.

**Methyl 5-(4-methoxyphenyl)-3a-(2,2,2-trichloroacetamido)-3,3a,8,8a-tetrahydropyrrolo[2,3-b]indole-1(2H)-carboxylate (3e)**

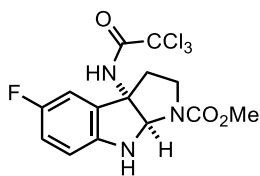




Following the **general procedure I**, N-hydroxyindole **1e** (40.0 mg, 0.118 mmol) afforded pyrroloindoline **3e** (37.6 mg, 68%) as a pale yellow oil after purification by flash column chromatography (silica gel, hexanes:EtOAc = 1:0 → 7:3).

$R_f$ =0.24 (silica gel, hexanes:EtOAc = 7:3);  $^1\text{H NMR}$  (400 MHz,  $\text{CDCl}_3$ ):  $\delta$  7.52 (s, 1H), 7.48 – 7.40 (m, 4H), 6.96 (d,  $J$  = 8.2 Hz, 2H), 6.87 and 6.84 (s, 1H), 6.74 (d,  $J$  = 8.2 Hz, 1H), 5.75 and 5.73 (s, 1H), 3.92 and 3.86 (t,  $J$  = 8.8 Hz, 1H), 3.84 (s, 3H), 3.79 and 3.72 (s, 3H), 3.20 (td,  $J$  = 10.2, 5.5 Hz, 1H), 3.00 (tt,  $J$  = 19.2, 9.8 Hz, 1H), 2.56 and 2.48 (dd,  $J$  = 12.4, 6.4 Hz, 1H);  $^{13}\text{C NMR}$  (101 MHz,  $\text{CDCl}_3$ ):  $\delta$  161.1, 158.9, 155.6, 154.7, 148.9, 148.7, 133.5, 133.5, 133.4, 133.2, 129.8, 129.8, 128.4, 127.8, 127.7, 122.0, 121.8, 114.4, 110.9, 110.7, 92.3, 78.6, 72.1, 71.0, 55.5, 53.0, 52.7, 45.5, 45.4, 33.0; **HRMS** calcd. for  $\text{C}_{21}\text{H}_{21}\text{Cl}_3\text{N}_3\text{O}_4^+$  [ $\text{M} + \text{H}$ ] $^+$  484.0592, found 484.0595.

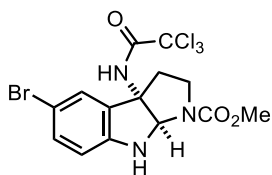
**Methyl 5-fluoro-3a-(2,2,2-trichloroacetamido)-3,3a,8,8a-tetrahydropyrrolo[2,3-b]indole-1(2H)-carboxylate (3f)**



Following the **general procedure J**, N-hydroxyindole **1f** (68.4 mg, 0.271 mmol) afforded pyrroloindoline **3f** (55.9 mg, 52%) as a pale yellow oil after purification by flash column chromatography (silica gel, hexanes:EtOAc = 1:0 → 6:4).

$R_f$ =0.30 (silica gel, hexanes:EtOAc = 1:1);  $^1\text{H NMR}$  (500 MHz,  $\text{CDCl}_3$ ):  $\delta$  7.09 and 7.04 (dd,  $J$  = 7.9, 2.6 Hz, 1H), 6.94 – 6.85 (m, 2H), 6.62 (dd,  $J$  = 8.9, 4.2 Hz, 1H), 5.69 and 5.66 (s, 1H), 3.89 and 3.79 (t,  $J$  = 9.7 Hz, 1H), 3.77 and 3.70 (s, 3H), 3.16 (td,  $J$  = 10.7, 6.4 Hz, 1H), 2.93 – 2.80 (m, 1H), 2.55 and 2.45 (dd,  $J$  = 12.7, 6.5 Hz, 1H);  $^{13}\text{C NMR}$  (126 MHz,  $\text{CDCl}_3$ ):  $\delta$  161.2, 160.2, 157.4 (d,  $J$  = 238.1 Hz), 157.3 (d,  $J$  = 238.1 Hz), 157.2, 155.5, 154.7, 146.0, 145.9, 128.2 (d,  $J$  = 7.6 Hz), 128.1 (d,  $J$  = 7.5 Hz), 117.7 (d,  $J$  = 22.5 Hz), 117.6 (d,  $J$  = 22.5 Hz), 111.3, 111.2 (d,  $J$  = 24.2 Hz), 110.8 (d,  $J$  = 24.2 Hz), 92.2, 79.6, 78.6, 72.1, 71.0, 53.0, 52.7, 45.4, 45.3, 33.6, 33.5;  $^{19}\text{F NMR}$  (376 MHz,  $\text{CDCl}_3$ ):  $\delta$  -123.6 (q,  $J$  = 8.1 Hz), -123.9 (td,  $J$  = 8.5, 4.1 Hz); **HRMS** calcd. for  $\text{C}_{14}\text{H}_{14}\text{Cl}_3\text{FN}_3\text{O}_3^+$  [ $\text{M} + \text{H}$ ] $^+$  396.0079, found 396.0081.

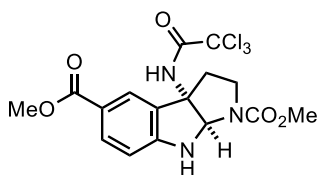
**Methyl 5-bromo-3a-(2,2,2-trichloroacetamido)-3,3a,8,8a-tetrahydropyrrolo[2,3-b]indole-1(2H)-carboxylate (3g)**



Following the **general procedure J**, N-hydroxyindole **1g** (63.1 mg, 0.201 mmol) afforded pyrroloindoline **3g** (58.0 mg, 63%) as a pale yellow oil after purification by flash column chromatography (silica gel, hexanes:EtOAc = 1:0 → 6:4).

$R_f=0.35$  (silica gel, hexanes:EtOAc = 1:1);  $^1\text{H NMR}$  (500 MHz,  $\text{CDCl}_3$ ):  $\delta$  7.45 and 7.40 (s, 1H), 7.31 (d,  $J = 6.2$  Hz, 1H), 6.82 and 6.80 (s, 1H), 6.57 (d,  $J = 8.3$  Hz, 1H), 5.70 and 5.67 (s, 1H), 5.29 and 4.88 (s, 1H), 3.90 and 3.80 (t,  $J = 9.6$  Hz, 1H), 3.78 and 3.71 (s, 3H), 3.16 (td,  $J = 10.8, 6.5$  Hz, 1H), 2.91 (ddd,  $J = 24.2, 13.1, 9.3$  Hz, 1H), 2.50 and 2.42 (dd,  $J = 13.0, 6.4$  Hz, 1H);  $^{13}\text{C NMR}$  (101 MHz,  $\text{CDCl}_3$ ):  $\delta$  161.2, 155.6, 154.6, 149.0, 134.0, 129.2, 129.0, 126.9, 126.7, 112.1, 111.9, 111.1, 92.2, 78.9, 78.0, 71.9, 70.7, 53.1, 52.8, 45.4, 45.3, 33.5, 33.4; **HRMS** calcd. for  $\text{C}_{14}\text{H}_{14}\text{BrCl}_3\text{N}_3\text{O}_3^+$   $[\text{M} + \text{H}]^+$  455.9279, found 455.9282.

**Dimethyl 3a-(2,2,2-trichloroacetamido)-3,3a,8,8a-tetrahydropyrrolo[2,3-b]indole-1,5(2H)-dicarboxylate (3h)**

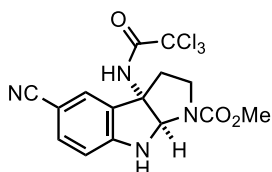


Following the **general procedure J**, N-hydroxyindole **1h** (32.9 mg, 0.113 mmol) afforded pyrroloindoline **3h** (25.1 mg, 51%) as a pale yellow oil after purification by flash column chromatography (silica gel, hexanes:EtOAc = 1:0 → 6:4).

$R_f=0.30$  (silica gel, hexanes:EtOAc = 1:1);  $^1\text{H NMR}$  (500 MHz,  $\text{CDCl}_3$ ):  $\delta$  8.00 and 7.98 (s, 1H), 7.95 (d,  $J = 8.4$  Hz, 1H), 6.76 (s, 1H), 6.65 (d,  $J = 8.4$  Hz, 1H), 5.80 and 5.79 (s, 1H), 3.92 and 3.81 (t,  $J = 9.8$  Hz, 1H), 3.88 (s, 3H) 3.79 and 3.72 (s, 3H), 3.15 (td,  $J = 10.6, 7.0$  Hz, 1H), 30.4 – 2.90 (m, 1H), 2.48 and 2.43 (dd,  $J = 12.8, 6.9$  Hz, 1H);  $^{13}\text{C NMR}$  (126 MHz,

CDCl<sub>3</sub>):  $\delta$  166.8, 161.1, 155.6, 154.5, 153.8, 153.6, 134.0, 126.9, 126.7, 125.8, 125.6, 121.6, 121.3, 109.2, 109.0, 92.2, 78.3, 71.5, 70.4, 53.1, 52.8, 52.1, 45.3, 45.2, 33.4, 33.4; **HRMS** calcd. for C<sub>16</sub>H<sub>17</sub>Cl<sub>3</sub>N<sub>3</sub>O<sub>5</sub><sup>+</sup> [M + H]<sup>+</sup> 436.0228, found 436.0227.

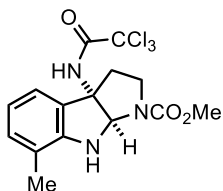
**Methyl 5-cyano-3a-(2,2,2-trichloroacetamido)-3,3a,8,8a-tetrahydropyrrolo[2,3-b]indole-1(2H)-carboxylate (3i)**



Following the **general procedure J**, N-hydroxyindole **1i** (30.1 mg, 0.116 mmol) afforded pyrroloindoline **3i** (25.8 mg, 55%) as a pale yellow oil after purification by flash column chromatography (silica gel, hexanes:EtOAc = 1:0 → 1:1).

**R<sub>f</sub>**=0.22 (silica gel, hexanes:EtOAc = 1:1); **<sup>1</sup>H NMR** (500 MHz, CDCl<sub>3</sub>):  $\delta$  7.61 and 7.55 (s, 1H), 7.49 (d, *J* = 8.3 Hz, 1H), 6.92 (s, 1H), 6.67 (d, *J* = 8.3 Hz, 1H), 5.78 and 5.75 (s, 1H), 3.93 and 3.83 (t, *J* = 9.8 Hz, 1H), 3.79 and 3.73 (s, 3H), 3.19 (td, *J* = 10.6, 6.5 Hz, 1H), 2.89 – 2.75 (m, 1H), 2.56 and 2.47 (dd, *J* = 12.9, 6.4 Hz, 1H); **<sup>13</sup>C NMR** (126 MHz, CDCl<sub>3</sub>):  $\delta$  161.3, 155.6, 154.4, 153.1, 153.0, 136.0, 128.1, 127.9, 127.8, 119.6, 109.9, 109.7, 102.0, 101.7, 92.1, 79.2, 78.4, 71.5, 70.3, 53.2, 52.9, 45.1, 34.9, 34.7; **HRMS** calcd. for C<sub>15</sub>H<sub>14</sub>Cl<sub>3</sub>N<sub>4</sub>O<sub>3</sub><sup>+</sup> [M + H]<sup>+</sup> 403.0126, found 403.0125.

**Methyl 7-methyl-3a-(2,2,2-trichloroacetamido)-3,3a,8,8a-tetrahydropyrrolo[2,3-b]indole-1(2H)-carboxylate (3j)**

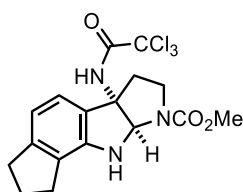


Following the **general procedure I**, N-hydroxyindole **1j** (57.0 mg, 0.230 mmol) afforded pyrroloindoline **3j** (42.3 mg, 47%) as a pale yellow oil after purification by flash column chromatography (silica gel, hexanes:EtOAc = 1:0 → 7:3).

**R<sub>f</sub>**=0.44 (silica gel, hexanes:EtOAc = 1:1); **<sup>1</sup>H NMR** (400 MHz, CDCl<sub>3</sub>):  $\delta$  7.18 and 7.14 (d,

$J = 7.6$  Hz, 1H), 7.05 (d,  $J = 7.4$  Hz, 1H), 6.81 – 6.76 (m, 2H), 5.75 and 5.73 (s, 1H), 5.09 and 4.64 (s, 1H), 3.89 and 3.79 (t,  $J = 9.6$  Hz, 1H), 3.79 and 3.71 (s, 3H), 3.13 (qd,  $J = 10.7$ , 6.3 Hz, 1H), 3.03 – 2.91 (m, 1H), 2.46 and 2.38 (dd,  $J = 12.2$ , 6.1 Hz, 1H), 2.16 and 2.15 (s, 3H);  $^{13}\text{C}$  NMR (101 MHz,  $\text{CDCl}_3$ ):  $\delta$  161.0, 155.6, 154.8, 148.6, 148.5, 132.0, 131.9, 126.4, 126.1, 121.0, 120.8, 120.3, 120.1, 120.0, 119.9, 92.3, 78.1, 72.5, 71.4, 53.0, 52.6, 45.5, 45.3, 33.0, 32.9, 16.8; HRMS calcd. for  $\text{C}_{15}\text{H}_{17}\text{Cl}_3\text{N}_3\text{O}_3^+$   $[\text{M} + \text{H}]^+$  392.0330, found 392.0330.

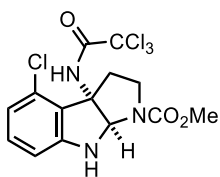
**Methyl 5b-(2,2,2-trichloroacetamido)-1,2,3,5b,6,7,8a,9-octahydro-8H-cyclopenta[g]pyrrolo[2,3-b]indole-8-carboxylate (3k)**



Following the **general procedure I**, N-hydroxyindole **1k** (41.0 mg, 0.149 mmol) afforded pyrroloindoline **3k** (34.4 mg, 55%) as a pale yellow oil after purification by flash column chromatography (silica gel, hexanes:EtOAc = 1:0  $\rightarrow$  7:3).

$R_f = 0.48$  (silica gel, hexanes:EtOAc = 1:1);  $^1\text{H}$  NMR (500 MHz,  $\text{CDCl}_3$ ):  $\delta$  7.12 and 7.09 (d,  $J = 7.6$  Hz, 1H), 6.77 – 6.74 (m, 2H), 5.75 and 5.74 (s, 1H), 5.06 and 4.60 (s, 1H), 3.89 and 3.79 (t,  $J = 9.6$  Hz, 1H), 3.79 and 3.71 (s, 3H), 3.19 – 3.09 (m, 1H), 3.00 (dtd,  $J = 20.0$ , 11.6, 8.6 Hz, 1H), 2.88 (m, 2H), 2.72 (m, 2H), 2.43 and 2.36 (dd,  $J = 12.1$ , 6.6 Hz, 1H), 2.11 (h,  $J = 7.4$  Hz, 2H);  $^{13}\text{C}$  NMR (126 MHz,  $\text{CDCl}_3$ ):  $\delta$  161.0, 160.9, 155.6, 154.8, 148.5, 146.1, 145.9, 125.8, 125.6, 124.7, 124.5, 121.4, 121.2, 116.2, 115.9, 92.4, 78.6, 72.3, 71.2, 53.0, 52.6, 45.5, 45.4, 33.1, 32.9, 32.8, 29.5, 25.5, 25.4; HRMS calcd. for  $\text{C}_{17}\text{H}_{19}\text{Cl}_3\text{N}_3\text{O}_3^+$   $[\text{M} + \text{H}]^+$  418.0487, found 418.0494.

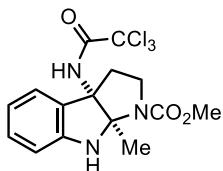
**Methyl 4-chloro-3a-(2,2,2-trichloroacetamido)-3,3a,8,8a-tetrahydropyrrolo[2,3-b]indole-1(2H)-carboxylate (3l)**



Following the **general procedure J**, N-hydroxyindole **11** (31.7 mg, 0.118 mmol) afforded pyrroloindoline **31** (27.8 mg, 57%) as a pale yellow oil after purification by flash column chromatography (silica gel, hexanes:EtOAc = 1:0 → 6:4).

$R_f$ =0.41 (silica gel, hexanes:EtOAc = 1:1); **<sup>1</sup>H NMR** (500 MHz, CDCl<sub>3</sub>): δ 7.12 (t,  $J$  = 8.0 Hz, 1H), 1.12 and 7.07 (s, 1H), 6.74 (dd,  $J$  = 7.9, 3.6 Hz, 1H), 6.55 (d,  $J$  = 8.0 Hz, 1H), 5.87 and 5.86 (s, 1H), 5.35 and 4.99 (s, 1H), 3.95 – 3.91 and 3.86 – 3.82 (m, 1H), 3.78 and 3.73 (s, 3H), 3.24 (q,  $J$  = 8.4 Hz, 1H), 2.80 (dd,  $J$  = 8.6, 5.9 Hz, 1H), 2.84 – 2.78 and 2.71 – 2.65 (m, 1H); **<sup>13</sup>C NMR** (126 MHz, CDCl<sub>3</sub>): δ 161.0, 160.8, 155.7, 154.7, 151.9, 151.8, 132.3, 130.3, 130.2, 122.9, 122.6, 120.2, 119.9, 108.7, 108.5, 92.4, 78.5, 77.9, 73.0, 71.8, 53.0, 52.8, 44.8, 33.8, 31.1; **HRMS** calcd. for C<sub>14</sub>H<sub>14</sub>Cl<sub>4</sub>N<sub>3</sub>O<sub>3</sub><sup>+</sup> [M + H]<sup>+</sup> 411.9784, found 411.9789.

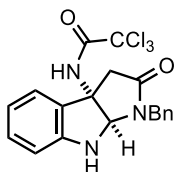
**Methyl 8a-methyl-3a-(2,2,2-trichloroacetamido)-3,3a,8,8a-tetrahydropyrrolo[2,3-b]indole-1(2H)-carboxylate (3m)**



Following the **general procedure I**, N-hydroxyindole **1m** (27.0 mg, 0.109 mmol) afforded pyrroloindoline **3m** (22.4 mg, 52%) as a pale yellow oil after purification by flash column chromatography (silica gel, hexanes:EtOAc = 1:0 → 7:3).

$R_f$ =0.63 (silica gel, hexanes:EtOAc = 1:1); **<sup>1</sup>H NMR** (500 MHz, CDCl<sub>3</sub>): δ 7.44 (d,  $J$  = 7.5 Hz, 1H), 7.18 (t,  $J$  = 7.7 Hz, 1H), 6.84 – 6.81 (m, 2H), 6.68 (d,  $J$  = 7.9 Hz, 1H), 5.87 (s, 1H), 3.64 (s, 3H), 3.09 – 3.03 (m, 1H), 2.95 (dd,  $J$  = 12.9, 6.6 Hz, 1H), 2.85 – 2.78 (m, 1H), 1.75 (s, 3H); **<sup>13</sup>C NMR** (126 MHz, CDCl<sub>3</sub>): δ 161.2, 154.8, 148.9, 130.7, 128.2, 124.6, 120.2, 110.8, 87.1, 71.5, 52.3, 45.5, 30.3, 19.5; **HRMS** calcd. for C<sub>15</sub>H<sub>17</sub>Cl<sub>3</sub>N<sub>3</sub>O<sub>3</sub><sup>+</sup> [M + H]<sup>+</sup> 392.0330, found 392.0333.

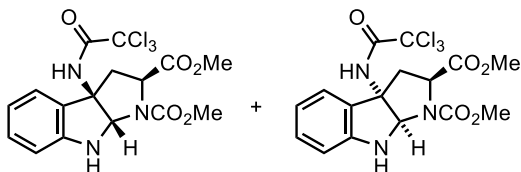
**N-(1-Benzyl-2-oxo-2,3,8,8a-tetrahydropyrrolo[2,3-b]indol-3a(1H)-yl)-2,2,2-trichloroacetamide (3n)**



Following the **general procedure I**, N-hydroxyindole **1n** (95.1 mg, 0.339 mmol) afforded pyrroloindoline **3n** (87.8 mg, 61%) as a pale yellow oil after purification by flash column chromatography (silica gel, hexanes:EtOAc = 1:0 → 7:3).

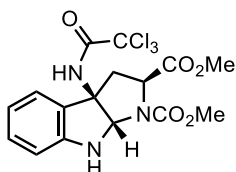
$R_f$ =0.50 (silica gel, hexanes:EtOAc = 6:4);  $^1\text{H NMR}$  (400 MHz,  $\text{CDCl}_3$ ):  $\delta$  7.39 – 7.27 (m, 6H), 6.96 (t,  $J$  = 7.5 Hz, 1H), 6.76 (s, 1H), 6.71 (d,  $J$  = 8.0 Hz, 1H), 5.43 and 5.42 (s, 1H), 4.95 (d,  $J$  = 15.4 Hz, 1H), 4.38 (d,  $J$  = 3.7 Hz, 1H), 4.31 (d,  $J$  = 15.4 Hz, 1H), 3.51 (d,  $J$  = 16.9 Hz, 1H), 3.03 (d,  $J$  = 16.8 Hz, 1H);  $^{13}\text{C NMR}$  (101 MHz,  $\text{CDCl}_3$ ):  $\delta$  170.6, 161.1, 148.4, 135.7, 131.6, 129.7, 129.1, 128.0, 127.8, 123.9, 121.7, 112.7, 92.0, 78.7, 65.3, 43.8, 40.1; **HRMS** calcd. for  $\text{C}_{19}\text{H}_{17}\text{Cl}_3\text{N}_3\text{O}_2^+$  [ $\text{M} + \text{H}$ ] $^+$  424.0381, found 424.0383.

**Dimethyl (2S)-3a-(2,2,2-trichloroacetamido)-3,3a,8,8a-tetrahydropyrrolo[2,3-b]indole-1,2(2H)-dicarboxylate (3o)**



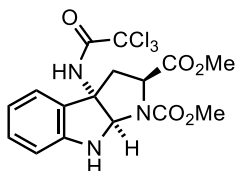
Following the **general procedure I**, N-hydroxyindole **1o** (108 mg, 0.369 mmol) afforded pyrroloindoline **3o** (77.4 mg, 48%, *syn-cis*: *anti-cis* = 1.3:1) as a pale yellow oil after purification by flash column chromatography (silica gel,  $\text{CH}_2\text{Cl}_2$ :acetone 1:0 → 97:3). Each diastereomers were isolated by preparative thin layer chromatography (silica gel,  $\text{CH}_2\text{Cl}_2$ :acetone 1:0 → 95:5) and characterized respectively.

**Dimethyl (2S,3aR,8aS)-3a-(2,2,2-trichloroacetamido)-3,3a,8,8a-tetrahydropyrrolo[2,3-b]indole-1,2(2H)-dicarboxylate (3o-1)**



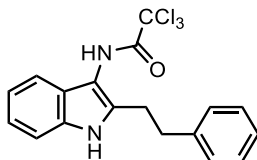
$R_f=0.72$  (silica gel,  $\text{CH}_2\text{Cl}_2$ :acetone 95:5);  $^1\text{H NMR}$  (500 MHz,  $\text{CDCl}_3$ ):  $\delta$  7.39 and 7.30 (d,  $J=7.5$  Hz, 1H), 7.21 (q,  $J=7.5$  Hz, 1H), 7.05 and 6.93 (s, 1H), 6.84 (t,  $J=7.4$  Hz, 1H), 6.69 (t,  $J=8.2$  Hz, 1H), 5.86 and 5.79 (s, 1H), 5.45 and 5.00 (s, 1H), 4.37 and 4.30 (dd,  $J=8.2$ , 5.8 Hz, 1H), 3.81 and 3.68 (s, 3H), 3.78 (s, 3H), 3.03 and 2.77 (dd,  $J=13.5$ , 6.2 Hz, 1H), 2.96–2.88 (m, 1H);  $^{13}\text{C NMR}$  (126 MHz,  $\text{CDCl}_3$ ):  $\delta$  172.2, 161.2, 155.3, 154.8, 148.7, 148.3, 131.0, 130.9, 127.6, 127.4, 124.0, 123.3, 120.3, 120.2, 110.9, 110.7, 92.2, 80.9, 80.5, 71.2, 69.8, 59.5, 59.1, 53.4, 53.0, 52.9, 52.9, 38.4, 37.8; **HRMS** calcd. for  $\text{C}_{16}\text{H}_{17}\text{Cl}_3\text{N}_3\text{O}_5^+$  [ $\text{M} + \text{H}$ ] $^+$  436.0228, found 436.0240.

**Dimethyl (2S,3aS,8aR)-3a-(2,2,2-trichloroacetamido)-3,3a,8,8a-tetrahydropyrrolo[2,3-b]indole-1,2(2H)-dicarboxylate (3o-2)**



$R_f=0.70$  (silica gel,  $\text{CH}_2\text{Cl}_2$ :acetone 95:5);  $^1\text{H NMR}$  (500 MHz,  $\text{CDCl}_3$ ):  $\delta$  7.25 – 7.19 (m, 2H), 6.80 (dt,  $J=14.9$ , 7.4 Hz, 1H), 6.74 – 6.65 (m, 1H), 5.77 (s, 1H), 4.75 and 4.63 (d,  $J=9.3$  Hz, 1H), 3.83 and 3.71 (s, 3H), 3.44 and 3.39 (dd,  $J=12.8$ , 9.4 Hz, 1H), 3.22 and 3.21 (s, 3H), 2.79 (t,  $J=12.1$  Hz, 1H);  $^{13}\text{C NMR}$  (126 MHz,  $\text{CDCl}_3$ ):  $\delta$  171.2, 171.1, 161.2, 161.2, 155.2, 154.6, 150.8, 150.5, 131.8, 131.7, 126.0, 125.9, 124.1, 124.1, 119.9, 119.6, 110.6, 92.2, 78.3, 70.9, 69.7, 59.2, 59.0, 53.3, 53.0, 52.4, 36.2, 35.7; **HRMS** calcd. for  $\text{C}_{16}\text{H}_{17}\text{Cl}_3\text{N}_3\text{O}_5^+$  [ $\text{M} + \text{H}$ ] $^+$  436.0228, found 436.0240.

**2,2,2-Trichloro-N-(2-phenethyl-1H-indol-3-yl)acetamide (3p)**

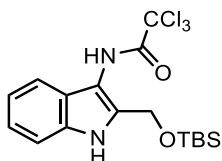


Following the **general procedure J**, N-hydroxyindole **1p** (38.0 mg, 0.160 mmol) afforded indole **3p** (32.4 mg, 53%) as a pale yellow oil after purification by flash column chromatography (silica gel, hexanes:EtOAc = 1:0  $\rightarrow$  9:1).

$R_f=0.27$  (silica gel, hexanes:EtOAc = 9:1);  $^1\text{H NMR}$  (500 MHz,  $\text{CDCl}_3$ ):  $\delta$  7.78 (br s, 1H), 7.54 (s, 1H), 7.39 (d,  $J = 7.8$  Hz, 1H), 7.29 – 7.22 (m, 3H), 7.17 (t,  $J = 7.5$  Hz, 1H), 7.14 – 7.11 (m, 3H), 3.01 (dq,  $J = 11.2, 6.0$  Hz, 4H);  $^{13}\text{C NMR}$  (126 MHz,  $\text{CDCl}_3$ ):  $\delta$  161.5, 140.8, 134.1, 133.9, 128.9, 128.7, 126.8, 124.3, 122.5, 120.6, 117.4, 111.1, 108.7, 92.9, 35.3, 28.2; **HRMS** calcd. for  $\text{C}_{18}\text{H}_{16}\text{Cl}_3\text{N}_2\text{O}^+$   $[\text{M} + \text{H}]^+$  381.0323, found 381.0323.

### N-(2-(((tert-Butyldimethylsilyloxy)methyl)-1H-indol-3-yl)-2,2,2-trichloroacetamide

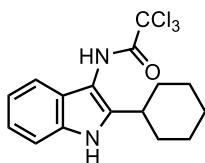
(3q)



Following the **general procedure J**, N-hydroxyindole **1q** (89.8 mg, 0.324 mmol) afforded indole **3q** (62.8 mg, 46%) as a pale yellow oil after purification by flash column chromatography (silica gel, hexanes:EtOAc = 1:0  $\rightarrow$  9:1).

$R_f=0.25$  (silica gel, hexanes:EtOAc = 9:1);  $^1\text{H NMR}$  (500 MHz, MeOD):  $\delta$  7.39 (t,  $J = 8.3$  Hz, 2H), 7.13 (t,  $J = 7.6$  Hz, 1H), 7.05 (t,  $J = 7.5$  Hz, 1H), 4.81 (s, 2H), 0.93 (s, 9H), 0.10 (s, 6H);  $^{13}\text{C NMR}$  (126 MHz, MeOD):  $\delta$  164.0, 136.1, 134.0, 125.1, 123.0, 120.5, 118.6, 112.5, 109.3, 79.3, 57.9, 26.4, -5.2; **HRMS** calcd. for  $\text{C}_{17}\text{H}_{24}\text{Cl}_3\text{N}_2\text{O}_2\text{Si}^+$   $[\text{M} + \text{H}]^+$  421.0667, found 421.0682.

### 2,2,2-Trichloro-N-(2-cyclohexyl-1H-indol-3-yl)acetamide (3r)



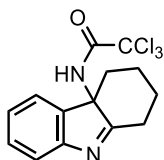
Following the **general procedure J**, N-hydroxyindole **1r** (26.2 mg, 0.122 mmol) afforded indole **3r** (19.3 mg, 44%) as a pale yellow oil after purification by flash column chromatography (silica gel, hexanes:EtOAc = 1:0  $\rightarrow$  9:1).

$R_f=0.26$  (silica gel, hexanes:EtOAc = 9:1);  $^1\text{H NMR}$  (500 MHz,  $\text{CDCl}_3$ ):  $\delta$  7.94 (s, 1H), 7.92 (s, 1H), 7.42 (d,  $J = 7.7$  Hz, 1H), 7.31 (d,  $J = 7.9$  Hz, 1H), 7.19 – 7.12 (m, 2H), 2.82 (tt,  $J = 11.9, 3.5$  Hz, 1H), 2.04 (d,  $J = 12.4$  Hz, 2H), 1.88 (dt,  $J = 12.8, 3.2$  Hz, 2H), 1.79 (d,  $J = 13.2$



Hz, 1H), 1.51 – 1.38 (m, 4H), 1.33 – 1.24 (m, 1H);  $^{13}\text{C}$  NMR (126 MHz,  $\text{CDCl}_3$ ):  $\delta$  161.6, 139.7, 133.6, 133.5, 124.7, 123.5, 122.3, 120.9, 120.6, 118.1, 117.1, 111.5, 111.2, 106.6, 56.9, 35.9, 32.4, 32.2, 26.6, 26.1, 25.6, 16.4; HRMS calcd. for  $\text{C}_{16}\text{H}_{18}\text{Cl}_3\text{N}_2\text{O}^+$   $[\text{M} + \text{H}]^+$  359.0479, found 359.0480.

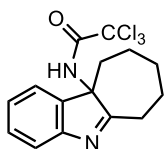
### 2,2,2-Trichloro-N-(1,2,3,4-tetrahydro-4aH-carbazol-4a-yl)acetamide (3s)



Following the **general procedure I**, N-hydroxyindole **1s** (126 mg, 0.673 mmol) afforded indolenine **3s** (129 mg, 58%) as a pale yellow oil after purification by flash column chromatography (silica gel, hexanes:EtOAc = 1:0  $\rightarrow$  1:1).

$R_f$ =0.29 (silica gel, hexanes:EtOAc = 1:1);  $^1\text{H}$  NMR (400 MHz,  $\text{CDCl}_3$ ):  $\delta$  7.60 (d,  $J$  = 7.7 Hz, 1H), 7.41 – 7.36 (m, 2H), 7.22 (t,  $J$  = 7.4 Hz, 1H), 6.97 (s, 1H), 2.97 (d,  $J$  = 12.9 Hz, 1H), 2.70 (dd,  $J$  = 14.5, 2.8 Hz, 1H), 2.50 (td,  $J$  = 13.1, 5.7 Hz, 1H), 2.25 – 2.20 (m, 1H), 1.80 – 1.70 (m, 3H), 1.58 – 1.47 (m, 3H), 1.35 – 1.25 (m, 1H);  $^{13}\text{C}$  NMR (101 MHz,  $\text{CDCl}_3$ ):  $\delta$  182.7, 160.1, 154.3, 139.1, 129.6, 126.0, 121.4, 121.0, 92.0, 67.9, 39.0, 29.5, 28.7, 21.1; HRMS calcd. for  $\text{C}_{14}\text{H}_{14}\text{Cl}_3\text{N}_2\text{O}^+$   $[\text{M} + \text{H}]^+$  331.0166, found 331.0167.

### 2,2,2-Trichloro-N-(7,8,9,10-tetrahydrocyclohepta[b]indol-10a(6H)-yl)acetamide (3t)



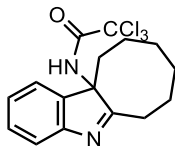
Following the **general procedure I**, N-hydroxyindole **1t** (105 mg, 0.523 mmol) afforded indolenine **3t** (136 mg, 75%) as a pale yellow oil after purification by flash column chromatography (silica gel, hexanes:EtOAc = 1:0  $\rightarrow$  1:1).

$R_f$ =0.25 (silica gel, hexanes:EtOAc = 1:1);  $^1\text{H}$  NMR (400 MHz,  $\text{CDCl}_3$ ):  $\delta$  7.48 (d,  $J$  = 7.7 Hz, 1H), 7.34 (t,  $J$  = 7.5 Hz, 1H), 7.25 – 7.17 (m, 2H), 7.11 (s, 1H), 3.09 – 3.01 (m, 1H), 2.85 (dt,  $J$  = 17.2, 5.2 Hz, 1H), 2.37 (dt,  $J$  = 14.9, 3.8 Hz, 1H), 1.97 – 1.40 (m, 7H);  $^{13}\text{C}$  NMR (101 MHz,  $\text{CDCl}_3$ ):  $\delta$  184.6, 159.7, 153.4, 139.9, 129.5, 126.2, 120.6, 120.5, 92.1, 71.8, 37.2,

32.5, 28.4, 26.0, 24.8; **HRMS** calcd. for  $C_{15}H_{16}Cl_3N_2O^+$   $[M + H]^+$  345.0323, found 345.0324.

### 2,2,2-Trichloro-N-(6,7,8,9,10,11-hexahydro-11aH-cycloocta[b]indol-11a-yl)acetamide

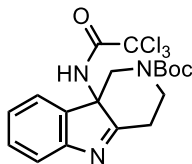
(**3u**)



Following the **general procedure I**, *N*-hydroxyindole **1u** (99.4 mg, 0.462 mmol) afforded indolenine **3u** (108 mg, 65%) as a pale yellow oil after purification by flash column chromatography (silica gel, hexanes:EtOAc = 1:0 → 1:1).

$R_f$ =0.38 (silica gel, hexanes:EtOAc = 1:1);  **$^1H$  NMR** (400 MHz,  $CDCl_3$ ):  $\delta$  7.54 (d,  $J$  = 7.7 Hz, 1H), 7.37 (t,  $J$  = 7.3 Hz, 1H), 7.26 – 7.19 (m, 2H), 6.94 (s, 1H), 2.87 – 2.80 (m, 2H), 2.65 (ddd,  $J$  = 13.9, 8.3, 5.5 Hz, 1H), 2.43 – 2.37 (m, 1H), 2.19 – 2.14 (m, 1H), 2.08 – 1.92 (m, 2H), 1.63 – 1.42 (m, 5H), 1.02 – 0.93 (m, 1H);  **$^{13}C$  NMR** (101 MHz,  $CDCl_3$ ):  $\delta$  184.8, 159.6, 154.2, 138.1, 129.7, 126.3, 121.1, 120.6, 92.0, 70.9, 34.3, 29.7, 27.4, 27.2, 24.7, 20.9; **HRMS** calcd. for  $C_{16}H_{18}Cl_3N_2O^+$   $[M + H]^+$  359.0479, found 359.0477.

### *tert*-Butyl 9b-(2,2,2-trichloroacetamido)-1,3,4,9b-tetrahydro-2H-pyrido[4,3-b]indole-2-carboxylate (**3v**)

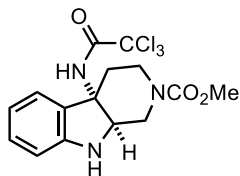


Following the **general procedure I**, *N*-hydroxyindole **1v** (55.3 mg, 0.203 mmol) afforded indolenine **3v** (46.6 mg, 53%) as a pale yellow oil after purification by flash column chromatography (silica gel, hexanes:EtOAc = 1:0 → 6:4).

$R_f$ =0.36 (silica gel, hexanes:EtOAc = 1:1);  **$^1H$  NMR** (500 MHz,  $CDCl_3$ ):  $\delta$  8.38 (br s, 1H), 7.64 (d,  $J$  = 7.7 Hz, 1H), 7.43 (t,  $J$  = 7.6 Hz, 1H), 7.38 (d,  $J$  = 7.3 Hz, 1H), 7.26 (t,  $J$  = 7.4 Hz, 1H), 5.00 (dd,  $J$  = 14.2, 2.5 Hz, 1H), 4.51 (dd,  $J$  = 12.5, 5.4 Hz, 1H), 2.94 (dd,  $J$  = 13.3, 2.3 Hz, 2H), 2.87 (td,  $J$  = 12.7, 3.2 Hz, 1H), 2.69 (td,  $J$  = 12.4, 6.3 Hz, 1H), 2.22 (d,  $J$  = 14.2 Hz, 1H), 1.54 (s, 9H);  **$^{13}C$  NMR** (126 MHz,  $CDCl_3$ ):  $\delta$  179.0, 160.8, 157.0, 154.7, 135.1, 130.2,

126.4, 121.7, 121.5, 91.5, 82.3, 70.6, 53.9, 46.9, 30.9, 28.6; **HRMS** calcd. for  $C_{18}H_{21}Cl_3N_3O_3^+ [M + H]^+$  432.0643, found 432.0641.

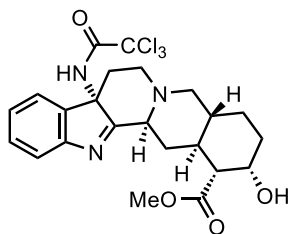
**Methyl 4a-(2,2,2-trichloroacetamido)-1,3,4,4a,9,9a-hexahydro-2H-pyrido[3,4-b]indole-2-carboxylate (3w)**



Following the **general procedure I**, N-hydroxyindole **1w** (50.6 mg, 0.205 mmol) afforded corresponding pyrroloindoline, which was then subsequently reduced due to its lability to afford indoline **3w** (32.2 mg, 40% for 2 steps) as a pale yellow oil after purification by flash column chromatography (silica gel, hexanes:EtOAc = 1:0 → 7:3).

$R_f=0.25$  (silica gel, hexanes:EtOAc = 1:1);  $^1H$  NMR (400 MHz,  $CDCl_3$ ):  $\delta$  7.31 (d,  $J = 7.6$  Hz, 1H), 7.19 (t,  $J = 7.8$  Hz, 1H), 6.83 (t,  $J = 7.4$  Hz, 1H), 6.72 (d,  $J = 7.9$  Hz, 1H), 4.84 (s, 1H), 3.88 (d,  $J = 10.4$  Hz, 1H), 3.80 (d,  $J = 10.4$  Hz, 1H), 3.64 (s, 3H), 3.35 – 3.11 (m, 2H), 2.55 – 2.49 (m, 1H), 2.30 – 2.23 (m, 1H);  $^{13}C$  NMR (101 MHz,  $CDCl_3$ ):  $\delta$  161.1, 157.2, 150.7, 130.3, 129.0, 123.1, 119.6, 110.9, 92.7, 65.0, 58.1, 52.3, 37.1, 36.7, 31.1; **HRMS** calcd. for  $C_{15}H_{17}Cl_3N_3O_3^+ [M + H]^+$  392.0330, found 392.0325.

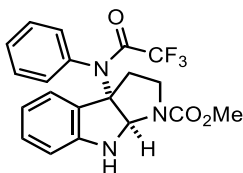
**Methyl (1R,2S,4aR,8aS,13bS,14aS)-2-hydroxy-8a-(2,2,2-trichloroacetamido)-1,2,3,4,4a,5,7,8,8a,13b,14,14a-dodecahydroindolo[2',3':3,4]pyrido[1,2-b]isoquinoline-1-carboxylate (3x)**



Following the **general procedure I**, N-hydroxyindole **1x** (40.0 mg, 0.108 mmol) afforded indolenine **3x** (24.5 mg, 44%) as a pale yellow oil after purification by flash column chromatography (silica gel,  $CH_2Cl_2$ :MeOH = 1:0 → 9:1).

$R_f=0.30$  (silica gel,  $\text{CH}_2\text{Cl}_2:\text{MeOH} = 9:1$ );  $^1\text{H NMR}$  (400 MHz,  $\text{CDCl}_3$ ):  $\delta$  7.67 (d,  $J = 7.6$  Hz, 1H), 7.43 – 7.37 (m, 2H), 7.23 (t,  $J = 7.4$  Hz, 1H), 6.89 (s, 1H), 4.19 (s, 1H), 3.77 (s, 3H), 3.15 (s, 1H), 2.94 (ddd,  $J = 20.8, 10.9, 3.0$  Hz, 2H), 2.83 (d,  $J = 12.0$  Hz, 1H), 2.68 (d,  $J = 14.5$  Hz, 1H), 2.60 (t,  $J = 12.9$  Hz, 1H), 2.38 (d,  $J = 11.1$  Hz, 1H), 2.18 (t,  $J = 10.8$  Hz, 1H), 2.12 – 2.07 (m, 1H), 1.96 (ddd,  $J = 13.6, 10.6, 2.7$  Hz, 2H), 1.93 – 1.81 (m, 2H), 1.64 – 1.35 (m, 5H);  $^{13}\text{C NMR}$  (101 MHz,  $\text{CDCl}_3$ ):  $\delta$  178.7, 176.0, 160.1, 154.3, 138.7, 129.9, 126.7, 121.9, 121.7, 92.1, 66.9, 66.8, 61.6, 60.3, 52.2, 52.1, 50.1, 40.5, 36.5, 36.4, 31.4, 31.2, 23.2; **HRMS** calcd. for  $\text{C}_{23}\text{H}_{27}\text{Cl}_3\text{N}_3\text{O}_4^+$   $[\text{M} + \text{H}]^+$  514.1062, found 514.1053.

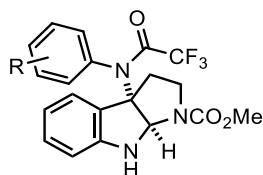
**Methyl 3a-(2,2,2-trifluoro-*N*-phenylacetamido)-3,3a,8,8a-tetrahydropyrrolo[2,3-*b*]indole-1(2H)-carboxylate (3y)**



Following the **general procedure K**, *N*-hydroxyindole **1a** (188 mg, 0.803 mmol) and imidoyl chloride **R1** (248 mg, 1.20 mmol) afforded pyrroloindoline **3y** (97.7 mg, 30%) as a pale yellow oil after purification by flash column chromatography (silica gel, hexanes:EtOAc = 1:0 → 8:2).

$R_f=0.42$  (silica gel, hexanes:EtOAc = 1:1);  $^1\text{H NMR}$  (400 MHz,  $\text{CDCl}_3$ , 60:40 mixture of rotamers):  $\delta$  8.00 and 7.92 (s, 1H), 7.49 (d,  $J = 8.3$  Hz, 2H), 7.42 – 7.34 (m, 2H), 7.10 (t,  $J = 7.7$  Hz, 1H), 7.02 (t,  $J = 6.9$  Hz, 1H), 6.81 – 6.72 (m, 1H), 6.68 (d,  $J = 7.8$  Hz, 1H), 5.46 and 5.41 (s, 1H), 5.21 and 4.79 (s, 1H), 3.92 and 3.80 (t,  $J = 9.1$  Hz, 1H), 3.78 and 3.71 (s, 3H), 3.20 – 3.09 (m, 1H), 2.69 – 2.55 (m, 2H);  $^{13}\text{C NMR}$  (101 MHz,  $\text{CDCl}_3$ ):  $\delta$  155.5, 154.9 (q,  $J = 36.9$  Hz), 154.6, 149.0, 148.8, 142.1, 142.0, 134.1, 134.0, 131.9, 131.8, 129.0, 128.9, 126.9, 126.8, 124.0, 123.9, 120.9, 119.9, 119.6, 115.8 (d,  $J = 288.7$  Hz), 110.3, 110.1, 82.9, 82.5, 61.2, 60.0, 52.9, 52.6, 46.5, 46.2, 36.1, 35.9;  $^{19}\text{F NMR}$  (376 MHz,  $\text{CDCl}_3$ ):  $\delta$  -75.7, -75.6; **HRMS** calcd. for  $\text{C}_{20}\text{H}_{19}\text{F}_3\text{N}_3\text{O}_3^+$   $[\text{M} + \text{H}]^+$  406.1373, found 406.1372.

**Methyl 3a-(*N*-(2,6-dimethylphenyl)-2,2,2-trifluoroacetamido)-3,3a,8,8a-tetrahydropyrrolo[2,3-*b*]indole-1(2H)-carboxylate (3z)**

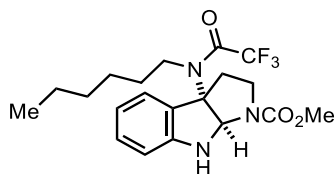


R= 2,6-Me<sub>2</sub>

Following the **general procedure K**, *N*-hydroxyindole **1a** (150 mg, 0.642 mmol) and imidoyl chloride **R2** (227 mg, 0.963 mmol) afforded pyrroloindoline **3z** (47.3 mg, 17%) as a pale yellow oil after purification by flash column chromatography (silica gel, hexanes:EtOAc = 1:0 → 8:2).

*R<sub>f</sub>*=0.24 (silica gel, hexanes:EtOAc = 7:3); <sup>1</sup>H NMR (500 MHz, CDCl<sub>3</sub>, 60:40 mixture of rotamers): δ 7.42 (s, 1H), 7.12 – 7.08 (m, 3H), 7.05 ad 7.03 (d, *J* = 7.4 Hz, 1H), 6.77 (td, *J* = 7.4, 3.0 Hz, 1H), 6.67 (d, *J* = 7.8 Hz, 1H), 5.48 and 5.42 (s, 1H), 5.20 and 4.76 (s, 1H), 3.91 and 3.79 (t, *J* = 8.6 Hz, 1H), 3.79 and 3.71 (s, 3H), 3.17 – 3.09 (m, 1H), 2.63 – 2.54 (m, 2H), 2.19 (s, 6H); <sup>13</sup>C NMR (126 MHz, CDCl<sub>3</sub>): δ 155.7 (q, *J* = 36.4 Hz), 155.5, 154.6, 149.1, 148.8, 144.3, 144.2, 135.6, 131.9, 131.8, 129.6, 128.9, 128.9, 126.1, 124.1, 124.0, 119.8, 119.5, 116.2 (q, *J* = 288.8 Hz), 110.3, 110.1, 83.0, 82.5, 61.2, 60.0, 52.9, 52.5, 46.5, 46.2, 36.5, 36.2, 18.4; <sup>19</sup>F NMR (471 MHz, CDCl<sub>3</sub>): δ -75.3; HRMS calcd. for C<sub>22</sub>H<sub>23</sub>F<sub>3</sub>N<sub>3</sub>O<sub>3</sub><sup>+</sup> [M + H]<sup>+</sup> 434.1686, found 434.1683.

**Methyl 3a-(2,2,2-trifluoro-*N*-hexylacetamido)-3,3a,8,8a-tetrahydropyrrolo[2,3-*b*]indole-1(2H)-carboxylate (3aa)**

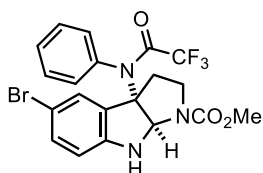


Following the **general procedure K**, *N*-hydroxyindole **1a** (129 mg, 0.551 mmol) and imidoyl chloride **R3** (178 mg, 0.825 mmol) afforded pyrroloindoline **3aa** (34.5 mg, 15%) as a pale yellow oil after purification by flash column chromatography (silica gel, hexanes:EtOAc = 1:0 → 8:2).

*R<sub>f</sub>*=0.65 (silica gel, hexanes:EtOAc = 1:1); <sup>1</sup>H NMR (500 MHz, CDCl<sub>3</sub>): δ 7.34 and 7.30 (d, *J* = 7.4 Hz, 1H), 7.23 – 7.19 (m, 1H), 6.83 (q, *J* = 8.2 Hz, 1H), 6.66 (d, *J* = 7.9 Hz, 1H), 5.71

and 5.70 (s, 1H), 3.92 – 3.86 and 3.80 – 3.76 (m, 1H), 3.76 and 3.68 (s, 3H), 3.29 (dq,  $J = 11.2, 6.5, 4.8$  Hz, 2H), 3.11 – 2.93 (m, 2H), 2.45 – 2.42 and 2.33 – 2.28 (m, 1H), 1.39 – 1.24 (m, 2H), 1.14 – 1.07 (m, 3H), 1.04 – 0.96 (m, 3H), 0.86 (t,  $J = 6.8$  Hz, 1H), 0.78 (t,  $J = 7.3$  Hz, 3H) 1Hxceed;  $^{13}\text{C NMR}$  (126 MHz,  $\text{CDCl}_3$ ):  $\delta$  157.6 (q,  $J = 35.6$  Hz), 155.6, 154.7, 151.0, 150.9, 133.9, 131.2, 131.1, 129.0, 126.7, 126.6, 125.6, 125.1, 124.0, 120.6, 119.6, 119.3, 116.5 (q,  $J = 288.4$  Hz), 111.5, 110.6, 110.6, 78.3, 52.9, 52.6, 46.6 (d,  $J = 3.3$  Hz), 46.5 (d,  $J = 3.6$  Hz), 46.1, 45.8, 33.5, 32.6, 31.0, 30.4, 26.1, 26.0, 22.4, 14.0;  $^{19}\text{F NMR}$  (471 MHz,  $\text{CDCl}_3$ ):  $\delta$  -69.4; **HRMS** calcd. for  $\text{C}_{20}\text{H}_{27}\text{F}_3\text{N}_3\text{O}_3^+$   $[\text{M} + \text{H}]^+$  414.1999, found 414.1991.

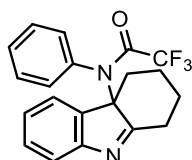
**Methyl 5-bromo-3a-(2,2,2-trifluoro-N-phenylacetamido)-3,3a,8,8a-tetrahydropyrrolo[2,3-b]indole-1(2H)-carboxylate (3ab)**



Following the **general procedure K**, N-hydroxyindole **1g** (0.150 g, 0.479 mmol) and imidoyl chloride **R1** (149 mg, 0.718 mmol) afforded pyrroloindoline **3ab** (48.7 mg, 21%) as a pale yellow oil after purification by flash column chromatography (silica gel, hexanes:EtOAc = 1:0 → 8:2).

$R_f$ =0.42 (silica gel, hexanes:EtOAc = 1:1);  $^1\text{H NMR}$  (500 MHz,  $\text{CDCl}_3$ ):  $\delta$  7.89 (br s, 1H), 7.51 (d,  $J = 8.7$  Hz, 1H), 7.39 – 7.35 (m, 2H), 7.10 – 7.08 (m, 1H), 6.56 (d,  $J = 8.3$  Hz, 1H), 5.47 and 5.42 (s, 1H), 3.94 and 3.81 (t,  $J = 9.3$  Hz, 1H), 3.78 and 3.72 (s, 3H), 3.17 (td,  $J = 10.8, 5.9$  Hz, 1H), 2.67 – 2.54 (m, 2H);  $^{13}\text{C NMR}$  (126 MHz,  $\text{CDCl}_3$ ):  $\delta$  155.5, 155.0, 154.6 (q,  $J = 33.9$  Hz), 148.1, 141.4, 141.3, 134.5, 134.3, 131.8, 131.7, 127.0, 126.9, 126.7, 126.7, 120.9, 111.7, 83.1, 82.7, 61.2, 60.0, 53.0, 52.7, 46.4, 46.1, 35.93, 35.7;  $^{19}\text{F NMR}$  (376 MHz,  $\text{CDCl}_3$ ):  $\delta$  -75.7; **HRMS** calcd. for  $\text{C}_{20}\text{H}_{18}\text{BrF}_3\text{N}_3\text{O}_3^+$   $[\text{M} + \text{H}]^+$  484.0478, found 484.0475.

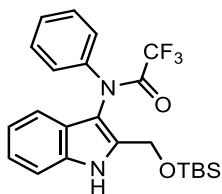
**2,2,2-Trifluoro-N-phenyl-N-(1,2,3,4-tetrahydro-4aH-carbazol-4a-yl)acetamide (3ac)**



Following the **general procedure K**, N-hydroxyindole **1s** (72.0 mg, 0.385 mmol) and imidoyl chloride **R1** (0.120 g, 0.578 mmol) afforded pyrroloindoline **3ac** (43.2 mg, 31%) as a pale yellow oil after purification by flash column chromatography (silica gel, hexanes:EtOAc = 1:0 → 1:1).

$R_f$ =0.29 (silica gel, hexanes:EtOAc = 1:1);  $^1\text{H NMR}$  (400 MHz,  $\text{CDCl}_3$ ):  $\delta$  7.84 (br s, 1H), 7.64 (d,  $J$  = 7.9 Hz, 1H), 7.52 (d,  $J$  = 8.3 Hz, 2H), 7.30 (td,  $J$  = 7.5, 1.4 Hz, 1H), 7.16 – 7.02 (m, 4H), 3.11 (d,  $J$  = 14.1 Hz, 1H), 2.96 (d,  $J$  = 13.1 Hz, 1H), 2.50 (td,  $J$  = 12.8, 5.9 Hz, 1H), 2.16 – 2.12 (m, 1H), 1.79 – 1.51 (m, 3H), 1.39 – 1.27 (m, 1H); lack of 1H  $^{13}\text{C NMR}$  (101 MHz,  $\text{CDCl}_3$ ):  $\delta$  188.6, 154.1, 147.2, 136.9, 134.1, 127.9, 127.4, 125.6, 122.4, 121.4, 120.8, 118.5 (q,  $J$  = 251.0 Hz), 62.6, 36.6, 30.7, 29.4, 22.0;  $^{19}\text{F NMR}$  (376 MHz,  $\text{CDCl}_3$ ):  $\delta$  -75.7; **HRMS** calcd. for  $\text{C}_{20}\text{H}_{18}\text{F}_3\text{N}_2\text{O}^+$  [ $\text{M} + \text{H}$ ] $^+$  359.1366, found 359.1366.

**N-(2-(((tert-Butyldimethylsilyl)oxy)methyl)-1H-indol-3-yl)-2,2,2-trifluoro-N-phenylacetamide (3ad)**

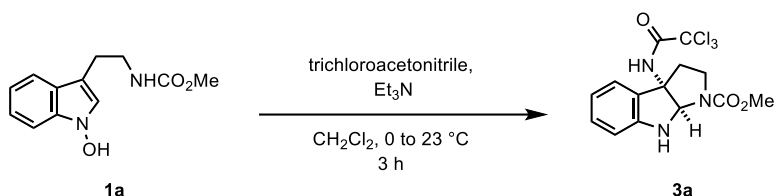


Following the **general procedure K**, N-hydroxyindole **1q** (55.0 mg, 0.198 mmol) and imidoyl chloride **R1** (61.7 mg, 0.297 mmol) afforded pyrroloindoline **3ad** (45.3 mg, 51%) as a pale yellow oil after purification by flash column chromatography (silica gel, hexanes:EtOAc = 1:0 → 95:5).

$R_f$ =0.24 (silica gel, hexanes:EtOAc = 7:3);  $^1\text{H NMR}$  (400 MHz, MeOD):  $\delta$  7.90 – 7.86 (m, 1H), 7.49 – 7.43 (m, 3H), 7.38 (td,  $J$  = 7.4, 1.4 Hz, 1H), 7.19 – 7.14 (m, 2H), 7.01 (td,  $J$  = 7.5, 7.0, 1.1 Hz, 1H), 4.78 (d,  $J$  = 12.5 Hz, 1H), 4.71 (d,  $J$  = 12.5 Hz, 1H), 0.86 (s, 9H), 0.00 and -0.01 (s, 6H);  $^{13}\text{C NMR}$  (126 MHz, MeOD):  $\delta$  154.7 (q,  $J$  = 37.3 Hz), 154.5, 136.3, 135.5, 134.1, 133.7, 131.8, 129.3, 128.6, 127.0, 126.0, 125.0, 123.1, 121.0, 119.0, 117.7, 115.7 (q,  $J$  = 288.8 Hz), 111.6, 107.0, 57.7, 26.0, 18.5, -5.4;  $^{19}\text{F NMR}$  (376 MHz, MeOD):  $\delta$  -77.5; **HRMS** calcd. for  $\text{C}_{23}\text{H}_{26}\text{F}_3\text{N}_2\text{O}_2\text{Si}^+$  [ $\text{M} - \text{H}$ ] $^-$  447.1721, found 447.1719.

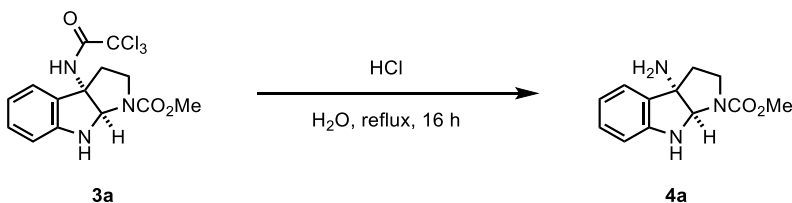
## 4.4. Evaluation of Practicality and Versatility of the C3-Amidaiton (Scheme 2.53)

### 4.4.1. Gram-scale Reaction



To an oven-dried round-bottom flask equipped with a stir bar and septum were added N-hydroxyindole **1a** (1.01 g, 4.31 mmol, 1.0 equiv) and CH<sub>2</sub>Cl<sub>2</sub> (50 mL) at 23 °C. The resulting solution was cooled to 0 °C, and trichloroacetonitrile (1.30 mL, 12.9 mmol, 3.0 equiv) and Et<sub>3</sub>N (60 μL, 0.1 equiv) were added to the solution. The reaction mixture was warmed up to rt and stirred for 3 h before it was quenched with H<sub>2</sub>O (30 mL). The layers were separated and the aqueous layer was extracted with CH<sub>2</sub>Cl<sub>2</sub> (3 × 20 mL). The combined organic layer was dried over anhydrous MgSO<sub>4</sub>, filtered, and concentrated under reduced pressure. The resulting residue was purified by flash column chromatography (silica gel, hexanes:EtOAc = 1:0 → 7:3) to afford pyrroloindoline **3a** (1.11 g, 68%) as a pale yellow oil.

### 4.4.2. Conversion to the 3-Aminopyrroloindoline



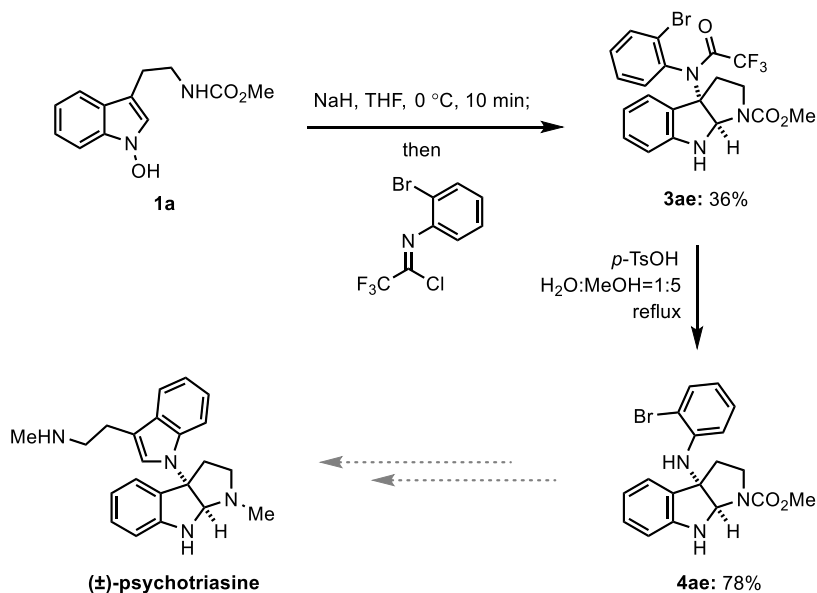
To an oven-dried round-bottom flask equipped with a stir bar and septum were added **3a** (0.100 g, 0.264 mmol, 1.0 equiv) and H<sub>2</sub>O (5 mL) at 23 °C, followed by HCl (35.0–37.0 wt% in H<sub>2</sub>O, 70 μL, 0.792 mmol, 3.0 equiv). The resulting mixture was heated to 100 °C in a pre-heated oil bath and stirred for 16 h. After the reaction mixture was cooled to 23 °C, the reaction mixture was diluted with EtOAc (5 mL) and quenched with NaHCO<sub>3</sub> (5 mL, sat. aq.). The layers were separated and the aqueous layer was extracted with EtOAc (3 × 20 mL). The combined organic layer was dried over anhydrous MgSO<sub>4</sub>, filtered, and concentrated under reduced pressure. The resulting residue was purified by flash column chromatography



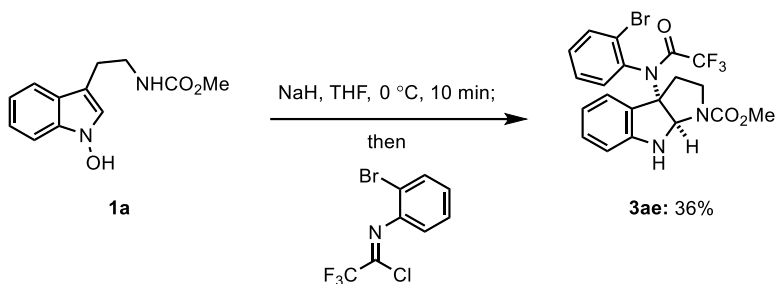
(silica gel, CH<sub>2</sub>Cl<sub>2</sub>:MeOH = 1:0 → 95:5) to afford pyrroloindoline **4a** (1.9143.0 mg, 70%) as a pale yellow oil. Analytic data is in agreement with the reported literature values.<sup>2</sup>

*R<sub>f</sub>*=0.35 (silica gel, CH<sub>2</sub>Cl<sub>2</sub>:MeOH = 9:1); <sup>1</sup>H NMR (500 MHz, CDCl<sub>3</sub>): δ 7.24 (d, *J* = 8.0 Hz, 1H), 7.13 (t, *J* = 7.6 Hz, 1H), 6.82 – 6.78 (m, 1H), 6.62 (dd, *J* = 8.0, 3.2 Hz, 1H), 5.12 and 4.71 (s, 1H), 5.09 and 5.05 (s, 1H), 3.77 and 3.69 (s, 3H), 3.67 – 3.62 (m, 1H), 3.17 – 3.09 (m, 1H), 2.40 – 2.33 (m, 1H), 2.25 – 2.16 (m, 1H); <sup>13</sup>C NMR (126 MHz, CDCl<sub>3</sub>): δ 155.8, 155.0, 149.1, 148.8, 131.8, 129.7, 123.3, 119.7, 119.5, 110.1, 110.0, 83.6, 83.3, 70.7, 69.6, 52.8, 52.5, 46.1, 45.7, 37.8, 37.7; HRMS calcd. for C<sub>12</sub>H<sub>16</sub>N<sub>3</sub>O<sub>2</sub><sup>+</sup> [M + H]<sup>+</sup> 234.1237, found 234.1238.

#### 4.4.3. Formal Synthesis of Psychotriasine



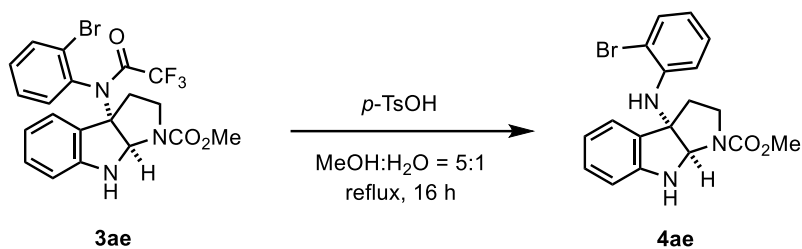
Methyl 3a-(N-(2-bromophenyl)-2,2,2-trifluoroacetamido)-3,3a,8,8a-tetrahydropyrrolo-[2,3-b]indole-1(2H)-carboxylate (**3ae**)



To an oven-dried round-bottom flask equipped with a stir bar and septum were added N-hydroxyindole **1a** (0.100 g, 0.427 mmol, 1.0 equiv) and THF (8 mL) at 23 °C. The resulting solution was cooled to 0 °C, and NaH (60% in mineral oil, 25.6 mg, 1.5 equiv, 0.641 mmol) was added to the solution. The reaction mixture was stirred for 10 min, then (Z)-N-(2-bromophenyl)-2,2,2-trifluoroacetimidoyl chloride (0.184 g, 0.641 mmol, 1.5 equiv,) was added. The resulting mixture was stirred for additional 1 h at 0 °C before it was quenched with H<sub>2</sub>O (10 mL). The layers were separated and the aqueous layer was extracted with EtOAc (3 × 10 mL). The combined organic layer was washed with brine (1 × 10 mL), dried over anhydrous MgSO<sub>4</sub>, filtered, and concentrated under reduced pressure. The resulting residue was purified by flash column chromatography (silica gel, hexanes:EtOAc = 1:0 → 8:2) to afford pyrroloindoline **3ae** (1.9174.0 mg, 36%) as a yellow oil.

*R<sub>f</sub>*=0.47 (silica gel, hexanes:EtOAc = 7:3); <sup>1</sup>H NMR (400 MHz, CDCl<sub>3</sub>): δ 8.38 (s, 1H), 8.22 (d, *J* = 8.6 Hz, 1H), 7.59 (dd, *J* = 7.8, 2.1 Hz, 1H), 7.41 – 7.38 (m, 1H), 7.12 (t, *J* = 7.5 Hz, 1H), 7.02 (t, *J* = 7.1 Hz, 1H), 6.80 – 6.76 (m, 1H), 6.69 (d, *J* = 7.8 Hz, 1H), 5.45 and 5.40 (s, 1H), 5.24 and 4.80 (s, 1H), 3.96 – 3.91 and 3.83 – 3.79 (m, 1H), 3.79 and 3.71 (s, 3H), 3.18 – 3.10 (m, 1H), 2.62 – 2.57 (m, 1H); <sup>13</sup>C NMR (101 MHz, CDCl<sub>3</sub>): δ 155.5, 154.76 (d, *J* = 37.1 Hz), 154.5, 149.0, 148.7, 143.4, 143.3, 132.1, 131.2, 130.0, 129.2, 126.2, 123.9, 123.8, 122.2, 122.1, 120.0, 119.7, 115.67 (q, *J* = 288.7 Hz), 114.5, 110.5, 110.3, 82.8, 82.3, 60.9, 59.7, 52.9, 52.6, 46.4, 46.1, 36.0, 35.7; <sup>19</sup>F NMR (471 MHz, CDCl<sub>3</sub>): δ –75.8; HRMS calcd. for C<sub>20</sub>H<sub>18</sub>BrF<sub>3</sub>N<sub>3</sub>O<sub>3</sub><sup>+</sup> [M + H]<sup>+</sup> 484.0478, found 484.0479.

**Methyl 3a-((2-bromophenyl)amino)-3,3a,8,8a-tetrahydropyrrolo[2,3-b]indole-1(2H)-carboxylate (4ae)**



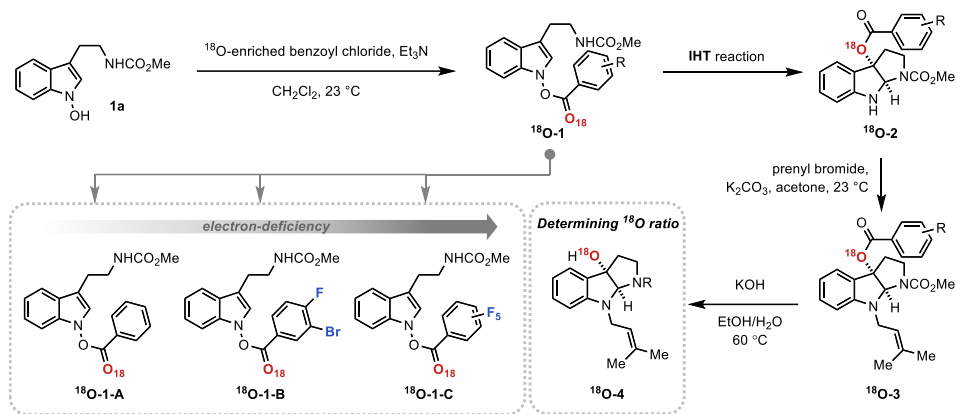
To an oven-dried round-bottom flask equipped with a stir bar and septum were added **3ae** (56.0 mg, 0.116 mmol, 1.0 equiv) and MeOH:H<sub>2</sub>O (5:1, 3 mL) at 23 °C, followed by *p*-TsOH (59.9 mg, 0.348 mmol, 3.0 equiv). The resulting mixture was heated to 60 °C in a pre-heated oil bath and stirred for 3 h. After the reaction mixture was cooled to 23 °C, the reaction mixture was diluted with CH<sub>2</sub>Cl<sub>2</sub> (10 mL) and quenched with NaHCO<sub>3</sub> (10 mL, sat. aq.). The layers were separated and the aqueous layer was extracted with CH<sub>2</sub>Cl<sub>2</sub> (3 × 10 mL). The combined organic layer was washed with brine (1 × 10 mL), dried over anhydrous MgSO<sub>4</sub>, filtered, and concentrated under reduced pressure. The resulting residue was purified by flash column chromatography (silica gel, hexanes:EtOAc = 1:0 → 8:2) to afford pyrroloindoline **4ae** (1.9135.0 mg, 78%) as a yellow oil. Analytic data is in agreement with the reported literature values.<sup>2</sup>

*R<sub>f</sub>* = 0.24 (silica gel, hexanes:EtOAc = 7:3); **<sup>1</sup>H NMR** (500 MHz, CDCl<sub>3</sub>): δ 7.41 (t, *J* = 8.1 Hz, 1H), 7.16 (t, *J* = 9.1 Hz, 2H), 6.98 (t, *J* = 7.9 Hz, 1H), 6.77 (q, *J* = 7.2 Hz, 1H), 6.65 (d, *J* = 7.8 Hz, 1H), 6.57 – 6.54 (m, 1H), 6.44 (dd, *J* = 16.5, 8.2 Hz, 1H), 5.73 and 5.66 (s, 1H), 5.14 and 4.82 (s, 1H), 4.81 and 4.77 (s, 1H), 3.90 – 3.85 and 3.79 – 3.75 (m, 1H), 3.77 and 3.74 (s, 3H), 3.35 – 3.28 (m, 1H), 2.65 – 2.55 (m, 1H), 2.42 – 2.36 (m, 1H); **<sup>13</sup>C NMR** (126 MHz, CDCl<sub>3</sub>): δ 156.1, 155.2, 149.1, 148.9, 142.2, 132.8, 132.7, 130.0, 129.1, 129.0, 128.4, 123.5, 123.4, 119.8, 119.6, 119.1, 119.0, 114.3, 114.0, 111.4, 111.3, 109.8, 109.7, 78.3, 73.5, 72.3, 52.9, 52.7, 44.7, 44.5, 39.2, 38.9; **HRMS** calcd. for C<sub>18</sub>H<sub>19</sub>BrN<sub>3</sub>O<sub>2</sub><sup>+</sup> [M + H]<sup>+</sup> 388.0655, found 388.0659.

## 5. Mechanistic Investigations

### 5.1. $^{18}\text{O}$ Isotope Experiment (Figure 2.10 and 2.11)

Scheme S2. Overview of the  $^{18}\text{O}$  labeling experiment.



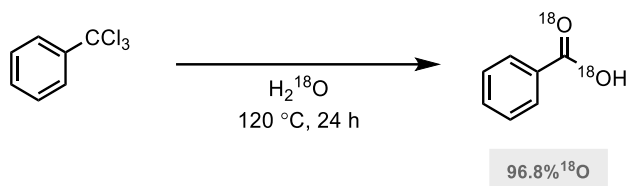
The general method for measuring  $^{18}\text{O}$  saturation is as follows: First,  $^{18}\text{O}$  enriched acyl chlorides were prepared according to the literature procedures.<sup>17</sup> Indolyl *N*-carboxylates, **18O-1-A** and **18O-1-B**, were synthesized using the prepared  $^{18}\text{O}$ -enriched acyl chlorides. These precursors were subsequently subjected to IHT reaction conditions to provide **18O-2-A** and **18O-2-B** respectively. In the case of **18O-1-C**, upon acylation, the intermediate immediately underwent the desired IHT reaction to provide **18O-2-C**. Independent HRMS analyses of acylation products of methanol with acyl chlorides used for the preparation of **18O-1-A** and **18O-1-B** had shown that the level of  $^{18}\text{O}$  enrichment in the acyl chloride is directly reflected the acylation products. Also, it was shown that the level of  $^{18}\text{O}$  enrichment for **18O-1-A** and **18O-1-B** remained unchanged after IHT reaction to provide **18O-2-A** and **18O-2-B** respectively. Therefore, the level of  $^{18}\text{O}$  enrichment for **18O-1-C** was estimated to be identical to that of **18O-2-C**.

Detailed synthetic schemes for preparation of compounds are presented below.

## 5.1.1. Preparation of $^{18}\text{O}$ Labeled Compounds

### 5.1.1.1 Benzoyl substituent

#### $^{18}\text{O}$ -Benzoic acid

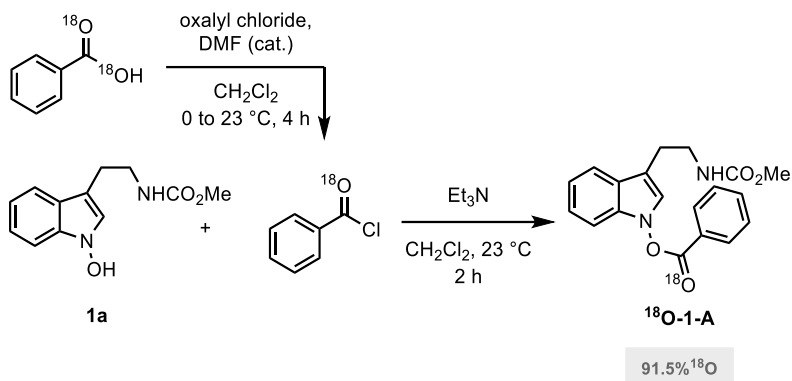


To an oven-dried heavy-wall pressure tube equipped with a stir bar and rubber septum were added  $\alpha,\alpha,\alpha$ -trichlorotoluene (1.40 mL, 10.0 mmol, 1.0 equiv) and  $\text{H}_2^{18}\text{O}$  (1.00 mL, 50.0 mmol, 5.0 equiv) at 23 °C. The rubber septum was replaced with a Teflon screw cap under  $\text{N}_2$  and the resulting mixture was heated to 120 °C in a pre-heated oil bath and stirred for 24 h. After the reaction mixture was cooled to 23 °C, the white solid was formed and precipitate was collected by filtration. The resulting filter cake was washed with  $\text{H}_2\text{O}$  ( $1 \times 3$  mL), and the solid was dried *in vacuo*, to afford  $^{18}\text{O}$ -benzoic acid (1.16 g, 92%) as a white solid. The resulting residue was used directly in the subsequent reaction without further purification. Analytic data is in agreement with the reported literature values.<sup>18</sup>

m.p. XX °C ;  $R_f$ =0.24 (silica gel, hexanes:EtOAc = 7:3);  $^1\text{H NMR}$  (500 MHz,  $\text{CDCl}_3$ ):  $\delta$  8.14 (dd,  $J$  = 8.3, 1.5 Hz, 2H), 7.63 (t,  $J$  = 7.5 Hz, 1H), 7.49 (t,  $J$  = 7.8 Hz, 2H);  $^{13}\text{C NMR}$  (126 MHz,  $\text{CDCl}_3$ ):  $\delta$  172.3, 134.0, 130.4, 129.5, 128.7; **HRMS** calcd. for  $\text{C}_7\text{H}_5^{18}\text{O}_2^-$  [ $\text{M} - \text{H}$ ] $^-$  125.0380, found 125.0380;

**Isotopic Incorporation:** [ $\text{M}+4$ ] 96.8%, [ $\text{M}+2$ ] 3.1%, [ $\text{M}+0$ ] 0.1%.

### 3-(2-((Methoxycarbonylamino)ethyl)-1H-indol-1-yl benzoate (<sup>18</sup>O-1-A)

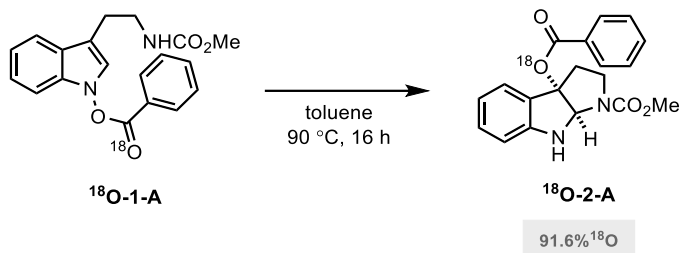


To an oven-dried two-neck round-bottom flask equipped with a stir bar, septum, and condenser were added <sup>18</sup>O-benzoic acid (126 mg, 1.00 mmol, 1.02 equiv), DMF (a few drops) and CH<sub>2</sub>Cl<sub>2</sub> (3 mL) at 23 °C. The resulting solution was cooled to 0 °C and oxalyl chloride (126 μL, 1.47 mmol, 1.5 equiv) was added dropwise. The reaction mixture was stirred for 4 h at 23 °C, before it was directly concentrated under reduced pressure. The resulting <sup>18</sup>O-benzoyl chloride was used directly in the subsequent reaction without further purification.

To an oven-dried round-bottom flask equipped with a stir bar and septum were added *N*-hydroxyindole **1a** (0.230 g, 0.982 mmol, 1.0 equiv) and CH<sub>2</sub>Cl<sub>2</sub> (10 mL) at 23 °C, followed by the crude benzoyl chloride and Et<sub>3</sub>N (0.178 mL, 1.28 mmol, 1.3 equiv). The resulting mixture was stirred for 2 h, before it was quenched with H<sub>2</sub>O (10 mL). The layers were separated, and the aqueous layer was extracted with CH<sub>2</sub>Cl<sub>2</sub> (3 × 20 mL). The combined organic layer was washed with brine (1 × 20 mL), dried over anhydrous MgSO<sub>4</sub>, filtered, and concentrated under reduced pressure. The resulting residue was purified by flash column chromatography (silica gel, hexanes:EtOAc = 1:0 → 7:3) to afford the product (237 mg, 71%) as a pale yellow oil. The spectral data matched to those of compound **2b-Int** (See section 3.1).

*R*<sub>f</sub>=0.65 (silica gel, hexanes:EtOAc = 1:1); <sup>1</sup>H NMR (500 MHz, CDCl<sub>3</sub>): δ 8.22 (d, *J* = 6.9 Hz, 2H), 7.72 (t, *J* = 7.5 Hz, 1H), 7.62 (d, *J* = 7.9 Hz, 1H), 7.57 (t, *J* = 7.8 Hz, 2H), 7.27 – 7.25 (m, 2H), 7.18 (ddd, *J* = 8.1, 4.7, 3.5 Hz, 1H), 7.10 (s, 1H), 4.83 (s, 1H), 3.67 (s, 3H), 3.55 (q, *J* = 6.6 Hz, 2H), 2.98 (t, *J* = 6.9 Hz, 2H); <sup>13</sup>C NMR (126 MHz, CDCl<sub>3</sub>): δ 164.9, 157.2, 135.9, 134.7, 130.4, 129.1, 126.6, 125.0, 124.2, 123.7, 121.1, 119.4, 112.0, 109.2, 52.2, 41.1, 25.9; HRMS calcd. for C<sub>19</sub>H<sub>18</sub>N<sub>2</sub>O<sub>3</sub><sup>18</sup>ONa<sup>+</sup> [M + Na]<sup>+</sup> 363.1201, found 363.1192; **Isotopic Incorporation**: [M+2] 91.5%, [M+0] 8.5%.

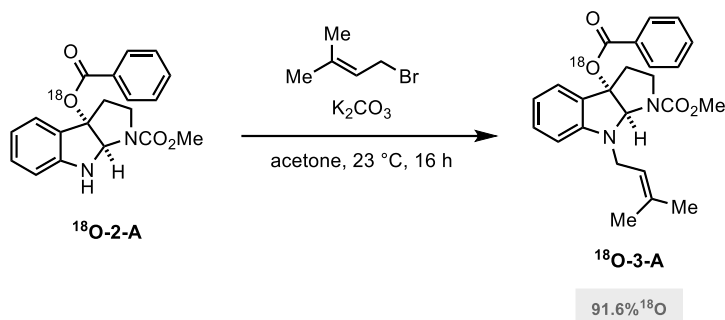
**Methyl 3a-(benzoyloxy)-3,3a,8,8a-tetrahydropyrrolo[2,3-b]indole-1(2H)-carboxylate (<sup>18</sup>O-1-A)**



To an oven-dried round-bottom flask equipped with a stir bar and septum were added **<sup>18</sup>O-1-A** (155 mg, 0.455 mmol, 1.0 equiv) and toluene (9 mL) at 23 °C. The resulting mixture was heated to 90 °C in a pre-heated oil bath and stirred for 16 h, before it was cooled to 23 °C and directly concentrated under reduced pressure. The resulting residue was purified by flash column chromatography (silica gel, hexanes:EtOAc = 1:0 → 7:3) to afford the product (98.3 mg, 63%) as a pale yellow oil.

*R<sub>f</sub>*=0.65 (silica gel, hexanes:EtOAc = 1:1); **<sup>1</sup>H NMR** (500 MHz, CDCl<sub>3</sub>, 55:45 mixture of rotamers): δ 7.99 (d, *J* = 7.7 Hz, 2H), 7.63 and 7.42 (d, *J* = 7.6 Hz, 1H), 7.54 (br t, *J* = 8.3 Hz, 1H), 7.41 (t, *J* = 7.6 Hz, 2H), 7.19 (t, *J* = 7.8 Hz, 1H), 6.80 (q, *J* = 6.9 Hz, 1H), 6.68 (d, *J* = 7.9 Hz, 1H), 5.78 (s, 1H), 3.93 and 3.80 (t, *J* = 9.7 Hz, 1H), 3.80 and 3.73 (s, 3H), 3.27 – 3.20 (m, 1H), 3.07 and 2.96 (dd, *J* = 12.9, 6.3 Hz, 1H), 2.78 – 2.64 (m, 1H); **<sup>13</sup>C NMR** (126 MHz, CDCl<sub>3</sub>): δ 165.3, 155.6, 154.8, 151.0, 150.7, 133.2, 131.0, 130.2, 129.8, 129.1, 128.4, 126.5, 126.3, 126.0, 119.6, 119.3, 110.3, 110.2, 94.5, 93.3, 80.4, 79.6, 52.8, 52.5, 45.5, 35.9, 35.8; **HRMS** calcd. for C<sub>19</sub>H<sub>19</sub>N<sub>2</sub>O<sub>3</sub><sup>18</sup>O<sup>+</sup> [M + H]<sup>+</sup> 341.1382, found 341.1373; **Isotopic Incorporation:** [M+2] 91.6%, [M+0] 8.4%.

**Methyl 3a-(benzoyloxy)-8-(3-methylbut-2-en-1-yl)-3,3a,8,8a-tetrahydropyrrolo[2,3-b]indole-1(2H)-carboxylate (<sup>18</sup>O-3-A)**

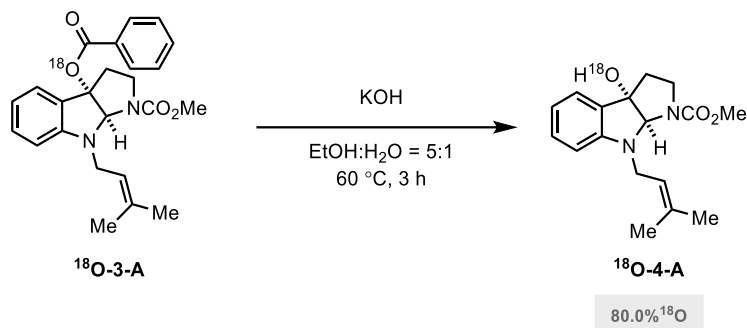


To an oven-dried round-bottom flask equipped with a stir bar and septum were added <sup>18</sup>O-2-A (98.3 mg, 0.289 mmol, 1.0 equiv) and acetone (7 mL) at 23 °C, followed by 1-bromo-3-methyl-2-butene (50  $\mu$ L, 0.434 mmol, 1.5 equiv) and K<sub>2</sub>CO<sub>3</sub> (0.120 g, 0.867 mmol, 3.0 equiv). The resulting mixture was stirred for 16 h, before it was directly concentrated under reduced pressure and re-dissolved in CH<sub>2</sub>Cl<sub>2</sub> (10 mL) and H<sub>2</sub>O (10 mL). The layers were separated, and the aqueous layer was extracted with CH<sub>2</sub>Cl<sub>2</sub> (3  $\times$  10 mL). The combined organic layer was washed with brine (1  $\times$  10 mL), dried over anhydrous MgSO<sub>4</sub>, filtered, and concentrated under reduced pressure. The resulting residue was purified by flash column chromatography (silica gel, hexanes:EtOAc = 1:0  $\rightarrow$  8:2) to afford the product (99.0 mg, 84%) as a pale yellow oil.

*R*<sub>f</sub>=0.38 (silica gel, hexanes:EtOAc = 7:3); <sup>1</sup>H NMR (400 MHz, CDCl<sub>3</sub>, 50:50 mixture of rotamers):  $\delta$  7.98 (d, *J* = 7.7 Hz, 2H), 7.54 (br t, *J* = 7.3 Hz, 1H), 7.53 and 7.46 (d, *J* = 7.2 Hz, 1H), 7.41 (t, *J* = 7.6 Hz, 2H), 7.20 (t, *J* = 7.7 Hz, 2H), 6.71 (t, *J* = 7.5 Hz, 2H), 6.53 (t, *J* = 8.5 Hz, 1H), 5.89 and 5.83 (s, 1H), 5.24 (s, 1H), 4.28 and 4.10 (dd, *J* = 16.3, 7.5 Hz, 1H), 4.07 (br t, *J* = 11.9, 10.4 Hz, 1H), 4.07 and 3.93 (br t, *J* = 9.8 Hz, 1H), 3.78 and 3.75 (s, 3H), 3.23 – 3.10 (m, 1H), 2.93 – 2.79 (m, 1H), 2.68 (t, *J* = 10.9 Hz, 1H), 1.78 (d, *J* = 14.6 Hz, 3H), 1.71 (s, 3H); <sup>13</sup>C NMR (101 MHz, CDCl<sub>3</sub>): 165.2, 155.9, 155.1, 152.1, 134.8, 134.4, 133.2, 131.1, 130.4, 129.8, 128.4, 127.0, 126.8, 126.0, 125.5, 121.3, 121.0, 118.2, 108.5, 108.0, 94.6, 93.7, 85.0, 84.4, 52.8, 45.6, 45.5, 45.3, 45.0, 37.6, 25.9, 18.3, 18.2; HRMS calcd. for C<sub>24</sub>H<sub>27</sub>N<sub>2</sub>O<sub>3</sub><sup>18</sup>O<sup>+</sup> [M + H]<sup>+</sup> 409.2008, found 409.2003; **Isotopic Incorporation:** [M+2] 91.6%, [M+0] 8.4%.



**Methyl 3a-hydroxy-8-(3-methylbut-2-en-1-yl)-3,3a,8,8a-tetrahydropyrrolo[2,3-b]indole-1(2H)-carboxylate (<sup>18</sup>O-4-A)**

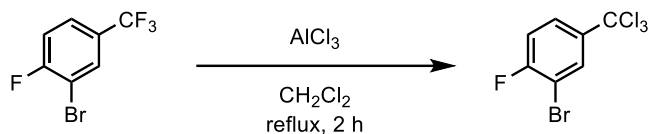


To an oven-dried round-bottom flask equipped with a stir bar and septum were added **<sup>18</sup>O-3-A** (99.0 mg, 0.242 mmol, 1.0 equiv) and EtOH: H<sub>2</sub>O (5:1, 6 mL) at 23 °C, followed by KOH (20.4 mg, 0.363 mmol, 1.5 equiv). The resulting mixture was heated to 60 °C in a pre-heated oil bath and stirred for 3 h, before it was cooled to 23 °C and re-dissolved with CH<sub>2</sub>Cl<sub>2</sub> (10 mL) and H<sub>2</sub>O (5 mL). The layers were separated, and the aqueous layer was extracted with CH<sub>2</sub>Cl<sub>2</sub> (3 × 10 mL). The combined organic layer was washed with brine (1 × 10 mL), dried over anhydrous MgSO<sub>4</sub>, filtered, and concentrated under reduced pressure. The resulting residue was purified by flash column chromatography (silica gel, hexanes:EtOAc = 1:0 → 7:3) to afford the product (57.2 mg, 78%) as a pale yellow oil.

*R<sub>f</sub>*=0.45 (silica gel, hexanes:EtOAc = 1:1); **<sup>1</sup>H NMR** (400 MHz, CDCl<sub>3</sub>, 50:50 mixture of rotamers): δ 7.25 (d, *J* = 8.4 Hz, 1H), 7.20 (t, *J* = 7.8 Hz, 1H), 6.74 (t, *J* = 7.4 Hz, 1H), 6.49 (s, 1H), 5.38 and 5.30 (s, 1H), 5.16 (s, 1H), 4.22 – 4.08 and 4.07 – 3.93 (m, 1H), 3.96 (br s, 1H), 3.96 and 3.83 (br s, 1H), 3.73 (s, 3H), 3.23 – 3.04 (m, 2H), 2.41 – 2.23 (m, 2H), 1.75 (d, *J* = 11.7 Hz, 3H), 1.69 (s, 3H); **<sup>13</sup>C NMR** (101 MHz, CDCl<sub>3</sub>): δ 150.4, 135.2, 130.8, 130.7, 130.5, 123.4, 123.2, 120.4, 120.3, 118.2, 108.4, 108.0, 87.7, 87.5, 86.9, 52.7, 45.8, 44.9, 44.4, 38.4, 25.9, 18.3; **HRMS** calcd. for C<sub>17</sub>H<sub>23</sub>N<sub>2</sub>O<sub>2</sub><sup>18</sup>O<sup>+</sup> [M + H]<sup>+</sup> 305.1746, found 305.1740; **Isotopic Incorporation:** [M+2] 80.0%, [M+0] 20.0%.

### 5.1.1.2 3-Bromo-4-fluorobenzoyl substituent

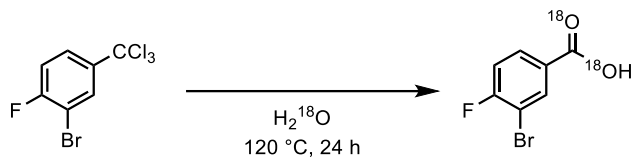
#### 2-Bromo-1-fluoro-4-(trichloromethyl)benzene



To an oven-dried round-bottom flask equipped with a stir bar and septum were added  $\text{AlCl}_3$  (1.73 g, 13.0 mmol, 1.3 equiv) and  $\text{CH}_2\text{Cl}_2$  (30 mL) at 23 °C. To a stirred mixture was added 3-bromo-4-fluorobenzotrifluoride (1.42 mL, 10.0 mmol, 1.0 equiv) dropwise via syringe. The reaction mixture was then heated to reflux in a pre-heated oil bath and stirred for 2 h, before it was cooled to rt and quenched with 0 °C  $\text{H}_2\text{O}$  (15 mL). The layers were separated, and the aqueous layer was extracted with  $\text{CH}_2\text{Cl}_2$  ( $3 \times 5$  mL). The combined organic layer was washed with brine ( $1 \times 5$  mL), dried over anhydrous  $\text{MgSO}_4$ , filtered, and concentrated under reduced pressure. The resulting residue was purified by flash column chromatography (silica gel, hexanes:EtOAc = 1:0  $\rightarrow$  9:1) to afford 3-bromo-4-fluorobenzotrifluoride (1.75 g, 60%) as a pale yellow liquid. Analytic data is in agreement with the reported literature values.

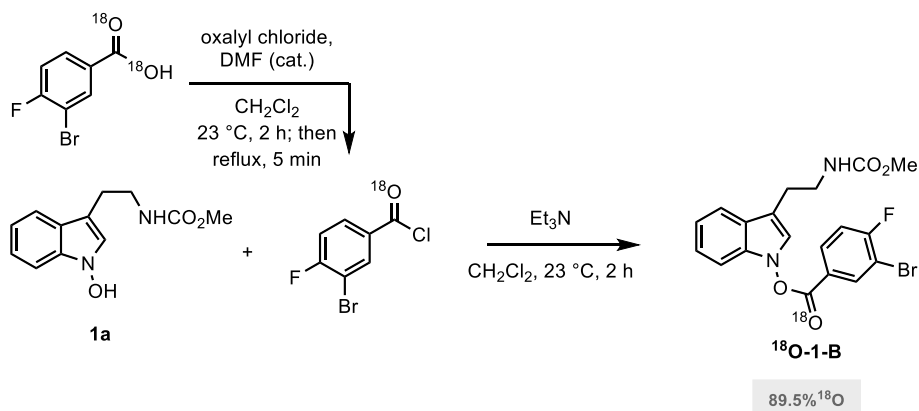
$R_f=0.75$  (silica gel, hexanes:EtOAc = 9:1);  $^1\text{H NMR}$  (400 MHz,  $\text{CDCl}_3$ ):  $\delta$  8.15 (dd,  $J = 6.2, 2.7$  Hz, 1H), 7.87 (ddd,  $J = 9.1, 4.4, 2.5$  Hz, 1H), 7.17 (ddd,  $J = 9.5, 7.8, 1.9$  Hz, 1H);  $^{13}\text{C NMR}$  (126 MHz,  $\text{CDCl}_3$ ):  $\delta$  160.0 (d,  $J = 253.1$  Hz), 141.6 (d,  $J = 3.8$  Hz), 131.4, 126.8 (d,  $J = 8.1$  Hz), 116.3 (d,  $J = 23.3$  Hz), 109.1 (d,  $J = 22.0$  Hz), 95.6;  $^{19}\text{F NMR}$  (376 MHz,  $\text{CDCl}_3$ ):  $\delta$  -103.7 – -104.3 (m); **HRMS** calcd. for  $\text{C}_7\text{H}_4\text{BrCl}_3\text{F}^+$   $[\text{M} + \text{H}]^+$  290.8541, found 290.8541.

### <sup>18</sup>O-3-Bromo-4-fluorobenzoic acid



To an oven-dried heavy-wall pressure tube equipped with a stir bar and rubber septum were added 3-bromo-4-fluorobenzotrichloride (0.230 g, 0.787 mmol, 1.0 equiv) and H<sub>2</sub><sup>18</sup>O (160 μL, 7.99 mmol, 10.2 equiv) at 23 °C. The rubber septum was replaced with a Teflon screw cap under N<sub>2</sub> and the resulting mixture was heated to 120 °C in a pre-heated oil bath and stirred for 24 h. After the reaction mixture was cooled to 23 °C, the white solid was formed and precipitate was collected by filtration. The resulting filter cake was washed with H<sub>2</sub>O (1 × 3 mL), and the solid was dried *in vacuo*, to afford <sup>18</sup>O-3-bromo-4-fluorobenzoic acid (70.8 mg, 40%) as a white solid. The resulting residue was used directly in the subsequent reaction without further purification. Analytic data is in agreement with the reported literature values. *R<sub>f</sub>*=0.24 (silica gel, hexanes:EtOAc = 7:3); <sup>1</sup>H NMR (500 MHz, CDCl<sub>3</sub>): δ 8.35 (dd, *J* = 6.6, 2.1 Hz, 1H), 8.07 (ddd, *J* = 8.6, 4.7, 2.1 Hz, 1H), 7.22 (t, *J* = 8.3 Hz, 1H); <sup>13</sup>C NMR (126 MHz, CDCl<sub>3</sub>): δ 169.9, 162.8 (d, *J* = 256.3 Hz), 136.2 (d, *J* = 1.8 Hz), 131.7 (d, *J* = 8.7 Hz), 126.8 (d, *J* = 3.6 Hz), 116.9 (d, *J* = 23.1 Hz), 109.7 (d, *J* = 21.8 Hz); <sup>19</sup>F NMR (471 MHz, CDCl<sub>3</sub>): δ -98.1 (dd, *J* = 12.4, 6.7 Hz); HRMS calcd. for C<sub>7</sub>H<sub>3</sub>BrF<sup>18</sup>O<sub>2</sub><sup>-</sup> [M - H]<sup>-</sup> 220.9391, found 220.9391; **Isotopic Incorporation:** [M+4] 96.6%, [M+2] 3.4%, [M+0] 0.0%.

**3-(2-((Methoxycarbonyl)amino)ethyl)-1H-indol-1-yl 3-bromo-4-fluorobenzoate (<sup>18</sup>O-1-B)**



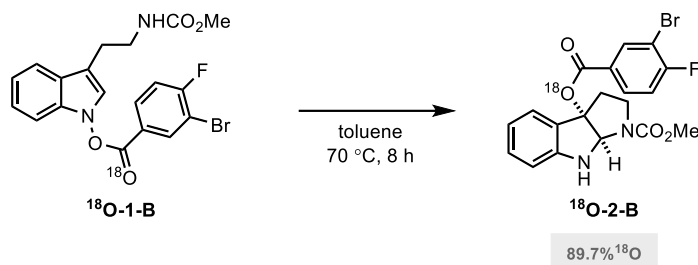
To an oven-dried two-neck round-bottom flask equipped with a stir bar, septum, and condenser were added <sup>18</sup>O-3-bromo-4-fluorobenzoic acid (70.8 mg, 0.317 mmol, 1.0 equiv) and CH<sub>2</sub>Cl<sub>2</sub> (3 mL) at 23 °C, followed by DMF (a few drops) and oxalyl chloride (136 μL, 1.59 mmol, 5.0 equiv). The reaction mixture was stirred for 2 h at 23 °C, then heated to reflux in a pre-heated oil bath and stirred for additional 5 min before it was directly concentrated under reduced pressure. The resulting <sup>18</sup>O-benzoyl chloride was used directly in the subsequent reaction without further purification.

To an oven-dried round-bottom flask equipped with a stir bar and septum were added *N*-hydroxyindole **1a** (72.9 mg, 0.311 mmol, 1.0 equiv) and CH<sub>2</sub>Cl<sub>2</sub> (10 mL) at 23 °C, followed by the crude benzoyl chloride and Et<sub>3</sub>N (56 μL, 0.402 mmol, 1.3 equiv). The resulting mixture was stirred for 2 h, before it was cooled to 23 °C and quenched with H<sub>2</sub>O (10 mL). The layers were separated, and the aqueous layer was extracted with CH<sub>2</sub>Cl<sub>2</sub> (3 × 10 mL). The combined organic layer was washed with brine (1 × 10 mL), dried over anhydrous MgSO<sub>4</sub>, filtered, and concentrated under reduced pressure. The resulting residue was purified by flash column chromatography (silica gel, hexanes:EtOAc = 1:0 → 7:3) to afford the product (107 mg, 79%) as a pale pink oil.

*R<sub>f</sub>* = 0.70 (silica gel, hexanes:EtOAc = 1:1); <sup>1</sup>H NMR (500 MHz, CDCl<sub>3</sub>): δ 8.47 (dd, *J* = 6.5, 2.2 Hz, 1H), 8.18 (ddd, *J* = 8.7, 4.7, 2.2 Hz, 1H), 7.64 (d, *J* = 7.8 Hz, 1H), 7.35 – 7.20 (m, 5H), 7.10 (s, 1H), 4.89 (s, 1H), 3.70 (s, 3H), 3.56 (q, *J* = 6.7 Hz, 2H), 2.99 (t, *J* = 6.9 Hz, 2H); <sup>13</sup>C NMR (126 MHz, CDCl<sub>3</sub>): δ 163.2 (d, *J* = 257.8 Hz), 162.9, 157.2, 136.2, 136.1 (d, *J* =

2.1 Hz), 131.6 (d,  $J = 8.8$  Hz), 125.2, 124.3, 124.1 (d,  $J = 3.7$  Hz), 123.8, 121.4, 119.5, 117.3 (d,  $J = 23.1$  Hz), 112.8, 110.3 (d,  $J = 21.9$  Hz), 109.3, 52.2, 41.0, 25.9;  **$^{19}\text{F}$  NMR** (471 MHz,  $\text{CDCl}_3$ ):  $\delta$  -98.1; **HRMS** calcd. for  $\text{C}_{19}\text{H}_{17}\text{BrFN}_2\text{O}_3^{18}\text{O}^+$   $[\text{M} + \text{H}]^+$  437.0393, found 437.0388; **Isotopic Incorporation:**  $[\text{M}+2]$  89.5%,  $[\text{M}+0]$  11.5%.

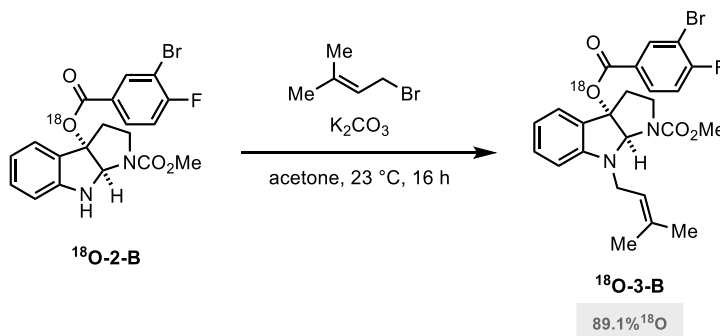
**Methyl 3a-((3-bromo-4-fluorobenzoyl)oxy)-3,3a,8,8a-tetrahydropyrrolo[2,3-b]indole-1(2H)-carboxylate (<sup>18</sup>O-2-B)**



To an oven-dried round-bottom flask equipped with a stir bar and septum were added <sup>18</sup>O-1-B (80.0 mg, 0.183 mmol, 1.0 equiv) and toluene (4 mL) at 23 °C. The resulting mixture was heated to 70 °C in a pre-heated oil bath and stirred for 8 h, before it was cooled to 23 °C and directly concentrated under reduced pressure. The resulting residue was purified directly by flash column chromatography (silica gel, hexanes:EtOAc = 1:0 → 7:3) to afford the product (47.3 mg, 59%) as a pale pink oil.

$R_f$ =0.70 (silica gel, hexanes:EtOAc = 1:1); <sup>1</sup>H NMR (500 MHz, CDCl<sub>3</sub>, 60:40 mixture of rotamers): δ 8.20 (dd,  $J$  = 6.6, 2.1 Hz, 1H), 7.95 – 7.88 (m, 1H), 7.60 and 7.54 (d,  $J$  = 7.5 Hz, 1H), 7.20 (t,  $J$  = 7.7 Hz, 1H), 7.14 (t,  $J$  = 8.3 Hz, 1H), 6.80 (q,  $J$  = 6.9 Hz, 1H), 6.69 (d,  $J$  = 7.9 Hz, 1H), 5.75 (d,  $J$  = 3.5 Hz, 1H), 3.93 and 3.81 (t,  $J$  = 9.7 Hz, 1H), 3.80 and 3.73 (s, 2H), 3.22 (ddd,  $J$  = 17.2, 8.5, 4.9 Hz, 1H), 3.07 and 2.98 (dd,  $J$  = 12.8, 6.2 Hz, 1H), 2.69 (tdd,  $J$  = 12.0, 8.7, 3.2 Hz, 1H); <sup>13</sup>C NMR (126 MHz, CDCl<sub>3</sub>): δ 163.4, 163.3, 155.7, 151.1, 150.8, 135.6, 131.4, 131.1 (d,  $J$  = 8.5 Hz), 127.9, 127.8, 126.7, 126.2, 125.5, 119.8, 119.6, 116.6 (d,  $J$  = 23.0 Hz), 110.5, 110.4, 109.4 (d,  $J$  = 21.7 Hz), 95.1, 93.8, 80.4, 79.6, 53.0, 52.7, 45.6, 35.8, 35.7; <sup>19</sup>F NMR (471 MHz, CDCl<sub>3</sub>): δ -99.3 (q,  $J$  = 7.1 Hz), -99.4 (q,  $J$  = 7.2 Hz); HRMS calcd. for C<sub>19</sub>H<sub>17</sub>BrFN<sub>2</sub>O<sub>3</sub><sup>18</sup>O<sup>+</sup> [M + H]<sup>+</sup> 437.0393, found 437.0397; **Isotopic Incorporation:** [M+2] 89.7%, [M+0] 11.3%.

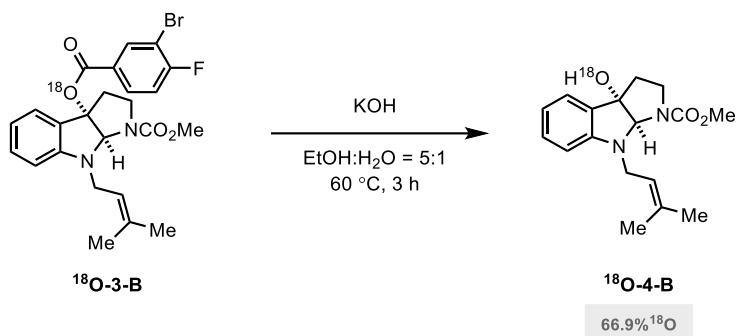
**Methyl 3a-((3-bromo-4-fluorobenzoyl)oxy)-8-(3-methylbut-2-en-1-yl)-3,3a,8,8a-tetrahydropyrrolo[2,3-b]indole-1(2H)-carboxylate (<sup>18</sup>O-3-B)**



To an oven-dried round-bottom flask equipped with a stir bar and septum were added <sup>18</sup>O-2-B (47.3 mg, 0.108 mmol, 1.0 equiv) and acetone (5 mL) at 23 °C, followed by 1-bromo-3-methyl-2-butene (19 μL, 0.162 mmol, 1.5 equiv) and K<sub>2</sub>CO<sub>3</sub> (44.2 mg, 0.320 mmol, 3.0 equiv). The resulting mixture was stirred for 16 h, before it was directly concentrated under reduced pressure and re-dissolved in CH<sub>2</sub>Cl<sub>2</sub> (5 mL) and H<sub>2</sub>O (5 mL). The layers were separated, and the aqueous layer was extracted with CH<sub>2</sub>Cl<sub>2</sub> (3 × 5 mL). The combined organic layer was washed with brine (1 × 5 mL), dried over anhydrous MgSO<sub>4</sub>, filtered, and concentrated under reduced pressure. The resulting residue was purified by flash column chromatography (silica gel, hexanes:EtOAc = 1:0 → 8:2) to afford the product (44.9 mg, 82%) as a pale pink oil.

*R<sub>f</sub>*=0.50 (silica gel, hexanes:EtOAc = 7:3); <sup>1</sup>H NMR (500 MHz, CDCl<sub>3</sub>, 55:45 mixture of rotamers): δ 8.18 (dd, *J* = 6.7, 2.1 Hz, 1H), 7.93 (ddd, *J* = 8.8, 4.8, 2.2 Hz, 1H), 7.49 and 7.44 (s, 1H), 7.21 (td, *J* = 7.8, 1.3 Hz, 1H), 7.14 (t, *J* = 8.4 Hz, 1H), 6.71 (t, *J* = 7.4 Hz, 1H), 6.54 (br s, 1H), 5.87 and 5.80 (s, 1H), 5.23 (t, *J* = 6.2 Hz, 1H), 4.29 – 4.19 (m, 1H), 4.12 – 4.00 (m, 2H), 3.97 – 3.90 (m, 1H), 3.78 and 3.75 (s, 3H), 3.16 (br s, 1H), 2.91 – 2.76 (m, 1H), 2.64 (td, *J* = 12.1, 8.4 Hz, 1H), 1.78 (d, *J* = 12.9 Hz, 3H), 1.72 (s, 3H); <sup>13</sup>C NMR (126 MHz, CDCl<sub>3</sub>): δ 163.3, 163.2, 161.3, 155.9, 155.1, 152.1, 135.6 (d, *J* = 1.1 Hz), 135.0, 134.5, 131.3, 131.1 (d, *J* = 8.4 Hz), 128.0, 126.5, 126.3, 126.0, 125.5, 121.1, 120.8, 118.3, 116.6 (d, *J* = 23.0 Hz), 109.4 (d, *J* = 21.8 Hz), 108.4, 108.0, 95.3, 94.3, 84.9, 84.3, 52.8, 45.4, 45.2, 45.0, 37.7, 37.6, 26.0, 18.3; <sup>19</sup>F NMR (471 MHz, CDCl<sub>3</sub>): δ -99.4, -99.5; HRMS calcd. for C<sub>24</sub>H<sub>25</sub>BrFN<sub>2</sub>O<sub>3</sub><sup>18</sup>O<sup>+</sup> [M + H]<sup>+</sup> 505.1019, found 505.1017; **Isotopic Incorporation:** [M+2] 89.1%, [M+0] 11.9%.

**Methyl 3a-hydroxy-8-(3-methylbut-2-en-1-yl)-3,3a,8,8a-tetrahydropyrrolo[2,3-b]indole-1(2H)-carboxylate (<sup>18</sup>O-4-B)**



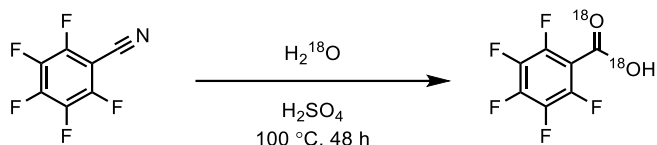
To an oven-dried round-bottom flask equipped with a stir bar and septum were added <sup>18</sup>O-3-B (44.9 mg, 0.089 mmol, 1.0 equiv) and EtOH: H<sub>2</sub>O (5:1, 6 mL) at 23 °C, followed by KOH (7.5 mg, 0.134 mmol, 1.5 equiv). The resulting mixture was heated to 60 °C in a pre-heated oil bath and stirred for 3 h, before it was cooled to 23 °C and diluted with CH<sub>2</sub>Cl<sub>2</sub> (5 mL) and H<sub>2</sub>O (5 mL). The layers were separated, and the aqueous layer was extracted with CH<sub>2</sub>Cl<sub>2</sub> (3 × 5 mL). The combined organic layer was washed with brine (1 × 5 mL), dried over anhydrous MgSO<sub>4</sub>, filtered, and concentrated under reduced pressure. The resulting residue was purified by flash column chromatography (silica gel, hexanes:EtOAc = 1:0 → 7:3) to afford the product (19.1 mg, 71%) as a pale yellow oil.

*R<sub>f</sub>*=0.44 (silica gel, hexanes:EtOAc = 1:1); <sup>1</sup>H NMR (400 MHz, CDCl<sub>3</sub>, 50:50 mixture of rotamers): δ 7.25 (d, *J* = 8.4 Hz, 1H), 7.20 (t, *J* = 7.8 Hz, 1H), 6.74 (t, *J* = 7.4 Hz, 1H), 6.49 (s, 1H), 5.38 and 5.30 (s, 1H), 5.16 (s, 1H), 4.22 – 4.08 and 4.07 – 3.93 (m, 1H), 4.07 – 3.93 (m, 1H), 4.07 – 3.93 and 3.87 – 3.79 (m, 1H), 3.73 (s, 3H), 3.23 – 3.04 (m, 2H), 2.41 – 2.23 (m, 2H), 1.75 (d, *J* = 11.7 Hz, 3H), 1.69 (s, 3H); <sup>13</sup>C NMR (101 MHz, CDCl<sub>3</sub>): δ 150.4, 135.2, 130.8, 130.7, 130.5, 123.4, 123.2, 120.4, 120.3, 118.2, 108.4, 108.0, 87.7, 87.5, 86.9, 52.7, 45.8, 44.9, 44.4, 38.4, 25.9, 18.3; HRMS calcd. for C<sub>17</sub>H<sub>23</sub>N<sub>2</sub>O<sub>2</sub><sup>18</sup>O<sup>+</sup> [M + H]<sup>+</sup> 305.1746, found 305.1740; **Isotopic Incorporation:** [M+2] 66.9%, [M+0] 33.1%.



### 5.1.1.3 Pentafluorobenzoyl substituent

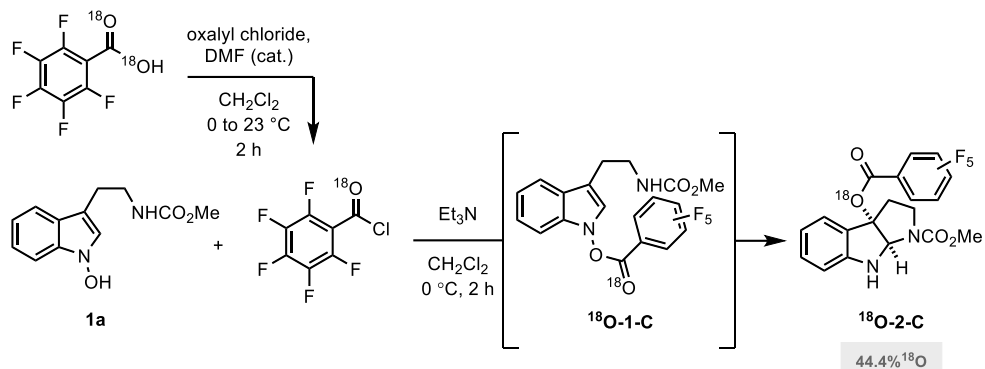
#### <sup>18</sup>O-2,3,4,5,6-Pentafluorobenzoic acid



To an oven-dried heavy-wall pressure tube equipped with a stir bar and rubber septum were added 2,3,4,5,6-pentafluorobenzonitrile (965 mg, 5.00 mmol, 1.0 equiv) and sulfuric acid (0.5 mL) at 23 °C, followed by H<sub>2</sub><sup>18</sup>O (500 μL, 25.0 mmol, 5.0 equiv). The rubber septum was replaced with a Teflon screw cap under N<sub>2</sub> and the resulting mixture was heated to 100 °C in a pre-heated oil bath. The reaction mixture was stirred for 48 h and cooled to 23 °C before it was diluted with CH<sub>2</sub>Cl<sub>2</sub> (20 mL). The layers were separated, and the aqueous layer was extracted with CH<sub>2</sub>Cl<sub>2</sub> (3 × 20 mL). The combined organic layer was dried over anhydrous MgSO<sub>4</sub>, filtered, and concentrated under reduced pressure to afford <sup>18</sup>O-pentafluorobenzoic acid (248 mg, 23%) as a white-beige solid. The resulting residue was used directly in the subsequent reaction without further purification.

*R<sub>f</sub>* = 0.10 (silica gel, hexanes:EtOAc = 9:1); <sup>13</sup>C NMR (126 MHz, CDCl<sub>3</sub>): δ 164.0, 147.6 – 145.2 (dm, *J* = 263.1 Hz), 145.5 – 143.0 (dm, d, *J* = 256.3 Hz), 139.2 – 136.7 (dm, d, *J* = 256.5 Hz), 106.8 (td, *J* = 14.4, 4.1 Hz); <sup>19</sup>F NMR (471 MHz, CDCl<sub>3</sub>): δ -136.2 (dt, *J* = 19.5, 5.5 Hz), -146.1 (td, *J* = 20.9, 5.9 Hz), -159.8 – -159.9 (m); HRMS calcd. for C<sub>7</sub>F<sub>5</sub><sup>18</sup>O<sub>2</sub><sup>-</sup> [M – H]<sup>-</sup> 214.9909, found 214.9910; **Isotopic Incorporation:** [M+4] 19.5%, [M+2] 49.6%, [M+0] 30.9%.

**Methyl 3a-((perfluorobenzoyl)oxy)-3,3a,8,8a-tetrahydropyrrolo[2,3-b]indole-1(2H)-carboxylate (<sup>18</sup>O-2-C)**



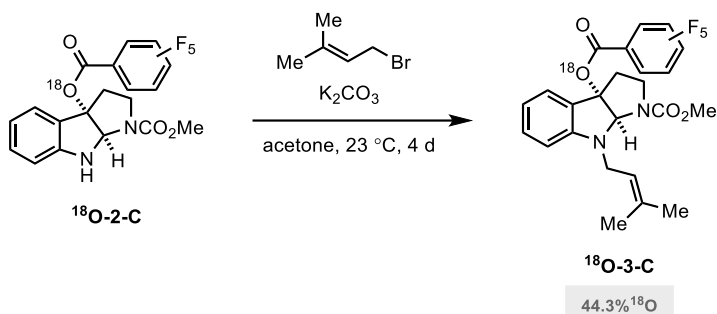
To an oven-dried round-bottom flask equipped with a stir bar and septum were added <sup>18</sup>O-2,3,4,5,6-pentafluorobenzoic acid (50 mg, 0.231 mmol, 1.04 equiv) and CH<sub>2</sub>Cl<sub>2</sub> (3 mL) at 23 °C. The resulting solution was cooled to 0 °C, and DMF (a few drops) and oxalyl chloride (19 μL, 0.222 mmol, 1.0 equiv) were successively added to the solution. The reaction mixture was warmed up to 23 °C and stirred for 2 h, before it was directly concentrated under reduced pressure. The resulting <sup>18</sup>O-benzoyl chloride was used directly in the subsequent reaction without further purification.

To an oven-dried round-bottom flask equipped with a stir bar and septum were added *N*-hydroxyindole **1a** (51.5 mg, 0.220 mmol, 1.0 equiv) and CH<sub>2</sub>Cl<sub>2</sub> (5 mL) at 23 °C. The solution was then cooled to 0 °C and the crude benzoyl chloride and Et<sub>3</sub>N (40 μL, 0.287 mmol, 1.3 equiv) was added to the solution. The reaction mixture was warmed up to 23 °C and stirred for 2 h, before it was quenched with H<sub>2</sub>O (5 mL). The layers were separated, and the aqueous layer was extracted with CH<sub>2</sub>Cl<sub>2</sub> (3 × 5 mL). The combined organic layer was washed with brine (1 × 5 mL), dried over anhydrous MgSO<sub>4</sub>, filtered, and concentrated under reduced pressure. The resulting residue was purified by flash column chromatography (silica gel, hexanes:EtOAc = 1:0 → 7:3) to afford the product (45.2 mg, 47%) as a pale yellow oil.

*R<sub>f</sub>* = 0.56 (silica gel, hexanes:EtOAc = 1:1); <sup>1</sup>H NMR (400 MHz, CDCl<sub>3</sub>, 60:40 mixture of rotamers): δ 7.56 and 7.53 (d, *J* = 8.7 Hz, 1H), 7.22 (t, *J* = 7.7 Hz, 1H), 6.83 (q, *J* = 7.2, 6.7 Hz, 1H), 6.69 (d, *J* = 8.0 Hz, 1H), 5.71 (d, *J* = 3.3 Hz, 1H), 3.92 and 3.82 (t, *J* = 9.7 Hz, 1H), 3.80 and 3.73 (s, 3H), 3.25 – 3.16 (m, 1H), 3.03 and 2.96 (dd, *J* = 12.6, 6.2 Hz, 1H), 2.70 (q, *J* = 10.7 Hz, 1H); <sup>13</sup>C NMR (101 MHz, CDCl<sub>3</sub>): δ 157.8, 155.6, 154.8, 151.2, 151.0, 147.2

– 144.0 (dm,  $J = 262.7$  Hz), 145.1 – 141.9 (dm,  $J = 260.2$  Hz), 139.5 – 136.1 (dm,  $J = 257.6$  Hz), 131.7, 126.4, 126.1, 124.8, 124.7, 122.6, 120.5, 120.0, 119.7, 110.7, 110.5, 108.2 (t,  $J = 15.7$  Hz), 96.6, 95.4, 80.1, 79.4, 53.0, 52.8, 45.5, 35.7, 35.6;  **$^{19}\text{F}$  NMR** (376 MHz,  $\text{CDCl}_3$ ):  $\delta$   $\delta$  –139.6 (dp,  $J = 17.0, 5.8$  Hz), –149.6 (dt,  $J = 57.4, 20.7, 4.8$  Hz), –161.8 – –162.0 (m); **HRMS** calcd. for  $\text{C}_{19}\text{H}_{14}\text{F}_5\text{N}_2\text{O}_3^{18}\text{O}^+$   $[\text{M} + \text{H}]^+$  431.0911, found 431.0907; **Isotopic Incorporation:**  $[\text{M}+2]$  44.4%,  $[\text{M}+0]$  55.6%.

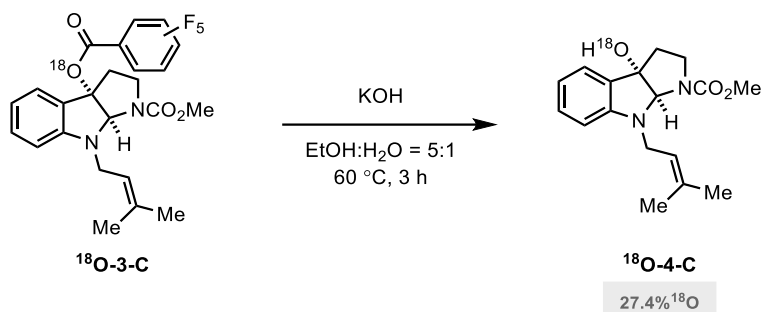
**Methyl 8-(3-methylbut-2-en-1-yl)-3a-((perfluorobenzoyl)oxy)-3,3a,8,8a-tetrahydropyrrolo[2,3-b]indole-1(2H)-carboxylate (<sup>18</sup>O-3-C)**



To an oven-dried round-bottom flask equipped with a stir bar and septum were added <sup>18</sup>O-2-C (45.2 mg, 0.105 mmol, 1.0 equiv) and acetone (3 mL) at 23 °C, followed by 1-bromo-3-methyl-2-butene (37  $\mu$ L, 0.315 mmol, 3.0 equiv) and K<sub>2</sub>CO<sub>3</sub> (87.0 mg, 0.629 mmol, 6.0 equiv). The resulting mixture was stirred for 4 d, before it was directly concentrated under reduced pressure and re-dissolved in CH<sub>2</sub>Cl<sub>2</sub> (5 mL) and H<sub>2</sub>O (5 mL). The layers were separated and the aqueous layer was extracted with CH<sub>2</sub>Cl<sub>2</sub> (3  $\times$  5 mL). The combined organic layer was washed with brine (1  $\times$  5 mL), dried over anhydrous MgSO<sub>4</sub>, filtered, and concentrated under reduced pressure. The resulting residue was purified by flash column chromatography (silica gel, hexanes:EtOAc = 1:0  $\rightarrow$  8:2) to afford the product (43.1 mg, 82%) as a pale yellow oil.

*R<sub>f</sub>*=0.66 (silica gel, hexanes:EtOAc = 1:1); <sup>1</sup>H NMR (500 MHz, CDCl<sub>3</sub>, 60:40 mixture of rotamers):  $\delta$  7.46 (d, *J* = 7.6 Hz, 1H), 7.22 (t, *J* = 7.9 Hz, 1H), 6.74 (t, *J* = 7.5 Hz, 1H), 6.53 (d, *J* = 7.7 Hz, 1H), 5.83 and 5.76 (s, 1H), 5.20 (s, 1H), 4.27 – 4.23 and 4.10 – 4.08 (m, 1H), 4.05 – 3.89 (m, 3H), 3.78 and 3.75 (s, 3H), 3.26 – 3.06 (m, 1H), 2.92 – 2.75 (m, 1H), 2.72 – 2.56 (m, 1H), 1.76 (s, 3H), 1.69 (s, 3H); <sup>13</sup>C NMR (126 MHz, CDCl<sub>3</sub>):  $\delta$  157.6, 155.8, 155.0, 152.1, 146.9 – 144.4 (dm, *J* = 264.7 Hz), 144.6 – 142.0 (dm, *J* = 260.6 Hz), 139.2 – 136.4 (dm, *J* = 250.5 Hz), 135.2, 134.7, 131.6, 128.2, 125.7, 125.6, 120.9, 120.5, 118.6, 108.7, 108.3, 97.0, 95.9, 84.7, 84.2, 52.9, 45.6, 45.5, 45.1, 44.9, 38.2, 37.6, 37.6, 25.8, 18.2; <sup>19</sup>F NMR (471 MHz, CDCl<sub>3</sub>):  $\delta$  –137.4 (dq, *J* = 17.5, 5.8 Hz), –137.8 (tdd, *J* = 26.9, 12.3, 7.0 Hz), –148.0 (dt, *J* = 43.5, 20.8 Hz), –148.2 (ddd, *J* = 25.5, 13.0, 4.7 Hz), –160.2 – –160.3 (m), –160.4 – –160.5 (m); HRMS calcd. for C<sub>24</sub>H<sub>22</sub>F<sub>5</sub>N<sub>2</sub>O<sub>3</sub><sup>18</sup>O<sup>+</sup> [M + H]<sup>+</sup> 499.1537, found 499.1535; **Isotopic Incorporation:** [M+2] 44.3%, [M+0] 55.7%.

**Methyl 3a-hydroxy-8-(3-methylbut-2-en-1-yl)-3,3a,8,8a-tetrahydropyrrolo[2,3-b]indole-1(2H)-carboxylate (<sup>18</sup>O-4-C)**

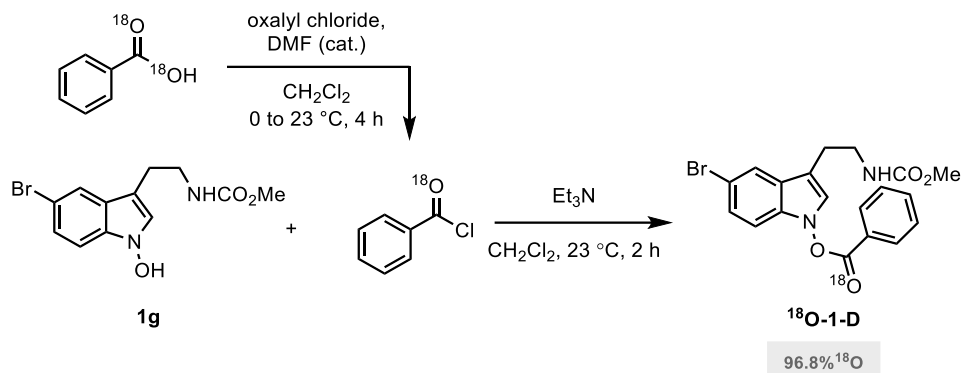


To an oven-dried round-bottom flask equipped with a stir bar and septum were added <sup>18</sup>O-3-C (43.1 mg, 0.086 mmol, 1.0 equiv) and EtOH: H<sub>2</sub>O (5:1, 4 mL) at 23 °C, followed by KOH (7.0 mg, 0.125 mmol, 1.5 equiv). The resulting mixture was heated to 60 °C in a pre-heated oil bath and stirred for 3 h, before it was cooled to 23 °C and diluted with CH<sub>2</sub>Cl<sub>2</sub> (5 mL) and H<sub>2</sub>O (5 mL). The layers were separated, and the aqueous layer was extracted with CH<sub>2</sub>Cl<sub>2</sub> (3 × 5 mL). The combined organic layer was washed with brine (1 × 5 mL), dried over anhydrous MgSO<sub>4</sub>, filtered, and concentrated under reduced pressure. The resulting residue was purified by flash column chromatography (silica gel, hexanes:EtOAc = 1:0 → 7:3) to afford the product (18.1 mg, 69%) as a pale yellow oil.

*R<sub>f</sub>*=0.45 (silica gel, hexanes:EtOAc = 1:1); <sup>1</sup>H NMR (400 MHz, CDCl<sub>3</sub>, 50:50 mixture of rotamers): δ 7.25 (d, *J* = 8.4 Hz, 1H), 7.20 (t, *J* = 7.8 Hz, 1H), 6.74 (t, *J* = 7.4 Hz, 1H), 6.49 (s, 1H), 5.38 and 5.30 (s, 1H), 5.16 (s, 1H), 4.22 – 4.08 and 4.07 – 3.93 (m, 1H), 4.07 – 3.93 (m, 1H), 4.07 – 3.93 and 3.87 – 3.79 (m, 1H), 3.73 (s, 3H), 3.23 – 3.04 (m, 2H), 2.41 – 2.23 (m, 2H), 1.75 (d, *J* = 11.7 Hz, 3H), 1.69 (s, 3H); <sup>13</sup>C NMR (101 MHz, CDCl<sub>3</sub>): δ 150.4, 135.2, 130.8, 130.7, 130.5, 123.4, 123.2, 120.4, 120.3, 118.2, 108.4, 108.0, 87.7, 87.5, 86.9, 52.7, 45.8, 44.9, 44.4, 38.4, 25.9, 18.3; HRMS calcd. for C<sub>17</sub>H<sub>23</sub>N<sub>2</sub>O<sub>2</sub><sup>18</sup>O<sup>+</sup> [M + H]<sup>+</sup> 305.1746, found 305.1740; **Isotopic Incorporation:** [M+2] 27.4%, [M+0] 72.6%.

#### 5.1.1.4 Bromotryptamine with benzoyl substituent

##### 5-Bromo-3-(2-((methoxycarbonyl)amino)ethyl)-1H-indol-1-yl benzoate (<sup>18</sup>O-1-D)



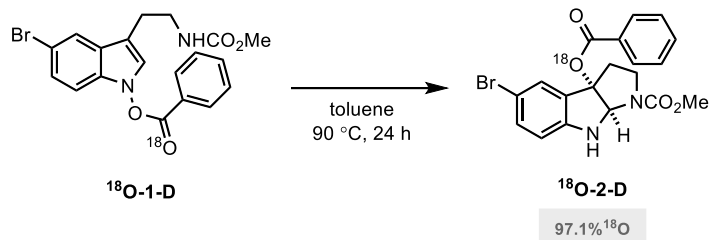
To an oven-dried two-neck round-bottom flask equipped with a stir bar, septum, and condenser were added <sup>18</sup>O- benzoic acid (31.8 mg, 0.252 mmol, 1.02 equiv), DMF (a few drops) and CH<sub>2</sub>Cl<sub>2</sub> (3 mL) at 23 °C. The resulting solution was cooled to 0 °C and oxalyl chloride (32 μL, 0.371 mmol, 1.5 equiv) was added dropwise. The reaction mixture was stirred for 4 h at 23 °C, before it was directly concentrated under reduced pressure. The resulting <sup>18</sup>O-benzoyl chloride was used directly in the subsequent reaction without further purification.

To an oven-dried round-bottom flask equipped with a stir bar and septum were added *N*-hydroxyindole **1g** (77.3 mg, 0.247 mmol, 1.0 equiv) and CH<sub>2</sub>Cl<sub>2</sub> (10 mL) at 23 °C, followed by the crude benzoyl chloride and Et<sub>3</sub>N (44 μL, 0.317 mmol, 1.3 equiv). The resulting mixture was stirred for 2 h, before it was quenched with H<sub>2</sub>O (10 mL). The layers were separated, and the aqueous layer was extracted with CH<sub>2</sub>Cl<sub>2</sub> (3 × 10 mL). The combined organic layer was washed with brine (1 × 10 mL), dried over anhydrous MgSO<sub>4</sub>, filtered, and concentrated under reduced pressure. The resulting residue was purified by flash column chromatography (silica gel, hexanes:EtOAc = 1:0 → 7:3) to afford the product (68.6 mg, 66%) as a pale yellow oil.

*R*<sub>f</sub>=0.48 (silica gel, hexanes:EtOAc = 6:4); <sup>1</sup>H NMR (400 MHz, CDCl<sub>3</sub>): δ 8.20 (d, *J* = 8.1 Hz, 2H), 7.76 – 7.68 (m, 1H), 7.73 (s, 1H), 7.57 (t, *J* = 7.5 Hz, 1H), 7.13 (d, *J* = 8.6 Hz, 2H), 7.10 (s, 1H), 3.69 (s, 3H), 3.51 (q, *J* = 6.7 Hz, 2H), 2.94 (t, *J* = 6.8 Hz, 2H); <sup>13</sup>C NMR (126 MHz, CDCl<sub>3</sub>): δ 164.7, 157.2, 134.9, 134.1, 130.4, 130.3, 129.2, 128.6, 126.5, 126.2, 125.0, 122.1, 114.2, 110.6, 52.3, 41.2, 25.7; HRMS calcd. for C<sub>19</sub>H<sub>18</sub>BrN<sub>2</sub>O<sub>3</sub><sup>18</sup>O<sup>+</sup> [M + H]<sup>+</sup>

419.0487, found 419.0496; **Isotopic Incorporation:** [M+2] 96.8%, [M+0] 3.2%.

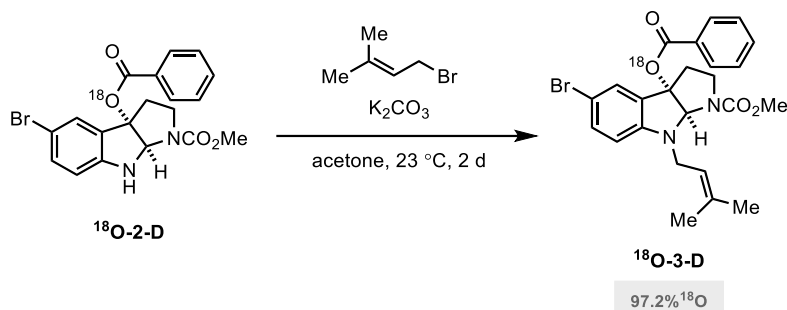
**Methyl 3a-(benzyloxy)-5-bromo-3,3a,8,8a-tetrahydropyrrolo[2,3-b]indole-1(2H)-carboxylate (<sup>18</sup>O-2-D)**



To an oven-dried round-bottom flask equipped with a stir bar and septum were added <sup>18</sup>O-1-D (68.6 mg, 0.164 mmol, 1.0 equiv) and toluene (3 mL) at 23 °C. The resulting mixture was heated to 90 °C in a pre-heated oil bath and stirred for 24 h, before it was cooled to 23 °C and directly concentrated under reduced pressure. The resulting residue was purified directly by flash column chromatography (silica gel, hexanes:EtOAc = 1:0 → 7:3) to afford the product (34.5 mg, 50%) as a pale yellow oil.

*R<sub>f</sub>*=0.48 (silica gel, hexanes:EtOAc = 6:4); <sup>1</sup>H NMR (500 MHz, CDCl<sub>3</sub>, 60:40 mixture of rotamers): δ 7.99 (dd, *J* = 8.2, 1.4 Hz, 2H), 7.72 and 7.63 (s, 1H), 7.56 (td, *J* = 7.6, 3.8 Hz, 2H), 7.43 (td, *J* = 7.9, 2.3 Hz, 1H), 7.30 – 7.26 (m, 1H), 6.56 (d, *J* = 8.4 Hz, 1H), 5.77 (s, 1H), 5.25 and 4.91 (s, 1H), 3.93 and 3.82 (t, *J* = 9.2 Hz, 1H), 3.79 and 3.73 (s, 3H), 3.24 (td, *J* = 10.9, 6.4 Hz, 1H), 3.01 and 2.90 (ddd, *J* = 12.9, 6.4, 1.8 Hz, 2H), 2.70 (ddd, *J* = 12.9, 10.9, 8.6 Hz, 1H); <sup>13</sup>C NMR (126 MHz, CDCl<sub>3</sub>): δ 165.4, 155.7, 154.8, 150.0, 149.7, 133.9, 133.6, 133.5, 129.9, 129.5, 128.9, 128.6, 128.3, 128.1, 111.8, 111.7, 111.2, 110.9, 94.0, 92.7, 80.7, 79.9, 53.0, 52.8, 45.5, 45.4, 36.1, 35.9; **HRMS** calcd. for C<sub>19</sub>H<sub>18</sub>BrN<sub>2</sub>O<sub>3</sub><sup>18</sup>O<sup>+</sup> [M + H]<sup>+</sup> 419.0487, found 419.0494; **Isotopic Incorporation:** [M+2] 97.1%, [M+0] 2.9%.

**Methyl 3a-(benzoyloxy)-5-bromo-8-(3-methylbut-2-en-1-yl)-3,3a,8,8a-tetrahydropyrrolo[2,3-b]indole-1(2H)-carboxylate (<sup>18</sup>O-3-D)**

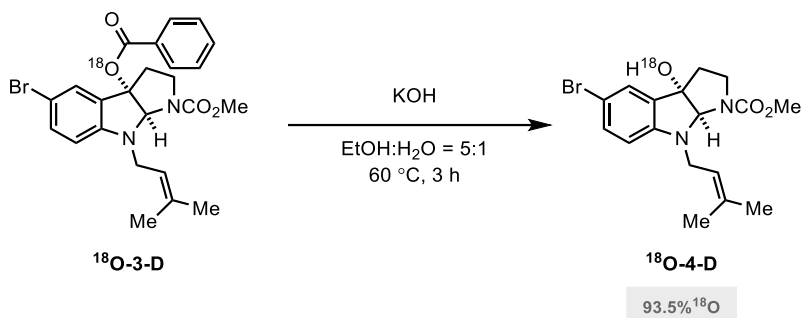


To an oven-dried round-bottom flask equipped with a stir bar and septum were added <sup>18</sup>O-2-D (34.5 mg, 0.082 mmol, 1.0 equiv) and acetone (4 mL) at 23 °C, followed by 1-bromo-3-methyl-2-butene (28 μL, 0.246 mmol, 3.0 equiv) and K<sub>2</sub>CO<sub>3</sub> (67.7 mg, 0.490 mmol, 6.0 equiv). The resulting mixture was stirred for 2 d, before it was directly concentrated under reduced pressure and re-dissolved in CH<sub>2</sub>Cl<sub>2</sub> (5 mL) and H<sub>2</sub>O (5 mL). The layers were separated, and the aqueous layer was extracted with CH<sub>2</sub>Cl<sub>2</sub> (3 × 10 mL). The combined organic layer was washed with brine (1 × 10 mL), dried over anhydrous MgSO<sub>4</sub>, filtered, and concentrated under reduced pressure. The resulting residue was purified by flash column chromatography (silica gel, hexanes:EtOAc = 1:0 → 8:2) to afford the product (29.0 mg, 73%) as a pale yellow oil.

*R<sub>f</sub>*=0.69 (silica gel, hexanes:EtOAc = 7:3); <sup>1</sup>H NMR (500 MHz, CDCl<sub>3</sub>, 50:50 mixture of rotamers): δ 7.98 (d, *J* = 7.6 Hz, 1H), 7.63 – 7.48 (m, 2H), 7.42 (t, *J* = 7.7 Hz, 2H), 7.28 (d, *J* = 2.1 Hz, 2H), 6.40 and 6.39 (s, 1H), 5.90 and 5.84 (s, 1H), 5.21 (s, 1H), 4.26 – 4.21 and 4.14 – 4.07 (m, 1H), 4.04 – 3.92 (m, 2H), 3.75 (s, 3H), 3.23 – 3.08 (m, 1H), 2.87 – 2.71 (m, 1H), 2.65 (q, *J* = 11.2, 10.5 Hz, 1H), 1.76 (d, *J* = 13.0 Hz, 3H); <sup>13</sup>C NMR (126 MHz, CDCl<sub>3</sub>): 165.2, 151.0, 133.7, 133.5, 130.1, 129.9, 129.1, 129.0, 128.5, 120.7, 120.5, 109.7, 109.5, 109.3, 93.9, 92.9, 85.2, 84.6, 52.9, 45.5, 45.2, 44.8, 37.8, 25.9, 18.2; **HRMS** calcd. for C<sub>24</sub>H<sub>26</sub>BrN<sub>2</sub>O<sub>3</sub><sup>18</sup>O<sup>+</sup> [M + H]<sup>+</sup> 487.1113, found 487.1107; **Isotopic Incorporation:** [M+2] 97.2%, [M+0] 2.8%.



**Methyl 5-bromo-3a-hydroxy-8-(3-methylbut-2-en-1-yl)-3,3a,8,8a-tetrahydropyrrolo-[2,3-b]indole-1(2H)-carboxylate (<sup>18</sup>O-4-D)**

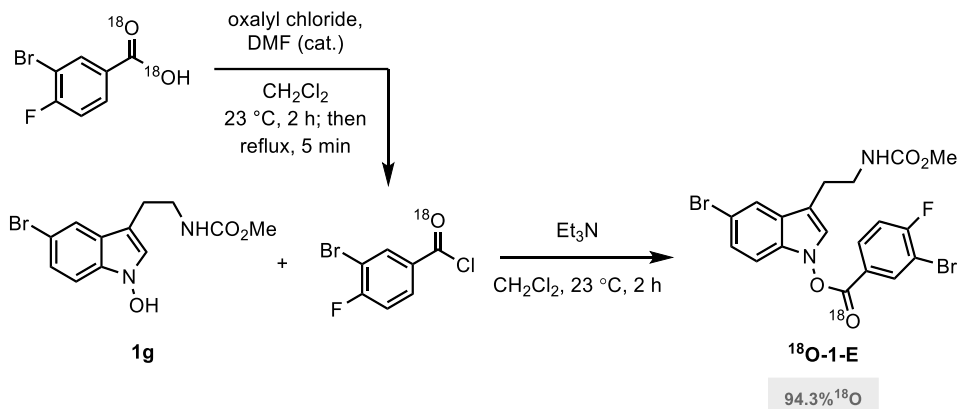


To an oven-dried round-bottom flask equipped with a stir bar and septum were added <sup>18</sup>O-3-D (29.0 mg, 0.060 mmol, 1.0 equiv) and EtOH: H<sub>2</sub>O (5:1, 3 mL) at 23 °C, followed by KOH (5.0 mg, 0.090 mmol, 1.5 equiv). The resulting mixture was heated to 60 °C in a pre-heated oil bath and stirred for 3 h, before it was cooled to 23 °C and diluted with CH<sub>2</sub>Cl<sub>2</sub> (2 mL) and H<sub>2</sub>O (2 mL). The layers were separated, and the aqueous layer was extracted with CH<sub>2</sub>Cl<sub>2</sub> (3 × 3 mL). The combined organic layer was washed with brine (1 × 3 mL), dried over anhydrous MgSO<sub>4</sub>, filtered, and concentrated under reduced pressure. The resulting residue was purified by flash column chromatography (silica gel, hexanes:EtOAc = 1:0 → 7:3) to afford the product (15.0 mg, 65%) as a pale yellow oil.

*R<sub>f</sub>*=0.55 (silica gel, hexanes:EtOAc = 1:1); <sup>1</sup>H NMR (400 MHz, CDCl<sub>3</sub>, 55:45 mixture of rotamers): δ 7.32 (d, *J* = 2.1 Hz, 1H), 7.27 (d, *J* = 2.1 Hz, 1H), 6.35 (t, *J* = 8.1 Hz, 1H), 5.39 and 5.31 (s, 1H), 5.13 and 5.09 (s, 1H), 4.16 – 4.10 and 3.99 – 3.96 (m, 1H), 3.96 – 3.83 (m, 3H), 3.73 (s, 3H), 3.25 – 3.05 (m, 2H), 2.39 – 2.22 (m, 2H), 1.74 (d, *J* = 14.0 Hz, 3H), 1.69 (s, 3H); <sup>13</sup>C NMR (101 MHz, CDCl<sub>3</sub>): δ 149.3, 135.7, 135.4, 133.4, 133.3, 126.5, 126.4, 119.9, 119.8, 109.8, 109.5, 88.3, 87.8, 87.1, 52.8, 45.8, 44.8, 44.3, 38.5, 25.9; HRMS calcd. for C<sub>17</sub>H<sub>22</sub>BrN<sub>2</sub>O<sub>2</sub><sup>18</sup>O<sup>+</sup> [M + H]<sup>+</sup> 383.0851, found 383.0838; **Isotopic Incorporation:** [M+2] 93.5%, [M+0] 6.5%.

### 5.1.1.5 Bromotryptamine with 3-bromo-4-fluorobenzoyl substituent

#### 5-Bromo-3-(2-((methoxycarbonyl)amino)ethyl)-1H-indol-1-yl 3-bromo-4-fluorobenzoate (<sup>18</sup>O-1-E)



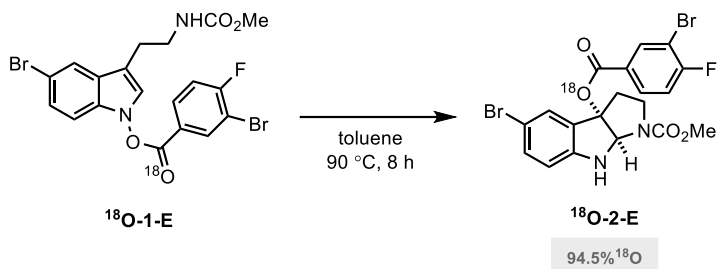
To an oven-dried two-neck round-bottom flask equipped with a stir bar, septum, and a reflux condenser were added <sup>18</sup>O-3-bromo-4-fluorobenzoic acid (60.0 mg, 0.269 mmol, 1.04 equiv) and CH<sub>2</sub>Cl<sub>2</sub> (3 mL) at 23 °C, followed by DMF (a few drops) and oxalyl chloride (111 μL, 1.29 mmol, 5.0 equiv). The reaction mixture was stirred for 2 h at 23 °C, then heated to reflux in a pre-heated oil bath and stirred for additional 5 min before it was directly concentrated under reduced pressure. The resulting <sup>18</sup>O-benzoyl chloride was used directly in the subsequent reaction without further purification.

To an oven-dried round-bottom flask equipped with a stir bar and septum were added *N*-hydroxyindole **1g** (80.8 mg, 0.258 mmol, 1.0 equiv) and CH<sub>2</sub>Cl<sub>2</sub> (10 mL) at 23 °C, followed by the crude benzoyl chloride and Et<sub>3</sub>N (47 μL, 0.337 mmol, 1.3 equiv). The resulting mixture was stirred for 2 h, before it was quenched with H<sub>2</sub>O (10 mL). The layers were separated, and the aqueous layer was extracted with CH<sub>2</sub>Cl<sub>2</sub> (3 × 20 mL). The combined organic layer was washed with brine (1 × 20 mL), dried over anhydrous MgSO<sub>4</sub>, filtered, and concentrated under reduced pressure. The resulting residue was purified by flash column chromatography (silica gel, hexanes:EtOAc = 1:0 → 7:3) to afford the product (77.2 mg, 58%) as a pale yellow oil.

*R*<sub>f</sub>=0.55 (silica gel, hexanes:EtOAc = 6:4); <sup>1</sup>H NMR (500 MHz, CDCl<sub>3</sub>): δ 8.43 (dd, *J* = 6.5, 2.2 Hz, 1H), 8.16 (ddd, *J* = 8.6, 4.6, 2.2 Hz, 1H), 7.73 (d, *J* = 1.8 Hz, 1H), 7.34 (dd, *J* = 8.6, 1.8 Hz, 1H), 7.31 (t, *J* = 8.3 Hz, 1H), 7.10 (d, *J* = 8.6 Hz, 1H), 7.08 (s, 1H), 4.80 (s, 1H), 3.68

(s, 3H), 3.51 (q,  $J = 6.8$  Hz, 2H), 2.93 (t,  $J = 6.8$  Hz, 2H);  $^{13}\text{C}$  NMR (126 MHz,  $\text{CDCl}_3$ ):  $\delta$  163.3 (d,  $J = 258.2$  Hz), 162.8, 157.2, 136.2, 134.4, 131.7 (d,  $J = 8.9$  Hz), 126.7, 125.1, 123.8 (d,  $J = 3.8$  Hz), 122.2, 117.5, 117.4 (d,  $J = 23.2$  Hz), 117.4, 114.5, 111.9, 110.6, 110.5, 110.3, 52.3, 41.1, 25.7;  $^{19}\text{F}$  NMR (471 MHz,  $\text{CDCl}_3$ ):  $\delta$  -95.8 (dd,  $J = 12.5, 5.7$  Hz); **HRMS** calcd. for  $\text{C}_{19}\text{H}_{15}\text{Br}_2\text{FN}_2\text{O}_3^{18}\text{ONa}^+$   $[\text{M} + \text{Na}]^+$  536.9317, found 536.9327; **Isotopic Incorporation:**  $[\text{M}+2]$  94.3%,  $[\text{M}+0]$  5.7%.

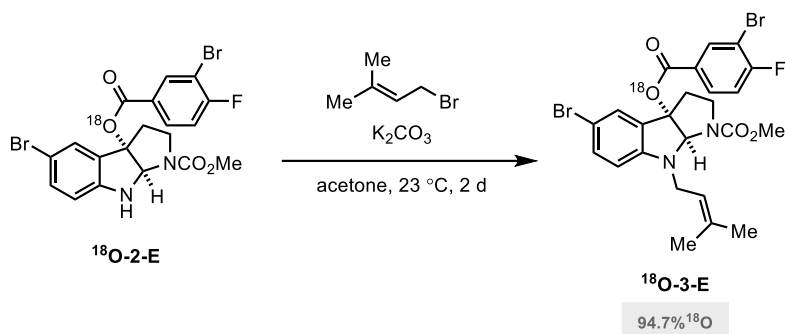
**Methyl 5-bromo-3a-((3-bromo-4-fluorobenzoyl)oxy)-3,3a,8,8a-tetrahydropyrrolo[2,3-b]indole-1(2H)-carboxylate (<sup>18</sup>O-2-E)**



To an oven-dried round-bottom flask equipped with a stir bar and septum were added <sup>18</sup>O-1-E (77.2 mg, 0.150 mmol, 1.0 equiv) and toluene (3 mL) at 23 °C. The resulting mixture was heated to 90 °C in a pre-heated oil bath and stirred for 8 h, before it was cooled to 23 °C and directly concentrated under reduced pressure. The resulting residue was purified directly by flash column chromatography (silica gel, hexanes:EtOAc = 1:0 → 7:3) to afford the product (42.6 mg, 55%) as a pale yellow oil.

*R<sub>f</sub>* = 0.55 (silica gel, hexanes:EtOAc = 6:4); <sup>1</sup>H NMR (500 MHz, CDCl<sub>3</sub>, 60:40 mixture of rotamers): δ 8.20 (dt, *J* = 6.5, 1.8 Hz, 1H), 7.98 – 7.89 (m, 1H), 7.69 and 7.63 (s, 1H), 7.29 (d, *J* = 8.4 Hz, 1H), 7.16 (t, *J* = 8.5 Hz, 1H), 6.57 (dd, *J* = 8.4, 1.4 Hz, 1H), 5.74 (d, *J* = 1.8 Hz, 1H), 5.27 and 4.91 (s, 1H), 3.93 and 3.82 (t, *J* = 9.8 Hz, 1H), 3.79 and 3.73 (s, 3H), 3.23 (q, *J* = 11.9, 10.8 Hz, 1H), 3.02 and 2.93 (dd, *J* = 13.2, 6.1 Hz, 1H), 2.67 (q, *J* = 10.9 Hz, 1H); <sup>13</sup>C NMR (126 MHz, CDCl<sub>3</sub>): δ 163.3, 162.4 (d, *J* = 254.9 Hz), 155.6, 154.7, 150.0, 149.8, 135.7, 134.1, 131.18 (d, *J* = 8.6 Hz), 129.5, 129.1, 127.7, 127.6, 127.5 (d, *J* = 3.4 Hz), 116.7 (d, *J* = 23.3 Hz), 111.9, 111.8, 111.2, 110.9, 109.6, 109.5, 94.4, 93.2, 80.6, 79.9, 53.1, 52.8, 45.5, 35.9, 35.8; <sup>19</sup>F NMR (471 MHz, CDCl<sub>3</sub>): δ -98.9 (q, *J* = 6.8 Hz), -99.0 (q, *J* = 6.9 Hz); HRMS calcd. for C<sub>19</sub>H<sub>16</sub>Br<sub>2</sub>FN<sub>2</sub>O<sub>3</sub><sup>18</sup>O<sup>+</sup> [M + H]<sup>+</sup> 514.9498, found 514.9486; **Isotopic Incorporation:** [M+2] 94.5%, [M+0] 5.5%.

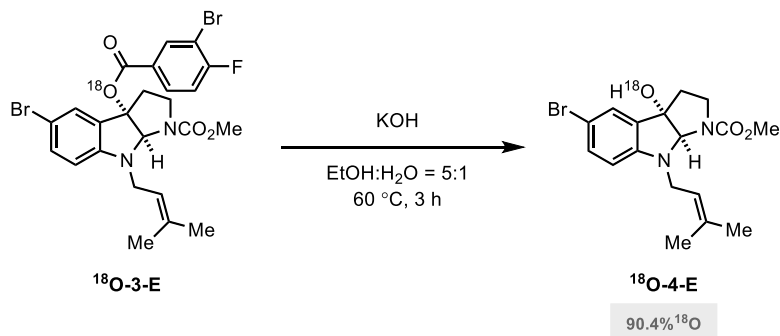
**Methyl 5-bromo-3a-((3-bromo-4-fluorobenzoyl)oxy)-8-(3-methylbut-2-en-1-yl)-3,3a,8,8a-tetrahydropyrrolo[2,3-b]indole-1(2H)-carboxylate (<sup>18</sup>O-3-E)**



To an oven-dried round-bottom flask equipped with a stir bar and septum were added <sup>18</sup>O-2-E (42.6 mg, 0.083 mmol, 1.0 equiv) and acetone (4 mL) at 23 °C, followed by 1-bromo-3-methyl-2-butene (29  $\mu$ L, 0.247 mmol, 3.0 equiv) and K<sub>2</sub>CO<sub>3</sub> (69.0 mg, 0.499 mmol, 6.0 equiv). The resulting mixture was stirred for 2 d, before it was directly concentrated under reduced pressure and re-dissolved in CH<sub>2</sub>Cl<sub>2</sub> (5 mL) and H<sub>2</sub>O (5 mL). The layers were separated, and the aqueous layer was extracted with CH<sub>2</sub>Cl<sub>2</sub> (3  $\times$  5 mL). The combined organic layer was washed with brine (1  $\times$  5 mL), dried over anhydrous MgSO<sub>4</sub>, filtered, and concentrated under reduced pressure. The resulting residue was purified by flash column chromatography (silica gel, hexanes:EtOAc = 1:0  $\rightarrow$  8:2) to afford the product (34.3 mg, 71%) as a pale yellow oil.

*R<sub>f</sub>* = 0.71 (silica gel, hexanes:EtOAc = 7:3); <sup>1</sup>H NMR (500 MHz, CDCl<sub>3</sub>, 60:40 mixture of rotamers):  $\delta$  8.18 (d, *J* = 6.1 Hz, 1H), 7.93 (s, 1H), 7.57 and 7.50 (s, 1H), 7.28 (d, *J* = 8.7 Hz, 1H), 7.16 (t, *J* = 8.3 Hz, 1H), 6.40 and 6.39 (s, 1H), 5.88 and 5.80 (s, 1H), 5.19 (s, 1H), 4.23 and 4.04 (dd, *J* = 15.8, 6.8 Hz, 1H), 4.13 – 3.92 (m, 3H), 3.77 and 3.75 (s, 3H), 3.24 – 3.05 (m, 1H), 2.89 – 2.71 (m, 1H), 2.61 (q, *J* = 10.3 Hz, 1H), 1.77 (d, *J* = 10.4 Hz, 3H); <sup>13</sup>C NMR (126 MHz, CDCl<sub>3</sub>): 163.0, 162.3 (d, *J* = 255.6 Hz), 161.3, 150.9, 135.5, 133.8, 131.0 (d, *J* = 8.6 Hz), 128.5, 128.4, 127.6, 120.4, 120.3, 118.2, 116.5 (d, *J* = 23.1 Hz), 109.5, 109.3, 94.4, 93.4, 84.9, 84.2, 64.5, 52.7, 45.2, 44.9, 44.7, 37.8, 25.8, 18.1, 18.0; <sup>19</sup>F NMR (471 MHz, CDCl<sub>3</sub>):  $\delta$  -99.0, -99.1; HRMS calcd. for C<sub>24</sub>H<sub>24</sub>Br<sub>2</sub>FN<sub>2</sub>O<sub>3</sub><sup>18</sup>O<sup>+</sup> [M + H]<sup>+</sup> 583.0124, found 583.0116; **Isotopic Incorporation:** [M+2] 94.7%, [M+0] 5.3%.

**Methyl 5-bromo-3a-hydroxy-8-(3-methylbut-2-en-1-yl)-3,3a,8,8a-tetrahydropyrrolo[2,3-b]indole-1(2H)-carboxylate (<sup>18</sup>O-4-E)**



To an oven-dried round-bottom flask equipped with a stir bar and septum were added <sup>18</sup>O-3-E (34.2 mg, 0.059 mmol, 1.0 equiv) and EtOH: H<sub>2</sub>O (5:1, 2 mL) at 23 °C, followed by KOH (5.0 mg, 0.089 mmol, 1.5 equiv). The resulting mixture was heated to 60 °C in a pre-heated oil bath and stirred for 3 h, before it was cooled to 23 °C and diluted with CH<sub>2</sub>Cl<sub>2</sub> (3 mL) and H<sub>2</sub>O (3 mL). The layers were separated, and the aqueous layer was extracted with CH<sub>2</sub>Cl<sub>2</sub> (3 × 3 mL). The combined organic layer was washed with brine (1 × 3 mL), dried over anhydrous MgSO<sub>4</sub>, filtered, and concentrated under reduced pressure. The resulting residue was purified by flash column chromatography (silica gel, hexanes:EtOAc = 1:0 → 7:3) to afford the product (15.6 mg, 69%) as a pale yellow oil.

*R<sub>f</sub>*=0.55 (silica gel, hexanes:EtOAc = 1:1); <sup>1</sup>H NMR (400 MHz, CDCl<sub>3</sub>, 55:45 mixture of rotamers): δ 7.32 (d, *J* = 2.1 Hz, 1H), 7.27 (d, *J* = 2.1 Hz, 1H), 6.35 (t, *J* = 8.1 Hz, 1H), 5.39 and 5.31 (s, 1H), 5.13 and 5.09 (s, 1H), 4.16 – 4.10 and 3.99 – 3.96 (m, 1H), 3.96 – 3.83 (m, 3H), 3.73 (s, 3H), 3.25 – 3.05 (m, 2H), 2.39 – 2.22 (m, 2H), 1.74 (d, *J* = 14.0 Hz, 3H), 1.69 (s, 3H); <sup>13</sup>C NMR (101 MHz, CDCl<sub>3</sub>): δ 149.3, 135.7, 135.4, 133.4, 133.3, 126.5, 126.4, 119.9, 119.8, 109.8, 109.5, 88.3, 87.8, 87.1, 52.8, 45.8, 44.8, 44.3, 38.5, 25.9; HRMS calcd. for C<sub>17</sub>H<sub>22</sub>BrN<sub>2</sub>O<sub>2</sub><sup>18</sup>O<sup>+</sup> [M + H]<sup>+</sup> 383.0851, found 383.0820; **Isotopic Incorporation:** [M+2] 90.4%, [M+0] 9.6%.

## 5.1.2. Determination of $^{18}\text{O}$ Saturation

### General information of HRMS

#### Reagents and Chemicals

MeCN (LC-MS grade),  $\text{H}_2\text{O}$  with 0.1% formic acid (LC-MS grade) were obtained from Samchun Chemical.

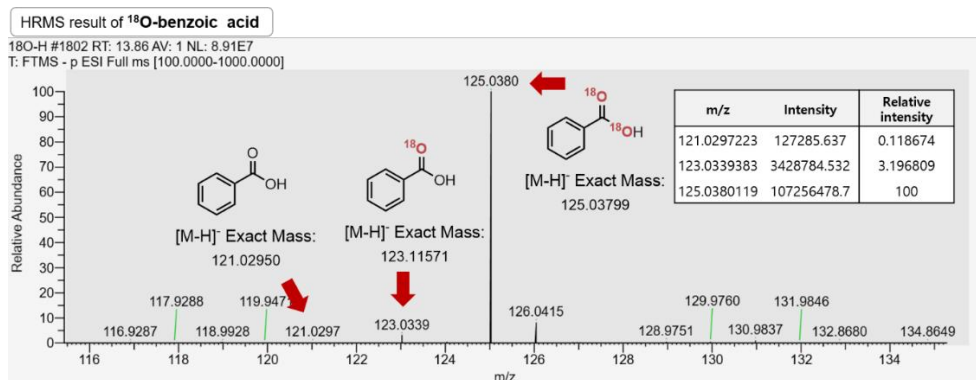
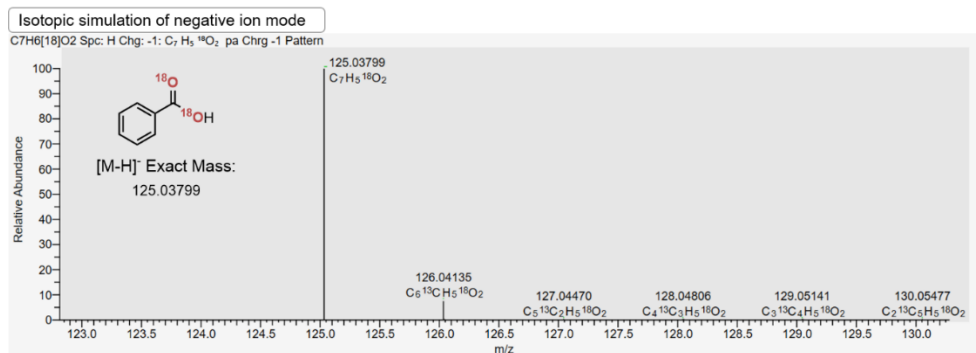
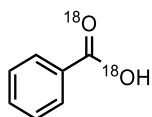
#### Instrumentation and Experimental

HRMS experiments were performed using a Thermo Scientific™ Orbitrap Exploris 120 equipped with a Hypersil GOLD™ C18 Selectivity HPLC column and Thermo Scientific™ mass spectrometer with Thermo Scientific™ Xcalibur™ software for instrument control and data processing. The aqueous mobile phase A is  $\text{H}_2\text{O}$  with 0.1% formic acid (v/v), and organic mobile phase B is MeCN with 0.1% formic acid (v/v). 20  $\mu\text{L}$  of samples were injected onto the column with a flow rate of 0.4 mL/min at 40 °C. The chromatographic conditions is as followed: 30 min method consisting with 5% B over 0.0–2.0 min, then a gradient of 5% B to 95% B over 2.0–20.0 min, then maintain 95% B over 20.0–24.9 min followed by a gradient of 95% B to 5% B over 24.9–25.0 min, then hold 5% B for 5 min. The eluents were monitored by a UV detector with a range of 210 nm to 400 nm, followed by HRMS detection in electrospray ionization with both positive and negative mode. The MS conditions were as followed: voltage for positive ion mode 3500 V, voltage for negative ion mode 3000 V, sheath gas flow rate 55 Arb; aux gas flow rate 15 Arb; sweep gas flow rate 1 Arb, ion transfer tube temperature 320 °C, vaporizer temperature 350 °C, orbitrap resolution 120000, m/z range 100–1000 Da.

#### **The conditions above were used for all the HRMS analysis in mechanistic section.**

The  $M + 2$  isotopic enrichment values ( $M$  = mass of unlabeled compound), and full isotopic incorporation data were calculated using the relative abundance in mass spectra for each  $M + n$  ( $n = 0, 2$ ) peak in HRMS.

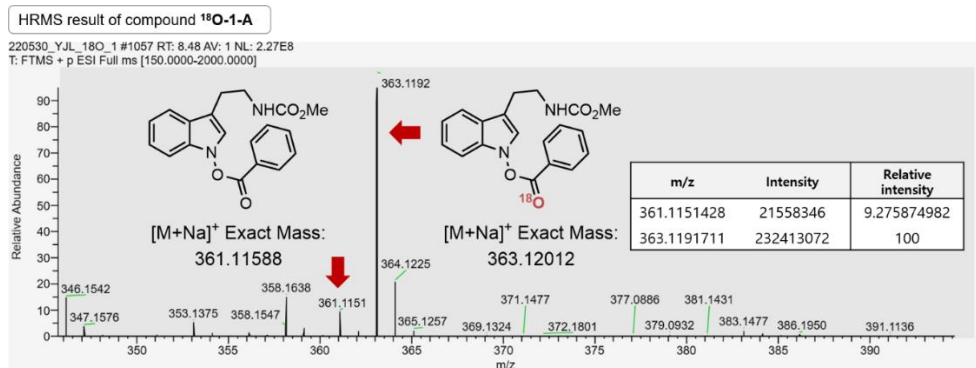
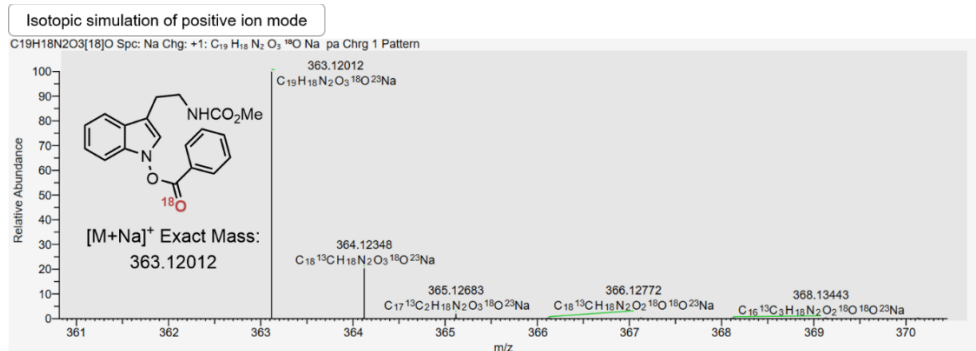
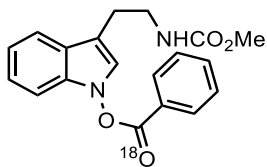
## <sup>18</sup>O-benzoic acid



<sup>18</sup>O enrichment: 96.8%

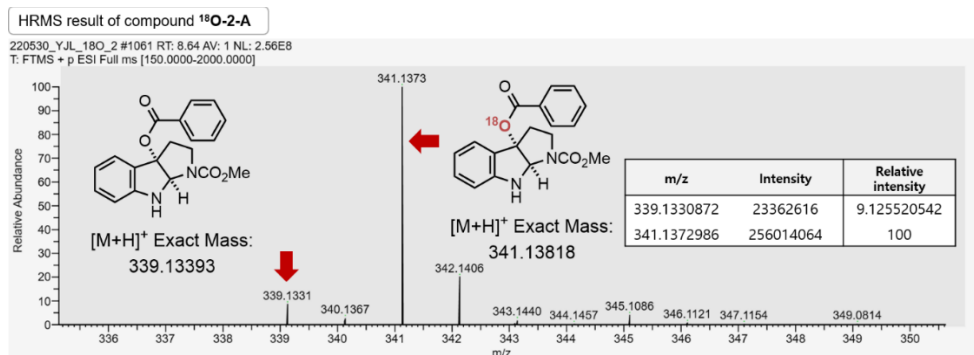
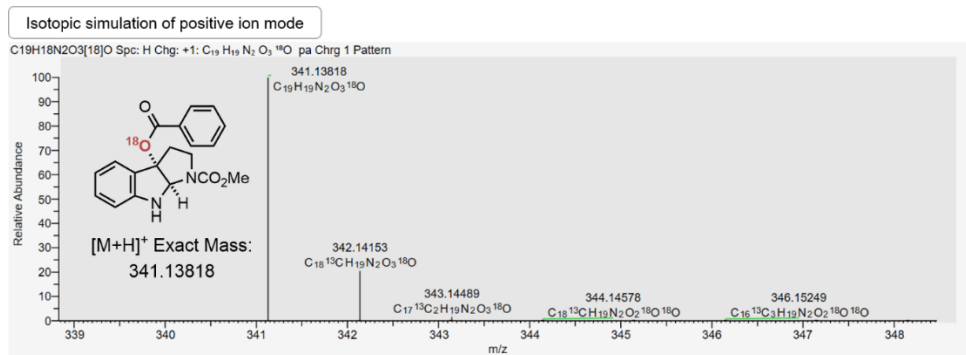
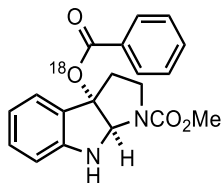


### 3-(2-((Methoxycarbonyl)amino)ethyl)-1H-indol-1-yl benzoate (<sup>18</sup>O-1-A)



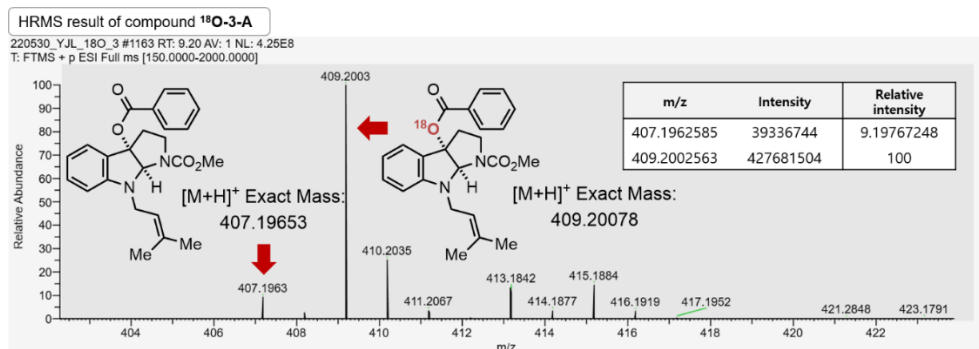
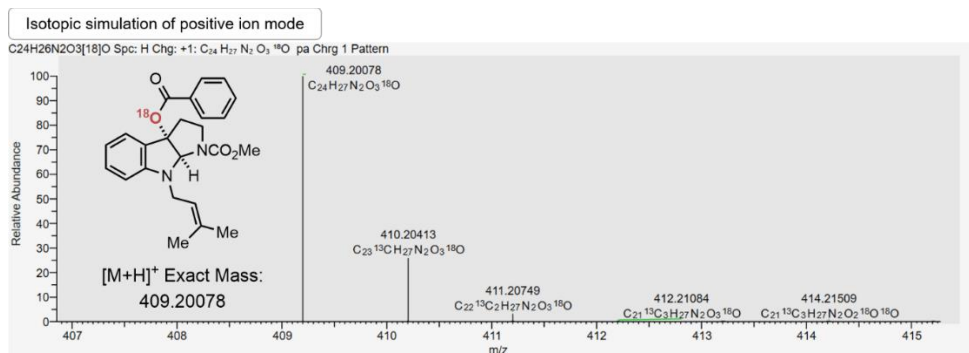
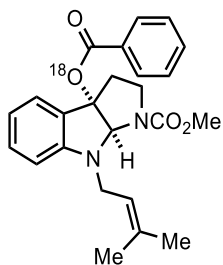
<sup>18</sup>O enrichment: 91.5%

**Methyl 3a-(benzoyloxy)-3,3a,8,8a-tetrahydropyrrolo[2,3-b]indole-1(2H)-carboxylate**  
(<sup>18</sup>O-2-A)



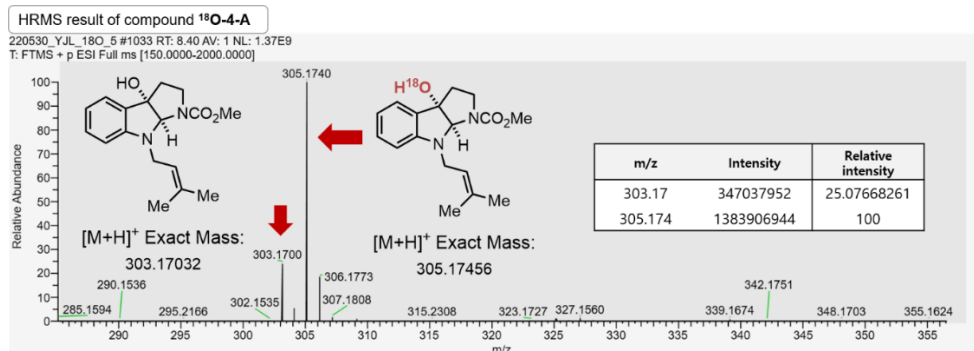
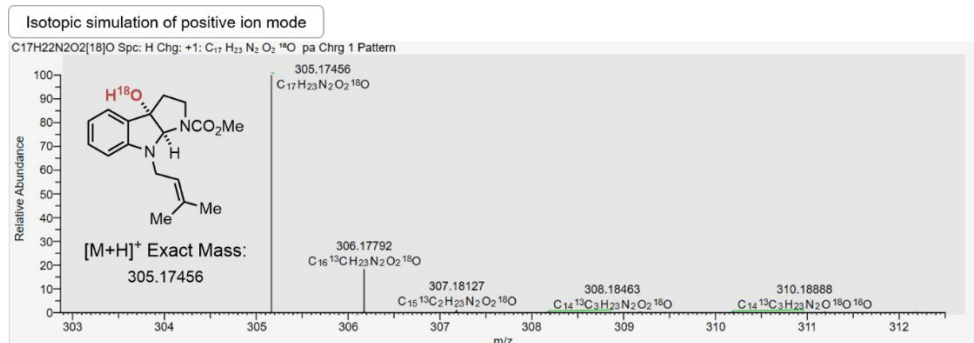
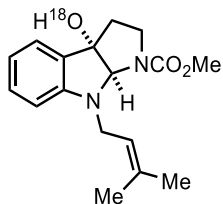
<sup>18</sup>O enrichment: 91.6%

**Methyl 3a-(benzoyloxy)-8-(3-methylbut-2-en-1-yl)-3,3a,8,8a-tetrahydropyrrolo[2,3-b]indole-1(2H)-carboxylate (<sup>18</sup>O-3-A)**



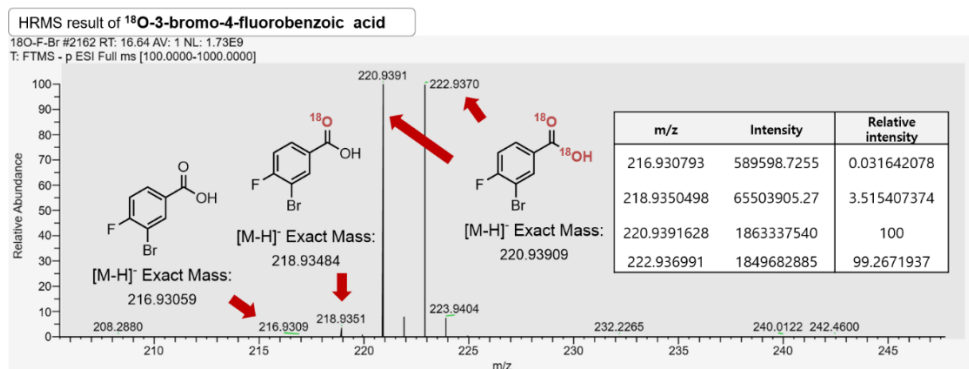
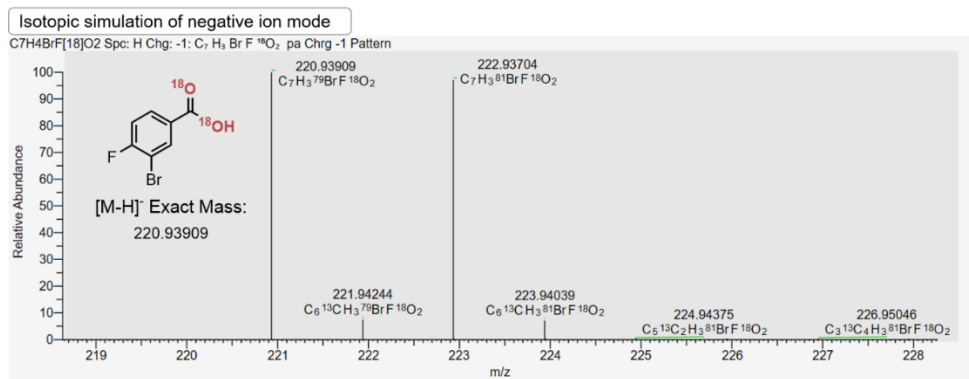
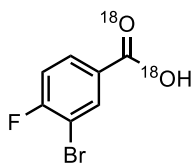
<sup>18</sup>O enrichment: 91.6%

**Methyl 3a-hydroxy-8-(3-methylbut-2-en-1-yl)-3,3a,8,8a-tetrahydropyrrolo[2,3-b]indole-1(2H)-carboxylate (<sup>18</sup>O-4-A)**

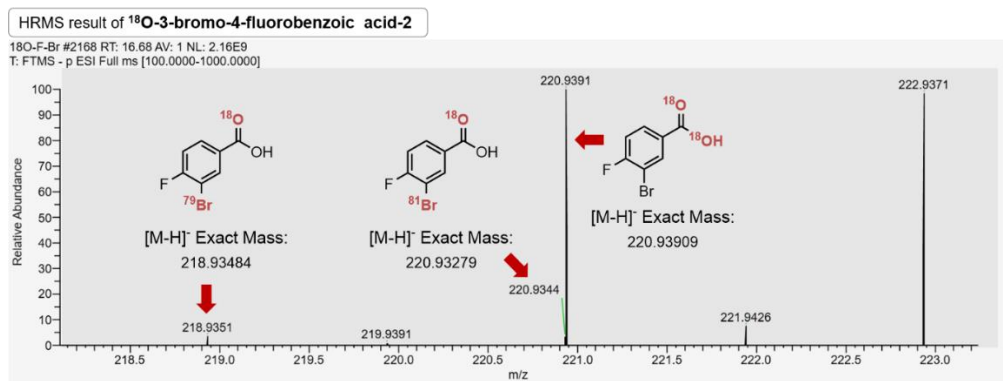


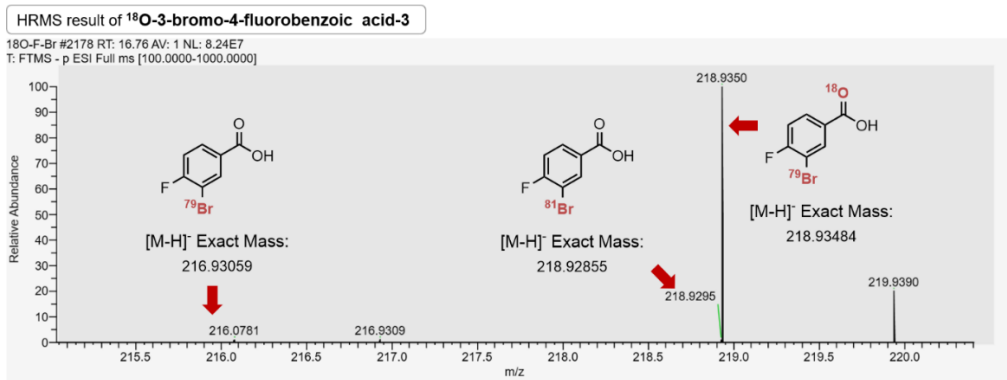
<sup>18</sup>O enrichment: 80.0%

# <sup>18</sup>O-3-Bromo-4-fluorobenzoic acid



<sup>18</sup>O enrichment: 96.6%

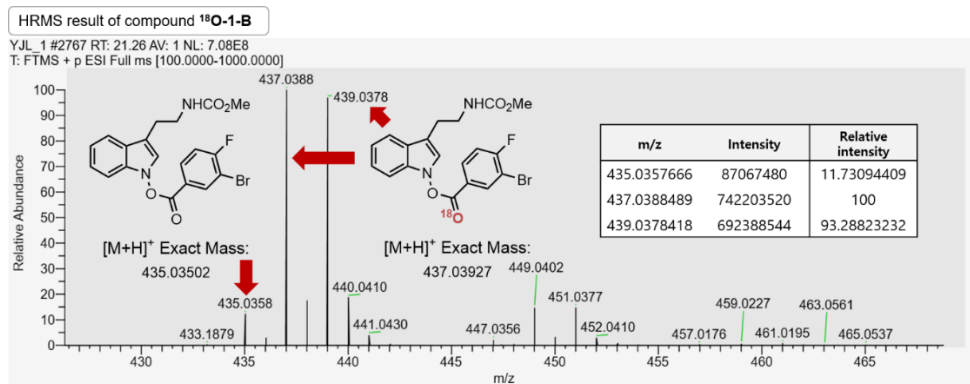
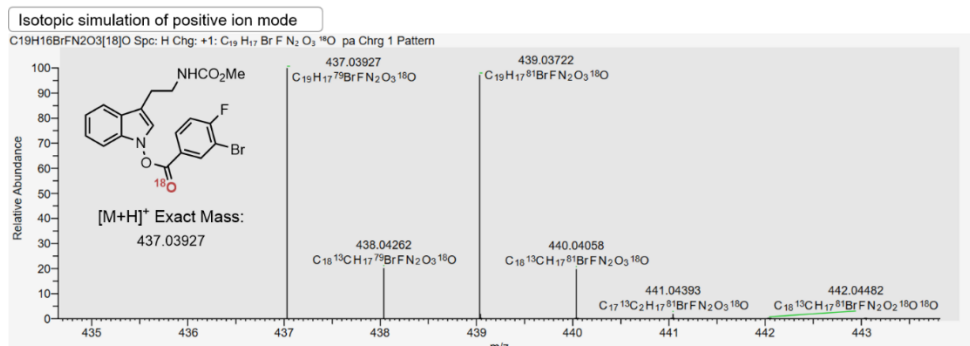
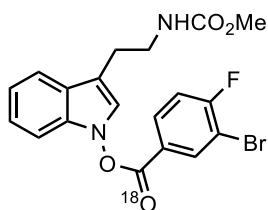




No overlap of isotopes (*i.e.* C<sub>7</sub>H<sub>4</sub><sup>81</sup>BrFO<sub>2</sub> and C<sub>7</sub>H<sub>4</sub><sup>79</sup>BrFO<sup>18</sup>O) on HRMS was observed.

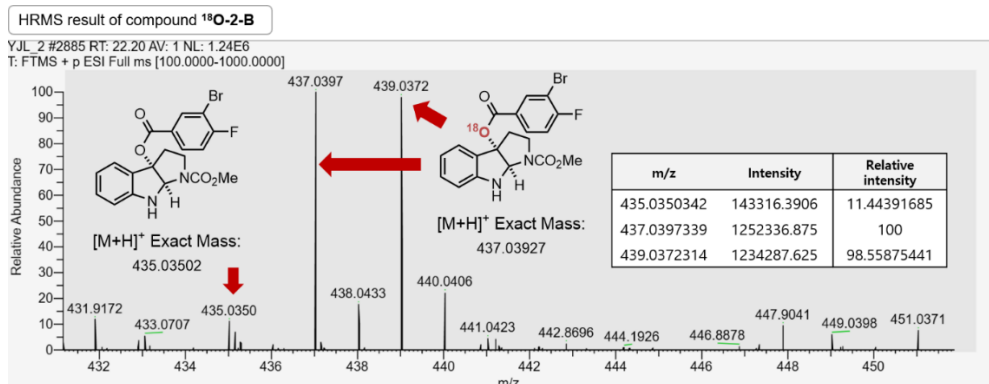
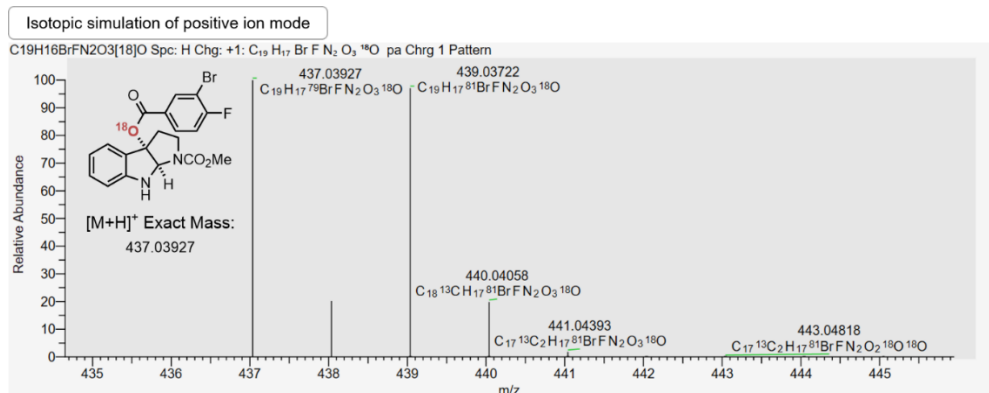
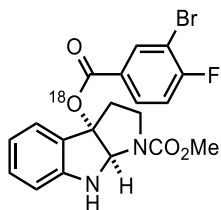
### 3-(2-((Methoxycarbonyl)amino)ethyl)-1H-indol-1-yl 3-bromo-4-fluorobenzoate (<sup>18</sup>O-1-

B)



<sup>18</sup>O enrichment: 89.5%

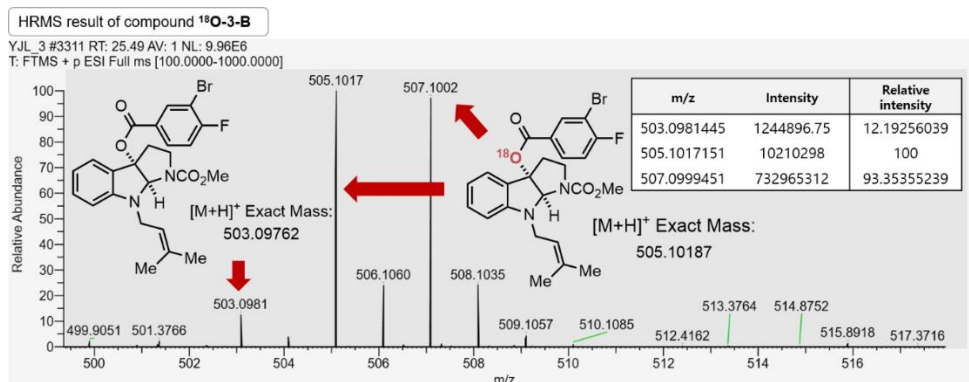
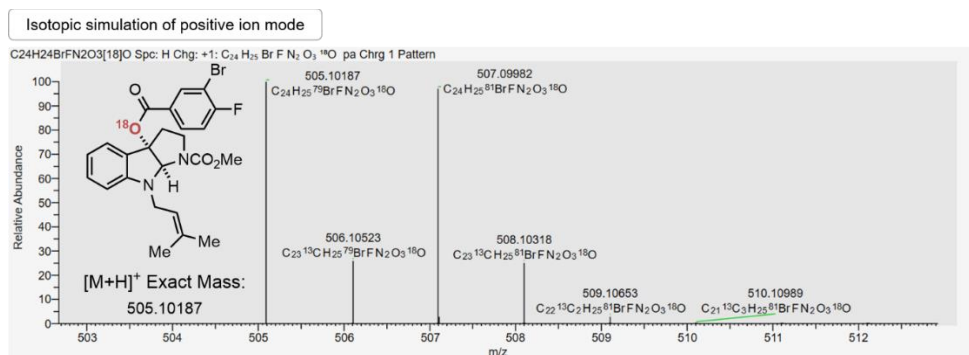
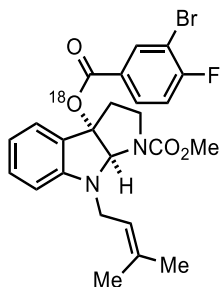
**Methyl 3a-((3-bromo-4-fluorobenzoyl)oxy)-3,3a,8,8a-tetrahydropyrrolo[2,3-b]indole-1(2H)-carboxylate (<sup>18</sup>O-2-B)**



<sup>18</sup>O enrichment: 89.7%

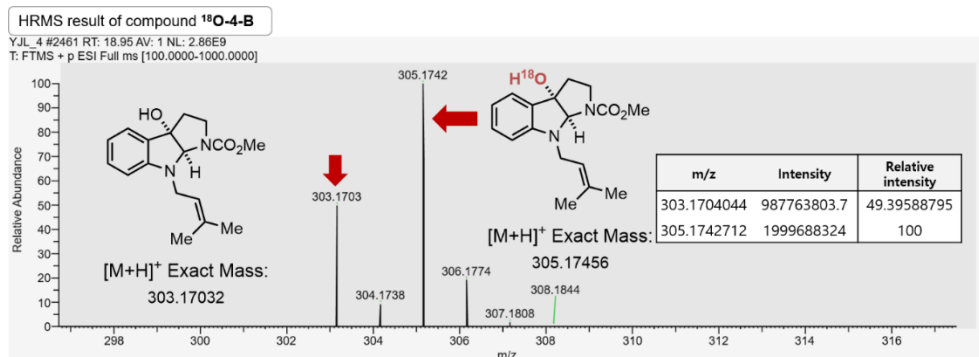
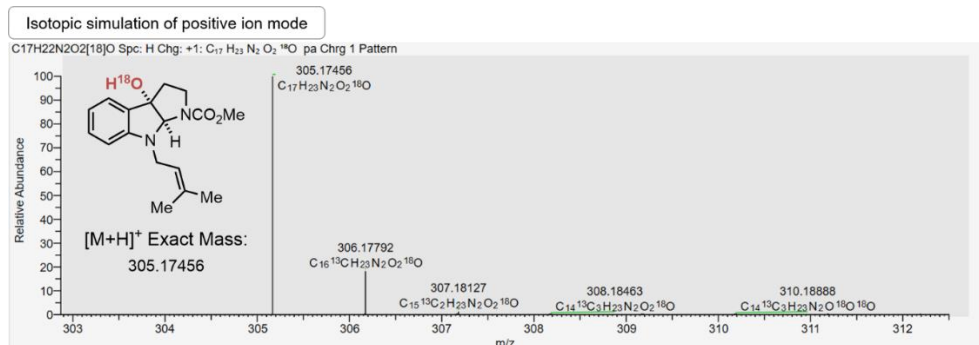
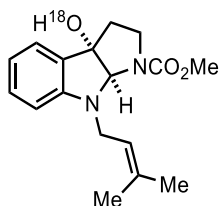


**Methyl 3a-((3-bromo-4-fluorobenzoyl)oxy)-8-(3-methylbut-2-en-1-yl)-3,3a,8,8a-tetrahydropyrrolo[2,3-b]indole-1(2H)-carboxylate (<sup>18</sup>O-3-B)**



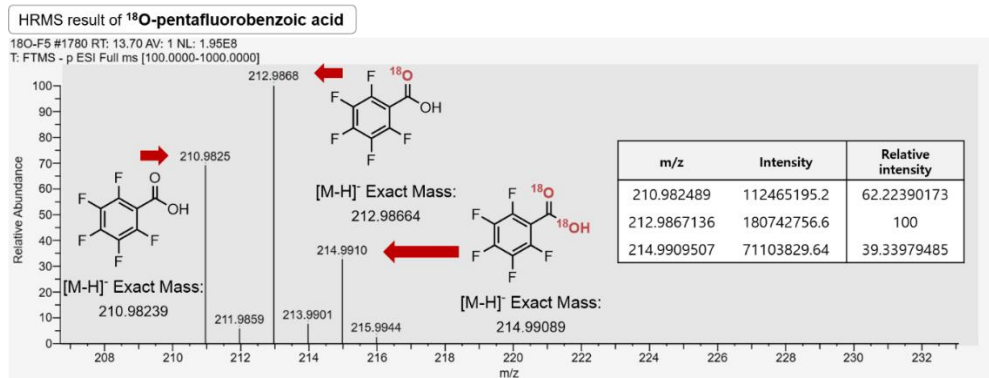
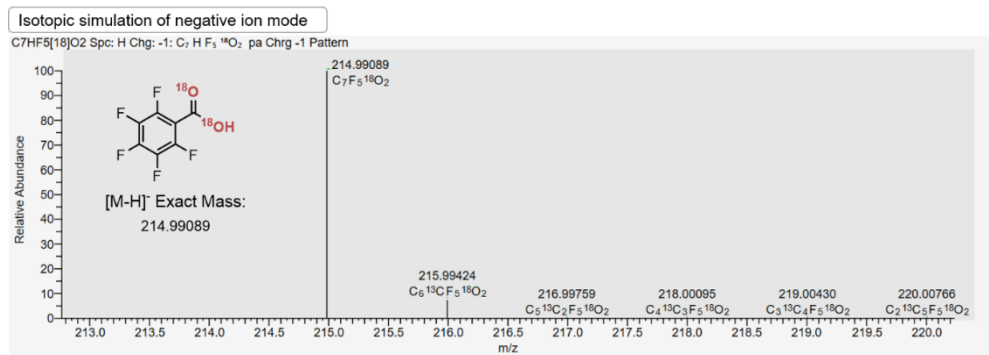
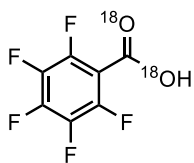
<sup>18</sup>O enrichment: 89.1%

**Methyl 3a-hydroxy-8-(3-methylbut-2-en-1-yl)-3,3a,8,8a-tetrahydropyrrolo[2,3-b]indole-1(2H)-carboxylate (<sup>18</sup>O-4-B)**

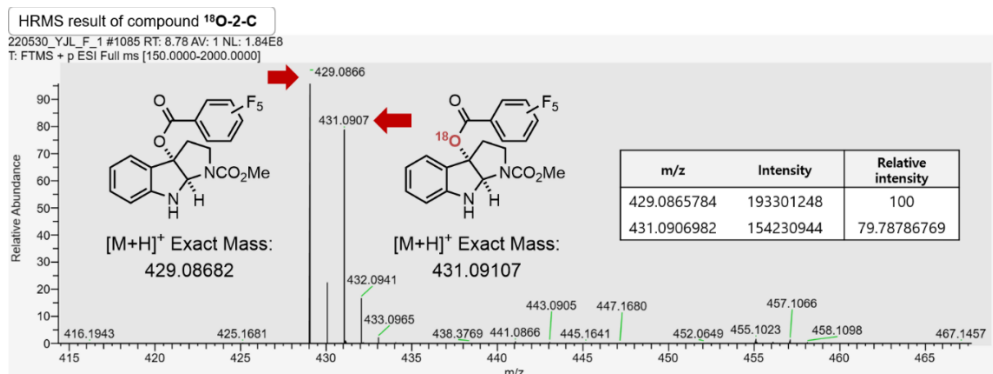
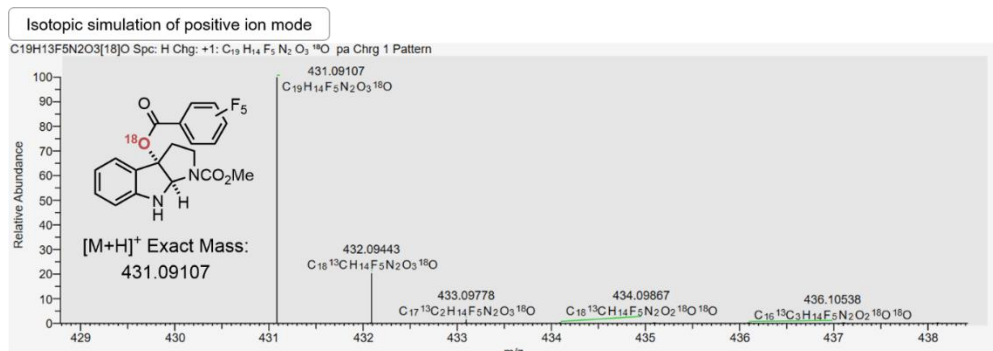
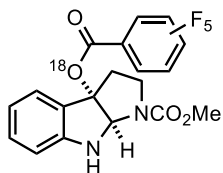


<sup>18</sup>O enrichment: 66.9%

# <sup>18</sup>O-2,3,4,5,6-Pentafluorobenzoic acid

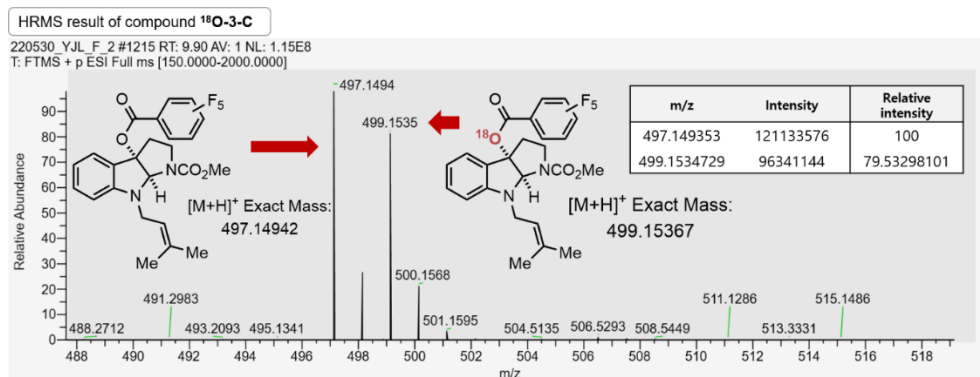
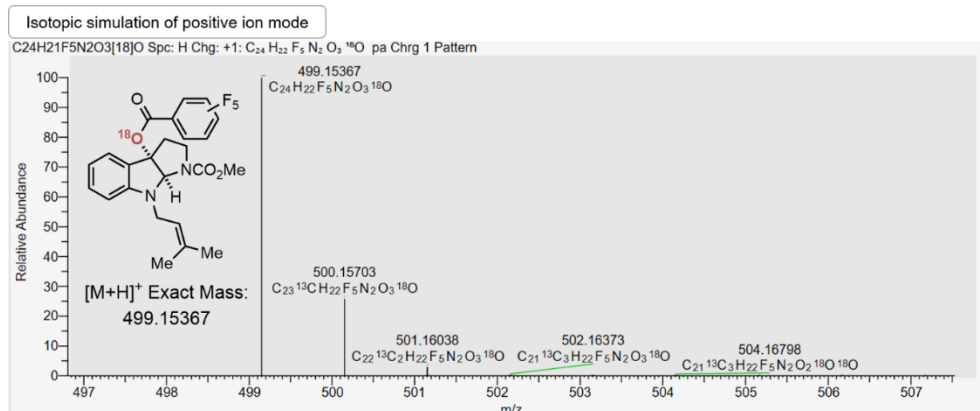
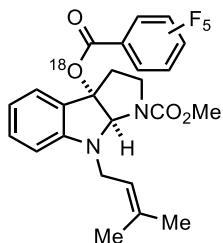


**Methyl 3a-((perfluorobenzoyl)oxy)-3,3a,8,8a-tetrahydropyrrolo[2,3-b]indole-1(2H)-carboxylate (<sup>18</sup>O-2-C)**



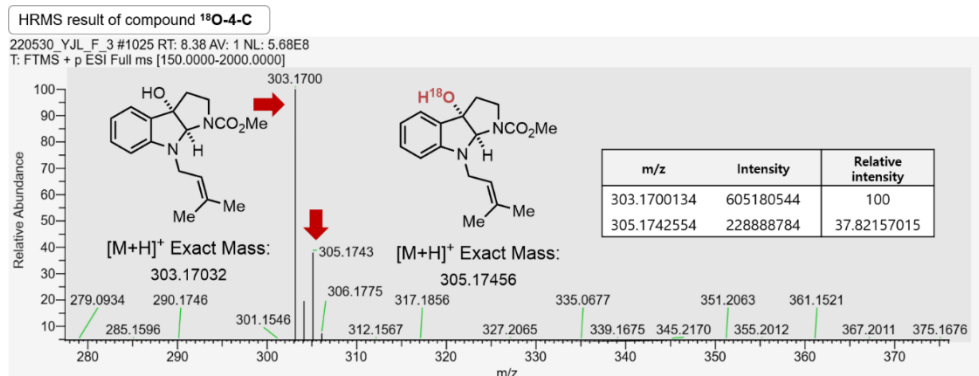
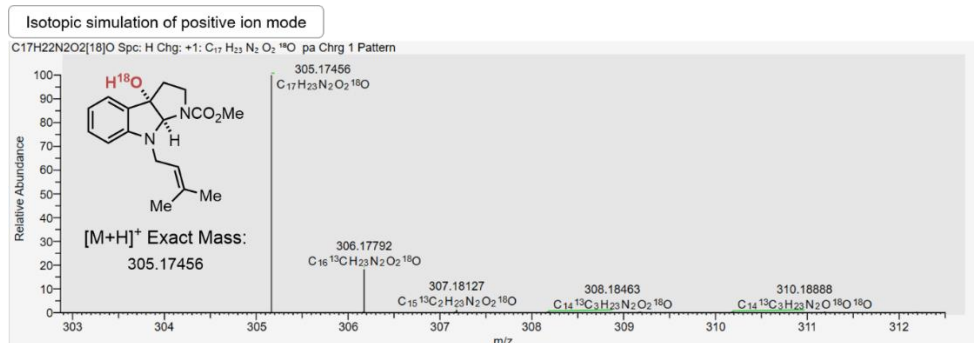
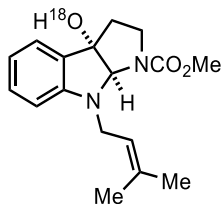
<sup>18</sup>O enrichment: 44.4%

**Methyl 8-(3-methylbut-2-en-1-yl)-3a-((perfluorobenzoyl)oxy)-3,3a,8,8a-tetrahydropyrrolo[2,3-b]indole-1(2H)-carboxylate (<sup>18</sup>O-3-C)**



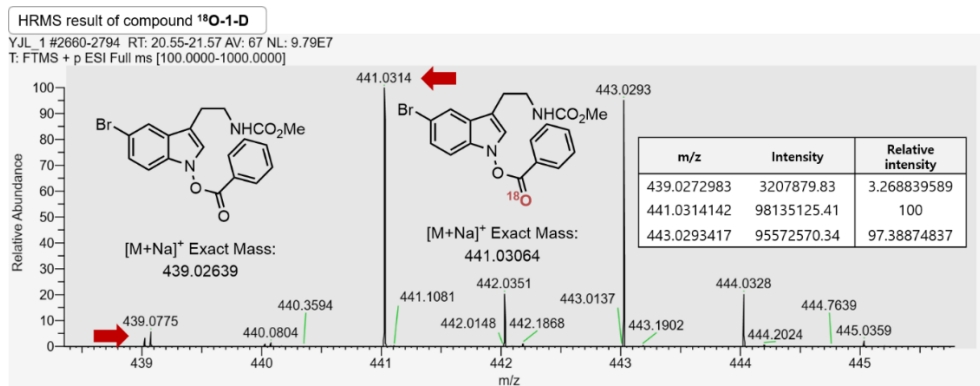
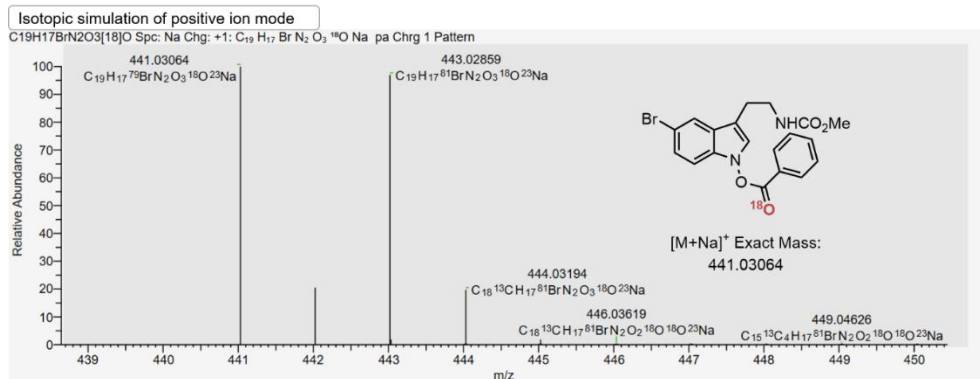
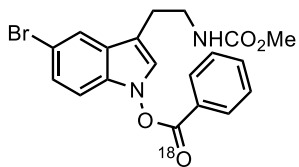
<sup>18</sup>O enrichment: 44.3%

**Methyl 3a-hydroxy-8-(3-methylbut-2-en-1-yl)-3,3a,8,8a-tetrahydropyrrolo[2,3-b]indole-1(2H)-carboxylate (<sup>18</sup>O-4-C)**



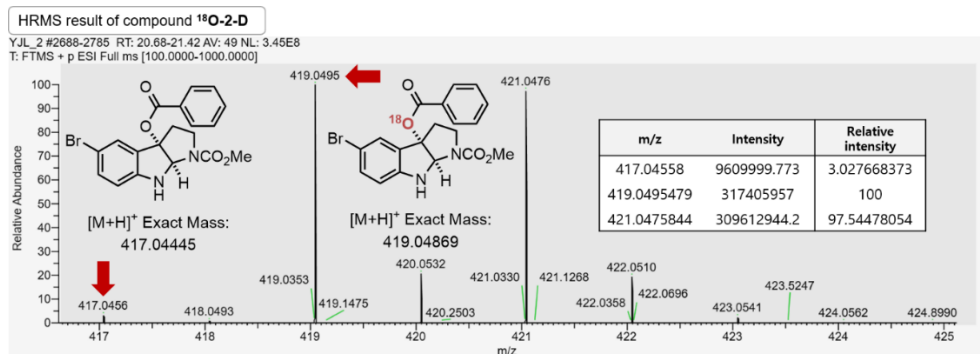
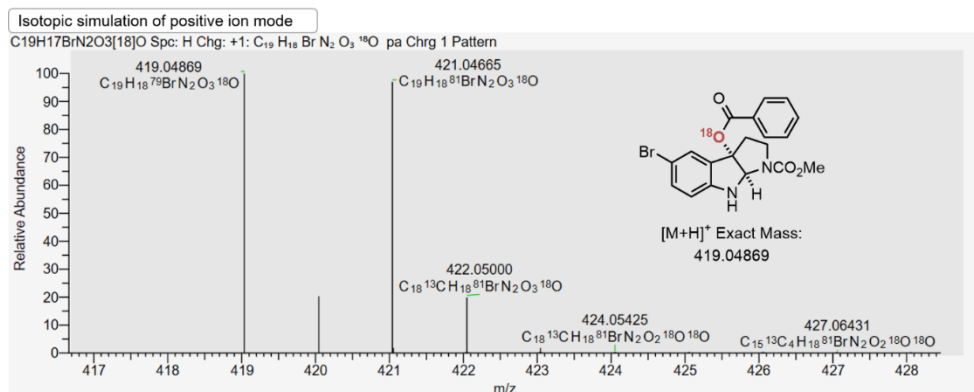
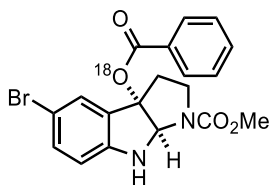
<sup>18</sup>O enrichment: 27.4%

### 5-Bromo-3-(2-((methoxycarbonyl)amino)ethyl)-1H-indol-1-yl benzoate (<sup>18</sup>O-1-D)



<sup>18</sup>O enrichment: 96.8%

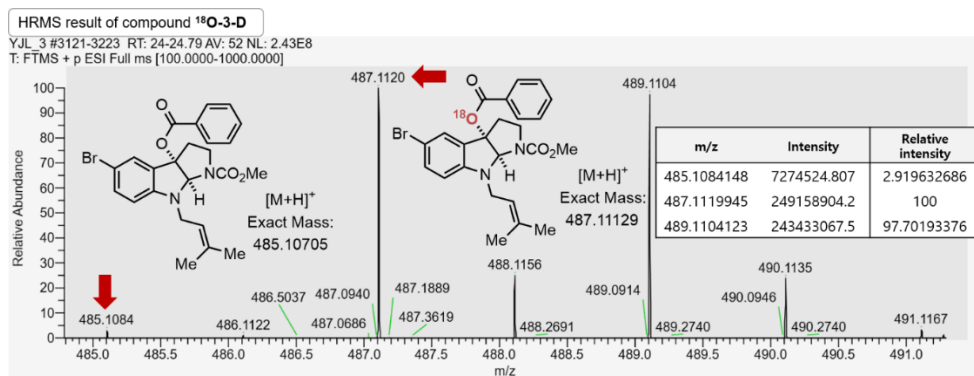
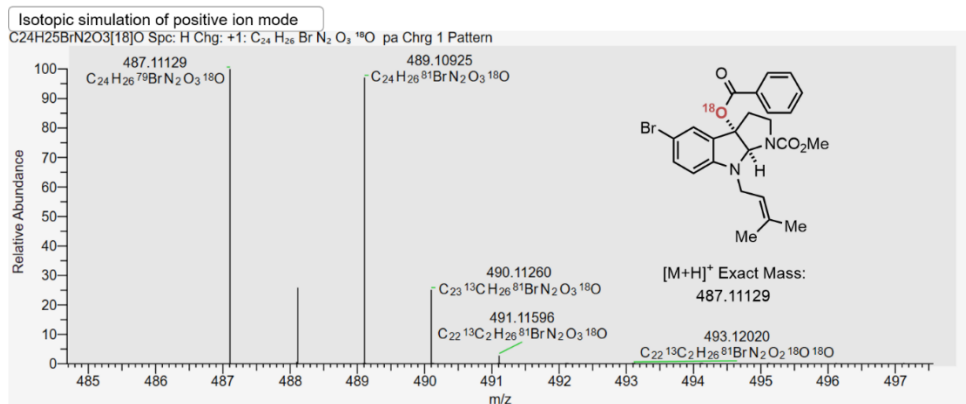
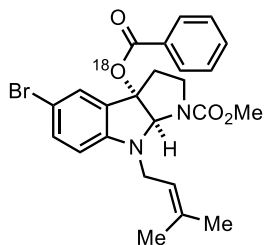
**Methyl 3a-(benzoyloxy)-5-bromo-3,3a,8,8a-tetrahydropyrrolo[2,3-b]indole-1(2H)-carboxylate (<sup>18</sup>O-2-D)**



<sup>18</sup>O enrichment: 97.1%

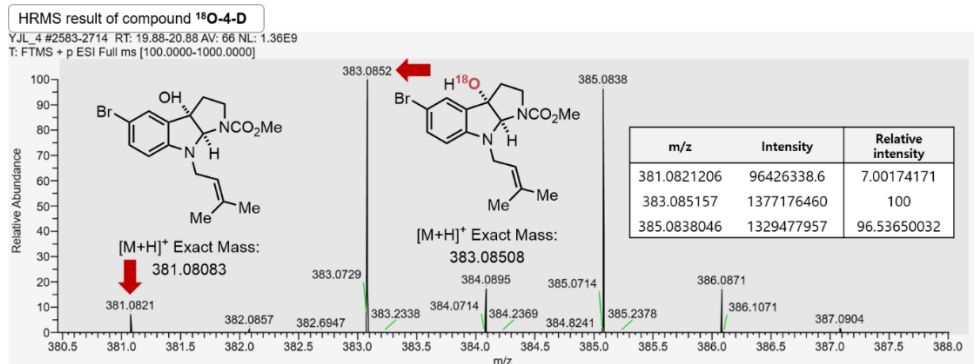
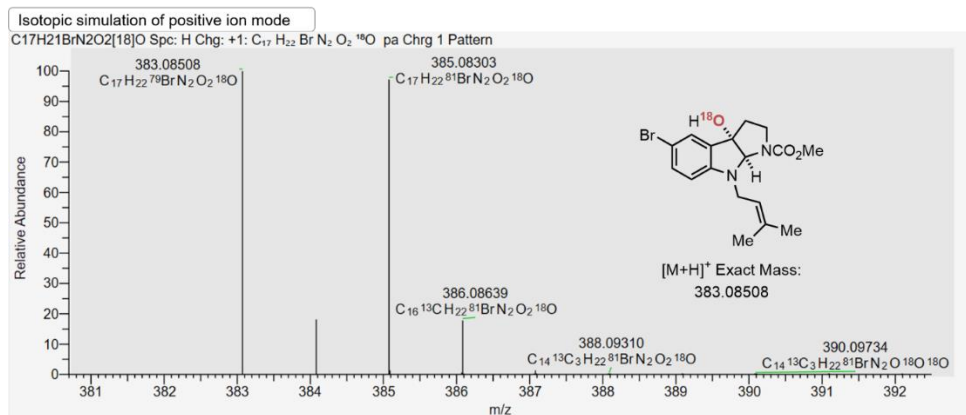
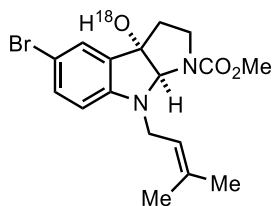


**Methyl 3a-(benzoyloxy)-5-bromo-8-(3-methylbut-2-en-1-yl)-3,3a,8,8a-tetrahydropyrrolo[2,3-b]indole-1(2H)-carboxylate (<sup>18</sup>O-3-D)**



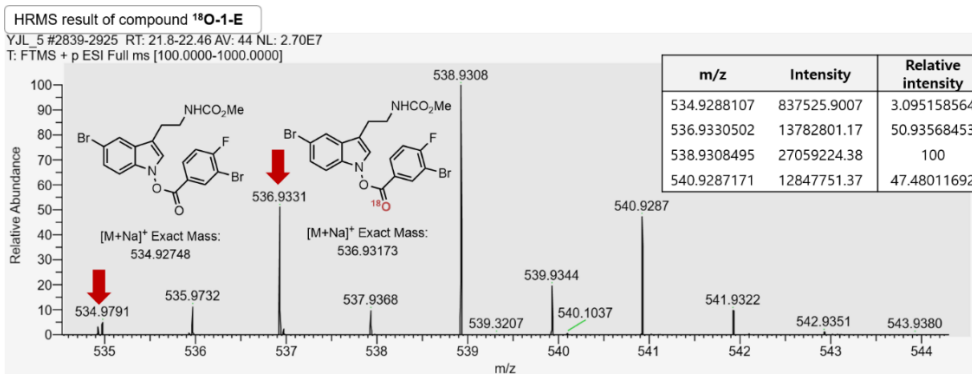
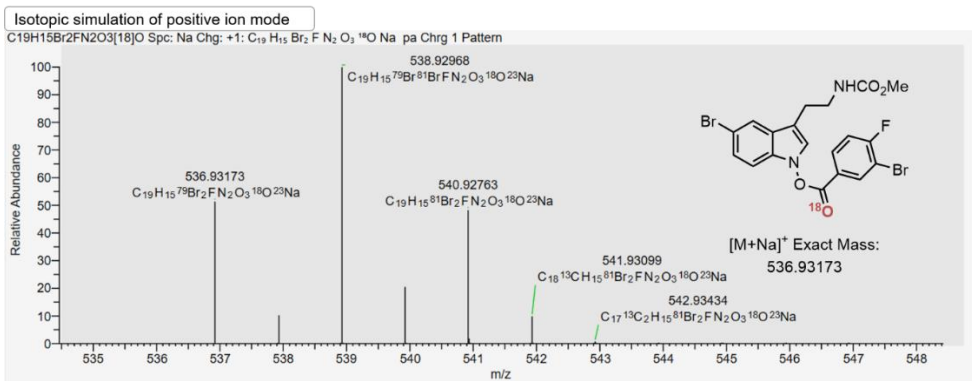
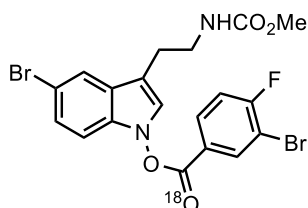
<sup>18</sup>O enrichment: 97.2%

**Methyl 5-bromo-3a-hydroxy-8-(3-methylbut-2-en-1-yl)-3,3a,8,8a-tetrahydropyrrolo[2,3-b]indole-1(2H)-carboxylate (<sup>18</sup>O-4-D)**



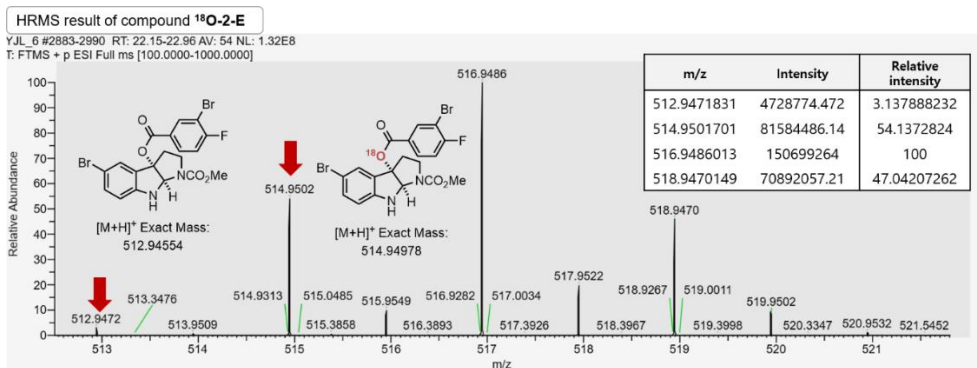
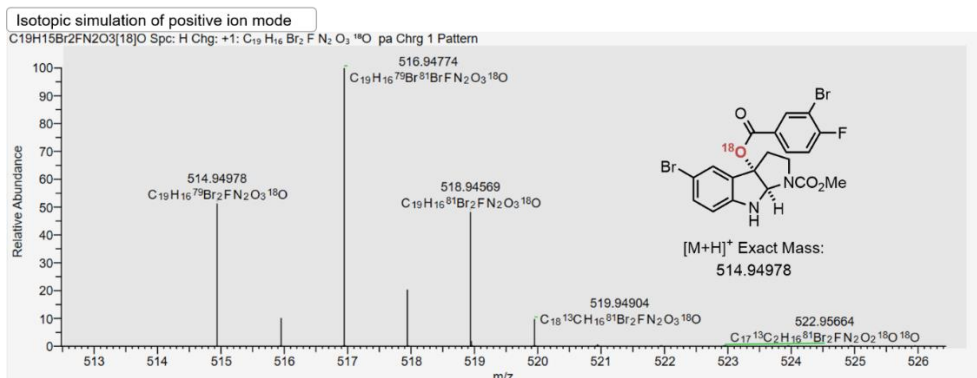
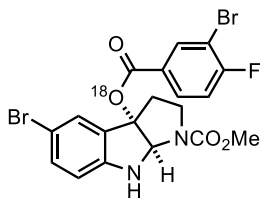
<sup>18</sup>O enrichment: 93.5%

**5-Bromo-3-(2-((methoxycarbonyl)amino)ethyl)-1H-indol-1-yl 3-bromo-4-fluorobenzoate (<sup>18</sup>O-1-E)**



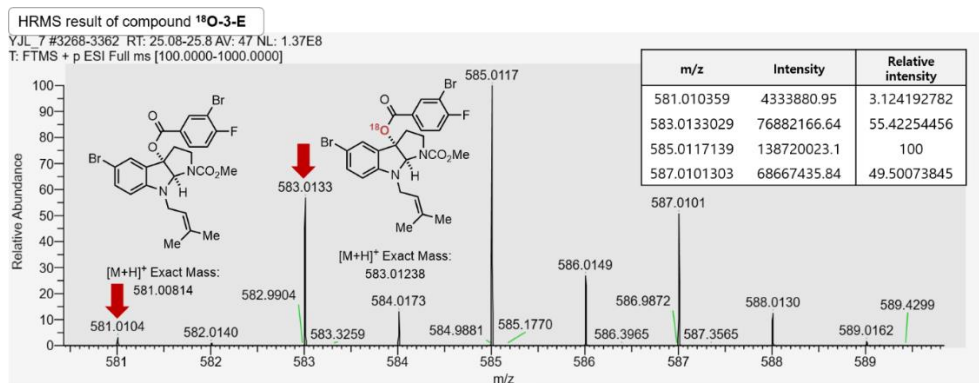
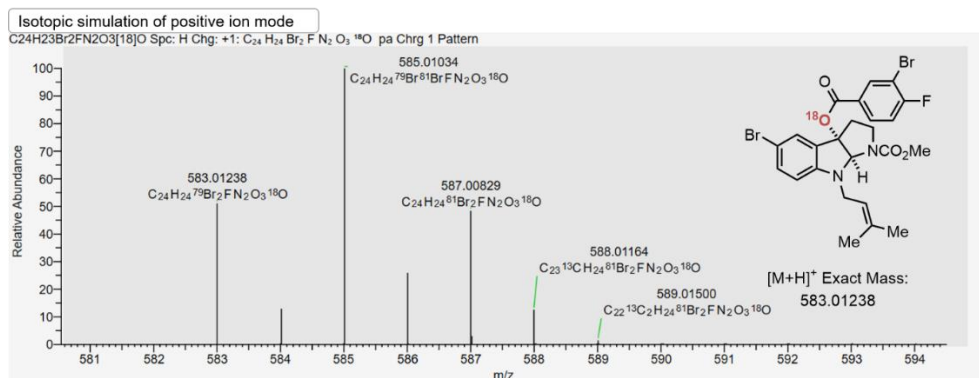
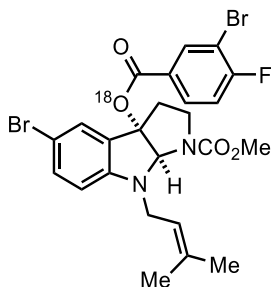
<sup>18</sup>O enrichment: 94.3%

**Methyl 5-bromo-3a-((3-bromo-4-fluorobenzoyl)oxy)-3,3a,8,8a-tetrahydropyrrolo[2,3-b]indole-1(2H)-carboxylate (<sup>18</sup>O-2-E)**



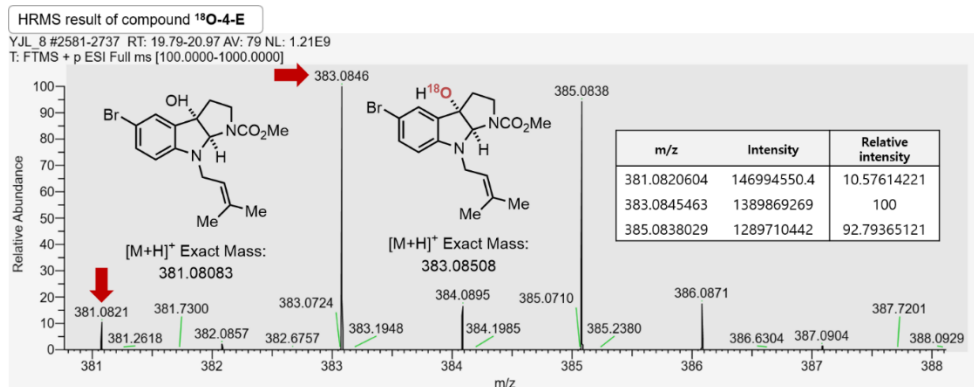
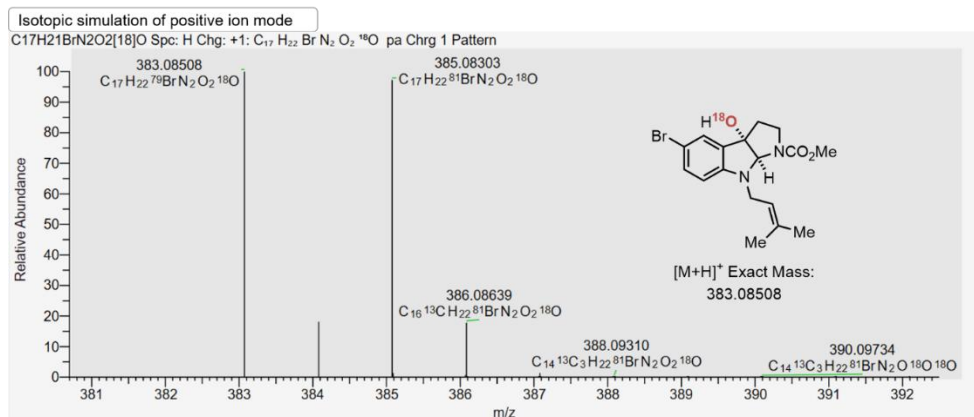
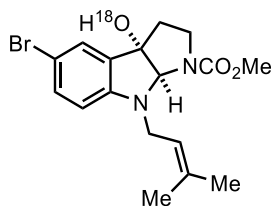
<sup>18</sup>O enrichment: 94.5%

**Methyl 5-bromo-3a-((3-bromo-4-fluorobenzoyl)oxy)-8-(3-methylbut-2-en-1-yl)-3,3a,8,8a-tetrahydropyrrolo[2,3-b]indole-1(2H)-carboxylate (<sup>18</sup>O-3-E)**



<sup>18</sup>O enrichment: 94.7%

**Methyl 5-bromo-3a-hydroxy-8-(3-methylbut-2-en-1-yl)-3,3a,8,8a-tetrahydropyrrolo[2,3-b]indole-1(2H)-carboxylate (<sup>18</sup>O-4-E)**

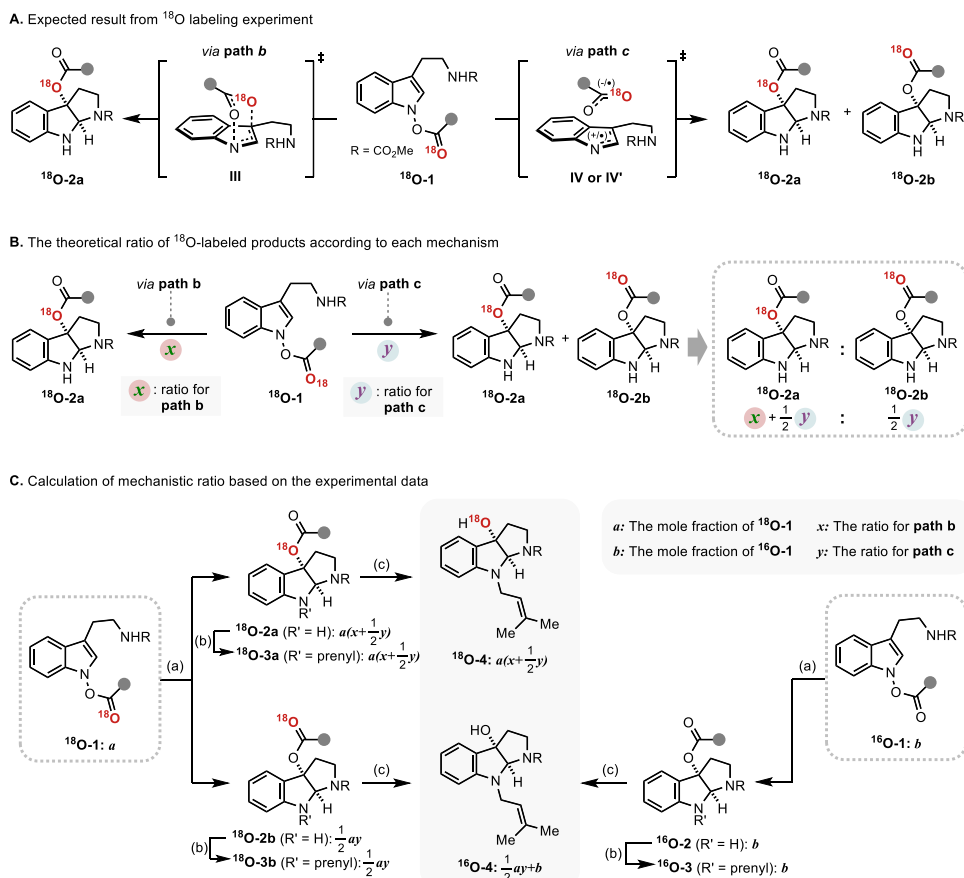


<sup>18</sup>O enrichment: 90.4%

### 5.1.3. Quantitative Analysis of $^{18}\text{O}$ -Labeling Experiment Results (Figures 2.12 and 2.13)

#### 5.1.3.1. Dependence of the electronic properties

Assuming **path b** and **path c** are primarily operating for the **IHT** process, the relative contribution of each pathway could be determined. The formation of  $^{18}\text{O}$ -**4** is attributed to the action of **path b** from  $^{18}\text{O}$ -**1** in total, and half the participation of **path c** from the identical starting material. The other half of the involvement of **path c** from  $^{18}\text{O}$ -**1**, along with the rearrangement from  $^{18}\text{O}$ -free starting material,  $^{16}\text{O}$ -**1**, generates the unlabeled oxygenation product  $^{16}\text{O}$ -**4**.



Conditions: (a) For  $^{18}\text{O}$ -**1-A**: toluene, 90 °C, 16 h, for  $^{18}\text{O}$ -**1-B**: toluene, 70 °C, 8 h, for  $^{18}\text{O}$ -**1-C**:  $\text{CH}_2\text{Cl}_2$ , 0 °C, 2 h; (b) For  $^{18}\text{O}$ -**2-A**,  $^{18}\text{O}$ -**2-B**: 1-bromo-3-methyl-2-butene (1.5 equiv),  $\text{K}_2\text{CO}_3$  (3.0 equiv), acetone, 23 °C, 16 h, for  $^{18}\text{O}$ -**2-C**: 1-bromo-3-methyl-2-butene (3.0 equiv),  $\text{K}_2\text{CO}_3$  (6.0 equiv), acetone, 23 °C, 4 d; (c) KOH (1.5 equiv),  $\text{EtOH}:\text{H}_2\text{O} = 5:1$ , 60 °C, 3 h

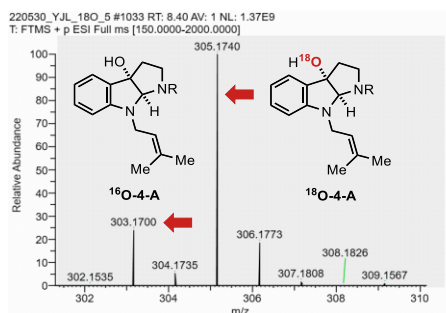
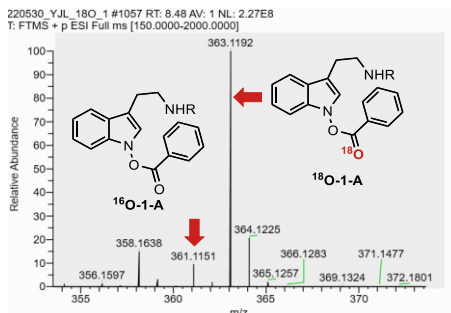
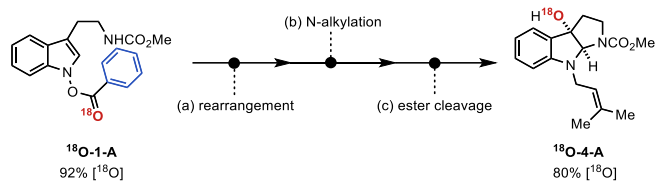
**Figure S6.** Schematic explanation for the calculation of the ratio of each pathway.

The relative contribution of each pathway for the formation of the **IHT** product was determined based on the following premises. **path b** will exclusively produce **<sup>18</sup>O-2a** as a sole product while **path c** will form **<sup>18</sup>O-2a** and **<sup>18</sup>O-2b** in a 1:1 ratio, respectively.

The mole fraction of **<sup>18</sup>O-1** is denoted as  $a$ , and since the <sup>18</sup>O enrichment is not 100%, the mole fraction of naturally existing **<sup>16</sup>O-1** is defined as  $b$ . Also, the relative contribution of **path b** for the formation of the product is denoted as  $x$ , and the relative contribution of **path c** for the formation of the product is defined as  $y$ . The ratio between **<sup>18</sup>O-4** and **<sup>16</sup>O-4** is expressed as  $a(x+\frac{1}{2}y) : \frac{1}{2}ay+b$  (Figure S3). Detailed calculation process is attached below.



(1) IHT reaction with benzoyl substituent



The system of equations is established by the two proportional expressions:

$$\begin{cases} a : b = 100 : 9.3 & (1) \\ a(x + \frac{1}{2}y) : \frac{1}{2}ay + b = 100 : 25.1 & (2) \end{cases}$$

From equation 1, **b** can be expressed as:

$$b = \frac{93}{1000} a \quad (3)$$

Insertion of the equation 3 into equation 2 gives equation 4:

$$a(x + \frac{1}{2}y) : \frac{1}{2}ay + \frac{93}{1000}a = 100 : 25.1 \quad (4)$$

$$\therefore x + \frac{1}{2}y : \frac{1}{2}y + \frac{93}{1000} = 100 : 25.1$$

$$\therefore 50y + 9.3 = 25.1x + \frac{251}{20}y$$

$$\therefore 25.1x - \frac{749}{20}y = 9.3 \quad (5)$$

Since **y** is defined in terms of 1-x, the equation 5 can be re-written as:

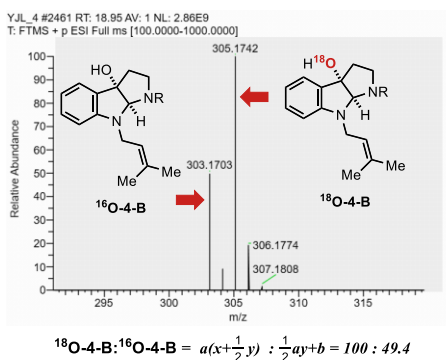
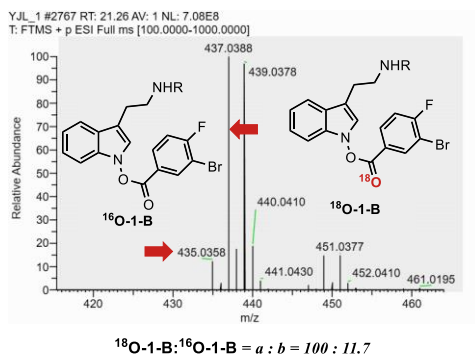
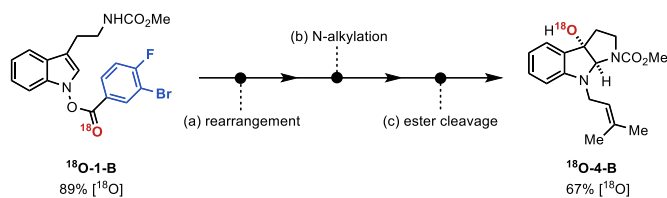
$$25.1x - \frac{749}{20}(1 - x) = 9.3$$

$$\therefore 62.6x = 46.8$$

$$\therefore x = 0.75 \quad (6)$$

$$\therefore y = 1 - x = 0.25 \quad (7)$$

(2) IHT reaction with 3-bromo-4-fluorobenzoyl substituent



The system of equations is established by the two proportional expressions:

$$\begin{cases} a : b = 100 : 11.7 & (1) \\ a(x + \frac{1}{2}y) : \frac{1}{2}ay + b = 100 : 49.4 & (2) \end{cases}$$

From equation 1,  $b$  can be expressed as:

$$b = \frac{117}{1000} a \quad (3)$$

Insertion of the equation 3 into equation 2 gives equation 4:

$$a(x + \frac{1}{2}y) : \frac{1}{2}ay + \frac{117}{1000}a = 100 : 49.4 \quad (4)$$

$$\therefore x + \frac{1}{2}y : \frac{1}{2}y + \frac{117}{1000} = 100 : 49.4$$

$$\therefore 50y + 11.7 = 49.4x + \frac{494}{20}y$$

$$\therefore 49.4x - \frac{506}{20}y = 11.7 \quad (5)$$

Since  $y$  is defined in terms of  $1-x$ , the equation 5 can be re-written as:

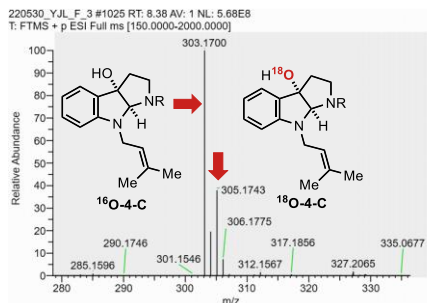
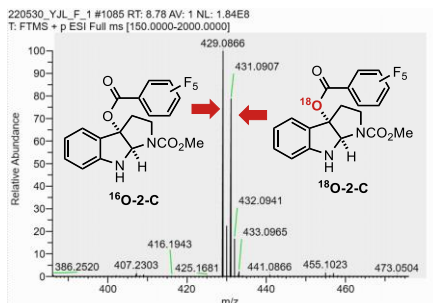
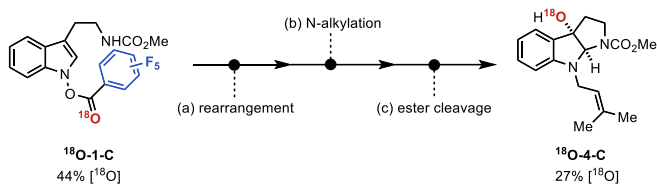
$$49.4x - \frac{506}{20}(1-x) = 11.7$$

$$\therefore 74.7x = 37$$

$$\therefore x = 0.49 \quad (6)$$

$$\therefore y = 1 - x = 0.51 \quad (7)$$

### (3) IHT reaction with pentafluorobenzoyl substituent



The system of equations is established by the two proportional expressions:

$$\begin{cases} a : b = 79.8 : 100 & (1) \\ a(x + \frac{1}{2}y) : \frac{1}{2}ay + b = 37.8 : 100 & (2) \end{cases}$$

From equation 1,  $b$  can be expressed as:

$$b = \frac{1000}{798} a \quad (3)$$

Insertion of the equation 3 into equation 2 gives equation 4:

$$a(x + \frac{1}{2}y) : \frac{1}{2}ay + \frac{1000}{798}a = 37.8 : 100 \quad (4)$$

$$\therefore x + \frac{1}{2}y : \frac{1}{2}y + \frac{1000}{798} = 37.8 : 100$$

$$\therefore 37.8(\frac{1}{2}y + \frac{1000}{798}) = 100x + 50y$$

$$\therefore 100x + 31.1y = \frac{37800}{798} = 47.4 \quad (5)$$

Since  $y$  is defined in terms of  $1-x$ , the equation 5 can be re-written as:

$$100x + 31.1(1 - x) = 47.4$$

$$\therefore 68.9x = 16.3$$

$$\therefore x = 0.24 \quad (6)$$

$$\therefore y = 1 - x = 0.76 \quad (7)$$

### 5.1.3.2. The influence of electronic properties of the indole backbone (Figure 2.14)

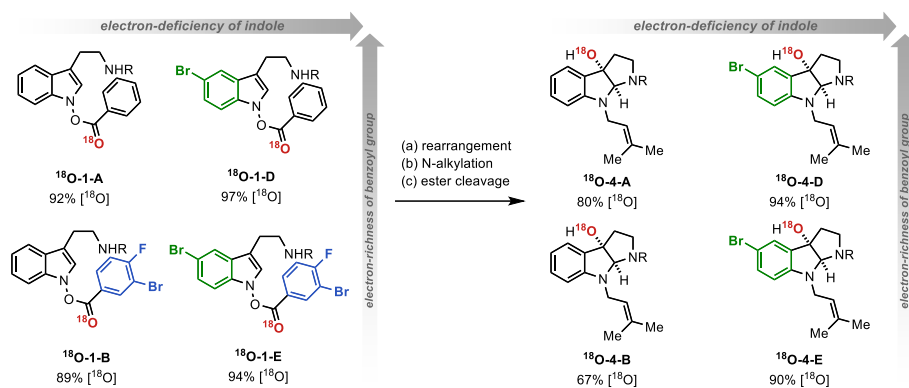
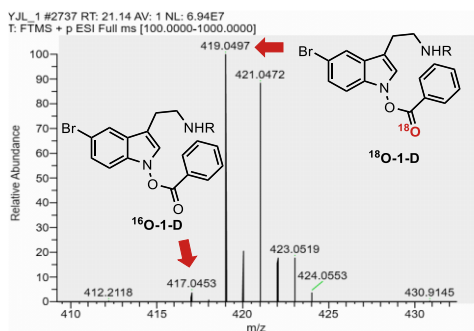
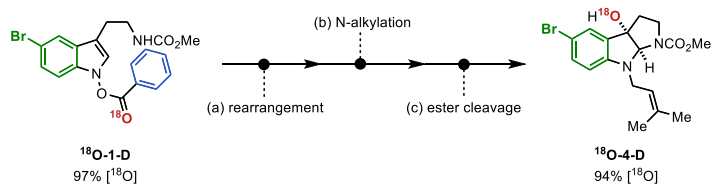


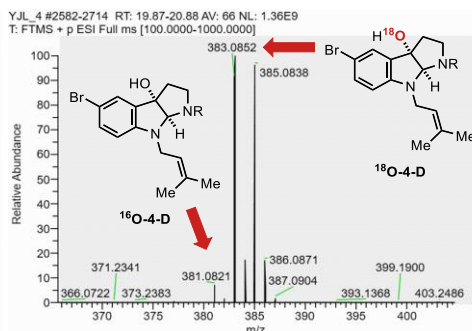
**Figure S7.** The influence of electronic properties of the indole backbone.

The determination of the relative contribution of **path b** and **path c** in each case was carried out via analogous calculations used for section 5.1.3.2.

(1) IHT reaction with benzoyl substituent



$$^{18}\text{O-1-D}:^{16}\text{O-1-D} = a : b = 100 : 3.1$$



$$^{18}\text{O-4-D}:^{16}\text{O-4-D} = a(x + \frac{1}{2}y) : \frac{1}{2}ay + b = 100 : 7.0$$

The system of equations is established by the two proportional expressions:

$$\begin{cases} a : b = 100 : 3.1 & (1) \\ a(x + \frac{1}{2}y) : \frac{1}{2}ay + b = 100 : 7.0 & (2) \end{cases}$$

From equation 1,  $b$  can be expressed as:

$$b = \frac{31}{1000} a \quad (3)$$

Insertion of the equation 3 into equation 2 gives equation 4:

$$a(x + \frac{1}{2}y) : \frac{1}{2}ay + \frac{31}{1000}a = 100 : 7.0 \quad (4)$$

$$\therefore x + \frac{1}{2}y : \frac{1}{2}y + \frac{31}{1000} = 100 : 7.0$$

$$\therefore 50y + 3.1 = 7x + 3.5y$$

$$\therefore 7x - 46.5y = 3.1 \quad (5)$$

Since  $y$  is defined in terms of  $1-x$ , the equation 5 can be re-written as:



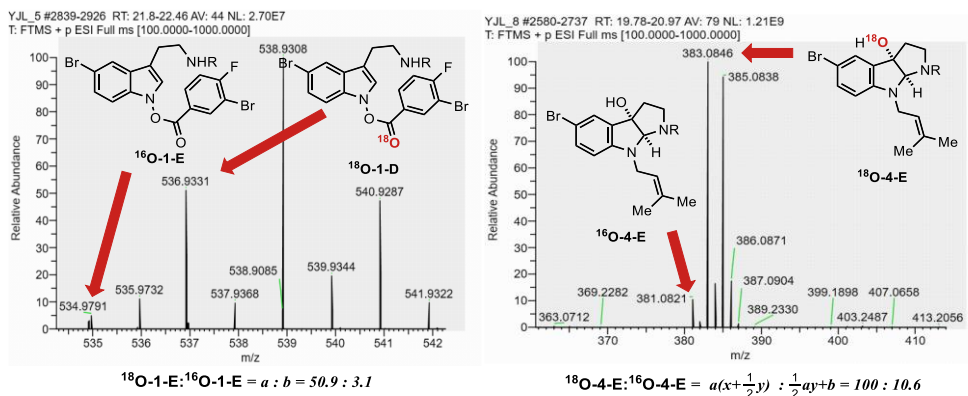
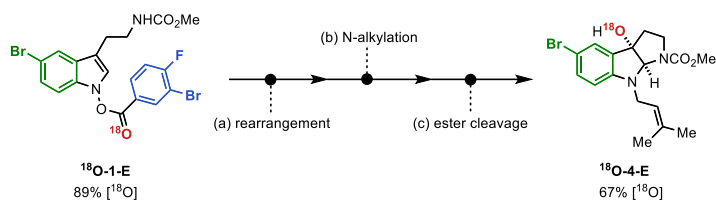
$$7x - 46.5(1 - x) = 3.1$$

$$\therefore 53.5x = 49.6$$

$$\therefore x = 0.93 \quad (6)$$

$$\therefore y = 1 - x = 0.7 \quad (7)$$

(2) IHT reaction with 3-bromo-4-fluorobenzoyl substituent



The system of equations is established by the two proportional expressions:

$$\begin{cases} a : b = 50.9 : 3.1 & (1) \\ a(x + \frac{1}{2}y) : \frac{1}{2}ay + b = 100 : 10.6 & (2) \end{cases}$$

From equation 1,  $b$  can be expressed as:

$$b = \frac{31}{509}a \quad (3)$$

Insertion of the equation 3 into equation 2 gives equation 4:

$$a(x + \frac{1}{2}y) : \frac{1}{2}ay + \frac{31}{509}a = 100 : 10.6 \quad (4)$$

$$\therefore x + \frac{1}{2}y : \frac{1}{2}y + \frac{31}{509} = 100 : 10.6$$

$$\therefore 50y + \frac{3100}{509} = 10.6x + 5.3y$$

$$\therefore 10.6x - 44.7y = \frac{3100}{509} \quad (5)$$

Since  $y$  is defined in terms of  $1-x$ , the equation 5 can be re-written as:

$$10.6x - 44.7(1 - x) = \frac{3100}{509}$$

$$\therefore 55.3x = 50.8$$

$$\therefore x = 0.92 \quad (6)$$

$$\therefore y = 1 - x = 0.08 \quad (7)$$

### 5.1.3.3. The influence of reaction temperature (Figure 2.15)

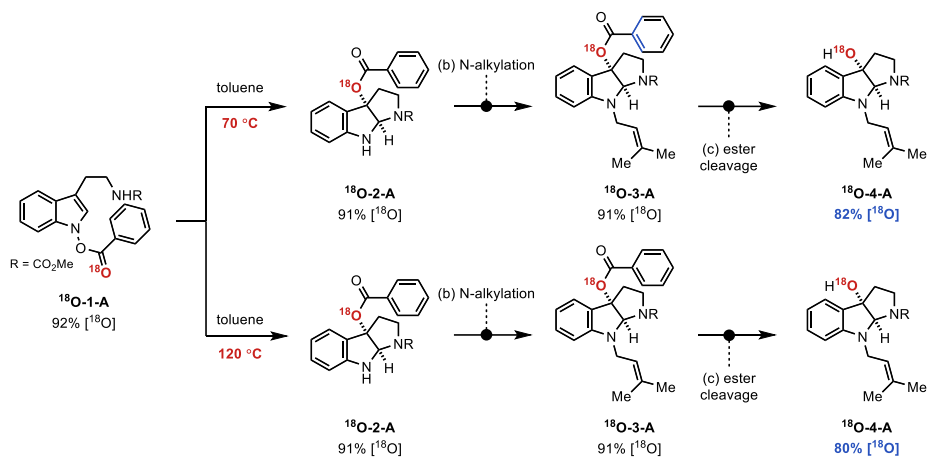
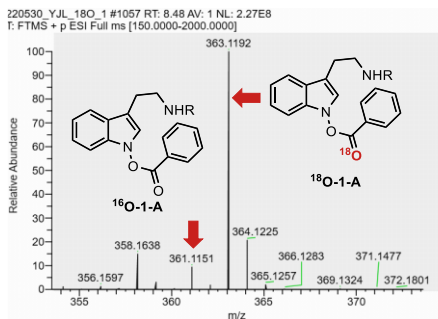
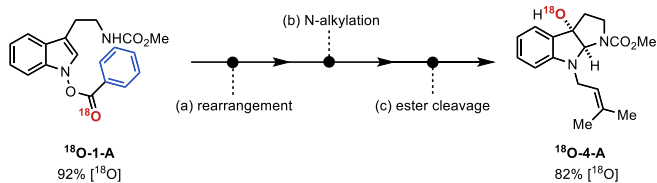


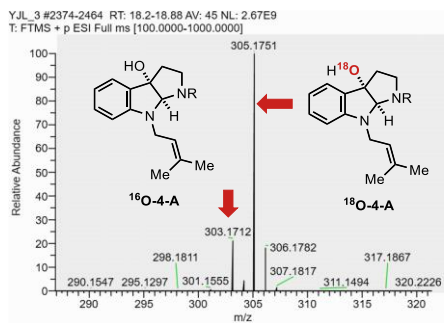
**Figure S8.** Evaluation of temperatures as factor affecting the level of <sup>18</sup>O-enrichment.

To the two oven-dried heavy-wall pressure tubes equipped with a stir bar and septum were added indolyl N-carboxylate **<sup>18</sup>O-1-A** (0.200 mmol, 1.0 equiv) and toluene (0.05 M in **<sup>18</sup>O-1-A**) at 23 °C, respectively. One of the prepared tubes was heated to 70 °C in a pre-heated oil bath and stirred for 60 h until full conversion was observed, while the other tube was heated to 120 °C in a pre-heated oil bath and stirred for 1 h before they were cooled to rt and directly concentrated under reduced pressure to obtain the crude product, respectively. The crude mixtures were then analyzed by HRMS. HRMS result of the resulting crude mixtures indicated no significant loss of <sup>18</sup>O enrichment.

(1) IHT reaction at 70 °C



$$^{18}\text{O-1-A}:^{16}\text{O-1-A} = a : b = 100 : 9.3$$



$$^{18}\text{O-4-A}:^{16}\text{O-4-A} = a(x + \frac{1}{2}y) : \frac{1}{2}ay + b = 100 : 21.7$$

The system of equations is established by the two proportional expressions:

$$\begin{cases} a : b = 100 : 9.3 & (1) \\ a(x + \frac{1}{2}y) : \frac{1}{2}ay + b = 100 : 21.7 & (2) \end{cases}$$

From equation 1,  $b$  can be expressed as:

$$b = \frac{93}{1000} a \quad (3)$$

Insertion of the equation 3 into equation 2 gives equation 4:

$$a(x + \frac{1}{2}y) : \frac{1}{2}ay + \frac{93}{1000}a = 100 : 21.7 \quad (4)$$

$$\therefore x + \frac{1}{2}y : \frac{1}{2}y + \frac{93}{1000} = 100 : 21.7$$

$$\therefore 50y + \frac{93}{10} = 21.7x + \frac{21.7}{2}y$$

$$\therefore 21.7x - \frac{78.3}{2}y = \frac{93}{10} \quad (5)$$

Since  $y$  is defined in terms of  $1-x$ , the equation 5 can be re-written as:

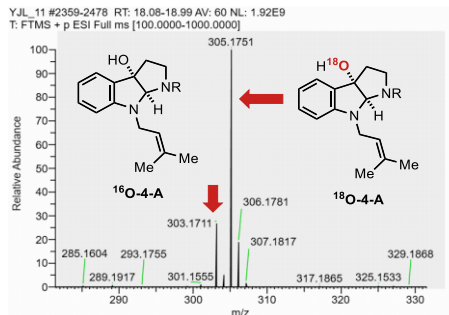
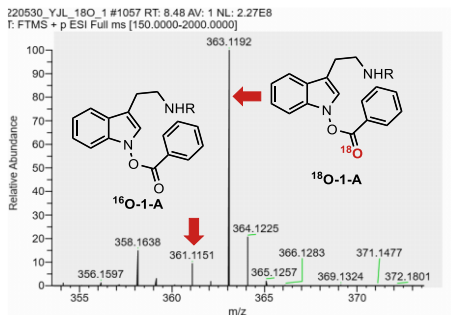
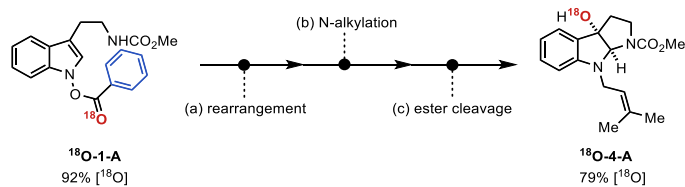
$$21.7x - \frac{78.3}{2}(1-x) = 9.3$$

$$\therefore 60.85x = 9.3 + 39.15 = 48.45$$

$$\therefore x = 0.8 \quad (6)$$

$$\therefore y = 1 - x = 0.2 \quad (7)$$

(2) IHT reaction at 120 °C



The system of equations is established by the two proportional expressions:

$$\begin{cases} a : b = 100 : 9.3 & (1) \\ a(x + \frac{1}{2}y) : \frac{1}{2}ay + b = 100 : 26.3 & (2) \end{cases}$$

From equation 1, **b** can be expressed as:

$$b = \frac{93}{1000} a \quad (3)$$

Insertion of the equation 3 into equation 2 gives equation 4:

$$a(x + \frac{1}{2}y) : \frac{1}{2}ay + \frac{93}{1000}a = 100 : 26.3 \quad (4)$$

$$\therefore x + \frac{1}{2}y : \frac{1}{2}y + \frac{93}{1000} = 100 : 26.3$$

$$\therefore 50y + \frac{93}{10} = 26.3x + \frac{26.3}{2}y$$

$$\therefore 26.3x - \frac{73.7}{2}y = \frac{93}{10} \quad (5)$$

Since  $y$  is defined in terms of  $1-x$ , the equation 5 can be re-written as:

$$26.3x - \frac{73.7}{2}(1-x) = 9.3$$

$$\therefore 63.15x = 9.3 + 36.85 = 46.15$$

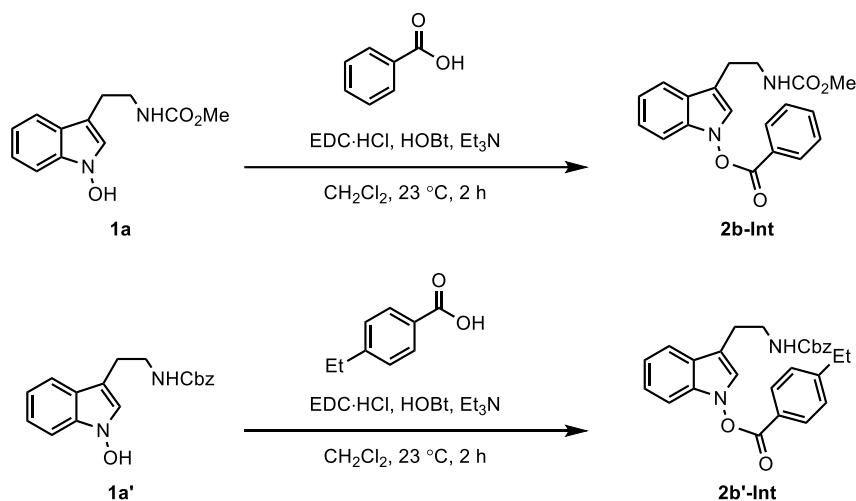
$$\therefore x = 0.73 \quad (6)$$

$$\therefore y = 1 - x = 0.27 \quad (7)$$



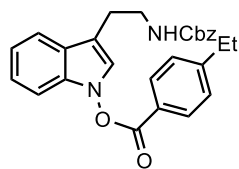
## 5.2. Crossover Experiment (Figure 2.16)

### 5.2.1 Preparation of Compound 2b-Int and 2b'-Int



To an oven-dried round-bottom flask equipped with a stir bar and septum were added *N*-hydroxyindole **1** (1.0 equiv) and CH<sub>2</sub>Cl<sub>2</sub> (0.05 M in **1**) at 23 °C, followed by benzoic acid (1.1 equiv), EDC·HCl (1.1 equiv), HOBT (1.1 equiv), and Et<sub>3</sub>N (2.2 equiv). The resulting mixture was stirred for 2 h, before it was quenched with H<sub>2</sub>O. The layers were separated, and the aqueous layer was extracted with CH<sub>2</sub>Cl<sub>2</sub> three times. The combined organic layer was washed with brine, dried over anhydrous MgSO<sub>4</sub>, filtered, and concentrated under reduced pressure. The resulting residue was purified by flash column chromatography (silica gel, hexanes:EtOAc = 1:0 → 1:1) to afford indolyl *N*-carboxylate **2-Int**.

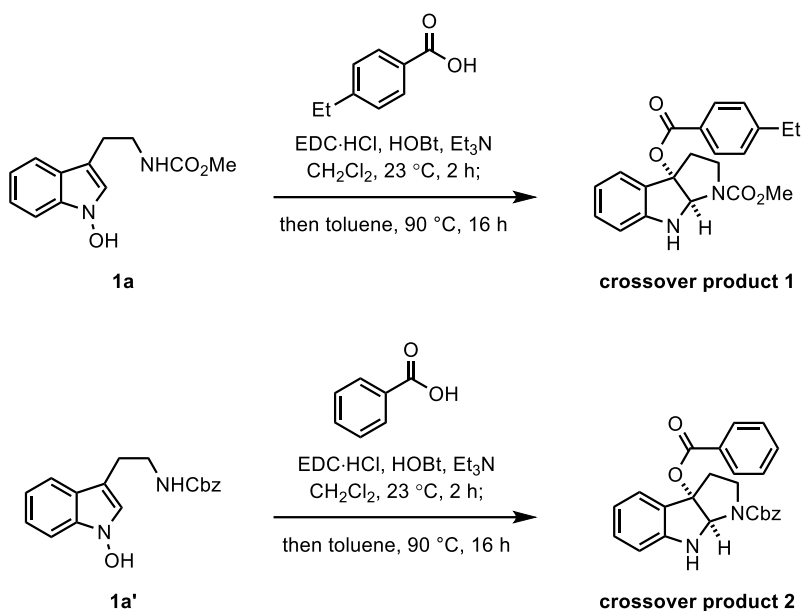
### 3-(2-(((Benzyloxy)carbamoyl)amino)ethyl)-1H-indol-1-yl 4-ethylbenzoate (**2b'-Int**)



$R_f$ =0.60 (silica gel, hexanes:EtOAc = 7:3); <sup>1</sup>H NMR (500 MHz, CDCl<sub>3</sub>): δ 8.13 (d,  $J$  = 8.2 Hz, 2H), 7.60 (d,  $J$  = 8.0 Hz, 1H), 7.39 (d,  $J$  = 8.0 Hz, 2H), 7.36 – 7.27 (m, 5H), 7.24 (d,  $J$  = 3.2 Hz, 2H), 7.16 (dt,  $J$  = 8.1, 3.8 Hz, 1H), 7.07 (s, 1H), 5.12 (s, 2H), 4.92 (s, 1H), 3.56 (q,  $J$  = 6.6 Hz, 2H), 2.99 (t,  $J$  = 6.8 Hz, 2H), 2.78 (q,  $J$  = 7.6 Hz, 2H), 1.31 (td,  $J$  = 7.6, 1.6 Hz, 3H); <sup>13</sup>C NMR (126 MHz, CDCl<sub>3</sub>): δ 164.9, 156.5, 152.0, 136.8, 135.8, 130.6, 128.6, 128.24,

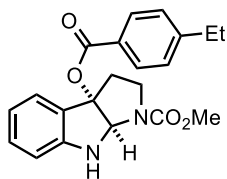
128.20, 124.9, 124.2, 123.9, 123.6, 121.0, 119.4, 111.7, 109.2, 66.8, 41.2, 29.8, 29.3, 25.8, 15.3; **HRMS** calcd. for  $C_{27}H_{27}N_2O_4^+$   $[M + H]^+$  443.1965, found 443.1961.

## 5.2.2. Preparation of Crossover Products



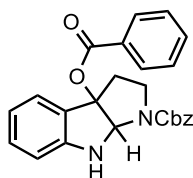
To an oven-dried round-bottom flask equipped with a stir bar and septum were added *N*-hydroxyindole **1** (1.0 equiv) and CH<sub>2</sub>Cl<sub>2</sub> (0.05 M in **1**) at 23 °C, followed by benzoic acid (1.1 equiv), EDC·HCl (1.1 equiv), HOBT (1.1 equiv), and Et<sub>3</sub>N (2.2 equiv). The resulting mixture was stirred for 2 h, before it was quenched with H<sub>2</sub>O. The layers were separated, and the aqueous layer was extracted with CH<sub>2</sub>Cl<sub>2</sub> three times. The combined organic layer was washed with brine, dried over anhydrous MgSO<sub>4</sub>, filtered, and concentrated under reduced pressure. The resulting crude was filtered through a short pad of silica gel using CH<sub>2</sub>Cl<sub>2</sub> as eluent, concentrated under reduced pressure and re-dissolved in toluene (0.05 M in **1**). The resulting solution was then heated to 90 °C in a pre-heated oil bath and stirred for 16 h, before it was cooled to 23 °C and directly concentrated under reduced pressure to provide the crude product. The crude product was purified by flash column chromatography (silica gel, hexanes:EtOAc = 1:0 → 7:3) to afford the product.

**Methyl 3a-((4-ethylbenzoyl)oxy)-3,3a,8,8a-tetrahydropyrrolo[2,3-b]indole-1(2H)-carboxylate (crossover product 1)**



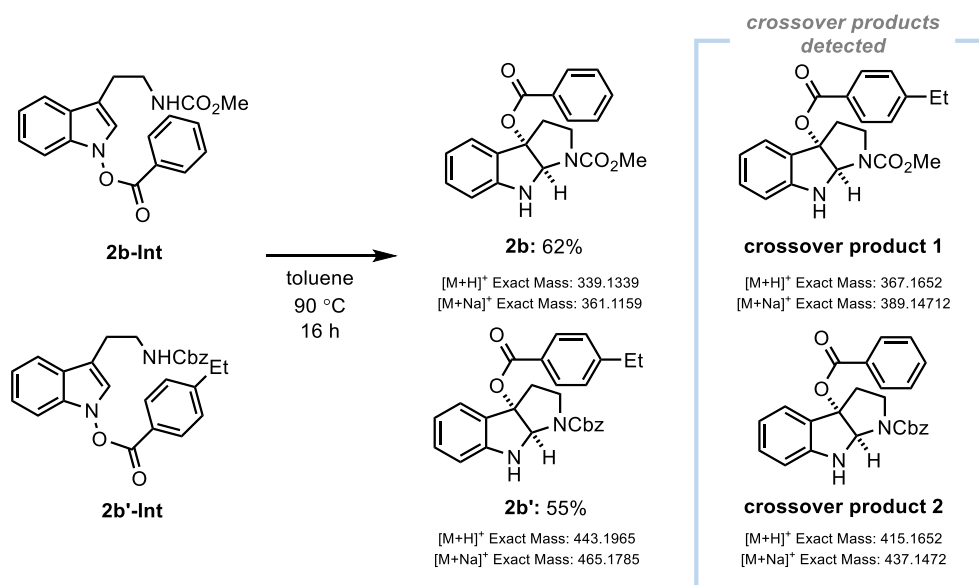
$R_f=0.43$  (silica gel, hexanes:EtOAc = 7:3);  $^1\text{H NMR}$  (500 MHz,  $\text{CDCl}_3$ , 60:40 mixture of rotamers):  $\delta$  7.90 (d,  $J = 7.8$  Hz, 2H), 7.62 and 7.54 (d,  $J = 7.6$  Hz, 1H), 7.23 (d,  $J = 7.9$  Hz, 2H), 7.18 (t,  $J = 7.6$  Hz, 1H), 6.79 (q,  $J = 6.8$  Hz, 1H), 6.68 (d,  $J = 7.9$  Hz, 1H), 5.77 (s, 1H), 3.92 and 3.81 (t,  $J = 9.7$  Hz, 1H), 3.79 and 3.73 (s, 3H), 3.22 (td,  $J = 10.9, 6.3$  Hz, 1H), 3.06 (dd,  $J = 12.9, 6.3$  Hz, 1H), 2.94 (dd,  $J = 12.8, 6.1$  Hz, 0H), 2.75 – 2.65 (m, 3H), 1.23 (t,  $J = 7.6$  Hz, 3H);  $^{13}\text{C NMR}$  (126 MHz,  $\text{CDCl}_3$ ):  $\delta$  165.5, 155.7, 154.9, 151.0, 150.8, 150.3, 131.1, 130.0, 128.0, 127.7, 126.7, 126.3, 126.1, 126.1, 119.7, 119.5, 110.4, 110.3, 94.3, 93.1, 80.5, 79.7, 52.9, 52.7, 45.6, 45.5, 36.0, 35.8, 29.1, 15.4; **HRMS** calcd. for  $\text{C}_{21}\text{H}_{23}\text{N}_2\text{O}_4^+$   $[\text{M} + \text{H}]^+$  367.1652, found 367.1647.

**Benzyl 3a-(benzoyloxy)-3,3a,8,8a-tetrahydropyrrolo[2,3-b]indole-1(2H)-carboxylate (crossover product 2)**



$R_f=0.56$  (silica gel, hexanes:EtOAc = 7:3);  $^1\text{H NMR}$  (500 MHz,  $\text{CDCl}_3$ , 55:45 mixture of rotamers):  $\delta$  7.99 and 7.98 (d,  $J = 7.6$  Hz, 2H), 7.63 and 7.55 (d,  $J = 7.5$  Hz, 1H), 7.54 (t,  $J = 8.3$  Hz, 1H), 7.44 – 7.28 (m, 7H), 7.19 (q,  $J = 6.7$  Hz, 1H), 6.80 (t,  $J = 7.5$  Hz, 2H), 6.69 and 6.63 (d,  $J = 7.9$  Hz, 1H), 5.81 and 5.79 (s, 1H), 5.25 and 5.20 (d,  $J = 12.3$  Hz, 1H), 5.21 and 5.12 (d,  $J = 12.3$  Hz, 1H), 3.94 and 3.87 (t,  $J = 9.1$  Hz, 1H), 3.32 – 3.20 (m, 1H), 3.07 and 2.98 (dd,  $J = 12.8, 5.3$  Hz, 1H), 2.77 – 2.67 (m, 1H);  $^{13}\text{C NMR}$  (126 MHz,  $\text{CDCl}_3$ ):  $\delta$  165.5, 165.4, 155.1, 154.3, 151.0, 150.7, 136.4, 134.4, 133.3, 133.3, 131.2, 131.1, 130.3, 130.2, 129.9, 129.9, 128.9, 128.7, 128.7, 128.5, 128.4, 128.3, 128.1, 126.7, 126.6, 126.2, 126.0, 126.0, 119.7, 119.5, 110.5, 110.3, 94.4, 93.3, 80.5, 79.7, 67.6, 67.2, 45.7, 45.6, 35.9, 35.8; **HRMS** calcd. for  $\text{C}_{25}\text{H}_{23}\text{N}_2\text{O}_4^+$   $[\text{M} + \text{H}]^+$  415.1652, found 415.1648.

## 5.2.2 Crossover Experiment

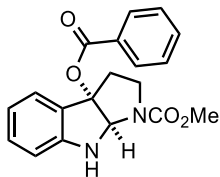


To a 10 mL oven-dried reaction tube equipped with a stir bar were added **2b-Int** (67.6 mg, 0.200 mmol, 1.0 equiv), **2b'-Int** (88.5 mg, 0.200 mmol, 1.0 equiv) and toluene (2 mL). The reaction tube was sealed under N<sub>2</sub> and the resulting mixture was heated to 90 °C in a pre-heated oil bath and stirred for 16 h, before it was cooled to 23 °C and directly concentrated under reduced pressure to provide the crude product. A small portion of the crude mixture was then analyzed by TLC and HRMS. The crude mixture of crossover experiment was purified by flash column chromatography (silica gel, hexanes:EtOAc = 1:0 → 7:3) to afford the product **2b** (41.7 mg, 62%) and **2b'** (48.9 mg, 55%).

From the TLC analysis, no appreciable amount of crossover products was detected.

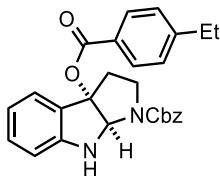
As a result of comparing the retention times of individually synthesized compounds by HPLC analysis performed simultaneously with HRMS analysis, it was concluded that **crossover product 1** and **crossover product 2** were not detected.

**Methyl 3a-(benzyloxy)-3,3a,8,8a-tetrahydropyrrolo[2,3-b]indole-1(2H)-carboxylate (2b)**



The spectral data matched to those of compound **<sup>18</sup>O-2-A** (See section 3.2.1.1.).  $R_f=0.38$  (silica gel, hexanes:EtOAc = 7:3); **<sup>1</sup>H NMR** (500 MHz, CDCl<sub>3</sub>):  $\delta$  7.99 (d,  $J = 7.7$  Hz, 2H), 7.63 and 7.58 (d,  $J = 7.6$  Hz, 1H), 7.54 (t,  $J = 8.4$  Hz, 1H), 7.41 (t,  $J = 7.6$  Hz, 2H), 7.19 (t,  $J = 7.7$  Hz, 1H), 6.80 (q,  $J = 7.0$  Hz, 1H), 6.68 (d,  $J = 7.9$  Hz, 1H), 5.78 (s, 1H), 3.93 and 3.81 (t,  $J = 9.7$  Hz, 1H), 3.80 and 3.73 (s, 3H), 3.26 – 3.20 (m, 1H), 3.07 and 2.96 (dd,  $J = 12.9$ , 6.1 Hz, 1H), 2.75 – 2.69 (m, 1H); **<sup>13</sup>C NMR** (126 MHz, CDCl<sub>3</sub>):  $\delta$  165.3, 155.6, 154.8, 151.0, 150.7, 133.2, 131.0, 130.2, 129.8, 129.1, 128.4, 126.5, 126.3, 126.1, 126.0, 119.6, 119.3, 110.3, 110.2, 94.5, 93.3, 80.4, 79.6, 52.8, 52.5, 45.5, 35.9, 35.8 ; **HRMS** calcd. for C<sub>19</sub>H<sub>18</sub>N<sub>2</sub>O<sub>4</sub>Na<sup>+</sup> [M + Na]<sup>+</sup> 361.1159, found 361.1160.

**3-(2-(((Benzyloxy)carbonyl)amino)ethyl)-1H-indol-1-yl 4-ethylbenzoate (2b')**



$R_f=0.76$  (silica gel, hexanes:EtOAc = 1:1); **<sup>1</sup>H NMR** (500 MHz, CDCl<sub>3</sub>):  $\delta$  7.89 (dd,  $J = 8.2$ , 3.8 Hz, 2H), 7.62 and 7.54 (d,  $J = 7.4$  Hz, 1H), 7.42 (d,  $J = 6.8$  Hz, 1H), 7.36 (d,  $J = 4.4$  Hz, 2H), 7.40 – 7.30 (m, 2H), 7.22 (d,  $J = 8.0$  Hz, 2H), 7.18 (tdd,  $J = 7.2$ , 5.6, 1.3 Hz, 1H), 6.79 (t,  $J = 7.5$  Hz, 1H), 6.68 and 6.63 (d,  $J = 7.9$  Hz, 1H), 5.80 and 5.78 (s, 1H), 5.24 and 5.20 (d,  $J = 12.2$  Hz, 1H), 5.20 and 5.12 (d,  $J = 12.3$  Hz, 1H), 3.93 and 3.87 (ddd,  $J = 10.6$ , 8.5, 1.8 Hz, 1H), 3.30 – 3.20 (m, 1H), 3.06 and 2.96 (ddd,  $J = 12.8$ , 6.4, 1.8 Hz, 1H), 2.76 – 2.68 (m, 1H), 2.68 (q,  $J = 7.5$  Hz, 2H), 1.23 (t,  $J = 7.6$  Hz, 3H); **<sup>13</sup>C NMR** (126 MHz, CDCl<sub>3</sub>):  $\delta$  165.5, 155.1, 154.3, 151.0, 150.7, 150.3, 150.3, 136.5, 131.1, 130.0, 128.9, 128.8, 128.5, 128.4, 128.3, 128.1, 128.0, 127.7, 127.7, 126.7, 126.2, 126.1, 119.7, 119.5, 110.4, 110.3, 94.2, 93.1, 80.5, 79.7, 67.5, 67.2, 45.7, 45.6, 35.9, 35.8, 29.1, 15.4; **HRMS** calcd. for C<sub>27</sub>H<sub>27</sub>N<sub>2</sub>O<sub>4</sub><sup>+</sup> [M + H]<sup>+</sup> 443.1965, found 443.1964.

### 5.2.3. Analysis of Crossover Experiment Results

#### 5.2.3.1. TLC analysis of the crossover experiment

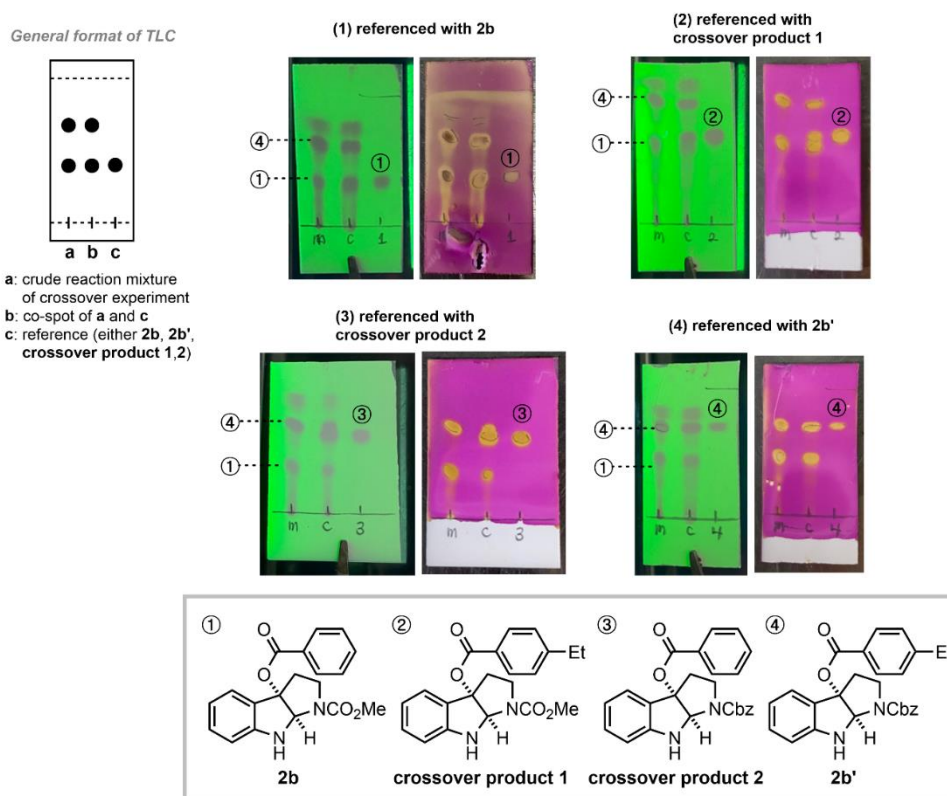
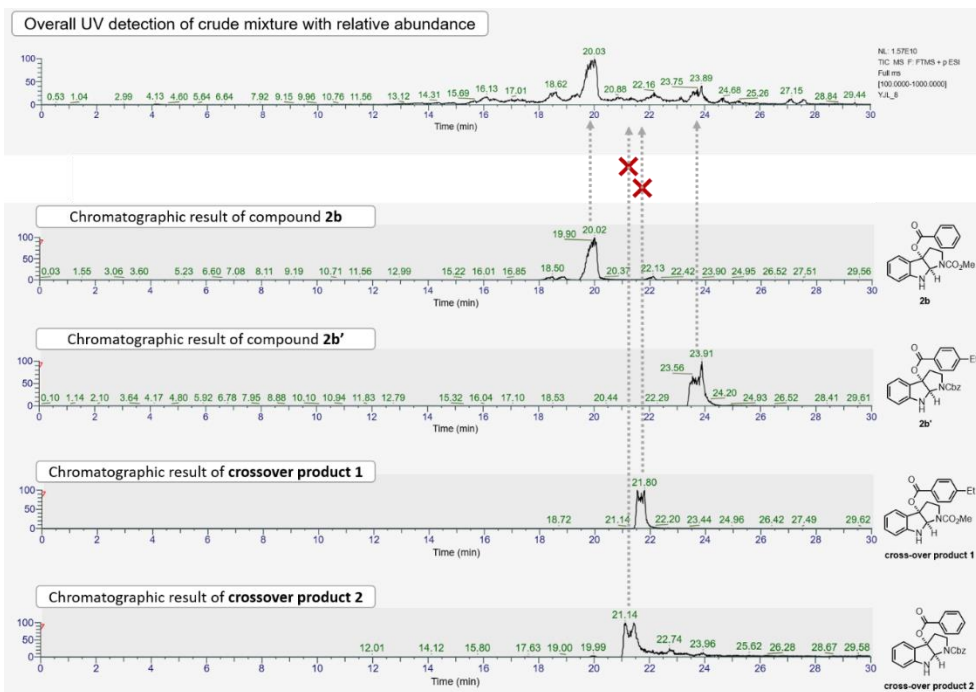


Figure S9. TLC analysis of crossover experiment.

TLC was checked with the reference compounds, which are the pyrroloindoline **2b**, **2b'**, **crossover product 1**, and **crossover product 2**. Each TLC sample was visualized by 254 nm UV lamp and stained with  $\text{KMnO}_4$  stain with heating. Among the photos of the TLC plates with two differently visualized forms, the one visualized by 254 nm UV lamp is on the left and the one stained with  $\text{KMnO}_4$  is on the right. TLC analysis indicates that no detectable spots corresponding to the **crossover product 1**, **2** were observed in each TLC while formation of **2b** and **2b'** was clearly detected.

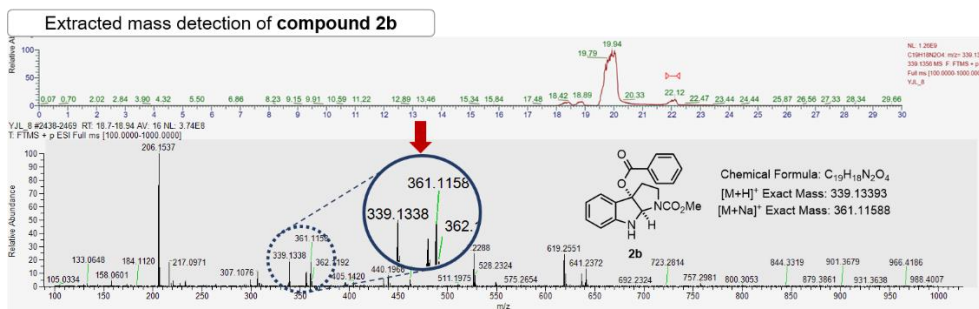
### 5.2.3.2. HRMS/HPLC analysis of the crossover experiment

(1) Result of UV detection for the crude mixture of the crossover experiment and the relative location of each product



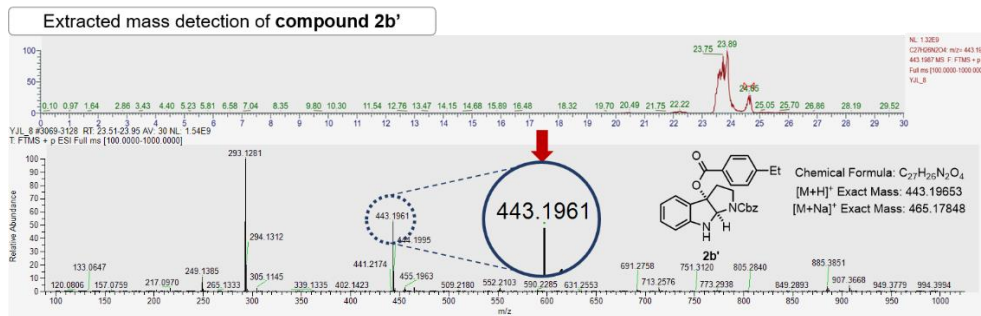
For all HRMS peaks shown below, the red arrow was used to indicate the detected mass of the desired products.

(2) Result of mass detection at peak corresponding to compound 2b



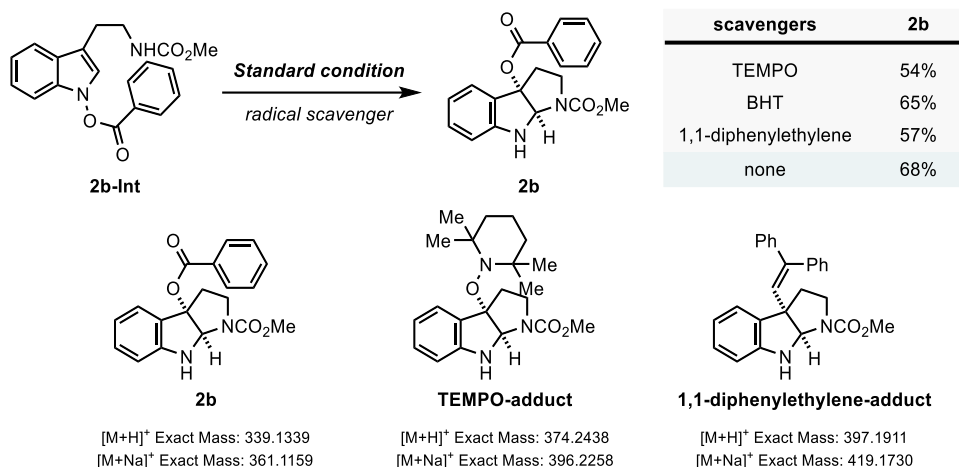


### (3) Result of mass detection at peak corresponding to compound **2b'**



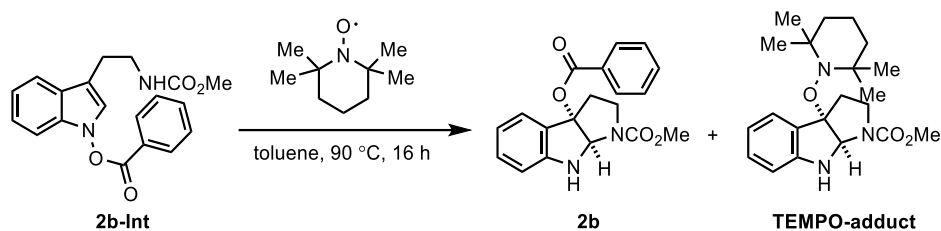
### 5.3. Radical-trapping Experiment (Figure 2.17)

#### 5.3.1. Radical-trapping Experiment with Indolyl *N*-Carboxylate **2b-Int**

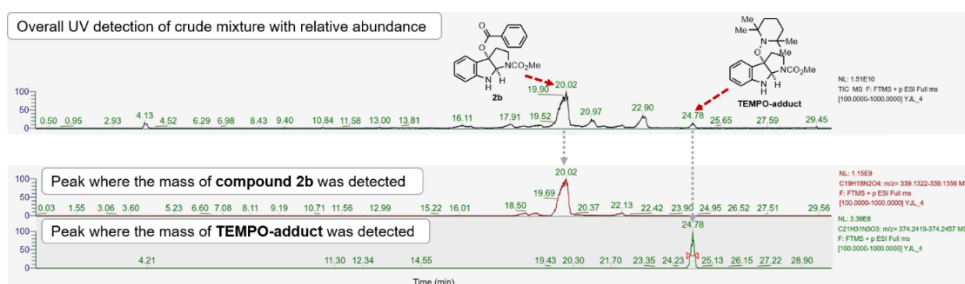


To a 10 mL oven-dried reaction tube equipped with a stir bar were added indolyl *N*-carboxylate **2b-Int** (67.6 mg, 0.200 mmol, 1.0 equiv) and toluene (4 mL, 0.05 M in **2b-Int**) at 23 °C, followed by radical-trapping reagent (2.0 equiv). The reaction tube was sealed under N<sub>2</sub> and the resulting mixture was heated to 90 °C in a pre-heated oil bath and stirred for 16 h, before it was cooled to 23 °C and directly concentrated under reduced pressure to provide the crude product. The crude mixture was then analyzed by HRMS. HRMS result of the resulting crude mixture indicated the formation of **TEMPO-adduct** or **1,1-diphenylethylene-adduct** when TEMPO or 1,1-diphenylethylene were used as a radical scavenger, even though no significant yield loss was observed for **2b**. Each crude mixture of radical-trapping experiment was purified by flash column chromatography (silica gel, hexanes:EtOAc = 1:0 → 1:1) to afford the product **2b** (when using TEMPO: 40.3 mg, 54%, when using BHT: 44.1 mg, 65%, when using 1,1-diphenylethylene: 38.6 mg, 57%)

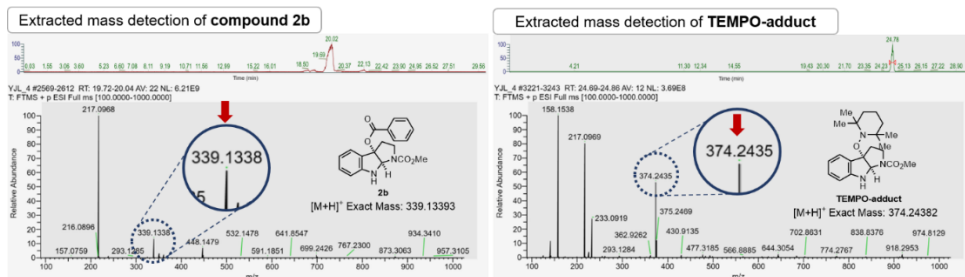
### 5.3.1.1. HRMS results using TEMPO as a radical scavenger



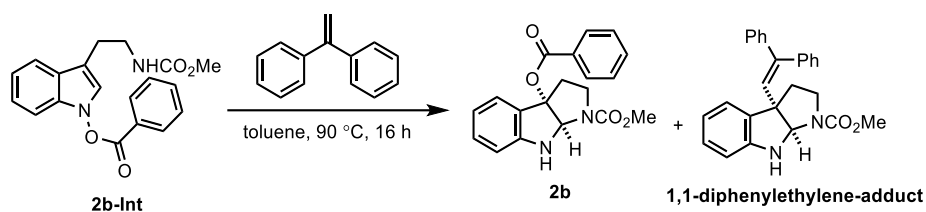
(1) Result of UV detection for the radical-trapping experiment and the relative location of each product detected



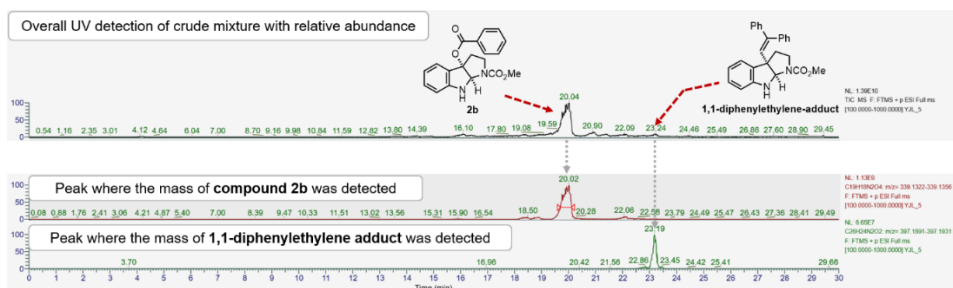
(b) Result of mass detection at peaks corresponding to compound **2b** and **TEMPO-adduct**



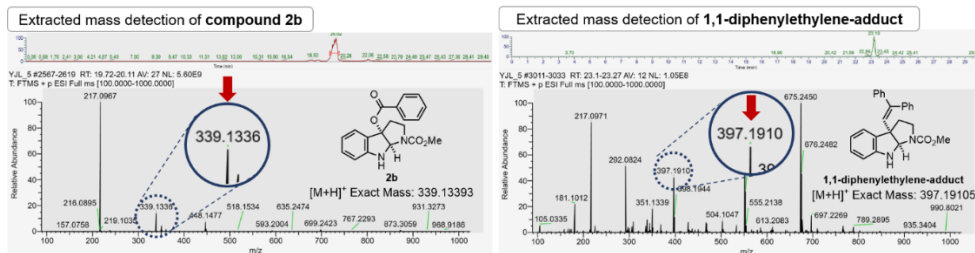
### 5.3.1.2. HRMS results using 1,1-diphenylethylene as a radical scavenger



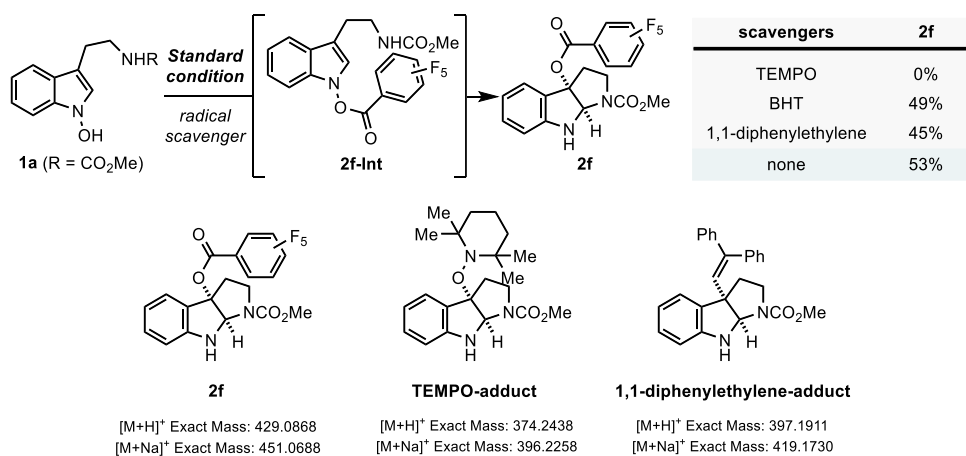
(1) Result of UV detection for the radical-trapping experiment and the relative location of each product detected



(2) Result of mass detection at peaks corresponding to compound 2b and 1,1-diphenylethylene-adduct

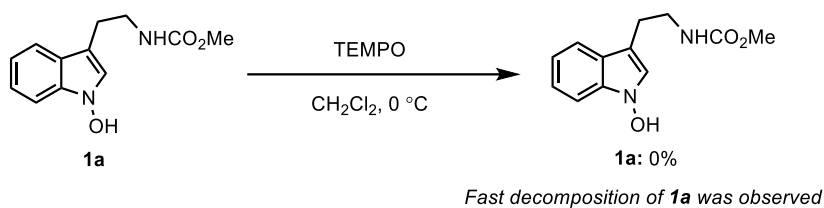


### 5.3.2. Radical-trapping Experiment with Electron-deficient Indolyl *N*-carboxylate



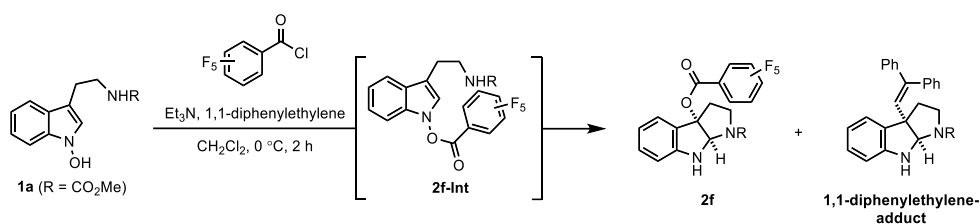
To an oven-dried round-bottom flask equipped with a stir bar and septum were added *N*-hydroxyindole **1a** (50.0 mg, 0.213 mmol, 1.0 equiv) and CH<sub>2</sub>Cl<sub>2</sub> (4.2 mL, 0.05 M in **1a**) at 23 °C. The resulting solution was cooled to 0 °C and 2,3,4,5,6-pentafluorobenzoyl chloride (1.1 equiv), Et<sub>3</sub>N (1.1 equiv) and radical-trapping reagent (2.0 equiv) were successively added to the solution. The reaction mixture was warmed up to 23 °C and stirred for 2 h, before it was quenched with H<sub>2</sub>O (2 mL). The layers were separated and the aqueous layer was extracted with CH<sub>2</sub>Cl<sub>2</sub> (3 × 3 mL). The combined organic layer was dried over anhydrous MgSO<sub>4</sub>, filtered, and concentrated under reduced pressure to provide the crude product. The crude mixture was then analyzed by HRMS. When 1,1-diphenylethylene was used as the radical scavenger, **1,1-diphenylethylene-adduct** was detected by HRMS analysis, while no significant decrease in the reaction yield was observed. On the other hand, the formation of **2f** was noticeably suppressed when TEMPO was used as the radical scavenger due to the rapid decomposition of **1a** induced by TEMPO. Each crude mixture of radical-trapping experiment was purified by flash column chromatography (silica gel, hexanes:EtOAc = 1:0 → 1:1) to afford the product **2f** (when using TEMPO: 0 mg, 0%, when using BHT: 44.7 mg, 49%, when using 1,1-diphenylethylene: 41.1 mg, 45%)

### 5.3.2.1. Control experiment using TEMPO as a radical scavenger

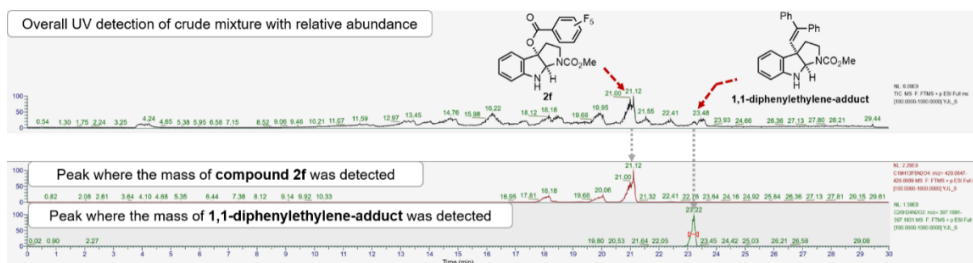


To confirm that the TEMPO is interacting with the *N*-hydroxyindole, *N*-hydroxyindole **1a** (50.0 mg, 0.213 mmol, 1.0 equiv) and CH<sub>2</sub>Cl<sub>2</sub> (4.2 mL, 0.05 M in **1a**) were added to an oven-dried round-bottom flask equipped with a stir bar and septum at 23 °C. The resulting solution was cooled to 0 °C, and TEMPO (2.0 equiv) was added to the solution. The reaction mixture was stirred while the reaction was monitored by TLC. TLC indicated that fast decomposition of **1a** occurred immediately after TEMPO was added. This clearly indicates that the result of radical-trapping experiment with TEMPO is derived from the decomposition of **1a**, not from the inhibition of the radical-involved reaction pathway.

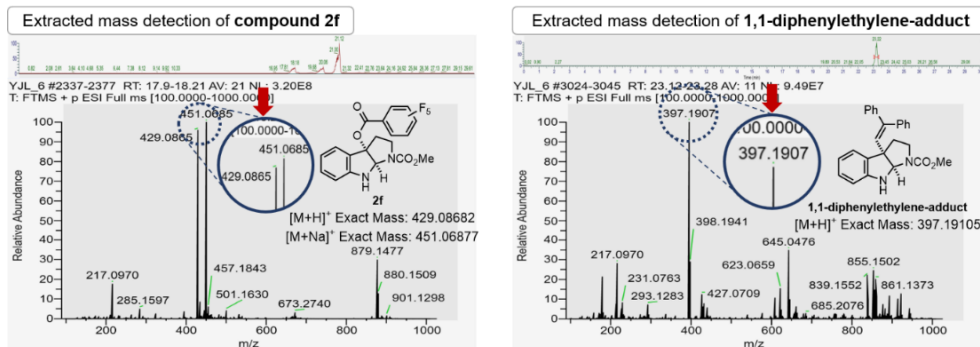
### 5.3.2.2. HRMS results using 1,1-diphenylethylene as a radical scavenger



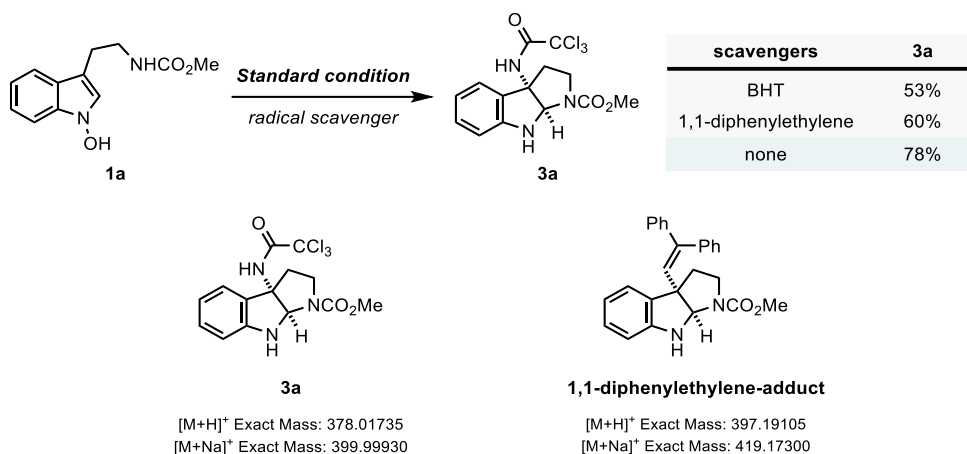
(1) Result of UV detection for the radical-trapping experiment and the relative location of each product detected



(b) Result of mass detection at peaks corresponding to compound 2f and 1,1-diphenylethylene-adduct



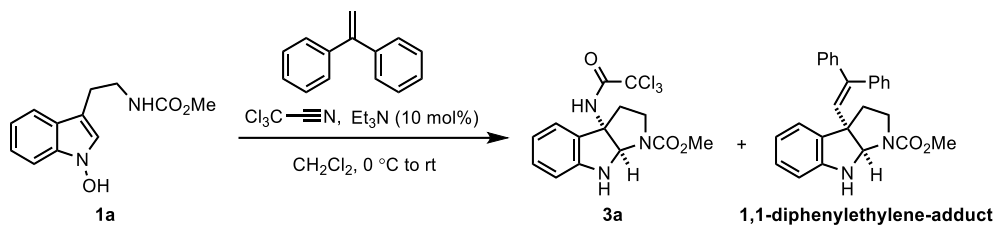
### 5.3.3. Radical-trapping Experiment with Indolyl Acetimide



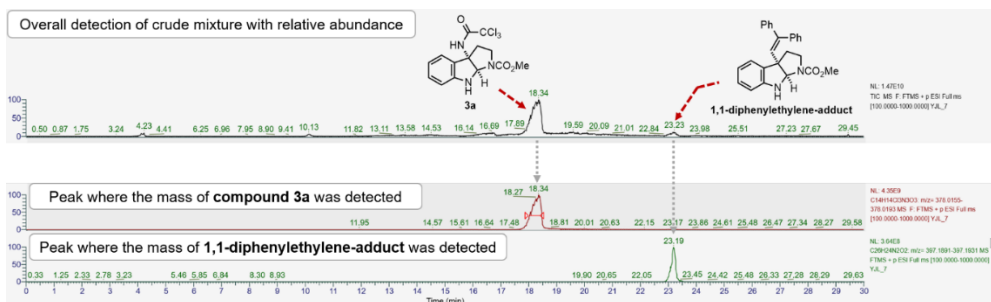
To an oven-dried round-bottom flask equipped with a stir bar and septum were added N-hydroxyindole **1a** (50.0 mg, 0.213 mmol, 1.0 equiv) and CH<sub>2</sub>Cl<sub>2</sub> (4.2 mL, 0.05 M in **1a**) at 23 °C. The resulting solution was cooled to 0 °C, and trichloroacetonitrile (3.0 equiv), Et<sub>3</sub>N (0.1 equiv), and radical-trapping reagent (2.0 equiv) were added to the solution. The reaction mixture was warmed up to rt and stirred for 3 h, before it was quenched with H<sub>2</sub>O (2 mL). The layers were separated and the aqueous layer was extracted with CH<sub>2</sub>Cl<sub>2</sub> (3 × 3 mL). The combined organic layer was dried over anhydrous MgSO<sub>4</sub>, filtered, and concentrated under reduced pressure to obtain the crude product, which was then analyzed by HRMS. When 1,1-diphenylethylene was used as the radical scavenger, **1,1-diphenylethylene-adduct** was detected by HRMS analysis while slight yield loss of **3a** was observed. Each crude mixture of radical-trapping experiment was purified by flash column chromatography (silica gel, hexanes:EtOAc = 1:0 → 1:1) to afford product **3a** (when using BHT: 42.8 mg, 53%, when using 1,1-diphenylethylene: 48.5 mg, 60%)



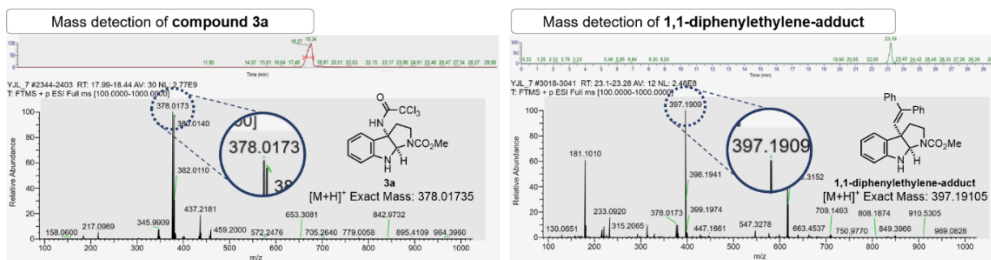
### 5.3.3.1. HRMS results using 1,1-diphenylethylene as a radical scavenger



(1) Result of UV detection for the radical-trapping experiment and the relative location of each product detected



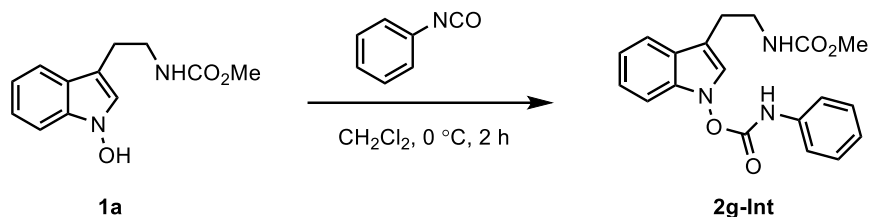
(2) Result of mass detection at peaks corresponding to compound **3a** and **1,1-diphenylethylene-adduct**



## 5.4. [3,3]-Sigmatropic Rearrangement of Indolyl Carbamate (Figure 2.19A)

### 5.4.1. Preparation of Indolyl Carbamate

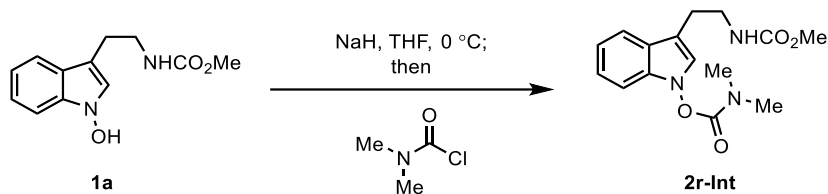
#### Methyl (2-(1-((phenylcarbamoyl)oxy)-1H-indol-3-yl)ethyl)carbamate (**2g-Int**)



To an oven-dried round-bottom flask equipped with a stir bar and septum were added *N*-hydroxyindole **1a** (318 mg, 1.36 mmol, 1.0 equiv) and CH<sub>2</sub>Cl<sub>2</sub> (14 mL, 0.1 M in **1a**) at 23 °C. The resulting solution was cooled to 0 °C, and phenyl isocyanate (155 μL, 1.42 mmol, 1.04 equiv) was added to the solution. The reaction mixture was stirred for 2 h, before it was quenched with H<sub>2</sub>O (10 mL). The layers were separated, and the aqueous layer was extracted with CH<sub>2</sub>Cl<sub>2</sub> (3 × 20 mL). The combined organic layer was washed with brine (1 × 20 mL), dried over anhydrous MgSO<sub>4</sub>, filtered, and concentrated under reduced pressure. The resulting residue was purified by flash column chromatography (silica gel, hexanes:EtOAc = 1:0 → 7:3) to afford indolyl *N*-carboxylate **2g-Int** (336 mg, 70%) as a pale yellow oil.

*R<sub>f</sub>*=0.47 (silica gel, hexanes:EtOAc = 1:1); **<sup>1</sup>H NMR** (500 MHz, CDCl<sub>3</sub>): δ 7.59 (d, *J* = 8.1 Hz, 1H), 7.47 (d, *J* = 8.0 Hz, 2H), 7.37 (t, *J* = 7.8 Hz, 2H), 7.33 – 7.26 (m, 2H), 7.17 (q, *J* = 7.1 Hz, 2H), 7.06 (s, 1H), 4.84 (s, 1H), 3.66 (s, 3H), 3.52 (q, *J* = 6.7 Hz, 2H), 2.95 (t, *J* = 6.9 Hz, 2H); **<sup>13</sup>C NMR** (126 MHz, CDCl<sub>3</sub>): δ 157.4, 151.8, 136.7, 135.7, 129.3, 124.7, 124.6, 124.0, 123.6, 122.2, 121.0, 119.3, 119.1, 111.5, 111.4, 109.0, 52.2, 41.1, 25.7; **HRMS** calcd. for C<sub>19</sub>H<sub>20</sub>N<sub>3</sub>O<sub>4</sub><sup>+</sup> [M + H]<sup>+</sup> 354.1448, found 354.1445.

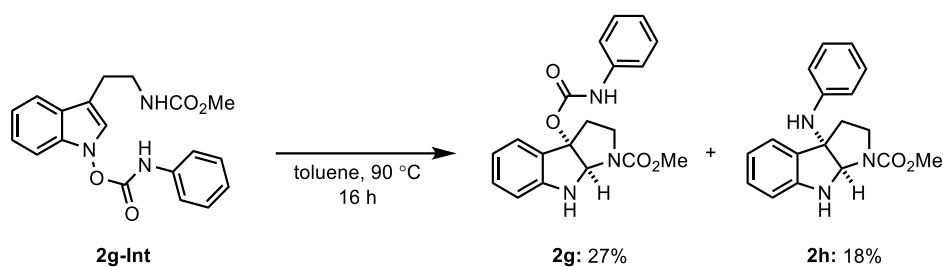
### 3-(2-((Methoxycarbonyl)amino)ethyl)-1H-indol-1-yl dimethylcarbamate (**2r-Int**)



To an oven-dried round-bottom flask equipped with a stir bar and septum were added N-hydroxyindole **1** (362 mg, 1.55 mmol, 1.0 equiv) and THF (20 mL, 0.08 M in **1a**) at 23 °C. The resulting solution was cooled to 0 °C, and NaH (60% in mineral oil, 93.0 mg, 2.32 mmol, 1.5 equiv) was added to the solution. The reaction mixture was stirred for 10 min, then dimethylcarbonyl chloride (0.21 mL, 2.32 mmol, 1.5 equiv) was added. The resulting mixture was stirred for additional 1 h at 0 °C before it was quenched with brine (20 mL). The layers were separated and the aqueous layer was extracted with EtOAc (3 × 20 mL). The combined organic layer was washed with brine (1 × 20 mL), dried over anhydrous MgSO<sub>4</sub>, filtered, and concentrated under reduced pressure. The resulting residue was purified by flash column chromatography (silica gel, hexanes:EtOAc = 1:0 → 1:1) to afford indolyl N-carboxylate **2r-Int** (288 mg, 61%) as a pale yellow oil.

*R<sub>f</sub>*=0.11 (silica gel, hexanes:EtOAc = 1:1); <sup>1</sup>H NMR (500 MHz, CDCl<sub>3</sub>): δ 7.60 (d, *J* = 8.0 Hz, 1H), 7.31 – 7.27 (m, 2H), 7.17 (ddd, *J* = 8.1, 5.7, 2.4 Hz, 1H), 7.06 (s, 1H), 4.98 (s, 1H), 3.69 (s, 3H), 3.52 (q, *J* = 6.6 Hz, 2H), 3.19 (s, 3H), 3.08 (s, 3H), 2.96 (t, *J* = 6.9 Hz, 2H); <sup>13</sup>C NMR (126 MHz, CDCl<sub>3</sub>): δ 157.1, 154.6, 135.3, 124.4, 123.9, 123.2, 120.5, 119.1, 110.6, 108.6, 52.0, 41.1, 37.6, 36.2, 25.7; HRMS calcd. for C<sub>15</sub>H<sub>20</sub>N<sub>3</sub>O<sub>4</sub><sup>+</sup> [M + H]<sup>+</sup> 306.1448, found 306.1456.

#### 5.4.2. [3,3]-Sigmatropic Rearrangement of indolyl *N*-carboxylate **2g-Int** (Figure 8A)



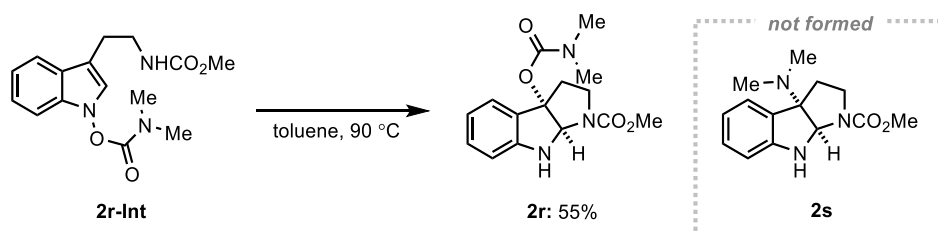
To a 10 mL oven-dried reaction tube equipped with a stir bar were added indolyl *N*-carboxylate **2g-Int** (0.120 g, 0.340 mmol, 1.0 equiv) and toluene (7 mL, 0.05 M in **2g-Int**) at 23 °C. The resulting mixture was heated to 90 °C in a pre-heated oil bath and stirred for 16 h, before it was cooled to 23 °C and directly concentrated under reduced pressure to provide the crude product. The resulting residue was purified by flash column chromatography (silica gel, hexanes:EtOAc = 1:0 → 7:3) to afford the product **2g** and **2h** (**2g**: 32.4 mg, 27%, **2h**: 18.9 mg, 18%) as a pale yellow oil.

**2g**:  $R_f$ =0.47 (silica gel, hexanes:EtOAc = 1:1);  $^1\text{H NMR}$  (500 MHz,  $\text{CDCl}_3$ ):  $\delta$  7.61 and 7.53 (d,  $J$  = 7.6 Hz, 1H), 7.36 – 7.26 (m, 5H), 7.19 (t,  $J$  = 7.6 Hz, 1H), 7.05 (t,  $J$  = 7.1 Hz, 1H), 6.81 (q,  $J$  = 7.4 Hz, 1H), 6.67 (d,  $J$  = 8.0 Hz, 1H), 6.65 – 6.61 (m, 1H), 5.68 and 5.63 (s, 1H), 5.21 and 4.85 (s, 1H), 3.89 and 3.79 (t,  $J$  = 9.8 Hz, 1H), 3.79 and 3.72 (s, 3H), 3.18 (td,  $J$  = 10.9, 6.3 Hz, 1H), 3.00 and 2.85 (dd,  $J$  = 12.9, 6.4 Hz, 1H), 2.70 (p,  $J$  = 11.6 Hz, 2H);  $^{13}\text{C NMR}$  (126 MHz,  $\text{CDCl}_3$ ):  $\delta$  155.7, 154.9, 152.0, 151.9, 150.9, 150.6, 137.7, 137.6, 131.2, 129.2, 126.6, 126.0, 125.9, 123.8, 119.8, 119.6, 119.0, 110.5, 110.4, 94.1, 92.8, 80.4, 79.6, 52.9, 52.7, 45.8, 45.6, 35.7, 35.5; **HRMS** calcd. for  $\text{C}_{19}\text{H}_{20}\text{N}_3\text{O}_4^+$  [ $\text{M} + \text{H}$ ] $^+$  354.1448, found 354.1445.

**2h**:  $R_f$ =0.45 (silica gel, hexanes:EtOAc = 1:1);  $^1\text{H NMR}$  (500 MHz,  $\text{CDCl}_3$ ):  $\delta$  7.18 (d,  $J$  = 7.6 Hz, 1H), 7.15 (d,  $J$  = 7.7 Hz, 1H), 7.10 (t,  $J$  = 7.0 Hz, 2H), 6.77 (q,  $J$  = 7.1 Hz, 1H), 6.72 (t,  $J$  = 7.3 Hz, 1H), 6.64 (d,  $J$  = 7.8 Hz, 1H), 6.51 (dd,  $J$  = 11.4, 8.0 Hz, 2H), 5.73 and 5.69 (s, 1H), 5.14 and 4.80 (s, 1H), 4.05 and 4.00 (s, 1H), 3.85 and 3.74 (ddd,  $J$  = 11.5, 7.7, 3.7 Hz, 1H), 3.76 and 3.73 (s, 3H), 3.27 (ddd,  $J$  = 19.8, 16.6, 9.3 Hz, 1H), 2.63 (ddt,  $J$  = 30.8, 12.8, 8.5 Hz, 1H), 2.37 – 2.29 (m, 1H);  $^{13}\text{C NMR}$  (126 MHz,  $\text{CDCl}_3$ ):  $\delta$  156.0, 155.3, 149.1, 148.9, 145.10, 145.09, 129.9, 129.4, 129.3, 123.6, 123.5, 119.6, 119.4, 118.7, 118.5, 115.5, 115.2, 109.9, 109.7, 73.6, 72.4, 52.9, 52.7, 44.8, 44.6, 37.8, 37.6; **HRMS** calcd. for  $\text{C}_{18}\text{H}_{20}\text{N}_3\text{O}_2^+$

[M + H]<sup>+</sup> 310.1550, found 310.1546.

### 5.4.3. [3,3]-Sigmatropic Rearrangement of indolyl *N*-carboxylate **2r-Int** (Figure 2.19B)



To a 10 mL oven-dried Schlenk tube equipped with a stir bar were added indolyl *N*-carboxylate **2r-Int** (61.0 mg, 0.200 mmol, 1.0 equiv) and toluene (4 mL, 0.05 M in **2r-Int**) at 23 °C. The resulting mixture was heated to 90 °C in a pre-heated oil bath and stirred for 16 h, before it was cooled to rt and directly concentrated under reduced pressure to obtain the crude product. The resulting residue was purified by flash column chromatography (silica gel, hexanes:EtOAc = 1:0 → 7:3) to afford product **2r** (33.7 mg, 55%) as a pale yellow oil.

$R_f=0.25$  (silica gel, hexanes:EtOAc = 1:1);  $^1\text{H NMR}$  (500 MHz,  $\text{CDCl}_3$ ):  $\delta$  7.58 and 7.48 (d,  $J=7.6$  Hz, 1H), 7.17 (td,  $J=7.6, 1.3$  Hz, 1H), 6.79 (q,  $J=7.1$  Hz, 1H), 6.64 (d,  $J=7.9$  Hz, 1H), 5.67 and 5.62 (s, 1H), 5.13 and 4.79 (s, 1H), 3.85 and 3.78 (t,  $J=9.1$  Hz, 1H), 3.77 and 3.71 (s, 3H), 3.15 (td,  $J=10.8, 6.4$  Hz, 1H), 2.85 (s, 6H), 2.91 and 2.75 (dd,  $J=13.2, 6.1$  Hz, 1H), 2.67 – 2.56 (m, 1H);  $^{13}\text{C NMR}$  (126 MHz,  $\text{CDCl}_3$ ):  $\delta$  155.8, 155.1, 155.0, 150.9, 150.6, 130.9, 126.9, 126.7, 126.6, 125.8, 119.6, 119.3, 110.4, 110.3, 93.7, 92.4, 80.6, 79.8, 52.8, 52.6, 45.6, 45.4, 36.4, 36.2, 36.0; **HRMS** calcd. for  $\text{C}_{15}\text{H}_{20}\text{N}_3\text{O}_4^+$   $[\text{M} + \text{H}]^+$  306.1448, found 306.1449.

## 6. References

- (1) Yi, J.-C.; Liu, C.; Dai, L.-X.; You, S.-L., Synthesis of C3-Methyl-Substituted Pyrroloindolines and Furoindolines via Cascade Dearomatization of Indole Derivatives with Methyl Iodide. *Chem. Asian. J.* **2017**, *12*, 2975.
- (2) Liu, C.; Yi, J.-C.; Zheng, Z.-B.; Tang, Y.; Dai, L.-X.; You, S.-L., Enantioselective Synthesis of 3a-Amino-Pyrroloindolines by Copper-Catalyzed Direct Asymmetric Dearomative Amination of Tryptamines. *Angew. Chem. Int. Ed.* **2016**, *55*, 751.
- (3) Liang, X.-W.; Liu, C.; Zhang, W.; You, S.-L., Asymmetric Fluorinative Dearomatization of Tryptamine Derivatives. *Chem. Commun.* **2017**, *53*, 5531.
- (4) Zhu, S.; MacMillan, D. W. C., Enantioselective Copper-Catalyzed Construction of Aryl Pyrroloindolines via an Arylation–Cyclization Cascade. *J. Am. Chem. Soc.* **2012**, *134*, 10815.
- (5) Wang, Y.; Ye, L.; Zhang, L., Au-catalyzed Synthesis of 2-Alkylindoles from *N*-Arylhydroxylamines and Terminal Alkynes. *Chem. Commun.* **2011**, *47*, 7815.
- (6) Gore, S.; Baskaran, S.; König, B., Fischer Indole Synthesis in Low Melting Mixtures. *Org. Lett.* **2012**, *14*, 4568.
- (7) Ye, J.; Wu, J.; Lv, T.; Wu, G.; Gao, Y.; Chen, H., Oxidative Rearrangement Coupling Reaction for the Functionalization of Tetrahydro- $\beta$ -carbolines with Aromatic Amines. *Angew. Chem. Int. Ed.* **2017**, *56*, 14968.
- (8) Ye, J.; Lin, Y.; Liu, Q.; Xu, D.; Wu, F.; Liu, B.; Gao, Y.; Chen, H., Biomimetic Oxidative Coupling Cyclization Enabling Rapid Construction of Isochromanoindolenines. *Org. Lett.* **2018**, *20*, 5457.
- (9) Gentry, E. C.; Rono, L. J.; Hale, M. E.; Matsuura, R.; Knowles, R. R., Enantioselective Synthesis of Pyrroloindolines via Noncovalent Stabilization of Indole Radical Cations and Applications to the Synthesis of Alkaloid Natural Products. *J. Am. Chem. Soc.* **2018**, *140*, 3394.
- (10) Arp, F. O.; Fu, G. C., Kinetic Resolutions of Indolines by a Nonenzymatic Acylation Catalyst. *J. Am. Chem. Soc.* **2006**, *128*, 14264.
- (11) Duan, Y.; Li, L.; Chen, M.-W.; Yu, C.-B.; Fan, H.-J.; Zhou, Y.-G., Homogenous Pd-Catalyzed Asymmetric Hydrogenation of Unprotected Indoles: Scope and Mechanistic Studies. *J. Am. Chem. Soc.* **2014**, *136*, 7688.
- (12) Touge, T.; Arai, T., Asymmetric Hydrogenation of Unprotected Indoles Catalyzed by  $\eta^6$ -

- Arene/N-Me-sulfonyldiamine–Ru(II) Complexes. *J. Am. Chem. Soc.* **2016**, *138*, 11299.
- (13) Somei, M.; Noguchi, K.; Yoshino, K., 1-Hydroxyyohimbine and Its Derivatives: New Potent  $\alpha$ 2-Blockers for the Treatment of Erectile Dysfunction. *Heterocycles* **2006**, *69*, 259.
- (14) Yamada, F.; Kawanishi, A.; Tomita, A.; Somei, M., The First Preparation of the Unstable 1-Hydroxy-2, 3-dimethylindole. *Arkivoc* **2003**, *8*, 102.
- (15) Tamura, K.; Mizukami, H.; Maeda, K.; Watanabe, H.; Uneyama, K., One-pot Synthesis of Trifluoroacetimidoyl Halides. *J. Org. Chem.* **1993**, *58*, 32.
- (16) P. Zhang, X.-M. Wang, Q. Xu, C.-Q. Guo, P. Wang, C.-J. Lu, R.-R. Liu, Enantioselective Synthesis of Atropisomeric Biaryls by Pd-Catalyzed Asymmetric Buchwald–Hartwig Amination, *Angew. Chem. Int. Ed.* **2021**, *60*, 21718-21722.
- (17) W. Xiong, Q. Shi, W. H. Liu, Simple and practical conversion of benzoic acids to phenols at room temperature, *J. Am. Chem. Soc.* **2022**, *144*, 15894-15902.
- (18) Wnuk, S. F.; Chowdhury, S. M.; Garcia, P. I.; Robins, M. J., Stereodefined Synthesis of O3'-Labeled Uracil Nucleosides. 3'-[<sup>17</sup>O]-2'-Azido-2'-deoxyuridine 5'-Diphosphate as a Probe for the Mechanism of Inactivation of Ribonucleotide Reductases. *J. Org. Chem.* **2002**, *67*, 1816.



## 초 록

인돌(Indole)은 다양한 헤테로원자 고리 구조들 사이에서도 독보적인 중요성을 지닌 구조체로, 유기 화학의 역사와 함께 해온 특별한 구조이다. 인돌 자체가 지니는 생물학적 및 약리학적 가치는 물론이고, 인돌의 탈방향족화 반응(dearomatization)을 통해 얻을 수 있는 다양한 분자 구조들이 인돌 연구의 가치를 더욱 높여주고 있다. 과학의 발전으로 말미암아 유기 화학 분야에서 다양한 기술과 혁신적인 도구들의 응용을 통해 이전에는 실현되지 않았던 아이디어들이 구체화하는 것이 가능해졌는데, 이러한 속도에 힘입어 인돌의 작용기화 반응 또한 다양한 접근 방법이 개발되고 있다.

이러한 다양한 연구 방향 가운데, *N*-하이드록시인돌(*N*-hydroxyindole)을 활용한 탈방향족화 반응에 대한 연구는 아직까지 소수에 지나지 않는다. 비록 최근 *N*-하이드록시인돌의 고유한 반응성이 다시 관심을 받아 관련 연구들이 적극적으로 진행되고 있으나, 아직까지 *N*-하이드록시인돌이 갖고 있는 잠재력이 완전히 드러나지 않은 상태이다. 본 논문은 그러한 *N*-하이드록시인돌을 [3,3]-시그마 결합 자리 옮김 반응의 기질로 활용하고, 이를 통해 전합성 연구 및 관련 방법론 개발 연구를 진행한 과정 및 결과를 보고하고자 한다.

1장에서는 라지말(Rhazimal)의 전합성을 위한 합성적 연구 과정을 소개한다. 먼저 인돌 중심부의 산화를 통해 형성된 *N*-하이드록실 가이소스키진(*N*-hydroxyl geissoschizine)이 분자 내 [3,3]-시그마 결합 자리 옮김 반응을 통해 선택적으로 C7-C16 결합을 형성한다는, 생합성 경로에 대한 새로운 가설을 제시하였다. 그리고 해당 가설의 실험적 증명을 위해 단계적으로 복잡성을 증가시키는 세 단계의 합성 계획을 구상하였으며, 이를 통해 궁극적으로 라지말의 생모방적 합성을 이루는 것을 목표로 하였습니다. 해당 세 단계의 합성 계획 중 총 두 단계까지는 확립하였으나, 분자 내 [3,3] 시그마

결합 자리 옮김 반응의 구현이 이루어지지 못하여 불가피하게 마지막 단계인 라지말의 생모방적 합성을 완성하지 못하였다.

2장에서는 라지말의 전합성에서 발견한, *N*-하이드록시인돌의 [3,3]-시그마 결합 자리 옮김 반응에 대한 반응성을 토대로, 해당 반응을 인돌 뼈대의 C3- 위치에 다양한 헤테로원자들을 도입하는 통합적 방법론으로 확장시킨 과정에 대해 소개한다. 또한 그 과정에서 두 개의 서로 다른 메커니즘이 동시에 작용하는 것을 확인하였으며, 반응 기질의 전자적 성질이 해당 메커니즘 경로들의 상대적인 기여도 및 각 경로의 에너지 장벽 레벨 등을 결정한다는 사실을 발견하였다.

**주요어** : 탈방향족화 반응 • *N*-하이드록시인돌 • 질소 헤테로원자 고리 • 치환기 효과 • 시그마 결합 자리 옮김 반응

**학 번** : 2018-39895